Identifications de nouvelles voies de régulation impliquées dans la résistance non enzymatique aux aminosides chez Pseudomonas aeruginosa

Arnaud Bolard

Doctoral thesis from UNIVERSITÉ BOURGOGNE FRANCHE-COMTÉ, prepared at UFR SCIENCES MÉDICALES ET PHARMACEUTIQUES

École doctorale Environnements-Santé n°554

Doctorate in Biochemistry and Molecular Biology

by

Arnaud BOLARD

Identification of novel regulatory pathways involved in non-enzymatic resistance to aminoglycosides in *Pseudomonas aeruginosa*

Thesis presented and defended at Besançon, France, on July 5th, 2019

Thesis committee:

Pr. Christophe BORDI	President
Dr. Ina ATTRÉE	Reviewer
Dr. Thierry NAAS	Reviewer
Dr. Thilo KÖHLER	Moderator
Dr. Katy JEANNOT	Moderator
Pr. Patrick PLÉSIAT	Thesis supervisor

UBFC
UNIVERSITÉ
BOURGOGNE FRANCHE-COMTÉ

Thèse de doctorat de l'UNIVERSITÉ BOURGOGNE FRANCHE-COMTÉ, préparée à l'UFR SCIENCES MÉDICALES ET PHARMACEUTIQUES

École doctorale Environnements-Santé n°554

Doctorat en Biochimie et Biologie moléculaire

par

Arnaud BOLARD

Identification de nouvelles voies de régulation impliquées dans la résistance non enzymatique aux aminosides chez Pseudomonas aeruginosa

---

Thèse présentée et soutenue à Besançon, France, le 5 juillet 2019

Composition du jury:

Pr. Christophe BORDI	Président
Dr. Ina ATTRÉE	Rapporteur
Dr. Thierry NAAS	Rapporteur
Dr. Thilo KÖHLER	Examinateur
Dr. Katy JEANNOT	Examinateur
Pr. Patrick PLÉSIAT	Directeur de thèse

ufr SMP sciences médicales & pharmaceutiques

Remerciements

Ce manuscrit de thèse est l'aboutissement de plusieurs années de travail qui ont pu se concrétiser grâce à l'expertise et au soutien sans faille de nombreuses personnes auxquelles j'adresse mes plus vifs remerciements.

Je tiens tout d'abord à remercier très sincèrement le Docteur Ina Attrée et le Docteur Thierry Naas pour m'avoir fait l'honneur d'accepter d'être les rapporteurs de ce manuscrit ainsi que pour leur participation au jury de soutenance de thèse.

Mes remerciements s'adressent également au Docteur Thilo Köhler qui a accepté de partager son expertise scientifique en examinant mon travail de thèse.

Je remercie avec beaucoup de respect le Professeur Christophe Bordi qui a contribué à la réalisation de cette thèse par ses précieux conseils et par les échanges que nous avons pu avoir au cours des comités annuels de suivi de thèse. Un grand merci pour avoir accepté de faire partie de mon jury de thèse.

Je remercie très chaleureusement le Docteur Delphine Destoumieux-Garzón pour son implication et sa contribution dans la maturation de mon doctorat lors des réunions annuelles de suivi de thèse. Je la remercie, ainsi que toute son équipe, et notamment Daniel Oyanedel pour m'avoir accueilli lors de mon séjour à Montpellier. J'ai été ravi de pouvoir passer ces quelques jours au sein de son équipe soudée et dynamique.

J'adresse mes remerciements à mon directeur de thèse, le Professeur Patrick Plésiat pour m'avoir permis d'effectuer mon doctorat au sein de son équipe. Je le remercie tout particulièrement pour son expertise précieuse et son implication apportées au cours de la rédaction de ce manuscrit.

Je remercie ma tutrice, le Docteur Katy Jeannot avec qui j'ai étroitement travaillé au cours de mon doctorat. Je la remercie tout particulièrement pour avoir initié une collaboration réussie avec le Docteur Yanyan Li.

J'adresse tout mon respect et mes remerciements éternels au Docteur Catherine Llanes. J'espère pouvoir suivre un jour ses pas.

Je remercie très amicalement le Docteur Benoît Valot pour m'avoir débloqué lorsque je pensais être dans une impasse.

Je dois avouer que ma thèse n'aurait pas été la même sans des collègues d'exception: Anaïs, Paulo, Loïs, Hélène, Mélanie, Alexandre, Eleni, Isabelle, Damien, Sophie, Jean-Baptiste, Camille, Gwendoline, Elisa, Antoine, Thomas, Maxime, Pauline, Amélie, Emilie, Steffi, Adeline, Audrey, Alice, Coralie, Chloé, Clothilde, Malik, Sandra, Marie, Didier, Charlotte, Jenny ; ce fut un réel plaisir de travailler avec vous et je vous remercie sincèrement pour votre soutien.

Pour finir, je remercie sans aucune commune mesure ma famille pour son soutien indéfectible depuis toujours et pour la liberté si précieuse qu'elle me procure. Vous êtes ma plus grande force.

Table of contents

List of figures

List of tables

Abbreviations

A_{530}: absorbance at 530 nm
A_{600}: absorbance at 600 nm
(p)ppGpp: guanosine pentaphosphate or tetraphosphate
$\Delta\psi$: membrane electrical potential
3OC12-HSL: N-3-oxododecanoyl-HSL
5FA: penta-acyl molecular species
6FA: hexa-acyl molecular species
A: adenylation
aa: aminoacyl
ACN: acetonitrile
AMB: L-2-amino-4-methoxy-trans-3-butenoic acid
AMK: amikacin
AMP: adenosine monophosphate
AMPs: antimicrobial peptides
Amp^r: ampicillin resistance
ANL: acyl-CoA synthetases, NRPS adenylation domains, and Luciferase enzymes
APH(3'): aminoglycoside O-3' phosphoryltransferase
AraN: aminoarabinose
arn: *arnBCADTEF-ugd*
A-site: aminoacyl-site
ATM: aztreonam
ATP: adenosine triphosphate
C: condensation
C4-HSL: N-butanoyl-HSL
CA: C-terminal catalytic and ATP binding
CAMPs: cationic antimicrobial peptides
CAZ: ceftazidime
c-di-GMP: bis-(3'-5')-cyclic dimeric GMP
cDNA: complementary DNA
CF: cystic fibrosis
CFU: colony forming unit
CHL: chloramphenicol
CIP: ciprofloxacin
CLSI: clinical and laboratory standards institute
Cm: carbamoyl
CST: colistin
Ct: cycle threshold
CTX: cefotaxime
Cy: hetero-cyclization
cyt c: MOPS-cytochrome *c* solution
D: aspartic acid
DABA: L-2,4-diaminobutyrate
DABA AT: L-2,4-diaminobutyrate:2-ketoglutarate 4-aminotransferase
DABA DC: L-2,4-diaminobutyrate decarboxylase
DHp: dimerization and histidine phosphotransfer
DMSO: dimethyl sulfoxide
DNA: deoxyribonucleic acid
DSF: cis-2-unsaturated fatty acids
E: epimerization
EARS-Net: european antimicrobial resistance surveillance network
ECDC: european centre for disease prevention and control
EDP: energy dependent phase
EEA: european economic area
EFF: effector
EPS: exopolysaccharides
E-site: exit-site
Etn: ethanolamine
EU: european union
FA: fatty acid
FEP: cefepime
FOF: fosfomycin
FucNAc: 2-acetamido-2-deoxy-D-fucose
GAF: c-GMP and c-GMP-stimulated phosphodiesterases, Anabaena adenylate cyclases and *E. coli* FhlA
GalN: 2-amino-2-deoxy-galactose
gDNA: genomic DNA
GEN: gentamicin
GI: genomic island
Glc: glucose
GlcN: 3-(acetylamino)-3-deoxy-D-glucose
Gm^r: gentamicin resistance
GTP: guanosine triphosphate
H: histidine
HAMP: linker domain
HATPase: histidine kinase-like ATPases
Hep: L-glycero-D-manno-heptose
HEPES: 4-(2-hydroxyethyl)-1-piperazineethanesulfonic acid
HHQ: 4-hydroxy-2-heptylquinoline
HisKA: dimerization and phosphoacceptor
HK: histidine kinase
Hpt: histidine-containing phosphotransfer
HSL: L-homoserine lactone
IM: inner membrane
IPM: imipenem
IPTG: isopropyl-β-D-thiogalactopyranoside
IQS: 2-(2-hydroxyphenyl)-thiazole-4-carbaldehyde

KAN: kanamycin
Kan^r: kanamycin resistance
Kdo: 3-deoxy-D-manno-oct-2-ulosonic acid
L-Ara-4N: 4-amino-4-desoxy-L-arabinose
L-ASA: L-aspartate β-semialdehyde
L-AZC: L-azetidine 2-carboxylic acid
LB: lysogeny broth
LC-ESI-MS: liquid chromatography-electrospray ionization-mass spectrometry
LC-HRMS: liquid chromatography coupled to high resolution mass spectrometry
L-Dab: L-2,4-diaminobutyrate
L-fOHOrn: L-N5-formyl-N5-hydroxyornithine
L-OHOrn: L-N5-hydroxyornithine
L-Orn: L-ornithine
LPS: lipopolysaccharide
m*/*z: mass/charge ratio
MALDI-TOF: matrix-assisted laser desorption/ionization with time-of-flight
ManNAc3NAcA: 2,3-diacetamido-2,3-dideoxy-D-mannuronic acid
ManNAc3NAmA: 2-acetamido-3-acetamidino-2,3-dideoxy-D-mannuronic acid
McF: McFarland
MDR: multidrug-resistant
MEM: meropenem
MHA: Mueller-Hinton agar
MHBc: Mueller-Hinton broth (cation-adjusted)
MIC: minimum inhibitory concentration
MOPS: 3-(N-morpholino)propanesulfonic acid
mRNA: messenger RNA
NA: non applicable
NADH: nicotinamide adenine dinucleotide
NADPH: nicotinamide adenine dinucleotide phosphate (reduced)
nd: not determined
N-Mt: N-methylation
NOV: novobiocin
NRP: nonribosomal peptide
NRPS: NRP synthetase
OM: outer membrane
OXA: oxacillinase
P: phosphate
PAS-like: Per (period circadian protein)-ARNT (vertebrate aryl hydrocarbon receptor nuclear translocator)-Sim (single-minded)
PATRIC: pathosystems resource integration center
PCP: peptidyl carrier protein
PCR: polymerase chain reaction
PDB: protein data bank
PDR: pandrug-resistant
PIA: *Pseudomonas* isolation agar
PIP: piperacillin
PKS: polyketide synthase
PLP: pyridoxal phosphate
Pmx: polymyxins
PPi: pyrophosphate
PQS: 2-heptyl-3-hydroxy-4-quinolone
P-site: peptidyl-site
PVD: pyoverdine
qPCR: quantitative PCR
QS: *quorum* sensing
REC: N-terminal receiver
Rec: recycled
Rha: rhamnose
RNA seq: high-throughput RNA sequencing
RNA: ribonucleic acid
RND: resistance nodulation cell division
rpm: revolutions per minute
RR: response regulator
rRNA: ribosomal RNA
RT: reverse transcription
SAM: S-adenosylmethionine
SDS-PAGE: sodium dodecyl sulphate-polyacrylamide gel electrophoresis
SMART: simple modular architecture research tool
STAC: solute carrier and two-component signal transduction associated component
STR: streptomycin
Str^r: streptomycin resistance
T: thiolation
TAE: tris-acetate 40 mM, EDTA 1 mM
TCS: two-component system
TE: thioesterase
TET: tetracycline
Tet^r: tetracycline resistance
TFA: trifluoroacetic acid
TIC: ticarcillin
TIM: ticarcillin-clavulanic acid
TM: transmembrane
TMAO: trimethylamine-N-oxide
TMP: trimethoprim
TMPP: N-succinimidyloxycarbonylmethyl)-tris-(2,4,6-trimethoxyphenyl)-phosphonium bromide
TOB: tobramycin
Trans_reg_C: transcriptional regulatory protein, C-terminal
tRNA: transfer RNA
TZP: piperacillin-tazobactam
U: enzyme unit
UV: ultraviolet
VAN: vancomycin
XDR: extensively drug-resistant
Zeo^r: zeocin resistance

I. Introduction

Pseudomonas aeruginosa is a Gram-negative bacillus with a remarkable ability to grow in a wide variety of environmental conditions such as soil, water as well as in plant-, animal- and human-host-associated environments (Kazmierczak *et al*., 2015; Sitaraman, 2015). This great adaptability may result in part from its relatively large genome (≈ 6.3 Mb) carrying a substantial number of genes enabling the utilization of various carbon sources, efficient energy metabolism, and encoding many regulatory systems (Stover *et al*., 2000).

In the clinical context, this non-fermentative bacillus is a major human opportunistic pathogen infecting immunocompromised patients, especially in intensive care units, as well as those suffering from chronic respiratory diseases such as cystic fibrosis (CF). In CF patients, the bronchial colonization by various microorganisms leads to significant alteration of respiratory function. Unfortunately, *P. aeruginosa* is difficult to treat because of its intrinsic resistance to several anti-Gram-negative antibiotic classes including β-lactams and aminoglycosides. This resistance is mainly due to the low permeability of the outer membrane, the action of enzymes which degrade or modify antibiotics (AmpC, OXA-50 and APH(3')-IIb) and finally the complementary action of two multi-drug efflux systems [MexAB-OprM and MexXY(OprM)] able to export a huge panel of antibacterials outside the cell (Lister *et al*., 2009).

In addition, resistance-associated genes may be acquired by *P. aeruginosa* from mobile genetic elements such as plasmids and transposons that can reduce ultimately the efficacy of all of the available antibiotic families (aminoglycosides, β-lactams, fluoroquinolones and polymyxins). Finally, the basal resistance levels of *P. aeruginosa* may also be increased through mutational processes altering the expression and/or function of chromosomally-encoded resistance-associated proteins. For example, mutational inactivation of MexR, a transcriptional repressor of the *mexAB-oprM* operon, is associated with a 4- to 8-fold increase in resistance to β-lactams (Cao *et al*., 2004).

As a result, the accumulation of several of these genetic events is the driving force of emergence of clinical isolates highly resistant to multiple antibiotic families. To characterize the different patterns of resistance, a standardized international terminology defined (i) multidrug-resistant (MDR) strains as presenting an acquired resistance to at least one agent in three or more antimicrobial categories, (ii) extensively drug-resistant

Table 1: Antimicrobial categories and agents used to define multidrug resistant (MDR), extensively drug-resistant (XDR) and pandrug-resistant (PDR) strains of *P. aeruginosa*.

Antimicrobial categories	Antimicrobial agents
Aminoglycosides	gentamicin, tobramycin, amikacin, netilmicin
Antipseudomonal carbapenems	imipenem, meropenem
Antipseudomonal cephalosporins	ceftazidime, cefepime
Antipseudomonal fluoroquinolones	ciprofloxacin, levofloxacin
Antipseudomonal penicillins/ β-lactamase inhibitors	ticarcillin/clavulanic acid, piperacillin/tazobactam
Monobactams	aztreonam
Phosphonic acids	fosfomycin
Polymyxins	colistin, polymyxin B

(Magiorakos *et al*., 2012)

(XDR) as those strains remaining susceptible to only one or two antimicrobial categories and (iii) pandrug-resistant (PDR), the ones resistant to all agents in all antimicrobial categories (Table 1) (Magiorakos *et al*., 2012).

Among the eight categories of antipseudomonal agents, aminoglycosides are widely used to treat acute and chronic infections (Krause *et al*., 2016). In CF patients, molecules such as tobramycin are administered by aerosols over long periods of time to eradicate or control lung colonization by *P. aeruginosa*. Identification of aminoglycoside resistance mechanisms is thus considered as a prerequisite for the development of novel and innovative inhibitory molecules. In general, therapeutic treatments often associate an aminoglycoside with an antibiotic from another family (β-lactams or fluoroquinolones) (Tamma *et al*., 2012). In addition to antimicrobial resistance mechanisms, *P. aeruginosa* counts on an arsenal of virulence factors to generate infections. Drug-resistant strains should be tackled in a global and integrated way to control and combat them.

While the main objective of this thesis was to identify and characterize novel non-enzymatic mechanisms developed by *P. aeruginosa* to resist aminoglycosides, we also assessed the impact of these mechanisms on resistance to other antibiotics, especially polymyxins. A specific attention was paid to decipher uncharacterized virulence-associated circuits, *via* the synthesis of non-ribosomal peptides, in our case, azetidine-containing alkaloids.

The review of the literature in this manuscript describes the mode of action of aminoglycosides and the known mechanisms causing resistance to these major antibiotics. It also makes the point on two-component systems (TCSs) and their implication in resistance to aminoglycosides and other antibiotic families. Furthermore, the virulence traits mediated by non-ribosomal peptide synthesis machineries are presented. The results are divided in four main chapters dealing with: (i) the role of elongation factor EF-G1A in aminoglycoside resistance of clinical strains, (ii) the cross-resistance to aminoglycosides and colistin conferred by PmrAB mutations, (iii) the participation of efflux pump MexXY(OprM) in acquired resistance to colistin and, (iv) the identification of two unusual bicyclic alkaloids produced by *P. aeruginosa*. A final discussion with a general conclusion ends this manuscript before a last section describing the materials and methods used to achieve these projects.

II. Bibliographic review

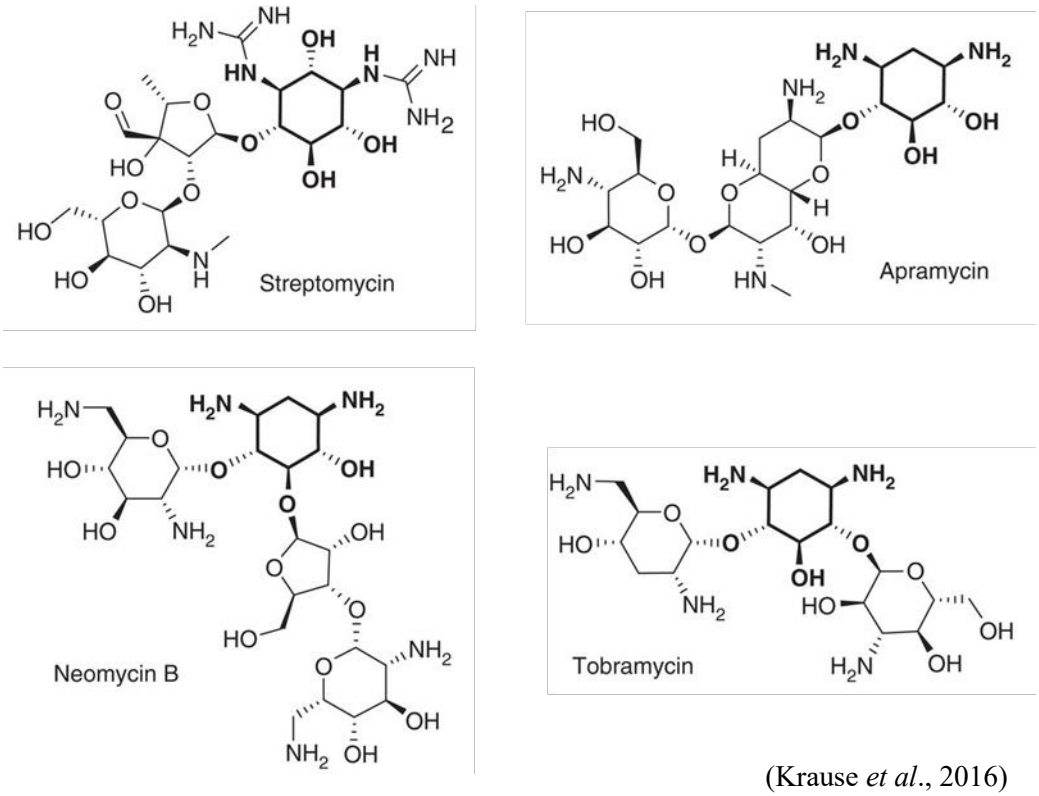

(Krause *et al*., 2016)

Figure 1: Structures of representative aminoglycosides from the four subclasses.

The deoxystreptamine (in streptomycin) and the streptidine rings (in apramycin, neomycin B and tobramycin) are in **bold**.

1. Aminoglycosides: overview

Aminoglycosides are natural antibacterial molecules produced by species from genus *Streptomyces* and *Micromonospora*. The first aminoglycoside to be discovered (streptomycin) was isolated in 1943 from *S. griseus* and was used to successfully treat tuberculosis (Becker and Cooper, 2013). After its introduction in antimicrobial chemotherapy in 1944, additional natural aminoglycosides were added to this family as neomycin, kanamycin, gentamicin, tobramycin and sisomycin. Subsequent chemical modifications of some of these natural molecules were then required to resolve the emergence of resistance and to prevent toxic side-effects. This second generation of semisynthetic derivatives includes dibekacin, amikacin, arbekacin, isepamicin and netilmicin. Like the natural molecules, these drugs of second generation target the ribosome and interferes with protein synthesis, leading to cell death.

1.1. Structure

The core structure of aminoglycosides consists of at least one amino sugar connected to a dibasic aminocyclitol *via* glycosidic linkages. The dibasic aminocyclitol inositol derivative is most often a 2-deoxystreptamine (Mingeot-Leclercq *et al*., 1999). The whole structure contains several free hydroxyl- and at least two amino-groups, which are important for the interaction with the ribosomal RNA of the 30S subunit (Becker and Cooper, 2013). Aminoglycosides are classified into four subclasses referring to the aminocyclitol moiety (Figure 1): (1) no deoxystreptamine (e.g., streptomycin, which has a streptidine ring); (2) a mono-substituted deoxystreptamine ring (e.g., apramycin); (3) a 4,5-di-substituted deoxystreptamine ring (e.g., neomycin, ribostamycin); or (4) a 4,6-di-substituted deoxystreptamine ring (e.g., gentamicin, amikacin, tobramycin and plazomicin) (Krause *et al*., 2016).

1.2. Aminoglycosides uptake

Aminoglycosides activity is dependent upon their penetration through bacterial membranes and accumulation into the cytoplasm, where the cellular target (ribosome) is located. The entry of the drug into bacterial cells occurs in three distinct stages, the first of which consists in a self-promoted uptake, whereas the second and the third are

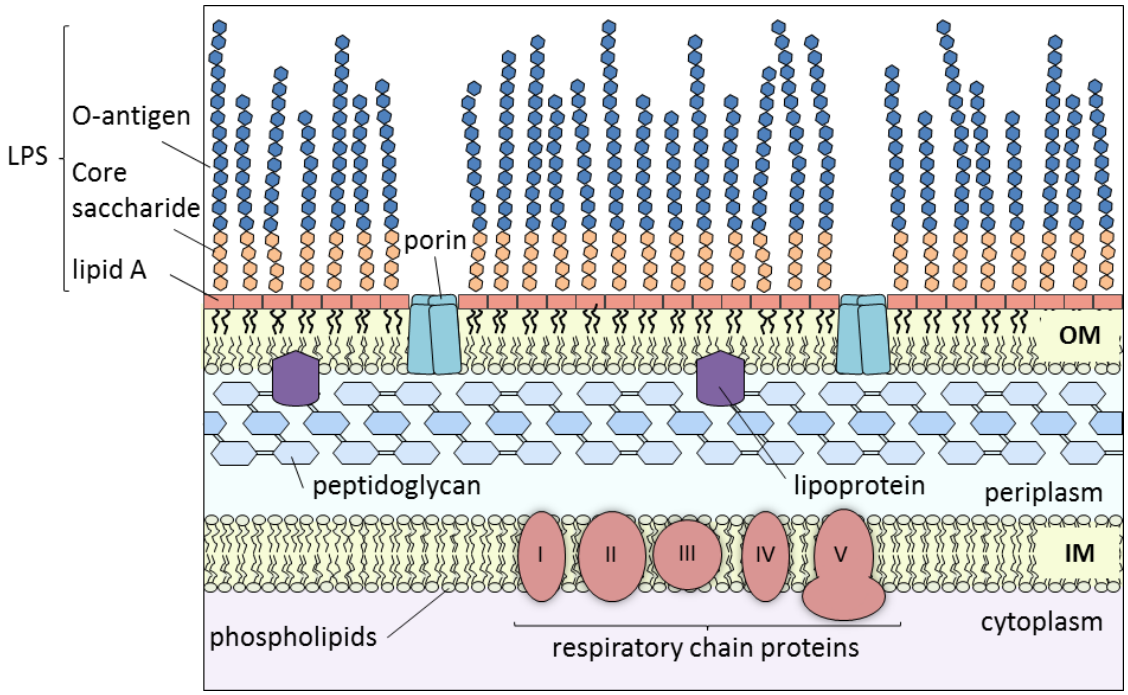

Figure 2: Schematic representation of the bacterial cell envelope of Gram-negative bacteria.

OM: outer membrane, IM: inner membrane, LPS: lipopolysaccharide.

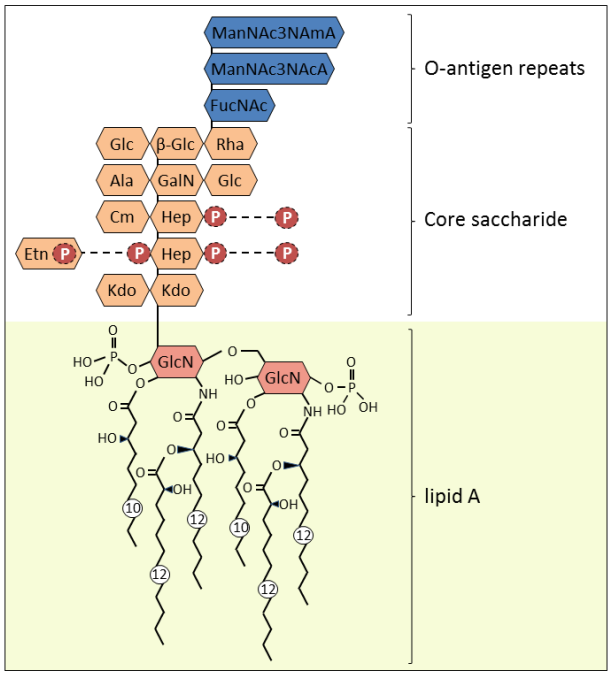

Figure 3: Lipopolysaccharide (LPS) structure of *P. aeruginosa*.

GlcN: 3-(acetylamino)-3-deoxy-D-glucose, Kdo: 3-deoxy-D-manno-oct-2-ulosonic acid, Hep: L-glycero-D-manno-heptose, Etn: ethanolamine, Cm: carbamoyl, GalN: 2-amino-2-deoxy-galactose, Ala: alanine, Glc: glucose, Rha: rhamnose, FucNAc: 2-acetamido-2-deoxy-D-fucose, ManNAc3NAcA: 2,3-diacetamido-2,3-dideoxy-D-mannuronic acid, ManNAc3NAmA: 2-acetamido-3-acetamidino-2,3-dideoxy-D-mannuronic acid, P: phosphate (King *et al*., 2009).

energy-dependent, and for this reason are named the Energy Dependent Phases I (EDPI) and II (EDPII) (Krause *et al*., 2016).

1.2.1. Cell envelope of Gram-negative bacteria

To reach the cytoplasm, aminoglycosides must cross the bacterial cell envelope which is a complex multi-layered structure (Figure 2). The cell wall of *P. aeruginosa* is composed of (i) an inner membrane (IM) constituted by a phospholipid bilayer surrounding the cytoplasm, (ii) a thin peptidoglycan layer and (iii) an outer membrane (OM) in part constituted of lipopolysaccharide (LPS) molecules (Silhavy *et al*., 2010). The two concentric membrane layers delimit an aqueous cellular compartment, known as the periplasm.

The OM, absent in Gram-positive bacteria, is an asymmetric bilayer. The inner leaflet mainly contains phosphatidylethanolamine, phosphatidylglycerol and diphosphatidyl-glycerol molecules (Lambert, 1988); while the outer leaflet is made of glycolipids, particularly LPS, which are essential in the barrier function of the OM. LPS consist of three covalently linked regions: the lipid A (a glucosamine disaccharide with six or seven acyl chains), a polysaccharide core, and an extended branched polysaccharide chain also called the O-antigen (Figure 3) (Lambert, 1988). LPS molecules are tightly bound to each other in a packing order *via* the bridging action of divalent cations, particularly Mg^{2+}, that neutralize the negative charge of LPS phosphate groups. Lipoproteins and β-barrel proteins are also major constituents of the OM. These latters, including porins, serve as a protection against hostile environments by contributing to the selective permeability of the OM (Silhavy *et al*., 2010).

The IM is a phospholipid bilayer containing enzymes, permeases and the components of the respiratory chains. The periplasm, delimited by the OM and IM, is rich in proteins whose activity is protected from harmful degradative enzymes such as RNAse or alkaline phosphatase (Silhavy *et al*., 2010). Periplasm features a peptidoglycan constituted of units of the disaccharide N-acetyl-glucosamine-N-acetyl-muramic acid, cross-linked by pentapeptide side chains (Lambert, 1988).

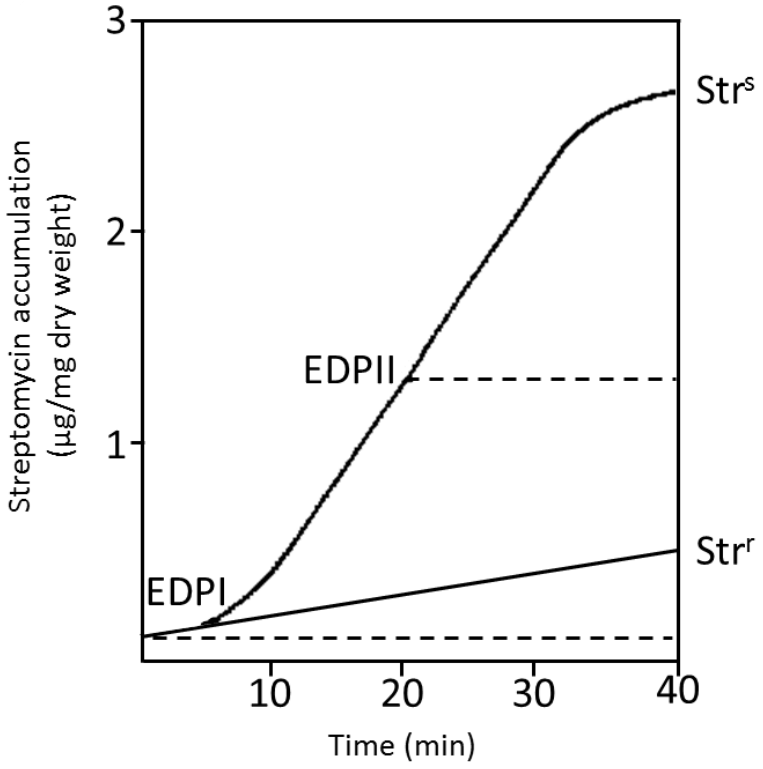

(Hancock, 1981)

Figure 4: Schematic representation of aminoglycoside (streptomycin) accumulation in *P. aeruginosa*.

Str^s: streptomycin susceptible strain, Str^r: *rpsL* mutant of Str^s.

1.2.2. Initial phase: ionic binding

In Gram-negative organisms, the first stage of aminoglycoside uptake consists of an electrostatic interaction between the polycationic aminoglycosides and the negatively charged components of the membrane (phospholipids, LPS and OM proteins). This electrostatic binding is reversible, concentration-dependent and uninfluenced by inhibitors of energized uptake. Ionic binding leads to a displacement of magnesium ions which are responsible for the cross bridging and stabilization of the membrane lipid components. Therefore, it follows a partial disruption of the OM continuum with local enhanced permeability and self-promoted uptake of aminoglycosides (Hancock *et al*. 1981; 1991; Hancock 1984; Ramirez and Tolmasky 2010). The two subsequent stages enable aminoglycosides to cross the IM: EDPI and EDPII (Figure 4).

1.2.3. Energy Dependent Phase I (EDPI)

Once aminoglycosides are in the periplasm, they need to cross the IM in order to reach their intracellular target. EDPI is characterized by a slow-rate energy-dependent uptake and is concentration-dependent. This phase precedes the loss of viability and the inhibition of protein synthesis (Becker and Cooper, 2013). It is assumed that during EDPI, aminoglycosides cross the IM in response to the membrane electrical potential ($\Delta\psi$). This transport might involve quinone-linked redox energy and/or components of the electron transport chains. That is why this active uptake can be blocked by inhibitors of oxidative phosphorylation (e.g., carbonyl cyanide-*m*-chlorophenylhydrazone) or electron transport inhibitors (cyanide) (Taber *et al*., 1987). According to some experimental results, EDPI could benefit from the inhibition of protein synthesis with mistranslated proteins being able to insert into the IM and thus to promote subsequent aminoglycoside entry (Nichols and Young 1985; Davis *et al*. 1986).

1.2.4. Energy Dependent Phase II (EDPII)

EDPI is followed by EDPII, the third stage of aminoglycoside uptake. It corresponds to a rapid energy-dependent accumulation of aminoglycosides in the cytoplasm increasing inhibition of protein synthesis, mistranslation, and accelerated cell death (Krause *et al*., 2016). This phase uses the energy from electron transport and possibly from adenosine triphosphate (ATP) hydrolysis, which explains why aminoglycoside uptake during

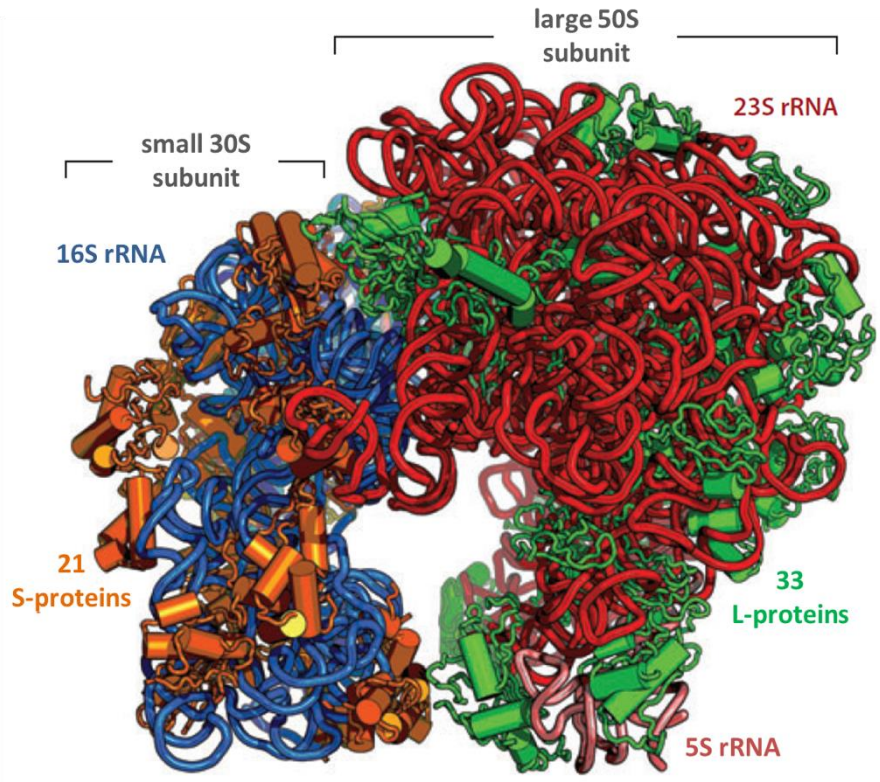

(Shajani *et al*., 2011)

Figure 5: Representation of the 70S ribosome of *E. coli*.

The small subunit 30S is composed of a single 16S rRNA (in blue) with 21 ribosomal proteins (S-proteins in orange). The large subunit 50S is formed by two rRNAs 5S and 23S (in red) with 33 ribosomal proteins (L-proteins in green). rRNA: ribosomal ribonucleic acid.

EDPII is blocked by cyanide, sulfhydryl reagents or other uncouplers of the oxidative phosphorylation (Taber *et al*., 1987). However, the exact mechanism of EDPII remains unclear because some inhibitors of protein synthesis can also reduce or completely abrogate EDPII, suggesting that this step requires protein synthesis. Aminoglycosides are ineffective against bacteria that grow anaerobically, as these microorganisms lack the membrane potential and the electron transport mechanisms necessary for EDPI and EDPII to occur.

1.3. Mode of action of aminoglycosides

Once aminoglycosides have reached the cytoplasm, their major antibacterial activity is due to the inhibition of protein synthesis. Indeed, aminoglycosides introduce errors in the sequence of newly elongated peptides and impact all four principle stages of the translation process (initiation, elongation, termination and recycling) (Prokhorova *et al*., 2017).

1.3.1. The ribosome, target of aminoglycosides

The ribosome is a ribonucleoprotein complex capable to decode the genetic information from the messenger RNA (mRNA) (Melnikov *et al*., 2012). Bacterial 70S ribosomes consist of two ribonucleoprotein subunits, a small subunit (30S) and a large one (50S) (Figure 5). In *Escherichia coli*, the 30S subunit is composed of 21 ribosomal proteins and a single 16S ribosomal RNA (rRNA) of 1,541 nucleotides, whereas the 50S subunit contains 33 ribosomal proteins and two rRNAs: 5S and 23S of 115 and 2,904 nucleotides, respectively (Figure 5) (Arenz and Wilson, 2016).

During the initiation of translation, the small subunit binds to mRNA and decodes the 3-nucleotides codon, to determine the amino acid to incorporate into the nascent polypeptide. The large subunit harbors the peptidyl transferase center, which is the site of peptide-bond formation (Shajani *et al*., 2011). The ribosome enables the binding of transfer RNAs (tRNAs), adaptor molecules able to recognize a specific codon of the mRNA with their anticodon arm. Next, the amino acid specific for the mRNA codon is covalently linked to the 3'-end of tRNA. The complete 70S ribosome (30S and 50S) contains three tRNA binding sites, termed the A-site, P-site and E-site (Figure 6) (Ling and Ermolenko, 2016).

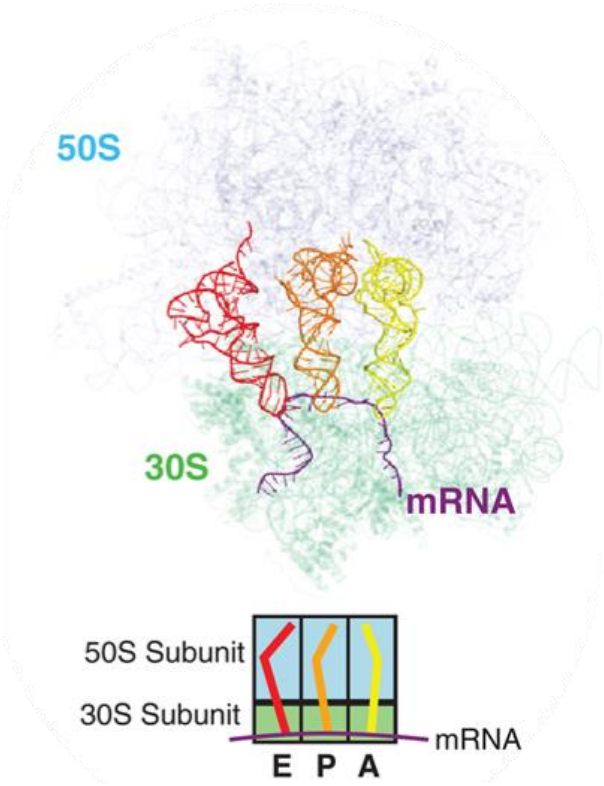

Figure 6: Functional organization of mRNA translation by the ribosome.

The 70S ribosome composed of the large 50S subunit (light blue) and small 30S subunit (light green) contains three tRNA binding sites, the aminoacyl (A) site, the peptidyl (P) site and the exit (E) site. Respective tRNAs are colored in yellow, orange and red. mRNA is in purple.

(Ling and Ermolenko, 2016)

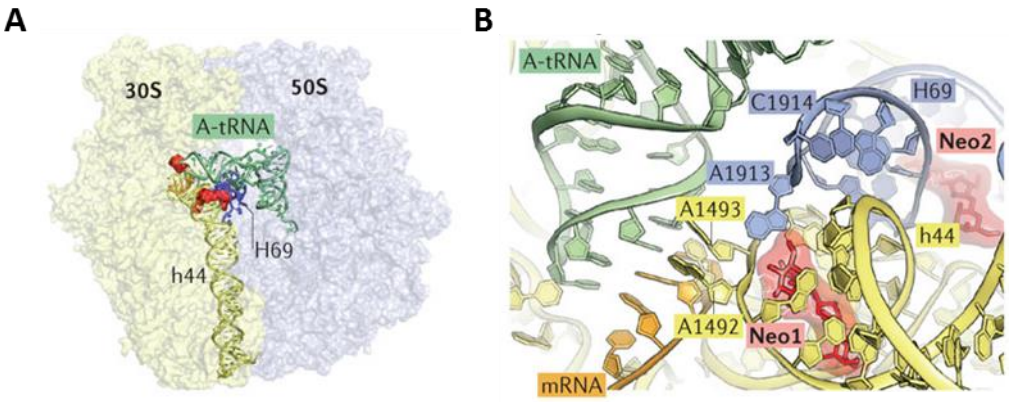

(Wilson, 2014)

Figure 7: Interactions of aminoglycoside molecule neomycin with the decoding center of the ribosome.

Large scale (A) and smaller scale (B) show that neomycin (in red) has two binding sites: h44 (yellow) of 30S subunit (neomycin molecule Neo1), and H69 (blue) of the 50S subunit (Neo2 molecule). A-site tRNA is in green.

The A-site binds the incoming aminoacylated or charged tRNA while the P-site (peptidyl-tRNA binding site) is occupied by the tRNA carrying the polypeptide chain in elongation (or the initiator tRNA during the initiation step). Finally, the E-site is the exit site which binds only outgoing deacylated or uncharged tRNA. During the stage of translation-elongation, the tRNAs successively pass through the A-, P-, and then E-sites (translocation process), before dissociating from the ribosome (Arenz and Wilson, 2016). Aminoglycosides interact with the ribosome at two distinct sites (Figure 7). The main drug target is at the A-site, on the 16S ribosomal RNA of 30S subunit (Krause *et al*., 2016). More precisely, this corresponds to highly conserved nucleotides of 16S rRNA helix 44 (h44) where monitoring of codon-anticodon interactions takes place (Gutierrez *et al*., 2013). Members of the aminoglycoside family exhibit affinity with different regions of the A-site (Carter *et al*., 2000). For example, it was shown that nucleotides C1407/G1494, A1408, A1493 and U1495 are important for paromomycin binding to the A-site (Fourmy *et al*., 1996). Finally, the majority of aminoglycosides alter the conformation of the ribosome, decreasing translational fidelity by inducing codon misreading on delivery of the aminoacyl transfer RNA (Krause *et al*., 2016). This results in the formation of erroneous proteins, that once released are assumed to cause damages to the cell membranes. However, some aminoglycosides do not cause misreading, such as apramycin (Matt *et al*., 2012) or spectinomycin (Vakulenko and Mobashery, 2003). In addition, some aminoglycosides are able to block one of the translation steps. For example, streptomycin blocks the initiation complex and decrease both the rate and the accuracy of translation (Davis, 1987); the 2-deoxystreptamine aminoglycosides are potent inhibitors of translocation (Wilson, 2014).

The second target site of aminoglycosides was identified within another functionally important region of the 50S subunit, the helix 69 (H69) of 23S rRNA (Gutierrez *et al*., 2013). H69 interacts with helix 44 (h44) of the 16S RNA to form one of the major intersubunit bridges B2a, a site of interaction at the interface between the small and large ribosomal subunits (Wilson, 2014). Following the termination of mRNA translation, the ribosome recycling factor together with elongation factor G (EF-G) disrupt the H69-h44 interaction enabling the two ribosomal subunits to separate. Aminoglycoside binding within H69 stabilizes the interbridge contacts and interfers with the subunit recycling process (Gutierrez *et al*., 2013).

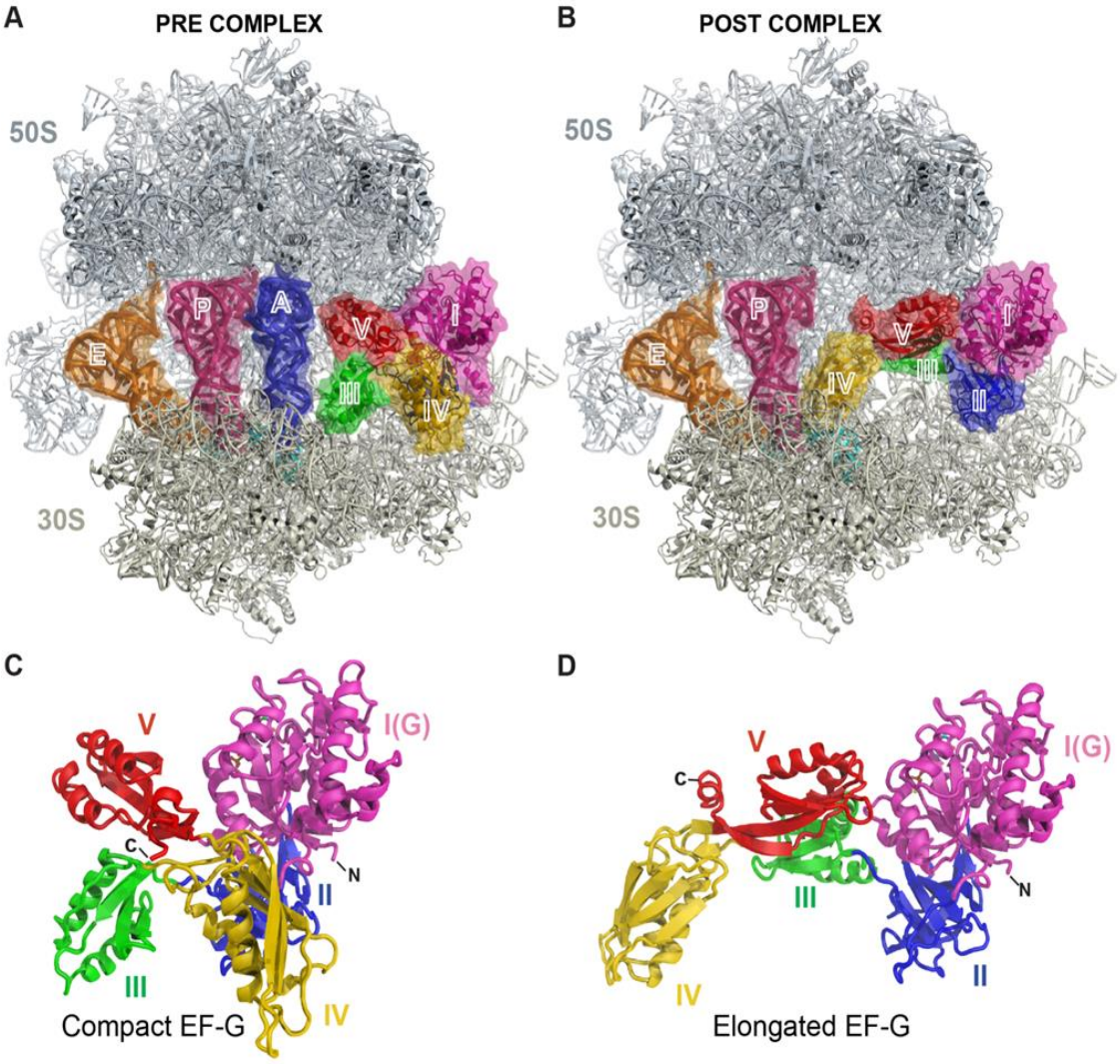

(Lin *et al*., 2015)

Figure 8: The structures of the elongation factor G in complex with the ribosome in pre- and post-translocational states.

EF-G conformations during pretranslocation (A and C) and posttranslocation (B and D) complexes are represented. The large ribosomal subunit 50S (gray) and the small subunit 30S (ivory) are shown with the A-site (blue), P-site (pink), and E-site (orange) tRNAs. The five domains of EF-G (I(G), II, II, IV and V) are represented with different colors.

1.3.2. Elongation factor G (EF-G)

The elongation factor G (EF-G) belongs to the GTPase superfamily. This enzyme triggers ribosome-dependent hydrolysis of GTP and thus participates in two different steps during protein synthesis: elongation and ribosome recycling (Palmer *et al*., 2013). During the elongation step, EF-G enables the translocation of mRNA and tRNA through the ribosome (Nyfeler *et al*., 2012). EF-G shows two conformations when the mRNA moves from one codon to another: a compact conformation during the pretranslocational state (Figure 8A and C) and an elongated conformation during the postranslocational state (Figure 8B and D) (Lin *et al*., 2015). Additionally, EF-G collaborates with ribosome recycling factor (RRF) to split the 70S ribosome into its two, 50S and 30S, subunits during a process called ribosome recycling (Borovinskaya *et al*., 2007). The ribosome subunits can then be utilized in another round of translation.

The genome of *P. aeruginosa* possesses two genes coding for two elongation factors G, namely *fusA1* (PA4266) and *fusA2* (PA2071). The *fusA1* gene is predicted to be part of a three-gene operon (PA4265-PA4266-PA4267). PA4265 (*tufA*) and PA4267 (*rpsG*) code for the elongation factor Tu and the 30S ribosomal protein S7, respectively. Palmer *et al*. named the *fusA1* encoded protein EF-G1A and the *fusA2* protein EF-G1B (Palmer *et al*., 2013). They consist of 706 and 702 amino acids, respectively. The two protein sequences share 84% identity and 90% similarity. Evidence was provided that EF-G1A plays a role in ribosome recycling while EF-G1B is involved in the translocation process (Palmer *et al*., 2013). Several mutations in the *fusA1* gene were reported to confer an increased resistance to argyrins (increasing the MICs from 16 to >256 µg ml^{-1} and from 8 to >128 µg ml^{-1}) in mutants selected *in vitro* from *P. aeruginosa* PA14 and PAO1, respectively (Table 2) (Bielecki *et al*., 2012; Nyfeler *et al*., 2012). These molecules are cyclic octapeptides produced by various *Myxobacteria spp* and *Actinomycetes spp*. They inhibit protein synthesis and are active against *P. aeruginosa* (Selva *et al*., 1996) through their interaction with EF-G1A (Gao *et al*., 2009). This is not the case of fusidic acid, another antibiotic compound targeting EF-G and active against *Staphylococcus* and *Streptococcus* species but not against *Pseudomonas* species. A putative argyrin-binding site was localized on the domain III of EF-G, opposite to that of fusidic acid (Bielecki *et al*., 2012).

Table 2: List of EF-G1A/B alterations in *in vitro*-selected and clinical strains of *P. aeruginosa*.

Reference strains[a]	EF-G1A substitutions[b]	EF-G1B substitutions[b]	References
	***in vitro* mutants**		
PAO1	$T_{493}I$		(Klockgether *et al*., 2010)
PA14	**$S_{417}L$** $I_{457}T$ **$S_{459}F$** $L_{663}M$ **$L_{663}Q$** $M_{685}R$		(Bielecki *et al*., 2012)
PAO1	$P_{414}S$ **$S_{417}L$** **$S_{459}F$** $P_{486}S$ **$L_{663}Q$** **$T_{671}A$** $Y_{683}C$		(Nyfeler *et al*., 2012)
ATCC 27853	$N_{592}I$		(Feng *et al*., 2016)
PAO1	$I_{61}M$ $E_{100}G$ **$T_{671}A$**		(López-Causapé *et al*., 2018)
	clinical strains		
LESB58	$A_{419}T$ $V_{538}A$ $G_{611}V$ **$Q_{678}R$**		(Chung *et al*., 2012)
DK2	$G_{148}D$ $V_{330}A$ $E_{372}K$ $D_{450}G$ $R_{491}C$ $R_{512}C$ **$Q_{678}R$** $A_{681}T$	$G_{571}D$	(Marvig *et al*., 2013)
DK1-P33F0	**$G_{118}S$** $D_{467}G$		(Markussen *et al*., 2014)
PA14	$L_{40}Q$ $G_{60}S$ $G_{60}V$ $V_{93}I$ **$V_{93}A$** $T_{96}A$ $E_{100}G$ $R_{104}C$ **$G_{118}S$** $P_{136}A$ $G_{181}D$ $Q_{182}R$ $V_{183}I$ $V_{183}A$ $D_{184}N$ $D_{184}G$ $L_{185}P$ $I_{186}V$ $A_{246}V$ $V_{262}A$ $N_{272}S$ $D_{280}N$ $D_{302}E$ $E_{306}D$ $F_{317}L$ $F_{335}L$ $N_{351}S$ $Q_{365}H$ $G_{387}D$ $K_{389}E$ **$K_{430}E$** $A_{439}T$ $T_{456}A$ $M_{461}V$ $L_{464}M$ $A_{481}V$ $G_{484}R$ $P_{486}L$ $V_{488}I$ **$K_{504}E$** $G_{516}S$ **$Y_{552}C$** $N_{566}K$ $S_{585}F$ **$D_{588}G$**[c] $N_{592}S$ $Q_{606}H$ $P_{618}Q$ **$T_{671}A$** **$T_{671}I$** $Q_{678}L$ $R_{680}S$	$E_{28}D$ $G_{74}D$ $P_{80}T$ **$L_{161}Q$** **$A_{176}S$** **$D_{197}A$** $Q_{199}K$ $T_{201}A$ $E_{207}D$ $A_{210}S$ Y_{238}Stop $A_{289}V$ $R_{297}K$ $K_{306}N$ $D_{315}N$ $T_{450}S$ Q_{456}Stop **$G_{479}S$** $E_{537}D$ $G_{566}S$ **$Q_{601}H$** $D_{632}V$ $A_{690}S$ **$A_{695}G$**	(Greipel *et al*., 2016)
PAO1	**$V_{93}A$** **$K_{430}E$** $N_{482}S$ **$K_{504}E$** **$Y_{552}C$** $P_{554}L$ **$D_{588}G$**[c] $P_{618}L$ **$T_{671}I$**	L104P $Nt_{889}\Delta1$ $N_{236}S$ $P_{329}L$ S_{445}Stop $N_{561}S$ $I_{640}L$	(López-Causapé *et al*., 2017)
PAO1	$V_{119}A$ $E_{401}D$ **$K_{430}E$** **$Y_{552}C$**	**$Q_{161}L$** **$S_{176}A$** **$A_{197}D$** $D_{373}E$ **$G_{479}S$** $I_{570}L$ **$Q_{601}H$** **$G_{695}A$** $V_{697}I$	(Del Barrio-Tofiño *et al*., 2017)

[a] reference strains used for sequencing alignments and for constructing *in vitro* mutants.
[b] substitutions identified in at least two independent studies and known to confer resistance to argyrin B are indicated in bold face and underlined, respectively.
[c] substitutions identified in strain LESB58.

Amino acid substitutions were indirectly identified in EF-G1A by studies investigating the genomic evolution of CF *P. aeruginosa* strains (Table 2). It was suggested that mutations in gene *fusA1* could contribute to the adaptation of *P. aeruginosa* to the CF lung environment by altering the (p)ppGpp levels and by downregulating the virulence factors of the pathogen (Chung *et al*., 2012). In another CF context, *fusA1* was identified as a pathoadaptive gene from the genomic analysis of clone DK2 prevalent in Denmark (Marvig *et al*., 2013), suggesting that this gene is important for bacterial persistence in CF patients. This conclusion was inferred from a longitudinal study on a CF patient, during a 32-year period. Two distinct sublineages were identified from the ancestral strain collected from paranasal sinuses; both sublineages were present in the lower airways and harbored alterations in EF-G1A, again highlighting the potential role of *fusA1* mutations in the persistence of *P. aeruginosa* in the CF lung (Markussen *et al*., 2014).

In Germany, characterization of 361 *P. aeruginosa* isolates collected from 258 CF patients revealed the presence of 52 and 22 nonsynonymous mutations in *fusA1* and *fusA2* genes, respectively (Greipel *et al*., 2016) (Table 2). Additionally, two stop mutations (Y_{238}Stop and Q_{456}Stop) were identified in *fusA2*. Thus, these results strongly suggested that *fusA1*/*fusA2* genes are under a high evolutionary pressure in the CF context. In another study, Antonio Oliver's group defined the resistome of isolates belonging to an international CF clone (CC274). Strains with MICs of tobramycin from 6 to >256 µg ml^{-1} turned out to harbor mutations in *fusA1* and *fusA2* genes, suggesting a role of these mutations in high-level aminoglycoside resistance of CF strains (López-Causapé *et al*., 2017). Finally, substitutions were identified in XDR isolates from Spain (Del Barrio-Tofiño *et al*., 2017) but their phenotypic impact was not further explored.

Not reported in clinical strains, an additional amino acid substitution in EF-G1A (N_{592}I) was identified in a *P. aeruginosa* strain subjected *in vitro* to increasing concentrations of tobramycin. Additional experiments using antibiotics of other families (ciprofloxacin, piperacillin/tazobactam, meropenem or ceftazidime) did not lead to the selection of *fusA1* mutants (Feng *et al*., 2016).

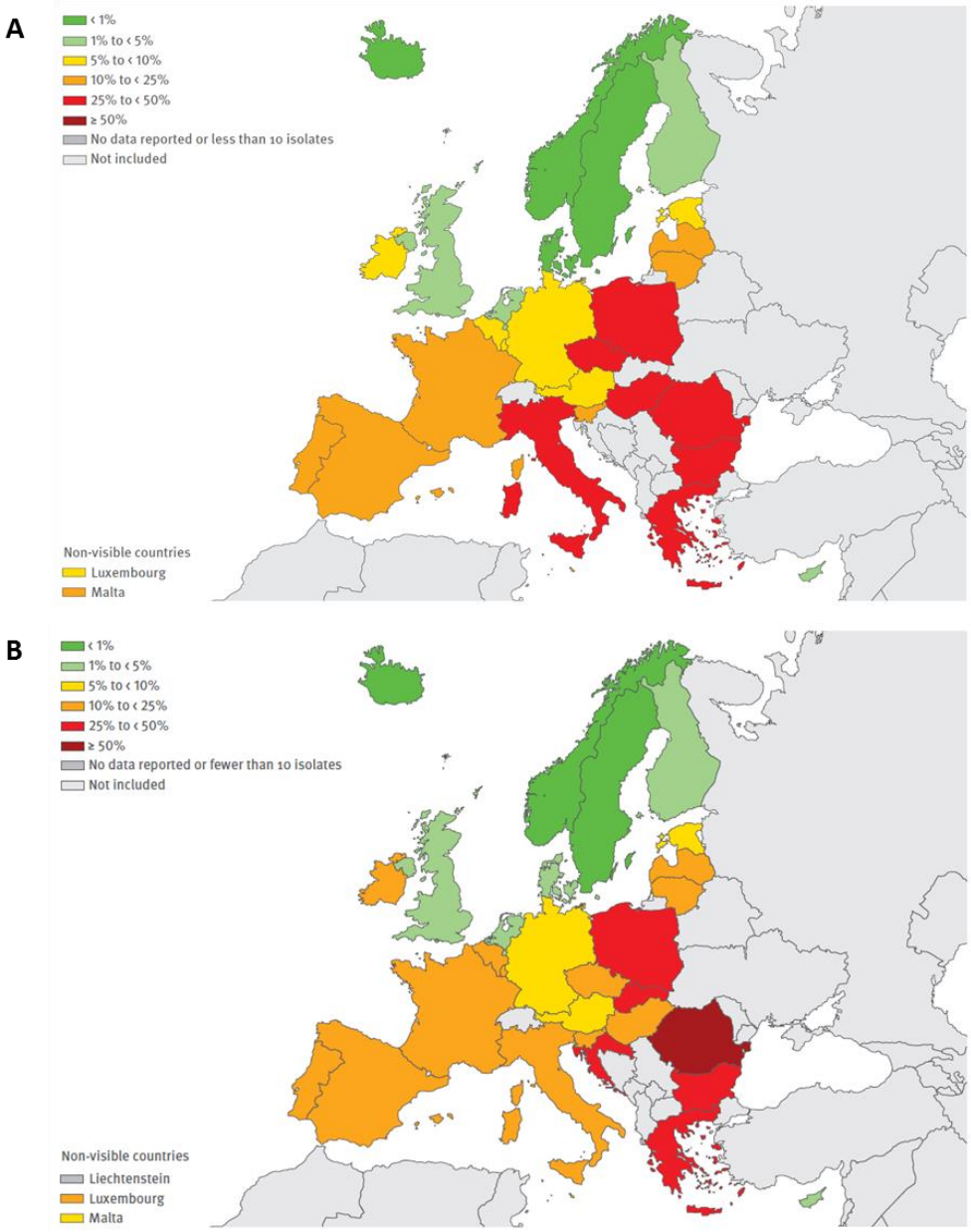

EARS-Net

Figure 9: Epidemiology of *P. aeruginosa* strains resistant to aminoglycosides in Europe.

Data are represented for years 2009 (A) and 2016 (B) (from the annual reports of the European Antimicrobial Resistance Surveillance Network (EARS-Net) 2009 and 2016).

1.4. Epidemiology of resistance

Antimicrobial resistance of Gram-negative bacteria, including *P. aeruginosa* is a global issue. Indeed, it was reported in 2011 that 8.9% and 7.1% of healthcare-associated infections were due to *P. aeruginosa* in Europe and in the United States, respectively (McCarthy, 2015). The development of MDR, XDR and PDR strains is alarming, making this organism a critical priority for the research and development of new antibiotics (Tacconelli *et al*., 2018).

Resistance to aminoglycoside molecules in invasive strains is monitored in France and in Europe by the European Centre for Disease Prevention and Control (ECDC), which publishes an annual report about the antimicrobial resistance surveillance in Europe [all 28 EU member states and two EEA countries (Iceland and Norway)] (Figure 9). These reports relate that in France 10.7% of the invasive isolates of *P. aeruginosa* were resistant to aminoglycosides in 2016. This rate is lower than in 2013 and 2009 where 15.5% and 22% were found resistant, respectively. This decreasing trend is also observed in some other European countries such as Italy and the Czech Republic. However, the percentage of aminoglycoside resistant strains remains high in Romania, Ireland and Belgium. Consequently, the ECDC recommends a prudent use of antibacterials and the implementation of infection control measures to prevent a deterioration of the situation.

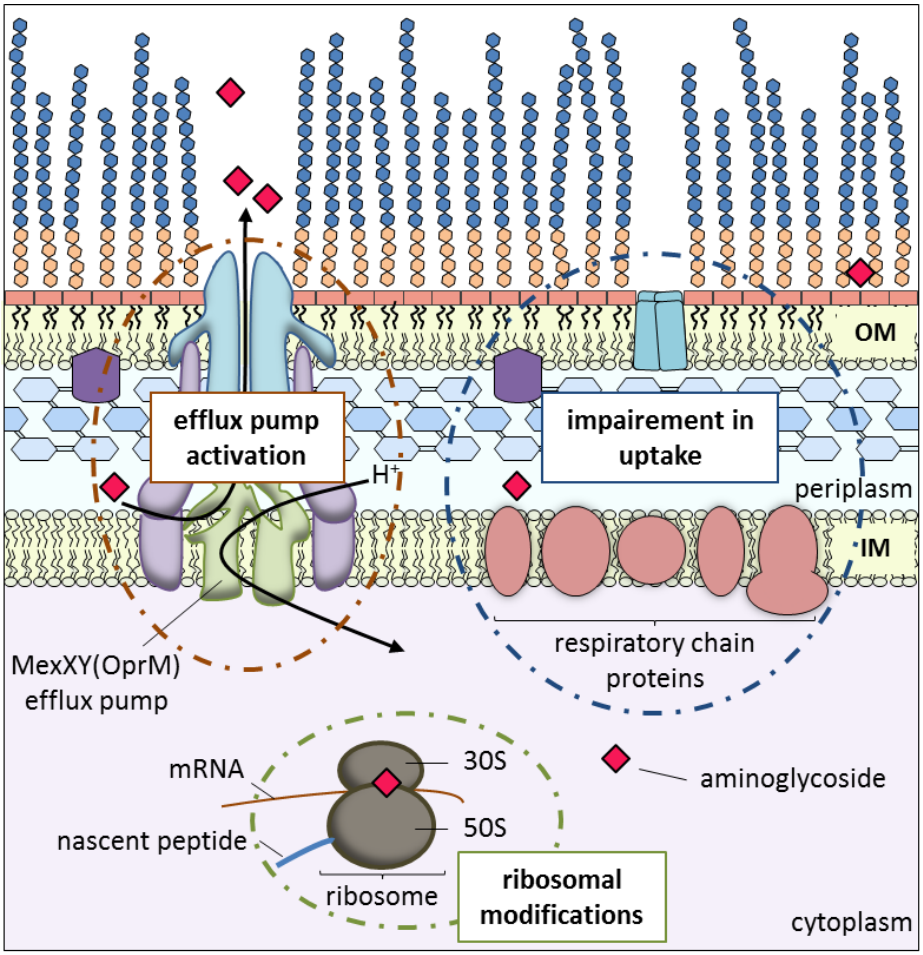

Figure 10: Schematic representation of global non-enzymatic resistance mechanisms to aminoglycosides developed by planktonic *P. aeruginosa* cells.

OM: outer membrane, IM: inner membrane.

2. Non-enzymatic resistance mechanisms to aminoglycosides

Several resistance mechanisms to aminoglycosides have been characterized in clinical strains of *P. aeruginosa*. A high level resistance to these agents can result from drug inactivation or modification by plasmid- or chromosome-encoded enzymes (Poole, 2005). However, this will not be described here as the aim of this research project focused on enzyme-independent resistance.

Non-enzymatic resistance to aminoglycosides in *P. aeruginosa* involve mechanisms such as aminoglycoside-target alterations, membrane modifications, and/or overproduction of the efflux pump MexXY(OprM) (Figure 10). Alternatively, the modification of the bacterial lifestyle *via* the formation of biofilm may also confer an increased resistance to aminoglycosides (Taylor *et al*., 2014).

2.1. Aminoglycosides resistance in biofilms

P. aeruginosa often develops in the lung of CF patients as biofilms (Taylor *et al*., 2014). Bacterial biofilms are dense microbial communities embedded within an extracellular matrix. The formation and dispersion of a biofilm is summarized in Figure 11. Cells living in biofilms exhibit phenotypic characteristics and a social behaviour quite different from that of planktonic cells. Antibiotic resistance conferred by the biofilm mode of life is a major therapeutic problem. Indeed, compared to planktonic cells, sessile bacteria can be up to 1,000-fold more resistant to antibiotics, including aminoglycosides (Taylor *et al*., 2014). Genetic determinants participating in this phenotype were investigated in several studies (Table 3). Whiteley *et al*. showed that 73 genes were differentially expressed in *P. aeruginosa* biofilms compared to planktonic counter parts. Among the 34 genes found to be overexpressed, *tolA* is supposed to decrease the affinity of aminoglycosides for the OM by impacting LPS structure. An increase amount of protein TolA might then contribute to the resistance of biofilms to these antibiotics (Whiteley *et al*., 2001). Among the repressed genes was *rpoS*, which codes for σ subunit of RNA polymerase. Biofilms formed by *rpoS* mutant are thicker and more resistant to tobramycin than those formed by wild-type strains (Whiteley *et al*., 2001).

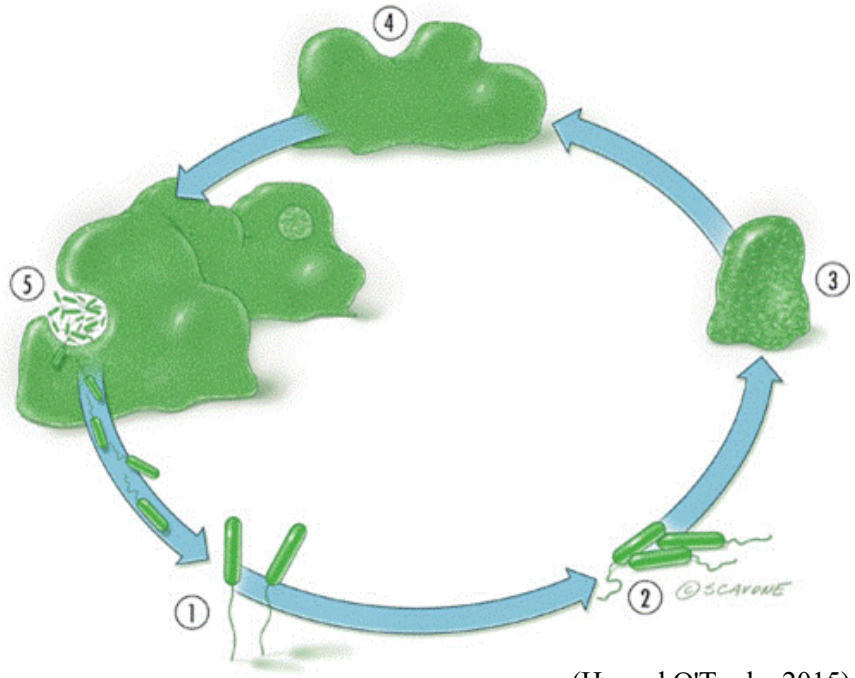

(Ha and O'Toole, 2015)

Figure 11: Schematic representation of the formation and dispersion of a *P. aeruginosa* biofilm.

The formation of a biofilm starts with a reversible attachment of planktonic bacteria to a cell or abiotic surface (1) followed by an irreversible attachment resulting in a monolayer of cells (2). Then, a microcolony is formed (3) and develops as a macrocolony (4). Finally, cells leave the macrocolony during the dispersion step (5).

Table 3: Genetic loci confirmed to be involved in the resistance of *P. aeruginosa* biofilms to aminoglycosides.

PA number	Gene name	Aminoglycosides	References
PA0084	*tssC1*	TOB, GEN	(Zhang *et al*., 2011)
PA0756-PA0757	-	TOB, GEN	(Zhang *et al*., 2013)
PA1163	*ndvB*	TOB, GEN	(Mah *et al*., 2003)
PA1875-PA1877	-	TOB, GEN	(Zhang and Mah, 2008)
PA2070	-	TOB, GEN	(Zhang *et al*., 2013)
PA2818	*arr*	TOB	(Hoffman *et al*., 2005)
PA3622	*rpoS*	TOB	(Whiteley *et al*., 2001)
PA5033	-	TOB, GEN	(Zhang *et al*., 2013)

-: no name, TOB: tobramycin, GEN: gentamicin.

Another study analyzed a library of about 4,000 random transposon insertion mutants of *P. aeruginosa* PA14 for suppression of antibiotic resistance when grown as biofilm (Mah *et al*., 2003). Amongst this collection, the *ndvB* mutant was more susceptible to tobramycin. The NdvB protein is involved in the synthesis of periplasmic glucans shown to interact with tobramycin, thus impairing their transport across the cytoplasmic membrane. However, it is worth to mention that the impact of NvdB varies among *P. aeruginosa* strains. Indeed, comparison of *ndvB* mutants highlighted a less important contribution in resistance of NdvB in the PAO1 and PAK genetic backgrounds than in PA14. For example, only a 2-fold decrease in resistance to tobramycin was observed in PAO1 *ndvB* knockout mutant compared with an 8-fold decrease in PA14 mutant (Mah *et al*., 2003). Later on, additional genetic loci identified from this mutant library were confirmed to participate in biofilm-associated aminoglycoside resistance, namely: (i) a putative efflux pump encoded by PA1875-PA1877 (Zhang and Mah, 2008), (ii) the *tssc1* encoded protein involved in type VI secretion (Zhang *et al*., 2011), (iii) a two-component system encoded by PA0756-PA0757 operon (Zhang *et al*., 2013), and (iv) two hypothetical proteins encoded by PA5033 and PA2070 (Zhang *et al*., 2013). Interestingly, the gene upstream of PA2070 (PA2071) encodes the elongation factor EF-G1B.

Finally, biofilm formation is now known to be induced by tobramycin. Gene *arr* (for aminoglycoside response regulator) was found responsible for biofilm-associated aminoglycoside resistance. Analysis of a transposon mutant library of PAO1 showed, indeed, that the inactivation of *arr* gene made the strain 100-fold more susceptible to the killing action of tobramycin. The Arr protein, predicted to be inserted in the IM *via* two transmembrane (TM) domains, contains a periplasmic domain and a EAL domain characteristic of putative phosphodiesterases involved in bis-(3'-5')-cyclic dimeric GMP (c-di-GMP) degradation (Hoffman *et al*., 2005).

2.2. Alteration of the cellular targets of aminoglycosides

Methylation of 16S rRNA in bacterial 30S ribosome is another mechanism of resistance to aminoglycosides. In *P. aeruginosa*, it results from the acquisition of gene *rmtA* encoding a 16S rRNA methylase (Yokoyama *et al*., 2003). RmtA shares high similarity with 16S rRNA methylases found in aminoglycoside-producing *Actinomycetes spp*

(Yokoyama *et al*., 2003). These bacteria protect themselves from intrinsic aminoglycosides by methylation of their own 16S rRNA. *P. aeruginosa* strains might have acquired this gene through intergeneric lateral transfer (Yokoyama *et al*., 2003). Of note, the transfer of a recombinant plasmid carrying gene *rmtA* in *E. coli* conferred an increased resistance to 4,6-di-substituted deoxystreptamines. The analysis of 1,113 clinical isolates of *P. aeruginosa* revealed the presence of gene *rmtA* in 9 of them (Yokoyama *et al*., 2003).

The modification of a second aminoglycoside target can lead to a deacrase of susceptibility. A specific resitance to streptomycin was associated with mutations in gene *rpsL*, encoding ribosomal protein S12 and which is the preferential target of this aminoglycoside (Hancock, 1981).

2.3. Membrane modifications

As aminoglycosides act intracellularly, any modification preventing their uptake and accumulation in the cytosol constitutes potentially a resistance mechanism. The analysis of clinical strains resistant to aminoglycosides revealed that some of them harbor modifications of LPS composition, remaining only with the A-band LPS (Hancock *et al*., 1983). Consequently, B-band LPS seem to have an impact on the intracellular uptake of aminoglycosides (gentamicin) although the exact mechanism remains unclear (Kadurugamuwa *et al*., 1993). In strains isolated from CF patients, deficiency in LPS O-side-chains is common (Hancock *et al*., 1983) and could be a widespread mechanism of resistance to aminoglycosides (Bryan *et al*., 1984).

In our laboratory, the screening of a Tn5-Hg insertional library constructed in reference strain PAO1 showed that the inactivation of the *galU* gene caused a 2-fold increase in resistance to aminoglycosides (gentamicin, amikacin, tobramycin and netilmicin) (El'Garch *et al*., 2007). The *galU* gene codes for an UDP-glucose pyrophosphorylase which catalyzes the conversion of glucose-1-phosphate to UDP-glucose. A previous work showed that the inactivation of *galU* leads to the synthesis of an incomplete LPS outer core, lacking both A- and B-band polysaccharides (Dean and Goldberg, 2002). The Tn5-Hg insertional library also revealed a role in resistance of a thirteen-gene operon (*nuoABDEFGHIJKLMN*) which codes for proton-translocating type I NADH

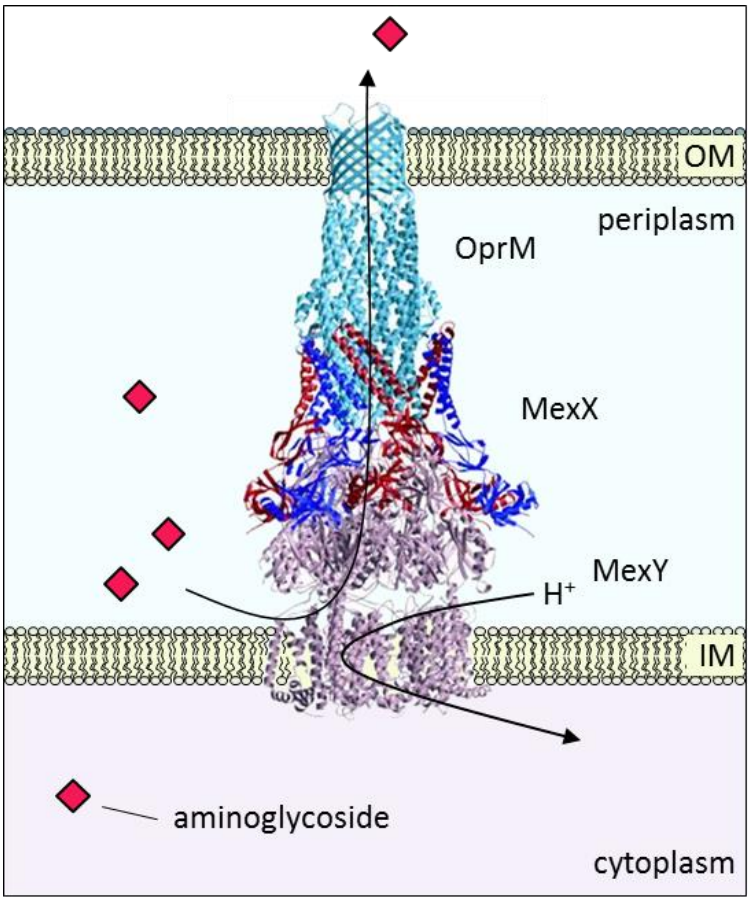

Figure 12: Structure of the RND efflux pump MexXY(OprM) based on the MexAB-OprM model from *P. aeruginosa*.

The OprM subunit is shown in light blue. The three pairs of MexX dimers are represented in red and deep blue. The MexY protein is represented in pink. OM: outer membrane, IM: inner membrane (Akama *et al*., 2004).

oxidoreductase. The PAO1 mutant FE10 harboring a Tn5-Hg transposon inserted in gene *nuoG* displayed a 2-fold higher aminoglycoside resistance, comparable to the level that of the *galU* mutant. Inactivation of this operon is believed to reduce the transport of aminoglycosides through the IM and thus to impair their accumulation in the cytoplasm (El'Garch *et al*., 2007).

Using the Harvard *P. aeruginosa* PA14 nonredundant library, Schurek *et al*. identified 135 genes whose inactivation by transposon insertion leads to a 2-fold increase in resistance to tobramycin (Schurek *et al*., 2008). Genes involved in the energy metabolism (PA1320 and PA1551) and LPS biosynthesis (PA5447 and PA5450) were noted. However, a transposon library does not include genes whose inactivation is lethal for bacteria and fails to detect those needing gain-of-function mutations to be activated and to generate an enhanced resistance.

2.4. Resistance mediated by the efflux pump MexXY(OprM)

Active efflux systems are major resistance mechanisms to antibiotics in Gram-negative species particularly those belonging to the Resistance Nodulation cell Division (RND) family. In *P. aeruginosa*, a single pump contributes to the intrinsic, adaptive and acquired resistance to aminoglycosides, namely MexXY(OprM).

2.4.1. The RND efflux pump structure and assembly

The MexXY system was simultaneously identified in 1999 by three research groups (Aires *et al*., 1999; Mine *et al*., 1999; Westbrock-Wadman *et al*., 1999). This homologue of the AmrAB-OprA system present in *Burkholderia pseudomallei* forms a channel spanning both membranes and functions by pumping molecules out of the cell (Piddock, 2006). MexXY(OprM), like all the members of the RND family, is organized as a tripartite machinery with: (i) a transporter protein in the IM (MexY), (ii) a periplasmic accessory protein (MexX) and (iii) an outer membrane protein (OprM) (Figure 12). MexXY proteins are coded by the *mexXY* operon and the OM factor OprM is encoded by *oprM*, located in the *mexAB-oprM* operon, which codes for another RND pump, MexAB-OprM. In order to allow concomitant functioning of MexAB-OprM and MexXY(OprM), gene *oprM* is partially transcribed from a second promoter situated within the *mexB* gene. Transporter MexY is supposed to capture substrates within the

phospholipid bilayer of the IM and transports them into the extracellular medium *via* OprM with the intervention of MexX. In addition to aminoglycosides, the substrates of MexXY(OprM) include antibiotic classes fluoroquinolones, β-lactams, tetracyclines, macrolides and chloramphenicol (Lister *et al*., 2009). As all RND efflux systems, MexXY(OprM) uses the proton gradient occurring in the IM to pump out one substrate molecule in exchange of one proton H^+.

2.4.2. Intrinsic resistance

The first work to be carried out on MexXY(OprM) showed that this pump contributes to the intrinsic resistance of *P. aeruginosa* to aminoglycosides (Aires *et al*., 1999). Indeed, a transposon insertion in *mexX* gene conferred a 4- to 8-fold increase in susceptibility to aminoglycosides (Aires *et al*., 1999).

To control the basal production of the pump, the *mexXY* operon is subjected to a transcriptional repressor belonging to the TetR family, named MexZ, encoded by the *mexZ* gene. This gene, located upstream of the *mexXY* operon, is transcribed divergently. MexZ binds as a homodimer to the *mexZ-mexXY* intergenic region and represses the expression of both *mexXY* and *mexZ* loci (Aires *et al*., 1999; Matsuo *et al*., 2004). Moreover, it was shown that the activity of MexZ is modulated by ArmZ, the product of the *armZ* gene which is cotranscribed with PA5470 (Hay *et al*., 2013; Yamamoto *et al*., 2009). The transcription of *armZ*-PA5470 operon is dependent upon a mechanism of attenuation itself dependent on PA5471.1, a leader peptide of 13 amino acids. Gene PA5471.1 is situated between the *armZ*-PA5470 operon and the PA5472 gene (Morita *et al*., 2009). The transcription of PA5471.1, together with the intergenic region (PA5471.1-*armZ*), results in an mRNA that can form a termination signal of transcription. Alteration of translation of this leader peptide, resulting from ribosomal stalling, causes a modification of the mRNA conformation and loss of the terminal signal of transcription. Subsequent transcription of the *armZ*-PA5470 operon takes place and enables ArmZ to interact with MexZ, that is no longer able to repress *mexXY* transcription. Ribosome stalling leading to *mexXY* transcription has been demonstrated to occur when bacteria are exposed to antibiotics affecting protein synthesis, including aminoglycosides. Indeed, ribosome-targeting antibiotics were shown to induce the *mexXY* operon expression (Jeannot *et al*., 2005). The induction of this operon was

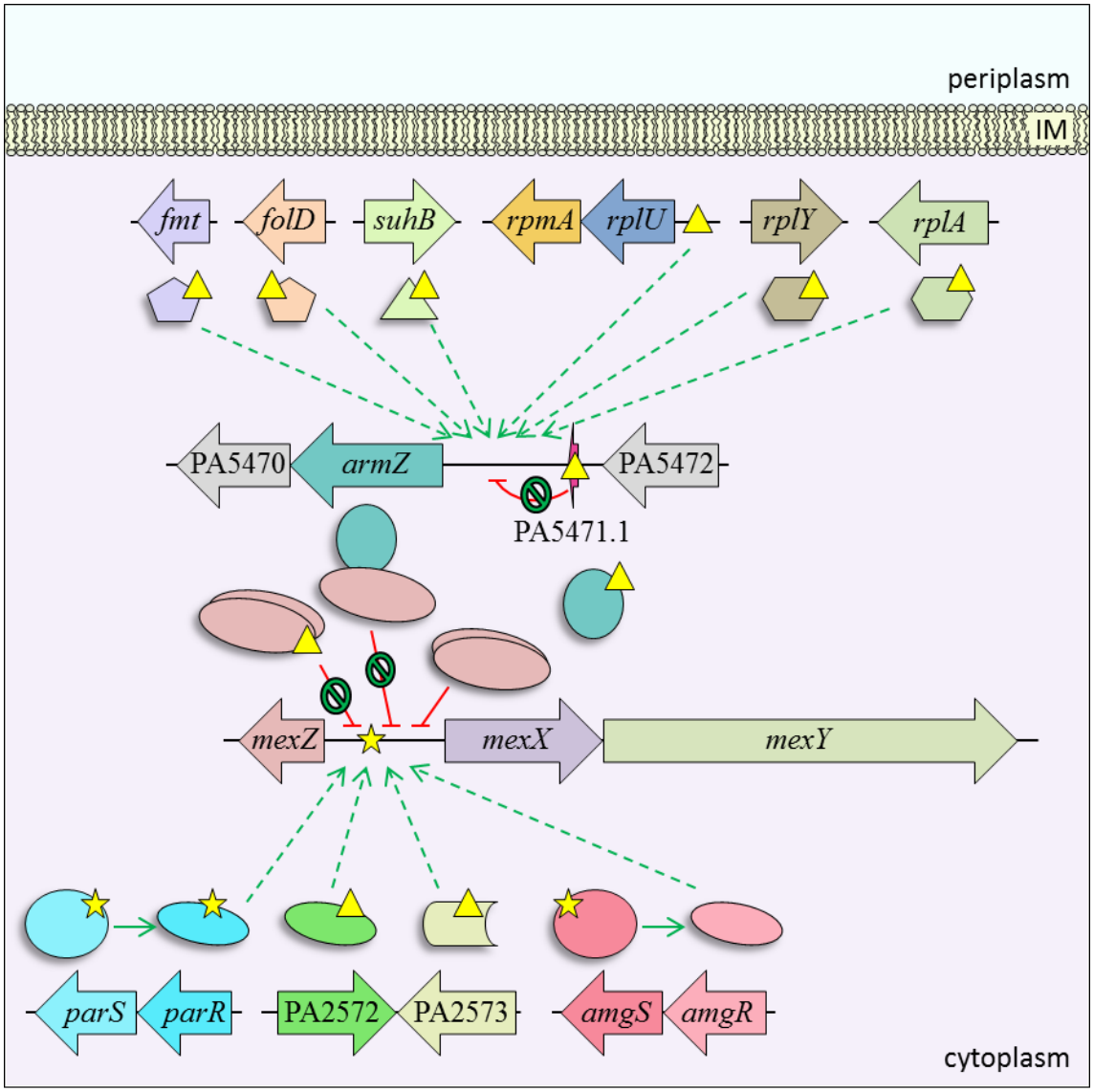

Figure 13: Schematic representation of the regulation of *mexXY* operon expression in *P. aeruginosa*.

Expression of *mexXY* operon can vary upon inactivating mutations (yellow triangles) or activating mutations (yellow stars). Green arrows represent an activation of *mexXY* expression. Red lines indicate repression. Solid and dotted lines indicate direct or indirect regulation pathways influencing expression of targeted genes, respectively. IM: inner membrane.

confirmed to contribute to the intrinsic resistance to aminoglycosides (Masuda *et al*., 2000). Nevertheless, *mexXY* operon can also be activated by non-ribosome targeting antibiotics. For example, the cationic peptides indolicidin, colistin and polymyxin B do so by an ArmZ-independent mechanism involving a two-component system named ParR-ParS (Muller *et al*., 2011). This will be discussed in the **3.** section of this review.

2.4.3. Adaptive resistance

The MexXY(OprM) efflux system is also known to contribute to the adaptive resistance of *P. aeruginosa* to aminoglycosides (Hocquet *et al*., 2003). This adaptive response occurs when bacteria are exposed to these antibiotics. After a rapid drug concentration-dependent killing phase, a transiently resistant subpopulation emerges, that exhibits a slow drug concentration-independent killing. Adaptive resistance disappears when the population is no longer in contact with the antibiotic. This process is of concern as it may compromise the efficacy of aminoglycosides *in vivo*. The role of the MexXY(OprM) pump was confirmed in a mutant of strain PAO1 defective in MexXY, which failed to become refractory to aminoglycosides (gentamicin) in comparison to the parental strain PAO1 (Hocquet *et al*., 2003). MexY was overproduced upon drug exposure, but not OprM (Hocquet *et al*., 2003). Recent work in our laboratory showed that a MexXY(OprM)-dependent response is induced when wild-type strain PA14 is exposed to electrophilic molecules (Juarez *et al*., 2017), but the molecular mechanism remains to be elucidated (Alexandre Tetard PhD thesis).

2.4.4. Acquired resistance

A MexXY(OprM)-mediated acquired resistance can be due to two distinct mechanisms: upregulation of the *mexXY* operon or greater efficacy of the MexY transporter consequently to gain-of-function mutations. An increased expression of the *mexXY* operon leads to overproduction of the pump and increased export of the antibiotic out of the cell. As a consequence, the amount of aminoglycoside molecules reaching their intra-cytoplasmic targets decreases with concomitant 2- to 8-fold higher resistance to these antibiotics (Caughlan *et al*., 2009; Hocquet *et al*., 2008; Muller *et al*., 2011; Westbrock-Wadman *et al*., 1999). Activation of *mexXY* expression was shown to result from either inactivating or activating mutations (Figure 13).

The first MexXY-overproducing mutants reported in the literature were of the *agrZ*-type (for *aminoglycoside resistance MexZ-dependent*) (Llanes *et al*., 2004). These mutants harbor either (i) an inactivated *mexZ* gene, (ii) mutations in the *mexZ-mexX* intergenic region or (iii) substitutions in the *mexZ* gene impairing the function of repressor MexZ. The *agrZ-type* mutants were successfully selected *in vitro* on media supplemented with any of MexXY(OprM) antibiotic substrates. More importantly, they were confirmed to be common in the clinical setting. Indeed, 44 strains out of a collection of 57 genotypically distinct strains characterized as MexXY(OprM)-overproducing strains carried one of the above mentioned alterations (Guénard *et al*., 2014). The remaining 13 strains harbored an intact *mexZ* gene. These strains were dubbed *agrW* mutants and were even subclassified into *agrW1* and *agrW2* mutants.

The *agrW1* strains are not mutated in one specific locus but carry genetic modifications that impair protein synthesis. For example, Westbrock-Wadman *et al*. reported the *in vitro* selection of a mutation in the *rplA* gene of strain PAO1, leading to the inactivation of the ribosomal protein L1 and to activation of the *mexXY* operon (Westbrock-Wadman *et al*., 1999). Other *in vitro*-selected mutations were also found to trigger *mexXY* overexpression, such as nucleotide changes in the promoter region of the *rplU-rpmA* operon (encoding ribosomal proteins L21 and L27), as well as indels in the *rplY* gene (encoding ribosomal protein L25 which binds to the 5S rRNA loop E) or the *suhB* gene (encoding a ribosome associated protein) (El'Garch *et al*., 2007; Lau *et al*., 2012; Shi *et al*., 2015). Moreover, an increase in *mexXY* expression was associated with mutations in the *fmt* or *folD* genes, that code for a methionyl-tRNA^{fmet} formyltransferase and a protein involved in biosynthesis of folate, respectively (Caughlan *et al*., 2009). In clinical strains, only one 7-bp deletion in the leader peptide PA5471.1 was identified so far (Guénard *et al*., 2014).

The *agrW2* mutants are characterized by a resistance phenotype distinct from that of *agrZ* and *agrW1* mutants. In addition to a higher resistance to MexXY(OprM) substrates, they exhibit a 2- to 8-fold decreased susceptibility to carbapenems and colistin (Muller *et al*., 2011). In strain PAO1, this phenotype results from amino acid substitutions either in the response regulator ParR (for example $M_{59}I$) or the histidine kinase ParS ($V_{101}M$) of TCS ParRS (Muller *et al*., 2011). The resistance to carbapenems is due to the downregulation of porin OprD, the main port of entry of carbapenems into

the bacterial cell (Trias and Nikaido, 1990). A concomitant activation of the *arnBCADTEF-ugd* (*arn*) operon protects the bacteria from colistin (Fernández *et al*., 2010). Proteins encoded by this operon are responsible of the addition of 4-amino-4-desoxy-L-arabinose (L-Ara-4N) molecules on the phosphate groups of the lipid A. More details will be provided in the **3.** section. In the collection of clinical strains analyzed by Guénard *et al*., 5 strains harboring mutations in sensor protein ParS were characterized as *agrW2* mutants, corresponding to 9% of the strains (Guénard *et al*., 2014).

In other studies, TCS AmgRS was shown to regulate operon *mexXY* (Lau *et al*., 2013; Lau *et al*., 2015). Inactivation of gene PA2572 (putative response regulator) or gene PA2573 (probable methyl-accepting chemotaxis protein) was associated with a higher expression of *mexXY* and aminoglycoside resistance in biofilms (McLaughlin *et al*., 2012).

Distinct from the aforementioned alterations, amino acid substitutions in transporter MexY are able to improve somehow the efflux of aminoglycosides. The $F_{1018}L$ change in MexY increases by 2-fold the MICs of aminoglycosides, cefepime and fluoroquinolones compared with wild-type protein (Vettoretti *et al*., 2009).

Other non-enzymatic mechanisms of resistance to aminoglycosides (MexXY-independent) are likely produced by *P. aeruginosa* that may play a role in the persistence of the pathogen *in vivo*, especially during chronic infections. In this context, TCSs represent an undeniable asset to better resist therapeutic treatments.

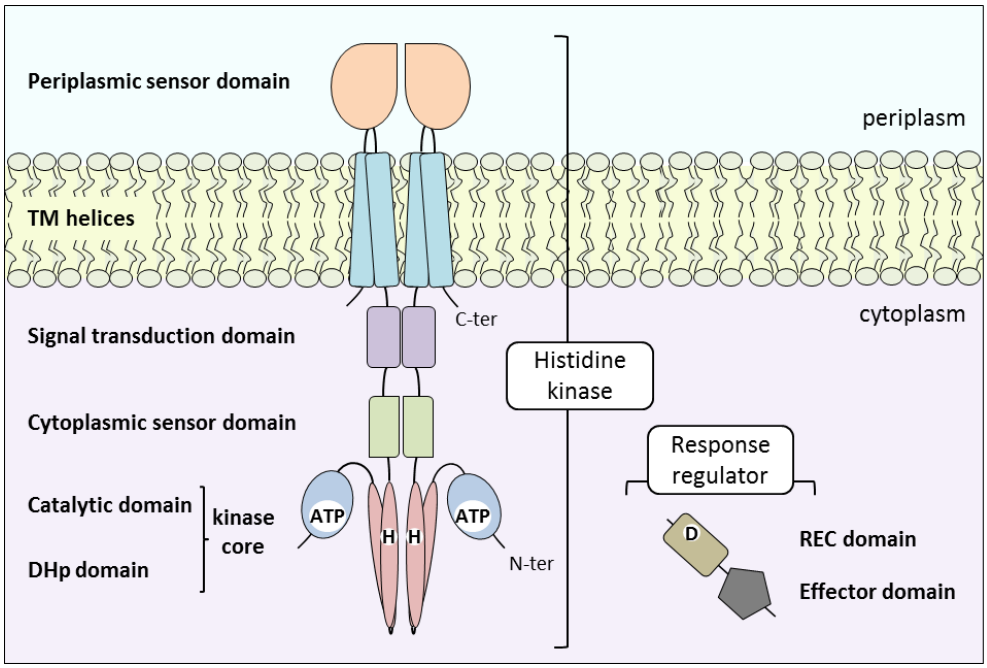

Figure 14: Schematic representation of a typical TCS.

The histidine kinase is represented as a dimer. TM: transmembrane, DHp: dimerization and histidine phosphotransfer, REC: N-terminal receiver, H: histidine, D: aspartic acid (Zschiedrich *et al*., 2016).

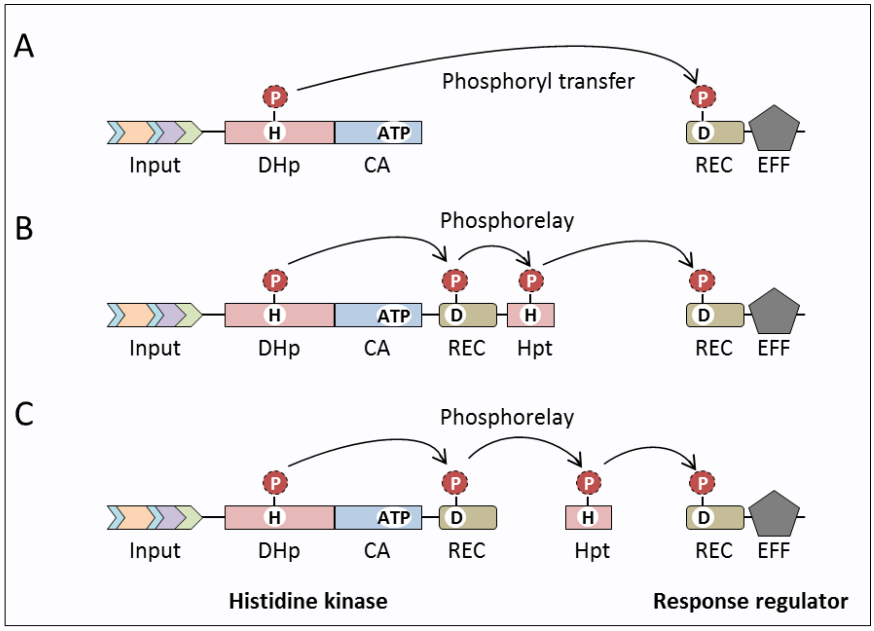

Figure 15: Schematic representation of His-Asp phosphotransfer between the sensor kinase and its cognate response regulator in classical (A), unorthodox (B) and hybrid (C) TCSs.

DHp: dimerization and histidine phosphotransfer, CA: C-terminal catalytic and ATP binding, REC: N-terminal receiver domain, Hpt: histidine-containing phosphotransfer, EFF: effector domain, H: histidine, D: aspartic acid, P: phosphate (Gao and Stock, 2009).

3. Two-component signal transduction

Fast adaptation is a prerequisite for *P. aeruginosa* to persist in hostile environments such as the CF lungs. Therefore, bacteria use two-component systems (TCSs) to orchestrate adaptive responses to stressful challenges (Rodrigue *et al*., 2000). A classical TCS is composed of : (i) a sensor histidine kinase (HK) anchored in the IM, which is in charge of the detection of one or several specific external signals, and (ii) a response regulator (RR), which after phosphorylation, in turn regulates the expression of specific target genes required for a coherent physiological response (Rodrigue *et al*., 2000) (Figure 14). The structure of the catalytic and the regulatory domains of TCSs are widely conserved. However, the diversity of both input signals and output responses resulted in a large variety of input and output domain structures (Zschiedrich *et al*., 2016).

3.1. Molecular mechanisms of signal transduction

In the presence of a specific signal, HK autophosphorylates at a conserved histidine residue, which generates a high-energy phosphoryl group; this latter is then transferred to the response regulator at a conserved aspartic acid residue. The phosphorylation of the RR induces a conformational change leading to adaptive responses (Gao and Stock, 2009) (Figure 15A).

The analysis of the genome of reference strain PAO1 allowed the identification of 63 HKs, 64 response regulators and 16 atypical kinases (Stover *et al*., 2000). Of the 63 histidine kinases identified, 42 display a putative classical conformation (Stover *et al*., 2000). Alternatively, some HKs harbor a receiver-domain adjacent to the transmitter domain itself linked to a histidine-containing phosphotransfer (Hpt) module (Figure 15B). Five of these unorthodox HKs were identified in *P. aeruginosa*. Finally, 11 sensor kinases are classified as hybrid kinases, which differ from the unorthodox HK by the presence of an independent Hpt domain (Figure 15C). The last five sensor proteins are homologous to the chemotaxis protein CheA. These five kinases contain a transmitter domain near the amino terminus; the amino acid sequence surrounding the conserved histidine is more closely related to Hpt domains than that of classical transmitters (Stover *et al*., 2000).

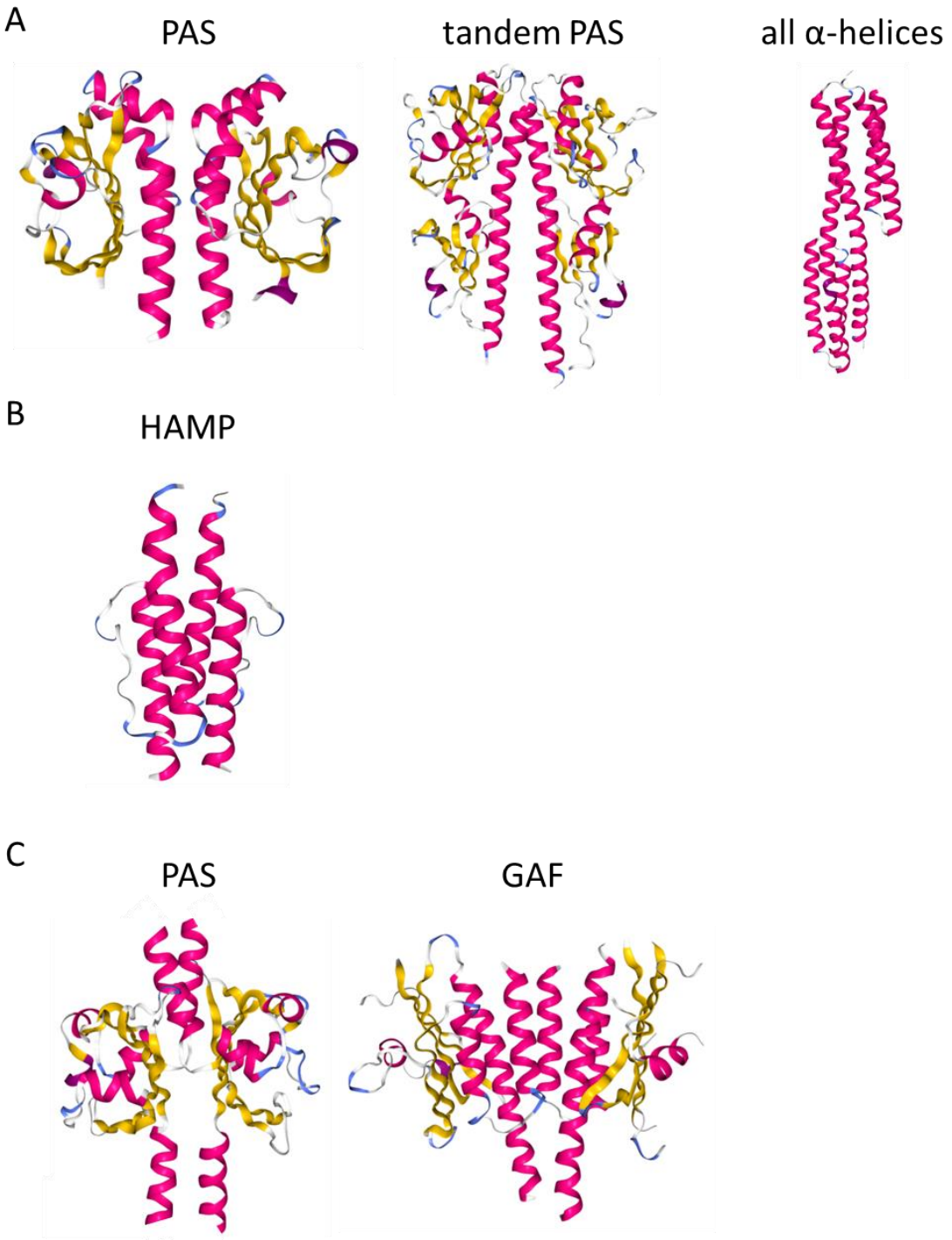

Figure 16: Structures of extra-cytoplasmic (A), HAMP signal transduction (B) and cytoplasmic (C) sensing domains.

The α-helices and β-sheets are represented in pink and yellow, respectively.

PDB ID from RCSB Protein Data Bank (https://www.rcsb.org): 2J80, 4JGO, 3I9Y, 2L7H, 4I5S and 4G3K.

3.1.1. The HK protein: signal detection and kinase activation

The histidine sensor protein is usually composed of two main domains: (i) a sensor domain which senses a signal and (ii) a transmitter domain carrying kinase activity. The typical kinase protein is a TM protein with signal detection occurring in the periplasm and with transmission happening in the cytoplasm (Zschiedrich *et al*., 2016). However, sensor domains can also be located inside the IM or in the cytosol (Bhate *et al*., 2015). HKs were shown to detect a large diversity of signals (both chemical and physical) but the molecular ligand or signal often remains unknown (Zschiedrich *et al*., 2016).

3.1.1.1. The periplasmic sensing domains

The diversity of HKs comes mainly from their sensor domains (Bhate *et al*., 2015). Except the intramembrane sensing kinases, that have only a small extracellular loop (Mascher, 2006), most kinases contain at least one periplasmic domain (Zschiedrich *et al*., 2016). A non-exhaustive list of conserved sensory domains with previously reported structures is presented below. The most common one is probably the PAS-like [Per (period circadian protein)-ARNT (vertebrate aryl hydrocarbon receptor nuclear translocator)-Sim (single-minded)] domain (Figure 16A). HK with a PAS-like domain bind their specific ligands in a ligand-binding pocket, as is the case of CitA citrate-sensing kinase from *Klebsiella pneumoniae* (Reinelt *et al*., 2003) and the DcuS fumarate sensor from *Escherichia coli* (Pappalardo *et al*., 2003), or bind their ligands without a ligand-binding pocket as for the PhoQ sensor from *Salmonella Typhimurium* which detects antimicrobial peptides through its membrane exposed surface (Bader *et al*., 2005).

A second type of periplasmic domain is known as the Tandem-PAS-like domain (Figure 16A). This latter is formed by two consecutive PAS domains as in LuxQ hybrid sensor kinase (Chen *et al*., 2002) and KinD sensor from *Bacillus subtilis* (Wu *et al*., 2013). As far as we know, the ligands are always detected by the membrane distal PAS domain leaving the proximal domain with uncharacterized function (Zschiedrich *et al*., 2016). The "all α-helical" domain is also a common HK extra-cytoplasmic domain (Figure 16A). This domain, reported as able to bind nitrates and nitrites, is present in proteins NarX from *E. coli* (Cheung and Hendrickson, 2009) and TorS from *Vibrio parahaemolyticus* (Moore and Hendrickson, 2012). TorS does not directly bind

to its stimulus signal TMAO (trimethylamine-N-oxide) but to the periplasmic protein TorT, to which TMAO binds (Baraquet *et al*., 2006). This characteristic is shared with LuxQ which binds an auto-inducer signal bound to protein LuxP (Chen *et al*., 2002).

3.1.1.2. The transmembrane helical segments

Once a stimulus is detected by the periplasmic domain it has to be transduced to the kinase core *via* the TM helical segment. The mechanism of transduction is still unclear (Goldberg *et al*., 2010), but for many HKs, it is believed that the TM domain forms a four-helical bundle in the membrane, with two TM helices from each monomer (Bhate *et al*., 2015). A water pocket created by an asparagine residue in the second TM helix was shown to be critical for signal transduction in the PhoQ sensor protein (Goldberg *et al*., 2010). In DesK, an HK activated once the temperature drops below 30°C, a monomer with five TM helices and a dimer with a ten TM helical segment are formed (Saita *et al*., 2016). However, temperature sensing is maintained even after reduction of the TM segments to a single TM helix (Cybulski *et al*., 2010), highlighting that this latter helix is responsible for the catalytic transitions along the signaling pathway in DesK (Cybulski *et al*., 2010).

3.1.1.3. The signal transduction domains: HAMP and STAC

The signal transduction domains HAMP (Histidine kinases, Adenylyl cyclases, Methylaccepting proteins, and other Prokaryotic signaling proteins) and STAC (Solute carrier and Two-component signal transduction Associated Component) serve to transmit the N-terminal signal to the catalytic domains and are thus located near to the C-terminal TM helix (Zschiedrich *et al*., 2016) (Figure 14). HAMP domains, present in about 31% of HKs (Gao and Stock, 2009), are parallel four-helical bundles with two helices from each monomer connected *via* a loop region (Zschiedrich *et al*., 2016) (Figure 16B). The first helix presents a highly conserved glycine followed by a loop that wraps around the structure (Bhate *et al*., 2015). The second helix is preceded by a conserved glutamate residue. Some HK require an HAMP domain for proper functioning but this is not the case of all HKs. The lack of HAMP domains in most TM HK might be compensated by other domains with analogous functions (Zschiedrich *et al*., 2016). The STAC domain is probably one of them. It was discovered in protein CbrA from *P. fluorescens* (Korycinski *et al*., 2015; Zhang and Rainey, 2008). The

STAC domain is a monomeric antiparallel four-helix bundle. However, it is not yet clear if it shares a similar function with the HAMP domains (Bhate *et al*., 2015). Additional domains connecting TM and cytoplasmic domains probably remain to be characterized (Bhate *et al*., 2015).

3.1.1.4. The cytoplasmic sensor domains: PAS and GAF

In addition to the input signal sensed by extra-cytoplasmic domains, many kinases present one or multiple domains which can integrate signals directly from the cytoplasm. Of which, nearly 33% of HKs contain at least one canonical PAS domain (Gao and Stock, 2009) which is a mixed α/β structure containing a five-stranded antiparallel β-sheets and several α-helices (Möglich *et al*., 2009) (Figure 16C). The ligand binds to the PAS domain inducing an alteration of the packing and dynamics of the flanking α-helices that transmit the signal (Bhate *et al*., 2015). PAS domains can bind small ligands and sense a variety of changes such as light, oxygen and redox potential (Taylor and Zhulin, 1999). Their identification remains however complicated because of the poor sequence homology among PAS domains (Möglich *et al*., 2009). Another common cytoplasmic sensing domain is GAF (c-GMP and c-GMP-stimulated phosphodiesterases, *Anabaena* adenylate cyclases and *E. coli* FhlA), present in around 9% of all HKs (Gao and Stock, 2009). It comprises six stranded anti-parallel β-sheets (Zschiedrich *et al*., 2016) (Figure 16C). GAF sensor domains detect a wide variety of small ligands (haeme, flavin, adenine and guanine) (Galperin, 2004).

3.1.1.5. The kinase core

In prototypical histidine kinases, the cytoplasmic kinase core is composed of two distinct domains: (i) a well-conserved C-terminal catalytic and ATP binding (CA) domain known as HATPase_c in the Pfam database (https://pfam.xfam.org/) and (ii) a less conserved dimerization and histidine phosphotransfer (DHp) domain, referred to as the His kinase A (HisKA) domain in Pfam (Figure 14). The DHp domain contains the conserved His residue necessary for phosphorylation, and the CA domain carries the catalytic site allowing the transfer of a phosphoryl group from ATP to the His residue (Gao and Stock, 2009). The CA domain is characterized by several conserved residues, that are implicated in ATP and metal ion coordination (Zschiedrich *et al*., 2016). It consists on a five-stranded β-sheet flanked by three parallel helices on the side of the

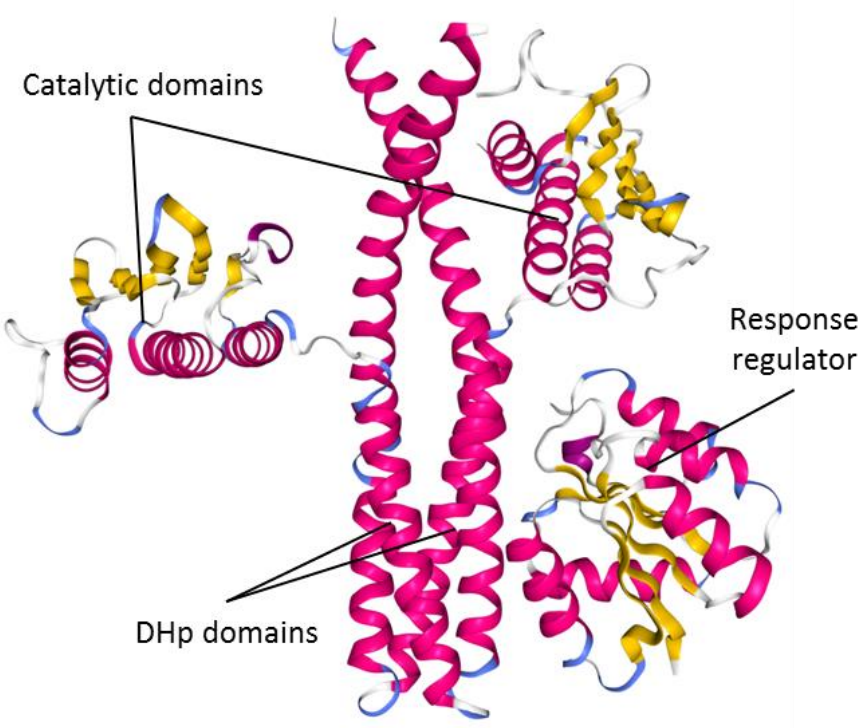

Figure 17: Structure of the kinase core in complex with RR during phosphotransfer. Example of the DesK-DesR system upon low Mg^{2+}.

The α-helices and β-sheets are represented in pink and yellow, respectively.

PDB ID from RCSB Protein Data Bank (https://www.rcsb.org): 5IUJ.

ATP-pocket (Zschiedrich *et al*., 2016). On the other side, the DHp domain usually forms a stable homodimer with a four-helix bundle architecture (Figure 14). However, functional monomeric architecture was also identified in a less frequent HisKA_2 structure (Rivera-Cancel *et al*., 2014). Two additional families are the HisKA_3 and the HisKA, different by their mechanism of autophosphorylation (Zschiedrich *et al*., 2016). In stable dimeric HK proteins, it is believed that the determinant for *cis* (each monomer phosphorylates itself) and *trans* (each monomer in the dimer phosphorylates the other) phosphorylation is the DHp loop connecting the two individual helices of the domain (Zschiedrich *et al*., 2016). Kinases with a left-handed four-helix bundle phosphorylate in *cis* and those with a right-handed four-helix bundle phosphorylate in *trans* (Zschiedrich *et al*., 2016).

3.1.1.6. The helical linker

Signal transmission from the sensing domains to the kinase core is mediated by a short helical linker with particular properties that facilitate asymmetric signaling (Bhate *et al*., 2015). The short linker interrupts a regular pattern of polar and apolar residues in the sequences of HAMP and DHp domains by insertion of a single residue. This prevents a connection of the two domains by an ideal coiled coil (Bhate *et al*., 2015). In contrast to the PAS/HAMP domains, these linkers are often rich in polar residues, buried at the dimer interface. The symmetric conformational changes of the HAMP/PAS domains are thus converted into an asymmetric conformation in the DHp (Zschiedrich *et al*., 2016).

3.1.2. The response regulator (RR): phosphotransfer and response

Once a signal sensed by HK domains is transduced to the kinase core, it is transferred to a RR (Figure 17). This interaction has to be specific to exclusively connect correct signal and response pairs (Zschiedrich *et al*., 2016). The typical RR is usually composed of two domains which are (i) a conserved N-terminal receiver domain (REC), connected with (ii) a highly diverse C-terminal effector domain by a variable linker.

3.1.2.1. The REC domain

The classical RR REC domain is about 120 amino acid long, featuring an α/β doubly wound fold (Zschiedrich *et al*., 2016). The active site of all typical RR harbors three

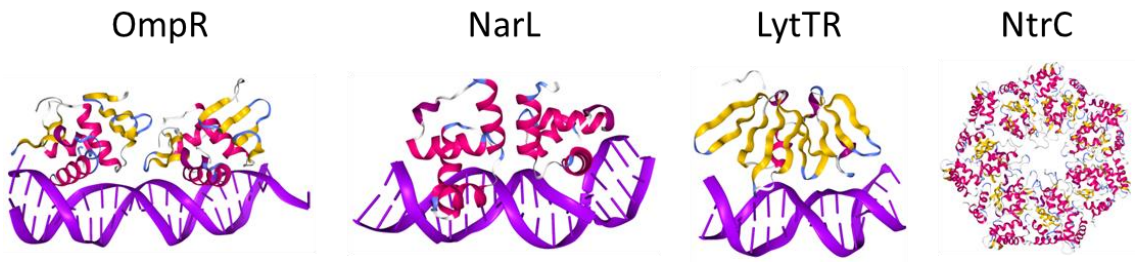

Figure 18: Structure of DNA-binding domain subfamilies of RRs.

The α-helices and β-sheets are represented in pink and yellow, respectively. Double stranded DNA is represented in purple.

PDB ID from RCSB Protein Data Bank (https://www.rcsb.org): 1GXP, 1JE8, 3BS1, 1NY6.

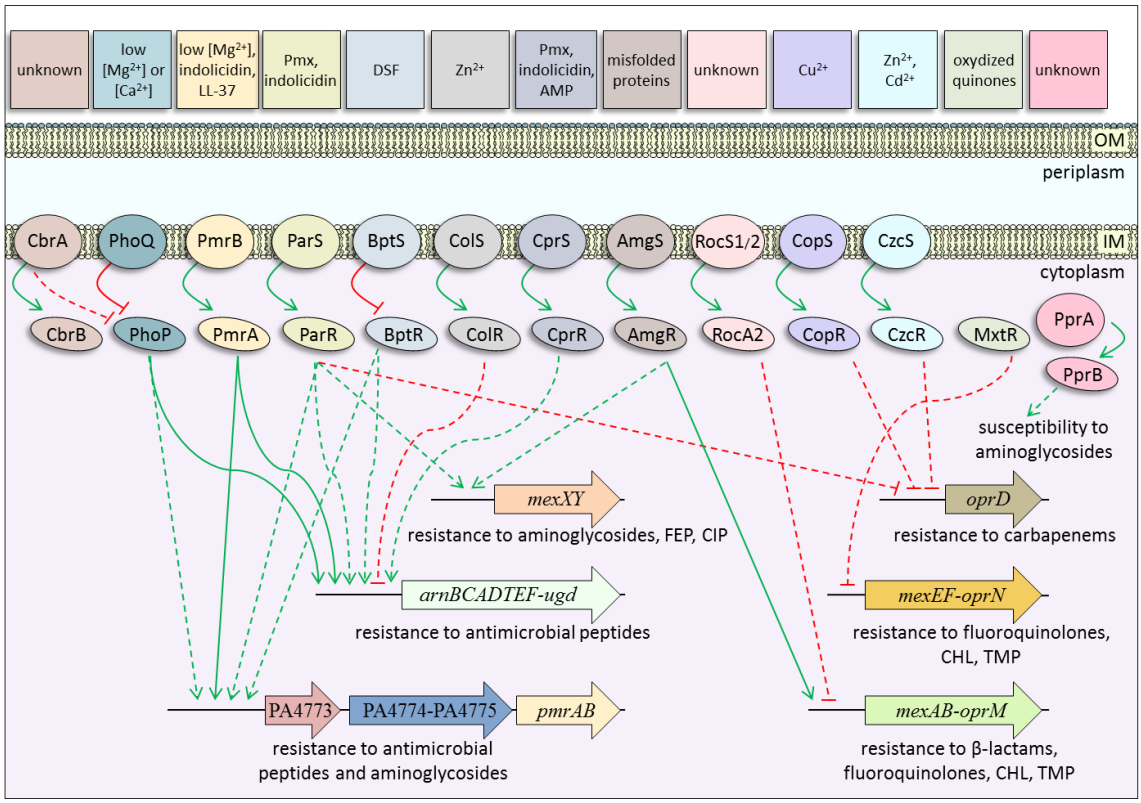

Figure 19: TCS contributing to antibiotic resistance in *P. aeruginosa*.

Green and red lines indicate an activation or repression, respectively. Solid lines represent a direct regulation whereas indirect routes are showed in dotted lines.

OM: outer membrane, IM: inner membrane, Pmx: polymyxins, DSF: cis-2-unsaturated fatty acids, AMP: antimicrobial peptides (including CP-26,-28,-29, pleuricidin, Bac2A, CRAMP, HHC36, IDR-1018, HH17), FEP: cefepime, CIP: ciprofloxacin, CHL: chloramphenicol, TMP: trimethoprim.

conserved residues: (i) the Asp residue at the end of the third β-strand receives the phosphoryl group from the conserved His residue of the specific HK, (ii) two acidic residues (aspartate-aspartate or glutamate-aspartate residues), within the loop connect β1 to α1 and are involved in Mg^{2+}-ion binding. This allows the coordination of the aspartic acid phosphorylation. For phosphoryl group transfer, the response regulator docks onto the DHp domain and catalyzes its own aspartyl phosphorylation, utilizing the phospho-histidine as a substrate and resulting in self-activation. Once activated, the effector domain of the RR in turn triggers the specific cellular output response (Zschiedrich *et al*., 2016).

3.1.2.2. The effector domain

A wide cellular output is allowed by a significant diversity in type and structure of the effector domains of RR proteins (Zschiedrich *et al*., 2016). The bacterial RR have been divided into six classes depending on their effector domain namely, the DNA-binding (65%), RNA binding (1%), enzymatic (11%), protein-binding (2%), stand-alone (14%) and other (7%) RR proteins (Gao *et al*., 2007).

The majority of RR belong to the DNA-binding class and are generally assumed to function as transcriptional regulators. In this case, phosphorylation of the REC domain usually leads to homo-oligomerization and most frequently to dimer formation. Dimerization of the RR is accompanied with increased affinity of the RR for specific DNA binding motifs, usually direct or inverted repeats. This principal mechanism has been observed for most DNA-binding RR subfamilies such as OmpR, NarL, LytTR and NtrC (Zschiedrich *et al*., 2016) (Gao and Stock, 2009) (Figure 18).

3.2. TCS and antibiotic resistance in *P. aeruginosa*

In bacteria, TCSs are implicated in the regulation of many physiological functions such as metabolism, motility, virulence and development (Gao and Stock, 2009). Some of them are able to regulate the expression of genes coding for antibiotic resistance mechanisms. Figure 19 summarizes the TCS of *P. aeruginosa* involved in susceptibility or resistance to antimicrobial peptides, aminoglycosides, β-lactams, carbapenems and/or fluoroquinolones.

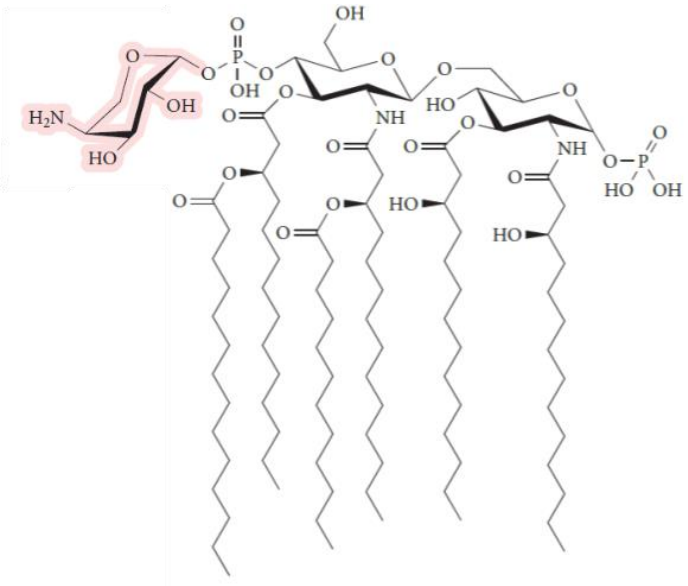

(Needham and Trent, 2013)

Figure 20: LPS modification by addition of 4-amino-4-desoxy-L-arabinose (L-Ara-4N) molecule on a phosphate group of the lipid A.

The L-Ara-4N molecule is highlighted in red.

3.2.1. TCS and resistance to colistin

Emergence of MDR and XDR strains of *P. aeruginosa* led clinicians to reintroduce colistin (polymyxin E), an old antibiotic rejected because of nephrotoxicity effects. Naturally produced by the bacterium *Paenibacillus polymyxa colistinus*, colistin belongs to the antimicrobial peptide family. This cyclic polycationic lipopeptide is often used as the last hope as less than 1% of clinical strains are resistant to this molecule. Despite its strong killing effect, resistant mutants of *P. aeruginosa* may emerge *in vitro* and under treatment. Analysis of these mutants allow the characterization of alterations in TCS, namely PhoPQ (Macfarlane *et al*., 1999), PmrAB (Moskowitz *et al*., 2004), ParRS (Fernández *et al*., 2010), CprRS (Fernández *et al*., 2012), ColRS (Gutu *et al*., 2013), BptSR and CbrAB (Yeung *et al*., 2011). Gain-of-function (e.g., in PmrB, ParR, ParS), as well as loss-of-function mutations (e.g., PhoQ, ColR, BptS) activate the expression of the *arnBCADTEF-ugd* (*arn*) operon. The encoded Arn proteins modify the LPS by adding L-Ara-4N molecules to the phosphate groups of the lipid A (Figure 20), thus decreasing the net negative charge of the cell surface. As a consequence, the interaction of cationic molecules with the OM is reduced and their penetration into the cell interior impaired (Gooderham and Hancock, 2009).

3.2.2. Aminoglycoside resistance mediated by TCS

Some TCS do contribute or are suspected to contribute to intrinsic, acquired or adaptive resistance of *P. aeruginosa* to aminoglycosides (Figure 19). The contribution of the envelope stress-responsive TCS AmgRS in intrinsic resistance of planktonic cells was discovered during the screening of PAO1 transposon mutants for those with an increased susceptibility to tobramycin (Lee *et al*., 2009b). Mutants inactivated in this system also exhibited a 4- to 16-fold decreased resistance to other aminoglycosides (gentamicin, kanamycin, paromomycin and streptomycin), and an increased bacterial susceptibility to tobramycin in biofilms (Lee *et al*., 2009b). Later on, the role of AmgRS in intrinsic pan-aminoglycoside resistance was confirmed (Krahn *et al*., 2012). The inactivation of *amgRS* reduced the virulence of wild-type strain PAO1 in a murine infection model and despite growth defect (Lee *et al*., 2009b). In addition, gain-of-function amino acid substitutions in sensor protein AmgS can mediate an acquired resistance to aminoglycosides in mutants isolated *in vitro* ($R_{182}C$) or in the clinical context ($V_{121}G$) (Lau *et al*., 2013). These variations increase aminoglycoside resistance

of 2-fold when genetically engineered in strain PAO1, and were associated with a 2- to 3-fold induction of the expression of genes *htpX* (presumed cytoplasmic membrane-associated protein) and PA5528 (membrane protein of unknown function) (Lau *et al*., 2013). Aminoglycoside-mediated mistranslated proteins or AmgS-mutational activation increase the expression of these two genes, leading to an overproduction of pump MexXY(OprM), and increased efflux of aminoglycosides (Lau *et al*., 2015).

The TCS ParRS can also enhance resistance to aminoglycosides. Distinct from AmgRS, this system does not contribute to intrinsic resistance to these drugs, but when constitutively activated by amino acid substitutions in ParR ($M_{59}I$), it mediates a 2- to 8-fold decrease of susceptibility to gentamicin, amikacin and tobramycin (Muller *et al*., 2011). In fact, alterations in this system activate the expression of the *mexXY* operon independently of ArmZ, leading to constitutive overproduction of MexXY(OprM) and thus, a higher resistance to aminoglycosides (Muller *et al*., 2011). Amino acid variations in TCS ParRS are clinically relevant as they represent 8.8% of MexXY(OprM)-dependent-aminoglycoside resistant strains (over a collection of 57 isolates) (Guénard *et al*., 2014). The identified amino acid changes in HK ParS ($A_{168}V$, $L_{99}P$, $L_{137}P$, $V_{152}A$ and $A_{138}T$) were confirmed to confer an up to 2-fold increased resistance in the PAO1 genetic background (Guénard *et al*., 2014).

Another TCS PhoPQ was claimed to play a similar role *via* a gene, *oprH*, cotranscribed with *phoP* and *phoQ*. The outer-membrane OprH, initialy thought to promote aminoglycoside resistance when overproduced (Macfarlane *et al*., 1999) seems to have a lower impact than anticipated (Macfarlane *et al*., 2000).

CbrAB plays a role in the metabolic regulation of carbon and nitrogen utilization (Nishijyo *et al*., 2001). Interestingly, inactivation of sensor CbrA was found to be associated with an augmentation of tobramycin MIC independently of CbrB response regulator (Yeung *et al*., 2011). This inactivation results in activation of *oprH-phoPQ*, *arn* and *pmrAB* operons (Yeung *et al*., 2011). The TCS PprAB, which is composed of two cytoplasmic monomers of PprA interacting with the cognate RR PprB, was in contrast shown to confer aminoglycoside susceptibility by increasing the permeability of the OM (Wang *et al*., 2003). Finally, the PmrAB system was also suspected to promote resistance to aminoglycosides (López-Causapé *et al*., 2018).

3.2.3. TCS-dependent susceptibility to carbapenems, fluoroquinolones and β-lactams

Modulation of the activity of some TCS influences the susceptibility of *P. aeruginosa* to antimicrobials (Figure 19). As previously mentioned, in addition to impacting polymyxin and aminoglycoside resistance, ParRS activation is associated with a slight increase in resistance (2-fold) to carbapenems (imipenem and meropenem) *via* down regulation of porin OprD (Muller *et al*., 2011). ParRS-dependent overexpression of operon *mexXY* also promotes resistance to cefepime and ciprofloxacin (Muller *et al*., 2011). Like ParRS, the TCS CopRS and CzcRS can provide *P. aeruginosa* with a higher resistance to carbapenems *via* the repression of gene *oprD* expression (Caille *et al*., 2007; Perron *et al*., 2004). Inactivation of CbrA from the CbrAB system enhances resistance to ciprofloxacin through a still unknown mechanism (Yeung *et al*., 2011).

Similarly, a stronger resistance to MexAB-OprM substrates is observed when the RR RocA2 is inactivated (Sivaneson *et al*., 2011) or when TCS AmgRS is activated as a result of operon *mexAB-oprM* upregulation (Fruci and Poole, 2018). Finally, transposon inactivation of the MxtR RR confers resistance to chloramphenicol, trimethoprim and fluoroquinolones *via* upregulation of the *mexEF-oprN* operon (Zaoui *et al*., 2012).

3.3. PmrAB two-component system

The *P. aeruginosa* PmrAB TCS was identified for the first time from a transposon insertion library constructed in strain PAO1 and cultivated in the presence of low Mg^{2+} concentrations (McPhee *et al*., 2003). This classic TCS is encoded by the *pmrAB* operon, with PmrA as the RR and PmrB as the HK, proteins which are homologous to PmrAB of *E. coli*, *S. Typhimurium*, *Yersinia spp*, *K. pneumoniae* and *A. baumannii*. Expression of *pmrAB* is activated by the RR PmrA upon low extracellular Mg^{2+} concentrations. Some antimicrobial peptides such as indolicidin, LL-37 and colistin also activate the expression of *pmrAB* (McPhee *et al*., 2003).

3.3.1. Structure of the TCS PmrAB

The HK PmrB from *P. aeruginosa* is a protein of 477 amino acids anchored in the IM by two TM domains. The periplasmic domain of PmrB is able to sense Mg^{2+}. However,

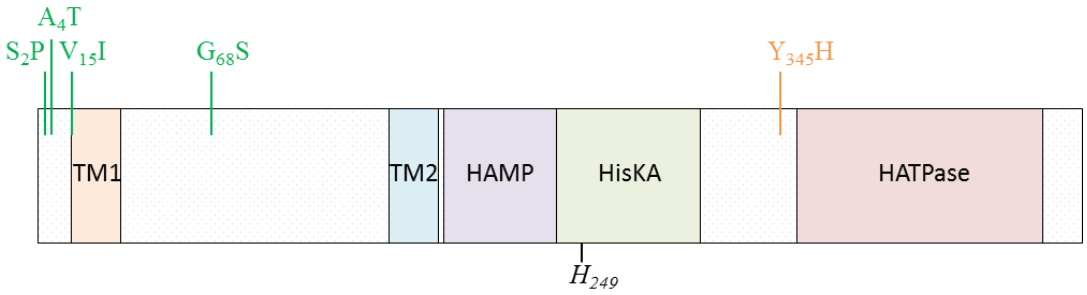

Figure 21: Schematic representation of functional domains of the PmrB sensor protein from *P. aeruginosa*.

Amino acid variations found in both strains PA14 and LESB58, or in strain PA14 only, are indicated (in orange and green, respectively) and are considered as polymorphism. TM1: transmembrane domain 1 (amino acids 15-37, in orange), TM2: transmembrane domain 2 (161-183, in blue), HAMP: linker domain (186-238, in purple), HisKA: dimerization and phosphoacceptor domain (239-304, in green), HATPase: Histidine kinase-like ATPases domain (348-459, in red). The putative active site histidine 249 (H_{249}) is indicated.

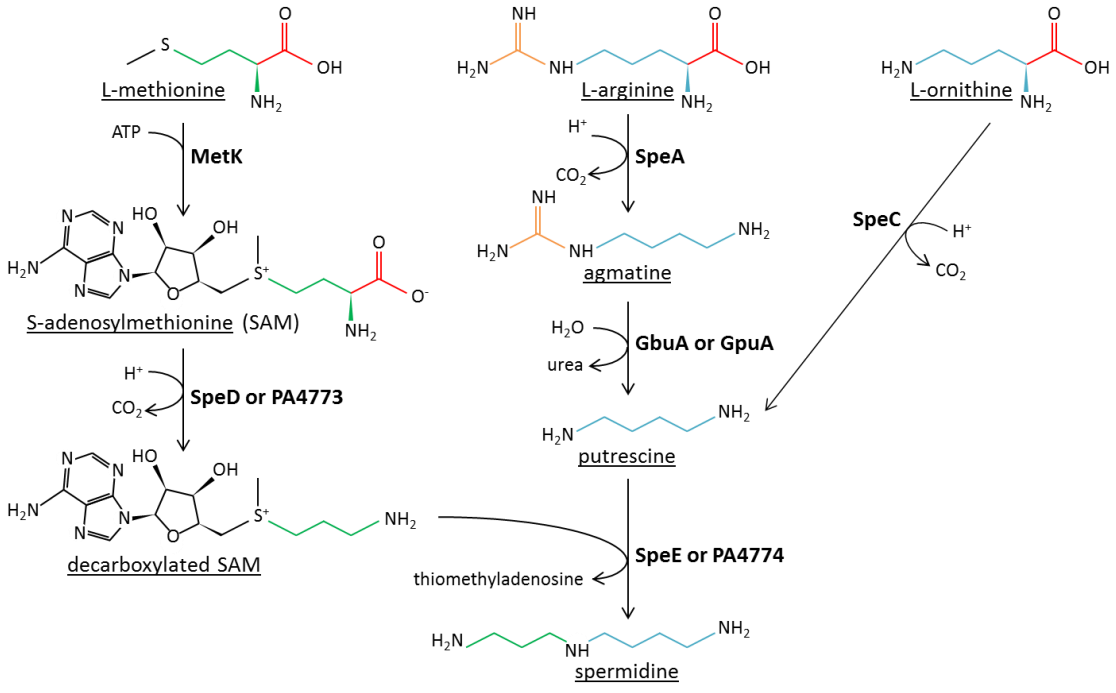

Figure 22: Pathways for spermidine biosynthesis in *P. aeruginosa*.

it was shown that peptide-induced activation of the *pmrAB* operon was only partially dependent of PmrAB (McPhee *et al*., 2003) and resulted from ParRS activation (Fernández *et al*., 2010). Prediction structure analysis using the SMART protein database (http://smart.embl-heidelberg.de/) identified three domains, an HAMP domain (from amino acid residues 186 to 238), a dimerization and phosphoacceptor domain HisKA (239-304) and an HATPase_c domain (348-459) (Figure 21). On the other hand, RR PmrA presents a N-terminal receiver domain (REC) (1-112) connected to a transcriptional regulatory protein, C-terminal (Trans_reg_C) domain (145-216) by a linker of 32 amino acids.

3.3.2. The regulon of PmrAB

Transcriptomic analysis of strain PAO1 and its transposon mutant *pmrA::xylE* grown with low Mg^{2+} concentration (0.02 mM) highlighted dysregulation of expression of 36 genes, of which 25 were at least 2-fold up-regulated (McPhee *et al*., 2006). In these conditions and in addition to operon *pmrAB*, protein PmrA activates the expression of the *arn* operon, causing an increased resistance to antimicrobial peptides. Moreover, it upregulates gene PA4773 and the PA4774-PA4775 operon located just upstream of *pmrAB*. PA4773 and PA4774 are considered as SpeD (PA0654) and SpeE (PA1687) homologs, respectively and they were proposed to determine an inducible pathway of spermidine biosynthesis (Johnson *et al*., 2012) (Figure 22). Spermidine production would contribute to the modification of the bacterial surface and thereby would have a protective role against aminoglycoside antibiotics, antimicrobial peptides and oxidative stress (Johnson *et al*., 2012). Predictive analysis of subcellular location using PSORT program (https://www.psort.org) indicated that the hypothetical protein of unknown function PA4775 harbors a signal peptide and a single predicted TM domain (Johnson *et al*., 2012). Based on a transcript length analysis, PA4775 appeared to be cotranscribed with PA4774 but not with PA4773 or *pmrAB* (Johnson *et al*., 2012). These five genes are activated when the bacteria are mixed with extracellular DNA, which chelates cations (Mulcahy *et al*., 2008) and acidifies biofilms (Wilton *et al*., 2016). Additional loci encoding transport systems, such as gene *mgtE*, operons PA4822-PA4826 (involved in Mg^{2+} uptake) and *feoAB*-PA4357 (ferrous iron uptake) were also up-regulated, as well as genes encoding various regulators (PA2359, *cueR*, PA4781 and *dnr*) (McPhee *et al*., 2006). Only 11 genes were down-regulated, including

Table 4: List of PmrAB substitutions identified *in vitro* and in clinical strains of *P. aeruginosa*.

Reference strains[a]	PmrB substitutions[b]	PmrA substitutions[b]	References
	***in vitro* mutants**		
PAK	$L_{243}Q$ $A_{248}V$		(Moskowitz *et al*., 2004)
PAO1	**$A_{247}T$ $M_{292}T$** $Y_{345}H$*		(Owusu-Anim and Kwon, 2012)
PAO1[c]	$L_{167}P$ $Y_{345}H$*		(Lee and Ko, 2014)
PAO1	V_9A $G_{52}S$ $L_{167}P$ $P_{175}L$ $W_{182}R$ $V_{212}M$ $A_{248}T$* $Q_{263}R$		(Jochumsen *et al*., 2016)
PA77	V_9A $L_{17}Q$ $N_{41}I$ $L_{90}Q$ $P_{169}X$ $P_{216}Q$ $P_{254}L$ $S_{257}N$ $H_{261}Y$ $M_{292}I$ $E_{320}K$		(Döβelmann *et al*., 2017)
PA83	S_8P V_9A $F_{51}L$ $L_{87}P$ $L_{96}R$ $G_{123}S$ $L_{167}P$ $L_{171}P$ $A_{248}T$ $R_{259}H$ $E_{320}K$ $V_{361}M$	$L_{11}P$ $L_{11}Q$ $G_{15}V$ $R_{159}L$ $N_{172}D$	(Döβelmann *et al*., 2017)
PAO1	$\Delta Nt_{131\text{-}133}$ $A_{247}T$ $S_{257}N$		(López-Causapé *et al*., 2018)
	clinical isolates		
non- CF strains			
PAO1	**$M_{292}T$**		(Abraham and Kwon, 2009)
PAO1	ΔD_{45} $Y_{345}H$*	$L_{71}R$*	(Schurek *et al*., 2009)
PAO1	**$A_{247}T$** $Y_{345}H$*		(Barrow and Kwon, 2009)
PAO1	$D_{47}N$ $V_{28}A$ $L_{162}P$ $Y_{345}H$*		(Sautrey *et al*., 2014)
PAO1	$V_{15}I$ $M_{48}L$ $A_{67}T$ $G_{68}D$ $D_{70}N$ $H_{340}R$ $T_{343}A$ $Y_{345}H$*	$L_{71}R$* $L_{157}Q$	(Lee and Ko, 2014)
	$V_{15}I$ $A_{67}T$ $L_{167}P$		(Lee *et al*., 2016)
PA14	T_4A $L_{323}H$	$L_{71}R$*	(Schniederjans *et al*., 2017)
CF strains			
PAK	$A_{211}V$* $A_{248}T$*		(Miller *et al*., 2011)
PAK	**$L_{14}P$ ΔD_{45} $A_{54}V$ $R_{57}H$** $R_{79}H$* $A_{95}T$* $R_{135}Q$* **$G_{188}D$** $A_{248}T$* $T_{253}M$* **$S_{257}N$** $R_{259}H$* **$M_{292}I$** $P_{456}S$*	$R_{71}L$*	(Moskowitz *et al*., 2012)
PAO1	$L_{31}P$ $F_{124}L$ $V_{185}I$ $E_{213}D$ $G_{221}D$ $R_{287}Q$		(López-Causapé *et al*., 2017)

[a] reference strains used for sequencing alignments and for constructing *in vitro* mutants.
[b] substitutions confirmed to induce polymyxin resistance are indicated in bold.
[c] *in vitro* mutants were selected from clinical strains (P5 and P155) and compared to PAO1 genome. *: polymorphism.

the operon of unknown function PA3515-PA3518, the copper-resistance associated operon *pcoAB*, the PA2274 gene encoding a putative flavin-dependent monooxygenase and the efflux pump operon *mexGHI-opmD* (McPhee *et al*., 2006).

3.3.3. Constitutive activation of PmrAB

Soon after the reintroduction of polymyxins in therapy, emergence of non-susceptible strains of *P. aeruginosa* was rapidly observed. Indeed, a citywide surveillance in Brooklyn revealed that 5% of *P. aeruginosa* isolates were resistant to these antibiotics in 2003 but zero in 2001 (Landman *et al*., 2005). Thus, the understanding of molecular mechanisms leading to resistance to this last resort antibiotics is important to design novel strategies of treatment.

Moskowitz *et al*. selected *in vitro* spontaneous polymyxin B-resistant mutants using strain PAK (Moskowitz *et al*., 2004). Sequencing of the *pmrB* gene in two of them revealed two variations ($L_{243}Q$ and $A_{248}V$) (Table 4), believed to impair PmrB phosphatase activity and therefore to result in constitutive activation of the RR PmrA. Moreover, analysis of the lipid A from these mutants showed that it contained one or two additional L-Ara-4N molecules compared to the LPS of parental strain PAK (Moskowitz *et al*., 2004). These data highlighted for the first time the fact that substitutions in PmrB can confer an acquired resistance to polymyxins in *P. aeruginosa*. Five years later, three groups described PmrAB alterations in polymyxin resistant isolates. In the first study, a variant in PmrB ($M_{292}T$) was identified in a resistant clinical isolate exhibiting polymyxin B resistance levels 4-fold higher than that of PAO1 (8 µg ml^{-1} *versus* 0.5 µg ml^{-1}) (Abraham and Kwon, 2009). The impact of this substitution was confirmed by measuring polymyxin MIC in a *pmrAB*-knockout mutant complemented with the mutated *pmrAB* allele. A second group identified three mutations in operon *pmrAB* causing two alterations in the PmrB sequence (ΔD_{45} and $Y_{345}H$) and one in that of PmrA ($L_{71}R$). As the $Y_{345}H$ and $L_{71}R$ variants were also found in susceptible strain LESB58 and/or wild-type strain PA14, these mutations do not participate in polymyxin resistance. Contribution of the remaining PmrB mutation ΔD_{45} remains to be confirmed (Schurek *et al*., 2009). The last study characterized five clonally unrelated strains isolated in a medical center of Brooklyn, that were resistant to polymyxin B (MICs = 8 µg ml^{-1}). In one of them, two substitutions ($A_{247}T$ and $Y_{345}H$)

were present in PmrB. Plasmid-mediated complementation of a *pmrAB*-null mutant of PAO1 with the mutated allele, confirmed the contribution of $A_{247}T$ in polymyxin B resistance (Barrow and Kwon, 2009). Interestingly, these variations $A_{247}T$ and $M_{292}T$ trigger higher levels of resistance to polymyxin with concomitant RR PhoQ loss-of-function mutations (Owusu-Anim and Kwon, 2012).

Additional mutations were identified in clinical strains from South Korea, resistant to colistin. However, their contribution to the phenotype was not confirmed, in particular the variant $L_{157}Q$ in PmrA (Lee and Ko, 2014).

In the CF context, molecular characterization of clinical strains isolated from patients treated with colistin, and exhibiting MICs higher than 512 µg ml^{-1}, detected two new PmrB alleles ($A_{211}V$ and $A_{248}T$). Nevertheless, expression of these alleles in strain PAK failed to increase bacterial resistance to colistin, and were thus considered as polymorphism (Miller *et al*., 2011). Later on, however, other PmrB mutations were shown to promote polymyxin resistance in CF strains from the United Kingdom or Denmark (Moskowitz *et al*., 2012). Interestingly, variants of PmrB harboring two mutations in the protein provided higher resistance levels than single mutation variants. Six other PmrB mutations ($L_{31}P$, $F_{124}L$, $V_{185}I$, $E_{213}D$, $G_{221}D$ and $R_{287}Q$) were identified in a study investigating the genetic evolution of a widespread CF clone (CC274) in Australia and in Spain (López-Causapé *et al*., 2017). These results illustrated the contribution of PmrAB to *P. aeruginosa* CF lung adaptation.

In vitro studies aiming to decipher the evolution of colistin resistance in *P. aeruginosa*, showed that it is a complex and multistep process. Indeed, in the PAO1 genetic background, mutations in at least five independent loci, including *pmrB*, are required for this evolution. Moreover, *pmrB* mutations potentiate evolution of high-level colistin resistance (Jochumsen *et al*., 2016). Additionally, Dößelmann *et al*. showed that clinical isolates (PA77 and PA83) cultured in a device adjusting colistin concentration continuously (morbidostat), also harbored mutations in PmrB (Dößelmann *et al*., 2017). Thus, PmrAB seems to be essential for *P. aeruginosa* to reach high-levels of colistin resistance and *de facto* could be a good cellular target for drug development.

Resistance to polymyxins could not be the only advantage provided by alterations in

PmrAB. López-Causapé *et al*. suggested that PmrB mutations might participate in aminoglycoside resistance (López-Causapé *et al*., 2018). However, comparison of MICs of tobramycin for PA14 mutants harboring variation T_4A in PmrB, alone, or combined with $L_{323}H$, showed no difference in one case and a 2-fold increase in the other one, respectively (Schniederjans *et al*., 2017). The authors concluded that the observed mutations in PmrAB did not influence tobramycin susceptibility.

Thus, despite the well established contribution of TCS PmrAB to polymyxin resistance, its role in aminoglycoside resistance and adaptation of *P. aeruginosa in vivo* remains to be assessed.

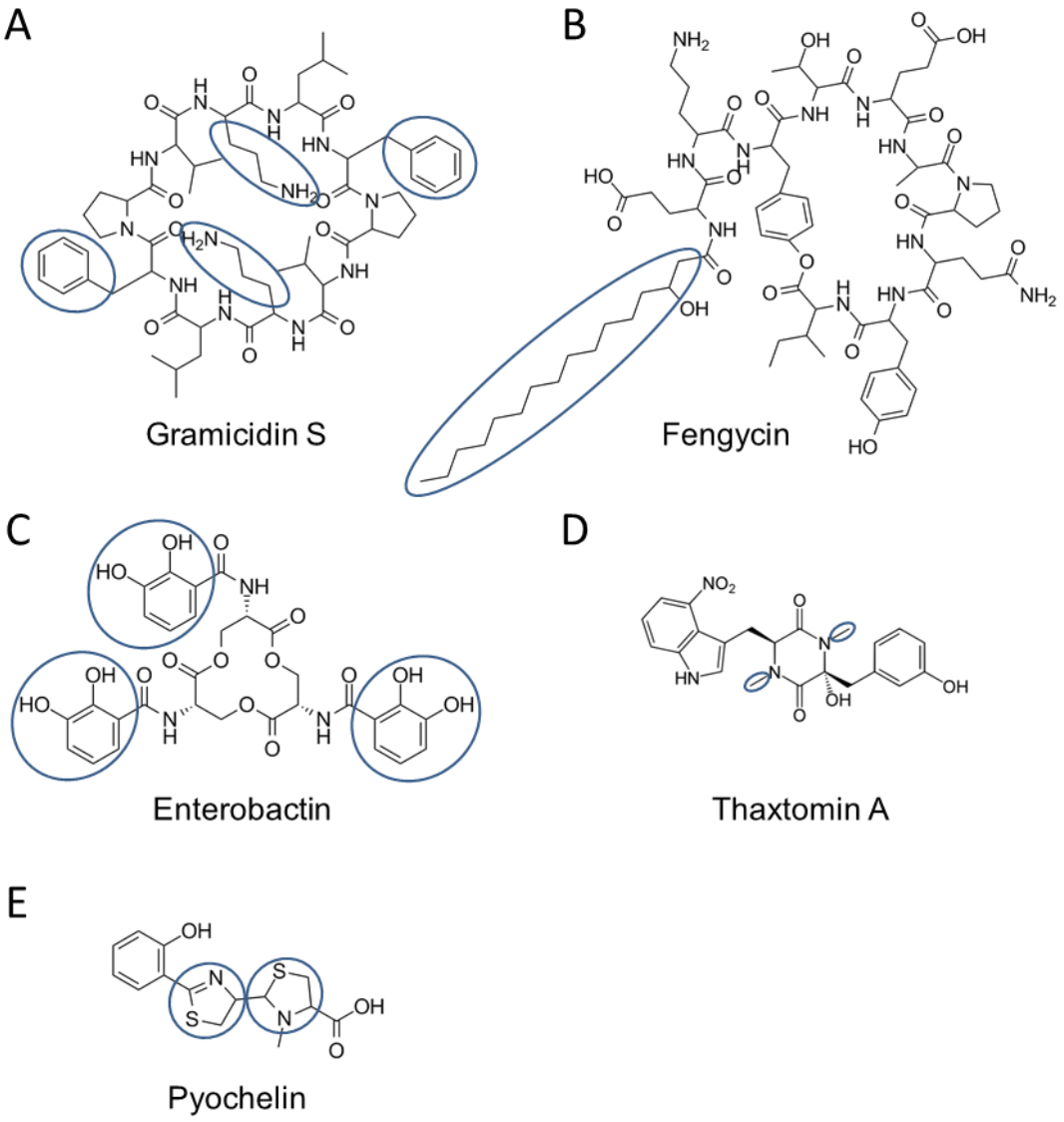

(Finking and Marahiel, 2004)

Figure 23: Nonribosomal peptides representing the diversity of monomers which can be incorporated by nonribosomal peptide synthetases.

Specific molecular features such as nonproteinogenic amino acids (A), fatty acids (B), carboxy acids (C), modified amino acids and heterocyclic rings (E) are surrounded in blue.

4. Nonribosomal peptides

Nonribosomal peptides (NRPs) are natural products synthesized independently of the ribosomal machinery, by large dedicated multimodular biocatalysts called NRP synthetases (NRPSs) (Gulick, 2017). The structures of NRPs are diverse and they have a broad spectrum of activity (Schwarzer *et al*., 2003). They are mainly produced by bacterial and fungal species and were shown to take part in a diversity of cellular processes as growth, nutrient acquisition, communication and virulence (Gulick, 2017). Many of the NRPs include drugs possessing anti-microbial activity (vancomycin, polymyxin, daptomycin and thienamycin).

4.1. NRPs biosynthesis

The modular organization of NRPSs drives the synthesis of the polypeptide. Each module contains catalytic domains responsible for the incorporation of an amino acid into the neopeptide. Additional proteins can be associated with NRPSs to participate in the synthesis of building blocks, peptide modification and export. The genes coding for NRPSs are often found in the same biosynthetic cluster. NRPs biosynthesis usually follows three phases: (i) building block assembly, (ii) NRPS-mediated peptide assembly and (iii) post-NRPS modifications and/or decoration (Süssmuth and Mainz, 2017).

4.1.1. The building block assembly

NRPs are synthesized by the consecutive condensation of building blocks by NRPSs. In addition to the twenty amino acids, NRPS can incorporate nonproteinogenic amino acids like heterocyclic amino acids, but also fatty acids, carboxy acids or α-hydroxy acids (Strieker *et al*., 2010) (Figure 23). Building blocks distinct from proteinogenic amino acids can be synthesized by specific enzymes encoded by genes either in operon with the NRPS gene or within the same genetic cluster. This characteristic participates in the high diversity of structures observed in NRPs and probably to their diverse bioactivity.

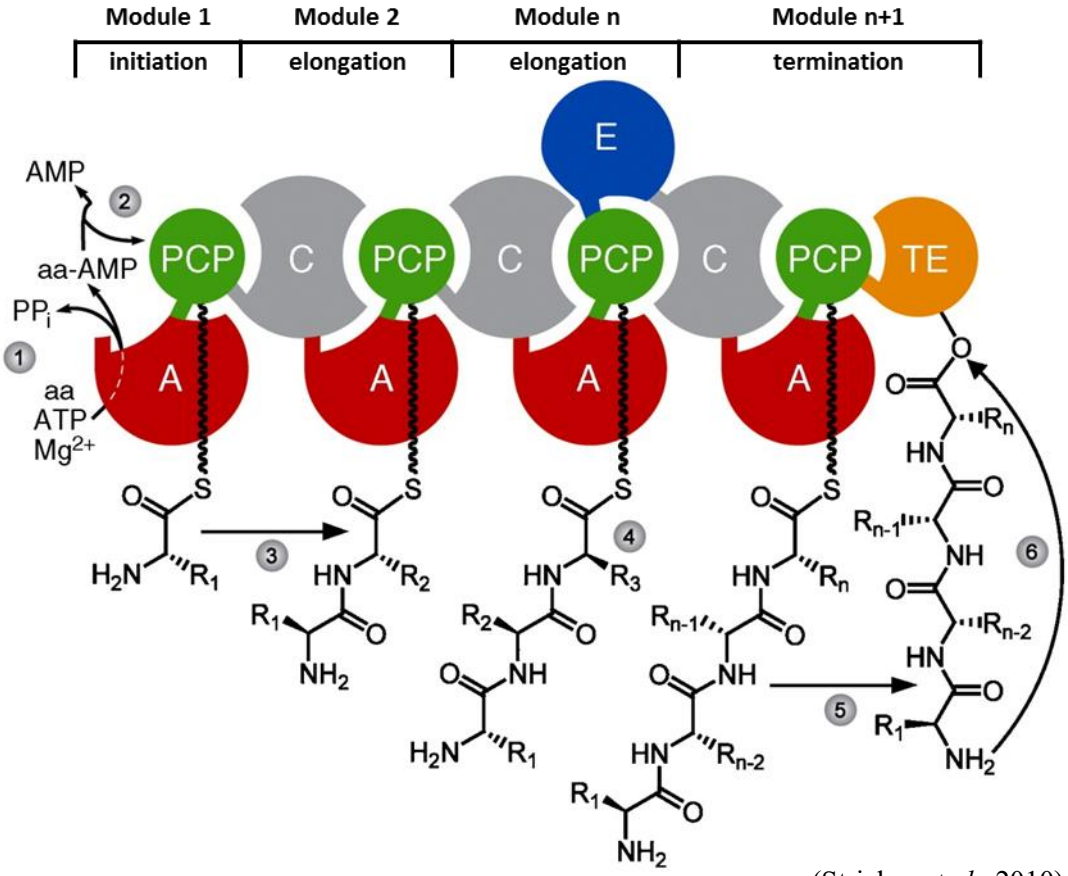

(Strieker *et al*., 2010)

Figure 24: NRP synthesis pathway.

A: adenylation, PCP: peptidyl carrier protein, C: condensation, E: epimerization, TE: thioesterase, ATP: adenosine triphosphate, AMP: adenosine monophosphate, aa: aminoacyl, PPi: pyrophosphate.

A domain	specificity signature										substrate
	1	2	3	4	5	6	7	8	9	10	
GrsA	D	A	W	T	I	A	A	I	C	K	Phe
ApnA-A1	D	V	E	S	I	G	V	I	A	K	Arg/Tyr
CytC1	D	F	w	n	i	G	g	V	F	K	D-Val
DltA	D	L	M	t	l	C	t	V	a	K	D-Ala
AB3403	D	I	l	q	l	g	v	V	W	K	Gly
SidNA3	D	V	L	G	G	G	V	I	G	K	cis-AMHO
VinN	D	F	k	p	t	S	m	K	R	K	β-MeAsp
DhbE	N	Y	S	a	q	G	V	–	V	K	DHBA
BadA	A	Y	g	y	s	A	g	H	I	K	BA
Alb1-A1	A	V	K	Y	V	A	N	D	A	K	pABA
BlmIV-A1	V	D	W	V	I	S	L	A	D	K	β-Ala
ESyn-A1	G	A	L	M	V	V	G	S	I	K	α-HIV
Vlm1-A1	A	A	L	W	I	A	V	S	G	K	α-KIV

(Süssmuth and Mainz, 2017)

Figure 25: Nonribosomal code.

Conserved Asp (D) and Lys (K) residues are highlighted in red, and residues which participate in substrate binding are in capital letters. A domain: adenylation domain.

4.1.2. The assembly of the polypeptide by NRPS

NRPS performs the activation and the assembly of a single amino acid to a growing peptide chain through the succession of several modules. In the modular organization of NRPSs, each module can be classified as an initiation, elongation (n) or termination (n+1) module (Finking and Marahiel, 2004) (Figure 24).

The NRP assembly begins with the selection and activation at the adenylation (A) domain of the first building block, by the initiation module. The A domain belongs to the Acyl-CoA synthetases, NRPS adenylation domains, and Luciferase enzymes (ANL) superfamily of adenylate forming enzymes (Süssmuth and Mainz, 2017). Thus, the amino acid is activated as aminoacyl-adenosine monophosphate (aminoacyl-AMP) by ATP (Finking and Marahiel, 2004) (Figure 24). The positioning of the amino acid is located in a consensus motif of ten residues of the A domain (Schwarzer *et al*., 2003). Among them, a highly conserved Asp (D1) residue stabilizes the amino group while a Lys (K10) residue stabilizes the carboxylate moiety (Süssmuth and Mainz, 2017). This strictly conserved Lys residue is required for adenylation while the Asp residue can vary or be repositioned along the binding pocket (Süssmuth and Mainz, 2017).

Analysis of crystal structures combined with amino acid sequence of A domains determined that up to 8 residues are involved in side chain recognition which led to the development of a nonribosomal code. This latter, in association with bioinformatics algorithms can predict the substrate of the A domain and the composition of NRP (Schwarzer *et al*., 2003) (Figure 25). Generally, the A domain is a part of the NRPSs but can be part of an independent enzyme (Schwarzer *et al*., 2003). The aminoacyl-AMP is transferred to the peptidyl carrier protein (PCP) also named thiolation (T) domain which carries a 4'-phosphopantetheine (4'-PP) prosthetic group at a highly conserved Ser residue (Schwarzer *et al*., 2003) (Figure 24).

The PCP domain with its 4'-PP extension corresponds to a flexible arm that covalently sequesters and transfers the aminoacyl/peptidyl thioester to the catalytic centers (Süssmuth and Mainz, 2017). The second substrate is activated at the A domain of the module next to the initiation module, named the elongation module. In addition to the initiation module, it contains a condensation (C) domain. This domain creates a peptide bound between the building blocks from the T domains of the initiation module and

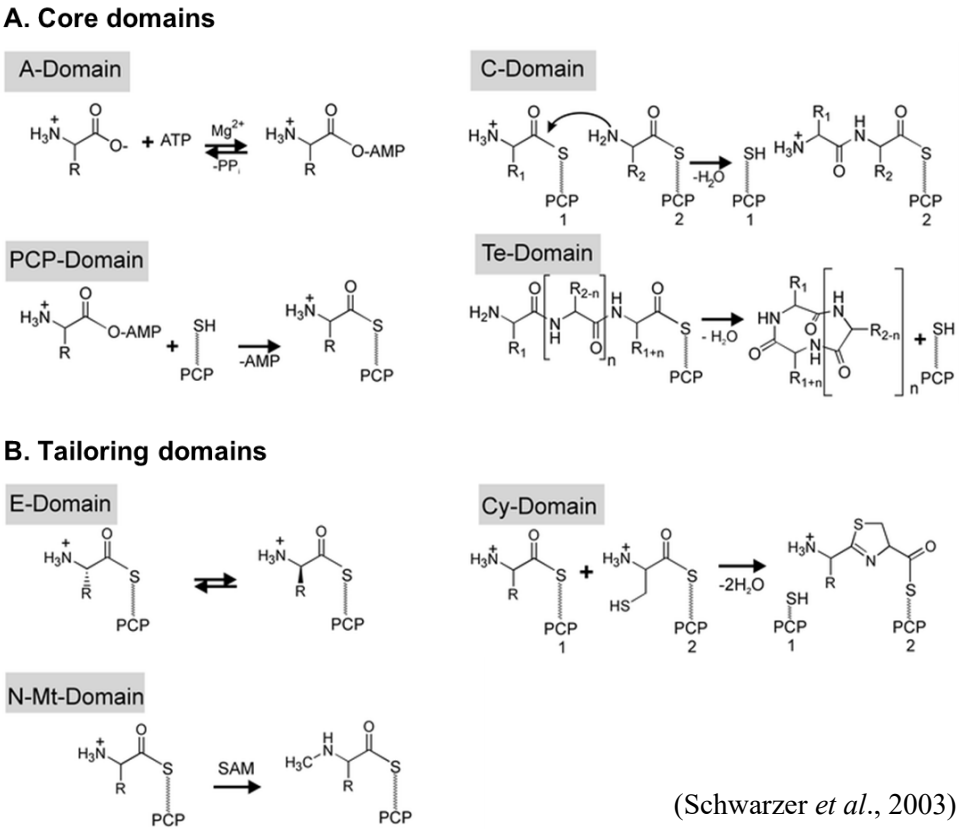

Figure 26: Examples of reactions catalyzed by NRPS domains.

A: adenylation, C: condensation, PCP: peptidyl carrier protein, Te: thioesterase, E: epimerization, Cy: hetero-cyclization, N-Mt: *N*-methylation.

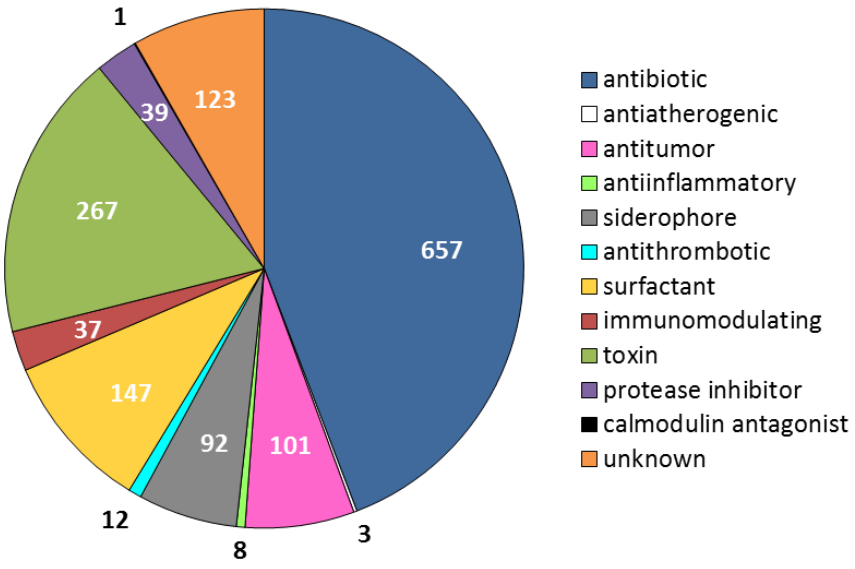

Figure 27: Pie chart repartition of the 1,190 NRPs listed in the Norine database according to their reported biological activities and therapeutic applications.

The total number of peptides (1,487) is higher than 1,190 due to dual activities of some peptides (https://bioinfo.lifl.fr/norine/subMod.jsp).

the nascent peptidyl intermediate generated by the elongation module. Despite exceptions, the C domain is present in all elongation modules of NRPSs and is characterized by its substrate specificity (Schwarzer *et al*., 2003). The catalytic domain is located at a conserved His residue. Interestingly, the C domain acts also as a proofreading backup to guarantee the synthesis of the correct polypeptide (Süssmuth and Mainz, 2017). NRP synthesis carries on with the incorporation of additional substrates through additional elongation modules (modules n). Elongation modules may harbor extra domains, called tailoring domains that modify the peptide upon synthesis as the epimerization (E), hetero-cyclization (Cy), N-methylation (N-Mt) domains (Figure 26B).

Once the NRP is complete, the PCP domain of the last module, called the termination module, transfers the NRP to the thioesterase (TE) domain which releases the NRP from the NRPS (Figure 24) (Schwarzer *et al*., 2003). Like α/β-hydrolases, the peptide is released either by hydrolysis (water as a nucleophile) or aminolysis (amine as a nucleophile) (Süssmuth and Mainz, 2017). Frequently, TE domains catalyze the formation of a cycle such as a lactone or lactam ring. TE domains can also catalyze amide bonds, branched-cyclic formation, epimerization and even oligomerization of peptide units (Finking and Marahiel, 2004). After the peptide is released, post-synthesis modifications by additional enzymes can occur.

4.1.3. The modifications and/or decoration

Peptides released from NRPSs can be modified by tailoring enzymes distinct from NRPS. These enzymes that act in *trans* can be glycosyl transferases, halogenases and hydroxylases (Schwarzer *et al*., 2003). This final step of NRP biosynthesis contributes to the elaboration of a variety of chemical structures and biological activities (Süssmuth and Mainz, 2017).

4.2. Biological activities of NRPs

NRPs represent an important source of therapeutic compounds exhibiting a wide range of biological activities (Figure 27). They are particularly interesting for their pharmacological behavior and stability *in vivo* (Kang and Suga, 2008). Unlike

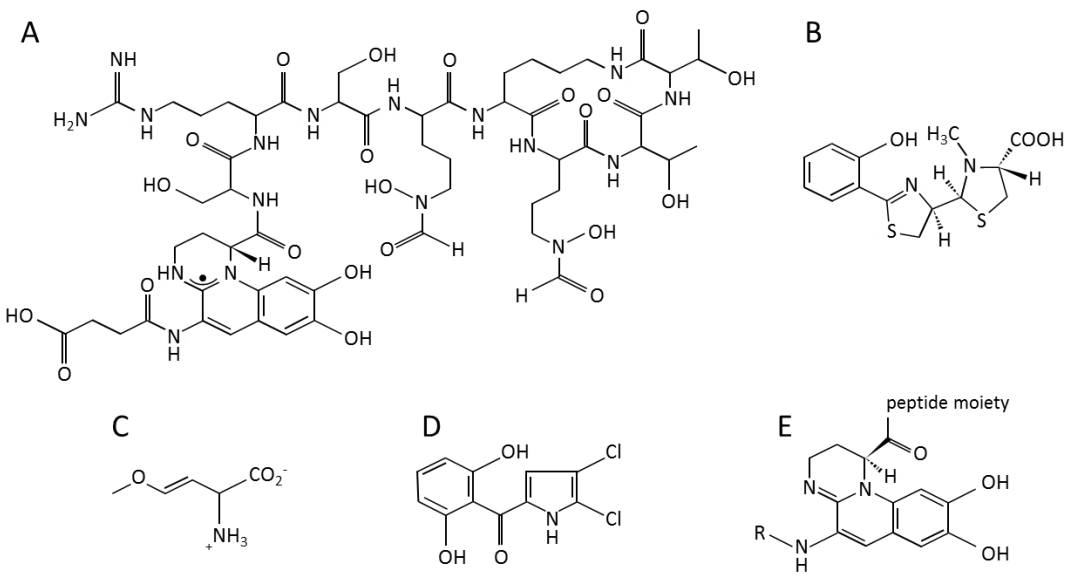

Figure 28: NRPs synthesized by *P. aeruginosa.*

P. aeruginosa may produce type I pyoverdine (A), pyochelin (B), AMB (C) and pyoluteorin (D). The conserved dihydroquinoline-type chromophore of pyoverdines is also represented (E).

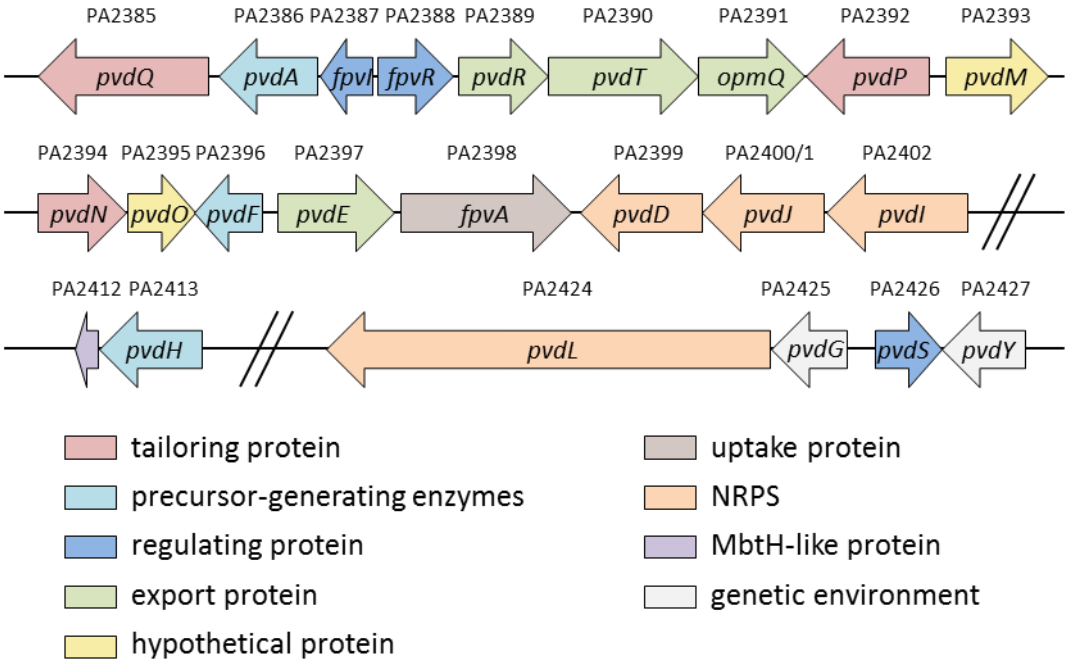

Figure 29: Genetic cluster responsible of type I pyoverdine biosynthesis and export in *P. aeruginosa* strain PAO1.

The orientation of open reading frames is indicated, as well as the PA numbers and gene names.

ribosomal peptides, NRPs are more stable to proteases, notably because of their composition that includes nonproteinogenic amino acids (Kang and Suga, 2008). The function of NRPs for producing organisms is not well established but some of them would participate in cell-to-cell communication, signal transduction or virulence (Süssmuth and Mainz, 2017). Production of NRPs siderophores such as enterobactin, vibriobactin, bacillibactin and pyoverdine enables microorganisms to grow under iron-limiting conditions (Schwarzer *et al*., 2003). Some NRP virulence factors such as the *Pseudomonads* pore-forming toxins syringomycin, syringostatin and syringopeptin participate in plant infections (Süssmuth and Mainz, 2017).

In medicine, several NRPs have been used for their antimicrobial activities against Gram-positive (daptomycin, vancomycin and novobiocin) and Gram-negative bacteria (polymyxins, thienamycin). Some have been employed as cytostatic agents (bleomycin A2 and epothilone), immunosuppressive drugs (cyclosporine A), as well as in obstetrics (ergometrine) and for pain treatment (ergotamine) (Strieker *et al*., 2010; Süssmuth and Mainz, 2017). Identification of new NRPs may potentially lead to interesting therapeutic alternatives.

4.3. NRPs in *P. aeruginosa*

Depending on their genetic background, strains of *P. aeruginosa* may possess up to eight NRPS clusters. In the genome of *P. aeruginosa* PAO1, six of such clusters have been identified of which only three were characterized. Two additional NRPS clusters are present in strains LESB58 and PA7 (Gulick, 2017). These large multifunctional enzymes are able to produce several peptides, including the well-known pyoverdine, pyochelin, L-2-amino-4-methoxy-trans-3-butenoic acid (AMB) and pyoluteorin (Figure 28). The function of four NRPS clusters remains to be investigated.

4.3.1. Pyoverdines

At least 60 different pyoverdines are produced by fluorescent *Pseudomonads* (Schalk and Guillon, 2013). They share similar characteristics: (i) a conserved dihydroquinoline-type chromophore (Figure 28E), (ii) a variable peptide bound to the carboxylic group of the chromophore and (iii) a dicarboxylic acid, an amide or an α-ketoglutaric acid linked to the NH_2 group of the chromophore (Hannauer *et al*., 2012).

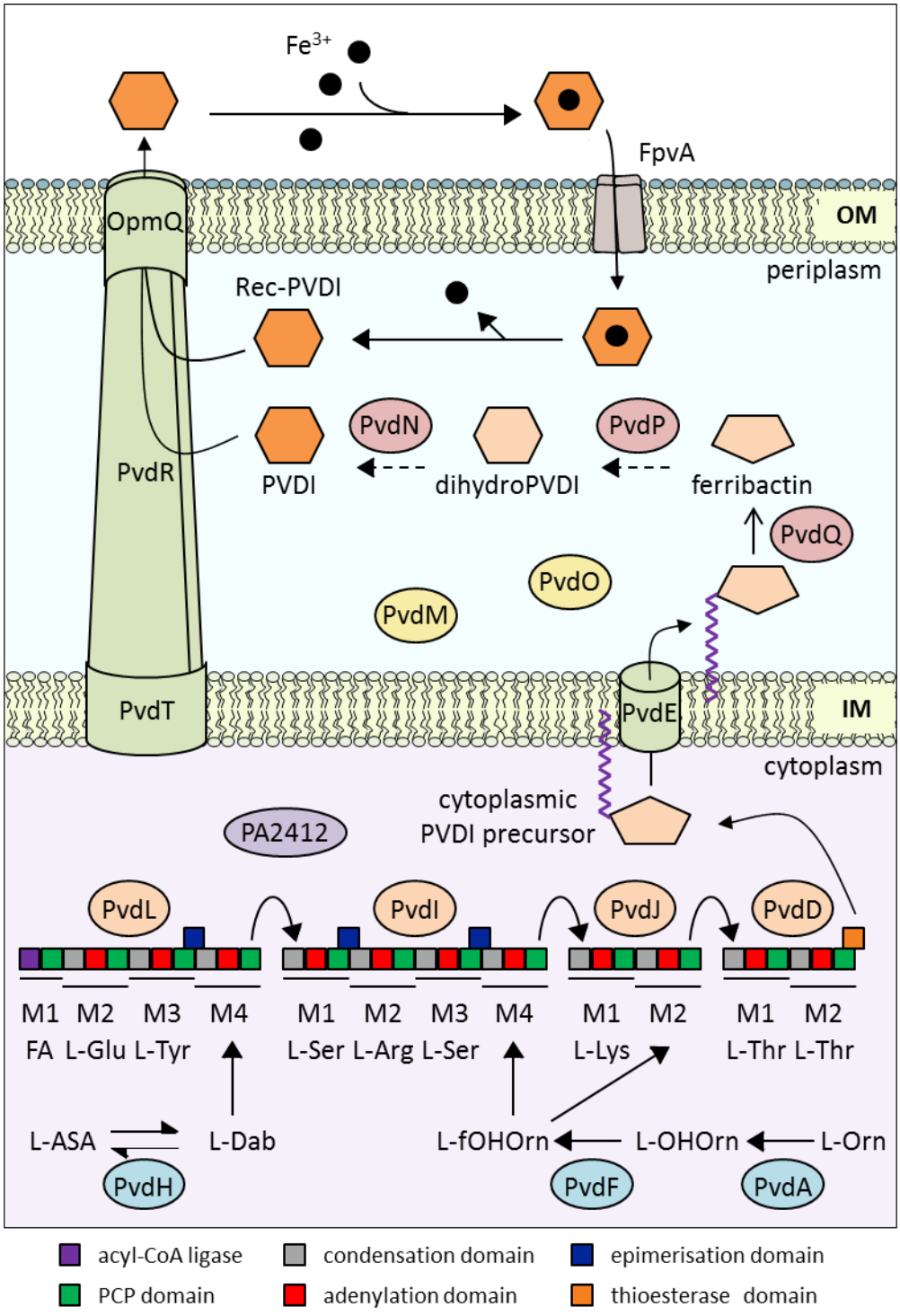

Figure 30: Schematic representation of pyoverdine synthesis, secretion and uptake in *P. aeruginosa*.

PVDI: pyoverdine I, Rec: recycled, FA: fatty acid, OM: outer membrane, IM: inner membrane.

Under iron-limiting conditions, pyoverdine molecules are secreted outside the cell to chelate ferric iron (Lamont *et al*., 2006). The siderophore-iron complex is then transported to the periplasm by the TM receptor protein FpvA (Dorrestein *et al*., 2003).

P. aeruginosa synthetizes three types of pyoverdine (PVDI, PVDII, and PVDIII), which differ from each other by their peptide moieties (Visca *et al*., 2007). PVDI biosynthesis in strain PAO1 requires four NRPS (PvdL, PvdI, PvdJ and PvdD) and the products of nine additional genes (*pvdH, pvdA, pvdF, pvdQ, pvdP, pvdM, pvdN, pvdO and* PA2412) located in the same genomic region (Figure 29) (Gulick, 2017). PVDI is made from two substrates, L-aspartate β-semialdehyde (L-ASA) and L-ornithine (L-Orn), which are modified by enzymes PvdH, PvdA and PvdF (Figure 30). PvdH converts L-ASA to L-2,4-diaminobutyrate (L-Dab) (Vandenende *et al*., 2004). L-ornithine-N^5-oxygenase PvdA interconverts L-Orn and L-N^5-hydroxyornithine (L-OHOrn) (Ge and Seah, 2006; Meneely *et al*., 2009).

L-OHOrn is then formylated by PvdF to produce L-N^5-formyl-N^5-hydroxyornithine (L-fOHOrn) (McMorran *et al*., 2001). These nonproteinogenic amino acids (L-Dab and L-fOHOrn) are then incorporated by the NRPS enzymes (PvdL, PvdI and PvdJ) which produce together with PvdD, the immature pyoverdine peptide. Protein PA2412 also participates in pyoverdine synthesis as an MbtH-like protein, to enhance the adenylation activity (Drake *et al*., 2007; Zhang *et al*., 2010).

The cytoplasmic PVDI precursor harbors a myristate or myristoleate chain on the first residue hanging it into the IM (Hannauer *et al*., 2012). This residue is removed by PvdQ in the periplasm after its transfer through PvdE, an export ABC transporter known to be required for PVDI production and secretion (Yeterian *et al*., 2010). Ferribactin is then hydroxylated by a copper-dependent tyrosinase, PvdP (Nadal-Jimenez *et al*., 2014) in dihydropyoverdine, an intermediate which differs from pyoverdine by one degree of unsaturation within the future chromophore moiety. Finally, N-terminal glutamic acid is converted into the succinamide moiety by PvdN (Ringel *et al*., 2016). Additional periplasmic enzymes PvdO and PvdM, with unknown functions, were shown to participate in pyoverdine synthesis or secretion (Ochsner *et al*., 2002). Newly synthesized PVDI is secreted *via* the ATP-dependent efflux pump PvdRT-OpmQ (Hannauer *et al*., 2010).

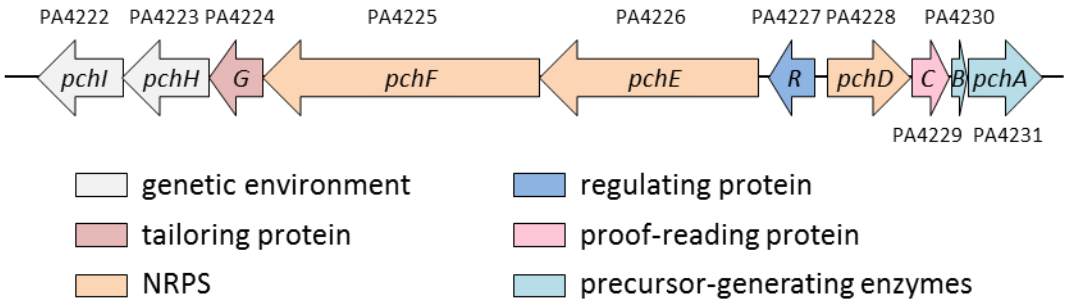

Figure 31: Genetic cluster for synthesis of pyochelin in *P. aeruginosa* strain PAO1.

The orientation of open reading frames is indicated, as well as the PA numbers and gene names.

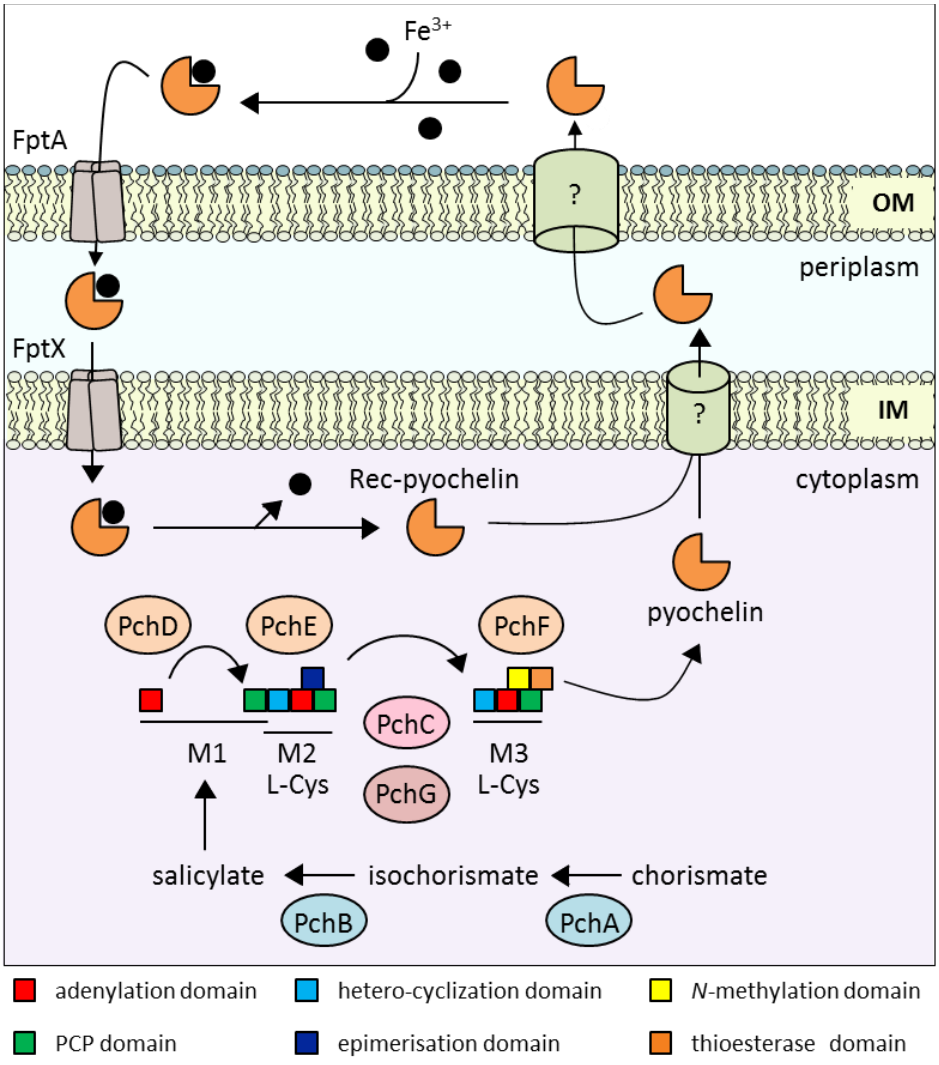

Figure 32: Schematic representation of pyochelin synthesis, secretion and uptake in *P. aeruginosa*.

Rec: recycled, ?: unknown transporter, OM: outer membrane, IM: inner membrane.

4.3.2. Pyochelin

P. aeruginosa produces a second NRP siderophore named pyochelin (Gulick, 2017). Pyochelin is however produced at lower levels than pyoverdine (Gulick, 2017). The affinity of pyochelin for Fe^{3+} (5.10^5 M^{-1}) (Braud *et al*., 2009) is lower than that of pyoverdine (10^{32} M^{-1}) (Gasser *et al*., 2015). In *P. aeruginosa* strain PAO1, pyochelin synthesis requires seven cytoplasmic enzymes, including three NRPSs, namely PchD, PchE, and PchF (Reimmann *et al*., 1998).

The substrate of the first module NRPS (PchD) is a nonproteinogenic building block. It comes from the conversion of chorismate by PchA and PchB to form salicylate (Figure 32). PchD activates salicylate incorporation by the N-terminal carrier protein domain of PchE. An L-Cys residue is incorporated into the nascent peptide by the elongation domain of PchE which further: (i) cyclizes the L-Cys to a thiazoline and, (ii) alters the stereochemistry with an epimerase tailoring domain (Patel *et al*., 2003). A second L-Cys residue is integrated by PchF which subsequently cycles it into a thiazoline ring. The proof-reading thioesterase PchC is in charge of the release of mischarged molecules from the PCP domains of PchE and PchF (Reimmann *et al*., 2004). The tailoring protein PchG proceeds to a NADPH-dependent reduction of the thiazolinyl group to a thiazolidinyl group (Reimmann *et al*., 2001). Thiazolidine is methylated by the N-methyltransferase domain of PchF (S-adenosylmethionine (SAM)-dependent reaction) (Patel and Walsh, 2001). Finally, PchF releases pyochelin through its TE-domain (Ronnebaum and Lamb, 2018). In contrast to pyoverdine, the transport system responsible for pyochelin secretion remains unknown but ferripyochelin is then transported across the OM by the TonB-dependent transporter FptA and across the IM by the proton-motive dependent permease FptX (Schalk and Cunrath, 2016).

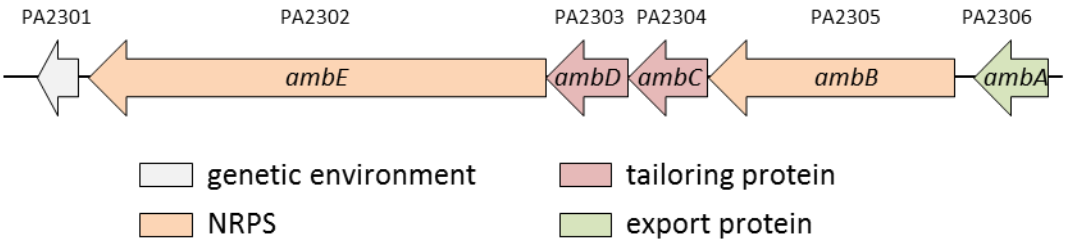

Figure 33: Genetic cluster for the biosynthesis of L-2-amino-4-methoxy-trans-3-butenoic acid in *P. aeruginosa* strain PAO1.

The orientation of open reading frames is indicated, as well as the PA numbers and gene names.

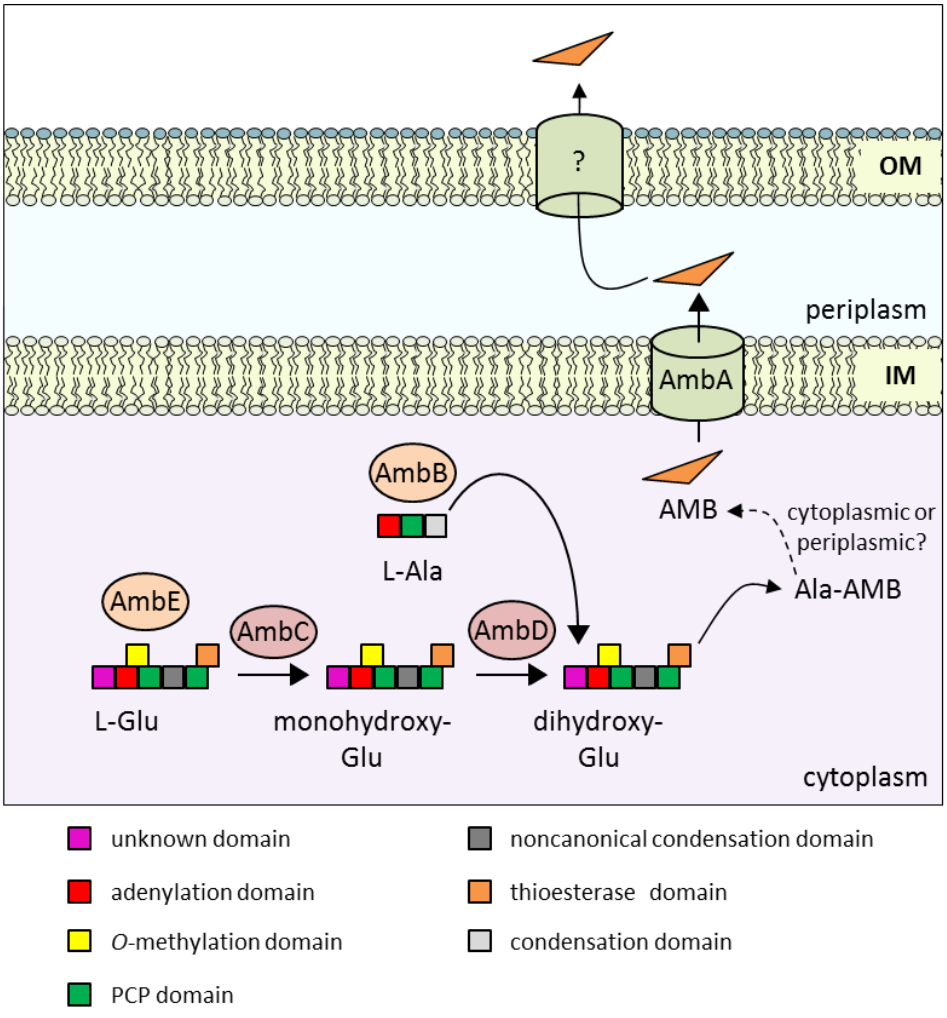

Figure 34: Schematic representation of L-2-amino-4-methoxy-trans-3-butenoic acid synthesis and export in *P. aeruginosa*.

AMB: L-2-Amino-4-methoxy-trans-3-butenoic acid, ?: unknown transporter, OM: outer membrane, IM: inner membrane.

4.3.3. L-2-Amino-4-methoxy-trans-3-butenoic acid (AMB)

AMB is a nonproteinogenic amino acid produced by *P. aeruginosa via* another NRPS pathway. This toxic antimetabolite was isolated for its capacity to inhibit the growth of *Bacillus subtilis* (Scannell *et al*., 1972) and *E. coli* (Sahm *et al*., 1973). AMB is active against bacteria and eukaryotic cells probably through the inhibition of pyridoxal phosphate (PLP)-dependent enzymes, an activity shared with other members of the γ-substituted vinylglycine family (Gulick, 2017). The genetic cluster responsible for its biosynthesis was identified by Lee *et al*. and named *ambABCDE* (Lee *et al*., 2010) (Figure 33). The genes *ambB* and *ambE* code respectively for a mono- and di-modular NRPSs while *ambC* and *ambD* encode proteins sharing sequence homologies with Fe(II)/α-ketoglutarate-dependent oxygenases (Gulick, 2017). Rojas Murcia *et al*. proposed a model for AMB biosynthesis involving an Ala-AMB-Ala tripeptide (Rojas Murcia *et al*., 2015). On the other hand, Patteson *et al*. recently suggested that a dipeptide, Ala-AMB, could be the precursor of AMB (Patteson *et al*., 2018) (Figure 34). This toxin is supposed to be exported by the LysE-type TM transporter encoded by *ambA*. However, whether AmbA exports AMB or the dipeptide form outside the cell is unknown.

The last model envisaged for AMB synthesis starts with the activation of an L-Ala and an L-Glu by AmbB and AmbE, respectively (Patteson *et al*., 2018). Methylation by the O-methyltransferase domain of AmbE takes place before the condensation with Ala by the C domain of AmbB. Then, Glu is subjected to two successive hydroxylations by AmbC and AmbD. The cryptic C_3 hydroxy of the resulting dipeptide is possibly removed by the non-canonical C domain of AmbE. Additional decarboxylation and isomerization generate a methoxy enol ether, by a still unknown route. The Ala-AMB peptide is believed to be released by the TE domain of AmbE before an uncharacterized source of peptidase activity cleaves AMB (Patteson *et al*., 2018).

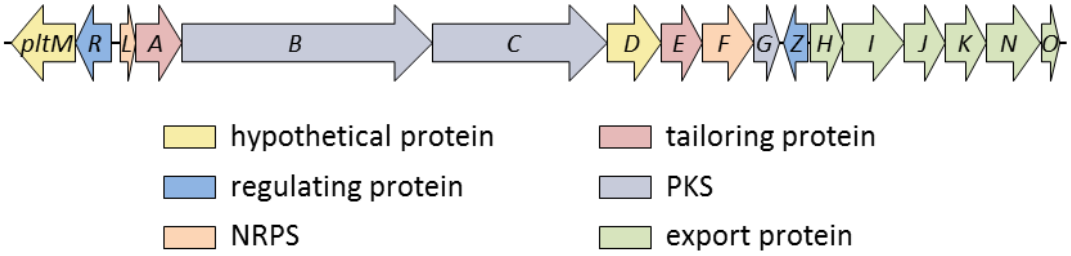

Figure 35: Genetic cluster for synthesis and export of pyoluteorin in *P. aeruginosa* strain M18.

The orientation of open reading frames is indicated, as well as gene names.

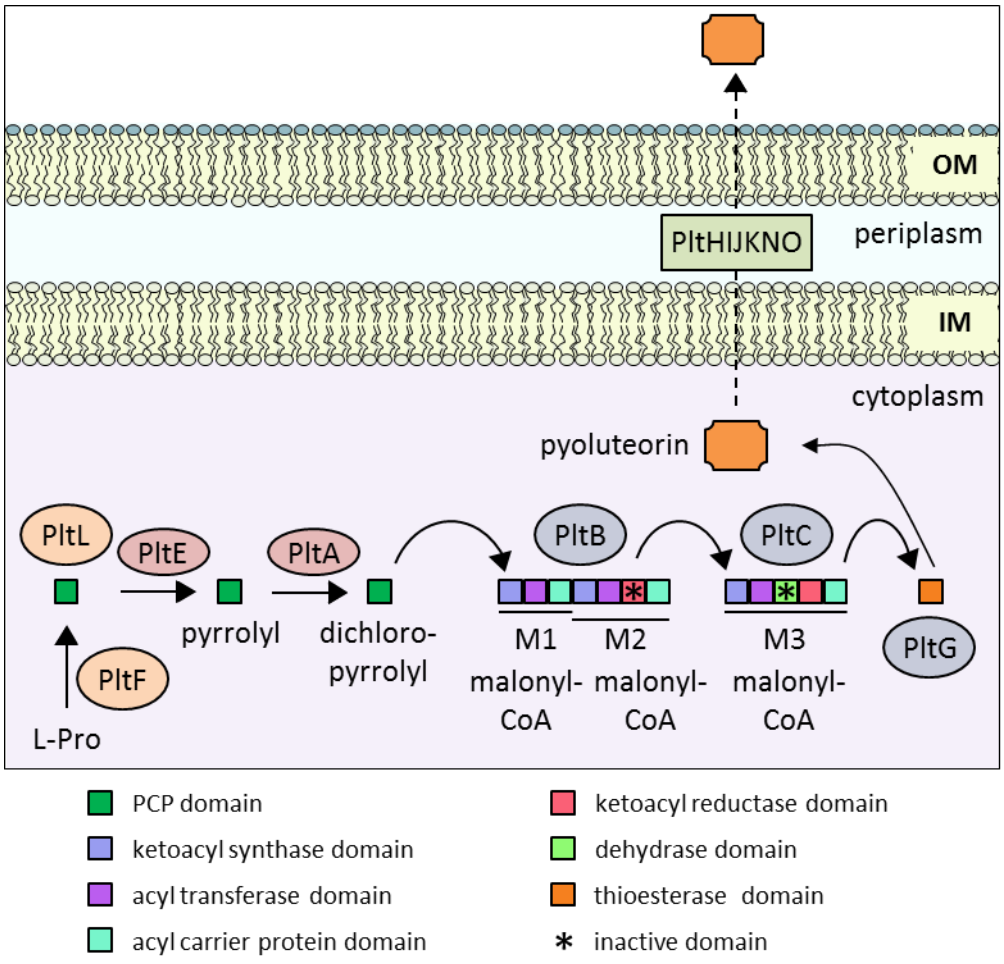

Figure 36: Schematic representation of pyoluteorin synthesis and export in *P. aeruginosa*.

OM: outer membrane, IM: inner membrane.

4.3.4. Pyoluteorin

Pyoluteorin was isolated for the first time from *P. aeruginosa* strains T-359 and IFO-3455 in 1958 by Takeda (Takeda, 1958). This antibiotic harbors a resorcinol moiety fused to a dihalogenated pyrrole derived from proline (Figure 28D). However, this inhibitor of fungi and oomycetes is not produced by all *P. aeruginosa* strains (Gulick, 2017). Reference strains PAO1 and PA14 are not producers of pyoluteorin due to the absence of the synthesis gene cluster. However, this latter cluster is present in Liverpool epidemic strains LES (Winstanley *et al*., 2009). This cluster belongs to a genomic island (GI), named LESGI-2, identified in the LES400, LES431 and LESB58 strains. Of note, the hypervirulent CF isolate LESB58 does not produce pyoluteorin because of a frameshifting mutation in gene *pltB* (Winstanley e*t al*., 2009). Pyoluteorin genes were identified in CF strains isolated at early and late stages of lung colonization (clonal pair PACS171b/PACS88) (Hayden *et al*., 2008), as well as in environmental strains (PaE2 and BE171) collected from plants and soil samples, respectively (Chugani *et al*., 2012).

The pyoluteorin biosynthesis locus was initially identified in another *Pseudomonas* species, *P. fluorescens* Pf-5 (Nowak-Thompson *et al*., 1999). It is composed of 10 genes, 8 of them being transcribed from a single operon, *pltLABCDEFG* (Figure 35). This operon is a hybrid NRPS/polyketide synthase (PKS) cluster (Gulick, 2017). It is regulated by the product of divergently transcribed gene *pltR* (Nowak-Thompson *et al*., 1999). Pyoluteorin synthesis begins with activation of L-Pro residue by the propyl-AMP ligase PltF, which transfers this amino acid as a thioester to PltL (Thomas *et al*., 2002) (Figure 36). L-Pro is successively transformed by PltE (Thomas *et al*., 2002) and PltA into dichloro-pyrrolyl (Dorrestein *et al*., 2005). PltB and PltC are believed to participate in formation of the pyoluteorin resorcinol moiety (Nowak-Thompson *et al*., 1997), and thioesterase PltG to the release of the antibiotic (Nowak-Thompson *et al*., 1999). The role of the remaining two proteins PltD and PltM remains unclear (Thomas *et al*., 2002). Putative ABC transporters PltHIJKNO in *P. aeruginosa* (Huang *et al*., 2006) and PltIJKNOP in *P. fluorescens* (Kidarsa *et al*., 2011) were shown to participate in pyoluteorin secretion. The genetic loci encoding these transporters are situated downstream from the biosynthesis genetic clusters, with in between, the regulatory gene *pltZ.*

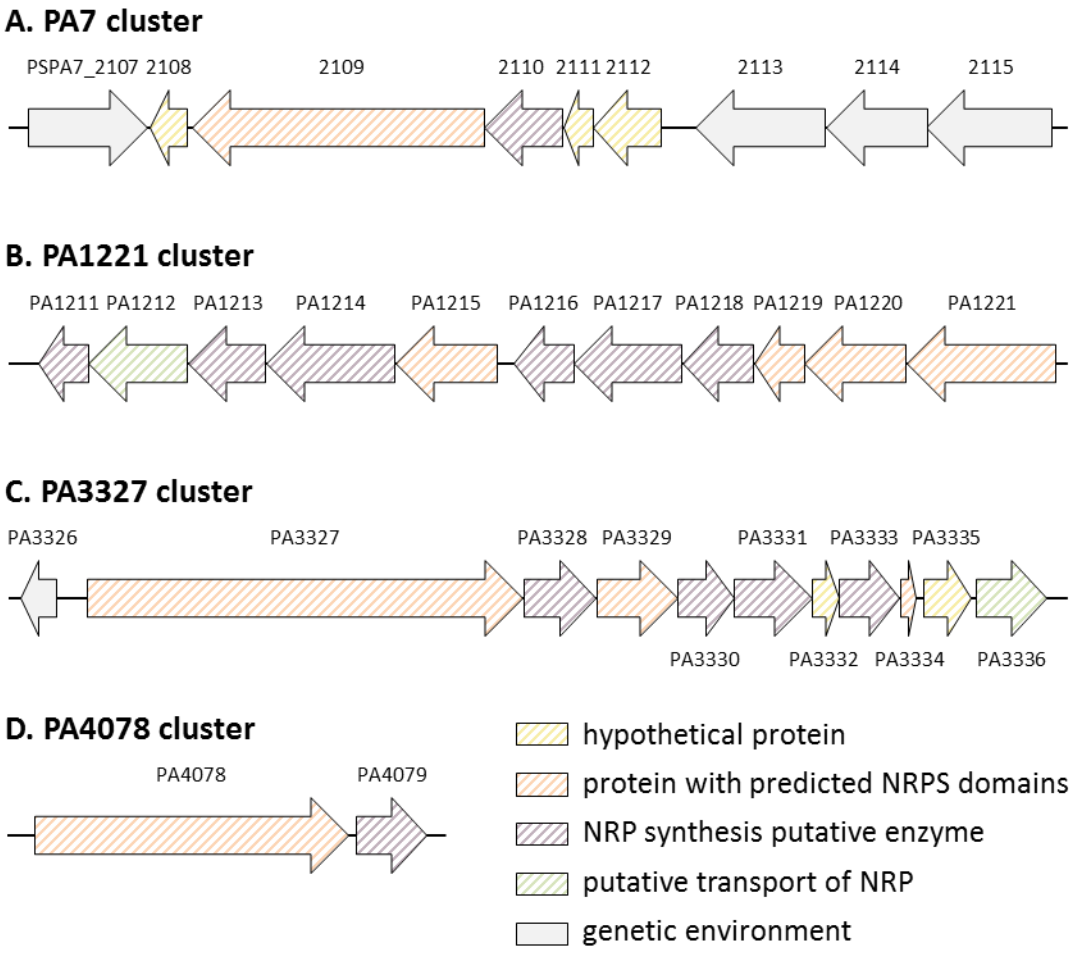

Figure 37: Genetic clusters of uncharacterized NRPS in *P. aeruginosa*.

The orientation of open reading frames is indicated, as well as the PA numbers.

4.3.5. Uncharacterized NRPS clusters

P. aeruginosa produces uncharacterized metabolites derived from four additional NRPS clusters. One is specific to clinical strain PA7 and the others are present in the majority of *P. aeruginosa* strains (Gulick, 2017). The identification of the compounds, their biosynthesis pathway and the characterization of their functions might increase our understanding of *P. aeruginosa* adaptability.

4.3.5.1. PA7-cluster

The NRPS cluster specifically identified in strain PA7 is encoded by a five-gene locus predicted to form two operons. The first one, composed of genes PSPA7_PA2108 and PSPA7_PA2109, codes for a hypothetical protein and a three domain NRPS, respectively. The second operon constituted of genes PSPA7_PA2110, PSPA7_PA2111 and PSPA7_PA2112 codes for an amine oxygenase and two hypothetical proteins, respectively (Figure 37). Moreover, Gulick *et al*. mentioned the presence of coding sequences in a close genetic environment that might participate in the synthesis of peptides derived from this NRPS. These genes encode an isopropylmalate synthase (LeuA1), an acyl-CoA dehydrogenase (PSPA7_PA2119), a protein with an adenylation domain (PSPA7_PA2121) and one with a thioesterase domain (PSPA7_PA2122) (Gulick, 2017). Both the natural products and the synthesis pathway remain to be characterized.

4.3.5.2. PA1221, PA3327 and PA4078 clusters

In *P. aeruginosa*, the compounds synthesized by the products of NRPS genes PA1221, PA3327 and PA4078 are unknown. Linear arrangement of these genes is represented by Figure 37. As demonstrated by transcriptomic analysis, some of these genes are positively regulated by *quorum* sensing (Schuster *et al*., 2003). Wagner *et al*. confirmed this induction by transcriptomic analysis of a *lasI*/*rhlI* knockout double mutant from strain PAO1, grown or not in the presence of both $3OC_{12}$-HSL and C_4-HSL (Wagner *et al*., 2003). Later on, inactivation of the TCS ParRS, was found to be associated with an increased expression of the two clusters PA1221 and PA3327 (Wang *et al*., 2013). PA1221 has an adenylating activity on valine; its crystal structure was resolved (Mitchell *et al*., 2012).

A putative *las-rhl* box was identified upstream of both genes PA1221 and PA3327. As a

matter of fact, an electrophoretic mobility shift assay confirmed that the *quorum* sensing transcription factor LasR binds to the PA3326-PA3327 intergenic region (Gilbert *et al*., 2009). Moreover, it appeared that proteins encoded by the PA3327-cluster (PA3327, PA3328 and PA3330) were quantitatively decreased upon conditions of low intracellular concentrations of c-di-GMP, a second messenger known to stimulate a sessile lifestyle and to increase biofilm formation (Chua *et al*., 2013). Transcriptome analysis of clinical isolate LES431 showed higher transcript levels of genes PA3326 to PA3335, in comparison with LES400 or PAO1 (Salunkhe *et al*., 2005). The differential expression levels between the two LES strains would be due to a 7-bp repetition that introduce a frameshift in the open reading frame of *lasR* gene in LES400 (Salunkhe *et al*., 2005). An additional transcriptomic analysis was performed to understand the molecular mechanisms by which *P. aeruginosa* colonizes the gut. For that purpose, the response of strain PAO1 in a nutrient-poor medium supplemented with the specific k-opioid receptor agonist U-50,488 was evaluated (to mimic the context of pathogenesis in the gut and during stress), that showed a transcriptional activation of the two clusters PA3327 and PA1221 (Zaborin *et al*., 2012). Interestingly, the increase in pyocyanin and pyoverdin production, as well as mortality in *Caenorhabditis elegans* induced by U-50,488 was attenuated by addition of phosphate or by inactivation of virulence regulator PqsE (Hazan *et al*., 2010).

Finally, cluster PA3327 was also mentioned in a study investigating the role of virulence genes in the pathogenesis of *P. aeruginosa* in different host models. Indeed, transposon-mediated inactivation of gene PA3327 led to attenuation of swarming motility, pyocyanin and protease production (Dubern *et al*., 2015). Furthermore, the PA3327 mutant showed a decreased pathogenicity in a *C. elegans* model while no alteration was observed in *Drosophila melanogaster* (Dubern *et al*., 2015). Regarding the PA3326 Clp peptidase encoded by upstream gene PA3326, it is required for microcolony formation at the initial phase of biofilm formation (Hall *et al*., 2017).

III. Results

Chapter 1. Mutations in *fusA1* confer aminoglycoside resistance in *P. aeruginosa*

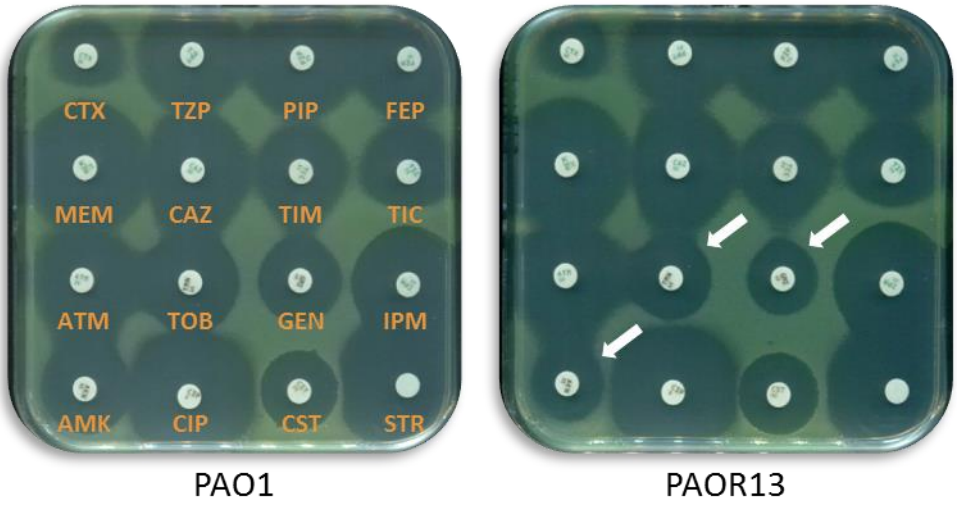

Figure 38: Antibiograms of PAO1 and PAOR13 derivative mutant.

CTX: cefotaxime, TZP: piperacillin-tazobactam, PIP: piperacillin, FEP: cefepime, MEM: meropenem, CAZ: ceftazidime, TIM: ticarcillin-clavulanic acid, TIC: ticarcillin, ATM: aztreonam, TOB: tobramycin, GEN: gentamicin, IPM: imipenem, AMK: amikacin, CIP: ciprofloxacin, CST: colistin, STR: streptomycin.

1. Context

Aminoglycosides are widely used to fight Gram-negative bacteria notably *P. aeruginosa* (Smith *et al*., 2017). Production of aminoglycoside modifying enzymes and constitutive overproduction of RND efflux pump MexXY(OprM) represent major causes of resistance to these agents amongst clinical strains, including those isolated from CF patients (Smith *et al*., 2017). However, these mechanisms do not explain the high levels of resistance observed in some clinical strains, suggesting that additional mechanisms might exist (Guénard *et al*., 2014). In this context, several mutations in gene *fusA1* coding for elongation factor EF-G1A, were suggested to confer an increased resistance to aminoglycosides (López-Causapé *et al*., 2017). In our laboratory, whole genome sequencing analysis of amikacin-resistant *in vitro*-selected mutants (e.g., PAOR13) highlighted mutations in this gene that supported this hypothesis (Figure 38).

2. Objective

The aim of this project was first to assess the impact of *in vitro*-selected amino acid substitutions in EF-G1A on susceptibility to antibiotics. The contribution of MexXY(OprM) to aminoglycoside resistance was also determined for these mutants. To get an insight into the relevance of such mutations in the clinical context, a collection of CF and non-CF clinical strains showing a non-enzymatic resistance profile to aminoglycosides was screened for mutations in *fusA1*. Finally, we evaluated if some of these mutations could contribute to particularly high levels of aminoglycoside resistance.

3. Results

3.1. Mutations in Gene *fusA1* as a Novel Mechanism of Aminoglycoside Resistance in Clinical Strains of *Pseudomonas aeruginosa*

Arnaud Bolard, Patrick Plésiat, Katy Jeannot
Antimicrobial Agents and Chemotherapy, 2018. Jan 25;62(2). pii: e01835-17.
doi: 10.1128/AAC.01835-17.

AMERICAN SOCIETY FOR MICROBIOLOGY | Antimicrobial Agents and Chemotherapy®

MECHANISMS OF RESISTANCE

Mutations in Gene *fusA1* as a Novel Mechanism of Aminoglycoside Resistance in Clinical Strains of *Pseudomonas aeruginosa*

Arnaud Bolard,[a,b] Patrick Plésiat,[a,b] Katy Jeannot[a,b]

[a]Centre National de Référence de la Résistance aux Antibiotiques, Laboratoire de Bactériologie, Centre Hospitalier Universitaire Jean Minjoz, Besançon, France

[b]UMR6249 CNRS Chronoenvironnement, Université de Franche-Comté, Besançon, France

ABSTRACT Resistance of clinical strains of *Pseudomonas aeruginosa* to aminoglycosides can result from production of transferable aminoglycoside-modifying enzymes, of 16S rRNA methylases, and/or mutational derepression of intrinsic multidrug efflux pump MexXY(OprM). We report here the characterization of a new type of mutant that is 4- to 8-fold more resistant to 2-deoxystreptamine derivatives (e.g., gentamicin, amikacin, and tobramycin) than the wild-type strain PAO1. The genetic alterations of three *in vitro* mutants were mapped on *fusA1* and found to result in single amino acid substitutions in domains II, III, and V of elongation factor G (EF-G1A), a key component of translational machinery. Transfer of the mutated *fusA1* alleles into PAO1 reproduced the resistance phenotype. Interestingly, *fusA1* mutants with other amino acid changes in domains G, IV, and V of EF-G1A were identified among clinical strains with decreased susceptibility to aminoglycosides. Allelic-exchange experiments confirmed the relevance of these latter mutations and of three other previously reported alterations located in domains G and IV. Pump MexXY(OprM) partly contributed to the resistance conferred by the mutated EF-G1A variants and had additive effects on aminoglycoside MICs when mutationally upregulated. Altogether, our data demonstrate that cystic fibrosis (CF) and non-CF strains of *P. aeruginosa* can acquire a therapeutically significant resistance to important aminoglycosides via a new mechanism involving mutations in elongation factor EF-G1A.

KEYWORDS EF-G1A, *Pseudomonas aeruginosa*, aminoglycosides, mechanisms of resistance

Aminoglycosides are widely used to treat acute and chronic infections caused by the opportunistic pathogen *Pseudomonas aeruginosa*. With polymyxins, these bactericidal antibiotics often remain the last therapeutic option to fight multidrug-resistant and extensively drug-resistant strains (1, 2). In patients with cystic fibrosis (CF), molecules such as tobramycin and amikacin are administered intravenously or by aerosol over long periods of time to try to eradicate or control lung colonization by *P. aeruginosa* (3). These inhibitors of protein synthesis interact with ribosomes to generate pleiotropic translational effects such as increased misreading rates, inhibition of translocation of the tRNA-mRNA complex, and impairment of ribosome recycling (4, 5). Aminoglycosides directly bind the decoding A site, an asymmetric internal loop present within helix 44 (H44) of small subunit 16S rRNA (6). Such a binding affects both tRNA selection and elongation factor G (EF-G)-catalyzed translocation (4, 7). Helix 69 (H69) of large subunit 23S rRNA is another molecular target of these inhibitors (8). At the end of translation process, a complex is formed between H44, H69, EF-G, and ribosome recycling factor (RRF) that enables the separation of the two ribosomal subunits and the recycling of ribosome (9). Aminoglycosides interfere with this recycling mechanism and

Received 1 September 2017 **Returned for modification** 25 September 2017 **Accepted** 5 November 2017

Accepted manuscript posted online 13 November 2017

Citation Bolard A, Plésiat P, Jeannot K. 2018. Mutations in gene *fusA1* as a novel mechanism of aminoglycoside resistance in clinical strains of *Pseudomonas aeruginosa*. Antimicrob Agents Chemother 62:e01835-17. https://doi.org/10.1128/AAC.01835-17.

Address correspondence to Katy Jeannot, katy.jeannot@univ-fcomte.fr.

prevent the release of the ribosomal subunits (9, 10). The presumed result is the overall reduction in the number of ribosomes, leading to severe reductions in bacterial growth rate and adaptive fitness (11).

Acquisition of resistance to antipseudomonal aminoglycosides (e.g., gentamicin, netilmicin, tobramycin, and amikacin) is common in clinical strains of *P. aeruginosa*. This can be achieved by the horizontal transfer of mobile elements carrying a variety of genes encoding either stereospecific aminoglycoside-modifying enzymes or 16S rRNA methyltransferases, which both prevent the interaction of antibiotics with their target (12). Aminoglycoside resistance may also result from nonenzymatic, mutation-driven intrinsic mechanisms that affect translation machinery (13) or that tend to reduce the intracellular accumulation of the drug molecules by limiting their diffusion across the bacterial membranes or by promoting their extrusion outside the bacterial cell (12). When upregulated by mutations, the efflux system MexXY(OprM) can provide clinical strains with low to moderate levels of resistance to various antibiotics, including aminoglycosides (14–16). For instance, mutational alteration of MexZ, a repressor of operon *mexXY*, is associated with a 2- to 8-fold increase in aminoglycoside MICs (14, 17). In CF patients, repeated administration of aminoglycosides to combat chronic lung colonization by *P. aeruginosa* tends to select subpopulations of mutants exhibiting an increasing resistance over time. *mexZ* was found to be the most frequently mutated gene of the bacterial chromosome (18–21). However, overproduction of the pump MexXY(OprM) cannot solely account for the high resistance levels displayed by late CF strains (14, 22).

As suggested previously, other mechanisms are likely to contribute to intrinsic and/or acquired resistance of *P. aeruginosa* to this important class of antibiotics (23). The present study was thus undertaken to find out new determinants involved in the evolution of clinical strains under aminoglycoside pressure.

RESULTS AND DISCUSSION

Single point mutations in the gene *fusA1* cause aminoglycoside resistance. As demonstrated previously, approximately 135 chromosomal genes may potentially contribute to the development of a low-level aminoglycoside resistance in *P. aeruginosa* when tagged by transposons (24). However, the relevance of such genes in the clinical setting has only been established for a few of them (12). In order to characterize new resistance determinants that could account for the resistance phenotype of strains isolated from patients, spontaneous mutants of reference strain PAO1 were selected *in vitro* on 6 μg ml^{-1} amikacin (3× MIC), with rates ranging from 8×10^{-8} to 7.7×10^{-7}. Three representative clones (PAOR10, PAOR13, and PAOR15) exhibiting a higher resistance than PAO1 to multiple aminoglycosides were retained for further investigations. Relative to the baselines, the MICs of apramycin (monosubstituted-2-deoxystreptamine), neomycin (4,5-disubstituted-2-deoxystreptamine), gentamicin, tobramycin, amikacin, and arbekacin (4,6-disubstituted-2-deoxystreptamines), spectinomycin (aminocyclitol), and streptomycin (streptamine) were increased from 2- to 16-fold (Table 1). In contrast, the three mutants exhibited wild-type susceptibility profiles to β-lactams (ceftazidime, cefepime, and imipenem), fluoroquinolones (ciprofloxacin), and tetracycline (data not shown).

Whole-genome sequencing with an average copy number of 80× revealed the presence of three different point mutations in gene *fusA1* (PA4266) compared to parent strain PAO1, resulting in single amino acid substitutions in domain II (Arg371Cys, PAOR15), III (Thr456Ala, PAOR13), and V (Arg680Cys, PAOR10) of elongation factor EF-G1A, respectively (Fig. 1 and Fig. 2). Gene *fusA1* is predicted to be cotranscribed with *rpsG* and *tufA*, the respective determinants of ribosomal protein S7 and elongation factor Tu (EF-Tu) (25). EF-G1A is crucial in protein synthesis since it mediates the translocation of mRNA and tRNA through the ribosome and participates in the ribosome recycling process (26, 27). To confirm the role of the observed mutations in aminoglycoside resistance, allelic exchanges were carried out in PAO1, leading to the replacement of wild-type *fusA1* with mutated genes from PAOR10, PAOR13, and

TABLE 1 Drug susceptibility of *in vitro* selected *fusA1* mutants[a]

Strain	EFG-1A[b]	MIC (μg ml^{-1})[c]							
		GEN	AMK	TOB	NEO	APR	ARB	STR	SPT
PAO1	WT	1	2	0.25	4	4	1	32	512
PAO1Δ*mexZ*	WT	2	**8**	0.5	**16**	**16**	**4**	**128**	1,024
PAO1Δ*mexXY*	WT	0.06	0.5	0.125	2	1	0.125	2	64
PAOR10	Arg680Cys	**4**	**16**	**2**	**32**	**32**	**8**	64	512
PAOR13	Thr456Ala	2	**8**	**1**	8	**16**	**4**	64	512
PAOR15	Arg371Cys	**4**	**16**	**2**	**16**	**16**	**8**	64	1,024
PAOR13Δ*mexZ*	Thr456Ala	**4**	**16**	**2**	**32**	**32**	**8**	**128**	1,024
PAOR13Δ*mexXY*	Thr456Ala	0.125	1	0.25	2	2	0.5	2	64
PAOR15Δ*mexZ*	Arg371Cys	**8**	**32**	**4**	**64**	**32**	**16**	**128**	**2,048**
PAOR15Δ*mexXY*	Arg371Cys	0.125	1	0.25	2	2	0.5	2	64
PAO1::*fusA1*$_{PAOR10}$	Arg680Cys	**4**	**16**	**2**	**32**	**32**	**8**	64	512
PAO1::*fusA1*$_{PAOR13}$	Thr456Ala	2	**8**	**1**	8	**16**	**4**	64	512
PAO1::*fusA1*$_{PAOR15}$	Arg371Cys	**4**	**16**	**2**	**16**	**16**	**8**	64	1,024

[a]Abbreviations: GEN, gentamicin; AMK, amikacin; TOB, tobramycin; NEO, neomycin; APR, apramycin; ARB, arbekacin; STR, streptomycin; SPT, spectinomycin.

[b]That is, the elongation factor EF-G1A sequence (the sequence of strain PAO1 is taken as the wild-type reference [WT]).

[c]The MIC data are representative of three independent experiments. Values in bold are at least four times higher than those for strain PAO1. Underlined values are above the EUCAST susceptibility breakpoints (gentamicin and tobramycin, >4 μg ml^{-1}; amikacin, $>$ 8 μg ml^{-1}).

PAOR15, yielding the constructs PAO1::*fusA1*$_{PAOR10}$, PAO1::*fusA1*$_{PAOR13}$, and PAO1::*fusA1*$_{PAOR15}$, respectively. As indicated in Table 1, these genetic manipulations caused a substantial increase in aminoglycoside MICs (up to 8-fold), highlighting a novel resistance mechanism in *P. aeruginosa*. The observation that the activity of aminocyclitol and streptamine molecules (spectinomycin and streptomycin, respectively) was poorly impacted by *fusA1* mutations is still unclear, since at least spectinomycin inhibits the EF-G-dependent translocation of the tRNA-mRNA complex (5, 28).

The *P. aeruginosa* genome actually encodes two closely related EF-G proteins that share 90% similarity at the sequence level (29). Gene *fusA2* (PA2071) is not essential for the growth of *P. aeruginosa* under laboratory conditions (30). In agreement with the notion that EF-G1A is key to ribosome activity, all attempts to delete *fusA1* in strain PAO1 and its mutants PAOR10, PAOR13, and PAOR15 were unsuccessful (data not shown).

***fusA1* mutations in clinical strains.** Elongation factor EF-G1A is subject to minor sequence polymorphism in *P. aeruginosa* as bioinformatic analysis of the PATRIC database (31) revealed that only 12 of 120 gentamicin-susceptible strains contained uncharacterized single amino acid substitutions in this protein. To gain an insight into the clinical relevance of *fusA1* mutations, we screened our laboratory collection in search of strains exhibiting a low to moderate resistance to gentamicin, tobramycin, and amikacin (data not shown). Isolates with increased resistance to ciprofloxacin and cefepime were not retained because of the probable involvement of the efflux system MexXY(OprM) in the phenotype (32, 33). PCR-sequencing experiments identified three isolates, recovered from the sputa (isolates 5910 and 6253) and urine (isolate 6233) of non-CF patients, that harbored one or two missense mutations in gene *fusA1* compared to PAO1 (Fig. 1). The related amino acid changes (Val93Ala and Ile186Val in isolate 6253,

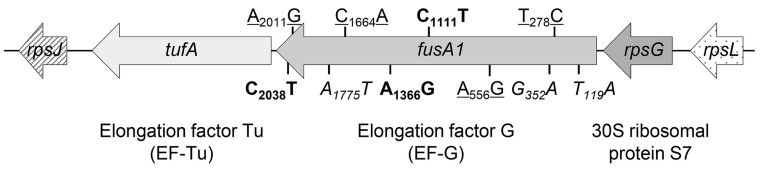

FIG 1 Aminoglycoside resistance-associated mutations in gene *fusA1*. Mutations identified in spontaneous *in vitro* mutants (in boldface type), clinical strains (underlined), and specifically engineered *in vitro* mutants (in italic type) are mapped on the gene sequence of strain PAO1.

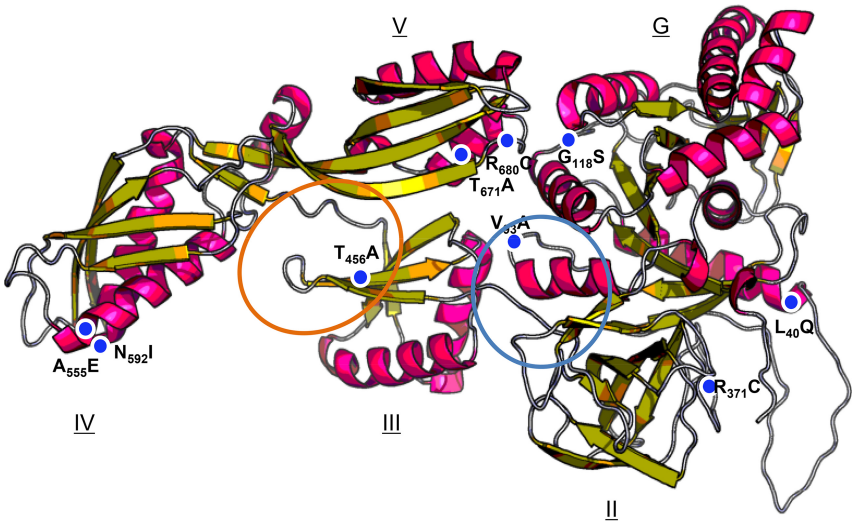

FIG 2 Three-dimensional structure of EF-G protein from strain PAO1, as predicted by RaptorX (http://raptorx.uchicago.edu/). EF-G domains were predicted by using Pfam database. The amino acid substitutions responsible for aminoglycoside resistance are indicated by blue spots. The blue and orange circles represent the fusidic acid and argyrin B binding sites, respectively.

Ala555Glu in isolate 5910, and Thr671Ala in isolate 6233) were different from those identified in the *in vitro* mutants. They were located in domains G (Val93Ala), IV (Ala555Glu), and V (Thr671Ala) of the protein, respectively, thus confirming that multiple mutations in EF-G1A can result in aminoglycoside resistance (Fig. 2). As for the *in vitro* mutants, replacement of wild-type *fusA1* in PAO1 by the mutated alleles from isolates 5910, 6233, and 6253 enhanced the MICs of deoxystreptamine derivatives significantly, up to 16-fold, whereas the activities of streptomycin and spectinomycin were poorly impacted (Table 2). According to the current EUCAST breakpoints (http://www.eucast.org), strains PAO1::*fusA1*$_{6233}$ and PAO1::*fusA1*$_{6253}$ were of intermediate susceptibility or resistant to gentamicin and amikacin, while PAO1::*fusA1*$_{5910}$ was intermediate to amikacin only (Table 2). None of the alleles conferred a therapeutically significant resistance to tobramycin, although the MICs of this antibiotic were close to the EUCAST resistance breakpoint (>4 μg ml^{-1}).

Correlation between genomic data and resistance phenotypes. A number of studies on the genomic evolution of *P. aeruginosa* strains in CF patients have reported that the *fusA1* gene is one of the most repeatedly hit by mutations. Thus, it was suggested that these genetic alterations could contribute to the development of a high resistance to aminoglycosides in the CF context (20, 34–36). For instance, 52 of 361 nonrelated CF isolates appeared to harbor nonsynonymous mutations in *fusA1* (34). In

TABLE 2 Drug susceptibility of clinical *fusA1* mutants[a]

Strain	EFG-1A	MIC (μg ml^{-1})							
		GEN	AMK	TOB	NEO	APR	ARB	STR	SPT
PAO1	WT	1	2	0.25	4	4	1	32	512
5910	Ala555Glu	**8**	**16**	**2**	**128**	**64**	**16**	64	1,024
6233	Thr671Ala	**8**	**32**	**2**	**32**	**64**	**16**	64	1,024
6253[b]	Val93Ala	**8**	**16**	**2**	**64**	**64**	**16**	64	1,024
PAO1::*fusA1*$_{5910}$	Ala555Glu	**4**	**16**	**2**	**32**	**32**	**8**	32	1,024
PAO1::*fusA1*$_{6233}$	Thr671Ala	**8**	**16**	**2**	**32**	**32**	**8**	64	512
PAO1::*fusA1*$_{6253}$	Val93Ala	**8**	**32**	**4**	**64**	**64**	**16**	64	512
PAO1::*fusA1*$_{T119A}$	Leu40Gln	2	**8**	**1**	8	8	**4**	64	1,024
PAO1::*fusA1*$_{G352A}$	Gly118Ser	2	4	0.5	8	8	2	32	512
PAO1::*fusA1*$_{A1775T}$	Asn592Ile	**8**	**32**	**2**	**128**	**64**	**8**	32	512

[a]Abbreviations and column headings are as described in the footnotes for Table 1.
[b]Strain 6253 also harbors an Ile186Val substitution in protein EF-G1A, which was considered nonsignificant.

another study, the gene was found to be mutated in 13 isolates belonging to international clone CC274, within a collection of 29 CF strains (20). Our analysis of the single nucleotide polymorphisms (SNPs) found in various CF and non-CF strains revealed that three of the amino acid substitutions predicted to occur in EF-G1A were identical to ones substitutions in the present study (Val93Ala, Thr456Ala, and Thr671Ala), thus reinforcing the notion that such variations represent a common mechanism of aminoglycoside resistance in *P. aeruginosa*. To assess the phenotypic impact of other reported *fusA1* mutations (34, 35, 37), site-directed mutagenesis experiments were carried out to generate *fusA1* alleles encoding EF-G1A variants with Leu40Gln (domain G), Gly118Ser (domain G), and Asn592Ile (domain IV) changes, respectively (Fig. 2). Substituting the wild-type *fusA1* gene with the mutated alleles provided PAO1 with a 2- to 16-fold higher resistance to gentamicin, amikacin, and tobramycin (compare strains PAO1::$fusA1_{T119A}$, PAO1::$fusA1_{G352A}$, and PAO1::$fusA1_{A1775T}$ with PAO1 in Table 2). These new results unambiguously demonstrate the role played by EF-G1A in the emergence of clinical mutants of *P. aeruginosa* exhibiting a reduced susceptibility to aminoglycosides.

Cross-resistance between aminoglycosides/argyrin and aminoglycosides/fusidic acid. EF-G1A is known as the cellular target of the bacteriostatic antistaphyloccocal antibiotic fusidic acid and of argyrin B, a natural cyclic peptide produced by *Myxobacteria* and *Actinomycetes*, exhibiting antipseudomonal activities (38). Fusidic acid binds to ribosome-bound EF-G in a pocket between domains II and III and the switch II region of domain G (39), whereas argyrin B interacts with EF-G at the interface of domains III and V (40) (Fig. 2). As shown elsewhere, mutations occurring in these binding domains may generate a high resistance to fusidic acid or argyrin (41, 42). A concomitant resistance to fusidic acid, kanamycin and spectinomycin was noted in 14 out of 18 *Salmonella* Typhimurium mutants selected *in vitro* (42). To the best of our knowledge, cross-resistance to argyrin B and aminoglycosides has not been reported so far in *P. aeruginosa* (40, 41). Of interest, one of the EF-G1A mutations able to promote argyrin B resistance, namely, Thr671Ala, was found here to significantly decrease the susceptibility of *P. aeruginosa* to aminoglycosides (see strains 6233 and PAO1::$fusA1_{6233}$ in Table 2). Thus, it is clear that some mutated forms of EF-G1A produced by clinical strains (e.g., urine isolate 6233) can provide a cross-resistance to argyrin B and aminoglycosides. Whether other amino acid variations in EF-G1A can also impair the binding of argyrin B or fusidic acid while conferring a resistance to aminoglycosides remains to be investigated.

EF-G1A and MexXY(OprM). A number of ribosomal alterations such as those affecting proteins L1 and L25, or methionyl-$tRNA^{fMet}$-formyl transferase can activate the expression of operon *mexXY*, which encodes two components of the multidrug efflux pump MexXY(OprM) (17, 43, 44). Since EF-G1A is involved in protein synthesis, one could argue that the resistance phenotype exhibited by *fusA1* mutants results from MexXY(OprM) being derepressed, and subsequent active efflux of aminoglycoside molecules. We therefore measured the transcript levels of gene *mexY* by reverse transcription-quantitative PCR in *fusA1* mutants PAOR13 and PAOR15. These levels were similar to that of parental strain PAO1 (data not shown). On the other hand, to investigate the contribution of MexXY(OprM) to the resistance phenotype conferred by *fusA1* mutations, the *mexXY* operon was deleted in PAOR13 and PAOR15. Interestingly, suppression of the efflux system was associated with a strong decrease in deoxystreptamine MICs, leaving a residual resistance (i.e., only due to EF-G1A) which was in general 2-fold higher than in strain PAO1Δ*mexXY* (see mutants PAOR13Δ*mexXY* and PAOR15Δ*mexXY* in Table 1). These results suggest that the effects of EF-G1A mutations are to some extent potentiated by the export of aminoglycosides via MexXY(OprM), although the pump itself is not upregulated by the effects of these mutations on protein synthesis.

Since mutation-driven upregulation of MexXY(OprM) is common in drug-resistant strains of *P. aeruginosa* (14–16), we evaluated the impact of this mechanism on

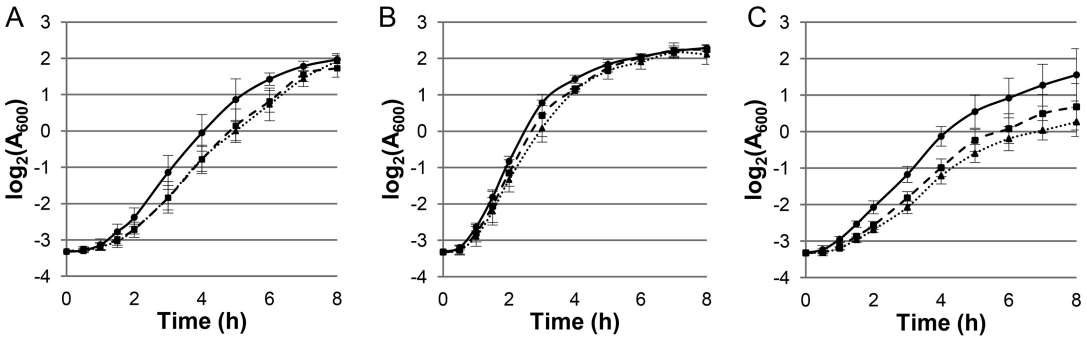

FIG 3 Growth curves of strain PAO1 (circles, solid line), mutants PAOR13 (squares, dashed line), and PAOR15 (triangles, dotted line) at 30°C (A), 37°C (B), and 44°C (C).

aminoglycoside MICs when associated with relevant *fusA1* mutations. As indicated in Table 1, MexXY(OprM) overproduction in the repressor MexZ-null mutant PAO1Δ*mexZ* increased aminoglycoside resistance from 2- to 4-fold relative to the wild-type parent PAO1. Similar results were obtained in mutants PAOR13 and PAOR15 upon deletion of *mexZ* (PAOR13Δ*mexZ* and PAOR15Δ*mexZ* in Table 1). So, while showing additive effects on aminoglycoside MICs when constitutively overproduced in *fusA1-mexZ* double mutants, the MexXY(OprM) pump contributes to the resistance provided by EF-G1A alterations through its *fusA1*-independent, drug-induced expression.

Impact of EF-G1A mutations on aminoglycoside resistance. Because aminoglycosides are not predicted to bind EF-G (45), resistance to these molecules seems to be an indirect consequence of EF-G alteration. The mutations characterized here impacted bacterial susceptibility to deoxystreptamines at different levels. Indeed, MIC changes were modest (2- to 4-fold) with alterations in domains G and III (Leu40Gln, Gly118Ser, and Thr456Ala) and higher (up to 16-fold) with mutations in domains II (Val93Ala, Arg371Cys), IV (Ala555Glu, Asn592Ile), and V (Thr671Ala, Arg680Cys) (Tables 1 and 2; Fig. 2). By modifying the conformation of EF-G, these amino acid substitutions could modify the interactions of the elongation factor with the ribosome recycling factor (RRF), 16S rRNA (helix 69), 23S rRNA (helix 44), P-site tRNA, mRNA, and/or associated ribosomal proteins L6, L11, L12, and S12 (45, 46). In *Escherichia coli*, kanamycin resistance was found to be associated with mutations strictly located in domain IV (47, 48). The *E. coli* mutants harboring such mutations were temperature sensitive and had a slower elongation rate than the parental strain (48). To assess the impact of representative *fusA1* mutations on protein synthesis, the growth rates of mutants PAOR13 and PAOR15 were compared to those of PAO1 at 30, 37, and 44°C. Although no significant difference was noted between the three strains at 37°C in Mueller-Hinton broth (MHB), the two mutants turned out to multiply more slowly at nonoptimal temperatures. Relative to PAO1, the doubling time was increased by 7 and 12 min for PAOR13 and by 9.5 to 20 min for PAOR15 at 30 and 44°C, respectively (Fig. 3). Feng et al. reported that *fusA1* mutants of *P. aeruginosa* selected on tobramycin had a lower μ_{max} value than the wild-type *P. aeruginosa* parent (ATCC 27853) (37). Similarly, in our study, *fusA1* mutations were associated with a significant decrease in μ_{max}, particularly at 44°C (0.78 h^{-1} for PAOR13; 0.71 h^{-1} for PAOR15), compared to PAO1 (0.93 h^{-1}) (Fig. 3). These data strongly suggest that *fusA1*-dependent aminoglycoside resistance has a cost for the cell.

During the translocation process, two highly conserved loops in domain IV of EF-G1A get inserted into the decoding center (DC) to override the hydrogen bonds between the DC nucleotides of 16S rRNA (mainly A1492 and A1493) (39), to which aminoglycosides bind (45). As a working hypothesis, it is possible that the structural modifications introduced by some mutations in EF-G1A prevent or loosen the binding of aminoglycosides to helix H44 or H69, resulting in a lower drug affinity for the ribosome. Whatever the molecular mechanism may be, the therapeutic implications of

TABLE 3 Bacterial strains and plasmids used in this study

Strain or plasmid	Relevant characteristics[a]	Source or reference
Strains		
Pseudomonas aeruginosa		
PAO1	Wild-type reference strain	51
PAOR10	PAO1 spontaneous *fusA1* mutant (Arg680Cys)	This study
PAOR13	PAO1 spontaneous *fusA1* mutant (Thr456Ala)	This study
PAOR15	PAO1 spontaneous *fusA1* mutant (Arg371Cys)	This study
5910	Clinical *fusA1* mutant (Ala555Glu)	This study
6233	Clinical *fusA1* mutant (Thr671Ala)	This study
6253	Clinical *fusA1* mutant (Val93Ala, Ile186Val)	This study
PAO1::*fusA1*$_{PAOR10}$	PAO1 with the *fusA1* allele from PAOR10	This study
PAO1::*fusA1*$_{PAOR13}$	PAO1 with the *fusA1* allele from PAOR13	This study
PAO1::*fusA1*$_{PAOR15}$	PAO1 with the *fusA1* allele from PAOR15	This study
PAO1::*fusA1*$_{5910}$	PAO1 with the *fusA1* allele from 5910	This study
PAO1::*fusA1*$_{6233}$	PAO1 with the *fusA1* allele from 6233	This study
PAO1::*fusA1*$_{6253}$	PAO1 with the *fusA1* allele from 6253	This study
PAO1::*fusA1*$_{T119A}$	PAO1 with a *fusA1* allele encoding Leu40Gln	This study
PAO1::*fusA1*$_{G352A}$	PAO1 with a *fusA1* allele encoding Gly118Ser	This study
PAO1::*fusA1*$_{A1775T}$	PAO1 with a *fusA1* allele encoding Asn592Ile	This study
PAO1Δ*mexXY*	PAO1 with in-frame deletion of operon *mexXY*	16
PAO1R13Δ*mexXY*	PAOR13 with in-frame deletion of operon *mexXY*	This study
PAO1R15Δ*mexXY*	PAOR15 with in-frame deletion of operon *mexXY*	This study
PAO1Δ*mexZ*	PAO1 with in-frame deletion of gene *mexZ*	49
PAO1R13Δ*mexZ*	PAOR13 with in-frame deletion of gene *mexZ*	This study
PAO1R15Δ*mexZ*	PAOR15 with in-frame deletion of gene *mexZ*	This study
Escherichia coli		
DH5α	F$^-$ ϕ80*lacZ*ΔM15 Δ(*lac*ZYA-argF)*U169 recA1 endA1 hsdR17*(r_K^- m_K^+) *phoA supE44 thi-1 gyrA96 relA1* λ$^-$	Thermo Fisher Scientific
CC118λ*pir*	Δ(*ara-leu*) *ara D* Δ*lacX74 galE galK phoA20 thi-1 rpsE rpoB argE*(Am) *recAI* lysogenized with λ*pir* phage	52
HB101	*supE44 hsdS20*(r_B^- m_B^-) *recA13 ara-14 proA2 lacY1 galK2 rpsL20 xyl-5 mtl-1 leuB6 thi-1*	53
DH5α-T1R	F$^-$ ϕ80*lacZ*ΔM15 Δ(*lacZYA-argF)U169 recA1 endA1 hsdR17*(r_K^- m_K^+) *phoA supE44 thi-1 gyrA96 relA1 tonA*	Thermo Fisher Scientific
Plasmids		
pKNG101	Marker exchange suicide vector in *P. aeruginosa*; *sac*BR *mob*RK2 *ori*R6K; Str^r	54
pRK2013	Helper plasmid for mobilization of non-self-transmissible plasmids; ColE1 Tra$^+$ Mob$^+$ Kan^r	50
pCR-Blunt	Blunt-end cloning vector *ccdB lacZ*α; Zeo^r Kan^r	Thermo Fisher Scientific
pKNG101::*fusA1*$_{C2038T}$	Gene *fusA1* from PAOR10 cloned in pKNG101	This study
pKNG101::*fusA1*$_{A1366G}$	Gene *fusA1* from PAOR13 cloned in pKNG101	This study
pKNG101::*fusA1*$_{C1111T}$	Gene *fusA1* from PAOR15 cloned in pKNG101	This study
pKNG101::*fusA1*$_{C1664A}$	Gene *fusA1* from 5910 cloned in pKNG101	This study
pKNG101::*fusA1*$_{A2011G}$	Gene *fusA1* from 6233 cloned in pKNG101	This study
pKNG101::*fusA1*$_{T278C'A556G}$	Gene *fusA1* from 6253 cloned in pKNG101	This study
pKNG101::*fusA1*$_{T119A}$	Gene *fusA1* with *in vitro*-engineered mutation T119A, cloned in pKNG101	This study
pKNG101::*fusA1*$_{G352A}$	Gene *fusA1* with *in vitro*-engineered mutation G352A, cloned in pKNG101	This study
pKNG101::*fusA1*$_{A1775T}$	Gene *fusA1* with *in vitro*-engineered mutation A1775T, cloned in pKNG101	This study
pKNGΔ*mexXY*	BamHI/ApaI 1,756-kb fragment composed of sequences flanking 5′ and 3′ ends of *mexXY*, cloned in pKNG101	16
pKNGΔ*mexZ*	BamHI/ApaI 1,111-kb fragment composed of sequences flanking 5′ and 3′ ends of *mexZ*, cloned in pKNG101	49

[a]Abbreviations: Str^r, streptomycin resistance; Kan^r, kanamycin resistance; Zeo^r, zeocin resistance.

fusA1 mutations need to be investigated. Whether mutations in EF-G1B encoded by gene *fusA2* have similar effects in EF-G1A also remains to be clarified.

MATERIALS AND METHODS

Bacterial strains, plasmids, and growth conditions. The features of bacterial strains and plasmids used in this study are presented in Table 3. Bacteria were cultivated in MHB with adjusted concentrations of divalent cations Ca^{2+} (from 20 to 25 mg ml^{-1}) and Mg^{2+} (from 10 to 12.5 μg ml^{-1}) or on Mueller-Hinton agar (MHA; Becton Dickinson, Sparks, MD). Maximal growth rates (μ_{max}) were calculated as the average growth rates of three independent replicates during exponential growth. Resistant mutants to aminoglycosides were selected by plating 10^8 CFU of log-phase PAO1 cells on MHA supplemented with 6 μg ml^{-1} amikacin (corresponding to 3× MIC for PAO1). *Escherichia coli* transformants were selected on MHA containing kanamycin at 50 μg ml^{-1} or streptomycin at 50 μg ml^{-1}. Unmarked deletion of gene *mexZ* and operon *mexXY* in PAO1 was performed using plasmids

pKNGΔ*mexZ* and pKNGΔ*mexXY*, respectively, as previously reported by Muller et al. and Guénard et al. (16, 49). The recombinant plasmids were introduced into strain PAO1 by triparental mating using mobilization properties of broad-host-range vector pRK2013 (50). Selection of transconjugants on *Pseudomonas* isolation agar (PIA; Becton Dickinson) and excision of pKNG101 from the bacterial chromosome were performed as described elsewhere (49).

Antimicrobial susceptibility testing. The MICs of selected antibiotics were determined by the standard microdilution method and interpreted in terms of bacterial susceptibility or resistance according to the guidelines of the European Committee on Antimicrobial Susceptibility testing (EUCAST [http://www.eucast.org]).

SNP identification. Single nucleotide polymorphisms (SNPs) occurring in *in vitro*-selected mutants PAOR10, PAOR13, and PAOR15 were identified using CLC Genomics Workbench software (v10.0.1; Qiagen, Aarhus, Denmark) after alignment of the genomic sequences of mutants to that of the PAO1 strain available in the laboratory and the PAO1 sequence deposited in GenBank (accession number NC_002516) (51). Genomic DNA was extracted from the mutants and purified with a Pure Link genomic DNA kit (Thermo Fisher Scientific, Waltham, MA). Genomic libraries (250 bp) and high-throughput sequencing were subsequently used with IonTorrent PGM technology (Thermo Fisher Scientific). Alignment of the sequence reads of PAOR10 (13,603,185 reads), PAOR13 (10,768,909 reads), and PAOR15 (11,708,879 reads) with the published PAO1 sequence led to the identification of potential SNPs. An SNP was considered significant if the coverage was >5-fold and its percentage was >90%. To eliminate putative variations between our PAO1 laboratory strain and the published PAO1 sequence, predicted SNPs were compared to the sequence reads of our PAO1 strain (12,289,792 reads) before confirmation by Sanger sequencing in a RUO3500 genetic analyzer (Applied Biosystems/Thermo Fisher Scientific).

Allelic replacement of *fusA1* in PAO1 chromosome. The *fusA1* genes of several *in vitro* and *in vivo* mutants were amplified by PCR from DNA extracts (Wizard genomic DNA purification kit; Promega Corporation, Charbonnières-les-Bains, France) with the specific primers PCR_fusA1_AB1 and PCR_fusA1_AB2 (see Table S1 in the supplemental material). The amplicons were cloned into vector pCR-Blunt, and 2,383-bp fragments carrying the *fusA1* alleles were subcloned into the SpeI/ApaI-linearized plasmid pKNG101. The recombinant plasmids were then transferred from *E. coli* CC118λ*pir* into strain PAO1 by conjugation, and selection of transconjugants was performed on PIA supplemented with 2,000 μg ml^{-1} streptomycin. Excision of pKNG101 was obtained by plating transconjugants on M9 plates containing 5% (wt/vol) sucrose. All of the allelic exchanges were checked by PCR and sequencing with primers PCR_screen_fusA1_AB1 and PCR_screen_fusA1_AB2 (RUO3500 genetic analyzer) (see Table S1 in the supplemental material). The same approach was applied to construct PAO1 mutants carrying *fusA1* alleles described in the literature, determining T119A, G352A, and A1775T substitutions in EF-G1A. The gene *fusA1* from PAO1 was cloned into pCR-Blunt to yield recombinant plasmid pCR-Blunt::*fusA1*$_{PAO1}$. The desired mutations were then introduced into *fusA1* by using a GENEART site-directed mutagenesis system kit (Thermo Fisher Scientific) and specific primers (see Table S1 in the supplemental material).

SUPPLEMENTAL MATERIAL

Supplemental material for this article may be found at https://doi.org/10.1128/AAC.01835-17.

SUPPLEMENTAL FILE 1, PDF file, 0.1 MB.

ACKNOWLEDGMENTS

This study was supported by the French Ministry of Health through the Santé Publique France Agency.

We authors thank Cédric Muller (Smaltis), Amandine Taquard, and Antoine Gouloumy for technical assistance.

REFERENCES

1. Cabot G, Ocampo-Sosa AA, Dominguez MA, Gago JF, Juan C, Tubau F, Rodriguez C, Moya B, Pena C, Martinez-Martinez L, Oliver A, Spanish Network for Research in Infectious Diseases. 2012. Genetic markers of widespread extensively drug-resistant *Pseudomonas aeruginosa* high-risk clones. Antimicrob Agents Chemother 56:6349–6357. https://doi.org/10.1128/AAC.01388-12.
2. Shortridge D, Castanheira M, Pfaller MA, Flamm RK. 2017. Ceftolozane-tazobactam activity against *Pseudomonas aeruginosa* clinical isolates from U.S. Hospitals: report from the PACTS Antimicrobial Surveillance Program, 2012 to 2015. Antimicrob Agents Chemother 61:e00465-17. https://doi.org/10.1128/AAC.00465-17.
3. Döring G, Flume P, Heijerman H, Elborn JS, Consensus Study Group. 2012. Treatment of lung infection in patients with cystic fibrosis: current and future strategies. J Cyst Fibros 11:461–479. https://doi.org/10.1016/j.jcf.2012.10.004.
4. Davies J, Davis BD. 1968. Misreading of ribonucleic acid code words induced by aminoglycoside antibiotics: the effect of drug concentration. J Biol Chem 243:3312–3316.
5. Wilson DN. 2014. Ribosome-targeting antibiotics and mechanisms of bacterial resistance. Nat Rev Microbiol 12:35–48. https://doi.org/10.1038/nrmicro3155.
6. Green R, Noller HF. 1997. Ribosomes and translation. Annu Rev Biochem 66:679–716. https://doi.org/10.1146/annurev.biochem.66.1.679.
7. Cabanas MJ, Vazquez D, Modolell J. 1978. Inhibition of ribosomal translocation by aminoglycoside antibiotics. Biochem Biophys Res Commun 83:991–997. https://doi.org/10.1016/0006-291X(78)91493-6.
8. Scheunemann AE, Graham WD, Vendeix FA, Agris PF. 2010. Binding of aminoglycoside antibiotics to helix 69 of 23S rRNA. Nucleic Acids Res 38:3094–3105. https://doi.org/10.1093/nar/gkp1253.
9. Borovinskaya MA, Pai RD, Zhang W, Schuwirth BS, Holton JM, Hirokawa

G, Kaji H, Kaji A, Cate JH. 2007. Structural basis for aminoglycoside inhibition of bacterial ribosome recycling. Nat Struct Mol Biol 14: 727–732. https://doi.org/10.1038/nsmb1271.
10. Wang L, Pulk A, Wasserman MR, Feldman MB, Altman RB, Cate JH, Blanchard SC. 2012. Allosteric control of the ribosome by small-molecule antibiotics. Nat Struct Mol Biol 19:957–963. https://doi.org/10.1038/nsmb.2360.
11. Levin BR, McCall IC, Perrot V, Weiss H, Ovesepian A, Baquero F. 2017. A numbers game: ribosome densities, bacterial growth, and antibiotic-mediated stasis and death. mBio 8:e02253-16. https://doi.org/10.1128/mBio.02253-16.
12. Poole K. 2005. Aminoglycoside resistance in *Pseudomonas aeruginosa*. Antimicrob Agents Chemother 49:479–487. https://doi.org/10.1128/AAC.49.2.479-487.2005.
13. Wilcox SK, Cavey GS, Pearson JD. 2001. Single ribosomal protein mutations in antibiotic-resistant bacteria analyzed by mass spectrometry. Antimicrob Agents Chemother 45:3046–3055. https://doi.org/10.1128/AAC.45.11.3046-3055.2001.
14. Vogne C, Aires JR, Bailly C, Hocquet D, Plésiat P. 2004. Role of the multidrug efflux system MexXY in the emergence of moderate resistance to aminoglycosides among *Pseudomonas aeruginosa* isolates from patients with cystic fibrosis. Antimicrob Agents Chemother 48: 1676–1680. https://doi.org/10.1128/AAC.48.5.1676-1680.2004.
15. Sobel ML, McKay GA, Poole K. 2003. Contribution of the MexXY multidrug transporter to aminoglycoside resistance in *Pseudomonas aeruginosa* clinical isolates. Antimicrob Agents Chemother 47:3202–3207. https://doi.org/10.1128/AAC.47.10.3202-3207.2003.
16. Guénard S, Muller C, Monlezun L, Benas P, Broutin I, Jeannot K, Plésiat P. 2014. Multiple mutations lead to MexXY-OprM-dependent aminoglycoside resistance in clinical strains of *Pseudomonas aeruginosa*. Antimicrob Agents Chemother 58:221–228. https://doi.org/10.1128/AAC.01252-13.
17. El'Garch F, Jeannot K, Hocquet D, Llanes-Barakat C, Plésiat P. 2007. Cumulative effects of several nonenzymatic mechanisms on the resistance of *Pseudomonas aeruginosa* to aminoglycosides. Antimicrob Agents Chemother 51:1016–1021. https://doi.org/10.1128/AAC.00704-06.
18. Marvig RL, Sommer LM, Molin S, Johansen HK. 2015. Convergent evolution and adaptation of *Pseudomonas aeruginosa* within patients with cystic fibrosis. Nat Genet 47:57–64. https://doi.org/10.1038/ng.3148.
19. Smith EE, Buckley DG, Wu Z, Saenphimmachak C, Hoffman LR, D'Argenio DA, Miller SI, Ramsey BW, Speert DP, Moskowitz SM, Burns JL, Kaul R, Olson MV. 2006. Genetic adaptation by *Pseudomonas aeruginosa* to the airways of cystic fibrosis patients. Proc Natl Acad Sci U S A 103: 8487–8492. https://doi.org/10.1073/pnas.0602138103.
20. Lopez-Causape C, Sommer LM, Cabot G, Rubio R, Ocampo-Sosa AA, Johansen HK, Figuerola J, Canton R, Kidd TJ, Molin S, Oliver A. 2017. Evolution of the *Pseudomonas aeruginosa* mutational resistome in an international cystic fibrosis clone. Sci Rep 7:5555. https://doi.org/10.1038/s41598-017-05621-5.
21. Feliziani S, Marvig RL, Lujan AM, Moyano AJ, Di Rienzo JA, Krogh Johansen H, Molin S, Smania AM. 2014. Coexistence and within-host evolution of diversified lineages of hypermutable *Pseudomonas aeruginosa* in long-term cystic fibrosis infections. PLoS Genet 10:e1004651. https://doi.org/10.1371/journal.pgen.1004651.
22. Islam S, Oh H, Jalal S, Karpati F, Ciofu O, Høiby N, Wretlind B. 2009. Chromosomal mechanisms of aminoglycoside resistance in *Pseudomonas aeruginosa* isolates from cystic fibrosis patients. Clin Microbiol Infect 15:60–66. https://doi.org/10.1111/j.1469-0691.2008.02097.x.
23. Fajardo A, Martinez-Martin N, Mercadillo M, Galan JC, Ghysels B, Matthijs S, Cornelis P, Wiehlmann L, Tümmler B, Baquero F, Martinez JL. 2008. The neglected intrinsic resistome of bacterial pathogens. PLoS One 3:e1619. https://doi.org/10.1371/journal.pone.0001619.
24. Schurek KN, Marr AK, Taylor PK, Wiegand I, Semenec L, Khaira BK, Hancock RE. 2008. Novel genetic determinants of low-level aminoglycoside resistance in *Pseudomonas aeruginosa*. Antimicrob Agents Chemother 52:4213–4219. https://doi.org/10.1128/AAC.00507-08.
25. Winsor GL, Griffiths EJ, Lo R, Dhillon BK, Shay JA, Brinkman FS. 2016. Enhanced annotations and features for comparing thousands of *Pseudomonas* genomes in the *Pseudomonas* genome database. Nucleic Acids Res 44:D646–D653. https://doi.org/10.1093/nar/gkv1227.
26. Rodnina MV, Savelsbergh A, Katunin VI, Wintermeyer W. 1997. Hydrolysis of GTP by elongation factor G drives tRNA movement on the ribosome. Nature 385:37–41. https://doi.org/10.1038/385037a0.
27. Zhang D, Yan K, Zhang Y, Liu G, Cao X, Song G, Xie Q, Gao N, Qin Y. 2015. New insights into the enzymatic role of EF-G in ribosome recycling. Nucleic Acids Res 43:10525–10533. https://doi.org/10.1093/nar/gkv901.
28. Carter AP, Clemons WM, Brodersen DE, Morgan-Warren RJ, Wimberly BT, Ramakrishnan V. 2000. Functional insights from the structure of the 30S ribosomal subunit and its interactions with antibiotics. Nature 407: 340–348. https://doi.org/10.1038/35030019.
29. Palmer SO, Rangel EY, Hu Y, Tran AT, Bullard JM. 2013. Two homologous EF-G proteins from *Pseudomonas aeruginosa* exhibit distinct functions. PLoS One 8:e80252. https://doi.org/10.1371/journal.pone.0080252.
30. Jones AK, Woods AL, Takeoka KT, Shen X, Wei JR, Caughlan RE, Dean CR. 2017. Determinants of antibacterial spectrum and resistance potential of the elongation factor G inhibitor argyrin B in key gram-negative pathogens. Antimicrob Agents Chemother 61:e02400-16. https://doi.org/10.1128/AAC.02400-16.
31. Wattam AR, Davis JJ, Assaf R, Boisvert S, Brettin T, Bun C, Conrad N, Dietrich EM, Disz T, Gabbard JL, Gerdes S, Henry CS, Kenyon RW, Machi D, Mao C, Nordberg EK, Olsen GJ, Murphy-Olson DE, Olson R, Overbeek R, Parrello B, Pusch GD, Shukla M, Vonstein V, Warren A, Xia F, Yoo H, Stevens RL. 2017. Improvements to PATRIC, the all-bacterial bioinformatics database and analysis resource center. Nucleic Acids Res 45: D535–D542. https://doi.org/10.1093/nar/gkw1017.
32. Hocquet D, Nordmann P, El Garch F, Cabanne L, Plésiat P. 2006. Involvement of the MexXY-OprM efflux system in emergence of cefepime resistance in clinical strains of *Pseudomonas aeruginosa*. Antimicrob Agents Chemother 50:1347–1351. https://doi.org/10.1128/AAC.50.4.1347-1351.2006.
33. Masuda N, Sakagawa E, Ohya S, Gotoh N, Tsujimoto H, Nishino T. 2000. Substrate specificities of MexAB-OprM, MexCD-OprJ, and MexXY-OprM efflux pumps in *Pseudomonas aeruginosa*. Antimicrob Agents Chemother 44:3322–3327. https://doi.org/10.1128/AAC.44.12.3322-3327.2000.
34. Greipel L, Fischer S, Klockgether J, Dorda M, Mielke S, Wiehlmann L, Cramer N, Tümmler B. 2016. Molecular epidemiology of mutations in antimicrobial resistance loci of *Pseudomonas aeruginosa* isolates from airways of cystic fibrosis patients. Antimicrob Agents Chemother 60: 6726–6734. https://doi.org/10.1128/AAC.00724-16.
35. Markussen T, Marvig RL, Gomez-Lozano M, Aanaes K, Burleigh AE, Høiby N, Johansen HK, Molin S, Jelsbak L. 2014. Environmental heterogeneity drives within-host diversification and evolution of *Pseudomonas aeruginosa*. mBio 5:e01592-14. https://doi.org/10.1128/mBio.01592-14.
36. Chung JC, Becq J, Fraser L, Schulz-Trieglaff O, Bond NJ, Foweraker J, Bruce KD, Smith GP, Welch M. 2012. Genomic variation among contemporary *Pseudomonas aeruginosa* isolates from chronically infected cystic fibrosis patients. J Bacteriol 194:4857–4866. https://doi.org/10.1128/JB.01050-12.
37. Feng Y, Jonker MJ, Moustakas I, Brul S, Ter Kuile BH. 2016. Dynamics of mutations during development of resistance by *Pseudomonas aeruginosa* against five antibiotics. Antimicrob Agents Chemother 60: 4229–4236. https://doi.org/10.1128/AAC.00434-16.
38. Selva E, Gastaldo L, Saddler GS, Toppo G, Ferrari P, Carniti G, Goldstein BP. 1996. Antibiotics A21459 A and B, new inhibitors of bacterial protein synthesis. I. Taxonomy, isolation, and characterization. J Antibiot (Tokyo) 49:145–149.
39. Gao YG, Selmer M, Dunham CM, Weixlbaumer A, Kelley AC, Ramakrishnan V. 2009. The structure of the ribosome with elongation factor G trapped in the posttranslocational state. Science 326:694–699. https://doi.org/10.1126/science.1179709.
40. Nyfeler B, Hoepfner D, Palestrant D, Kirby CA, Whitehead L, Yu R, Deng G, Caughlan RE, Woods AL, Jones AK, Barnes SW, Walker JR, Gaulis S, Hauy E, Brachmann SM, Krastel P, Studer C, Riedl R, Estoppey D, Aust T, Movva NR, Wang Z, Salcius M, Michaud GA, McAllister G, Murphy LO, Tallarico JA, Wilson CJ, Dean CR. 2012. Identification of elongation factor G as the conserved cellular target of argyrin B. PLoS One 7:e42657. https://doi.org/10.1371/journal.pone.0042657.
41. Bielecki P, Lukat P, Husecken K, Dötsch A, Steinmetz H, Hartmann RW, Muller R, Haussler S. 2012. Mutation in elongation factor G confers resistance to the antibiotic argyrin in the opportunistic pathogen *Pseudomonas aeruginosa*. Chembiochem 13:2339–2345. https://doi.org/10.1002/cbic.201200479.
42. Johanson U, Hughes D. 1994. Fusidic acid-resistant mutants define three regions in elongation factor G of *Salmonella typhimurium*. Gene 143: 55–59. https://doi.org/10.1016/0378-1119(94)90604-1.
43. Westbrock-Wadman S, Sherman DR, Hickey MJ, Coulter SN, Zhu YQ, Warrener P, Nguyen LY, Shawar RM, Folger KR, Stover CK. 1999. Characterization of a *Pseudomonas aeruginosa* efflux pump contrib-

uting to aminoglycoside impermeability. Antimicrob Agents Chemother 43:2975–2983.
44. Caughlan RE, Sriram S, Daigle DM, Woods AL, Buco J, Peterson RL, Dzink-Fox J, Walker S, Dean CR. 2009. Fmt bypass in *Pseudomonas aeruginosa* causes induction of MexXY efflux pump expression. Antimicrob Agents Chemother 53:5015–5021. https://doi.org/10.1128/AAC.00253-09.
45. Gutierrez B, Douthwaite S, Gonzalez-Zorn B. 2013. Indigenous and acquired modifications in the aminoglycoside binding sites of *Pseudomonas aeruginosa* rRNAs. RNA Biol 10:1324–1332. https://doi.org/10.4161/rna.25984.
46. Tourigny DS, Fernandez IS, Kelley AC, Ramakrishnan V. 2013. Elongation factor G bound to the ribosome in an intermediate state of translocation. Science 340:1235490. https://doi.org/10.1126/science.1235490.
47. Mogre A, Sengupta T, Veetil RT, Ravi P, Seshasayee AS. 2014. Genomic analysis reveals distinct concentration-dependent evolutionary trajectories for antibiotic resistance in *Escherichia coli*. DNA Res 21:711–726. https://doi.org/10.1093/dnares/dsu032.
48. Hou Y, Lin YP, Sharer JD, March PE. 1994. *In vivo* selection of conditional-lethal mutations in the gene encoding elongation factor G of *Escherichia coli*. J Bacteriol 176:123–129. https://doi.org/10.1128/jb.176.1.123-129.1994.
49. Muller C, Plésiat P, Jeannot K. 2011. A two-component regulatory system interconnects resistance to polymyxins, aminoglycosides, fluoroquinolones, and beta-lactams in *Pseudomonas aeruginosa*. Antimicrob Agents Chemother 55:1211–1221. https://doi.org/10.1128/AAC.01252-10.
50. Ditta G, Stanfield S, Corbin D, Helinski DR. 1980. Broad host range DNA cloning system for Gram-negative bacteria: construction of a gene bank of *Rhizobium meliloti*. Proc Natl Acad Sci U S A 77:7347–7351. https://doi.org/10.1073/pnas.77.12.7347.
51. Stover CK, Pham XQ, Erwin AL, Mizoguchi SD, Warrener P, Hickey MJ, Brinkman FSL, Hufnagle WO, Kowalik DJ, Lagrou M, Garber RL, Goltry L, Tolentino E, Westbrock-Wadman S, Yuan Y, Brody LL, Coulter SN, Folger KR, Kas A, Larbig K, Lim R, Smith K, Spencer D, Wong GK-S, Wu Z, Paulsen IT, Reizer J, Saier MH, Hancock RE, Lory S, Olson MV. 2000. Complete genome sequence of *Pseudomonas aeruginosa* PAO1, an opportunistic pathogen. Nature 406:959–964. https://doi.org/10.1038/35023079.
52. Herrero M, de Lorenzo V, Timmis KN. 1990. Transposon vectors containing nonantibiotic resistance selection markers for cloning and stable chromosomal insertion of foreign genes in gram-negative bacteria. J Bacteriol 172:6557–6567. https://doi.org/10.1128/jb.172.11.6557-6567.1990.
53. Lacks S, Greenberg B. 1977. Complementary specificity of restriction endonucleases of *Diplococcus pneumoniae* with respect to DNA methylation. J Mol Biol 114:153–168. https://doi.org/10.1016/0022-2836(77)90289-3.
54. Kaniga K, Delor I, Cornelis GR. 1991. A wide-host-range suicide vector for improving reverse genetics in Gram-negative bacteria: inactivation of the *blaA* gene of *Yersinia enterocolitica*. Gene 109:137–141. https://doi.org/10.1016/0378-1119(91)90599-7.

SUPPLEMENTARY DATA.

TABLE S1. Primers used in this study

Primer	Sequence (5'→3')
Primers for SNP identification and complementation of *fusA1*	
PCR_fusA1_AB1	TCAAGAAGCGTGAAGACGTG
PCR_fusA1_AB2	GTTGACGTGCGGTTTGTTAC
Seq_fusA1_AB1	AGGAAGGCCTGCGTCTG
Seq_fusA1_AB2	GGTCGGTAGCGATCTTGAAC
PCR_screen_fusA1_AB1	TGCCAAGACGTCGTGTAGC
PCR_screen_fusA1_AB2	GCGAACTTCCATCTCGACCA
Primers for site-directed mutagenesis	
Mut_L40Q_AB1	GCGTCAACCACAAGC**A**GGGCGAAGTGCATGA
Mut_L40Q_AB2	TCATGCACTTCGCCC**T**GCTTGTGGTTGACGC
Mut_G118S_AB1	TTCTGTGGCACCTCC**A**GCGTAGAGCCGCAGT
Mut_G118S_AB2	ACTGCGGCTCTACGC**T**GGAGGTGCCACAGAA
Mut_N592I_AB1	ATGACGTCGACTCCA**T**CGAGATGGCGTTCAA
Mut_N592I_AB2	TTGAACGCCATCTCG**A**TGGAGTCGACGTCAT

Strains	EF-G1A substitutions[a]
Reference strains	
PAO1	-
PA14	-
LESB58	$D_{588}G$
Environmental strains	
591	-
142951	-
1053	-
2140	-
114793	-
1033	-
2531	-
986-36	-
201	$A_{175}S$
1281G	$I_{186}V$
2112	-
1972G	-
2910	-
2998x	-

Table 5: Determination of polymorphic mutations in EF-G1A by DNA sequencing of environmental strains.

[a] gene sequences were aligned to the published genome (http://www.pseudomonas.com/) of PAO1 and then translated in predicted proteins.

Table 6: Characterization of a collection of non-CF clinical strains from the University Hospital of Besançon.

Strains	Origin	MIC (µg ml^{-1})[a]				EF-G1A substitutions[b]
		TOB	AMK	FEP	CIP	
Reference strain						
PAO1	environment	0.5	4	2	<0.125	-
Clinical strains not retained for *fusA1* sequencing						
6051	unknown	0.5	4	2	<0.125	ns
6083	urine	0.5	4	2	<0.125	ns
6087	blood culture	0.5	4	2	<0.125	ns
6107	unknown	0.5	4	2	<0.125	ns
6128	urine	0.5	4	2	4	ns
6238	unknown	0.5	<2	2	<0.125	ns
6269	bronchoalveolar lavage	0.5	4	1	<0.125	ns
6285	blood culture	0.5	4	2	<0.125	ns
6289	catheter	0.5	4	1	<0.125	ns
Clinical strains retained for *fusA1* sequencing						
5910	expectoration	**2**	**16**	8	<0.125	$A_{555}E$
6106	urine	**1**	**8**	2	<0.125	-
6232	urine	**2**	**16**	8	<0.125	-
6233	urine	**2**	**16**	2	<0.125	$T_{671}A$
6253	bronchial aspirate	**2**	**16**	2	0.25	$V_{93}A$ $I_{186}V$
6256	unknown	**1**	4	1	<0.125	-
6284	urine	**2**	**16**	4	<0.125	-

[a] MICs were determined using Sensititre® microplates. Compared to PAO1, a 2-fold increase in MIC of TOB and AMK is indicated in bold face. TOB: tobramycin, AMK: amikacin, FEP: cefepime, CIP: ciprofloxacin.

[b] sequences were aligned to the published genome of PAO1, ns: not sequenced.

3.2. Supplementary results

3.2.1. Genetic polymorphism of *fusA1* among environmental strains of *P. aeruginosa*

To assess the relevance of amino acid substitutions in elongation factor EF-G1A, we first investigated the natural polymorphism of gene *fusA1* and its product. Comparison of *fusA1* coding sequences from three susceptible reference strains (PAO1, PA14 and LESB58) showed that the $D_{588}G$ variation is a common polymorphism (Table 5). Additionally, *fusA1* sequence analysis of 14 environmental strains showing a wild-type susceptibility to antibiotics (β-lactams, carbapenems, aminoglycosides and fluoroquinolones) characterized two other non-significant substitutions ($A_{175}S$ and $I_{186}V$) (Table 5). Of note, $D_{588}G$ and $I_{186}V$ had been identified in CF strains but actually do not impact bacterial susceptibility to aminoglycosides (Greipel *et al*., 2016; López-Causapé *et al*., 2017) (Table 2).

3.2.2. Prevalence of *fusA1* mutations in a collection of isolates exhibiting a non-enzymatic resistance to aminoglycosides

We showed that engineered substitutions in EF-G1A confer high resistance levels to the four aminoglycoside subclasses (e.g., a 4- to 8-fold increase in tobramycin MIC) (Bolard *et al*., 2018). To get an insight of the prevalence of *fusA1* mutations in clinical strains, we selected isolates showing a resistance profile (antibiogram method) to aminoglycosides that could not be explained by known mechanisms (e.g., production of modifying enzymes or MexXY(OprM) dysregulation). Thus, 16 strains were retained for further analysis (Table 6). Determination of the MICs of tobramycin, amikacin, cefepime and ciprofloxacin led us to select 7/16 of these bacteria. Sequencing of their *fusA1* genes revealed substitutions ($A_{555}E$, $T_{671}A$ or $V_{93}A/I_{186}V$) in EF-G1A for 3/7 strains. The three variations were confirmed to confer resistance to aminoglycosides (from 8- to 16-fold increase in tobramycin MIC) (Bolard *et al*., 2018). Since the $I_{186}V$ substitution was present in environmental strain 1281G, aminoglycosides resistance conferred by the $fusA1_{6253}$ allele results probably from mutation $V_{93}A$. Mechanisms underlying aminoglycoside resistance in the 4 remaining strains were not explored further. It might result from previously characterized mechanisms such as *galU* mutant (El'Garch *et al*., 2007) or from mutations in probable-aminoglycoside-resistance genes (López-Causapé *et al*., 2018).

Table 7: Sequence analysis of *fusA1* gene in a clinical collection of previously characterized *agrZ* and *agrW1* mutants.

Strains	Genotype[a]	MIC (µg ml^{-1})[ab]				EF-G1A substitutions
		TOB	AMK	FEP	CIP	
Reference strains						
PAO1		0.5	4	4	0.25	-
PAO1Δ*mexZ*	*agrZ*	1	8	8	0.5	-
PAOW1	*agrW1*	2	16	16	0.5	-
agrZ-type strains						
2404	*agrZ*	1	**16**	32	1	-
2696	*agrZ*	1	**16**	32	1	-
2752	*agrZ*	1	**16**	32	32	-
2855	*agrZ*	1	**16**	32	32	-
3103	*agrZ*	**4**	**32**	16	1	-
3197	*agrZ*	**4**	**32**	8	8	-
3215	*agrZ*	**2**	**16**	8	0.5	-
3245	*agrZ*	**2**	**16**	16	32	-
4194	*agrZ*	**4**	**32**	32	1	-
4364	*agrZ*	**2**	**16**	8	1	-
4465	*agrZ*	**2**	**16**	8	0.125	-
4484	*agrZ*	**2**	**16**	16	0.5	-
4753	*agrZ*	1	**16**	32	0.5	-
4891	*agrZ*	**2**	**16**	8	4	-
agrW1-type strains						
2405	*agrW1*	**4**	**64**	8	0.5	-
3452	*agrW1*	**4**	**32**	8	32	-
3564	*agrW1*	**4**	**32**	8	0.5	-

[a] genotypes and MICs were previously reported (Guénard *et al*., 2014).
[b] a minimum 2-fold increase in MICs compared to PAO1Δ*mexZ* or PAO1W1 strain is indicated in bold face. TOB: tobramycin, AMK: amikacin, FEP: cefepime, CIP: ciprofloxacin.

Table 8: Phenotypic characterization of engineered EF-G1A mutants.

Strains[a]	MIC (µg ml^{-1})[b]								
	TOB	AMK	STR	SPT	CAZ	FEP	IPM	CIP	TET
PAO1	0.25	2	32	512	2	2	1	0.125	32
PAO1::*fusA1*$_{PAOR10}$	**2**	**16**	**64**	512	2	2	1	0.125	32
PAO1::*fusA1*$_{PAOR13}$	**1**	**8**	**64**	512	2	2	1	0.125	32
PAO1::*fusA1*$_{PAOR15}$	**2**	**16**	**64**	**1,024**	2	2	1	0.125	32
PAO1::*fusA1*$_{5910}$	**2**	**16**	32	**1,024**	2	2	1	0.125	32
PAO1::*fusA1*$_{6233}$	**2**	**16**	**64**	512	2	2	1	0.125	32
PAO1::*fusA1*$_{6253}$	**4**	**32**	**64**	512	2	2	1	0.125	32
PAO1::*fusA1*$_{T119A}$	**1**	**8**	**64**	**1,024**	2	2	1	0.125	32
PAO1::*fusA1*$_{G352A}$	**0.5**	**4**	32	512	2	2	1	0.125	32
PAO1::*fusA1*$_{A1775T}$	**2**	**32**	32	512	2	2	1	0.125	32

[a] alleles PAOR10, PAOR13 and PAOR15 are from *in vitro*-selected mutants. Additionnal alleles are from non-CF (5910, 6233, 6253) and CF (T119A, G352A, A1775T) strains.
[b] a minimum 2-fold increase in MICs compared to PAO1 is indicated in bold face. TOB: tobramycin, AMK: amikacin, STR: streptomycin, SPT: spectinomycin, CAZ: ceftazidime, FEP: cefepime, IPM: imipenem, CIP: ciprofloxacin, TET: tetracycline.

3.2.3. *fusA1* mutations do not contribute to high aminoglycoside resistance in a collection of *agrZ* and *agrW1* mutants isolated from patients

Amino acid substitutions in EF-G1A can confer a substantial resistance to aminoglycosides when associated with constitutive overexpression of operon *mexXY* (Bolard *et al*., 2018). Thus, we wondered if the higher (2- to 4-fold) resistance levels observed in a previous study (Guénard *et al*., 2014), evaluating the prevalence of *agrZ* and *agrW* mutants among clinical strains of *P. aeruginosa* could be, at least partially, explained by mutations in *fusA1*.

In the collection from Guénard *et al*., we selected *agrZ* and *agrW1* mutants exhibiting a resistance to tobramycin and/or amikacin higher than that of mutants PAO1Δ*mexZ* and PAOW1 (MICs of tobramycin = 1/2 and amikacin = 8/16 µg ml^{-1}). Based on these criteria, 17 strains were selected and their gene *fusA1* sequenced (Table 7). None of them showed substitutions in factor EF-G1A as compared with that of PAO1, indicating that still unknown mechanisms decrease susceptibility of the bacteria to aminoglycosides. On the other hand, variations in the amino acid sequence of proteins MexXY or very high production of this pump might account for the resistance phenotype of selected strains as well.

3.2.4. Susceptibility to β-lactams, carbapenems, fluoroquinolones and tetracycline is unchanged in *fusA1* mutants

Some resistance mechanisms compromise the activity of different families of antibiotics. For example, substitutions in sensor protein ParS of the TCS ParRS, confer a resistance to β-lactams (including carbapenems), aminoglycosides, fluoroquinolones and polymyxins. Thus, the impact of *fusA1* gain-of-function mutations on the MICs of selected β-lactams, fluoroquinolones and tetracyclines was analyzed (Table 8). Our results demonstrated that only aminoglycosides are impacted by mutations in gene *fusA1*. No cross-resistance with other antibiotic classes was observed.

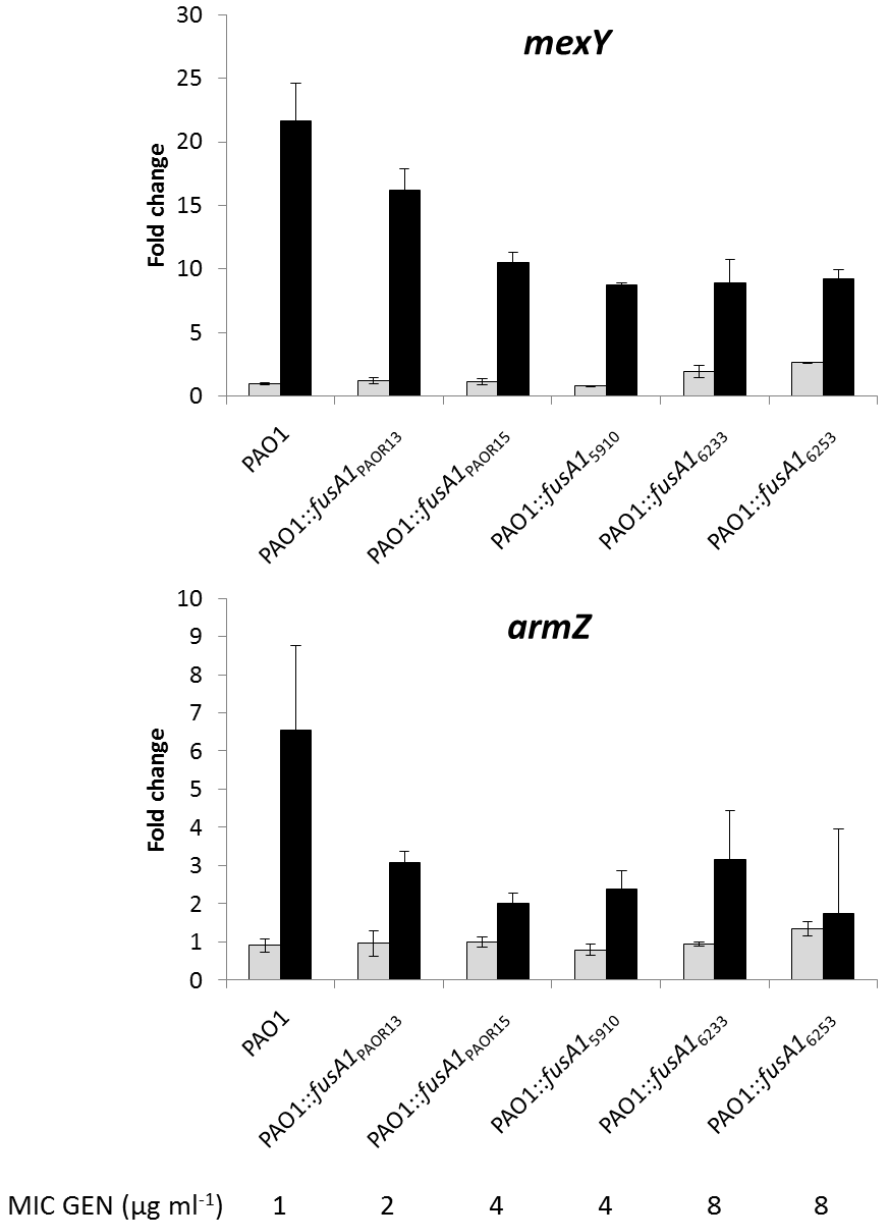

Figure 39: Effects of *fusA1* mutations on gene *mexY* and gene *armZ* expression in strain PAO1 submitted to gentamicin exposure.

Untreated cells and cells exposed to 0.5 µg ml^{-1} of gentamicin are represented with grey and black bars, respectively. GEN: gentamicin.

3.2.5. *fusA1* mutations decrease gentamicin-induced expression of *mexY* and *armZ*

Acquired resistance of *fusA1* mutants to aminoglycosides is independent of efflux pump MexXY(OprM) (Bolard *et al*., 2018). However, a previous work from the laboratory showed that, in strain PAO1 the *mexXY* and *armZ* genes are activated by agents targeting the ribosome such as gentamicin (Jeannot *et al*., 2005). To know whether EF-G1A mutations somehow increase the aminoglycoside-induced expression of *mexXY*, we cultured strain PAO1 and several *fusA1* mutants in the presence or absence of gentamicin at 0.5 µg ml^{-1}. Total RNAs were extracted and genes *mexY* and *armZ* were quantified by RT-qPCR (Figure 39).

First, our data confirmed the reported activation of *mexY* and *armZ* in wild-type bacteria exposed to gentamicin (21.6-fold and 7.2-fold, respectively). Second, both loci were activated in *fusA1* mutants in the presence of the antibiotic, indicating that induction of *mexXY* also occurs in these mutants. However, it is important to note that the induced expression of *mexXY* was lower in the mutants than in PAO1. A trivial explanation would be that the resistance to gentamicin conferred by the EF-G1A alteration partially protects the ribosomal machinery from stalling and thus limits activation of operon *mexXY via* the ArmZ pathway. Our RT-qPCR experiments were performed with a fixed concentration of gentamicin (0.5 µg ml^{-1}) and could likely have provided different results by using the antibiotic as a fixed fraction of the MIC for each strain considered.

4. Conclusion

Taken together, these results unambiguously confirm that some amino acid substitutions in elongation factor EF-G1A lead to a decreased susceptibility of CF and non-CF strains of *P. aeruginosa* to aminoglycosides. This phenotype is independent of MexXY(OprM), a pump known to participate in intrinsic, acquired and adaptive resistance to aminoglycosides. While this has not been observed in clinical isolates, we found that the coexistence of the two mechanisms [EF-G1A alteration and constitutive overproduction of MexXY(OprM)] has additive effects on aminoglycoside MICs. The EF-G1A mutations studied impaired the bacterial fitness *in vitro*, suggesting that these deficient bacteria may have an advantage (or a lower handicap) in the CF lung where they mostly live in biofilms.

Chapter 2. Mutations in *pmrAB* mediate aminoglycoside resistance in *P. aeruginosa*

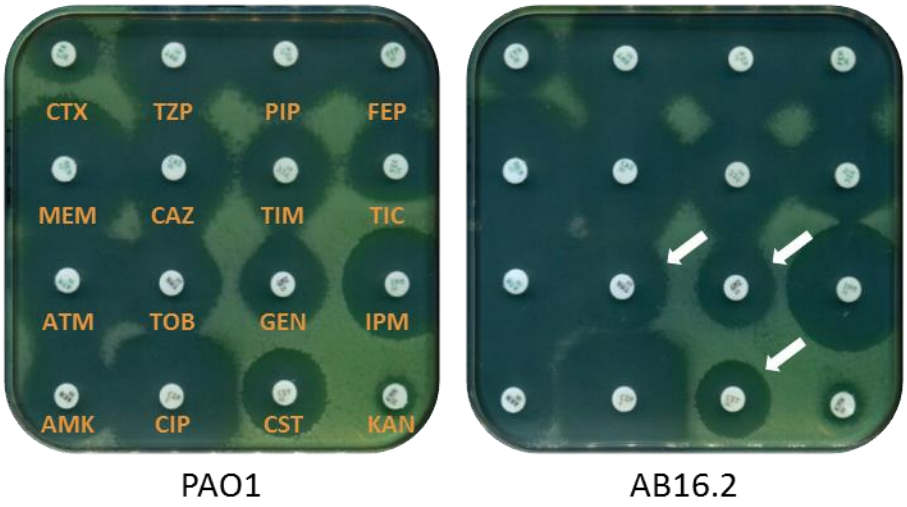

Figure 40: Antibiograms of PAO1 and AB16.2 derivative mutant.

CTX: cefotaxime, TZP: piperacillin-tazobactam, PIP: piperacillin, FEP: cefepime, MEM: meropenem, CAZ: ceftazidime, TIM: ticarcillin-clavulanic acid, TIC: ticarcillin, ATM: aztreonam, TOB: tobramycin, GEN: gentamicin, IPM: imipenem, AMK: amikacin, CIP: ciprofloxacin, CST: colistin, KAN: kanamycin.

1. Context

The TCS PmrAB plays a key role in the development of resistance to polymyxins in *P. aeruginosa*. Indeed, several amino acid substitutions in sensor protein PmrB were shown to result in an increased resistance to colistin through the activation of operon *arnBCADTEF-ugd*. Recently, analysis of the mutational resistome of *P. aeruginosa* to aminoglycosides suggested that alterations in sensor HK PmrB could also provide a resistance to these antibiotics in addition to polymyxins (López-Causapé *et al*., 2018). However, the mutations identified in *pmrB* were not investigated further and the underlying molecular mechanism(s) remained to be characterized. In our laboratory, sequence analysis of the *pmrAB* loci from 10 *in vitro*-selected mutants resistant to colistin revealed the presence of three different mutations in gene *pmrB*, respectively. The mutants harboring these mutations (e.g., AB16.2) were resistant to both colistin and aminoglycosides (Figure 40).

2. Objective

The main objective of this project was to identify the mechanism determining a cross-resistance to colistin and aminoglycosides in *in vitro*-selected *pmrAB* mutants and clinical strains. The role played by the genes PA4773 to PA4775 was studied. Some investigators had proposed that genes PA4773 and PA4774 encode SpeD and SpeE homologs, respectively, two enzymes implicated in the biosynthesis of spermidine. Spermidine would modify bacterial surface properties and confer a protection against aminoglycosides, antimicrobial peptides and oxidative stress (Johnson *et al*., 2012). To analyze more precisely the cellular effects caused by the aforementioned *pmrB* mutations in cross-resistant mutants, we compared the transcriptome of one of these mutants with that of parental strain PAO1.

3. Results

3.1. Article in preparation

Production of norspermidine contributes to aminoglycoside resistance in *pmrAB* mutants of *Pseudomonas aeruginosa*

Arnaud BOLARD[1,2], Monika SCHNIEDERJANS[3], Susanne HAUSSLER[3], Pauline TRIPONNEY[1], Benoît VALOT[2], Patrick PLESIAT[1,2], Katy JEANNOT[1,2]*

[1] Centre National de Référence de la Résistance aux Antibiotiques, Centre Hospitalier Universitaire de Besançon, France

[2] UMR6249 Chrono-environnement, Faculté de Médecine-Pharmacie, Université de Bourgogne-Franche Comté, Besançon, France

[3] Molecular Bacteriology, Twincore, Centre for Experimental and Clinical Infection Research, a joint venture of the Helmholtz Centre for Infection Research, Braunschweig and the Hannover Medical School, Feodor-Lynen-Straße 7, D-30265 Hannover, Germany

*Corresponding author : Katy Jeannot

katy.jeannot@univ-fcomte.fr

tel : +33 3 70 63 21 69/ fax : +33 3 70 63 23 64

Address. Centre National de Référence de la Résistance aux Antibiotiques, Laboratoire de Bactériologie, CHU Jean Minjoz, Boulevard Fleming, 25030 Besançon, France

Running title :

Key Words : *Pseudomonas aeruginosa* / colistin resistance /aminoglycosides/ norspermidine

Abstract (202 words)

Emergence of resistance to polymyxins in *Pseudomonas aeruginosa* is mainly due to mutations in two-components systems, that promote addition of 4-amino-4-deoxy-L-arabinose to the lipopolysaccharide (LPS) molecules that cover the bacterial surface, by upregulating operon *arnBCADTEF-ugd* (*arn*) expression. Here, we demonstrate that mutations occurring in different domains of histidine kinase PmrB or in response regulator PmrA result in coresistance to aminoglycosides and colistin. Seventeen clinical strains exhibiting such a cross-resistance phenotype were found to be *pmrAB* mutants. As shown by gene deletion experiments, the decreased susceptibility of the mutants to aminoglycosides is independent from operon *arn* but requires the efflux system MexXY(OprM) and the products of three genes, PA4773-PA4774-PA4775, that are cotranscribed and activated with genes *pmrAB*. Gene PA4773 (annoted as *speD2* in PAO1 genome) and PA4774 (*speE2*) are predicted to encode enzymes involved in biosynthesis of polyamines. Comparative analysis of cell surface extracts of an *in vitro* selected *pmrAB* mutant, called AB16.2, and derivatives lacking PA4473, PA4774 and PA4775, respectively revealed that these genes are needed for norspermidine production via a pathway that likely uses 1,3-diaminoprane. Altogether, our results suggest that norspermidine decreases the self-promoted uptake pathway of aminoglycosides across the outer membrane and thereby potentiates the activity of efflux pump MexXY(OprM).

Introduction

Pseudomonas aeruginosa is a common cause of healthcare-associated infections (1). Because of an increasing number of extensively drug-resistant (XDR) strains, polymyxins (colistin and polymyxin B) and aminoglycosides are more and more used as the last-line antibiotics to treat infected patients (2, 3). Therefore, emergence of resistance to one or both of these antibiotic families under treatment may leave clinicians with very few or no more therapeutic options, and result in clinical failures.

Though still infrequent (3), polymyxin resistance in *P. aeruginosa* is due to enzymatic addition of 4-amino-4-deoxy-L-arabinose (Ara4N) to lipid A of lipopolysaccharide (LPS), with subsequent decrease in the electrostatic interaction between the polycationic polymyxins and the negatively-charged outer membrane (4, 5). Ara4N modification of LPS is determined by an operon, *arnBCADTEF-ugd* (thereafter called *arn*), whose expression is controlled by several two-component regulatory systems (TCS) including PmrAB, PhoPQ, ParRS, ColRS and CprRS. Various mutations in these phospho-relays have been demonstrated or more simply suspected to activate *arn* transcription and thereby to enhance colistin resistance in clinical strains of *P. aeruginosa* (6). Sensor PmrB is a hot spot for such mutations (7-13).

Three genes of the PmrAB regulon (PA4773, PA4774 and PA4775) are activated when planktonic bacteria are grown upon Mg^{2+} starvation, at acidic pH, in the presence of extracellular DNA (eDNA) or with antimicrobial peptides such as colistin, indolicidin and CP11 (14-17). Inactivation of gene PA4774 (annotated as spermidine synthase gene *speE2* in the *Pseudomonas* Genome database; (18) was found to alter the outer membrane permeability barrier to polymyxin B, CP10A and aminoglycoside gentamicin (14). Another study revealed that the resistance developed by *P. aeruginosa* towards polymyxin B, gentamicin and tobramycin when cultured with eDNA or at acidic pH, required functional PA4773 and *arn* genes (16). It was concluded that genes PA4773 (S-adenosyl methionine transferase gene

speD2 in the *Pseudomonas* Genome database) and PA4774 are part of an alternative spermidine biosynthesis pathway, which once activated via TCS PmrAB protects *P. aeruginosa* against antimicrobial peptides and aminoglycosides by increasing the amounts of the positively-charged spermidine at the cell surface (14).

Non-enzymatic resistance of clinical strains of *P. aeruginosa* to aminoglycosides is often associated with constitutive upregulation of efflux system MexXY(OprM) (19). Loss-of-function mutations in gene *mexZ* which encodes a TetR-like repressor of operon *mexXY*, alteration of components of the protein synthesis machinery, or amino acid substitutions in TCS ParRS can positively impact *mexXY* activity and thus promote resistance to pump MexXY(OprM) substrates such as aminoglycosides, cefepime and fluoroquinolones, from 2- to 4-fold. In addition, ParRS mutants exhibit an increased resistance to colistin as a result of operon *arn* induction, and to carbapenems due to repressed transcription of porin OprD gene (20).

The present study investigates a novel type of aminoglycosides-colistin cross resistant *pmrB* mutants that overexpress both the *mexXY* operon and the PA4773-4775 gene cluster.

Results

Alteration of sensor PmrB provides cross-resistance to aminoglycosides and colistin

Characterisation of resistant mutants of reference strain PAO1 selected on agar plates containing 8 µg ml^{-1} (MIC x 16; mutant rates = 9.10^{-7}) and 16 µg ml^{-1} (MIC x 32; 6.10^{-8}) of colistin, showed that all the analysed clones were coresistant to colistin and aminoglycosides (256-fold and up to 8-fold more than PAO1, respectively), while some of them were slightly more susceptible (2-fold) to β-lactams (Table 1). Sequencing of genes *pmrA*, *pmrB*, *parS*, *parR*, *cprS*, *cprR*, *phoP*, *phoQ*, *colS* and *colR* known to be involved in regulation of operon *arn* expression revealed the presence of single amino acid substitutions in histidine kinase PmrB of randomly chosen mutants AB8.2 (V28G) and AB16.1 (F408L), and an amino acid deletion in the protein of mutant AB16.2 (ΔL172) (Figure 1). To confirm the impact of these alterations on aminoglycoside resistance, we complemented the *pmrAB* negative strain PAO1Δ*pmrAB* with plasmid vector pME6012 carrying the *pmrAB* alleles from PAO1, AB8.2, AB16.1 and AB16.2 (yielding constructs pABWT, pAB8.2, pAB16.1, pAB16.2, respectively). Compared with the wild-type control, all the mutated *pmrB* genes conferred a significant resistance to gentamicin (8 µg ml^{-1}; MIC x 8), amikacin (8 µg ml^{-1}; MIC x 4), and tobramycin (2 µg ml^{-1}; MIC x 8) in addition to colistin (128 µg ml^{-1}; MIC x 256) (Table 1). On the other hand, deletion of gene *pmrA* or *pmrB* restored a wild-type susceptibility phenotype in mutant AB16.2, thus providing further evidence that the cross-resistance of *pmrB* mutants requires both components of the signal transducing system PmrAB (Table 2). The observation that mutants PAO1Δ*pmrA* and PAO1Δ*pmrB* exhibited the same resistance levels as that of parent strain PAO1, also indicates that PmrAB does not play a role in the intrinsic resistance of *P. aeruginosa* to antibiotics including polymyxins (Table 2). To assess a possible contribution of LPS modification operon *arn* to aminoglycoside resistance of *pmrB* mutants, we measured gene *arnA* expression by RT-qPCR in AB8.2, AB16.1 and AB16.2,

and removed the whole *arn* locus from PAO1 and AB16.2 genomes (yielding derivatives PAO1Δ*arn* and AB16.2Δ*arn*, respectively). All the three studied mutants were found to overexpress gene *arnA* strongly (from 424 to 657-fold *versus* PAO1). Whereas the parental susceptibility to colistin was almost completely restored in mutant AB16.2Δ*arn* (MIC = 1 µg ml^{-1}; Table 2), MICs of aminoglycosides remained unchanged, confirming our hypothesis of an Arn-independent mechanism of aminoglycoside resistance in *pmrB* mutants. In a previous work, we showed that mutational activation of TCS ParRS results in constitutive upregulation of operon *mexXY* and increased resistance to various pump MexXY(OprM) substrates such as aminoglycosides (20). To assess the role played by this TCS is aminoglycoside-colistin cross-resistance, we deleted operon *parRS* in AB16.2 (yielding strain AB16.2Δ*parRS*) and PAO1 (PAO1Δ*parRS*). As indicated in Table 2, these deletions only impacted colistin MICs with a 16-fold reduction in AB16.2Δ*parRS* as compared with AB16.2 (4 *versus* 64 µg ml^{-1}), and a two-fold decrease in PAO1 (as already reported in (20)). Altogether, these results supported the notion that other PmrAB-dependent mechanisms are responsible for the resistance of *pmrB* mutants to aminoglycosides.

Aminoglycoside-colistin cross-resistant pmrB mutants occur in the clinical setting

To get an insight into the *in vivo* relevance of such mutants, we selected 28 colistin non-susceptible clinical strains (MIC from 4 to 256 µg ml^{-1}) from our lab collection. Seventeen of them (60.7%) appeared to be at least 4-fold more resistant to gentamicin, tobramycin and amikacin that wild-type strain PAO1 (Table 3). Sequencing of gene *pmrB* in these 17 strains revealed the presence of several non-synonymous mutations relative to the PAO1 gene sequence (Table 3). A number of predicted amino acid variations in protein PmrB were identical to that of aminoglycoside-colistin susceptible strains PA14 (S2P, A4T, G68S, V15I, Y345H) and LESB58 (Y345H), and were considered as common polymorphism. Four *pmrAB*

alleles encoding five so far uncharacterised amino acid variations in PmrB were amplified from isolates 2243 (Q105P), 3092 (V6A/L37P), 3795 (G188D) and 3890 (D45E), and cloned in vector pME6012. In addition, we cloned the *pmrAB* locus of a drug susceptible clinical strain (3095), that codes for a PmrB variant exhibiting a V6A substitution along with several nonsignificant amino acid changes. The resulting recombinant plasmids were used to complement strain PAO1Δ*pmrAB* (Table 3). Reminiscent of our previous findings, the non-polymorphic mutations in PmrB (L37P, D45E, Q105P, G188D) except V6A led to cross-resistance to aminoglycosides and colistin in transcomplemented mutant PAO1Δ*pmrAB* (Table 3).

Since response regulator PmrA can also be constitutively activated by mutations (4), we sequenced its gene in the two strains showing nonsignificant amino acid variations in sensor PmrB, namely 3091 and 4586. Beside the L71R change also present in strain LESB58, isolate 3091 harboured a L21I substitution in PmrA. Cloning and expression of the *pmrAB* genes from 3091 in PAO1Δ*pmrAB* caused an increase in MICs of gentamicin (8 μg ml^{-1}; 8-fold the wild-type level), amikacin (8 μg ml^{-1}; 4-fold), tobramycin (2 μg ml^{-1}; 8-fold) and colistin (128 μg ml^{-1}; 256-fold), demonstrating that coresistance to aminoglycosides and polymyxins can arise when either PmrB or PmrA is mutationally activated. Since the PmrA protein from strain 4586 displayed the same sequence as PAO1, we considered its resistance phenotype to aminoglycosides and polymyxins as being independent of PmrAB.

MexXY(OprM) is required for aminoglycoside resistance and contributes to colistin resistance in pmrB mutants

The transcript levels of gene *mexY* that codes for RND transporter MexY were measured in strain PAO1Δ*pmrAB* complemented with different *pmrAB* alleles described above (i.e., carrying PmrAB activating mutations). Compared with PAO1Δ*pmrAB* overexpressing the

161 wild-type *pmrAB* genes from plasmid pABWT, *mexY* transcription was found to be only
162 marginally increased (from 1.4 to 2.8-fold) upon complementation with 6 of the 7 mutated
163 alleles (Figure S1), while the resistance to aminoglycosides (from 4- to 8-fold; Tables 1 and
164 3), and other MexXY(OprM) substrates ciprofloxacin and cefepime (2-fold, data not shown)
165 augmented significantly. The allele from the remaining strain 2243 (that encodes a Q105P
166 PmrB variant) was associated with a 16.6-fold upregulation of *mexY* relative to
167 PAO1Δ*pmrAB*(pABWT), and a stronger increase in MICs of aminoglycosides (from 16- to
168 32-fold), ciprofloxacin and cefepime (4-fold, data not shown). To further investigate the role
169 of MexXY(OprM) in the phenotype of *pmrB* mutants, we deleted operon *mexXY* in mutant
170 AB16.2 and in PAO1. Because this efflux system contributes to the natural resistance of
171 *P. aeruginosa* to aminoglycosides (21), the *mexXY* deletion rendered PAO1 hypersusceptible
172 to these antimicrobials (compare mutant PAO1Δ*mexXY* with PAO1 in Table 2). Very similar
173 results were obtained when genes *mexXY* were removed from AB16.2 (AB16.2Δ*mexXY*
174 *versus* AB16.2 in Table 2). MICs of aminoglycosides dropped from 32-fold (amikacin,
175 tobramycin) to 128-fold (gentamicin), clearly indicating that the elevated resistance of *pmrB*
176 mutants to these antibiotics depends on the activity of MexXY(OprM), though operon *mexXY*
177 expression remains unaffected by the *pmrB* mutations (Figure S1). We therefore hypothetized
178 that another mechanism could potentiate the extrusion of aminoglycosides out of bacteria by
179 MexXY(OprM). Indeed, synergistic interplays between efflux systems and factors modulating
180 the outer membrane permeability to antibiotics, such as porins, are common in multidrug
181 resistant Gram-negative bacteria (19).
182 Unexpectedly, inactivation of operon *mexXY* strongly reduced colistin MIC (16-fold) leaving
183 a residual resistance of 4 μg ml^{-1} in AB16.2Δ*mexXY* while it had virtually no effects on the
184 susceptibility level of parent PAO1 (Table 2). Although polymyxins are not in the list of
185 known substrates of MexXY(OprM) (22), our data supported the notion that aminoglycosides

and colistin might be pumped out more efficiently outside bacteria if their intracellular penetration was impaired by a decreased permeability of the cell envelope.

Aminoglycoside resistance is linked to genes PA4773-PA4774-PA4775 in pmrB mutants

To identify the mechanisms that could synergise MexXY(OprM) activity in our mutants, we compared the transcriptomes of AB16.2 and PAO1. A total of 233 genes turned out to be dysregulated, of which 201 exhibited an increased expression and 32 a reduced expression ≥ 3-fold linked to PmrAB activation (Table S1). As expected, operon *arn* and all the genes of the *pmrAB* cluster that includes PA4773 (*speD2*), PA4774 (*speE2*), PA4775, PA4776 (*pmrA*) and PA4777 (*pmrB*) were strongly activated in AB16.2. In most *P. aeruginosa* genomes (18), genes PA4773 to PA4777 form a single transcriptional unit. Protein PA4773 shares 24.2% sequence identity with S-adenosyl methionine decarboxylase SpeD (encoded by gene PA0654 in strain PAO1), and PA4774 has a sequence 38.3% identical to that of spermidine synthase SpeE (gene PA1687). Protein PA4775 has no known homologs. Involvement of these three proteins in the resistance phenotype of *pmrB* mutants was examined by deleting each encoding gene in AB16.2 and PAO1. We obtained no evidence of the contribution of these proteins to the natural resistance of *P. aeruginosa* to aminoglycosides or polymyxins (compare PAO1 and its PAO1Δ derivatives in Figures 2A, 2B and S2). However, while it did not affect colistin resistance significantly, inactivation of any of these proteins restored a wild-type susceptibility to aminoglycosides in AB16.2. On the other hand, mutants AB16.2ΔPA4773, AB16.2ΔPA4774 and AB16.2ΔPA4775 recovered the initial phenotype of AB16.2 when a DNA fragment carrying genes PA4773-PA4774-PA4775 was inserted in chromosomal site *attB* (Figures 2A and S2). At this point, our results showed that the elevated resistance of *pmrB* mutants to aminoglycosides was dependent upon PA4773-PA4774-PA4775 and efflux system MexXY(OprM).

211

212 ***Norspermidine contributes to aminoglycoside resistance***

213 Since genes PA4773 and PA4774 are predicted to encode enzymes involved in synthesis of
214 polyamines, we measured the amounts of 1,3-diaminopropane (a precursor of polyamines),
215 putrescine, cadaverine, norspermidine, spermidine and spermine bound to the cell surface of
216 strains PAO1, AB16.2, AB16.2ΔPA4773, AB16.2ΔPA4774 and AB16.2ΔPA4775, by using
217 LC-ESI-MS. As shown Figure S3, we found no significant differences in the areas under the
218 peaks of cadaverine, putrescine and spermine between the strains. In contrast, 15.8-fold more
219 spermidine was detected in the extracts from mutant AB16.2 (10.6 $\log_{10}$) relative to strain
220 PAO1 (9.4 $\log_{10}$) (Figure 3A), as previously observed in bacteria grown under conditions of
221 Mg^{2+} deficiency or at acidic pH (14). These amounts were only partially reduced in the
222 mutants lacking PA4773, PA4774 or PA4775, suggesting that the major part of the
223 spermidine present in the extracts had been elaborated via another pathway. More
224 importantly, the LC-ESI-MS analysis revealed the presence of much higher quantities
225 (>1,000-fold) of norspermidine at the surface of AB16.2 (10.7 $\log_{10}$) than that of PAO1
226 (7.6 $\log_{10}$, a value close to the limit of detection) (Figure 3B). The observation that the
227 deletion of genes PA4773 (8.6 $\log_{10}$), PA4774 (7.8 $\log_{10}$) or PA4775 (9.0 $\log_{10}$) was
228 associated with lower norspermidine levels in AB16.2 (126-, 794- and 50-fold, respectively)
229 (Figure 3B) supports the notion that when overexpressed in *pmrB* mutants the three genes
230 enable the formation of this polyamine and contribute to aminoglycoside resistance. Finally,
231 1,3-diaminopropane turned out to be 3.2-fold more abundant in extracts from mutant
232 AB16.2ΔPA4775 (11.2 $\log_{10}$) in comparison with AB16.2 (10.7 $\log_{10}$) (Figure 3C), which
233 might suggest that protein PA4775 converts this precursor to fuel the norspermidine
234 biosynthesis pathway.

235

Impact of norspermidine synthesis on bacterial growth

Addition of exogenous norspermidine is known to inhibit bacterial growth in various species including *P. aeruginosa* (23). Since mutant AB16.2 forms smaller colonies than parental strain PAO1 on MH agar medium, we compared the growth curves of the two strains with that of mutants AB16.2ΔPA4773, AB16.2ΔPA4774 and AB16.2ΔPA4775. As shown Figure 4, these experiments confirmed the impaired development of mutant AB16.2. Suppression of genes PA4773 and PA4774 in this mutant completely restored the parental fitness, while the deletion of PA4775 only partially improved its growth, consistent with the hypothesis that norspermidine production in mutant AB16.2 is deleterious.

Discussion

Mutations in TCS PmrAB are a well-known cause of colistin resistance in *P. aeruginosa* (6). However, their impact on bacterial susceptibility to aminoglycosides has not been addressed specifically until the present study. Lopez-Causapé *et al.* observed the emergence of *pmrB* mutations in strain PAO1 submitted to increasing concentrations of tobramycin in addition to other gene alterations (e.g., *fusA1*, *nuoD*), but the role of mutated PmrB proteins in coresistance to aminoglycosides and polymyxins was not investigated further (24). In another study, a concomitant increase in tobramycin (2-fold) and colistin MICs (64-fold) was noted in strain PA14 upon complementation with an A4T/L323H PmrB variant provided by allelic replacement (25).

Our work demonstrates that mutations affecting the histidine kinase PmrB or response regulator PmrA elicit a cross-resistance to these antibiotics in *in vitro*-selected mutants and clinical strains. Alteration of this TCS has been reported to result in a wide range of colistin MICs in *P. aeruginosa* (from 2 to 128 mg/L), due to different levels of operon *arn* activation (4, 10). All the PmrAB variants described here conferred a quite high resistance to colistin

(MIC $\geq$ 16 µg ml^{-1}) when expressed in strain PAO1Δ*pmrAB*, which might suggest that aminoglycoside resistance arises only when the TCS is activated by specific mutations. However, our observation that various amino acid substitutions occurring in different domains of PmrB (Figure 1) and in PmrA provide the same cross-resistance profile does not support this assumption. Furthermore, this phenotype was also observed in mutants selected on lower concentrations of colistin (4 µg ml^{-1} instead of 8 or 16 µg ml^{-1}) (data not shown). Thus, aminoglycoside resistance seems to be a common feature of *pmrAB* mutants.

As highlighted by gene deletion experiments, aminoglycoside resistance of *pmrB* mutants is independent from the LPS modification pathway determined by operon *arn* (i.e., independent from the mechanism of polymyxin resistance), and does not result from constitutive overexpression of genes *mexXY*. Intriguingly, a Q105P change in PmrB increased *mexXY* expression and aminoglycoside resistance (2-fold) in PAO1Δ*pmrAB* as compared with other PmrB variations (Figure S1 and Table 3). This PmrAB-dependent activation of pump MexXY(OprM) remains to be investigated. It could potentially involve ParRS, as cross talks between TCS are common in bacteria to allow adapted stress responses (26). Operon *mexXY* transcription is indeed upregulated when ParRS is activated by mutations or bacterial exposure to colistin (20). Though gene deletion experiments established that this TCS does not mediate aminoglycoside resistance in mutant AB16.2, they have to be done on PAO1Δ*pmrAB*(pAB2243) to rule out any implication of ParRS in *mexXY* dysregulation linked to PmrB Q105P variant.

As stated above, the presence of efflux pump MexXY(OprM) is required for aminoglycoside resistance in *pmrAB* mutants, but genes *mexXY* do not need to be constitutively activated (Figure S1). Since protein synthesis inhibitors induce *mexXY* transcription through the ArmZ/MexZ regulatory pathway when ribosomes stall (27), we envisaged that aminoglycosides could be more stronger inducers of *mexXY* expression in *pmrAB* mutants

than in wild-type bacteria (data not shown). However, deletion of genes PA4773, PA4774 and PA4775 in mutant AB16.2 provided a simpler explanation in line with amounts of several polyamines extracted from the cell surface (Figure 3A). Several lines of evidence suggest that this three gene cluster which is cotranscribed and under the control of *pmrAB* genes is involved in norspermidine biosynthesis. To our knowledge, this linear and flexible aliphatic molecule that carries three amine groups positively charged at physiological pH has never been detected before in *P. aeruginosa*. In contrast to spermidine, a triamine involved in multiple physiological functions, norspermidine is considered as rather uncommon in bacteria except in *Vibrionales* (28). In *Vibrio cholerae*, norspermidine is synthesized from 1,3-diaminopropane through the aspartate β-semialdehyde-dependent pathway involving enzymes carboxyspermidine dehydrogenase (CASDH) and carboxyspermidine decarboxylase (CANSDC) (29) (Figure 5). BLAST searches failed to find evident homologs encoded by the *P. aeruginosa* genome (30). Some bacteria such as the hyperthermophiles *Thermus thermophilus* and *Thermotoga maritima* are able to produce norspermidine through a S-adenosylmethionine-dependent route (31, 32). This pathway relies on the activity of an aminopropyltransferase enzyme able to add an aminopropyl residue from decarboxylated S-adenosylmethionine to various polyamines including 1,3-diaminopropane. This metabolic route is widely used in bacteria to form spermidine from putrescine (31). However, its role in synthesis of other polyamines has been reported only in *T. thermophilus*, and *T. maritima* which produce an aminopropyltransferase enzyme (named triamine/agmatine aminopropyl transferase; TAAPT) able to cope with other substrates than putrescine (33, 34). One explanation for the presence of norspermidine in *P. aeruginosa* might be that the putative enzyme SpeE2 encoded by gene PA4774 promotes the transfer of an aminopropyl residue to 1,3-diaminopropane to form norspermidine (Figure 5). Supporting this hypothesis, we found that, with a sequence identity of 60%, protein PA4774 is the closest homolog of

311 aminopropyltransferase from *T. thermophilus* HB8 (1UIR_A) (34). Additional experiments
312 are necessary to confirm that the substrate specificity of PA4774 includes 1,3-
313 diaminopropane. If correct, this scenario could explain why higher amounts of this metabolite
314 were detected in cell extracts of mutant AB16.2ΔPA4775 as compared with AB.16.2.
315 While norspermidine is strongly overproduced in *pmrAB* mutants through the PA4773-
316 PA4774-PA4775 pathway, spermidine synthesis is also increased to similar levels via another
317 route. The presence of high spermidine amounts at the cell surface was reported to have a
318 protective role against aminoglycosides when bacteria are exposed to an acid environment or
319 to eDNA, through the activation of TCS PmrAB (16). That the decreased resistance of
320 mutants AB16.2ΔPA4773, AB16.2Δ4774 and AB16.2Δ4775 to aminoglycosides correlated
321 with reduced norspermidine levels (while that of spermidine remain almost unchanged)
322 strongly suggest that norspermidine plays the main protective role against these antibiotics in
323 *pmrAB* mutants. An attractive hypothesis supported by some experimental data (16) would be
324 that norspermidine and spermidine inhibit the self-promoted uptake pathway of
325 aminoglycosides through the outer membrane, by reducing the net negative charge of the cell
326 surface. Whether these two structurally-close polyamines individually confer a resistance to
327 specific inhibitors sharing a polycationic structure is an interesting issue that warrants further
328 studies.
329 Mutation-driven activation of PmrAB is associated with therapeutically significant levels of
330 aminoglycoside and polymyxin resistance in *in vitro* mutants, according EUCAST
331 breakpoints (Tables 1 and 3). Consistent with these results, 16 of 17 clinical strains exhibiting
332 a cross-resistance to both antibiotic families turned out to be *pmrAB* mutants. The impaired
333 growth of these bacteria *in vitro*, due to polyamine production, might reduce their ability to
334 cause acute infections. However, their presence in clinical samples evidently shows that their
335 survival in patients is not compromised by mutations in PmrAB.

Materials and Methods

Bacterial strains, plasmids, and growth conditions. Bacterial strains and plasmids used in this study are listed in Table 4. Bacteria were routinely grown in Mueller-Hinton broth (MHB) with adjusted concentrations of divalent cations Ca^{2+} (from 20 to 25 μg ml^{-1}) and Mg^{2+} (from 10 to 12.5 μg ml^{-1}) (Becton, Dickinson and Company, Sparks, MD), or on Mueller-Hinton agar (MHA; Becton, Dickinson and Company, Sparks, MD). Eighteen clinical strains of *P. aeruginosa* isolated between 2015 and 2018 in 14 French hospitals were studied, of which 17 were colistin resistant (MIC >2 μg ml^{-1}). Wild-type reference strain PAO1 (from K. Stover's laboratory) was used to select colistin-resistant mutants and to perform gene complementation experiments. Unless otherwise stated, bacterial cultures were performed at 37°C.

PmrAB mutants were selected by spreading 10^8 colony-forming units (CFU) of log-phase PAO1 cells on MHA plates supplemented with 8 and 16 μg ml^{-1} colistin, respectively. Plasmid vectors were maintained in subcultures of *E. coli* with 50 μg ml^{-1} kanamycin, 15 μg ml^{-1} tetracycline, 100 μg ml^{-1} ampicillin or 50 μg ml^{-1} streptomycin as selection markers. Transconjugants and transformants of *P. aeruginosa* were selected on MHA or *Pseudomonas* Agar Isolation medium (PAI; Becton, Dickinson and Company, Sparks, MD) by using 200 μg ml^{-1} tetracycline, 2,000 μg ml^{-1} streptomycin or 150 μg ml^{-1} ticarcillin. Bacterial growth curves were established in triplicates from freshly diluted cultures in 30 ml of MHB (initial absorbance $A_{600nm} = 0.1$), incubated at 37°C with vigorous shaking. The absorbance was monitored hourly up to 8 h. Standard deviations were calculated at each time point.

Antimicrobial susceptibility testing. The MICs of selected antibiotics were determined by microdilution in MHB and interpreted according to the guidelines of European Committee on Antimicrobial Susceptibility Testing (EUCAST 2018) (http://www.eucast.org).

Transcomplementation of mutant PAO1Δ*pmrAB*. The *pmrAB* loci from strain PAO1, *in vitro*-selected mutants and clinical strains were amplified by PCR from genomic DNA extracts (Wizard genomic DNA purification kit, Promega Corporation, Charbonnières-les-Bains, France) with specific primers PCRpmrAB1 and PCRpmrAB4 (Table S2). The amplicons were first cloned into vector pCR-Blunt. Then, 2,286-bp fragments carrying the *pmrAB* alleles were subcloned into EcoRI-linearised plasmid pME6012 (35). Sequence of cloned alleles was checked on both strands by using specific primers (3130, Genetic Analyzer, Applied Biosystems) (Table S2). Recombinant plasmids were introduced by electrotransformation into mutant PAO1Δ*pmrAB* (36) and the resulting transformants were selected on MHA supplemented with 200 µg ml^{-1} tetracycline.

Complementation with PA4773-PA4774-PA4775 gene cluster. The locus with its promoter region was amplified by PCR from a whole DNA extract of strain PAO1, with primers PCRiPA4773A1 and PCRiPA4775A4 (Table S2). The 3,231-bp amplicon was cloned into vector pCR-Blunt and then subcloned into plasmid mini-CTX1 previously cleaved with endonucleases BamHI/NotI (37). The recombinant plasmid was transferred from *E. coli* CC118 to *P. aeruginosa* strains by conjugation as previously reported (37), and the transconjugants were selected on PAI medium containing 200 µg ml^{-1} tetracycline. Excision of the tetracycline resistance cassette was achieved by expressing recombinase Flp from of plasmid pFLP2. This plasmid which carries levansucrase gene *sacB* was finally cured by growing bacteria on minimal agar medium M9 containing 5% sucrose. Insertion of the PA4773-PA4774-PA4775 fragment in chromosomal site *attB* was confirmed by PCR-sequencing experiments (Table S2).

Construction of deletion mutants in strain PAO1. Gene deletion mutants were obtained by using overlapping PCRs and recombination events, as previously described by Kaniga *et al* (38). Briefly, using the primers indicated in Table S2, the DNA regions flanking the target

386 genes were amplified as single DNA fragments. These fragments were subsequently cloned
387 into plasmid pCR-Blunt and subcloned into suicide vector pKNG101, in *E. coli* CC118λ*pir*
388 (38). The resulting plasmids were introduced into *P. aeruginosa* strains by triparental mating
389 using helper strain *E. coli* HB101(pRK2013) (39). Transconjugants were selected on PAI
390 supplemented with streptomycin 2,000 µg ml^{-1}. Excision of pKNG101 was obtained by
391 selection on M9 minimal agar medium supplemented with 5% sucrose. The deletions were
392 checked by PCR and sequencing using specific primers (Table S2).
393 **RT-qPCR.** Total RNA was extracted and purified (RNeasy plus kit, Qiagen) from cultures of
394 strain PAO1 or its mutants grown to mid-log phase ($A_{600nm} = 0.8$) in MHB, as previously
395 reported by (40). Two µg of RNA extracts treated with DNAse (Qiagen) were reverse
396 transcribed into cDNA with ImpromII reverse transcriptase (RT) according to the
397 manufacturer's recommendations (Promega, Madison, WI). The mRNA amounts of target
398 genes were estimated by real-time quantitative PCR (RT-qPCR) in a Rotor Gene RG6000
399 instrument (Qiagen, Courtaboeuf, France) by using the QuantiFast SYBR Green PCR kit
400 (Qiagen), specific RT-qPCR primers (listed in Table S2) and 1:10 dilution of cDNA as
401 template. Absolute values of gene expression were normalised for each strain with those of
402 housekeeping gene *uvrD*, and expressed as a ratio (fold change) to that of wild-type strain
403 PAO1, used as reference (41). Mean gene expression values were calculated from two
404 independent cultures, each assayed in duplicate.
405 **RNA-Seq transcriptome.** Strain PAO1 and mutant AB16.2 were incubated at 35°C with
406 shaking (250 rpm) in drug-free MHB until an absorbance of $A_{600nm} = 0.8 \pm 0.05$. RNA was
407 extracted from cell pellets (duplicates for each sample) using the RNeasy Mini Kit (Qiagen)
408 in combination with Qiashredder columns (Qiagen). The preparation and sequencing of the
409 cDNA libraries were done as described previously (42). Libraries were sequenced with 50
410 cycles in single end mode on an Illumina HiSeq 2500 device. Computational analysis was

done according to the method reported by Dotsch *et al.*(42), with some modifications. The reads were aligned to the PAO1 reference genome using *stampy* (43).

LC-ESI-MS analysis of cell surface extracts. Overnight cultures in MHB were diluted in fresh medium and grown at 35°C with shaking to mid-log phase (A_{600nm}=0.8). Surface-associated polyamines were extracted as previously described, except that the pellet was resuspended in a final 500 µl volume of buffer (14). Analysis of polyamines was performed on the plateform of BioPark (Archamps Technopole, France) from 100 µl of bacterial extract added to 90 µl of N-(succinimidyloxycarbonylmethyl)tris (2,4,6-trimethoxyphenyl)phosphonium bromide 20 mM (TMPP, Sigma-Aldrich, Saint Louis, MO). The primary amines were labelled with TMPP, which is known to make amines more amenable to detection by mass spectrometry by improving the molecules ionization in the electrospray. Addition of TMPP increased the mass of 572.18 Da to the nominal mass of any molecule with a primary or secondary amine. The mixture was incubated one hour at room temperature and the reaction was stopped by addition of 150 µL of NH_4OH (1 M). After 30 min of incubation at room temperature, 160 µl of trifluoroacetic acid (TFA) (10%) were added, and the samples were desalted by a solid phase extraction (SPE) (Omics bond elut C18 100 µl tip, Waters) according to the manufacturer's protocol. Amines were eluted using 50 µl of mix containing 60% acetonitrile and 0.1% of TFA, and dried down by speed-vacuum. The pellet was re-suspended in 20 µl of 2% ACN and 0.1% TFA, and 2 µl of the mixture were loaded on a standard reverse-phase chromatography column using an Ultimate 300 nanoflow high performance liquid chromatography system coupled to a Q-Exactive Orbitrap with a 75µm x 150 mm Acclaim Pepmap 100, C18, 3 µm nanoviper column (Thermo Scientific, Bremen, Germany). The amines were eluted by a gradient from 2 to 35% ACN in 0.1% (v/v) formic acid, and subsequently from 35 to 85% over a period of 35 min. Then, the amines were detected by a mass spectrometer connected at the column exit to an electrospray ionization

interface (ES-MS). The Q-Exactive Orbitrap acquired a full-range scan from 310 to 2 000 Th (70,000 resolution, AGC target 3.10^6, maximum IT 200 ms). An equimolar mix of 1,3-diaminopropane, putrescine dihydrochloride, cadaverine, norspermidine, spermidine and spermine was analysed in similar conditions and used as standard. Extracted ions chromatograms were used to identify the m/z ions expected for the TMPP amines. Areas under the peaks were collected to compare the amounts of amines in different strains.

Statistical analysis

The reported gene read counts were used to estimate differential gene expression between mutant AB16.2 and PAO1, making use of package DESeq in R (Project for statistical computing). Comparison of polyamine levels were performed using R software (v 3.3.3). The three independent replicates were normalised to remove block effects and then $\log_{10}$ transformed. For each polyamine and strain tested, an Anova test was applied. Statistically significant ($p<0.05$) differences between the strains were checked with a tukey HSD test.

Acknowledgments.

We are grateful to Loïs Andrey for his excellent technical assistance. This work was supported by the French ministry of Health through the Santé publique France agency.

References

1. Luyt CE, Hekimian G, Koulenti D, Chastre J. 2018. Microbial cause of ICU-acquired pneumonia: hospital-acquired pneumonia versus ventilator-associated pneumonia. Curr Opin Crit Care 24:332-338.

2. Del Barrio-Tofino E, Lopez-Causape C, Cabot G, Rivera A, Benito N, Segura C, Montero MM, Sorli L, Tubau F, Gomez-Zorrilla S, Tormo N, Dura-Navarro R, Viedma E, Resino-Foz E, Fernandez-Martinez M, Gonzalez-Rico C, Alejo-Cancho I, Martinez JA, Labayru-Echverria C, Duenas C, Ayestaran I, Zamorano L, Martinez-Martinez L, Horcajada JP, Oliver A. 2017. Genomics and Susceptibility Profiles of Extensively Drug-Resistant *Pseudomonas aeruginosa* Isolates from Spain. Antimicrob Agents Chemother 62.pii: e01589-17.

3. Sader HS, Huband MD, Castanheira M, Flamm RK. 2017. *Pseudomonas aeruginosa* antimicrobial susceptibility results from four years (2012 to 2015) of the international network for optimal resistance monitoring program in the United States. Antimicrob Agents Chemother 61(3). pii: e02252-16.

4. Moskowitz SM, Ernst RK, Miller SI. 2004. PmrAB, a two-component regulatory system of *Pseudomonas aeruginosa* that modulates resistance to cationic antimicrobial peptides and addition of aminoarabinose to lipid A. J Bacteriol 186:575-579.

5. Nummila K, Kilpelainen I, Zahringer U, Vaara M, Helander IM. 1995. Lipopolysaccharides of polymyxin B-resistant mutants of *Escherichia coli* are extensively substituted by 2-aminoethyl pyrophosphate and contain aminoarabinose in lipid A. Mol Microbiol 16:271-278.

6. Jeannot K, Bolard A, Plésiat P. 2017. Resistance to polymyxins in Gram-negative organisms. Int J Antimicrob Agents 49:526-535.

7. Abraham N, Kwon DH. 2009. A single amino acid substitution in PmrB is associated with polymyxin B resistance in clinical isolate of *Pseudomonas aeruginosa*. FEMS Microbiol Lett 298:249-254.

8. Barrow K, Kwon DH. 2009. Alterations in two-component regulatory systems of phoPQ and pmrAB are associated with polymyxin B resistance in clinical isolates of *Pseudomonas aeruginosa*. Antimicrob Agents Chemother 53:5150-5154.

9. Schurek KN, Sampaio JL, Kiffer CR, Sinto S, Mendes CM, Hancock RE. 2009. Involvement of pmrAB and phoPQ in polymyxin B adaptation and inducible resistance in non-cystic fibrosis clinical isolates of *Pseudomonas aeruginosa*. Antimicrob Agents Chemother 53:4345-4351.

10. Moskowitz SM, Brannon MK, Dasgupta N, Pier M, Sgambati N, Miller AK, Selgrade SE, Miller SI, Denton M, Conway SP, Johansen HK, Hoiby N. 2012. PmrB mutations promote polymyxin resistance of *Pseudomonas aeruginosa* isolated from colistin-treated cystic fibrosis patients. Antimicrob Agents Chemother 56:1019-1030.

11. Miller AK, Brannon MK, Stevens L, Johansen HK, Selgrade SE, Miller SI, Hoiby N, Moskowitz SM. 2011. PhoQ mutations promote lipid A modification and polymyxin resistance of *Pseudomonas aeruginosa* found in colistin-treated cystic fibrosis patients. Antimicrob Agents Chemother 55:5761-5769.

12. Sautrey G, Zimmermann L, Deleu M, Delbar A, Souza Machado L, Jeannot K, Van Bambeke F, Buyck JM, Decout JL, Mingeot-Leclercq MP. 2014. New amphiphilic neamine derivatives active against resistant *Pseudomonas aeruginosa* and their interactions with lipopolysaccharides. Antimicrob Agents Chemother 58:4420-4430.

13. Lee JY, Ko KS. 2014. Mutations and expression of PmrAB and PhoPQ related with colistin resistance in *Pseudomonas aeruginosa* clinical isolates. Diagn Microbiol Infect Dis 78:271-276.

14. Johnson L, Mulcahy H, Kanevets U, Shi Y, Lewenza S. 2012. Surface-localized spermidine protects the *Pseudomonas aeruginosa* outer membrane from antibiotic treatment and oxidative stress. J Bacteriol 194:813-826.

15. McPhee JB, Bains M, Winsor G, Lewenza S, Kwasnicka A, Brazas MD, Brinkman FS, Hancock RE. 2006. Contribution of the PhoP-PhoQ and PmrA-PmrB two-component

regulatory systems to Mg2+-induced gene regulation in *Pseudomonas aeruginosa*. J Bacteriol 188:3995-4006.

16. Wilton M, Charron-Mazenod L, Moore R, Lewenza S. 2016. Extracellular DNA acidifies biofilms and induces aminoglycoside resistance in *Pseudomonas aeruginosa*. Antimicrob Agents Chemother 60:544-553.

17. McPhee JB, Lewenza S, Hancock RE. 2003. Cationic antimicrobial peptides activate a two-component regulatory system, PmrA-PmrB, that regulates resistance to polymyxin B and cationic antimicrobial peptides in *Pseudomonas aeruginosa*. Mol Microbiol 50:205-217.

18. Winsor GL, Griffiths EJ, Lo R, Dhillon BK, Shay JA, Brinkman FS. 2016. Enhanced annotations and features for comparing thousands of *Pseudomonas* genomes in the *Pseudomonas* genome database. Nucleic Acids Res 44:D646-653.

19. Li XZ, Plésiat P, Nikaido H. 2015. The challenge of efflux-mediated antibiotic resistance in Gram-negative bacteria. Clin Microbiol Rev 28:337-418.

20. Muller C, Plésiat P, Jeannot K. 2011. A two-component regulatory system interconnects resistance to polymyxins, aminoglycosides, fluoroquinolones, and beta-lactams in *Pseudomonas aeruginosa*. Antimicrob Agents Chemother 55:1211-1221.

21. Aires JR, Köhler T, Nikaido H, Plésiat P. 1999. Involvement of an active efflux system in the natural resistance of *Pseudomonas aeruginosa* to aminoglycosides. Antimicrob Agents Chemother 43:2624-2628.

22. Masuda N, Sakagawa E, Ohya S, Gotoh N, Tsujimoto H, Nishino T. 2000. Contribution of the MexX-MexY-OprM efflux system to intrinsic resistance in *Pseudomonas aeruginosa*. Antimicrob Agents Chemother 44:2242-2246.

23. Qu L, She P, Wang Y, Liu F, Zhang D, Chen L, Luo Z, Xu H, Qi Y, Wu Y. 2016. Effects of norspermidine on *Pseudomonas aeruginosa* biofilm formation and eradication. Microbiologyopen 5:402-412.

24. Lopez-Causape C, Rubio R, Cabot G, Oliver A. 2018. Evolution of the *Pseudomonas aeruginosa* aminoglycoside mutational resistome *in vitro* and in the cystic fibrosis setting. Antimicrob Agents Chemother 62.pii: e02583-17.

25. Schniederjans M, Koska M, Haussler S. 2017. Transcriptional and mutational profiling of an aminoglycoside-resistant *Pseudomonas aeruginosa* small-colony variant. Antimicrob Agents Chemother 61.pii: e01178-17.

26. Agrawal R, Sahoo BK, Saini DK. 2016. Cross-talk and specificity in two-component signal transduction pathways. Future Microbiol 11:685-697.

27. Jeannot K, Sobel ML, El Garch F, Poole K, Plésiat P. 2005. Induction of the MexXY efflux pump in *Pseudomonas aeruginosa* is dependent on drug-ribosome interaction. J Bacteriol 187:5341-5346.

28. Hamana K. 1997. Polyamine distribution patterns within the families *Aeromonadaceae*, *Vibrionaceae*, *Pasteurellaceae*, and H*alomonadaceae*, and related genera of the gamma subclass of the *Proteobacteria*. J Gen Appl Microbiol 43:49-59.

29. Lee J, Sperandio V, Frantz DE, Longgood J, Camilli A, Phillips MA, Michael AJ. 2009. An alternative polyamine biosynthetic pathway is widespread in bacteria and essential for biofilm formation in *Vibrio cholerae*. J Biol Chem 284:9899-9907.

30. Stover CK, Pham XQ, Erwin AL, Mizoguchi SD, Warrener P, Hickey MJ, Brinkman FSL, Hufnagle WO, Kowalik DJ, Lagrou M, Garber RL, Goltry L, Tolentino E, Westbrock-Wadman S, Yuan Y, Brody LL, Coulter SN, Folger KR, Kas A, Larbig K, Lim R, Smith K, Spencer D, Wong GK-S, Wu Z, Paulsen IT, Reizer J, Saier MH, Hancock REW, Lory S, Olson MV. 2000. Complete genome sequence of *Pseudomonas aeruginosa* PAO1, an opportunistic pathogen. Nature 406:959-964.

31. Michael AJ. 2016. Biosynthesis of polyamines and polyamine-containing molecules. Biochem J 473:2315-2329.

32. Michael AJ. 2016. Polyamines in Eukaryotes, Bacteria, and Archaea. J Biol Chem 291:14896-14903.

572 33. Korolev S, Ikeguchi Y, Skarina T, Beasley S, Arrowsmith C, Edwards A, Joachimiak A, Pegg
573 AE, Savchenko A. 2002. The crystal structure of spermidine synthase with a multisubstrate
574 adduct inhibitor. Nat Struct Biol 9:27-31.
575 34. Ohnuma M, Ganbe T, Terui Y, Niitsu M, Sato T, Tanaka N, Tamakoshi M, Samejima K,
576 Kumasaka T, Oshima T. 2011. Crystal structures and enzymatic properties of a
577 triamine/agmatine aminopropyltransferase from Thermus thermophilus. J Mol Biol 408:971-
578 986.
579 35. Heeb S, Itoh Y, Nishijyo T, Schnider U, Keel C, Wade J, Walsh U, O'Gara F, Haas D. 2000.
580 Small, stable shuttle vectors based on the minimal pVS1 replicon for use in Gram-negative,
581 plant-associated bacteria. Mol Plant Microbe Interact 13:232-237.
582 36. Choi KH, Kumar A, Schweizer HP. 2006. A 10-min method for preparation of highly
583 electrocompetent *Pseudomonas aeruginosa* cells: application for DNA fragment transfer
584 between chromosomes and plasmid transformation. J Microbiol Methods 64:391-397.
585 37. Hoang TT, Kutchma AJ, Becher A, Schweizer HP. 2000. Integration-proficient plasmids for
586 *Pseudomonas aeruginosa*: site-specific integration and use for engineering of reporter and
587 expression strains. Plasmid 43:59-72.
588 38. Kaniga K, Delor I, Cornelis GR. 1991. A wide-host-range suicide vector for improving
589 reverse genetics in Gram-negative bacteria: inactivation of the *bla*A gene of *Yersinia*
590 *enterocolitica*. Gene 109:137-141.
591 39. Ditta G, Stanfield S, Corbin D, Helinski DR. 1980. Broad host range DNA cloning system for
592 Gram-negative bacteria: construction of a gene bank of *Rhizobium meliloti*. Proc Natl Acad
593 Sci U S A 77:7347-7351.
594 40. Dumas JL, van Delden C, Perron K, Köhler T. 2006. Analysis of antibiotic resistance gene
595 expression in *Pseudomonas aeruginosa* by quantitative real-time-PCR. FEMS Microbiol Lett
596 254:217-225.
597 41. Jo JT, Brinkman FS, Hancock RE. 2003. Aminoglycoside efflux in *Pseudomonas aeruginosa*:
598 involvement of novel outer membrane proteins. Antimicrob Agents Chemother 47:1101-1111.

42. Dotsch A, Eckweiler D, Schniederjans M, Zimmermann A, Jensen V, Scharfe M, Geffers R, Haussler S. 2012. The *Pseudomonas aeruginosa* transcriptome in planktonic cultures and static biofilms using RNA sequencing. PLoS One 7:e31092.

43. Lunter G, Goodson M. 2011. Stampy: a statistical algorithm for sensitive and fast mapping of Illumina sequence reads. Genome Res 21:936-939.

44. Manoil C, Beckwith J. 1985. TnphoA: a transposon probe for protein export signals. Proc Natl Acad Sci U S A 82:8129-8133.

45. Herrero M, de Lorenzo V, Timmis KN. 1990. Transposon vectors containing non-antibiotic resistance selection markers for cloning and stable chromosomal insertion of foreign genes in gram-negative bacteria. J Bacteriol 172:6557-6567.

46. Lacks S, Greenberg B. 1977. Complementary specificity of restriction endonucleases of *Diplococcus pneumoniae* with respect to DNA methylation. J Mol Biol 114:153-168.

47. Guénard S, Muller C, Monlezun L, Benas P, Broutin I, Jeannot K, Plésiat P. 2014. Multiple mutations lead to MexXY-OprM-dependent aminoglycoside resistance in clinical strains of *Pseudomonas aeruginosa*. Antimicrob Agents Chemother 58:221-228.

48. Hoang TT, Karkhoff-Schweizer RR, Kutchma AJ, Schweizer HP. 1998. A broad-host-range Flp-FRT recombination system for site-specific excision of chromosomally-located DNA sequences: application for isolation of unmarked *Pseudomonas aeruginosa* mutants. Gene 212:77-86.

TABLE 1. Effects of *pmrB* mutations on antibiotic susceptibility.

Strain	Plasmid	Protein PmrB [b]	MIC (μg ml^{-1}) [a]							
			CST	GEN	AMK	TOB	TCC	CAZ	IPM	CIP
PAO1	-	wild-type	0.5	1	2	0.25	16	2	1	0.12
AB8.2	-	V28G	**128**	**8**	**8**	**2**	4	1	0.5	0.25
AB16.1	-	F408L	**128**	**8**	**8**	**2**	16	2	1	0.12
AB16.2	-	ΔL172	**128**	**8**	**8**	**2**	8	1	0.5	0.12
PAO1Δ*pmrAB*	-	Δ	0.5	1	2	0.25	16	2	1	0.12
PAO1Δ*pmrAB*	pME6012	-	0.5	1	2	0.25	16	2	1	0.12
PAO1Δ*pmrAB*	pABWT	wild-type	0.5	1	2	0.25	16	2	1	0.12
PAO1Δ*pmrAB*	pAB8.2	V28G	**128**	**8**	**8**	**2**	8	1	0.5	0.25
PAO1Δ*pmrAB*	pAB16.1	F408L	**128**	**8**	**8**	**2**	8	1	0.5	0.25
PAO1Δ*pmrAB*	pAB16.2	ΔL172	**128**	**8**	**8**	**2**	8	1	0.5	0.25

[a] The MIC data are representative of three independent experiments. Values in bold are at least 4-fold higher than those of strain PAO1.

[b] Amino acid sequence refers to PmrB protein of strain PAO1.

CST, colistin; GEN, gentamicin; AMK, amikacin; TOB, tobramycin; TCC, ticarcillin (plus clavulanic acid at a fixed concentration of 2 μg ml^{-1}); CAZ, ceftazidime; IPM, imipenem; CIP, ciprofloxacin.

627 **TABLE 2.** Drug susceptibility of PAO1 and derived mutants.

Strain	Gene deletion	MIC (μg ml^{-1}) [a]			
		CST	GEN	AMK	TOB
PAO1	-	0.5	1	2	0.25
	pmrA	0.5	1	2	0.25
	pmrB	0.5	1	2	0.25
	arn	0.5	1	2	0.25
	parRS	0.25	1	2	0.25
	mexXY	0.5	0.06	0.5	0.125
AB16.2	-	**64**	**8**	**8**	**2**
	pmrA	0.5	1	2	0.25
	pmrB	0.5	1	2	0.25
	arn	1	**8**	**8**	**2**
	parRS	**4**	**8**	**8**	**2**
	mexXY	**4**	0.06	0.25	0.06

628

629 [a] Values in bold (underlined) are at least 4-fold higher (lower) than those of strain PAO1.

630 CST, colistin; GEN, gentamicin; AMK, amikacin; TOB, tobramycin.

631

632 **TABLE 3**. Effects of *pmrB* mutations on susceptibility of *P. aeruginosa* clinical strains to
633 colistin and aminoglycosides.

Strain (plasmid)	Sequence variation(s) in protein PmrB [a]	MIC (μg ml^{-1}) [b]			
		CST	GEN	AMK	TOB
Clinical strains					
543	S2P, A4T, G68S, **G86V**, Y345H, **G362S**	**8**	**>256**	**>256**	**>256**
2243	**Q105P**, Y345H	**128**	**>256**	**>256**	**>256**
2739	S2P, A4T, **V6A**, V15I, G68S, **V264A,** Y345H	**16**	**>256**	**>256**	**>256**
3038	**D47N**, Y345H	**64**	**4**	**8**	**16**
3091	S2P, A4T, **V6A**, V15I, G68S, Y345H	**128**	**>256**	**32**	**>256**
3092	S2P, A4T, **V6A**, V15I, **L37P**, G68S, Y345H	**128**	**>256**	**128**	**>256**
3795	**G188D**, Y345H	**128**	**8**	**32**	**2**
3890	S2P, A4T, **D45E**, Y345H	**>128**	**4**	**32**	**2**
3921	Y345H	**>128**	**>256**	**>256**	**>256**
4536	**V136E,** Y345H	**4**	**>256**	**8**	**16**
4586	Y345H	**64**	**32**	**>256**	**64**
4660	**G121P, V313A**, Y345H	**64**	**16**	**64**	**>256**
4782	S2P, A4T, V15I, **H33Y**, G68S, Y345H	**4**	**4**	**64**	**64**
5058	S2P, A4T, **D45N**, G68S, Y345H, **G362S**	**4**	**>256**	**16**	**32**
5071	**F168L**, Y345H	**16**	**4**	**16**	**>256**
5101	**R92H**, **G123S**, Y345H	**32**	**>256**	**>256**	**>256**
5115	**R92H**, **G123S**, Y345H	**16**	**4**	**16**	**64**
3095	S2P, A4T, **V6A**, V15I, G68S, Y345H	1	1	2	0.25
PAO1 constructs					
PAO1	-	0.5	1	2	0.25
PAO1Δ*pmrAB*	-	0.5	1	2	0.25
PAO1Δ*pmrAB*(pAB2243)	**Q105P**, Y345H	**128**	**16**	**32**	**4**
PAO1Δ*pmrAB*(pAB3092)	S2P, A4T, **V6A**, V15I, **L37P**, G68S, Y345H	**128**	**8**	**8**	**2**
PAO1Δ*pmrAB*(pAB3795)	**G188D**, Y345H	**128**	**8**	**8**	**2**
PAO1Δ*pmrAB*(pAB3890)	S2P, A4T, **D45E**, Y345H	**16**	**4**	**8**	**2**
PAO1Δ*pmrAB*(pAB3095)	S2P, A4T, **V6A**, V15I, G68S, Y345H	0.5	1	2	0.25

634

635 [a] The PmrB sequence of reference strain PAO1 was used as reference. The amino acid
636 changes highlighted in boldface are absent from strains PAO1, PA14 and LESB58.
637 [b] MIC values are representative of three independent experiments. Values in bold are at least
638 fourfold higher than those of strain PAO1 or its mutant PAO1Δ*pmrAB*.
639 CST, colistin; GEN, gentamicin; AMK, amikacin; TOB, tobramycin.
640

641 **TABLE 4**. Strains and plasmids used in the study.

Strain or plasmid	Relevant characteristics	Source or reference
Strains		
E. coli		
DH5α	F$^-$ Φ80*lac*ZΔM15 Δ(*lacZYA-argF*) U169 *recA1 endA1 hsdR17*(r_k^-, m_k^+) *phoA supE44 thi*-1 *gyrA96 relA1* λ^-	Invitrogen
CC118	Δ(*ara-leu*) *araD* Δ*lac*X74 *galE galK phoA20 thi-1 rpsE rpoB argE*(Am) *recAl*	(44)
CC118 λ*pir*	CC118 lysogenized with λ*pir* phage	(45)
HB101	*supE44 hsdS20*(r_B^-, m_B^-) *recA13 ara-14 proA2 lacY1 galK2 rpsL20 xyl-5 mtl-1 leuB6 thi-1*	(46)
P. aeruginosa		
PAO1	Wild-type reference strain	(30)
AB8.2	PAO1 spontaneous *pmrB* mutant (V28G)	This study
AB16.1	PAO1 spontaneous *pmrB* mutant (F408L)	This study
AB16.2	PAO1 spontaneous *pmrB* mutant (ΔL172)	This study
PAO1Δ*pmrB*	PAO1 with in-frame deletion of gene *pmrB*	This study
PAO1Δ*pmrA*	PAO1 with in-frame deletion of gene *pmrA*	This study
PAO1Δ*pmrAB*	PAO1 with in-frame deletion of operon *pmrAB*	(20)
PAO1ΔPA4773	PAO1 with in-frame deletion of gene PA4773	This study
PAO1ΔPA4774	PAO1 with in-frame deletion of gene PA4774	This study
PAO1ΔPA4775	PAO1 with in-frame deletion of gene PA4775	This study
PAO1Δ*arn*	PAO1 with in-frame deletion of operon *arnBCADTEF-ugd* (*arn*)	This study
PAO1Δ*mexXY*	PAO1 with in-frame deletion of operon *mexXY*	(47)
PAO1Δ*parRS*	PAO1 with in-frame deletion of operon *parRS*	(20)
AB16.2Δ*pmrB*	AB16.2 with in-frame deletion of gene *pmrB*	This study
AB16.2Δ*pmrA*	AB16.2 with in-frame deletion of gene *pmrA*	This study
AB16.2ΔPA4773	AB16.2 with in-frame deletion of gene PA4773	This study
AB16.2ΔPA4774	AB16.2 with in-frame deletion of gene PA4774	This study
AB16.2ΔPA4775	AB16.2 with in-frame deletion of gene PA4775	This study
AB16.2Δ*arn*	AB16.2 with in-frame deletion of operon *arnBCADTEF-ugd* (*arn*)	This study
AB16.2Δ*mexXY*	AB16.2 with in-frame deletion of operon *mexXY*	This study
AB16.2Δ*parRS*	AB16.2 with in-frame deletion of operon *parRS*	This study
AB16.2ΔPA4773::73-75	AB16.2ΔPA4773 complemented with PA4773 to PA4775 locus	This study
AB16.2ΔPA4774::73-75	AB16.2ΔPA4774 complemented with PA4773 to PA4775 locus	This study
AB16.2ΔPA4775::73-75	AB16.2ΔPA4775 complemented with PA4773 to PA4775 locus	This study

Plasmids

pKNG101	Marker exchange suicide vector in *P. aeruginosa*; *sac*BR *mob*RK2 *ori*R6K; Str^r	(38)
pRK2013	Helper plasmid for mobilization of non-self-transmissible plasmids; ColE1 Tra^+ Mob^+; Kan^r	(39)
pCR-Blunt	Blunt-end cloning vector; *ccdB lacZ*α; Zeo^r Kan^r	Life technologies
pME6012	Broad host-range expression plasmid; Tet^r	(35)
mini-CTX1	Self-proficient integration vector, Ω-FRT-*attP*-MCS, *ori*, *int*, *oriT*; Tet^r	(37)
pFLP2	Source of FLP recombinase; Tic^r	(48)
pABWT	pME6012 carrying genes *pmrAB* from strain PAO1	This study
pAB8.2	pME6012 carrying genes *pmrAB* from mutant 8.2	This study
pAB16.1	pME6012 carrying genes *pmrAB* from mutant 16.1	This study
pAB16.2	pME6012 carrying genes *pmrAB* from mutant 16.2	This study
pAB2243	pME6012 carrying genes *pmrAB* from strain 2243	This study
pAB3092	pME6012 carrying genes *pmrAB* from strain 3092	This study
pAB3795	pME6012 carrying genes *pmrAB* from strain 3795	This study
pAB3890	pME6012 carrying genes *pmrAB* from strain 3890	This study
pAB3095	pME6012 carrying genes *pmrAB* from strain 3095	This study
pAB3091	pME6012 carrying genes *pmrAB* from strain 3091	This study
pKNGΔ*pmrAB*	BamHI/ApaI 1,028-kb fragment composed of sequences flanking the 5' and 3' ends of *pmrAB*, cloned in pKNG101	(20)
pKNGΔ*pmrB*	BamHI/XbaI 1,074-kb fragment composed of sequences flanking the 5' and 3' ends of *pmrB*, cloned in pKNG101	This study
pKNGΔ*pmrA*	ApaI 851-bp fragment composed of sequences flanking the 5' and 3' ends of *pmrA*, cloned in pKNG101	This study
pKNGΔPA4773	BamHI/ApaI 1,045-kb fragment composed of sequences flanking the 5' and 3' ends of PA4773, cloned in pKNG101	This study
pKNGΔPA4774	BamHI/ApaI 1,070-kb fragment composed of sequences flanking the 5' and 3' ends of PA4774, cloned in pKNG101	This study
pKNGΔPA4775	BamHI/ApaI 1,027-kb fragment composed of sequences flanking the 5' and 3' ends of PA4775, cloned in pKNG101	This study
pKNGΔ*arn*	BamHI/ApaI 1,135-kb fragment composed of sequences flanking the 5' and 3' ends of *arnBCADTEF-ugd (arn)*, cloned in pKNG101	This study
pKNGΔ*mexXY*	BamHI/ApaI 1,756-kb fragment composed of sequences	(47)

	flanking the 5’ and 3’ ends of *mexXY*, cloned in pKNG101	
pKNGΔ*parRS*	ApaI 1,045-kb fragment composed of sequences the flanking 5’ and 3’ ends of *parRS*, cloned in pKNG101	(20)
mini-CTX::*PA4773-75*	PA4773 to PA4775 locus cloned in mini-CTX1 at sites BamHI/NotI	This study

642 Str^r, marker of streptomycin resistance; Kan^r, kanamycin resistance; Zeo^r, zeocin resistance; Tet^r,

643 tetracycline resistance; Tic^r, ticarcillin resistance.

TABLE S1 PmrB-dependent genes

PA number[a]	Gene name	Description	Fold change[b]
PA0007	-	hypothetical protein	*-3,36*
PA0036	*trpB*	tryptophan synthase beta chain	3,29
PA0050	-	hypothetical protein	5,20
PA0112	-	hypothetical protein	*-7,20*
PA0122	*rahU*	rahU	8,23
PA0165	-	hypothetical protein	*-4,03*
PA0224	-	probable aldolase	*-5,45*
PA0251	-	hypothetical protein	*-11,35*
PA0447	*gcdH*	glutaryl-CoA dehydrogenase	3,56
PA0453	-	hypothetical protein	*-6,06*
PA0546	*metK*	methionine adenosyltransferase	8,50
PA0547	-	probable transcriptional regulator	9,87
PA0572	-	hypothetical protein	3,48
PA0612	*ptrB*	repressor; PtrB	3,19
PA0613	-	hypothetical protein	3,02
PA0615	-	hypothetical protein	3,30
PA0617	-	probable bacteriophage protein	3,03
PA0618	-	probable bacteriophage protein	3,35
PA0619	-	probable bacteriophage protein	3,12
PA0620	-	probable bacteriophage protein	3,84
PA0621	-	conserved hypothetical protein	3,97
PA0622	-	probable bacteriophage protein	3,82
PA0623	-	probable bacteriophage protein	4,47
PA0624	-	hypothetical protein	3,59
PA0625	-	hypothetical protein	3,22
PA0626	-	hypothetical protein	3,33
PA0630	-	hypothetical protein	3,73
PA0633	-	hypothetical protein	3,53
PA0634	-	hypothetical protein	3,76
PA0635	-	hypothetical protein	3,09
PA0638	-	probable bacteriophage protein	3,23
PA0640	-	probable bacteriophage protein	3,00
PA0641	-	probable bacteriophage protein	3,11
PA0642	-	hypothetical protein	3,80
PA0643	-	hypothetical protein	3,64
PA0644	-	hypothetical protein	3,51
PA0645	-	hypothetical protein	3,33
PA0646	-	hypothetical protein	3,40
PA0647	-	hypothetical protein	3,21
PA0713	-	hypothetical protein	3,67
PA0744	-	probable enoyl-CoA hydratase/isomerase	3,76
PA0746	-	probable acyl-CoA dehydrogenase	3,89
PA0747	-	probable aldehyde dehydrogenase	3,11
PA0751	-	conserved hypothetical protein	*-5,53*
PA0752	-	conserved hypothetical protein	*-3,97*
PA0753	-	hypothetical protein	*-4,60*
PA0754	-	hypothetical protein	*-3,21*
PA0755	*opdH*	cis-aconitate porin OpdH	*-3,25*
PA0796	*prpB*	carboxyphosphonoenolpyruvate phosphonomutase	3,08
PA0805	-	hypothetical protein	3,05
PA0852	*cbpD*	chitin-binding protein CbpD precursor	10,05

PA0924	-	hypothetical protein	*-3,52*
PA0996	*pqsA*	PqsA	24,83
PA0997	*pqsB*	PqsB	23,79
PA0998	*pqsC*	PqsC	17,25
PA0999	*pqsD*	3-oxoacyl-[acyl-carrier-protein] synthase III	17,73
PA1000	*pqsE*	Quinolone signal response protein	25,31
PA1001	*phnA*	anthranilate synthase component I	26,07
PA1002	*phnB*	anthranilate synthase component II	12,84
PA1041	-	probable outer membrane protein precursor	3,58
PA1123	-	hypothetical protein	4,02
PA1245	*aprX*	AprX	4,87
PA1249	*aprA*	alkaline metalloproteinase precursor	3,38
PA1250	*aprI*	alkaline proteinase inhibitor AprI	3,47
PA1395	-	hypothetical protein	*-3,06*
PA1431	*rsaL*	regulatory protein RsaL	5,68
PA1435	-	probable Resistance-Nodulation-Cell Division (RND) efflux membrane fusion protein precursor	*-5,19*
PA1555	*ccoP2*	Cytochrome c oxidase; cbb3-type; CcoP subunit	3,35
PA1555.1	*ccoQ2*	Cytochrome c oxidase; cbb3-type; CcoQ subunit	3,09
PA1556	*ccoO2*	Cytochrome c oxidase; cbb3-type; CcoO subunit	3,45
PA1557	*ccoN2*	Cytochrome c oxidase; cbb3-type; CcoN subunit	5,17
PA1559	-	hypothetical protein	143,34
PA1560	-	hypothetical protein	77,73
PA1568	-	conserved hypothetical protein	*-8,96*
PA1656	*hsiA2*	HsiA2	7,24
PA1657	*hsiB2*	HsiB2	6,96
PA1658	*hsiC2*	HsiC2	5,36
PA1659	*hsiF2*	HsiF2	5,16
PA1660	*hsiG2*	HsiG2	4,40
PA1662	*clpV2*	ClpV2	4,22
PA1663	*sfa2*	Sfa2	3,24
PA1665	*fha2*	Fha2	4,69
PA1666	*lip2*	Lip2	4,52
PA1667	*hsiJ2*	HsiJ2	3,16
PA1668	*dotU2*	DotU2	4,26
PA1669	*icmF2*	IcmF2	3,14
PA1869	-	probable acyl carrier protein	16,09
PA1871	*lasA*	LasA protease precursor	5,48
PA1899	*phzA2*	probable phenazine biosynthesis protein	4,57
PA1901	*phzC2*	phenazine biosynthesis protein PhzC	9,14
PA1902	*phzD2*	phenazine biosynthesis protein PhzD	15,29
PA1903	*phzE2*	phenazine biosynthesis protein PhzE	6,34
PA1904	*phzF2*	probable phenazine biosynthesis protein	7,93
PA1905	*phzG2*	probable pyridoxamine 5'-phosphate oxidase	9,98
PA2012	*liuD*	methylcrotonyl-CoA carboxylase; alpha-subunit (biotin-containing)	3,43
PA2013	*liuC*	putative 3-methylglutaconyl-CoA hydratase	4,10
PA2014	*liuB*	methylcrotonyl-CoA carboxylase; beta-subunit	3,58
PA2015	*liuA*	putative isovaleryl-CoA dehydrogenase	4,87
PA2016	*liuR*	regulator of liu genes	4,51
PA2069	-	probable carbamoyl transferase	4,63
PA2124	-	probable dehydrogenase	*-7,34*
PA2193	*hcnA*	hydrogen cyanide synthase HcnA	46,74
PA2194	*hcnB*	hydrogen cyanide synthase HcnB	16,84
PA2195	*hcnC*	hydrogen cyanide synthase HcnC	12,14
PA2205	-	hypothetical protein	*-4,07*
PA2248	*bkdA2*	2-oxoisovalerate dehydrogenase (beta subunit)	3,06
PA2252	-	probable AGCS sodium/alanine/glycine symporter	*-5,11*

PA2265	-	gluconate dehydrogenase	*-3,19*
PA2288	-	hypothetical protein	3,30
PA2300	*chiC*	chitinase	3,83
PA2302	*ambE*	AmbE	3,65
PA2305	*ambB*	AmbB	3,83
PA2321	*gntK*	GntK	*-5,19*
PA2322	*gntP*	GntP	*-6,04*
PA2329	-	probable ATP-binding component of ABC transporter	5,25
PA2330	-	hypothetical protein	4,40
PA2349	-	conserved hypothetical protein	*-9,43*
PA2381	-	hypothetical protein	7,23
PA2386	*pvdA*	L-ornithine N5-oxygenase	4,88
PA2396	*pvdF*	pyoverdine synthetase F	3,29
PA2423	-	hypothetical protein	4,19
PA2426	*pvdS*	sigma factor PvdS	4,41
PA2442	*gcvT2*	glycine cleavage system protein T2	3,02
PA2443	*sdaA*	L-serine dehydratase	3,14
PA2445	*gcvP2*	glycine cleavage system protein P2	3,60
PA2477	-	probable thiol:disulfide interchange protein	4,00
PA2552	-	probable acyl-CoA dehydrogenase	3,17
PA2553	-	probable acyl-CoA thiolase	6,85
PA2554	-	probable short-chain dehydrogenase	4,87
PA2563	-	probable sulfate transporter	*-5,21*
PA2587	*pqsH*	probable FAD-dependent monooxygenase	4,78
PA2588	-	probable transcriptional regulator	3,92
PA2591	*vqsR*	VqsR	4,35
PA2592	-	probable periplasmic spermidine/putrescine-binding protein	3,30
PA2622	*cspD*	cold-shock protein CspD	4,35
PA2659	-	hypothetical protein	3,86
PA2761	-	hypothetical protein	3,36
PA3007	*lexA*	repressor protein LexA	3,65
PA3008	-	hypothetical protein	3,89
PA3022	-	hypothetical protein	7,02
PA3040	-	conserved hypothetical protein	3,34
PA3049	*rmf*	ribosome modulation factor	6,54
PA3100	*xcpU*	General secretion pathway outer membrane protein H precursor	3,25
PA3101	*xcpT*	general secretion pathway protein G	3,07
PA3104	*xcpP*	secretion protein XcpP	3,55
PA3161	*himD*	integration host factor beta subunit	3,09
PA3326	*clpP2*	ClpP2	21,21
PA3327	-	probable non-ribosomal peptide synthetase	10,80
PA3328	-	probable FAD-dependent monooxygenase	13,70
PA3329	-	hypothetical protein	8,04
PA3330	-	probable short chain dehydrogenase	22,73
PA3331	-	cytochrome P450	12,03
PA3332	-	conserved hypothetical protein	22,91
PA3333	*fabH2*	3-oxoacyl-[acyl-carrier-protein] synthase III	23,29
PA3334	-	probable acyl carrier protein	26,37
PA3335	-	hypothetical protein	7,24
PA3356	*pauA5*	Glutamylpolyamine synthetase	3,14
PA3397	*fprA*	FprA	3,86
PA3413	-	conserved hypothetical protein	3,76
PA3442	-	probable ATP-binding component of ABC transporter	13,94
PA3450	*lsfA*	1-Cys peroxiredoxin LsfA	4,56
PA3476	*rhlI*	autoinducer synthesis protein RhlI	8,74
PA3477	*rhlR*	transcriptional regulator RhlR	6,94
PA3478	*rhlB*	rhamnosyltransferase chain B	6,55

PA3479	*rhlA*	rhamnosyltransferase chain A	7,31
PA3530	*bfd*	bacterioferritin-associated ferredoxin Bfd	3,33
PA3552	*arnB*	ArnB	257,90
PA3553	*arnC*	ArnC	112,03
PA3554	*arnA*	ArnA	157,97
PA3555	*arnD*	ArnD	70,21
PA3556	*arnT*	inner membrane L-Ara4N transferase ArnT	73,11
PA3557	*arnE*	ArnE	37,42
PA3558	*arnF*	ArnF	272,41
PA3559	-	probable nucleotide sugar dehydrogenase	103,65
PA3607	*potA*	polyamine transport protein PotA	*-4,42*
PA3609	*potC*	polyamine transport protein PotC	*-3,85*
PA3622	*rpoS*	sigma factor RpoS	4,63
PA3623	-	conserved hypothetical protein	4,55
PA3661	-	hypothetical protein	*-3,62*
PA3712	-	hypothetical protein	3,18
PA3724	*lasB*	elastase LasB	19,55
PA3784	-	hypothetical protein	4,28
PA3785	-	conserved hypothetical protein	6,72
PA3786	-	hypothetical protein	9,36
PA3790	*oprC*	Putative copper transport outer membrane porin OprC precursor	4,08
PA3791	-	hypothetical protein	3,78
PA3904	-	hypothetical protein	4,36
PA3905	-	hypothetical protein	4,09
PA3906	-	hypothetical protein	3,47
PA3907	-	hypothetical protein	3,49
PA3930	*cioA*	cyanide insensitive terminal oxidase	5,70
PA4067	*oprG*	Outer membrane protein OprG precursor	5,30
PA4099	-	hypothetical protein	*-7,22*
PA4129	-	hypothetical protein	21,01
PA4130	-	probable sulfite or nitrite reductase	12,19
PA4131	-	probable iron-sulfur protein	19,75
PA4132	-	conserved hypothetical protein	15,86
PA4133	-	cytochrome c oxidase subunit (cbb3-type)	30,63
PA4134	-	hypothetical protein	14,62
PA4141	-	hypothetical protein	7,17
PA4179	-	probable porin	*-4,30*
PA4209	*phzM*	probable phenazine-specific methyltransferase	4,83
PA4210	*phzA1*	probable phenazine biosynthesis protein	14,65
PA4211	*phzB1*	probable phenazine biosynthesis protein	13,09
PA4212	*phzC1*	phenazine biosynthesis protein PhzC	9,05
PA4213	*phzD1*	phenazine biosynthesis protein PhzD	14,84
PA4214	*phzE1*	phenazine biosynthesis protein PhzE	6,01
PA4215	*phzF1*	probable phenazine biosynthesis protein	8,22
PA4216	*phzG1*	probable pyridoxamine 5'-phosphate oxidase	9,42
PA4217	*phzS*	flavin-containing monooxygenase	15,00
PA4357	-	conserved hypothetical protein	19,87
PA4358	*feoB*	FeoB	18,07
PA4359	-	conserved hypothetical protein	17,77
PA4493	*roxR*	RoxR	3,49
PA4494	*roxS*	RoxS	3,83
PA4607	-	hypothetical protein	3,63
PA4629	-	hypothetical protein	*-3,03*
PA4714	-	conserved hypothetical protein	3,82
PA4773	*speD2*	hypothetical protein	340,79
PA4774	*speE2*	hypothetical protein	336,83
PA4775	-	hypothetical protein	154,25

PA4776	*pmrA*	PmrA: two-component regulator system response regulator PmrA	160,54
PA4777	*pmrB*	PmrB: two-component regulator system signal sensor kinase PmrB	46,04
PA4778	*cueR*	CueR	6,11
PA4781	-	cyclic di-GMP phosphodiesterase	12,40
PA4782	-	hypothetical protein	96,27
PA4817	-	hypothetical protein	*-3,66*
PA4917	*nadD2*	nicotinate mononucleotide adenylyltransferase NadD2	3,02
PA4922	*azu*	azurin precursor	3,40
PA5219	-	hypothetical protein	3,07
PA5220	-	hypothetical protein	7,63
PA5468	-	probable citrate transporter	*-5,97*
PA5469	-	conserved hypothetical protein	*-5,41*

[a] PA gene numbers are annotated according to the Pseudomonas Genome Project (www.pseudomonas.com).

[b] Gene expression in AB16.2 relative to that in PAO1. Only genes with a variation of 3-fold ($p \leq 0.01$) are shown.

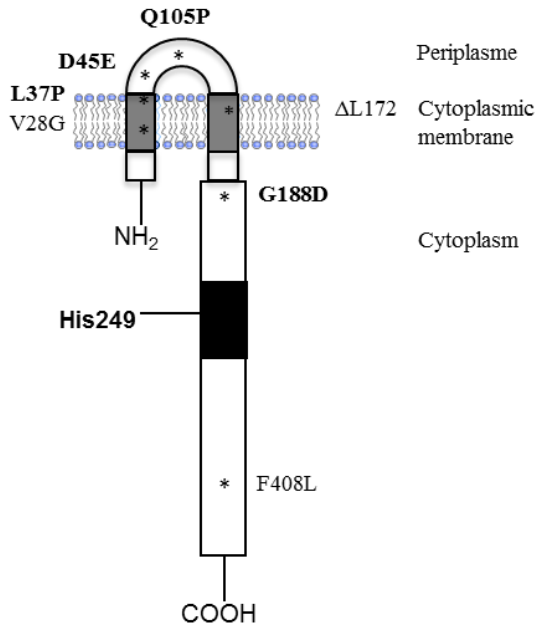

FIG 1 Schematic representation of histidine kinase (HK) PmrB. The mutations responsible for cross-resistance to aminoglycosides and colistin in *in* vitro-selected mutants and clinical strains are marked with asterisks. The first and second transmembrane domains of PmrB are colored in gray (from amino acid position 15 to 37, and from 161 to 183, respectively). Are also represented the periplasmic domain (from 38 to 160), the HAMP linker domain (from 186 to 238), the dimerization/phosphoacceptor (HisKA) domain (from 239 to 304, colored in black) that contains the conserved active site histidine 249, and the histidine kinase-like ATPase (HATPase) domain (from 348 to 459). The domains are available from the SMART protein database (http://smart.embl-heidelberg.de).

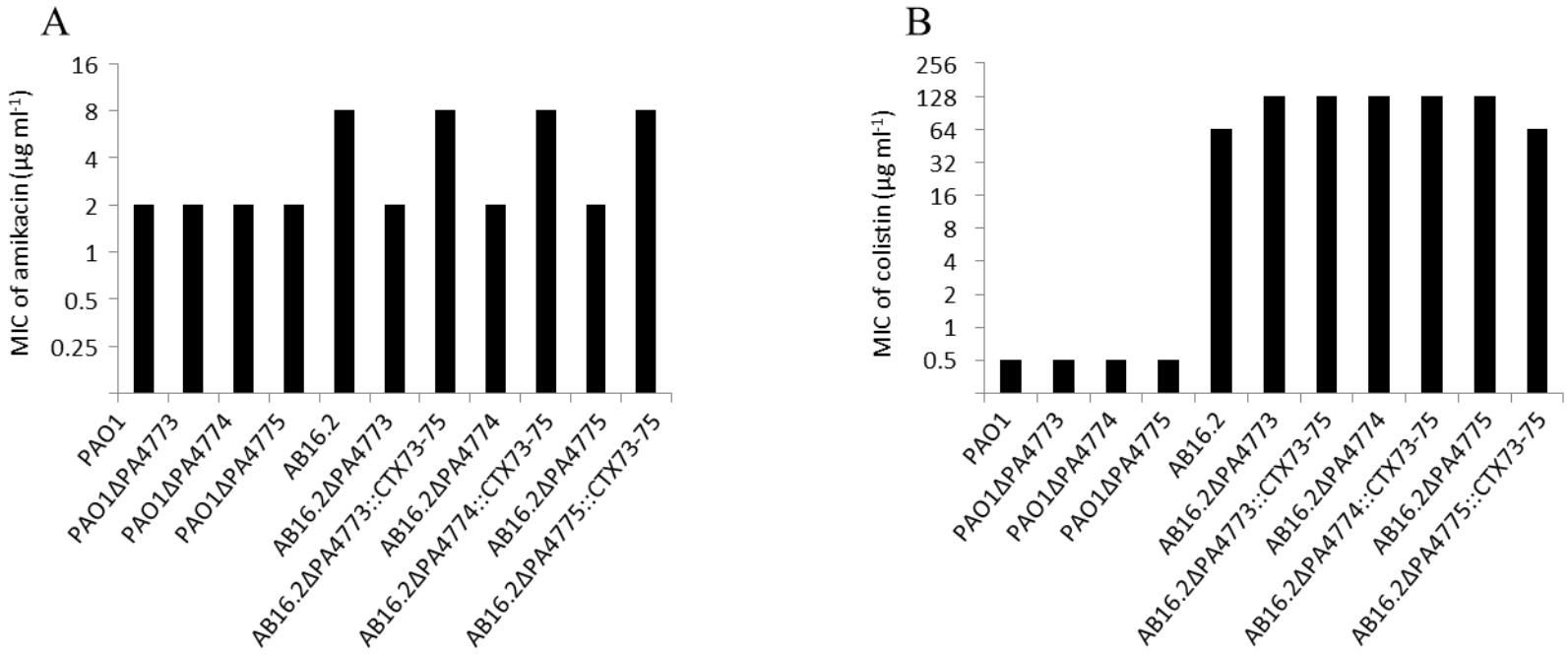

FIG 2 Contribution of genes PA4773, PA4774 and PA4775 to amikacin (A) and colistin (B) resistance. Deletion mutants AB16.2ΔPA4773, AB16.2ΔPA4774 and AB16.2ΔPA4775 were transcomplemented with a DNA fragment carrying the wild-type genes PA4773-PA4774-PA4775 inserted in chromosomal site *attB* (yielding constructs AB16.2ΔPA4773::CTX73-75, AB16.2ΔPA4774::CTX73-75 and AB16.2ΔPA4775::CTX73-75, respectively). The data presented are representative of 3 independent MIC determinations.

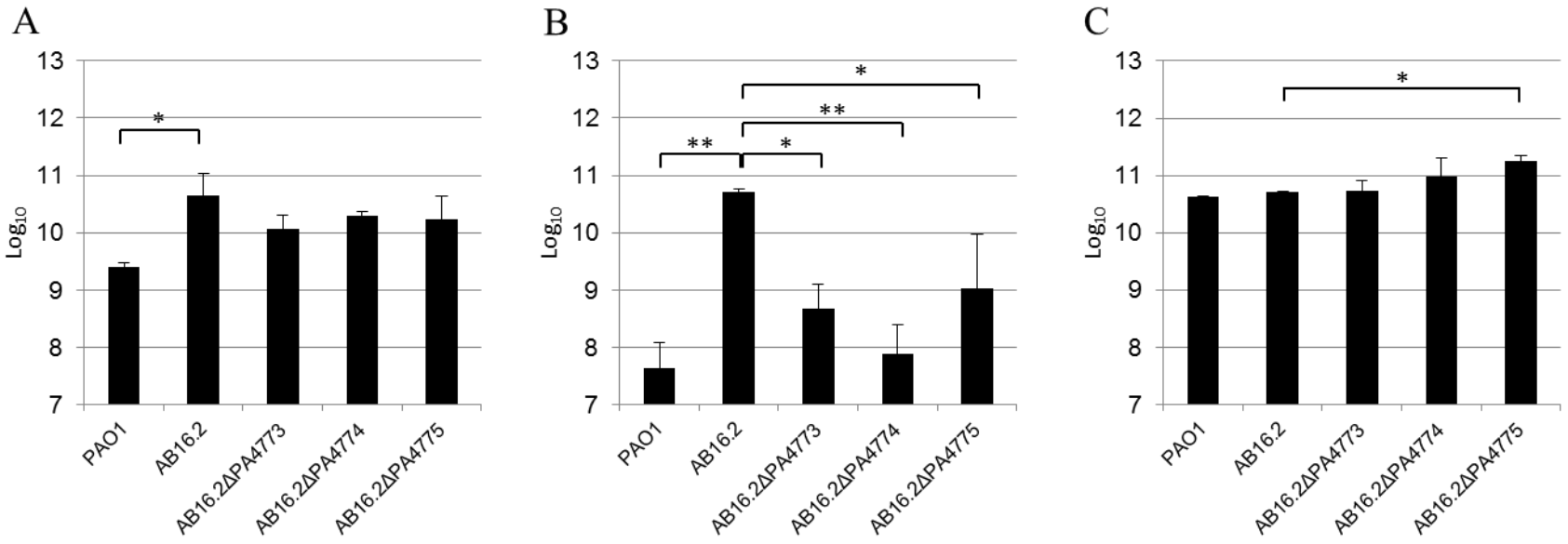

FIG 3 Amounts of spermidine (A), norspermidine (B) and 1,3-diaminopropane (C) in cell surface extracts of strain PAO1 and derived mutants. The histograms represent the area under the peak values of each compound as determined by LC-ESI-MS. The data correspond to means of normalized values (log scale) ± SD of three independent experiments. Tukey's test results are indicated as *P<0.05, **P<0.01.

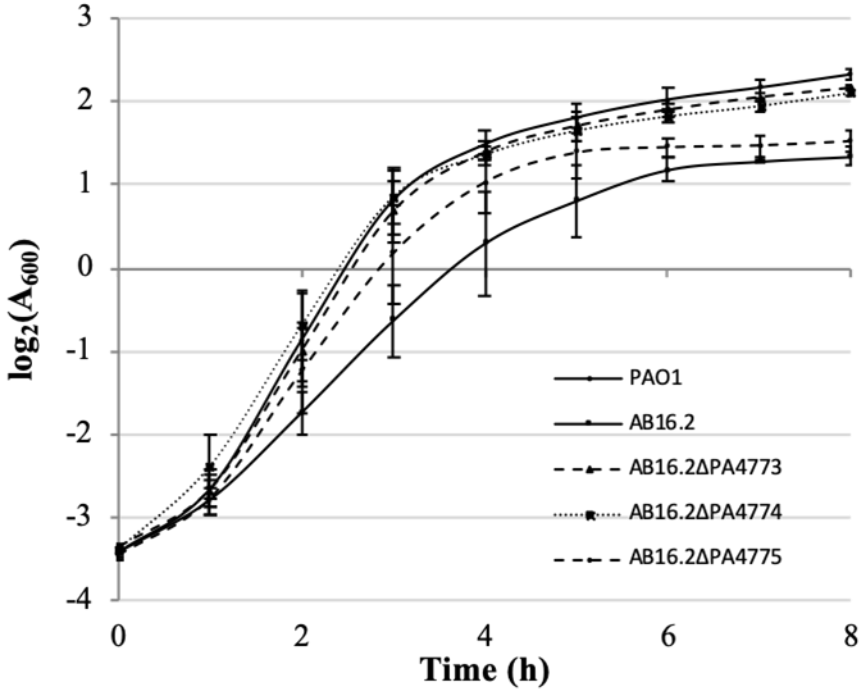

FIG 4 Effects of gene PA4773, PA4774 and PA4775 overexpression on bacterial growth. Growth of strains PAO1 (circles, solid line), AB16.2 (squares, solid line), AB16.2ΔPA4773 (triangles, dashed line), AB16.2ΔPA4774 (squares, dotted line) and AB16.2ΔPA4775 (circles, dashed line) in Mueller Hinton broth at 37°C was measured spectrophotometrically at A_{600nm}. Error bars indicate SD of three biological replicates.

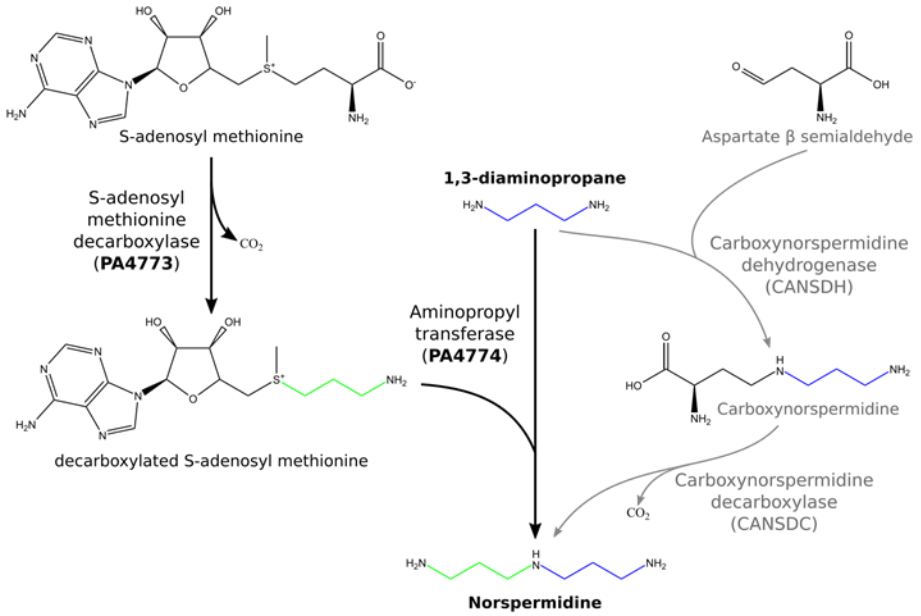

FIG 5 Norspermidine biosynthesis.

The putative pathway of norspermidine synthesis in *P. aeruginosa* and the previously identified pathway of norspermidine biosynthesis in *Vibrionales* are represented with black and grey lines respectively.

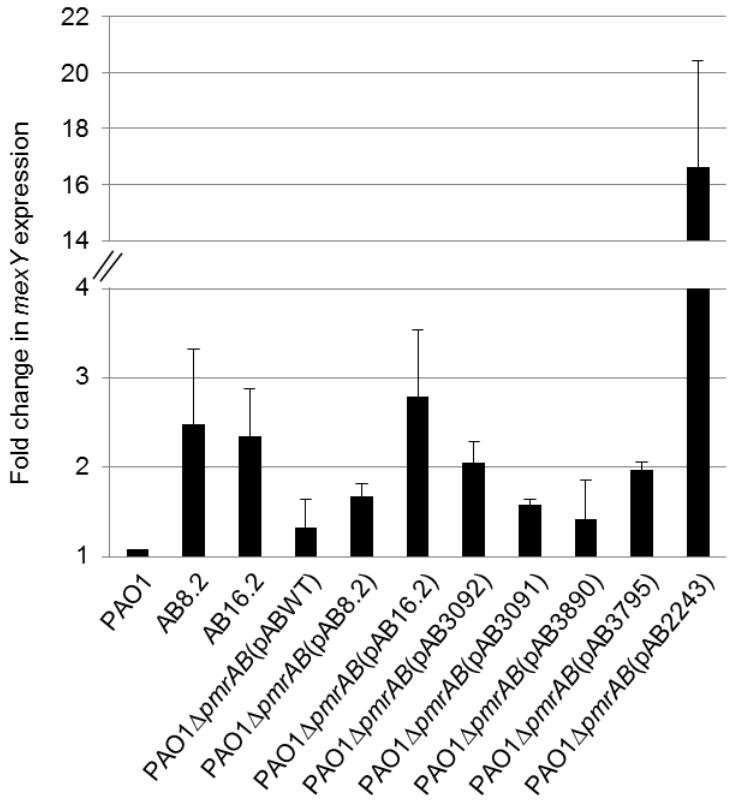

FIG S1. Effects of various mutations occurring in gene *pmrA* or *pmrB* on *mexY* expression. The mRNA amounts of gene *mexY* were determined by RT-qPCR from log-phase bacteria grown in Mueller Hinton broth (A_{600nm} = 0.8). Mean values of *mexY* were calculated from two independent experiments each including two determinations. These transcription levels were then normalized by reference to housekeeping gene *uvrD* activity in each strain. They are presented here as a ratio (fold change) to the values of PAO1 (± SD) .

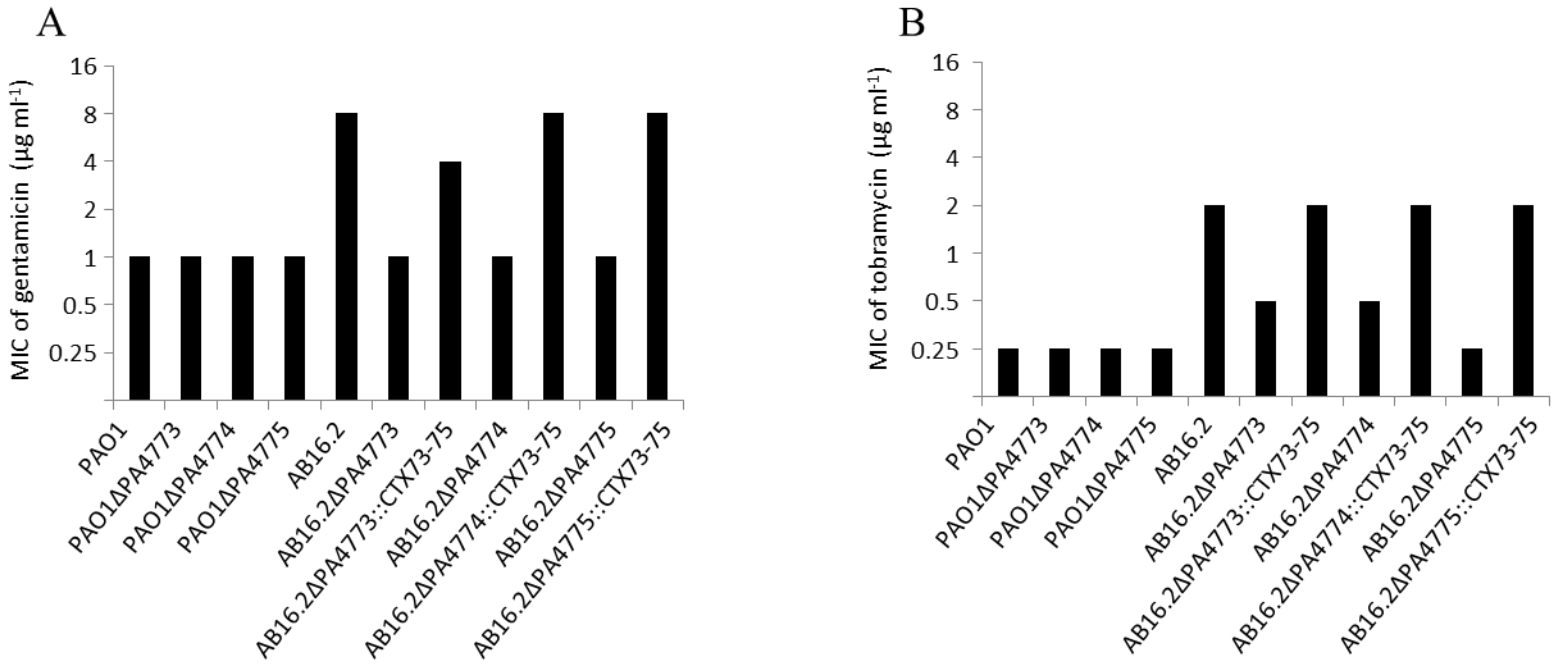

FIG S2 Contribution of genes PA4773, PA4774 and PA4775 to gentamicin (A) and tobramycin (B) resistance. Deletion mutants AB16.2ΔPA4773, AB16.2ΔPA4774 and AB16.2ΔPA4775 were transcomplemented with a DNA fragment carrying the wild-type genes PA4773-PA4774-PA4775 inserted in chromosomal site *attB* (yielding constructs AB16.2ΔPA4773::CTX73-75, AB16.2ΔPA4774::CTX73-75 and AB16.2ΔPA4775::CTX73-75, respectively). The data presented are representative of 3 independent MIC determinations.

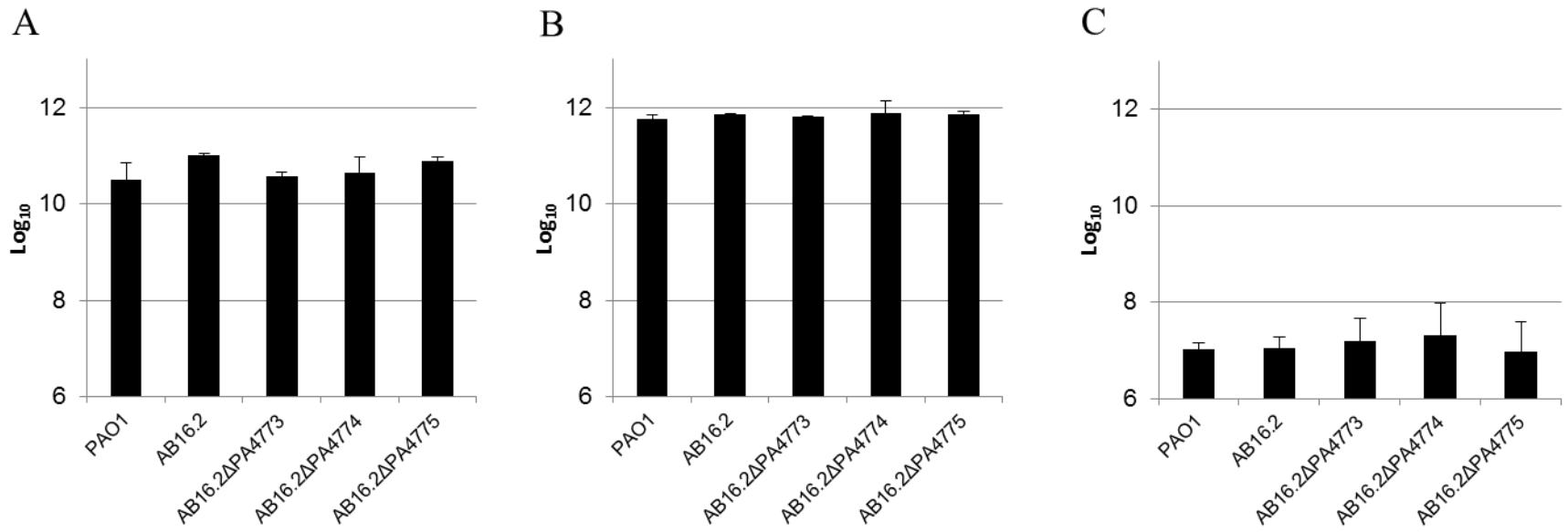

FIG S3 Amounts of cadaverine (A), putrescine (B) and spermine (C) in cell surface extracts of strain PAO1 and derived mutants. The histograms represent the area under the peak values of each compound as determined by LC-ESI-MS. The data correspond to means of normalized values (log scale) ± SD of three independent experiments. Tukey's test results are indicated as *P<0.05, **P<0.01.

Table 9: Characterization of a collection of colistin-resistant clinical strains.

Strains[a]	Origin	Protein substitutions[b]							
		PmrA	PmrB	ParR	ParS	PhoP	PhoQ	CprR	CprS
3095	bronchial aspiration	$L_{71}R$	$S_{2}P$ $A_{4}T$ $V_{6}A$ $V_{15}I$ $G_{68}S$ $Y_{345}H$	-	$L_{137}P$ $H_{398}R$	-	-		
3094	bronchial aspiration	$L_{71}R$	$S_{2}P$ $A_{4}T$ $V_{6}A$ $V_{15}I$ $G_{68}S$ $Y_{345}H$	-	$L_{137}P$ $H_{398}R$	-	-	-	-
3093	bronchial aspiration	$L_{71}R$	$S_{2}P$ $A_{4}T$ $V_{6}A$ $V_{15}I$ $L_{37}P$ $G_{68}S$ $Y_{345}H$	-	$L_{137}P$ $H_{398}R$	-	-	-	-
3092	bronchial aspiration	$L_{71}R$	$S_{2}P$ $A_{4}T$ $V_{6}A$ $V_{15}I$ $L_{37}P$ $G_{68}S$ $Y_{345}H$	-	$L_{137}P$ $H_{398}R$	-	-	-	-
3091	bronchial aspiration	$L_{12}I$ $L_{71}R$	$S_{2}P$ $A_{4}T$ $V_{6}A$ $V_{15}I$ $G_{68}S$ $Y_{345}H$	-	$L_{137}P$ $H_{398}R$	-	-	-	-
3090	bronchial aspiration	$L_{12}I$ $L_{71}R$	$S_{2}P$ $A_{4}T$ $V_{6}A$ $V_{15}I$ $G_{68}S$ $Y_{345}H$	-	$L_{137}P$ $H_{398}R$	-	-	-	-
3089	bronchial aspiration	$L_{12}I$ $L_{71}R$	$S_{2}P$ $A_{4}T$ $V_{6}A$ $V_{15}I$ $G_{68}S$ $Y_{345}H$	-	$L_{137}P$ $H_{398}R$	-	-	-	-
2243	bronchoalveolar lavage	-	$Q_{105}P$ $Y_{345}H$	$E_{87}K$	$H_{398}R$	-	-	-	-
3795	expectoration	$L_{71}R$	$G_{188}D$ $Y_{345}H$	-	$A_{82}T$ $H_{398}R$	-	$D_{334}G$		
3890	expectoration	$L_{71}R$	$S_{2}P$ $A_{4}T$ $D_{45}E$ $Y_{345}H$	-	$F_{171}L$ $H_{398}R$	-	-	-	-
3917	unknown			-	$A_{345}T$ $H_{398}R$	-	Q_{280}Stop		-
3921	unknown	$L_{71}R$	$Y_{345}H$	$E_{234}K$	$H_{398}R$	-	-	-	$H_{331}Y$ $E_{386}D$ $L_{411}M$
3936	unknown	$L_{71}R$	$Y_{345}H$	-	$H_{398}R$	-	-	-	-
3561	unknown	-	$Y_{345}H$	-	$H_{398}R$	-	$S_{300}R$	-	$T_{16}S$
4363	unknown		$Y_{345}H$	-	$V_{152}A$ $H_{398}R$	-	$S_{300}R$	-	$T_{16}S$

[a] isolates from the same patient are highlighted in grey.
[b] mutations found in colistin susceptible reference strains PA14, LESB58 or both are indicated in green, orange or blue, respectively. Other mutations are indicated in black.

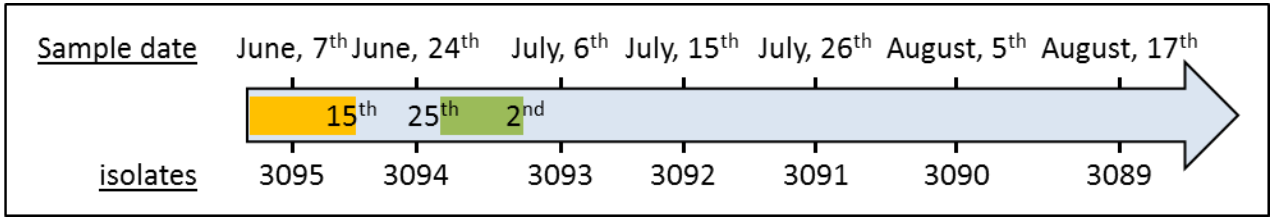

Figure 41: Timeline of isolation of strains 3095 to 3089, and periods of antibiotic treatement.

Periods of treatment with tazocillin plus colistin, or colistin only, are highlighted in yellow and green, respectively.

3.2. Supplementary results

3.2.1. Characterization of a collection of *P. aeruginosa* clinical strains resistant to colistin

Mutations in *pmrB* were reported to increase resistance to colistin in non-CF and CF strains of *P. aeruginosa* (Barrow and Kwon, 2009; Moskowitz *et al*., 2012). In our work, *pmrB* mutants selected *in vitro* turned out to be also more resistant (4- to 8-fold increase) to aminoglycosides (Chapter 2, **3.1.** *article in preparation*). In order to determine if similar mutations exist in clinical strains, we analyzed 31 colistin-resistant strains from our laboratory collection (MIC $\geq$ 4 µg ml^{-1}). Sanger DNA sequencing of *pmrAB* in 20 of them revealed that 18 and 3 strains had potentially significant amino acid substitutions in PmrB (e.g. V_6A, $L_{37}P$, $D_{45}E$, $Q_{105}P$, $G_{188}D$) and PmrA ($L_{12}I$), respectively. Complementation of mutant PAO1Δ*pmrAB* with various *pmrAB* alleles showed that substitution V_6A belongs to a common polymorphism (Chapter 2, **3.1.** *article in preparation*). More interestingly, substitutions $L_{37}P$, $D_{45}E$, $Q_{105}P$, $G_{188}D$ in PmrB and $L_{12}I$ in PmrA appeared to provide a cross-resistance to colistin (up to 128-fold increase) and aminoglycosides (Chapter 2, **3.1.** *article in preparation*). These mutations were responsible for a so far uncharacterized mechanism of resistance.

Interestingly, 7 of these isolates (3095 to 3089) were collected from a same patient, treated twice with colistin over a 71-day period (Figure 41 and Table 9). Two isolates recovered at the onset of infection (3095 and 3094) harbored the V_6A change in PmrB and the $L_{137}P$ substitution in ParS. Two further strains (3093 and 3092) showed an additional PmrB mutation ($L_{37}P$). Finally, the last three isolates (3091, 3090 and 3089) were found to contain a substitution in PmrA ($L_{12}I$) but not the $L_{37}P$ mutation in PmrB. Theses data suggest that two populations emerged from the initial strain: a subpopulation with a substitution in PmrB and a second one, with a substitution in PmrA. In addition, our findings highlight that mutations in *pmrA* can also contribute to the persistence of strains upon colistin treatment.

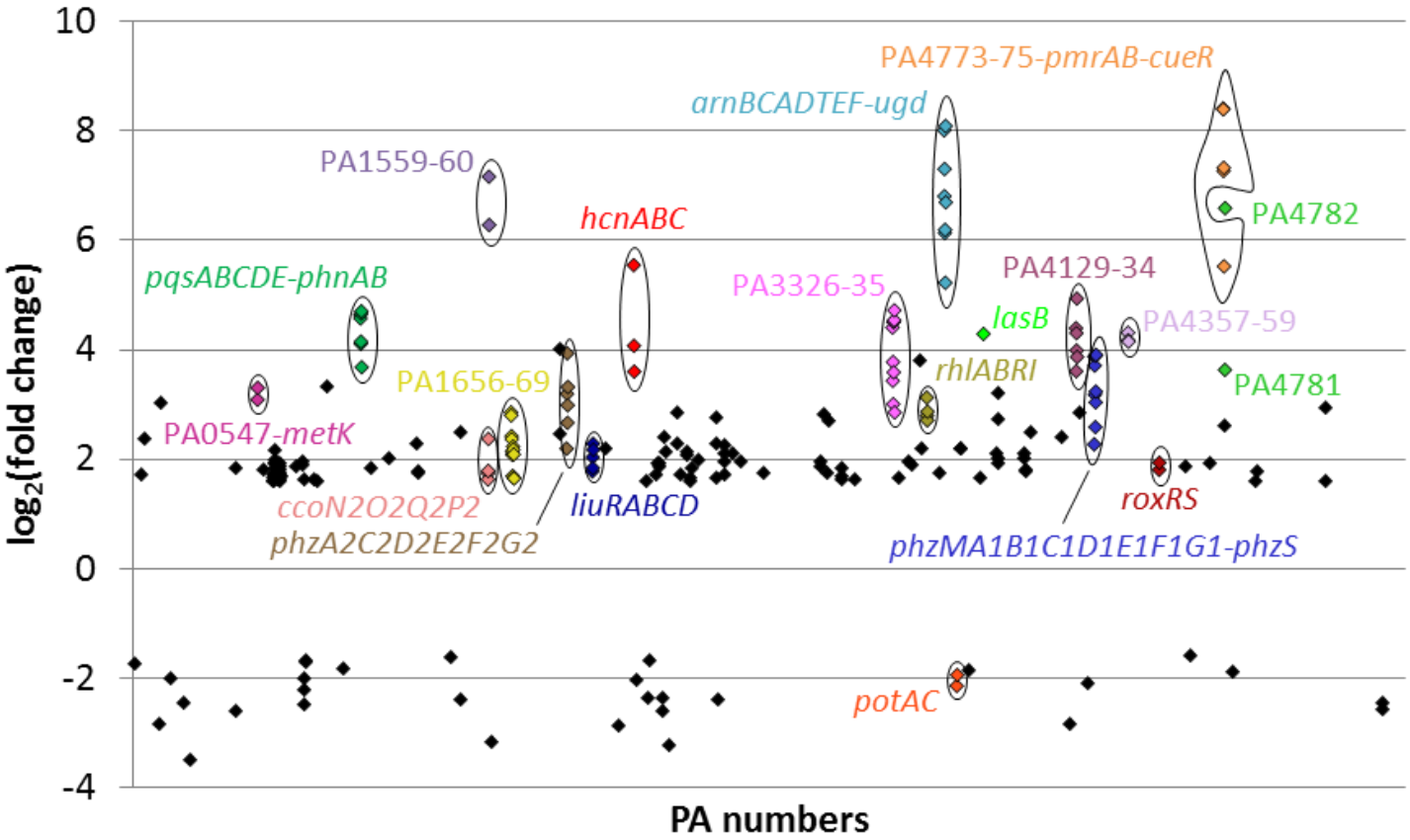

Figure 42: Comparison of global gene expression of AB16.2 *versus* PAO1.

Only genes exhibiting a differential expression ≥ 3-fold between the two bacteria are represented ($p \leq 0.01$).

3.2.2. Transcriptional analysis of mutant AB16.2 compared to PAO1 reveals a high number of PmrAB-regulated genes

A number of genes regulated by RR PmrA were previously identified by comparing the transcription levels of strain PAO1 and a *pmrA::xylE* transposon mutant grown in the presence of low Mg^{2+} concentration (0.02 mM) (McPhee *et al*., 2006). Among the genes positively regulated by PmrA, the loci *arnBCADTEF-ugd*, PA4773-*pmrAB*, *cprA* [a gene inactivated by a frameshift mutation in strain PAO1 (Gutu *et al*., 2015)], PA4781 (encoding a c-di-GMP phosphodiesterase) and PA4782 were identified.

In order to get more information on the physiological functions responding to mutationally activated sensor PmrB, we compared the transcriptional profiles of mutant AB16.2 and strain PAO1. The mRNA levels of 233 genes (as quantified by RNA seq) were dysregulated at least 3-fold ($p \leq 0{,}01$) in the mutant, 201 of them being upregulated and 32 downregulated (Figure 42). As previously reported from the analysis of PmrA-regulon (McPhee *et al*., 2006), operons PA4773-75-*pmrAB*, *arnBCADTEF-ugD* and PA1559-60 (disrupted gene *cprA*) were the most activated. Mutant AB16.2 also overexpressed locus *pqsABCDE-phnAB* (involved in the synthesis of signaling molecule PQS), *hcnABC* (synthesis of hydrogen cyanide, a potent inhibitor of cytochrome *c* oxidases) and the *phzMA1B1C1D1E1F1G1-phzS* and *phzA2B2C2D2E2F2G2* loci (synthesis of phenazine compounds). Interestinlgy, the expression of PA3326-35 locus encoding a probable NRPS (PA3327) was increased from 7.2- to 26.4-fold. The gene cluster *ccoN2O2Q2P2* that determines a cytochrome *c* cbb_3-2 oxidase, an enzyme with high affinity for oxygen, was also upregulated (Hamada *et al*., 2014). Another upregulated operon was PA0547-*metK*. MetK is a methionine adenosyltransferase that synthesizes S-adenosylmethionine (SAM) from L-methionine at the expense of ATP in the initial step of spermidine synthesis. Gene PA0547 encodes a probable transcriptional regulator of the ArsR family, named SahR in *Pseudomonadaceae*. According to some investigators, the regulon of SahR would encompass the operon *sahR-metK* itself and operon *ahcY-metF* (Novichkov *et al*., 2014); however, no change in *ahcY* or *metK* expression was observed in mutant AB16.2.

Finally, two genes of the *potABCD* operon were repressed, encoding proteins involved in spermidine uptake in *E. coli* (Kashiwagi *et al*., 1993).

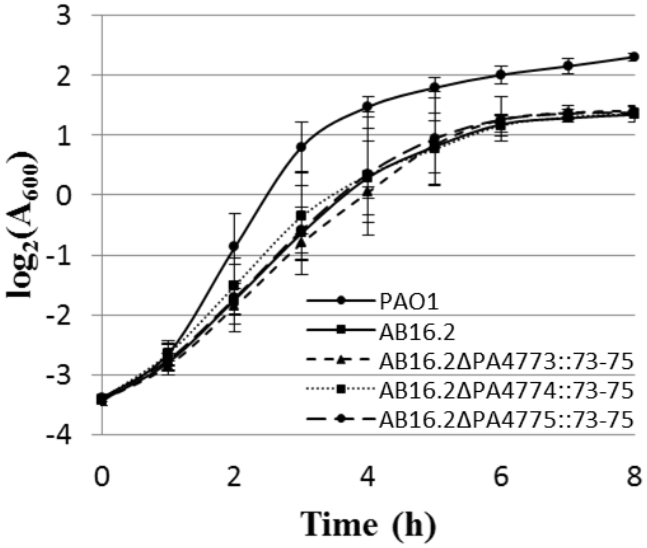

Figure 43: Growth curves of complemented-AB16.2 knockout mutants cultivated in Mueller-Hinton broth at 37°C with shacking (250 rpm).

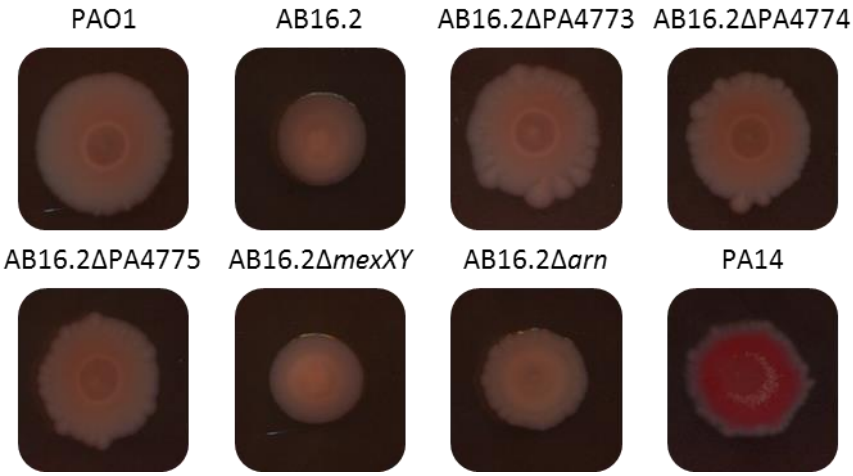

Figure 44: Congo red binding assay with AB16.2 and derivative mutants.

Strain PA14 was included as a control producing exopolysaccharides.

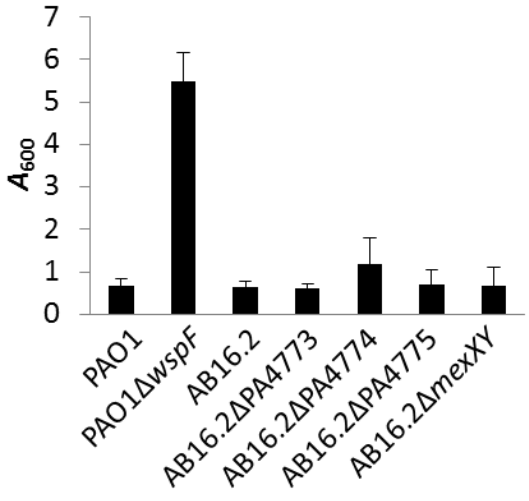

Figure 45: Capacity of *pmrB* mutant AB16.2 and derivatives to adhere to a plastic surface.

Sessile bacteria were stained with a crystal violet solution (1%). The bound pigment was redissolved in ethanol and quantified by measuring A_{600}. Mutant PAO1Δ*wspF* was used as a positive control as *wspF* inactivation stimulates production of Pel and Psl exopolysaccharides (Borlee *et al*., 2010).

3.2.3. Role of PA4773, PA4774 and PA4775 genes in AB16.2: growth curves, colony morphology and surface attachement

Analysis of transcriptomic data showed that genes PA4773, PA4774 and PA4775 were highly upregulated in AB16.2 compared with PAO1 (Figure 42). In PAO1, transposon inactivation of PA4774 was reported to increase the OM permeabilizing activity of gentamicin, polymyxin B and CP10A (an antimicrobial peptide derived from indolicidin) (Johnson *et al*., 2012). Here, we found that the three genes provide the resistance to aminoglycosides but not to colistin, when overexpressed due to *pmrB* mutations (Chapter 2, **3.1.** *article in preparation*). Indeed, *trans*-complementations with genes PA4773 to PA4775 increased the resistance to aminoglycosides of AB16.2 susceptible mutants with in-frame deletion in any of the three genes. Of note, the growth defect of AB16.2 was completely or partially abolished when gene PA4773/PA4774 or PA4775 was inactivated, respectively (Chapter 2, **3.1.** *article in preparation*). As expected, complemented mutants grew as AB16.2 (Figure 43). The poor growth of AB16.2 might thus result from a high production of polyamines, known to modulate cell growth and proliferation (Miller-Fleming *et al*., 2015).

Bacteria growing in biofilms are more resistant to antibiotics including aminoglycosides. Exopolysaccharides (EPS) are important components of biofilms as they serve as a matrix structure. Solid media containing the cationic dye Congo red were used to study (i) the morphology of bacterial colonies, and (ii) capacity of strains to produce EPS (Strehmel *et al*., 2015). Compared with PAO1, colonies of AB16.2 were smaller (Figure 44). Inactivation of either PA4773, PA4774 or PA4775 increased their size in agreement with the results of growth experiments in liquid broth. It is worth mentioning the apparition of small protuberances at the colony extremity that are not observed for PAO1. Regarding production of EPS, no difference was observed between AB16.2 and PAO1.This is consistent with our observation that AB16.2 displayed the same capacity to adhere to a plastic surface (Figure 45). Overall, no evidence was obtained that the higher resistance of AB16.2 to aminoglycosides results from a biofilm mode of life.

Table 10: *PmrB* mutants susceptibility to β-lactams.

Strains	MIC (µg ml^{-1})[a]									
	TIM	TZP	CAZ	FEP	ATM	IPM	MEM	FOF	NOV	VAN
PAO1	16	4	2	2	4	1	0.5	128	512	>2,048
AB8.2	4	2	0.5	2	1	0.5	0.25	64	64	2,048
AB16.1	16	4	2	2	4	1	0.5	64	256	>2,018
AB16.2	8	2	0.5	2	2	0.5	0.25	64	128	2,048
AB16.2ΔPA4773	nd	nd	2	2	nd	1	nd	nd	nd	nd
AB16.2ΔPA4774	nd	nd	2	2	nd	1	nd	nd	nd	nd
AB16.2ΔPA4775	nd	nd	1	2	nd	1	nd	nd	nd	nd

[a] MIC values for mutants ≥2-fold less than for PAO1 are underlined. TIM: ticarcillin-clavulanic acid, TZP: piperacillin-tazobactam, CAZ: ceftazidime, FEP: cefepime, ATM: aztreonam, IPM: imipenem, MEM: meropenem, FOF: fosfomycin, NOV: novobiocin, VAN: vancomycin, nd: not determined.

Table 11: Effect of *pmrB* mutations on the susceptibility to β-lactams.

PAO1Δ*pmrAB* transformed with pME6012 derivates[a]	PmrA substitution	PmrB substitution	MIC (µg ml^{-1})[b]		
			CAZ	FEP	IPM
-	Δ	Δ	2	2	1
pME6012	Δ	Δ	2	2	1
pABWT	-	-	2	2	1
pAB8.2	-	$V_{28}G$	1	1	0.5
pAB16.1	-	$F_{408}L$	1	1	0.5
pAB16.1.1	-	$F_{408}L$ $(K_{428}$-$V_{431})$[c]	2	4	1
pAB16.1.2	-	$F_{408}L$ ΔNtG_{1175}	2	4	1
pAB16.2	-	ΔL_{172}	1	1	0.5

[a] pME6012 plasmids carrying the *pmrAB* alleles from strain PAO1 (WT), *in vitro* mutants (8.2, 16.1, 16.2) or AB16.1 revertants (16.1.1, 16.1.2).
[b] compared to PAO1, a 2-fold decrease of MIC was underlined. CAZ: ceftazidime, FEP: cefepime, IPM: imipenem.
[c] *pmrAB* allele contains a 12-bp insertion leading to a K_{428} to V_{431} insertion.
Δ: absence of protein.

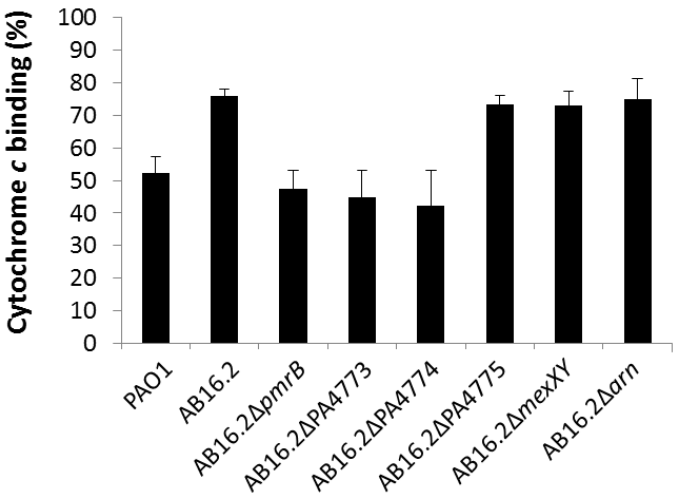

Figure 46: Assessment of net negative charges present at the bacterial surface by a binding test using cationic probe cytochrome *c*.

Higher is the binding of the probe, higher is the number of negative charges at the cell surface.

3.2.4. Polyamines and cell surface modifications

AB8.2 and AB16.2 *pmrB* mutants were cross-resistant to aminoglycosides and colistin, and hypersusceptible (2- to 4-fold) to β-lactams (Table 10). We confirmed that this phenotype was dependent upon the *pmrB* mutations (Table 11) and due to overexpression of genes PA4773-75 (Table 10). β-lactam antibiotics block the crosslinking of peptidoglycan units by inhibiting the formation of peptide bonds catalyzed by penicillin-binding proteins, which ultimately leads to cell death (Kohanski *et al*., 2010). An increased susceptibility to β-lactams could result from repression of β-lactamase AmpC or downregulation of MexAB-OprM, a pump known to export a number of β-lactam molecules except imipenem. Hypersusceptibility to carbapenems could be due to overexpression of porin OprD encoding gene *oprD*. However, based on our transcriptomic data, *ampC*, *mexAB-oprM* and *oprD* were not dysregulated in AB16.2. One could assume that the OM modification in AB16.2 that confers aminoglycoside resistance might increase the OM permeability to β-lactams.

To test this hypothesis, we assessed the net charge of the cell surface of AB16.2 by measuring the capacity of living bacteria to bind a cationic probe (Figure 46). The binding of equine heart cytochrome *c* to whole cells was found to be higher for AB16.2 than for PAO1, suggesting the presence of more negative charge at the surface of AB16.2. Inactivation of *pmrB*, PA4773 and PA4774, respectively in the mutant confirmed the role of these genes in this OM modification. In contrast, deletion of PA4775 and *mexXY* respectively did not impact the results of cytochrome *c* binding experiments. Surprisingly enough, despite the fact that the addition of L-Ara-4N molecules to LPS has been demonstrated to decrease the net negative charges of the OM, inactivation of operon *arn* (AB16.2Δ*arn*) did not reduced the OM-cytochrome *c* interaction either. Overall, these data support the notion that the PA4773-PA4774-associated modifications of OM have inverse effects on bacterial susceptibility to aminoglycosides and β-lactams. Nevertheless, it cannot be ruled out that some defects in peptidoglycan synthesis also exist in *pmrB* mutants.

As genes PA4773 and PA4774 were predicted to participate in an alternative biosynthesis pathway of spermidine, we quantified the amounts of polyamines bound to the cell surface of PAO1 and AB16.2 by Liquid Chromatography-ElectroSpray

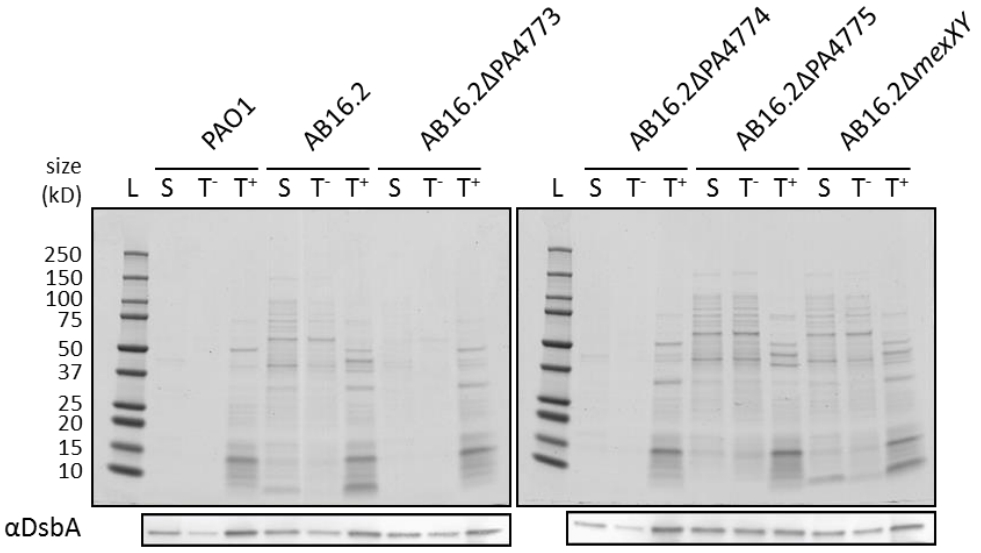

Figure 47: SDS-PAGE analysis of samples used for characterization of surface-bound polyamines.

L: protein ladder, S: sample containing polyamines recovered from bacterial surface by NaCl treatement, T^-: same as S but without NaCl, T^+: whole cell lysate. A western blot αDsbA was achieved as a marker of periplasmic leakage.

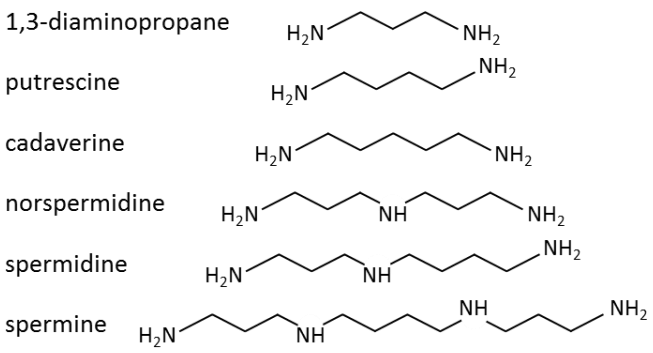

Figure 48: Structures of several polyamines.

Amino groups are protonated at physiological pH.

Putrescine is a precursor of spermidine in *P. aeruginosa*.

1,3-diaminopropane is a precursor of norspermidine synthesis in *V. cholera* (Lee *et al*., 2009a).

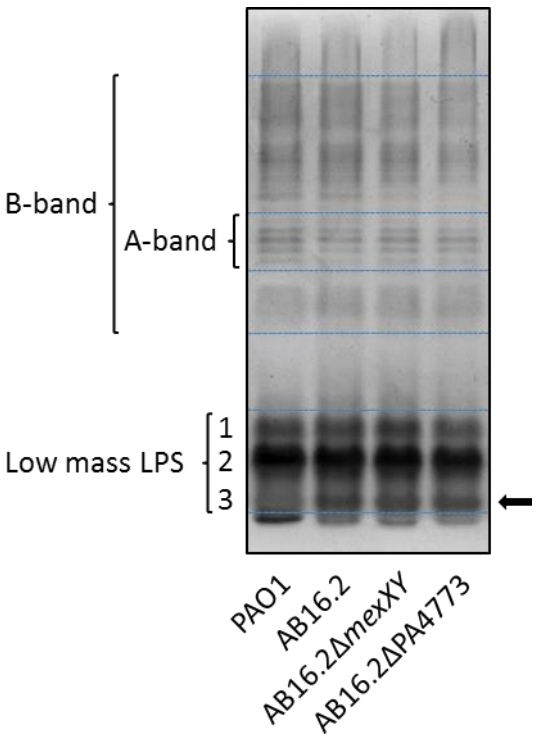

Figure 49: Comparison of LPS profiles by SDS-PAGE.

1: might correspond to molecules constituted of lipid A and a complete oligosaccharide core with one or two O-chain units
2: might correspond to molecules constituted of lipid A and a complete oligosaccharide core
3: might correspond to molecules with a truncated core oligosaccharide

Ionization-Mass Spectrometry (LC-ESI-MS). This work was performed in collaboration with the Plateforme BioPark d'Archamps of the Archamps Technopole located in Saint-Julien-en-Genevois, France (Chapter 2, **3.1.** *article in preparation*). Membrane-attached polyamines were collected according to the protocol indicated in Materials and Methods and proteins in the extracts were analyzed by SDS-PAGE to check whether a leakage of cellular components across bacterial cell wall occurred during the extraction process (Figure 47). Two main protein profiles were obtained by SDS-PAGE from the samples subsequently analyzed by LC-ESI-MS. First, amounts of proteins in samples from mutant AB16.2, AB16.2ΔPA4775 and AB16.2Δ*mexXY* were higher than that from PAO1, AB16.2ΔPA4773 and AB16.2ΔPA4774 (Figure 47, S lanes), consistent with the notion that AB16.2 has an altered cell wall and hypersusceptibility to β-lactams (Figure 46 and Table 10). Samples treated with HEPES buffer only contained higher amounts of proteins from AB16.2 than from PAO1 (Figure 47, T^- lanes).

Spermidine and various structural analogs such as the shorter molecules norspermidine, putrescine, cadaverine, 1,3-diaminopropane and the longer polyamine spermine (Figure 48) were quantified in the cell extracts. Amounts of spermidine and norspermidine appeared to be higher in AB16.2 than in PAO1, while inactivation of genes PA4773, PA4774 and PA4775, respectively led to a significant decrease in norspermidine levels and a moderate reduction in spermidine levels (Chapter 2, **3.1.** *article in preparation*). Furthermore, 1,3-diaminopropane (a norspermidine synthesis precursor in *Vibrio cholerae*) was found to be quantitatively higher in AB16.2ΔPA4775. Overall, these data suggest that proteins PA4773, PA4774 and PA4775 are required for the biosynthesis of norspermidine and possibly spermidine.

Johnson *et al*. reached the conclusion that spermidine binding to the LPS protects the OM against antibiotics (Johnson *et al*., 2012). Analysis of LPS molecules by SDS-PAGE showed the presence of both A-band and B-band LPS in PAO1 and AB16.2, eliminating the loss of B-band LPS as a cause of aminoglycoside resistance (Kadurugamuwa *et al*., 1993) (Figure 49). The sole difference observed between PAO1 and AB16.2 was the presence of an additional band (indicated by an arrow, Figure 49) in AB16.2. This band might correspond to molecules containing a truncated core (Lam *et al*., 2011). Inactivation of gene PA4773 or operon *mexXY* in AB16.2 had no effects on the presence of this band. Overall, SDS experiments did not reveal a PA4773-

Table 12: Antibiotic susceptibility of AB16.2 derivatives.

Strains	MIC (µg ml^{-1})			
	CST	**GEN**	**CAZ**	**IPM**
PAO1	0.5	1	2	1
PAO1Δ*armZ*	0.5	0.125	2	1
AB16.2	64	8	1	0.5
AB16.2Δ*pmrA*	0.5	1	2	1
AB16.2Δ*pmrB*	0.5	1	2	1
AB16.2Δ*cueR*	64	8	1	0.5
AB16.2ΔPA4781	64	8	1	0.5
AB16.2ΔPA4782	128	8	1	0.5
AB16.2Δ*pqsA*	64	8	1	0.5
AB16.2Δ*hcnB*	64	8	1	0.5
AB16.2Δ*rmf*	64	8	1	0.5
AB16.2Δ*oprC*	64	8	1	0.5
AB16.2ΔPA4133	64	8	1	0.5
AB16.2Δ*pslB*	32	8	1	0.5
AB16.2Δ*pelB*	64	8	1	0.5
AB16.2Δ*cdrA*	64	8	1	0.5
AB16.2ΔPA0547	64	4	1	1
AB16.2Δ*mexXY*	4	0.06	1	0.5
AB16.2Δ*mexZ*	128	16	1	0.5
AB16.2Δ*armZ*	64	0.5	1	0.5

CST: colistin, GEN: gentamicin, CAZ: ceftazidime, IPM: imipenem.

dependent modification of LPS, and the contribution of LPS changes to aminoglycoside resistance remains to be characterized.

3.2.5. Contribution of additional genetic loci to antibiotic resistance of AB16.2

The role of addititonal genes in antibiotic susceptibility of AB16.2 was assessed by the disk diffusion method and by MIC determination on a series of AB16.2 derived deletion mutants (Table 12). These experiments demonstrated that the upregulated genes *cueR*, PA4781, PA4782, *pqsA*, *hcnB*, *rmf*, *oprC* and PA4133 were not involved in the resistance of AB16.2 to colistin and gentamicin, nor in its hypersusceptibility phenotype to β-lactams.

4. Conclusion

Our work on the TCS PmrAB confirmed that some amino acid substitutions in protein sensor PmrB lead to a decreased susceptibility to aminoglycosides, an antibiotic class widely used to treat patients infected by *P. aeruginosa*. These substitutions were localized in all domains of the protein (transmembrane, HAMP, HisKA and HATPase domains). These PmrB mutants exhibited an impaired fitness that may compromise their survival in the infected host, and a higher resistance to colistin due to activation of the *arnBCADTEF-ugd* operon with subsequent addition of L-Ara-4N molecules to the phosphate groups of lipid A. PmrB-dependent overexpression of genes PA4773, PA4774 and PA4775 accounted for the resistance of the mutants to aminoglycosides. Likely because of their low transcription in wild-type cells, these genes do not contribute to the intrinsic resistance of *P. aeruginosa* to these drugs.

LC-ESI-MS quantitative analysis of amine molecules present at the cell surface revealed significantly higher amounts of both spermidine and norspermidine in the *pmrB* mutant AB16.2 compared to PAO1. Altogether our data suggest that genes PA4773-PA4774-PA4775 determine the synthesis of norspermidine in the AB16.2 mutant, a polyamine conferring an increased resistance to aminoglycosides. The RND pump MexXY(OprM) contributed through its ArmZ-dependent activation to this phenotype.

Chapter 3. The efflux pump MexXY(OprM) contributes to acquired resistance to colistin in *P. aeruginosa*

1. Context

The contribution of RND efflux pumps to antimicrobial resistance of Gram-negative bacteria is well established (Li *et al*., 2015). However, whether these transporters may influence bacterial susceptibility to cationic antimicrobial peptides (CAMPs) including colistin has been poorly investigated. Shafer *et al*. showed that MtrCDE modulates the susceptibility of *Neisseria gonorrhoeae* to human protegrin-1 and LL-37 (Shafer *et al*., 1998). In *N. meningitidis*, the pump homologous to MtrCDE was also reported to mediate intrinsic resistance to these two CAMPs and to polymyxin B as well (Tzeng *et al*., 2005). In this last study, the MtrCDE system might be as important as LPS modification with phosphoethanolamine, both mechanisms working synergistically to protect the bacterium against CAMPs. Two other efflux pumps, VexAB-TolC and AcrAB-TolC, are active on polymyxin B in *Vibrio cholerae* and *Klebsiella pneumoniae*, respectively (Bina *et al*., 2008; Padilla *et al*., 2010). In *P. aeruginosa*, resistance to polymyxins mainly relies on activation of the *arn* operon and subsequent addition of L-Ara-4N molecules to the phosphate groups of the lipid A. Several TCSs modulate the expression of this operon in response to still unknown environmental signals and to membrane damaging agents (for a review, see Jeannot *et al*., 2018 in appendix). Tolerance of bacteria growing in biofilm not only depends on genes *arn* but also *mexAB-oprM* transcription (Pamp *et al*., 2008). In contrast, system MexAB-OprM is dispensable in planktonic bacteria exposed to CAMPs (LL-37, HNP-1-3) (Rieg *et al*., 2009). In our laboratory, we found that the inactivation of *mexXY* in *pmrB* mutant AB16.2 was associated with an increased suceptibility to colistin, a result that suggested for the first time that MexXY(OprM) could promote resistance to colistin (Hélène Puja PhD thesis).

2. Objective

We have contributed to investigate the role of RND efflux pumps in modulation of colistin susceptibility in *P. aeruginosa*.

3. Results

Table 13: Contribution of several TCSs and RND efflux pumps in acquired resistance to colistin.

Strains	Transformed with plasmid	MIC (µg ml^{-1})[a]			
		CST	GEN	AMK	TOB
PAO1	-	0.5	1	2	0.25
PAO1Δ*pmrAB*	-	0.5	1	2	0.25
PAO1Δ*parRS*	-	0.25	1	2	0.25
PAO1Δ*phoPQ*	-	0.5	1	2	0.25
PAO1Δ*cprRS*	-	0.5	1	2	0.25
PAO1Δ*arn*	-	0.5	1	2	0.25
PAO1Δ*mexXY*	-	0.5	0.06	0.5	0.125
PAO1Δ*oprM*	-	0.5	0.06	0.5	0.125
PAO1Δ*armZ*	-	0.5	0.125	0.5	0.125
PAO1Δ*mexZ*	-	0.5	**2**	**4**	**0.5**
PAO1Δ*mexAB*	-	0.5	1	2	0.25
PAO1Δ*mexCD-oprJ*	-	0.5	1	2	0.25
AB16.2	-	**64**	**8**	**8**	**2**
AB16.2Δ*pmrAB*	-	0.5	1	2	0.25
AB16.2Δ*parRS*	-	**4**	**8**	**8**	**2**
AB16.2Δ*phoPQ*	-	**64**	**8**	**8**	**2**
AB16.2Δ*cprRS*	-	**64**	**8**	**8**	**2**
AB16.2Δ*arn*	-	**1**	**8**	**8**	**2**
AB16.2Δ*mexXY*	-	**4**	0.06	0.25	0.06
AB16.2Δ*mexXY*	pAK1900	**4**	0.06	0.25	0.06
AB16.2Δ*mexXY*	pAGH97[b]	**>128**	**16**	**16**	**4**
AB16.2Δ*oprM*	-	**4**	0.125	0.5	0.125
AB16.2Δ*armZ*	-	**64**	0.5	2	0.25
AB16.2Δ*mexZ*	-	**>128**	**16**	**16**	**4**
AB16.2Δ*mexAB*	-	**64**	**8**	**8**	**2**
AB16.2Δ*mexCD-oprJ*	-	**128**	**8**	**8**	**2**
AB8.2	-	**64**	**8**	**8**	**2**
AB8.2Δ*mexXY*	-	**4**	0.06	0.5	0.125

[a] compared to PAO1, a 2-fold increase or decrease of MIC was highlighted in bold or underlined, respectively. CST: colistin, GEN: gentamicin, AMK: amikacin, TOB: tobramycin.
[b] pAK1900-derived *mexXY* expression vector.

3.1. Colistin resistance in *pmrB* mutants is partially dependent upon MexXY(OprM)

While we analyzed the contribution of MexXY(OprM) to aminoglycoside resistance in *pmrB* mutants, we could observe that the inactivation of *mexXY* in mutants AB8.2 and AB16.2 partially abolished colistin resistance (MIC from 64 to 4 µg ml^{-1}) (Table 13). As expected, complementation of the knockout mutant AB16.2Δ*mexXY* with *mexXY* restored the initial phenotype (MIC >128 µg ml^{-1}). Although the MexXY pump is involved in *pmrB*-dependent resistance to colistin, it does not play a similar role in wild-type bacteria (by comparing PAO1 *versus* PAO1Δ*mexXY*). We hypothesized that in *P. aeruginosa*, as in *N. meningitidis*, modification of the core of lipid A by aminoarabinose (phosphoethanolamine in *N. meningitidis*) is necessary but not sufficient to confer a high resistance to colistin, and that MexXY contributes to this phenotype as MtrCDE does in meningococcal strains. Further experiments with mutant AB16.2Δ*oprM* indicated that OM protein OprM also mediates colistin resistance likely by interacting with protein MexXY to form a functional tripartite efflux system (Table 13).

Expression of *mexXY* is known to be induced in colistin-treated bacteria through the TCS ParRS (Muller *et al*., 2011). Inactivation of *parRS* operon in AB16.2 partially reversed the resistance to the antibiotic just as the *mexXY* and *oprM* deletions did. On the other hand, constitutive upregulation of *mexXY* expression in mutant AB16.2Δ*mexZ* was associated with a 2-fold higher MIC of colistin as compared with AB16.2. All these data support the notion that both the modification of lipid A by aminoarabinose and the induced or constitutive activation of *mexXY* are required to promote high resistance levels to colistin in *P. aeruginosa*. As shown in Table 13, TCSs PhoPQ and CprRS, as well as the *mexXY*-activator ArmZ do not contribute to this phenotype. Since deletion of operon *mexXY* (or *oprM*) drastically reduced the resistance of AB16.2 to colistin, as stated above (from 64 to 4 µg ml^{-1}), a plausible explanation is that *mexXY* expression is induced by an ArmZ-independent regulatory pathway in colistin exposed bacteria, most probably *via* ParRS activation.

Finally, we evaluated the contribution of additional RND efflux pumps known to mediate antimicrobial resistance in *P. aeruginosa*. Neither MexAB nor MexCD-OprJ

Table 14: Analysis of the synergy between lipid A modification and efflux.

Strains	Transformed with plasmid	*arnA* transcript level[a]	MIC colistin (µg ml^{-1})
PAO1	-	0.8 ± 0.2	0.5
PAO1	pAK1900	0.9 ± 0.0	0.5
PAO1	pAK1900*::arn*	115.4 ± 47.5	64
PAO1Δ*mexXY*	-	nd	0.5
PAO1Δ*mexXY*	pAK1900	nd	0.5
PAO1Δ*mexXY*	pAK1900*::arn*	nd	2
PAO1Δ*mexZ*	-	0.7 ± 0.0	0.5
PAO1Δ*mexZ*	pAK1900	0.8 ± 0.2	0.5
PAO1Δ*mexZ*	pAK1900*::arn*	126.4 ± 39.5	128
AB16.2	-	656.7 ± 190.1	64
AB16.2Δ*mexXY*	-	775.5 ± 49.8	4

[a] data are expressed as a fold-change ratio to the value from reference strain PAO1.

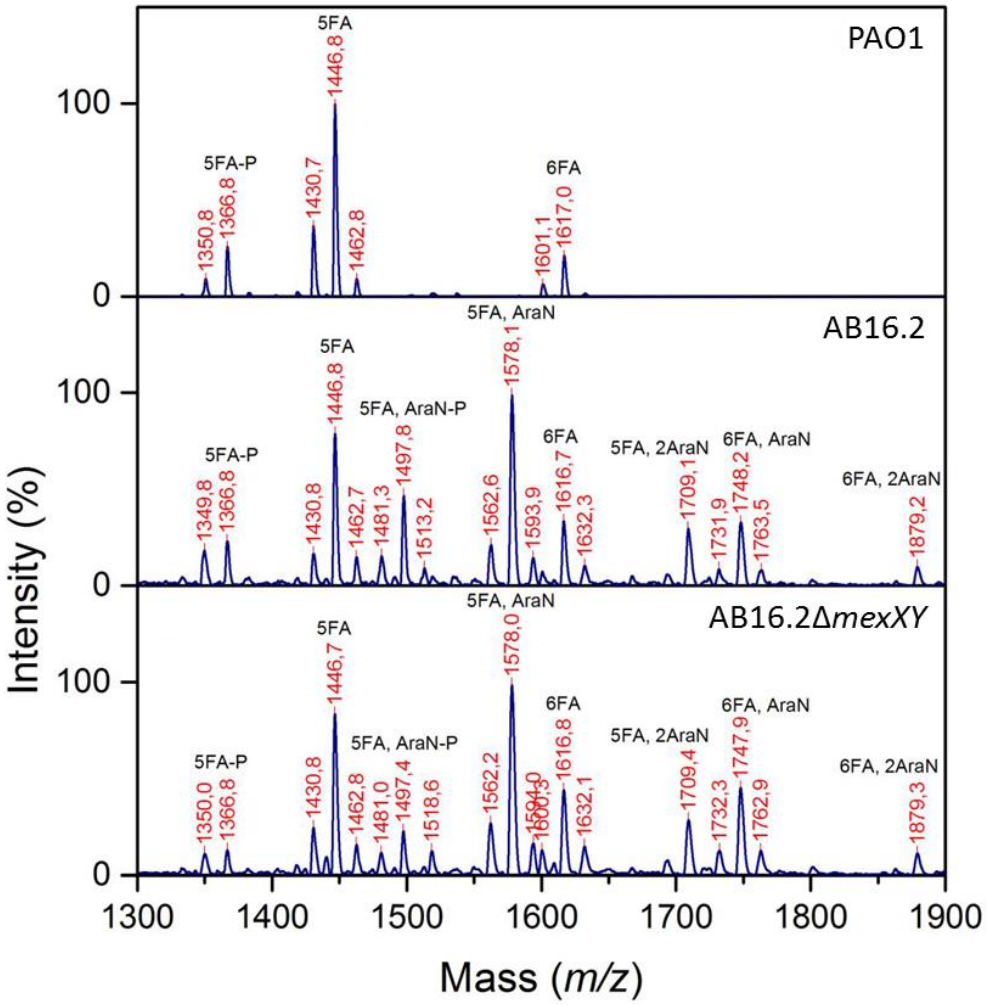

Figure 50: MALDI-TOF mass spectra of lipid A from strains PAO1, AB16.2 and AB16.2Δ*mexXY*.

5FA: penta-acyl molecular species, P: phosphate, 6FA: hexa-acyl molecular species, AraN: aminoarabinose.

modulated colistin MICs when inactivated by gene deletion. The so called MexAB-OprM-dependent tolerance of biofilms to colistin (Pamp *et al*., 2008) as demonstrated previously by deletion of the whole operon can thus be explained by the sole inactivation of gene *oprM*, and impairement of MexXY(OprM) pump.

3.2. Aminoarabinose modification of lipid A is independent of MexXY(OprM)

Inactivation of operon *arn* in AB16.2 restored almost completely the wild-type susceptibility to colistin, demonstrating that LPS modification with aminoarabinose is the major mechanism of colistin resistance in *pmrB* mutants (Table 13). However, the observation that MexXY(OprM) contributes partially to this phenotype raised the issue of whether an interconnection exists between the two mechanisms.

Neither operon *mexXY* nor the ParRS-regulated PA1797 gene appeared to be activated in the transcriptome of mutant AB16.2 (not exposed to colistin or aminoglycosides). These data strongly suggest that the MexXY(OprM) system participates in the high resistance level of AB16.2 to colistin through its activation *via* the TCS ParRS itself activated in response to colistin exposure.

We checked whether operon *arn* expression is at least partially dependent on *mexXY* expression in mutant AB16.2 by comparing *arnA* levels and colistin MICs in AB16.2 and its derivative AB16.2Δ*mexXY* (Table 14). Data demonstrated that MexXY(OprM) does not contribute to the high expression of *arn*. However, this did not rule out the possibility that *mexXY* inactivation might indirectly perturb the effective modification of lipid A by aminoarabinose. To address this question, lipid A from strains PAO1, AB16.2 and AB16.2Δ*mexXY* was extracted and analyzed by MALDI-TOF (in collaboration with the *LPS-BioSciences* company in Orsay, France). Interestingly, MALDI mass spectra showed similar patterns of molecular species substituted with aminoarabinose in AB16.2 and *mexXY*-null mutant AB16.2Δ*mexXY* (Figure 50), clearly indicating that lipid A modification is independent of MexXY(OprM) activity.

To determine if cooperativity between the LPS modification pathway Arn and the efflux pump MexXY(OprM) is strictly dependent or independent from a *pmrB* mutation, we overexpressed operon *arn* (115-fold *versus* the baseline) from plasmid pAK1900 in

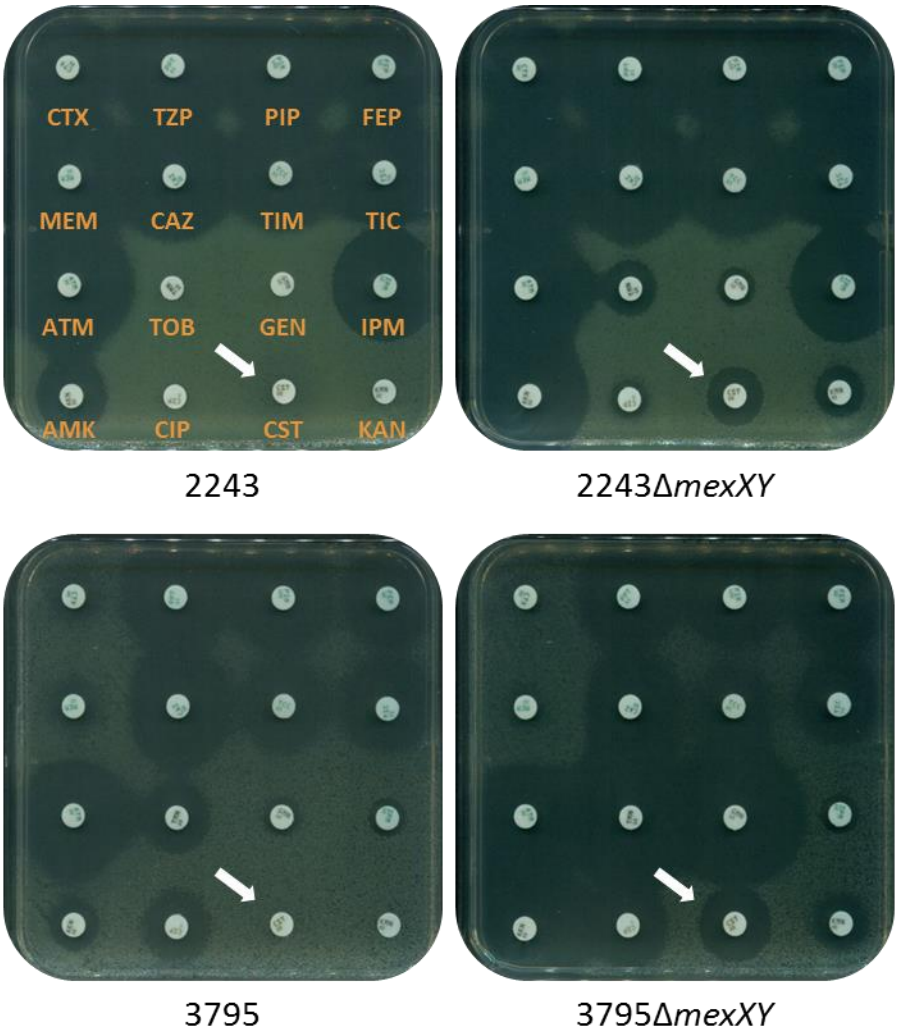

Figure 51: Antibiograms of clinical isolates 2243 and 3795, and their respective *mexXY*-inactivated mutants.

CTX: cefotaxime, TZP: piperacillin-tazobactam, PIP: piperacillin, FEP: cefepime, MEM: meropenem, CAZ: ceftazidime, TIM: ticarcillin-clavulanic acid, TIC: ticarcillin, ATM: aztreonam, TOB: tobramycin, GEN: gentamicin, IPM: imipenem, AMK: amikacin, CIP: ciprofloxacin, CST: colistin, KAN: kanamycin.

PAO1 (Table 14). The high colistin resistance conferred by plasmid pAK1900*::arn* (MIC = 64 µg ml^{-1}) was partially reversed (MIC = 2 µg ml^{-1}) in a Δ*mexXY* background reminiscent of the result obtained in mutant AB16.2. Therefore, we can conclude that the Arn pathway and system MexXY have interplays in colistin resistance independently of the TCS PmrAB (Table 14).

3.3. MexXY(OprM) is required for high resistance levels to colistin in clinical strains exhibiting *pmrB* mutations

Acquired resistance to colistin in clinical strains of *P. aeruginosa* results from mutations in genes encoding TCSs, mostly *pmrAB*. In order to evaluate the contribution of system MexXY(OprM) to colistin resistance in clinical strains, we deleted operon *mexXY* in isolates 2243 (harboring the $Q_{105}P$ substitution in PmrB and $E_{87}K$ in ParR) and 3795 ($G_{188}D$ in PmrB, $A_{82}T$ in ParS and $D_{334}G$ in PhoQ). These gene inactivations increased the susceptibility of both strains to colistin as highlighted by antibiograms (Figure 51) and MIC values (MIC from >128 to 8 µg ml^{-1}) (data not shown), an indication of MexXY(OprM) participation in this resistance. Additionnal investigations are required to evaluate, in this context, if this contribution of MexXY(OprM) is independent from *pmrB* mutations.

4. Conclusion

This project clearly demonstrated that MexXY(OprM) is required for a high colistin resistance in Arn-overexpressing mutants selected *in vitro* or *in vivo*. Previously known for its contribution to intrinsic, acquired and adaptive resistance to aminoglycosides, MexXY(OprM) is also able to promote the development of high resistance to colistin in conjunction with LPS modification. Consequently, the proposed role of MexAB-OprM in tolerance of biofilms to colistin (Pamp *et al*., 2008) deserves to be reconsidered as it might result from a wrong interpretation of data due to the inactivation of gene *oprM*. Identification of MexXY-inhibitors would be helpful to restore the susceptibility of some clinical isolates of *P. aeruginosa* to both aminoglycosides and colistin.

Chapter 4. Identification of new azetidine-containing alkaloids produced by *P. aeruginosa*

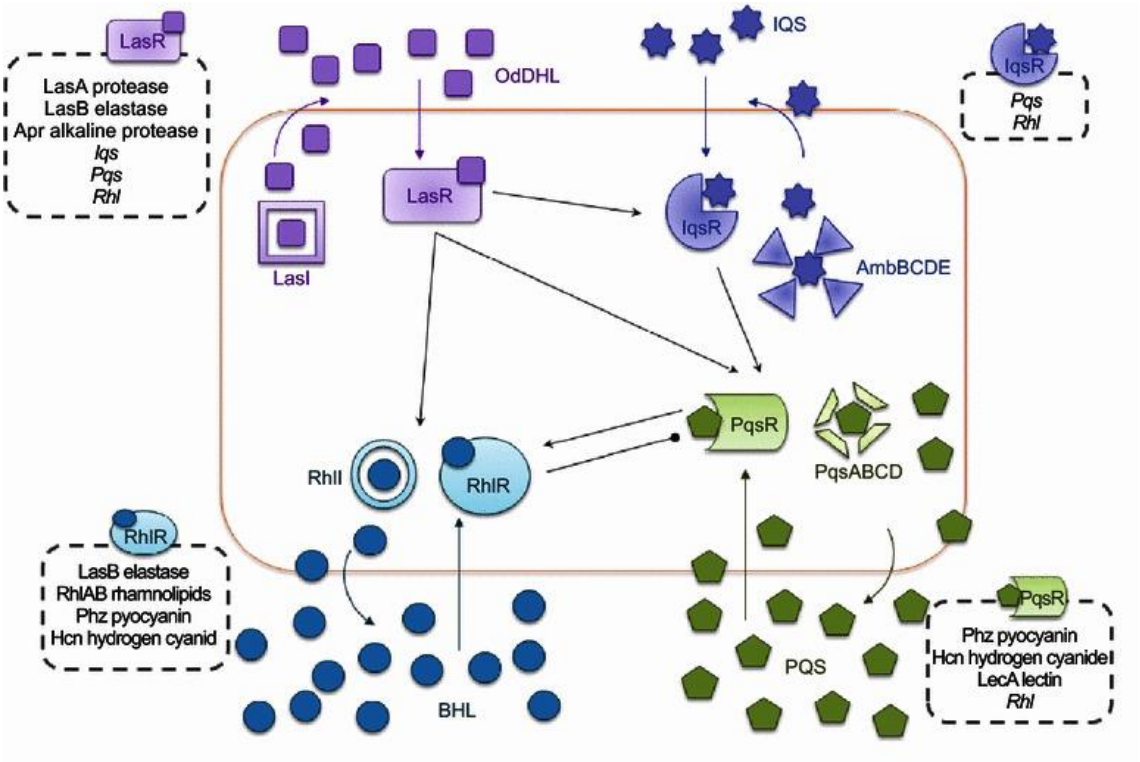

(Lee and Zhang, 2015)

Figure 52: Schematic representation of *quorum* sensing-dependent signaling in *P. aeruginosa*.

In *P. aeruginosa*, QS signaling is based on two acyl-homoserine lactone (acyl-HSL) QS systems (LasI-LasR and RhlI-RhlR), and two systems using either PQS (2-heptyl-3-hydroxy-4-quinolone) or IQS (2-(2-hydroxyphenyl)-thiazole-4-carbaldehyde). LasI and RhlI are responsible for the synthesis of N-3-oxododecanoyl-HSL (3OC12-HSL) and N-butanoyl-HSL (C4-HSL), respectively; while LasR responds to 3OC12-HSL, and RhlR to C4-HSL. The PQS molecule is synthesized by the product of genes *pqsABCD*, *phnAB* and *pqsH*; IQS production is dependent on the NRPS gene cluster *ambBCDE* (Lee and Zhang, 2015).
Arrows indicate an effect.

1. Context

The impressive capacity of *P. aeruginosa* to infect a large range of hosts is in part due to a remarkable cell density-based intracellular communication network named *Quorum* sensing (QS). QS-based gene regulation relies on at least four interconnected signaling pathways detailed in Figure 52 (Lee and Zhang, 2015). The QS network responds to environmental stress signals which are known to be sensed by TCSs. Sensor histidine kinase PhoQ was shown to modulate the virulence of *P. aeruginosa* (Gooderham *et al*., 2009) through a large regulon (Gooderham *et al*., 2009). Transcriptome analysis of *pmrB* mutant AB16.2 revealed the activation of locus *pqsABCDE* and of an uncharacterized cluster PA3326-PA3335 containing a gene encoding a bimodular NRPS (PA3327) (Figure 42).

2. Objective

NRPs are bacterial molecules exhibiting specific activities in nutrient acquisition, cell-to-cell communication and virulence. Many NRPs have medical applications as antibiotics, antitumoral drugs, immunosuppressants. For these reasons, characterization of NRPs produced by the biosynthesis gene cluster PA3326-PA3335 was undertaken through a collaboration with Zhilai Hong and Dr Yanyan Li from the MCAM unit at the *Muséum National d'Histoire Naturelle* in Paris. The possible regulation of the gene cluster by QS and its contribution to antibiotic resistance profile of a *pmrB* mutant were evaluated.

3. Results

3.1. Azetidine-containing alkaloids produced by a *quorum*-sensing regulated non-ribosomal peptide synthetase pathway in *Pseudomonas aeruginosa*

Zhilai Hong, **Arnaud Bolard**, Caroline Giraud, Sébastien Prévost, Grégory Genta-Jouve, Christiane Deregnaucourt, Susanne Häussler, Katy Jeannot, Yanyan Li
Angewandte Chemie (International ed. in English), 2019. Mar 4;58(10):3178-3182.
doi: 10.1002/anie.201809981.

Natural Products

Deutsche Ausgabe: DOI: 10.1002/ange.201809981
Internationale Ausgabe: DOI: 10.1002/anie.201809981

Azetidine-Containing Alkaloids Produced by a Quorum-Sensing Regulated Nonribosomal Peptide Synthetase Pathway in *Pseudomonas aeruginosa*

Zhilai Hong, Arnaud Bolard, Caroline Giraud, Sébastien Prévost, Grégory Genta-Jouve, Christiane Deregnaucourt, Susanne Häussler, Katy Jeannot, and Yanyan Li**

Abstract: *Pseudomonas aeruginosa displays an impressive metabolic versatility, which ensures its survival in diverse environments. Reported herein is the identification of rare azetidine-containing alkaloids from P. aeruginosa PAO1, termed azetidomonamides, which are derived from a conserved, quorum-sensing regulated nonribosomal peptide synthetase (NRPS) pathway. Biosynthesis of the azetidine motif has been elucidated by gene inactivation, feeding experiments, and biochemical characterization in vitro, which involves a new S-adenosylmethionine-dependent enzyme to produce azetidine 2-carboxylic acid as an unusual building block of NRPS. The mutants of P. aeruginosa unable to produce azetidomonamides had an advantage in growth at high cell density in vitro and displayed rapid virulence in Galleria mellonella model, inferring functional roles of azetidomonamides in the host adaptation. This work opens the avenue to study the biological functions of azetidomonamides and related compounds in pathogenic and environmental bacteria.*

Pseudomonas aeruginosa is a highly adaptable Gram-negative bacterium which thrives in diverse environments, including soil, water, plant, and animal hosts. This microorganism is a prominent nosocomial human pathogen which is associated with acute pulmonary infections in immunocompromised patients, particularly in intensive care units. It is also well-known in cystic fibrosis patients for the deleterious impact on lung function. The ecological success of *P. aeruginosa* is largely attributed to its metabolic plasticity and versatility, frequently linked to quorum-sensing (QS) regulation. QS is a cell–cell communication mechanism allowing bacteria to sense cell density and to coordinate gene expression at the community level in response to environmental conditions. *P. aeruginosa* has evolved complex QS systems to control critical processes including biofilm formation, virulence factor production, and antimicrobial resistance. The knowledge of the chemical nature and biological function of QS-regulated specialized metabolites is thus of prime importance and would provide new biomarkers or therapeutic strategies to progress in combating *P. aeruginosa* infection.[1]

The core genome of *P. aeruginosa* encodes six nonribosomal peptide synthetase (NRPS) biosynthetic gene clusters (BGCs) as major components of the specialized metabolism.[2] Among them, three are involved in the production of siderophores such as pyoverdine and pyochelin, as well as an antibacterial antimetabolite, L-2-amino-4-methoxy-*trans*-3-butenoic acid.[3] Although extensively studied, products of other NRPS pathways remain elusive. During the course of investigating new physiological functions associated with polymyxin resistance, we generated a spontaneous mutant from *P. aeruginosa* reference strain PAO1 on colistin ($16\ mg\,L^{-1}$), named AB16.2, and performed the whole genome expression profile. Among genes that are most up-regulated in the mutant AB16.2 in comparison with the parental strain PAO1, we identified the operons *pmrAB* encoding a two-component system, PmrA-PmrB, involved in

[*] Z. Hong, Dr. G. Genta-Jouve, Dr. C. Deregnaucourt, Dr. Y. Li
Unité Molécules de Communication et Adaptation des Microorganismes (MCAM), Muséum National d'Histoire Naturelle (MNHN), Centre National de la Recherche Scientifique (CNRS), CP 54
57 rue Cuvier, 75005 Paris (France)
E-mail: yanyanli@mnhn.fr

A. Bolard, Dr. K. Jeannot
Laboratoire de Bactériologie, Centre National de Référence (CNR) de la Résistance aux Antibiotiques, Centre Hospitalier Régional Universitaire (CHRU) de Besançon, UMR4269 "Chrono-Environnement"
Boulevard Fleming, 25030 Besançon (France)
E-mail: katy.jeannot@univ-fcomte.fr

Dr. C. Giraud
U2RM Stress/Virulence, Normandy University, UNICAEN
14000 Caen (France)

Dr. S. Prévost
Laboratoire de Synthèse Organique, UMR 7652, CNRS, Ecole Polytechnique, ENSTA ParisTech, Université Paris-Saclay
828 Bd des Maréchaux, 91128 Palaiseau (France)

Dr. G. Genta-Jouve
C-TAC, UMR 8638, CNRS, Faculté de Pharmacie de Paris, Université Paris Descartes, Sorbonne Paris Cité
4 Avenue de l'Observatoire, 75006 Paris (France)

Prof. Dr. S. Häussler
Institute for Molecular Bacteriology, TWINCORE, Centre for Experimental and Clinical Infection Research
Hannover (Germany)
and
Department of Molecular Bacteriology, Helmholtz Centre for Infection Research, Braunschweig (Germany)

Supporting information and the ORCID identification number(s) for the author(s) of this article can be found under: https://doi.org/10.1002/anie.201809981.

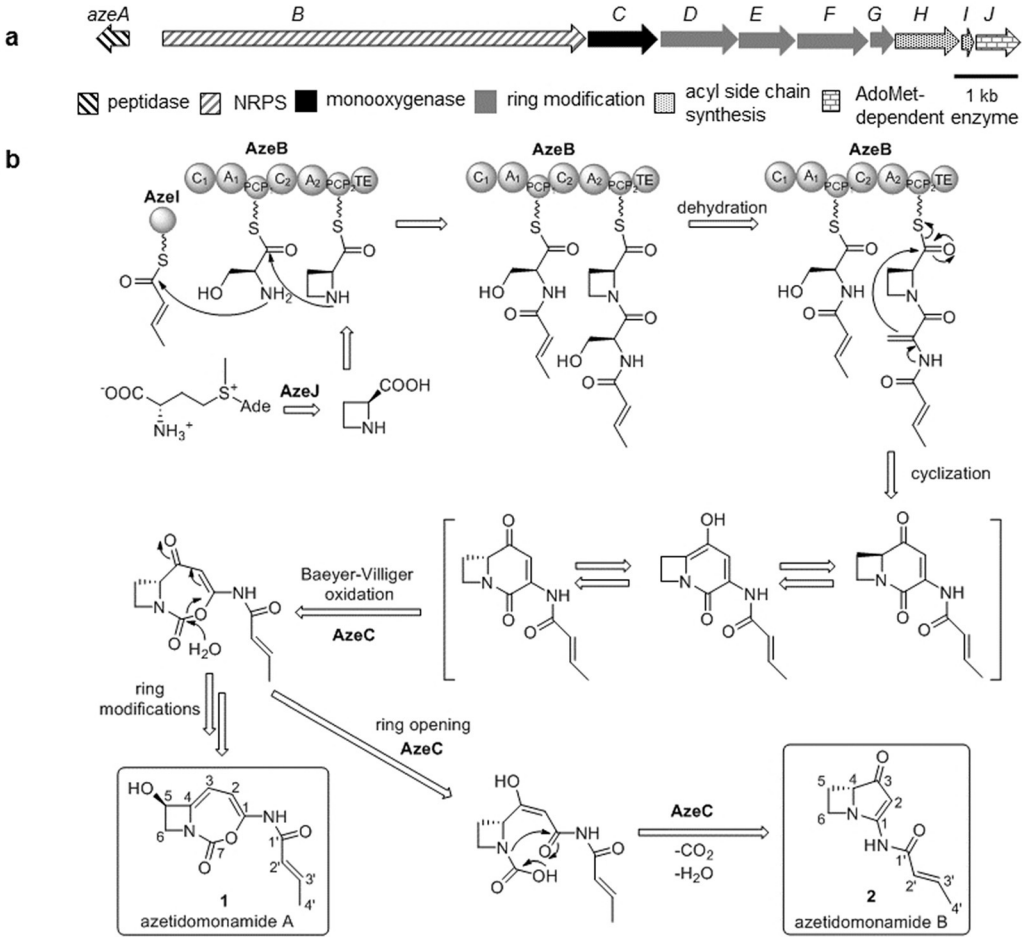

Figure 1. a) Gene organization of the *aze* cluster. b) Structure and proposed biosynthetic pathway of azetidomonamides.

polymyxin resistance,[4] *pqsABCDE* coding the pseudomonas quinolone signal (PQS) belonging to the QS system and one uncharacterized BGC for nonribosomal peptide synthesis (see Table S1 in the Supporting Information). This BGC comprises 10 genes (PA3326–PA3335) encoding notably a bimodular NRPS (the product of PA3327) and modification enzymes (Figure 1 a; see Table S2). Worthy of note, this BGC is strictly conserved in all sequenced *P. aeruginosa* genomes, with only few exceptions in other *Pseudomonas* species, in the *Pseudomonas* genome database.[5] Moreover, some genes of this BGC, including PA3326, 3327, 3329, and 3332, have been shown to be part of the core regulon of the *las*/*rhl* QS systems using acyl-homoserine lactone as signals.[6] Given that *pqs* genes are overexpressed in the mutant AB16.2, we assessed if the cluster is also regulated by *pqs* QS. Quantitative real-time PCR with reverse transcription analysis showed that in-frame deletion of *pqsA* in the mutant AB16.2 resulted in a significant decrease of PA3327 transcription (see Figure S1). Therefore, this BGC is under the control of three QS systems operating in *P. aeruginosa.* Taken together, this data suggests that the metabolites derived from this pathway play an important role in the pathogen's physiology.

To facilitate compound identification, a PA3327-deficient mutant of AB16.2 was constructed. After media screening, AB16.2 and AB16.2Δ27 were grown in selected E2 medium and their metabolic profiles were compared by liquid chromatography coupled to high-resolution mass spectrometry (LC-HRMS). Two major peaks with a $[M+H]^+$ ion at m/z 237.0868 (**1**) and 193.0969 (**2**) were present only in the extract of AB16.2 (see Figure S2). The exact masses indicated molecular formulas of $C_{11}H_{12}N_2O_4$ for **1** and $C_{10}H_{12}N_2O_2$ for **2**, indicating a CO_2 loss in the latter. Fermentation and subsequent purification allowed the full elucidation of their structures by HR-MS/MS, UV, and NMR spectroscopy (see Table S3 and Figures S3–S19). The compound **1**, named azetidomonamide A, features a [5.2.0]bicyclocarbamate ring system, whereas **2**, termed azetidomonamide B, has an azetidopyrroline scaffold (Figure 1 b). Based on specific rotation and the comparison between the measured and theoretical electronic circular dichroism (ECD) spectra, the absolute configuration was determined to be 5*R* for **1** and 4*R* for **2** (see Figures S20 and S21).

The four-membered azetidine heterocycle presented in the azetidomonamides is rare in natural products (see Figure S22), and raised the question about its biosynthetic origin. Structurally, **1** and **2** are related to bacterial lipocyclocarbamates[7] and pyrrolizidine alkaloids[8] (see Figure S23). Biosynthesis of these compounds has been characterized to involve a bimodular NRPS that ligates either a serine (Ser) or threonine (Thr) to a proline (Pro) residue, and a Baeyer–

Villiger monooxygenase whose action leads to two bicyclic skeletons.[8,9] Predicted functions of now designated *aze* genes (see Table S2) suggested that azetidomonamide biogenesis would operate in a similar way, except the activation by NRPS of either an azetidine 2-carboxylic acid (AZC) or a derivative thereof instead of Pro. To prove this proposal, in vivo isotope-labelling experiments with L-Ser, L-methionine (Met), and L-AZC were performed using an inverse feeding approach.[10] The rational to feed Met was that Met-derived *S*-adenosyl-methionine (AdoMet) could be a key precursor of AZC, similar to the synthesis of plant nicotianamine.[11] LC-HRMS and MS/MS analysis showed the incorporation of all three amino acids into **2** (see Figures S24 and S25). As for **1**, its labelling by L-Ser and L-Met was observed, but addition of L-AZC appeared to reduce significantly its production level which prevented the detection (see Figures S26 and S27). Furthermore, in silico analysis of the adenylation (A) domains of AzeB was carried out. This analysis predicted that AzeB_A1 activates Ser, whereas the specificity of AzeB_A2 could be Pro but without certainty (see Table S4). To unambiguously establish the building blocks of AzeB, both A domains together with their cognate condensation (C) and peptidyl-carrier-protein (PCP) were produced and purified from *Escherichia coli* for characterization in vitro (see Figure S28). Twenty proteinogenic amino acids together with additional ones (i.e., L-AZC, D-Pro, AdoMet and homoserine) were tested as substrates. Using a hydroxylamine-trapping assay,[12] it was shown that AzeB_A2 displayed the highest activity towards L-AZC and showed substrate promiscuity, notably to the structural mimics of AZC such as L-Pro and L-Ala (Figure 2a). By a more specific ATP-release assay,[13] we could further confirm the substrate preference of AzeB_A1 and AzeB_A2 for L-Ser and L-AZC, respectively (see Figures S29 and S30). Together, these data established that the azetidine motif comes from L-AZC, which is derived from the Met cycle, and is subsequently incorporated into the NRPS assembly line.

AZC has been known as a non-proteinogenic amino acid in some plants for 60 years.[14] However, its biosynthetic route still remains unknown, although feeding studies similarly showed a link of AZC and the Met metabolism.[15] We envisioned that L-AZC can result from the intramolecular cyclization of AdoMet, as in the plant nicotianamine biosynthesis.[11] Inspection of the *aze* cluster identified *azeJ* encoding an AdoMet-dependent enzyme as a candidate for this reaction. Indeed, inactivation of *azeJ* in the mutant AB16.2 disrupted completely the production of both azetidomonamides, while complementation of *azeJ* back to the mutant restored the production, albeit at a much lower level (Figure 2b). Interestingly, supply of L-AZC to the medium

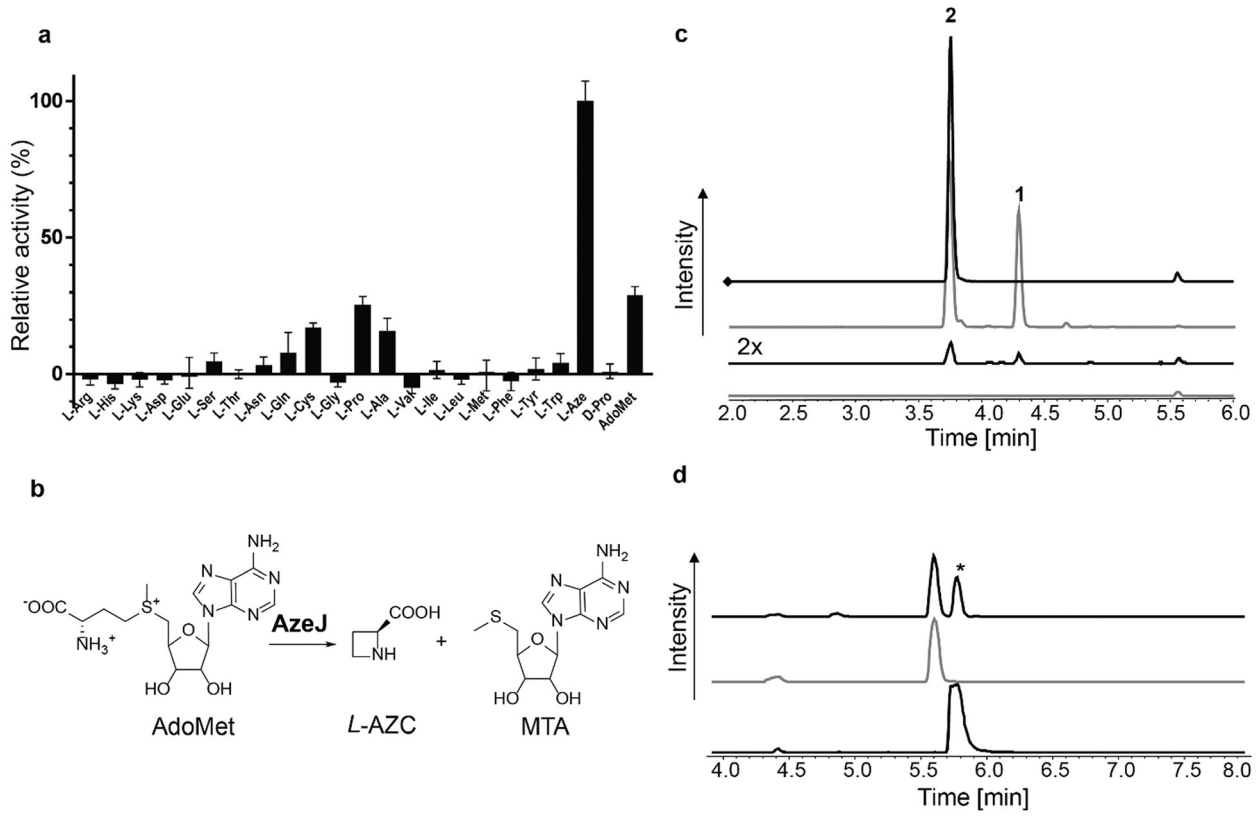

Figure 2. Biosynthetic origin of the azetidine motif. a) The substrate specificity of AzeB_A2 domain determined in vitro. b) Reaction Scheme of AzeJ. c) LC-MS analysis of azetidomonamide production in *P. aeruginosa* AB16.2 (grey), the *azeJ*-deficient strain AB16.2Δ35 (dotted line), AB16.2Δ35 supplemented with AZC (black) and the complementation strain AB16.2Δ35 *attB*:PA3335 (dashed line). Extracted ion chromatograms (EICs) of ions *m/z* 237.0867 ($[M+H]^+$ of **1**) and *m/z* 193.0968 ($[M+H]^+$ of **2**) are shown. For clarity, the trace of the complementation strain is enlarged twofold. Addition of AZC disrupted the production of **1**. d) LC-MS analysis of AZC production in AzeJ assays in vitro. EICs of *m/z* 258.0729 ($[M+Na]^+$ of the derivatized AZC product): AZC standard (dashed line), AzeJ reaction (black) and a control with boiled AzeJ (grey).

yielded only **2**, and is consistent with the feeding experiments. It thus appeared that AZC availability regulates directly the product outcome. To provide direct evidence of the AzeJ function, recombinant AzeJ was purified from *E. coli* and characterized in vitro (see Figure S28). Incubation of AdoMet with AzeJ led to the production of 5′-methylthioadenosine (MTA), as revealed by HPLC coupled to UV/Vis spectrophotometry (see Figure S31). Detection of AZC was achieved by derivatization with benzyl chloroformate followed by LC-HRMS analysis. AZC was observed in the AzeJ reaction and absent in the control with the heat-inactivated enzyme (Figure 2d). Moreover, AZC was found only in the extract of *E. coli* expressing the *azeJ* gene, compared to that of control cells with an empty vector (see Figure S32). These experiments showed unambiguously that AzeJ is an AZC synthase. Under our conditions, AzeJ displayed K_m^{app}-(AdoMet) of 1.3 ± 0.1 mM and k_{cat}^{app} of $16.7 \pm 0.7\ min^{-1}$, indicating a rather low catalytic efficiency (see Figure S33). Worthy of note, a similar enzyme (VioH) proposed to catalyze the same reaction as AzeJ, has been identified very recently by gene inactivation in the myxobacterial vioprolide pathway.[16] Sequence analysis using profile hidden Markov models pointed out that AzeJ homologues can be found in disparate bacteria, and occasionally in eukaryotes (e.g. algae) or archaea (see Table S5). The discovery of AZC synthases from bacteria adds a new reaction to AdoMet-dependent enzymes and may inform the biosynthetic origin of AZC in plants.

Overall, the ensemble of our data consolidates the proposed biosynthetic route to azetidomonamides (Figure 1), which is similar to that of related bacterial alkaloids (see Figure S34).[8,9] Our data also extends the current model. The crotonyl side chain in azetidomonamides is delivered to the NRPS on a dedicated ACP, contrary to other pathways that use CoA esters. On-line cyclization would operate on a dipeptide intermediate containing a serine-derived dehydroalanine (Dha), a process likely assisted by the TE domain.[8,9] A plausible cyclization mechanism would involve nucleophilic attack of the Dha β-carbon atom to the carbonyl group, and is enabled by delocalization of the lone pair of electrons of the enamine nitrogen. Upon cyclization, the azetidopyridin-2-one intermediate would undergo keto–enol tautomerization to generate an R-configured substrate for AzeC, which catalyzes Baeyer–Villiger oxidation in a stereospecific manner. This resembles the biosynthesis of brabantamide A.[9b]

More minor products derived from the *aze* BGC could be identified by LC-HRMS. In particular, the compounds **3** ($[M+H]^+$ at *m*/*z* 207.1124) and **4** ($[M+H]^+$ at *m*/*z* 251.1024) are analogues of **1** and **2**, respectively (see Figures S35 and S36). The pyrrolizidine structure of **3** was confirmed by a synthetic reference (see the Supporting Information). These molecules are generated by incorporating Pro instead of AZC during the assembly-line synthesis. Such diversity-oriented biosynthesis would imply distinct or/and synergetic functional roles of these metabolites in the physiology of *P. aeruginosa.*

The compounds **1**, **2**, and **3** showed no antibacterial activities to tested Gram-negative and Gram-positive bacteria (*E. coli*, *Micrococcus luteus*, *Staphylococcus aureus*), no inhibition of human phospholipase A2, an activity reported for the related 5,5- or 5,7-lipocyclocarbamate,[7,17] as well as no cytotoxicity to murine macrophages cell line J774A.1. This data indicates that, at least, these metabolites are less likely to be involved in microbial competition or acute virulence. To gain insight into their biological function in *P. aeruginosa*, the mutants AB16.2 and AB16.2Δ27 were subject to phenotypic characterization. No significant difference between them could be observed with regard to biofilm formation, microcolony morphology, and antibiotic resistance. However, the mutant AB16.2 displayed a reduced growth at high cell density as compared to AB16.2Δ27 in vitro (Figure 3a). The

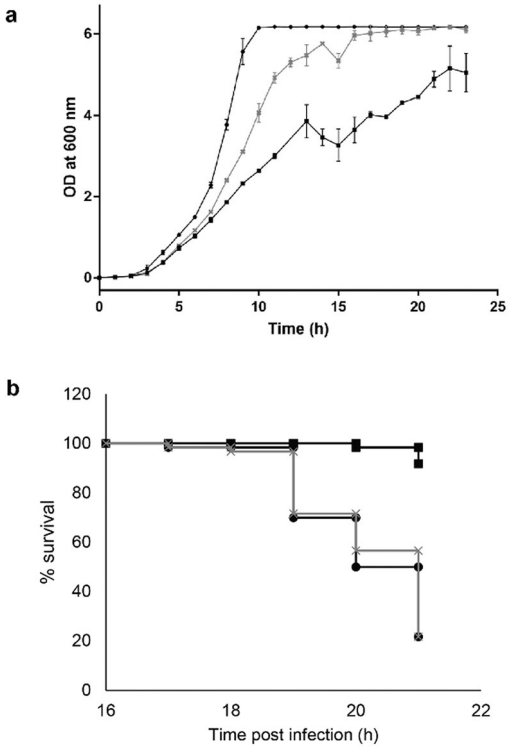

Figure 3. Characterization of the functional roles of azetidomonamides. a) Growth curve in LB medium at 37°C. b) Kaplan-Meier survival curves of *Galleria mellonella* infected with *P. aeruginosa* strains with an inoculum of 25(±5) CFU per larvae. $p < 0.001$ (log-rank test with Bonferroni correction). PAO1 (black circles), AB16.2 (black squares) and AB16.2Δ27 (grey crosses).

deviation typically started at the mid- or late logarithmic phase, corroborating with the growth phase-dependent QS-regulation of these *aze* genes.[6b] To note, both strains showed a slower growth rate than the parental PAO1. When microinjected into a caterpillar host, *Galleria mellonella*, the mutant AB16.2 had a delayed killing phenotype, whereas AB16.2Δ27 killed as rapidly and efficiently as the wildtype PAO1 (Figure 3b). This attenuated virulence effect manifested by the presence of the *aze* BGC, likely by the growth modulation, is reminiscent of a QS-controlled virulence reduction in an insect endosymbiotic bacterium, following its infection of insects.[18] The direct implication for *P. aeruginosa* would be to establish a long-term stable relationship

with the host, as under the chronic infection conditions.[19] The underlining molecular mechanisms are being investigated.

Genome mining revealed that identical *aze* BGC is present in two strains of human pathogens, namely *Acinetobacter baumannii* AB32_M and *Enterobacter cloacae* e403 (see Figure S37), indicating a horizontal gene-transfer event from *P. aeruginosa.* Using the combined presence of *azeB*, *azeC*, and *azeJ* as an indication, related *aze* BGCs can be identified in a handful of bacteria, some of them are plant-associated (see Figure S37). Consistently, phylogenetic analysis showed that, A2 domains of the AzeB-like NRPSs, which would activate AZC, form a distinct group from the Pro-utilizing ones involved in the biosynthesis of bacterial pyrrolizidine alkaloids and cyclocarbamates[8] (see Figure S38). Together, these analyses open the avenue to study the diversity and biological functions of azetidomonamide-like compounds in various ecological settings, particularly in human pathogens.

In conclusion, this work identifies a novel class of specialized metabolites in the major opportunist human pathogen *P. aeruginosa*, elucidates their biosynthesis which involves a new family of AdoMet-dependent enzymes, and provides first insight into their physiological functions. Further studies of exact roles of azetidomonamides in host–pathogen interactions with regard to QS regulation would lead to important mechanistic discoveries.

Experimental Section

Experimental details are given in the Supporting Information.

Acknowledgements

The bioorganic analytical platform of MNHN and the bacteriology service in the MCAM unit are acknowledged for giving access to necessary instruments. We thank Yoann Negre for technical assistance in caterpillar killing assays, Dr. Gérard Lambeau (Université Côte d'Azur, France) for providing radioactive *E. coli* membranes for phospholipase tests, and Dr. Stéphane Mann (MNHN, France) for helpful discussions. Z. H. was supported by a China Scholarship Council PhD fellowship. This work was partially supported by the French Ministry of Health through the Santé publique France agency.

Conflict of interest

The authors declare no conflict of interest.

Keywords: alkaloids · biosynthesis · enzymes · natural products · quorum sensing

How to cite: *Angew. Chem. Int. Ed.* **2019**, *58*, 3178–3182
Angew. Chem. **2019**, *131*, 3210–3214

[1] J. Lee, L. Zhang, *Protein Cell* **2015**, *6*, 26–41.
[2] B. Valot, C. Guyeux, J. Y. Rolland, K. Mazouzi, X. Bertrand, D. Hocquet, *PLoS ONE* **2015**, *10*, e0126468.
[3] A. M. Gulick, *Nat. Prod. Rep.* **2017**, *34*, 981–1009.
[4] S. M. Moskowitz, R. K. Ernst, S. I. Miller, *J. Bacteriol.* **2004**, *186*, 575–579.
[5] G. L. Winsor, E. J. Griffiths, R. Lo, B. K. Dhillon, J. A. Shay, F. S. Brinkman, *Nucleic Acids Res.* **2016**, *44*, D646–D653.
[6] a) S. Chugani, B. S. Kim, S. Phattarasukol, M. J. Brittnacher, S. H. Choi, C. S. Harwood, E. P. Greenberg, *Proc. Natl. Acad. Sci. USA* **2012**, *109*, E2823–2831; b) V. E. Wagner, D. Bushnell, L. Passador, A. I. Brooks, B. H. Iglewski, *J. Bacteriol.* **2003**, *185*, 2080–2095; c) A. M. Firoved, V. Deretic, *J. Bacteriol.* **2003**, *185*, 1071–1081; d) P. Salunkhe, C. H. M. Smart, J. A. W. Morgan, S. Panagea, M. J. Walshaw, C. A. Hart, R. Geffers, B. Tuemmler, C. Winstanley, *J. Bacteriol.* **2005**, *187*, 4908–4920.
[7] D. J. Busby, R. C. Copley, J. A. Hueso, S. A. Readshaw, A. Rivera, *J. Antibiot.* **2000**, *53*, 670–676.
[8] a) S. Huang, J. Tabudravu, S. S. Elsayed, J. Travert, D. Peace, M. H. Tong, K. Kyeremeh, S. M. Kelly, L. Trembleau, R. Ebel, M. Jaspars, Y. Yu, H. Deng, *Angew. Chem. Int. Ed.* **2015**, *54*, 12697–12701; *Angew. Chem.* **2015**, *127*, 12888–12892; b) O. Schimming, V. L. Challinor, N. J. Tobias, H. Adihou, P. Grun, L. Poschel, C. Richter, H. Schwalbe, H. B. Bode, *Angew. Chem. Int. Ed.* **2015**, *54*, 12702–12705; *Angew. Chem.* **2015**, *127*, 12893–12896.
[9] a) C. W. Johnston, R. Zvanych, N. Khyzha, N. A. Magarvey, *ChemBioChem* **2013**, *14*, 431–435; b) Y. Schmidt, M. van der Voort, M. Crusemann, J. Piel, M. Josten, H. G. Sahl, H. Miess, J. M. Raaijmakers, H. Gross, *ChemBioChem* **2014**, *15*, 259–266.
[10] H. B. Bode, D. Reimer, S. W. Fuchs, F. Kirchner, C. Dauth, C. Kegler, W. Lorenzen, A. O. Brachmann, P. Grun, *Chem. Eur. J.* **2012**, *18*, 2342–2348.
[11] J. F. Ma, T. Shinada, C. Matsuda, K. Nomoto, *J. Biol. Chem.* **1995**, *270*, 16549–16554.
[12] B. P. Duckworth, D. J. Wilson, C. C. Aldrich, *Methods Mol. Biol.* **2016**, *1401*, 53–61.
[13] A. J. Lloyd, N. J. Potter, C. W. Fishwick, D. I. Roper, C. G. Dowson, *ACS Chem. Biol.* **2013**, *8*, 2157–2163.
[14] L. Fowden, *Nature* **1955**, *176*, 347.
[15] E. Leete, G. E. Davis, C. R. Hutchinson, K. W. Woo, M. R. Chedekel, *Phytochemistry* **1974**, *13*, 427–433.
[16] F. Yan, D. Auerbach, Y. Chai, L. Keller, Q. Tu, S. Huttel, A. Glemser, H. A. Grab, T. Bach, Y. Zhang, R. Müller, *Angew. Chem. Int. Ed.* **2018**, *57*, 8754–8759; *Angew. Chem.* **2018**, *130*, 8890–8895.
[17] J. Thirkettle, E. Alvarez, H. Boyd, M. Brown, E. Diez, J. Hueso, S. Elson, M. Fulston, C. Gershater, M. L. Morata, P. Perez, S. Ready, J. M. Sanchez-Puelles, R. Sheridan, A. Stefanska, S. Warr, *J. Antibiot.* **2000**, *53*, 664–669.
[18] S. Enomoto, A. Chari, A. L. Clayton, C. Dale, *Cell Host Microbe* **2017**, *21*, 629–636.
[19] a) X. Qin, *Crit. Rev. Microbiol.* **2016**, *42*, 144–157; b) G. Jansen, L. L. Crummenerl, F. Gilbert, T. Mohr, R. Pfefferkorn, R. Thanert, P. Rosenstiel, H. Schulenburg, *Mol. Biol. Evol.* **2015**, *32*, 2883–2896.

Manuscript received: August 30, 2018
Revised manuscript received: November 8, 2018
Accepted manuscript online: December 11, 2018
Version of record online: January 14, 2019

Angewandte Chemie
Eine Zeitschrift der Gesellschaft Deutscher Chemiker

Supporting Information

Azetidine-Containing Alkaloids Produced by a Quorum-Sensing Regulated Nonribosomal Peptide Synthetase Pathway in *Pseudomonas aeruginosa*

Zhilai Hong, Arnaud Bolard, Caroline Giraud, Sébastien Prévost, Grégory Genta-Jouve, Christiane Deregnaucourt, Susanne Häussler, Katy Jeannot, and Yanyan Li**

anie_201809981_sm_miscellaneous_information.pdf

Author Contributions

Z.H. Data curation: Lead; Formal analysis: Lead; Investigation: Lead; Methodology: Equal; Writing – original draft: Supporting
A.B. Investigation: Equal
C.G. Investigation: Equal; Methodology: Supporting
S.P. Investigation: Supporting
G.G. Investigation: Supporting
C.D. Investigation: Supporting
S.H. Data curation: Supporting
K.J. Conceptualization: Equal; Funding acquisition: Lead; Methodology: Equal; Supervision: Lead; Writing – original draft: Equal; Writing – review & editing: Equal
Y.L. Conceptualization: Equal; Formal analysis: Lead; Funding acquisition: Lead; Methodology: Equal; Project administration: Lead; Supervision: Lead; Writing – original draft: Lead; Writing – review & editing: Lead.

Table of Contents

Experimental Procedures

Bacterial strains, plasmids and growth conditions

The bacterial strains and plasmids used or constructed in this study are listed in the supplemental Table S5. *P. aeruginosa* were routinely grown in Mueller Hinton Broth (MHB) with adjusted concentrations of divalent cations Ca^{2+} and Mg^{2+} (Beckton Dickinson, Microbiology Systems, Cockeysville), or in Lysogeny Broth (LB), or on Mueller Hinton Agar (MHA) (Bio-Rad, Marnes-la-Coquette, France). For azetidomonamide production, *P. aeruginosa* were grown in E2 medium containing 3.5 g/L $NaNH_4HPO_4 \cdot 4H_2O$, 7.5 g/L $K_2HPO_4 \cdot 3H_2O$, 3.7 g/L KH_2PO_4, 0.2% glycerol and supplemented with 1 mL of 1M $MgSO_4$ and 1 mL of MT microelements stock solution (for MT stock: 2.78 g/L $FeSO_4 \cdot 7H_2O$, 1.98 g/L $MnCl_2 \cdot 4H_2O$, 2.81 g/L $CoSO_4 \cdot 7H_2O$, 0.47 g/L $CaCl_2 \cdot 2H_2O$, 0.17 g/L $CuCl_2 \cdot 2H_2O$ and 0.29 g/L $ZnSO_4$ in 1 N HCl).[1] *E. coli* were routinely grown in LB. Plasmids and primers are listed in Table S6-7.

Selection of colistin resistant mutant and transcriptomics analysis

From the *P. aeruginosa* reference strain PAO1, isolation of one-step mutants with increased colistin resistance was performed by plating 100 μL aliquots of log phase *P. aeruginosa* cultures ($A_{600\ nm}$ equal to 1) on MHA supplemented with 16 mg/L of colistin sulfate (Sigma-Aldrich Chimie, Lyon, France). The selected mutant AB16.2 and its PAO1 parental strain were grown in drug-free MHB, until an absorbance of A_{600nm}=1 ± 0.05 (full transcriptomics study will be reported elsewhere).

Construction of *P. aeruginosa* mutants

Primers used in this study were listed in Table S6. Single disruption of PA3327, PA3335 and *pqsA* genes in *P. aeruginosa* was performed by homologous recombination events as previously described[2]. Brefly, two flanking regions of 0.5 kb of the fragment to be deleted were assembled by overlapping PCR and cloned into the suicide vector, pKNG101. To construct the plasmid for PA3335 complementation, the complete sequence of gene PA3335 was amplified from genomic DNA of the PAO1 strain, cloned into the shuttle vector pCR-blunt, and subsequently subcloned into the plasmid mini-CTX1[3]. Recombinant plasmids were introduced into *P. aeruginosa* strains by triparental conjugation by using mobilisation properties of broad-host range helper plasmid pRK2013. Transconjugants were selected on *Pseudomonas* Isolation Agar (PIA) or MHA supplemented with tetracyclin 15 mg/L and streptomycin 50 mg/L for *E. coli*; tetracyclin 200 mg/L and streptomycin 2 000 mg/L for *P. aeruginosa*. The chromosomal deletions and complementation were confirmed by PCR and nucleotide sequencing.

Reverse Transcription quantitative PCR (RT-qPCR).

Overnight cultures of the strain PAO1 and its mutants AB16.2, AB16.2Δ*pqsA*, and AB16.2Δ27 were diluted in 1:100 into fresh medium and incubated with vigorously shaking at 37°C to an A_{600} value of 0.8 ± 0.05. Total RNA extraction and reverse transcription were performed as previously described[4]. The cDNA of genes PA3327 was quantified in a Rotor Gene RG6000 Real Time PCR machine (RG6000, Qiagen, Courtaboeuf, France) in the presence of QuantiFast SybrGreen kit (Qiagen) and specific primers designed from the sequence of *Pseudomonas*[5]. The transcript levels of the selected genes were normalized with those of the *uvrD* gene[6] and expressed as a ratio to that for the wild type strain PAO1 used as a reference.

LC-MS and MS/MS analysis

LC-MS and LC-MS/MS data were acquired on an ultra-high performance LC system (Ultimate 3000 RSLC, Thermo Scientific) coupled to a high resolution electrospray ionization-quadrupole-time of flight (ESI-Q-TOF) mass spectrometer (MaXis II ETD, Bruker Daltonics). An Acclaim RSLC Polar Advantage II column (2.2 µm, 2.1 × 100 mm, Thermo Scientific) was used for LC separation with a flow rate of 0.3 mL/min. The gradient of solvent A (MilliQ water with 0.1% (v/v) formic acid) and solvent B (HPLC-MS grade acetonitrile with 0.08% formic acid) over a total runtime of 12 min was: linear increase from 5% to 100% B over 10 mins, staying at 100% B for 1 min then decrease to 5% in 1 min. In the first half minute of each run, a sodium formate solution was injected directly as an internal reference for calibration. The mass range *m/z* from 50 to 1300 in positive ion mode were acquired. The acquisition parameters of the ESI source were set up as follows: nebulizer gas 2.4 bar, dry heater 200 ºC, dry gas 8.0 L/min, capillary voltage 3500 V, end plate offset 500 V and charging voltage 2000 V. For LC-MS/MS, the auto MS/MS mode (collision energy 40.0 eV) was chosen with the same parameters as the MS method. The data were treated with Data Analysis 4.3 (Bruker Daltonics).

Extraction and isolation of azetidomonamides

For metabolic profiling: *P. aeruginosa* strains were grown in 1 mL of E2 medium in a 10 mL capped glass cell culture tubes (Wheaton) at 37 °C with rigorous shaking for 24 h. One mL of ethyl acetate was added to the culture and shaken for 30 min. After centrifugation, the organic phase was dried and the pellet was resuspended in 200 μL 80% acetonitrile. One μL of this extract was injected for LC-MS analysis.

For compound isolation: *P. aeruginosa* AB16.2 strain was grown in liquid LB medium at 37 °C with rigorous shaking overnight. The pellet was collected from pre-culture, washed twice with E2 medium and 1 to 100 diluted into 1 L fresh E2 medium. After growth at 37 °C for 24 h, the cell culture was extracted three times by a total volume of 3 L ethyl acetate. The organic phase was combined and the solvent was removed under vacuum to get around 80 mg crude extracts. The crude extract was resuspended in 30 mL H_2O and then loaded to a C18 Sep-Pak 35cc SPE column (Waters). Azetidomonamides were eluted by 40% acetonitrile and further purified on a semi-preparative reverse phase HPLC column, Luna C-18 (250 × 10 mm, 5 μm, 100 Å, Phenomenex). Elution with isocratic acetonitrile-H_2O (22:78) at 5.0 mL/min afforded 1 mg of azetidomonamide A and 0.3 mg of B.

Structural characterization

Purified compounds were characterized by HR-MS and tandem MS, UV and NMR spectroscopy (detailed description see Supplementary Note). NMR spectra were recorded on a Bruker AVANCE III HD 600 MHz spectrometer equipped with a triple resonance TCI cryoprobe at 298 K. Chemical shifts are expressed in δ (ppm) and referenced to the residual non-deuterated solvent signals, and coupling constants (*J*) are reported in Hertz (Hz). The analysis of the NMR data was performed in MestReNova/Topspin3.5 software. Specific rotations were measured by a MCP 100 polarimeter (Anton-Paar) at 25 ºC. Electronic circular dichroism (ECD) spectra were recorded by a Jasco J-810 spectropolarimeter. The absolute configuration (C-5 in **1**; C-4 in **2**) was assigned by comparing between the measured and calculated ECD spectra.

Azetidomonamide A (**1**) was isolated as a pale yellowish powder that gave a $[M+H]^+$ ion at *m/z* 237.0868 (calcd 237.0870) by HR-MS, corresponding to a molecular formula of $C_{11}H_{12}N_2O_4$. The ^1H, ^{13}C and HSQC NMR data (Table S3) in DMSO-d_6 indicated the presence of two exchangeable protons, one vinyl methyl group, one methylene, five methines including four olefinic methines, as well as four quaternary carbons including two olefinic and two carbonyl carbons. Subsequent interpretation of 2D NMR (COSY and HMBC) spectra allowed to establish the connectivity. The ^1H-^1H COSY spectrum indicated three sets of spin-coupling systems: [–CH=CH(CH_3)], [=CH–CH=] and [–CH_2–CH(OH)–]. The key HMBC correlations from H-3′ to C-1′/C-2′/C-4′, and NH-1 to C-1/C-2/C-1′, indicated that a conjugated side chain crotonic acid containing one of the spin-coupling systems was linked to another spin-coupling system by an amide bond. The latter spin-coupling system was placed at the alpha position of the last spin-coupling system, an azetidine ring according to the HMBC correlations from H-2 to C-4, H-3 to C-5, OH-5 to C-4/C-5/C-6 and H-6 to C-4/C-5/C-7. The molecular formula implied 7 degrees of unsaturation. Apart from 3 double bonds and 2 amides, the remaining two degrees of unsaturation indicated the presence of a bicyclic structure in azetidomonamide A. In this case, C-7 was linked to C-1 by an ester bond. Thus, the planar structure of **1** was established as azetido-1,3-oxazepinan-2-one. These assignments were consistent with those of similar compounds such as SB-315021[7]. The trans-geometries of the double bond in the side chain was determined based on the coupling constant between H-2′ and H-3′ (*J*= 15.3 Hz).

Azetidomonamide B (**2**) was obtained as a colorless powder. The molecular formula was determined as $C_{10}H_{12}N_2O_2$ according to the accurate mass data of $[M+H]^+$ ion at *m/z* 193.0969 (calcd 193.0972), indicated a CO_2 less than azetidomonamide A. Its UV data vary from that of **1**, referring to the change of the skeleton. The ^1H NMR spectrum showed a N, C2-disubstituted azetidine ring and a singlet olefinic proton, in addition to a similar side chain as in azetidomonamide A. Two [–CH=CH(CH_3) and –CH_2–CH_2–CH–] moieties were proved in ^1H-^1H COSY NMR spectrum. Unlike the downfield of azetidomonamide A in ^{13}C data (Table S3), compound **2** showed a characteristic conjugated ketone group. Further HMBC analysis showed key ^3J correlations from H-5 to C-3, H-6 to C-1, and H-2 to C-3, which established the skeleton as 1-azabicyclo[3.2.0]heptane. Aforementioned evidences implied that **2** is an analog of known compound pyrrolizixenamide A[8]. Subsequent detailed analysis of chemical shifts verified that the side chain crotonic acid is linked to NH-1 by an amide bond. Taken all together, the planar structure of azetidomonamide B (**2**) was determined unambiguously.

Azetidomonamide A (**1**): yellow solid, $[\alpha]_D^{25}$ = –91.0º (*c*=0.1, MeOH); ^1H NMR (600 MHz, DMSO-d_6): δ 9.99 (s, 1H), 6.74 (dq, *J* =15.2, 6.9 Hz, 1H), 6.24 (d, *J*=6.2, 1H), 6.18 d (d, *J*=7.9 Hz, 1H), 6.08 (dq, *J*=15.3, 1.7 Hz, 1H), 5.46 (dd, *J*=6.3, 1.5 Hz, 1H), 4.96 (m, 1H), 4.19 (dd, *J*=8.2, 6.7 Hz, 1H), 3.75 (dd, *J*=8.2, 3.7 Hz, 1H), 1.81 (dd, *J*=6.9, 1.6 Hz, 3H); ^{13}C NMR (150 MHz, DMSO-d_6): δ 163.10, 155.73, 148.04, 140.91, 137.78, 124.86, 101.62, 98.22, 66.04, 58.87, 17.57; UV/Vis: λ_{max} 222 nm; HRESIMS (*m/z*): $[M+H]^+$ $C_{11}H_{13}N_2O_4$ calcd, 237.0870; found, 237.0868.

Azetidomonamide B (**2**): colorless solid, $[\alpha]_D^{25}$ = –12.0º (*c*=0.05, MeOH); ^1H NMR (600 MHz, DMSO-d_6): δ 10.74 (s, 1H), 6.91 (dq, *J* =15.2, 6.9 Hz, 1H), 6.16 (dq, *J*=15.4, 1.7 Hz, 1H), 5.94 (s, 1H), 4.20 (dd, *J*=9.8, 6.2 Hz, 1H), 4.03 (dt, *J*=9.1, 8.9 Hz, 1H), 3.38 (m, 1H), 2.60 (m, 1H), 2.11 (m, 1H), 1.87 (dd, *J*=6.9, 1.6 Hz, 3H); ^{13}C NMR (150 MHz, DMSO-d_6): δ 204.36, 174.28, 163.91, 143.75, 124.31, 99.10, 65.84, 53.35, 20.27, 17.81; UV/Vis: λ_{max} 242 nm; HRESIMS (*m/z*): $[M+H]^+$ $C_{10}H_{13}N_2O_2$ calcd, 193.0972; found, 193.0969.

Computational details

All density functional theory (DFT) calculations have been performed using Gaussian16[9]. After a conformational analysis with GMMX package using the MMFF94 force field with a 3.5 kcal/mol threshold. 15 conformers were obtained for compound **1** and only 1 for compound **2**. After geometry optimization using DFT at the b3lyp/6-31g(d) level followed by a frequency calculation in order to confirm the presence of a minimum, time-dependent (TD) DFT prediction was performed using the b3lyp/6-311+g(d,p) method for 20 excited states for compound **1**, only 3 excited states were calculated for compound **2**. Visualization of the spectra was realized after Boltzmann weighing using GaussView 6. UV correction was applied for both compounds with a shift of 12 and 15 nm for **1** and **2** respectively.

Isotope labelling experiments

Isotope labelling: An inverse feeding approach was applied[10]. *P. aeruginosa* AB16.2 cells from an overnight culture in LB was washed and diluted (1 to 100) into a 1 mL fresh E2 medium with 0.2% U-$^{13}C_3$-glycerol (Cambridge Isotope Laboratories) as sole carbon source. *L*-Ser, *L*-Met and *L*-AZC were added to a final concentration of 1 mM, respectively, and cells were allowed to grow for 30 hour at 37 °C. Extraction and LC-HRMS analysis were performed as described above.

Construction of protein expression plasmids

Genes to be expressed were amplified from the genomic DNA of the PAO1 strain by PCR using the Phusion DNA polymerase and corresponding primers (Table S6). For *azeJ* expression, the gene was cloned between the *Nde*I and *Xho*I sites of pET28a(+) or pET29b(+) (Novagen) to afford pET28-PA3335N or pET29-PA3335C, respectively. For A domain expression, coding regions of C1-A1-PCP1 (A1L, 1-1046 amino acid of AzeB) and C2-A2-PCP2 (A2L, 1024-2072 amino acid of AzeB) were amplified and cloned between the *Nde*I and *Hind* Ⅲ sites of pET28a(+), yielding pET28-PA3327A1L and pET28-PA3327A2L. Lastly, the 4'-phosphopantetheinyltransferase gene *sfp* from *Bacillus subtilis*, excised from pET28a_Sfp[11], was inserted between the *Nde*I and *Xho*I sites of pACYCDuet-1 (Novagen) to generate pACYC-SFP.

Expression and purification of A domains

E. coli BL21(DE3) harbouring pACYC-SFP and each A domain expression plasmid were grown in 1 L LB medium supplemented with kanamycin (50 μg/mL) and chloramphenicol (25 μg/mL) at 37 °C with shaking until optical density at 600 nm (OD_{600}) reached 0.7-1. The culture was cold shocked on ice for 30 min before the addition of isopropyl-β-*D*-thiogalactopyranoside (IPTG) to a final concentration of 0.05 mM for induction. Cells were allowed to grow at 16 °C overnight before being harvested. The pellets were resuspended in 25 mL buffer A (50 mM Tris-HCl, pH 7.8, 300 mM NaCl, 10 mM imidazole, 10% glycerol) supplemented with 0.1 mg/mL DNAase I and 0.1 mg/mL RNAase A, followed by lysis by French Press. After centrifugation at 13000 rpm for 45 min to get rid of cell debris, the supernatant was purified by nickel-affinity chromatography using an AKTA FPLC system equipped with a HisTrap HP 5 mL column (GE Healthcare Biosciences). Proteins were eluted by a step-wise program using buffer A and B (same as A except with 300 mM imidazole) as mobile phases. N-His_6-tagged AzeB_A1L and AzeB_A2L were eluted out starting from 100 mM imidazole (Figure S28). Correct fractions were combined and concentrated using a Vivaspin 15R concentrator (Sartorius). The protein was then desalted using a PD-10 column (GE Healthcare Biosciences), exchanged into the storage buffer (20 mM Tris-HCl, pH 7.5, 100 mM NaCl and 10% glycerol) and further concentrated. Aliquots of the purified protein were flash frozen in liquid N_2 and stored at –80 °C until use. From 1 L culture, we could obtain 12 mg AzeB_A1L and 30 mg AzeB_A2L.

Expression and purification of AzeJ

E. coli BL21(DE3) transformed with pET28-PA3335N or pET28-PA3335C were grown in 1 L LB medium supplemented with kanamycin (50 μg/mL) at 37 °C until OD_{600} reached 0.7-1. Then IPTG was added to the culture at a final concentration of 0.1 mM and protein induction was carried out at 37 °C for 4 h. Protein purification followed the procedure as described above, with the modifications of buffer B which contained 500 mM imidazole. The protein was eluted by 300 mM imidazole. From 1 L culture, about 5 mg N-His_6 AzeJ and 30 mg C-His_6 AzeJ could be obtained. Both versions were found to be active. For the reason of simplicity, C-His_6-tagged AzeJ was used throughout this study, unless otherwise stated.

Hydroxylamine trapping assays for AzeB_A2 domain

The assay was performed as described in a 96-well microplate format[12]. A reaction of 150 μL contained 25 mM Tris-HCl (pH 8.0), 15 mM $MgCl_2$, 2.25 mM freshly prepared ATP, 150 mM NH_2OH (the stock solution was prepared as 2 M NH_2OH in 3.5 M NaOH and the pH was subsequently adjusted to 8 by 6 M HCl), 3 mM amino acid and 8.5 μM purified AzeB_A2L. Negative controls were set up using the boiled protein or without amino acid. The reaction for each amino acid was performed in triplicate. After incubation at 30 °C for 1 h, assays were stopped by the addition of 150 μL stopping solution (10% (w/v) $FeCl_3 \cdot 6H_2O$ and 3.3% (v/v) trichloroacetic acid). After centrifugation, the supernatant was transferred to a new microplate and OD_{540} was recorded immediately by a microplate reader (PolarStar Omega, BMG Labtech).

Continuous ATP-releasing assay for A domains

Given the hydroxylamine method required large amount of proteins, a continuous ATP-releasing assay using adenosine tetraphosphoadenosine (Ap4A) was used for the AzeB_A1L[13]. This method is adapted for cognate amino acid, because the use of an ATP analog reduces the enzyme activity. A total 200 μL reaction was composed of 50 mM Hepes (pH 7.6), 10 mM $MgCl_2$, 50 mM KCl, 1 mM DTT, 10% DMSO, 10 mM D-glucose, 0.5 mM $NADP^+$, 2.5 mM amino acid, 0.5 mM pyrophosphate, 2.5 μM AzeB_A2L, 3.4 U yeast hexokinase and 1.7 U glucose 6-phosphate dehydrogenase (Roche). A reaction with boiled protein and a reaction without amino acid were used as negative controls. Each reaction was performed in triplicate. The microplate was incubated at 30 ºC and the absorbance at 340 nm was measured continuously for 100 min by a microplate reader (PolarStar, BMG Labtech). This method was also applied for AzeB_A2L to confirm the result from the hydroxylamine assay.

Determination of AzeJ activity *in vitro*

A total 100 μL reaction contained 50 mM Tris-HCl (pH 7.5), 2 mM Tris(2-carboxyethyl)phosphine hydrochloride (TCEP), 1 mM AdoMet, 3.5 μM AzeJ with or without 0.5 μM MTA nucleosidase (G-Biosciences) and was incubated at 30 ºC for 4 h. A negative control was set up with the boiled protein. After reaction, 50 μL of the mixture was added 50 μL methanol to inactive the protein. Production of MTA or adenosine was analyzed by HPLC on an Ultimate 3000 system (Thermo Scientific) equipped with a Luna HILIC column (5 μm, 200 Å, 250 × 4.6 mm, Phenomenex) and UV detection at 254 nm. The gradient used was with solvent A (10 mM ammonium formate, 0.1% formic acid, pH 5) and solvent B (10 mM ammonium formate, pH 5, in 80% methanol): linear increase from 3% to 30% B over 10 min, then increase to 100% B in 0.5 min and keep at 100% B for 5 min. The other 50 μL reaction was derivatized by benzyl chloroformate using the following protocol[14]: after addition of 2 μL 1M NaOH and 1 μL benzyl chloroformate, the mixture was kept at 0 ºC for 1 h and then at room temperature for 1 h. The final product was extracted by 50 μL ethyl acetate. The organic phase was dried and the product was dissolved in 80% acetonitrile prior to LC-MS analysis.

Kinetic parameters were determined in a 50 µL reaction with 0.5 µM MTA nucleosidase, 174 nM AzeJ and varying concentration of AdoMet. A background control with inactivated protein was set up for each amino acid concentration. The reaction was carried out at 30 °C for 20 min and 50 µL methanol was added. Ten µL of the mixture was subject to analysis by HPLC as described above, using the following gradient for a better separation with buffer A (10% 50 mM ammonium acetate, pH 5.8, 50% acetonitrile) and buffer B (10% 50 mM ammonium acetate, pH 5.8, 90% acetonitrile): 100% B for 2.5 min, 100% B to 0% B over 10 min and then 0% B for 2.5 min. The UV peak area of adenosine was integrated and then quantified according to a standard curve. The kinetic data were treated with Prism (GraphPad software).

Extraction of AZC from *E. coli* expressing *azeJ*

E. coli cells expression *azeJ* under IPTG induction (500 µL) were extracted with 500 µL ethyl acetate followed by votexing for 2 min and centrifuged. The aqueous phase (50 µL) was used for derivatization with benzyl chloroformate using the procedure as indicated above. A negative control was set-up with cells harbouring the empty vector.

Biological activity tests

Antibacterial tests were performed by a disc diffusion assay on MHA or LB plates. Tested strains were *E. coli* ATCC® 25922™, *Micrococcus luteus* ATCC® 9341™, *Staphylococcus aureus* ATCC® 25923™ and ATCC® 700699™. Inhibition assay with recombinant human group IIA phospholipase A2 was performed using the ^{3}H-oleic acid-labeled *E. coli* membranes test, as described[15]. Lactate dehydrogenase release assay (cytotoxicity detection kit, Roche) was used to measure the cytotoxicity effect of the mutants AB16.2, AB16.2Δ27, and their parental strain PAO1 on the murine macrophage cell line J774A.1 (ATCC TIB-67), as previously described[16].

Virulence assays in *Galleria mellonella*

In house reared *Galleria mellonella* larvae were infected subcutaneously using a syringe pump (KD scientific) with *P. aeruginosa* strains from an overnight culture washed and resuspended in physiological water (25± 5 CFU per larvae) and the larvae were incubated at 37°C. In each test, 20 insects were infected and the experiments were repeated at least three times. Larvae killing was then monitored between 16 and 21 hours post infection. Data analysis was done using the Kaplan-Meier R package and statistical analysis was done using the log-rank test with Bonferroni correction.

Growth curve measurement

From an overnight culture, *P. aeruginosa* strains were diluted to OD_{600} equaled 0.01 in 1 mL LB or MHII and grown in a 24-well microplate at 37 °C inside a microtiter plate reader (PolarStar Omega, BMG Labtech) with continuous shaking. The OD_{600} was measured over 24 h. Three independent experiments were performed.

Bioinformatic methods

Homologous sequences of AzeB and AzeJ were retrieved using pBLAST search against available genome sequences with *P. aeruginosa* excluded, respectively. Next, the two hits tables were compared in order to identify genomes containing homologs of both proteins. Genomic regions flanking these *azeB*-like genes were then inspected manually to confirm the presence of *azeC* encoding a monooxygenase and *azeJ*. Subsequently, domain organization and A domain specificity of AzeB-like proteins in the identified BGCs were analyzed by antiSMASH.[17] This confirmed that all A1 domains are specific for Ser/Thr, whereas A2 domains prefer Pro-like substrates. These analyses led to 13 bacterial genomes containing similar *aze* clusters, including two strains of *Pseudomonas palleroniana* (Figure S37). To construct the phylogenetic tree of A2 domains, 33 other sequences from the AzeB homolog hits were selected using 30% identity cutoff and the specificity of their A2 domains was verified to be Pro using antiSMASH. A total of 45 A2 domain sequences were then subject to phylogenetic analysis using the BioNJ algorithm (Poisson model, 1000 bootstrap replicates) in SeaView.[18] Furthermore, to appreciate distribution of AzeJ in all domains of life, its remote sequence homologues were also identified using profile hidden Markov models. Homologues with E-value < 0.01 were considered.

Chemical synthesis of the pyrrolizidine alkaloid 3

All reactions were carried out in flame-dried vessels under an atmosphere of nitrogen and in anhydrous solvents. Unless otherwise stated, all reagents were purchased from commercial suppliers and used without further purification. All solvents used in the reactions were distilled from appropriate drying agents prior to use. Reactions were monitored by TLC on Merck silica gel 60-F_{254} aluminium sheets, using UV absorption then vanillin-H_2SO_4 (1% vanillin in ethanol + 2% H_2SO_4) or basic permanganate (1% $KMnO_4$ + 15% Na_2CO_3 in water) as staining system. The products were purified by silica gel column chromatography (Geduran silica gel Si 60, 40-63 µm). NMR spectra were recorded on a Bruker Avance 400 MHz spectrometer. Proton chemical shifts are reported in ppm (δ) with the solvent resonance employed as the internal standard ($CDCl_3$ δ 7.26, CD_3OD δ 3.31). Data are reported as follows: chemical shift, multiplicity (s = singlet, d = doublet, t = triplet, q = quartet, m = multiplet, br = broad), coupling constants (Hz) and integration. Carbon chemical shifts are reported in ppm with the solvent resonance as the internal standard ($CDCl_3$ δ 77.16, CD_3OD δ 49.00). High resolution mass spectra (HR-MS) were measured by positive electron impact on a double-focusing high-resolution mass spectrometer (JEOL JMS-GCmate II mass spectrometer). Melting points were measured on a Stuart SMP3 apparatus. Hydrogenation reactions were carried out with an H-Cube ThalesNano.

_t_-Butyl 3-Amino-5,6,7,7a-tetrahydro-1-oxo-1_H_-pyrrolizine-2-carboxylate (5):

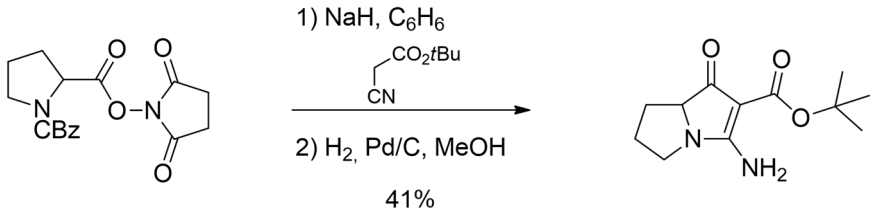

4 **5**

According to a procedure developed by Snider *et al.*,[19] to a solution of sodium hydride (192 mg, 2.5 eq., 4.80 mmol, 60% dispersion in mineral oil) in anhydrous benzene (11.7 mL) was added *t*-butylcyanoacetate (823 µL, 3 eq., 5.76 mmol) at rt. The mixture was stirred at rt for 1 h and a solution of **4** (665 mg, 1 eq., 1.92 mmol) in anhydrous benzene (2.9 mL) was added dropwise. The mixture was stirred for an additional 2 h 30 min at rt and H_2O (20 mL) was added. The aqueous layer was washed with Et_2O (2 x 30 mL), acidified with a 1N aqueous solution of HCl and extracted with CH_2Cl_2 (3 x 20 mL). The combined organic layers were dried over $MgSO_4$ and concentrated under vacuum.

A solution of crude in MeOH (30 mL) was hydrogenated with an H-cube (catalyst 10% Pd/C, flow = 1 mL/min, p_{H2} = 10 bar, T = 25 °C). The mixture was concentrated under vacuum and let 24 h at rt for cyclization. The residue was purified by flash chromatography (SiO_2, AcOEt/MeOH 95:5) to obtain **5** (188 mg, 0.79 mmol, 41% yield) as a white solid.

^{1}H NMR (400 MHz, $CDCl_3$) δ_H = 7.99 (br s, 1H), 5.50 (br s, 1H), 3.86 (dd, *J* = 9.8, 7.1 Hz, 1H), 3.41-3.32 (m, 1H), 3.29-3.19 (m, 1H), 2.27-2.00 (m, 3H), 1.62-1.50 (m, 1H), 1.54 (s, 9H).

Spectroscopic properties are in agreement with those previously reported.[19]

3-(2*E*-butenoylamino)-5,6,7,7a-tetrahydro-1*H*-pyrrolizin-1-one (3):

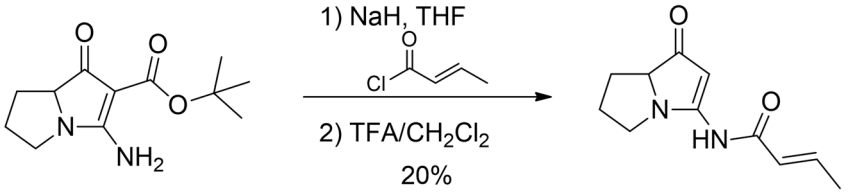

5 **3**

According to a procedure developed by Snyder *et al.*,[19] to a solution of **5** (40 mg, 1 eq., 0.17 mmol) in anhydrous THF (3.9 mL) was added sodium hydride (17 mg, 2.5 eq., 0.42 mmol, 60% dispersion in mineral oil). After 10 min at rt, a solution of freshly distilled acyl chloride (37 µL, 2.3 eq., 0.39 mmol) in anhydrous THF (1.2 mL) was added dropwise. The solution was stirred for an additional 2 h at rt and then quenched with brine (5 mL). The aqueous layer was extracted with CH_2Cl_2 (3 x 10 mL) and the combined organic layers were dried over $MgSO_4$ and concentrated under vacuum.

A solution of the crude in CH_2Cl_2/TFA (3.9 mL, 9:1) was stirred at r.t for 17 h. Then, a saturated aqueous solution of $NaHCO_3$ (5 mL) and brine (5 mL) were added. The aqueous layer was extracted with EtOAc (3 x 10 mL) and the combined organic layers were dried over $MgSO_4$ and concentrated under vacuum. The residue was purified by flash chromatography (SiO_2, CH_2Cl_2/MeOH 95:5) to obtain **3** (7 mg, 0.034 mmol, 20% yield) as a pale yellow solid.

M_p = 117 °C.

^{1}H NMR (400 MHz, CD_3OD) δ_H = 7.08 (dq, *J* = 15.1, 6.9 Hz, 1H), 6.21 (dq, *J* = 15.1, 1.6 Hz, 1H), 5.74 (s,1H), 3.97-3.89 (m, 1H), 3.47-3.38 (m, 1H), 3.24-3.15 (m, 1H), 2.24-2.06 (m, 3H), 1.94 (dd, *J* = 6.9, 1.6 Hz, 3H), 1.59-1.46 (m, 1H).

^{13}C NMR (101 MHz, CD_3OD) δ_C = 204.8, 173.3, 165.8, 146.6, 124.9, 93.9, 70.5, 54.8, 28.9, 27.4, 18.2.

HRMS (*m/z*) calcd for $C_{11}H_{14}N_2O_2$ [M^+] 206.1055, found 206.1060.

Results

Figure S1. Transcript levels of gene PA3327 in strain PAO1 and its mutants determined by RT-qPCR. The experiments were performed in quadruple.

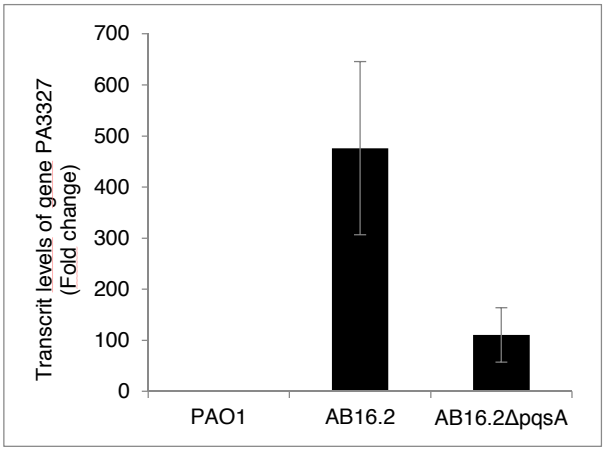

Figure S2. Comparison of metabolic profiles by LC-MS. Total ion chromatography is shown. Red: AB16.2 extract, black: AB16.2Δ27 extract. * denotes major peaks that are absent in the mutant (1: azetidomonamide A; 2: azetidomonamide B).

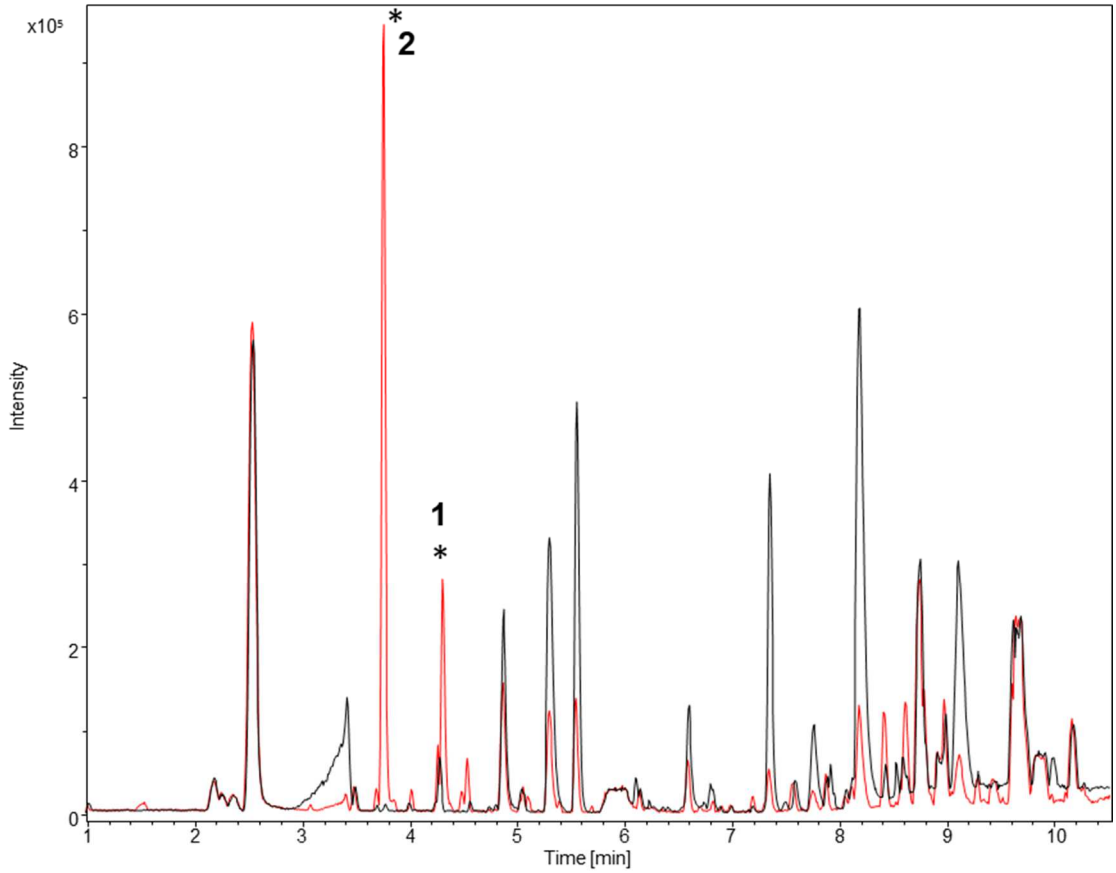

Figure S3. Key COSY (▬) and HMBC (H→C) correlations of azetidomonamides (600 MHz, DMSO-d_6).

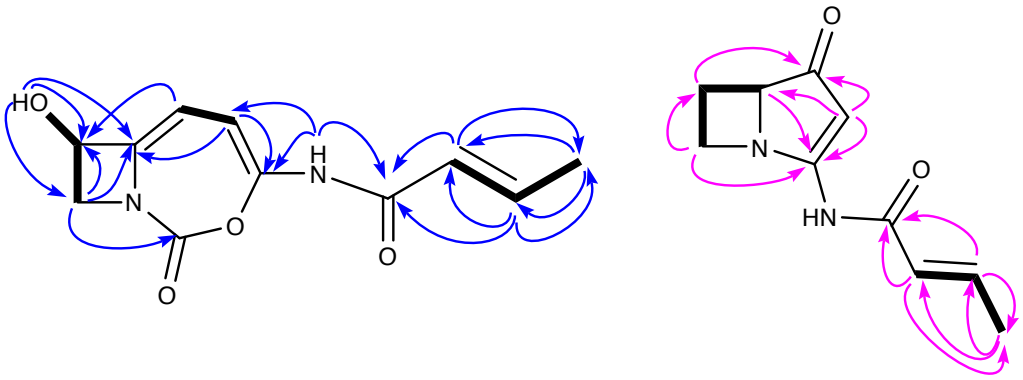

azetidomonamide A (**1**) azetidomonamide B (**2**)

Figure S4. ^{1}H-NMR spectrum of azetidomonamide A (**1**) (DMSO-d_6, 600 MHz).

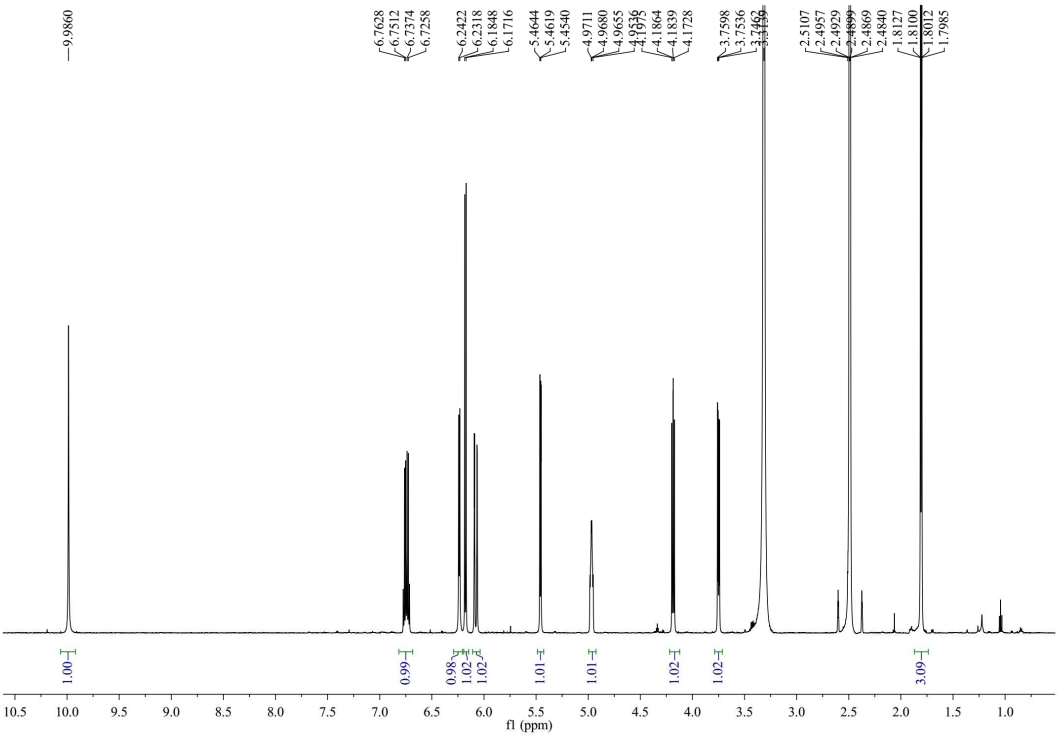

Figure S5. DEPTQ ^{13}C-NMR spectrum of azetidomonamide A (1) (DMSO-d_6, 600 MHz).

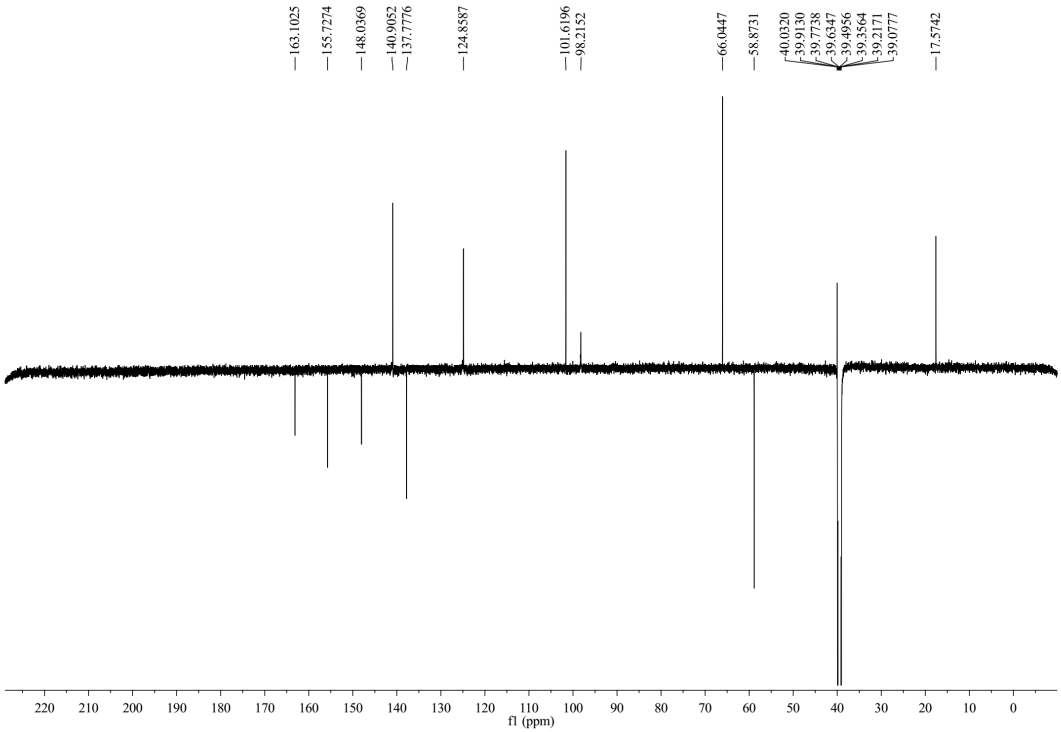

Figure S6. ^{1}H-^{1}H COSY spectrum of azetidomonamide A (**1**) (DMSO-d_6, 600 MHz).

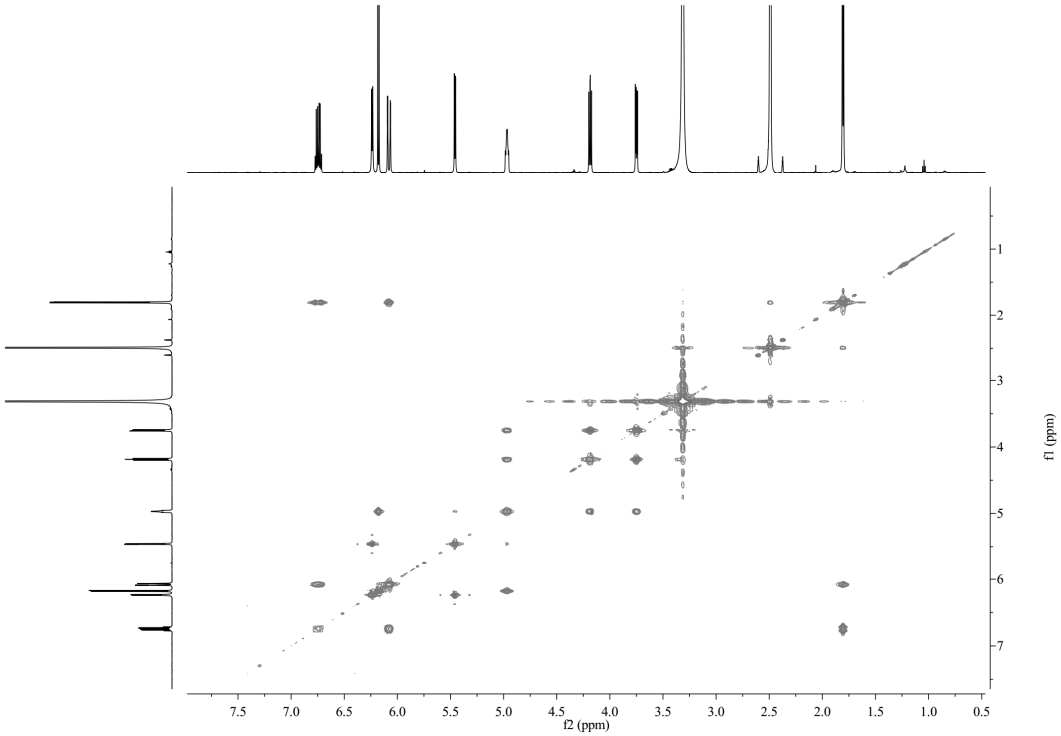

Figure S7. HSQC spectrum of azetidomonamide A (1) (DMSO-d_6, 600 MHz).

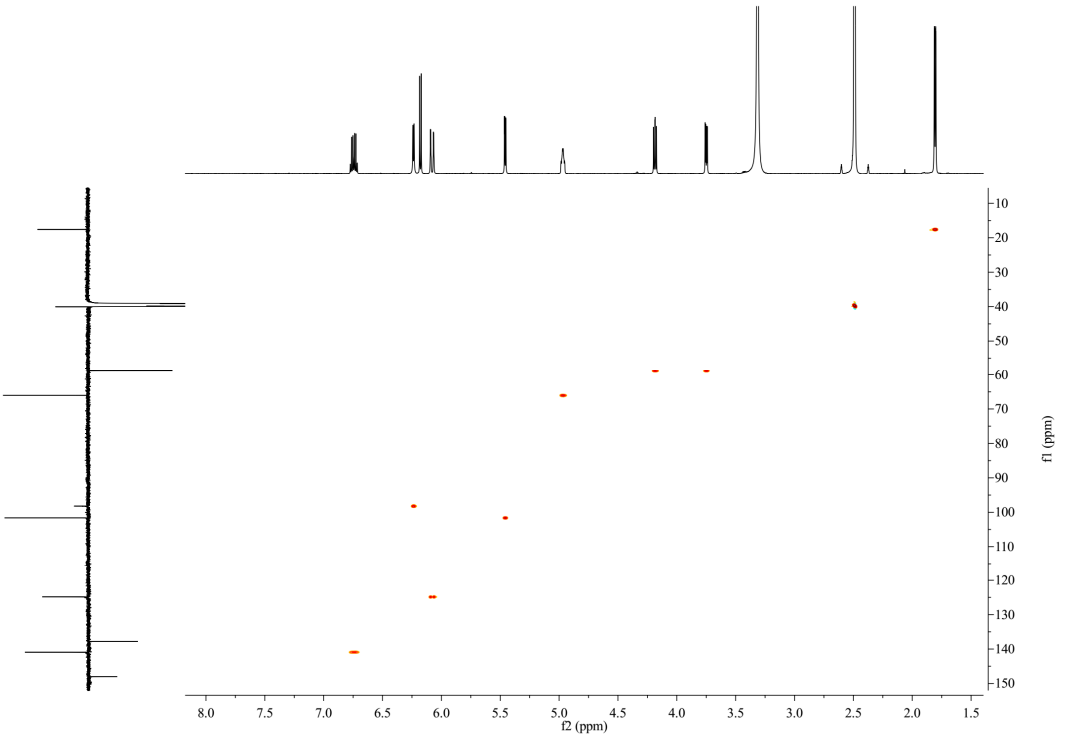

Figure S8. HMBC spectrum of azetidomonamide A (**1**) (DMSO-d_6, 600 MHz).

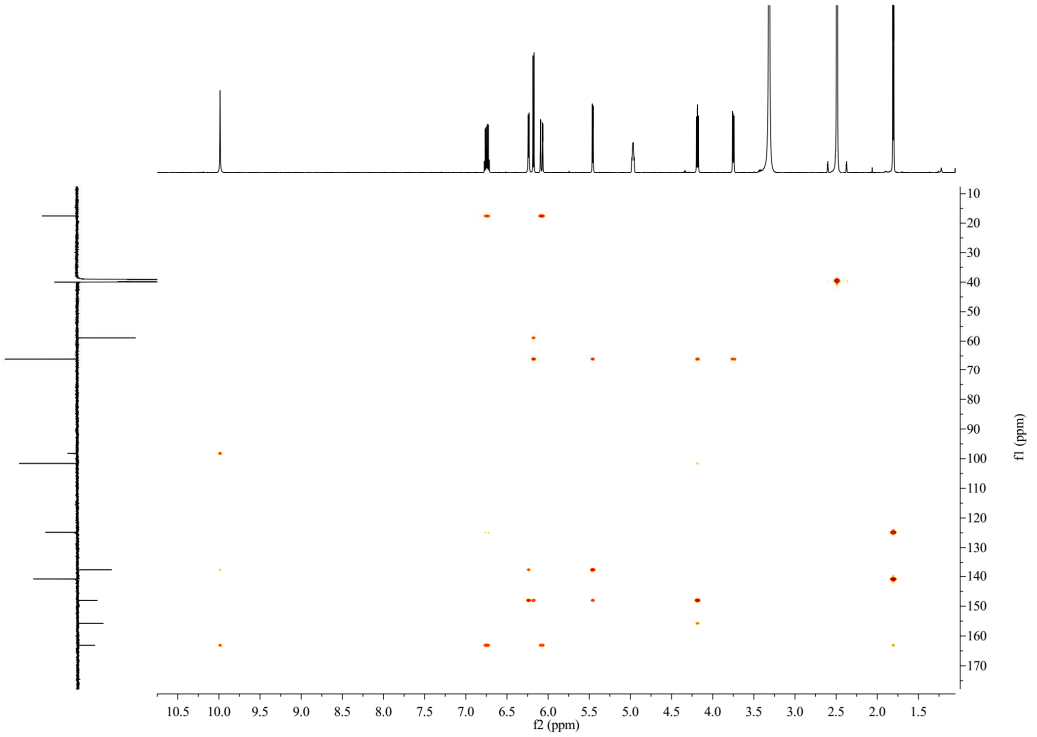

Figure S9. NOESY spectrum of azetidomonamide A (**1**) (DMSO-d_6, 600 MHz).

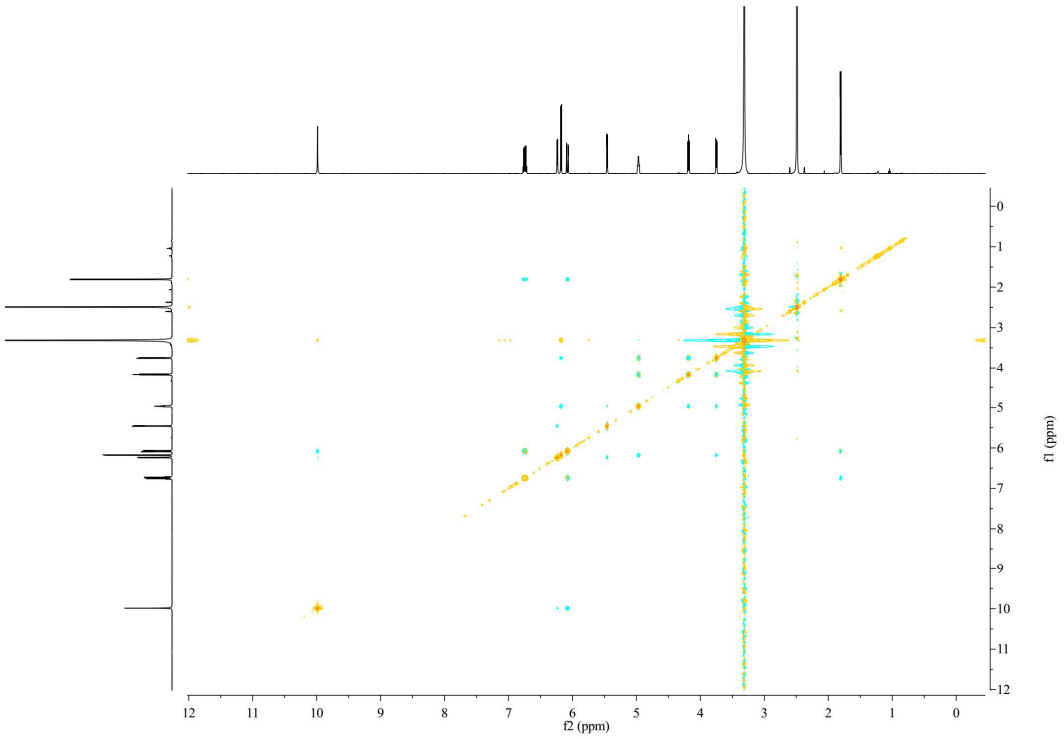

Figure S10. ^{1}H-NMR spectrum of azetidomonamide B (**2**) (DMSO-d_6, 600 MHz).

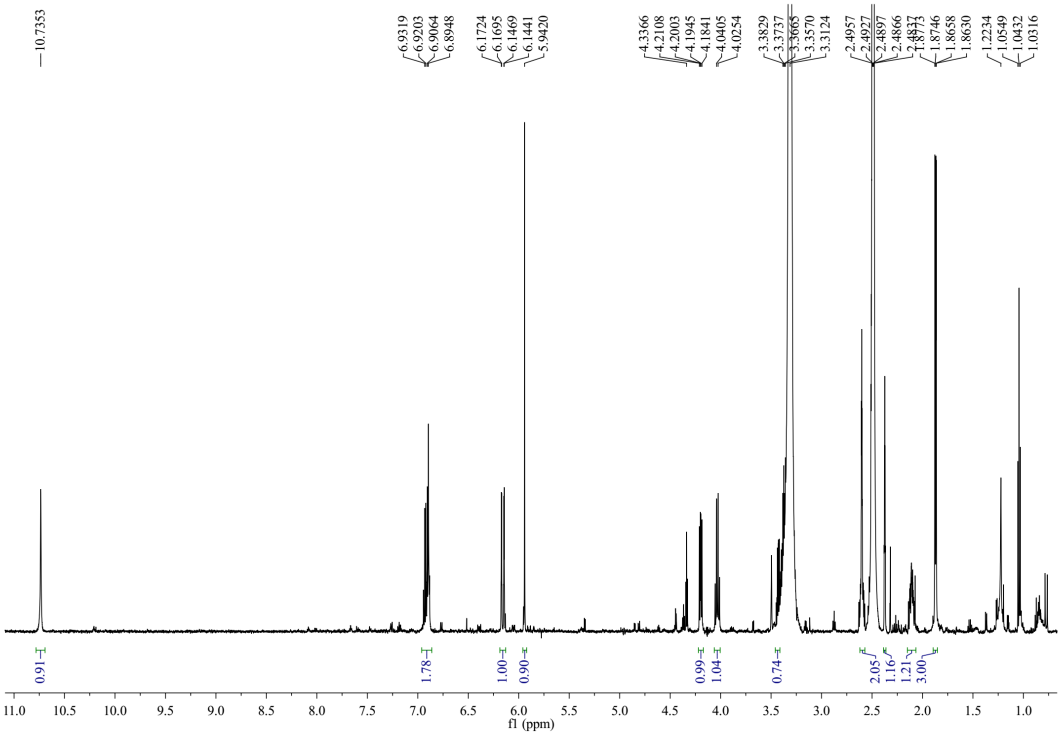

Figure S11. DEPTQ ^{13}C-NMR spectrum of azetidomonamide B (**2**) (DMSO-d_6, 600 MHz).

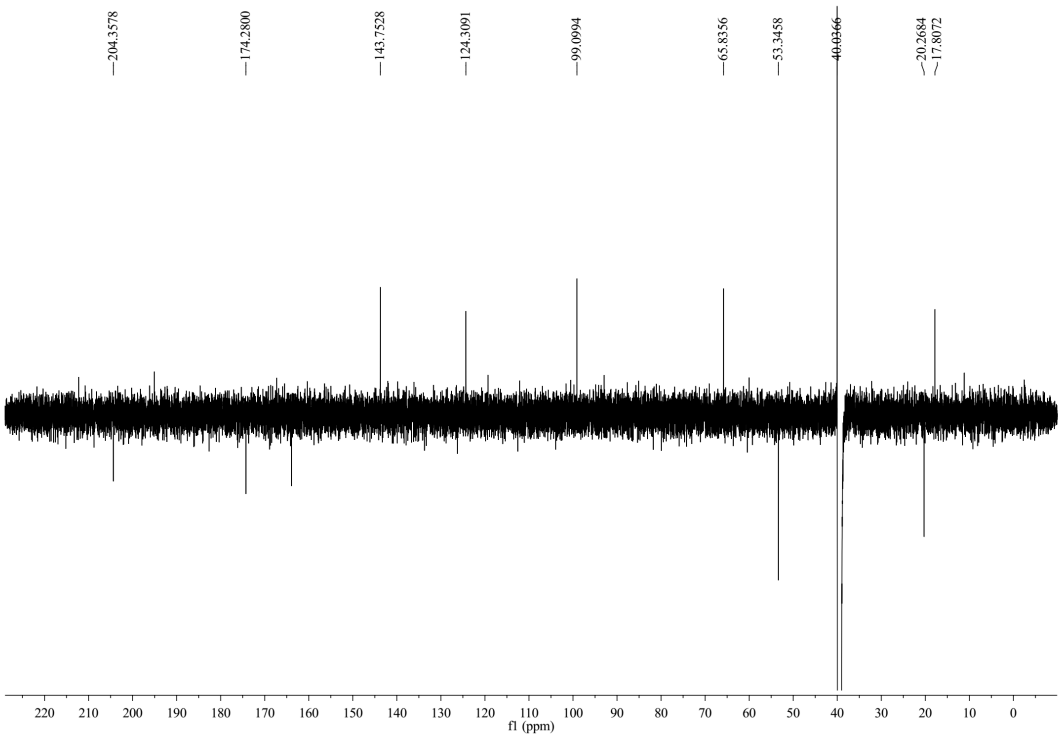

Figure S12. ^{1}H-^{1}H COSY spectrum of azetidomonamide B (**2**) (DMSO-d_6, 600 MHz).

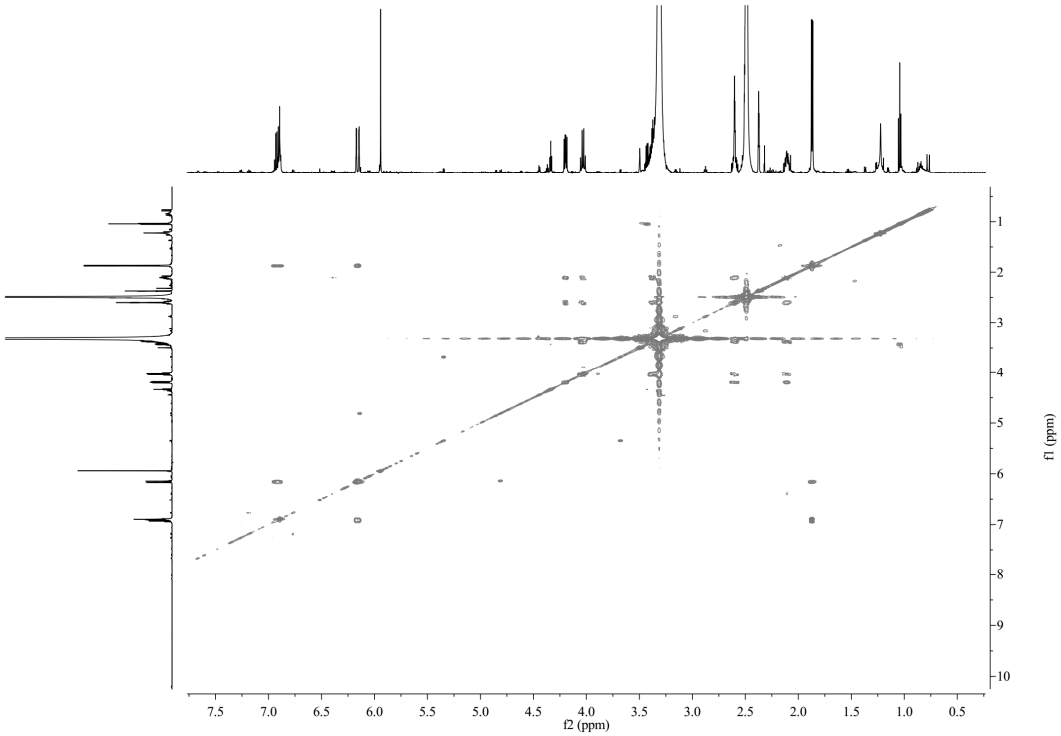

Figure S13. HSQC spectrum of azetidomonamide B (**2**) (DMSO-d_6, 600 MHz).

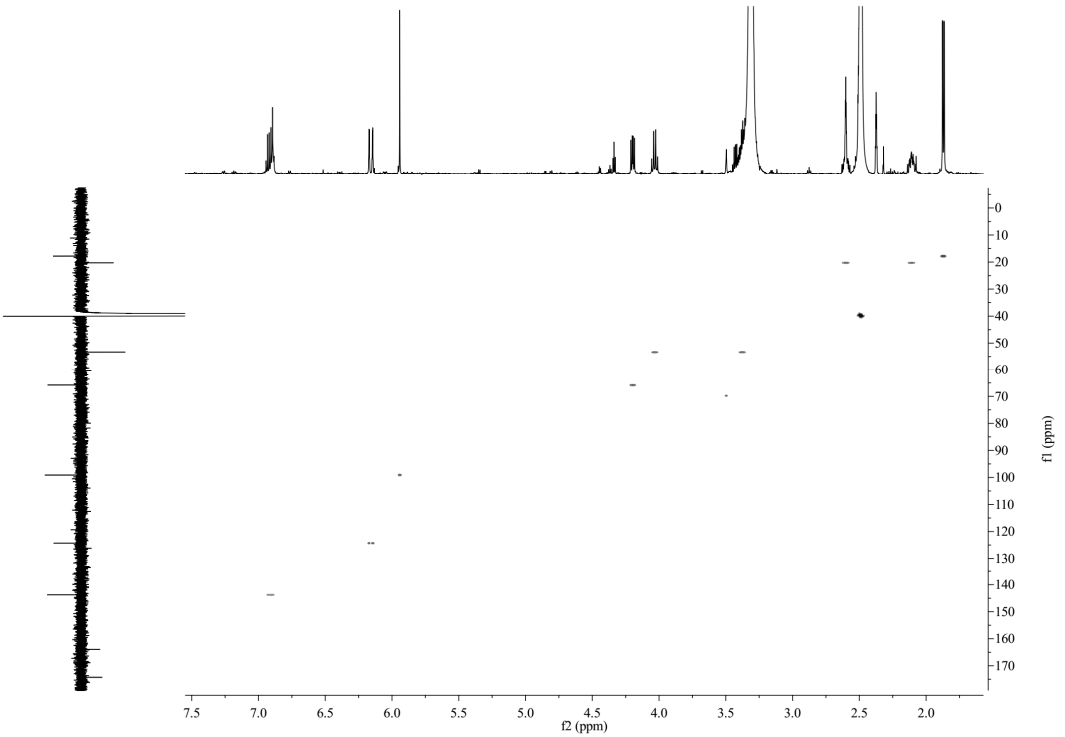

Figure S14. HMBC spectrum of azetidomonamide B (**2**) (DMSO-d_6, 600 MHz).

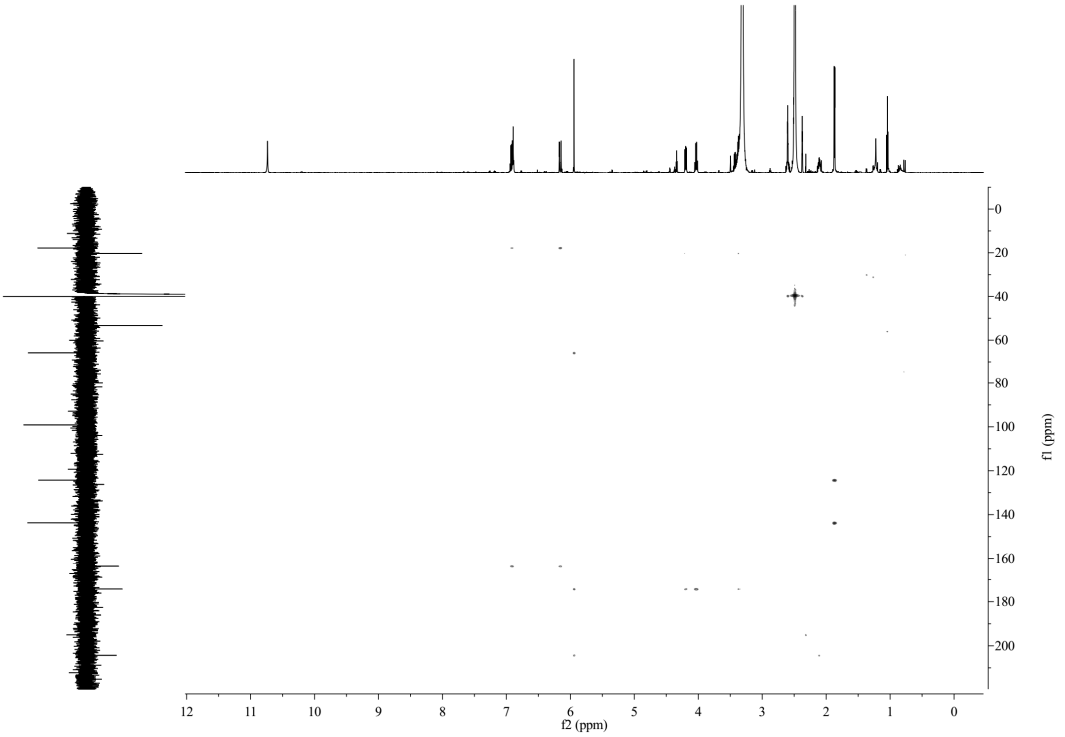

Figure S15. NOESY spectrum of azetidomonamide B (**2**) (DMSO-d_6, 600 MHz).

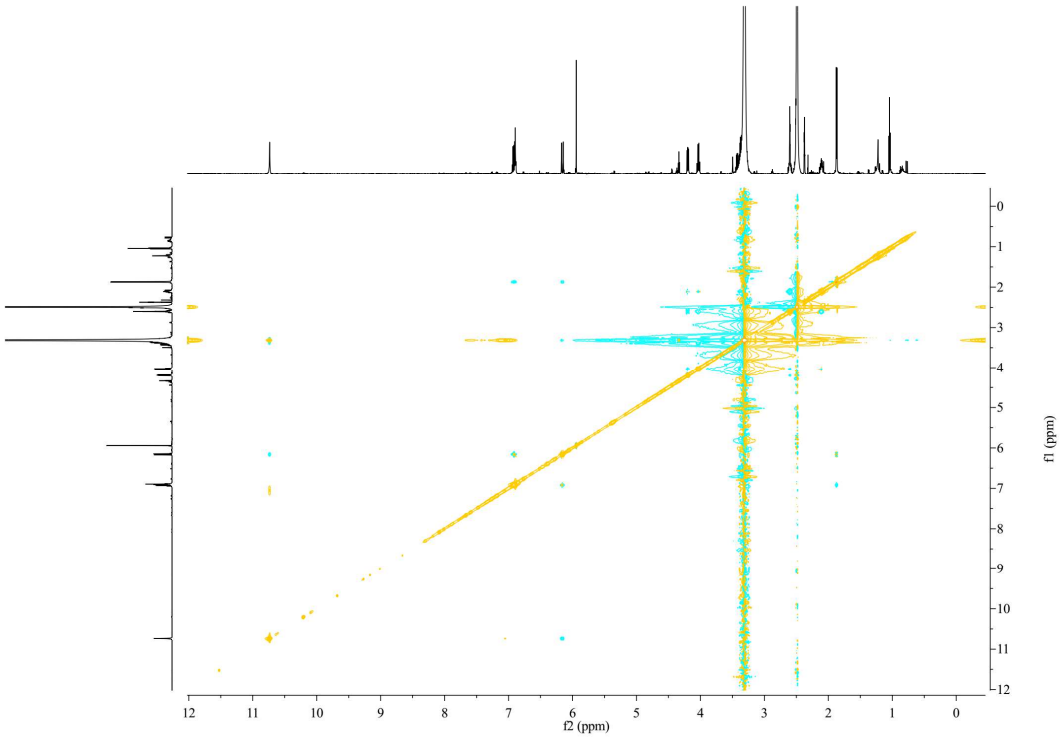

Figure S16. HR-MS spectrum of azetidomonamide A (**1**). Upper panel: extracted ion chromatography (EIC) of *m/z* 237.0868. Lower panel: HR-ESI-MS data (RT 4.3 min).

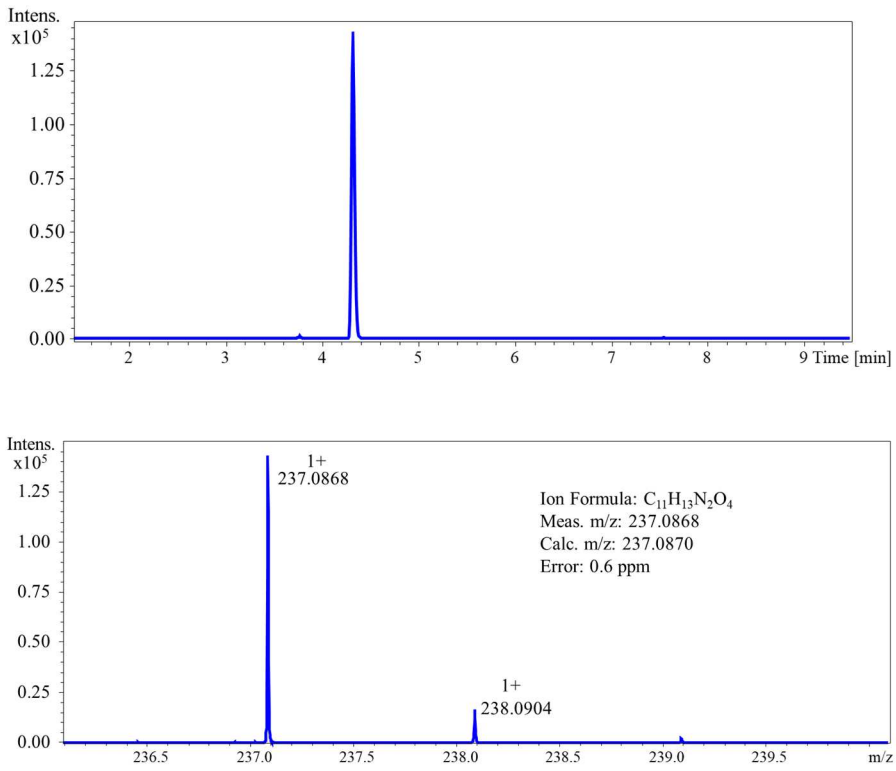

Figure S17. HR-MS spectrum of azetidomonamide B (**2**). Upper panel: extracted ion chromatography (EIC) of *m/z* 193.0967. Lower panel: HR-ESI-MS data (RT 3.8 min).

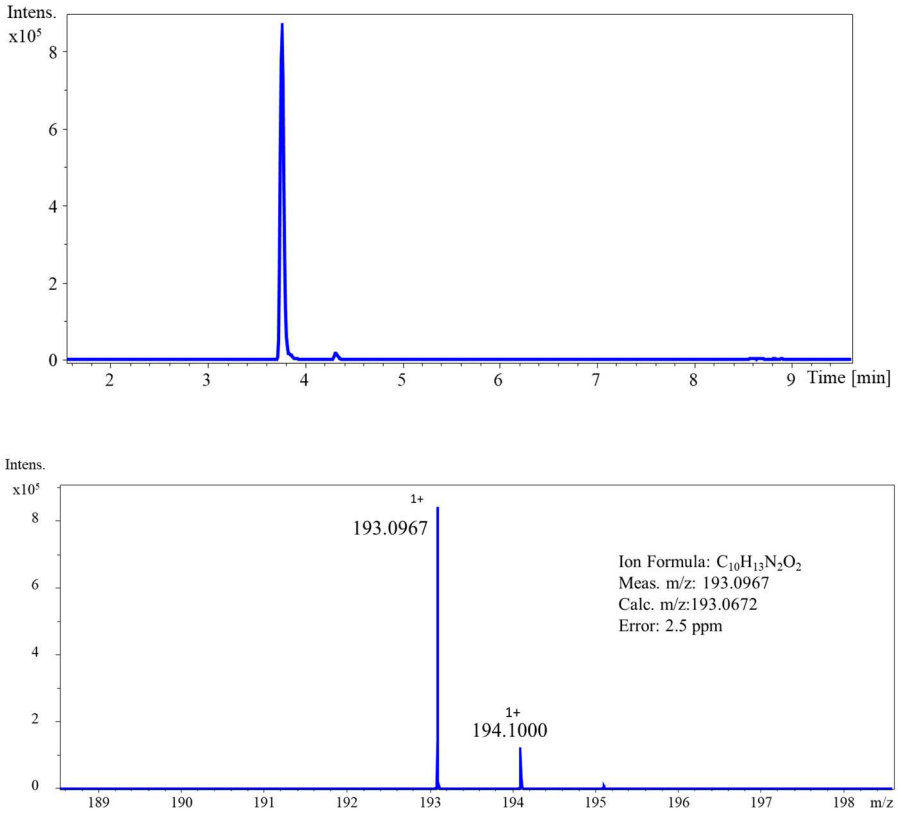

Figure S18. UV absorbance and measured ECD spectra of azetidomonamide A (**1**).

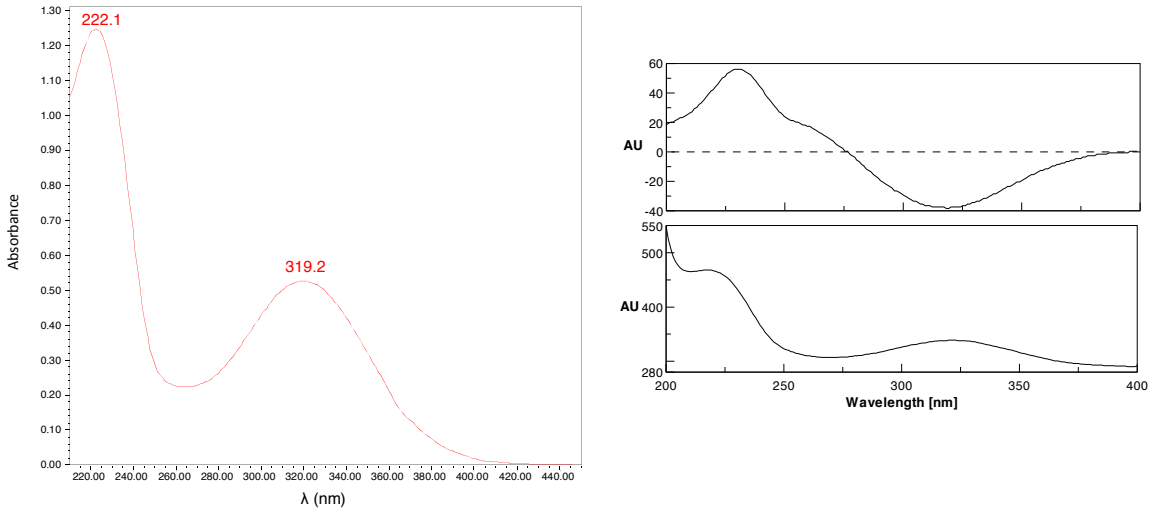

Figure S19. UV absorbance and measured ECD spectra of azetidomonamide B (**2**).

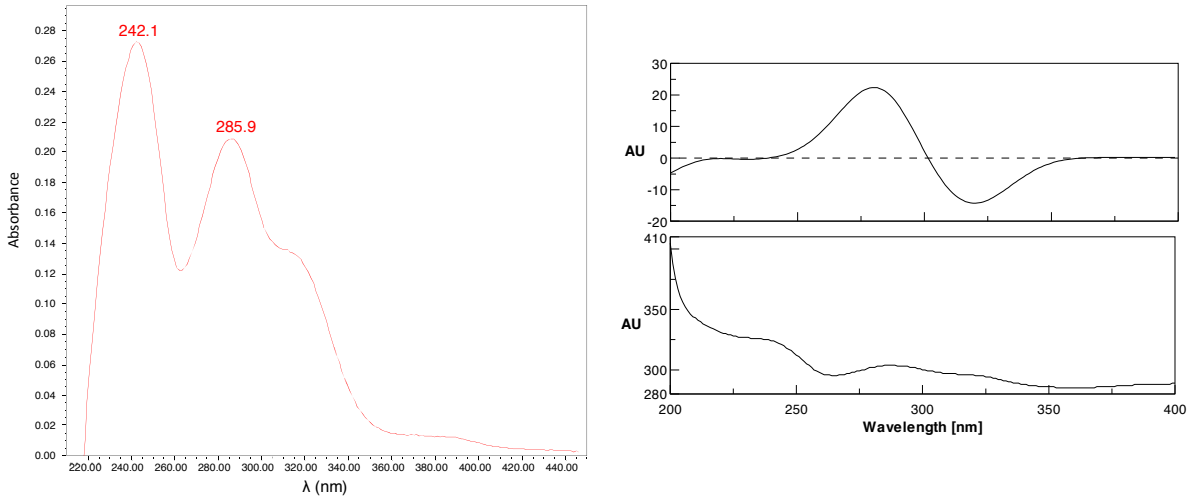

Figure S20. Experimental and theoretical ECD spectra of azetidomonamide A (**1**).

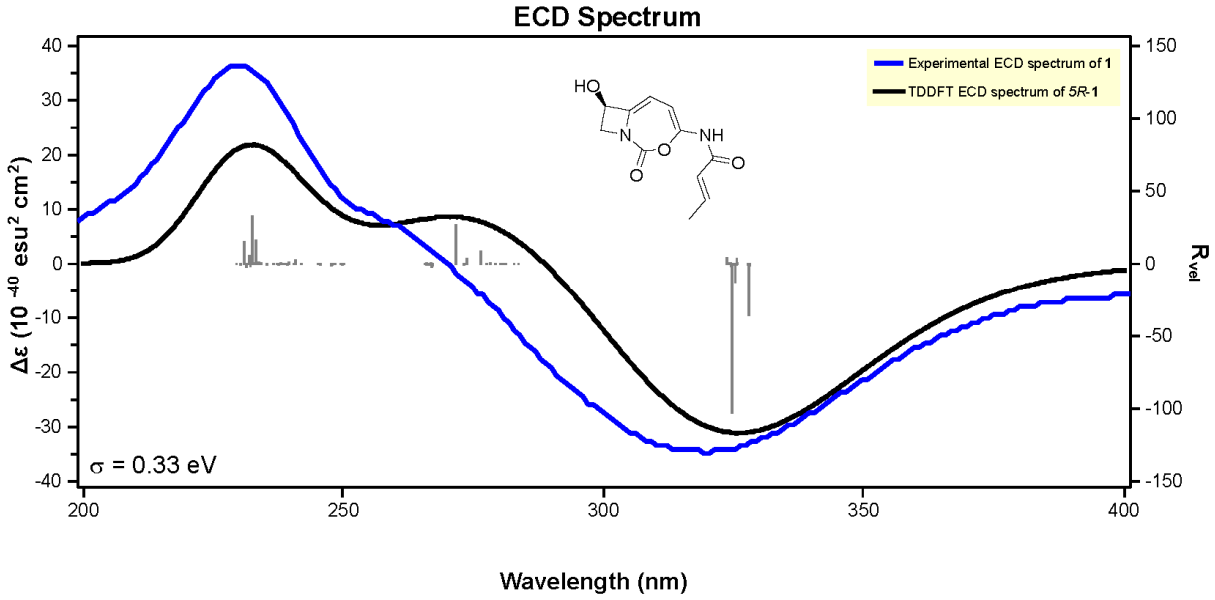

Figure S21. Experimental and theoretical ECD spectra of azetidomonamide B (**2**).

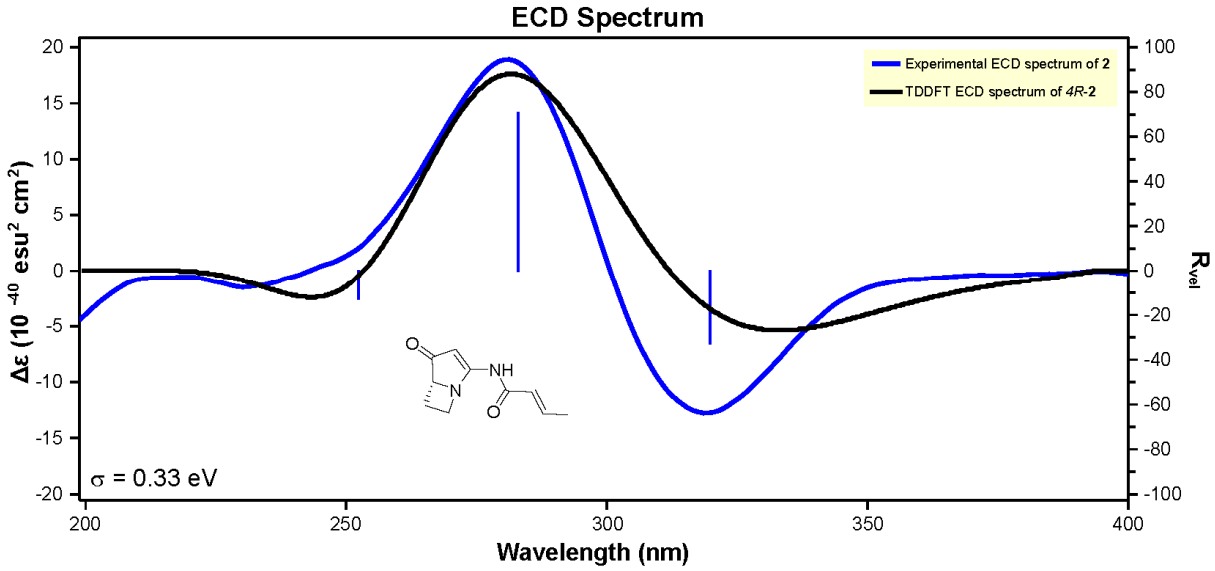

Figure S22. Structures of known natural products containing the azetidine moiety (β-lactam compounds are excluded).[24]

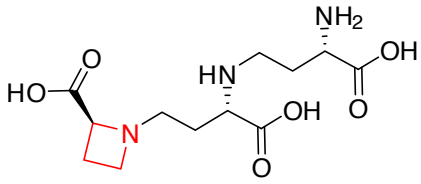

nicotianamine
Higuchi, K. *et al*. 1999

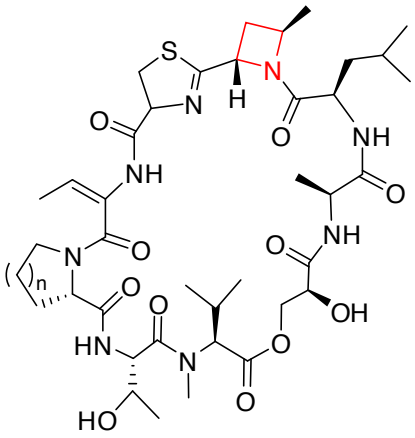

vioprolide A(n=2)/B(n=1)
Yan, F. *et al*. 2018

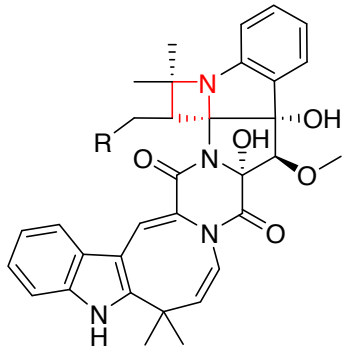

okaramine B(R=H)/D(R=OH)
Lai, C. Y. *et al*. 2017

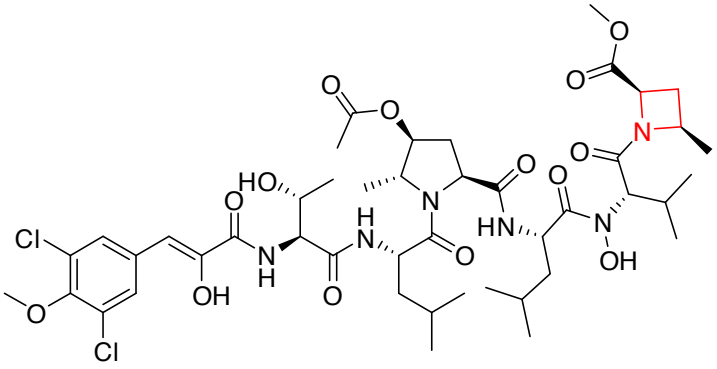

bonnevillamide A
Wu, G. *et al.* 2017

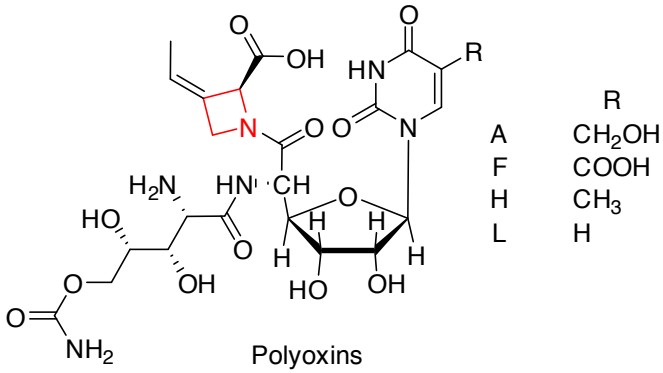

	R
A	CH_2OH
F	COOH
H	CH_3
L	H

Polyoxins
Isono, K. *et al*. 1968

Figure S23. An overview of structures of bacterial pyrrolizidine and cyclocarbamate alkaloids that are likely derived from similar NRPS pathways.[25]

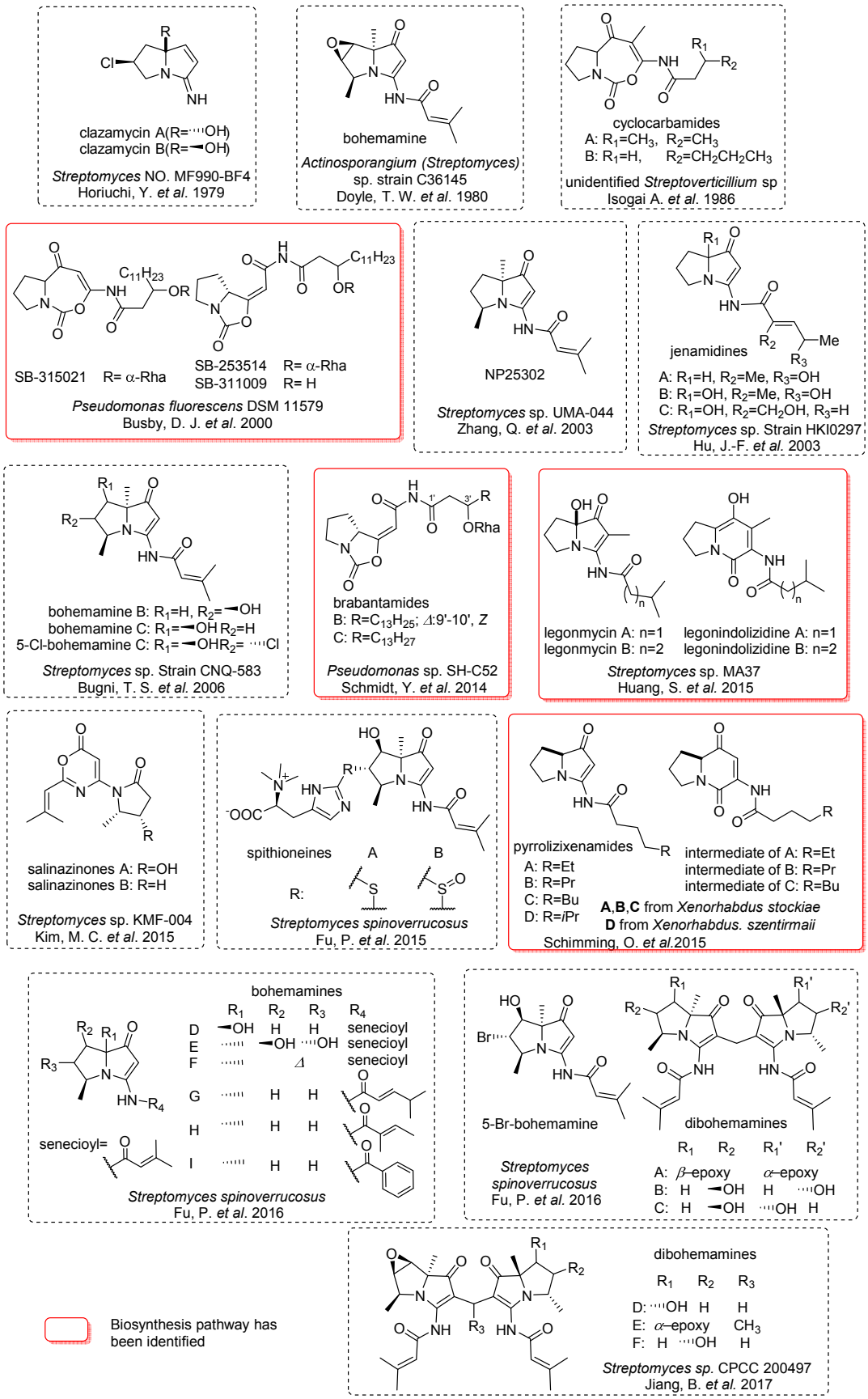

Figure S24. Mass spectra of azetidomonamide B (**2**) in inverse isotope labelling experiments. Azetidomonamide B was fully labelled with ^{13}C atoms in ^{13}C-E2 medium (blue). A 4 Da down shift was observed when ^{12}C-*L*-AZC (red) or ^{12}C-*L*-Met was fed (green). Partial ^{12}C-*L*-Ser incorporation showed a peak of 2 Da less (purple). The ^{13}C atoms in the structures were marked with *.

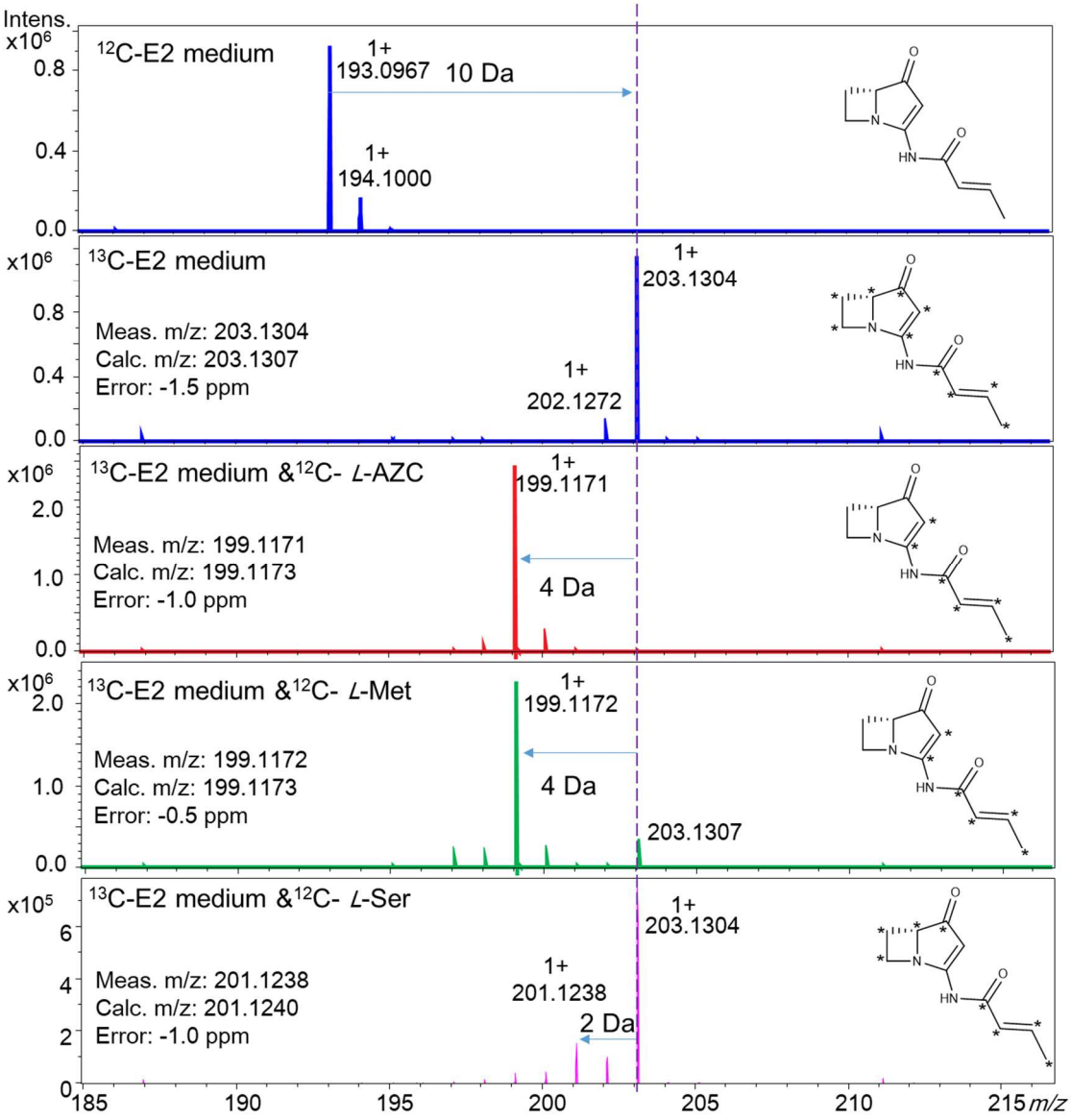

Figure S25. MS/MS spectra and fragment annotation of azetidomonamide B (**2**) in inverse isotope labelling experiments. Same color code as in Fig. S24 is used.

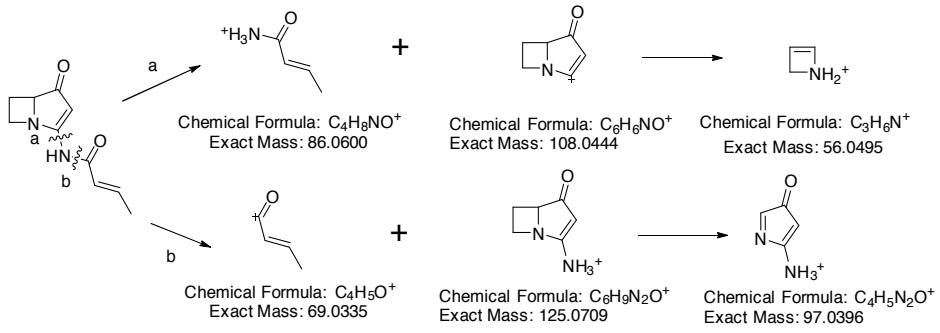

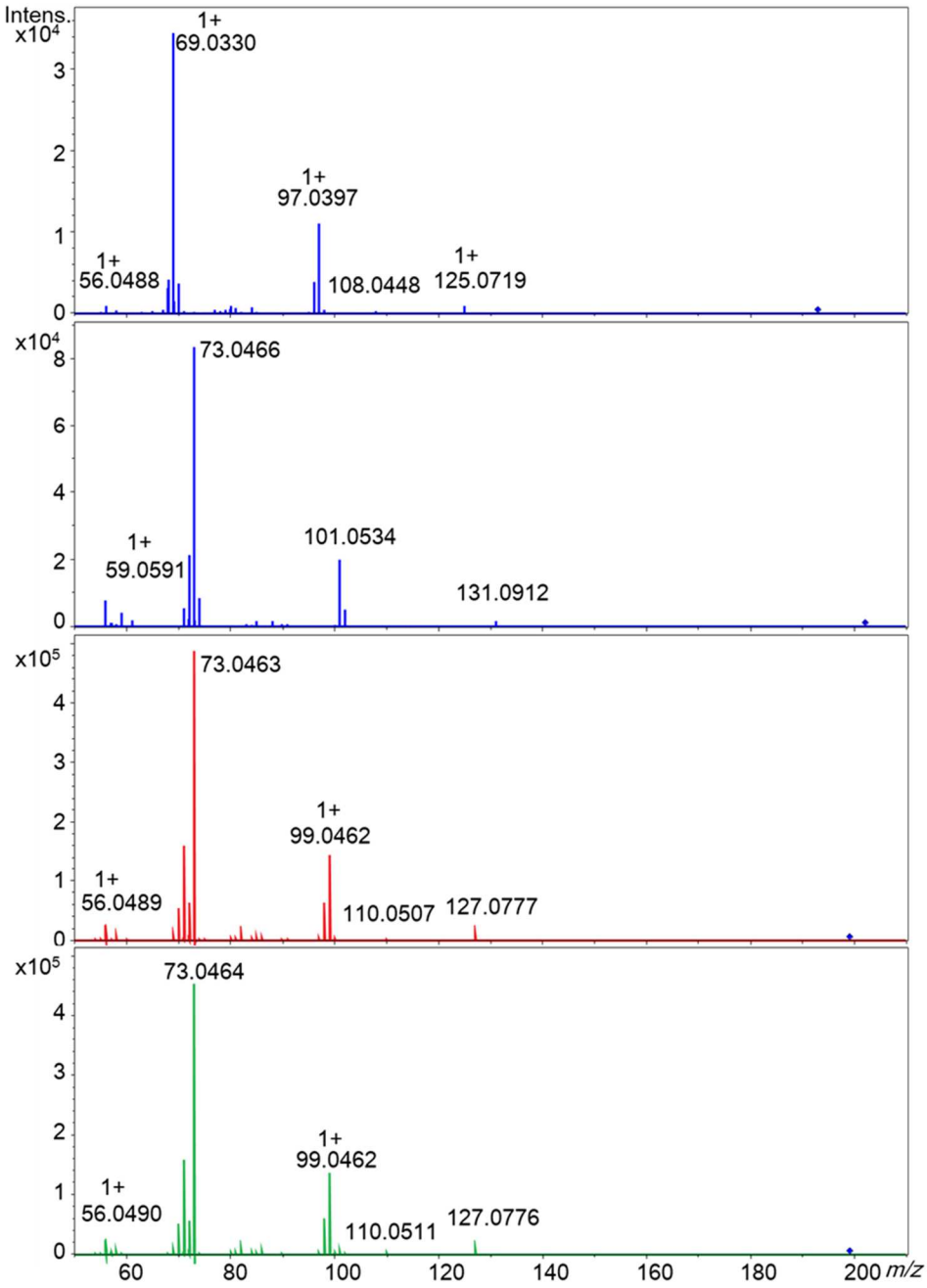

Figure S26. Mass spectra of azetidomonamide A (**1**) in inverse isotope labelling experiments. Azetidomonamide A was fully labelled with ^{13}C atoms in ^{13}C-E2 medium (blue). When ^{12}C-*L*-Met was fed, 4 Da down shift was observed (green). Partial ^{12}C-*L*-Ser incorporation showed a peak of 3 Da less. Production of **1** was inhibited when feeding ^{12}C-*L*-AZC (data not shown). The ^{13}C atoms in the structures were marked with *.

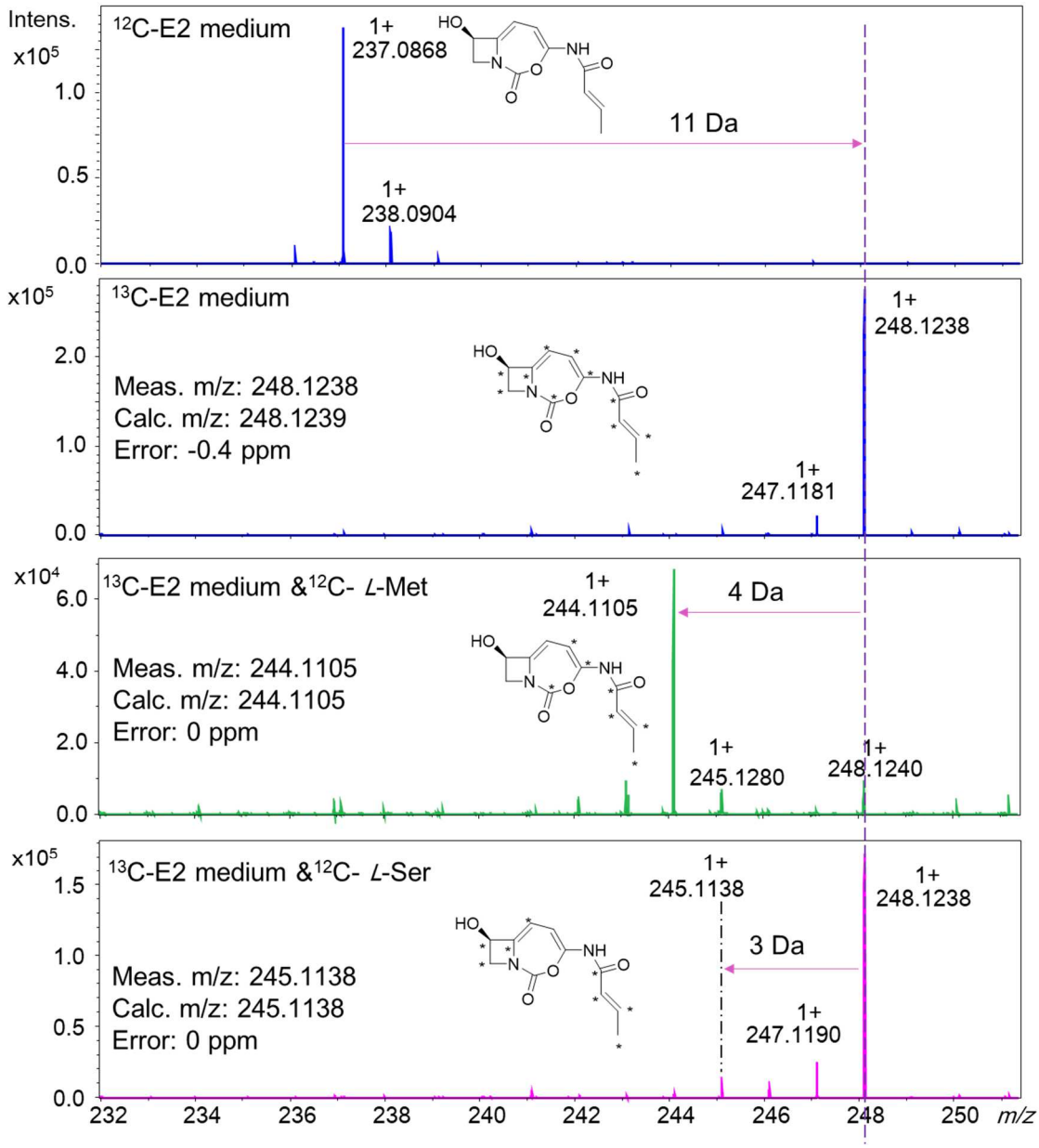

Figure S27. MS/MS spectra and fragment annotation of azetidomonamide A (**1**) in inverse isotope labelling experiments. Same color code as in Fig. S26 is used.

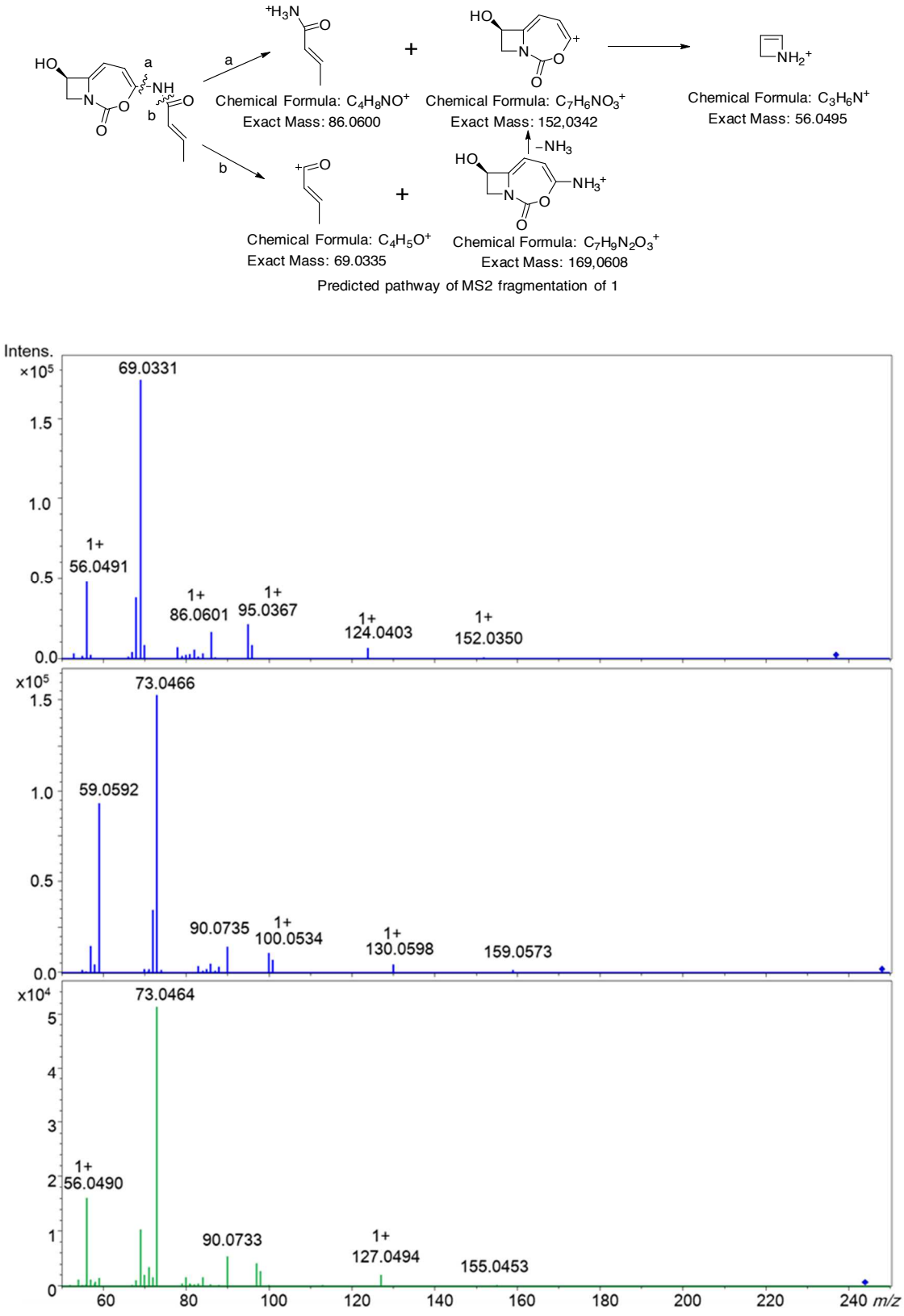

Figure S28. Purified proteins on SDS-PAGE gels stained with Coomassie blue. (**A**) FPLC purification of AzeJ. N-His_6 tagged AzeJ (29.8 kDa): fraction at 60, 150, 300 and 500 mM imidazole, concentrated stock (lane 1-5); ladder (lane 6); C-His_6 tagged AzeJ (28.7 kDa): concentrated stock, fraction at 150, 300 and 500 mM imidazole (lane 7-10). (**B**) FPLC purification of AzeB_A1L (117.8 kDa). ladder (lane 1), fraction at 300 mM (lane 2), 150 mM (lane 3-4) and 100 mM (lane 5) imidazole. (**C**) FPLC purification of AzeB_A2L (118.1 kDa). ladder (lane 1), fraction at 300 mM (lane 2), 150 mM (lane 3-4) and 100 mM (lane 5) imidazole. The ladder used was PageRuler™ Unstained Protein Ladder (Thermo Fisher Scientific).

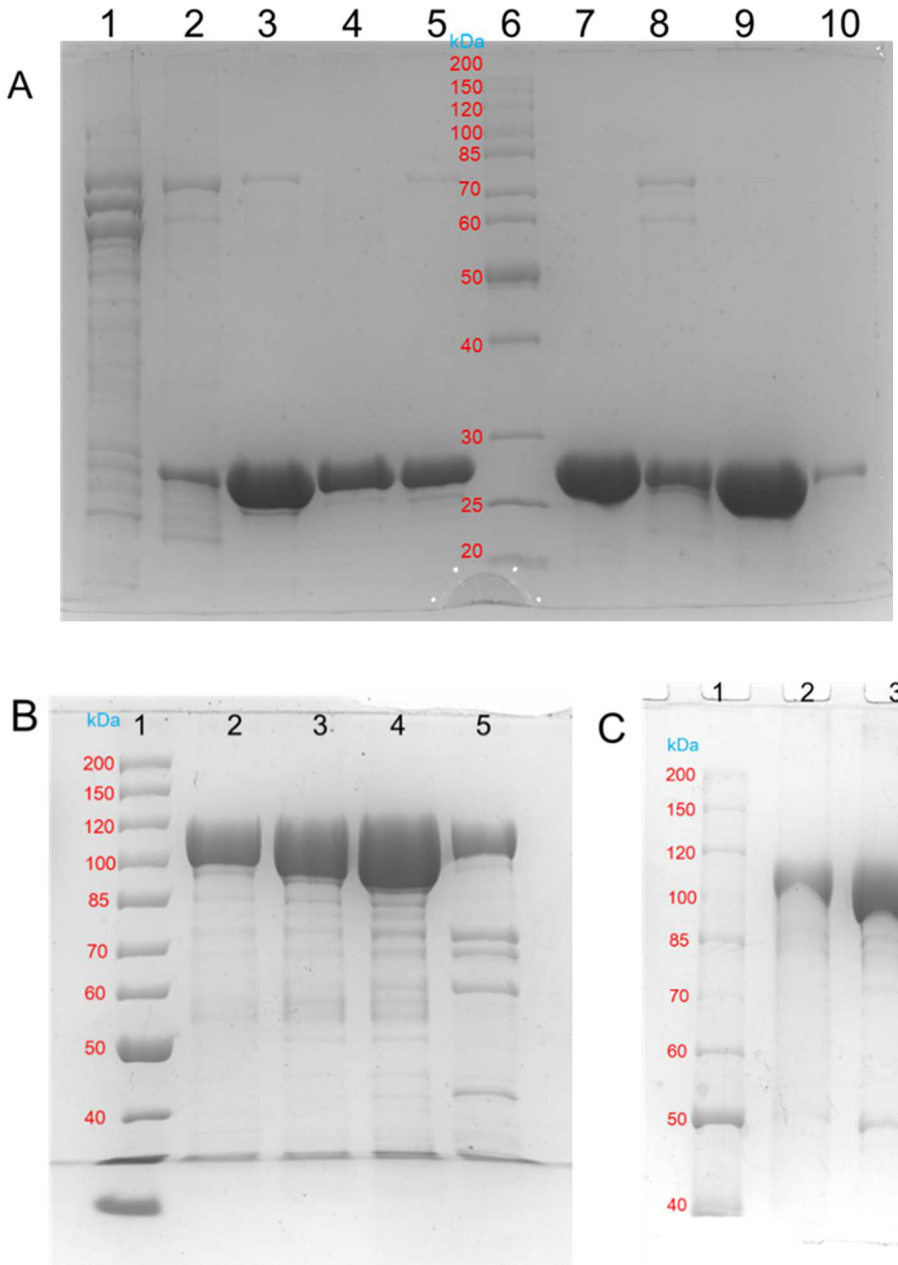

Figure S29. Time-course of AzeB_A1L catalysing pyrophosphorolysis of Ap4A with twenty proteinogenic amino acids and *L*-homoserine.

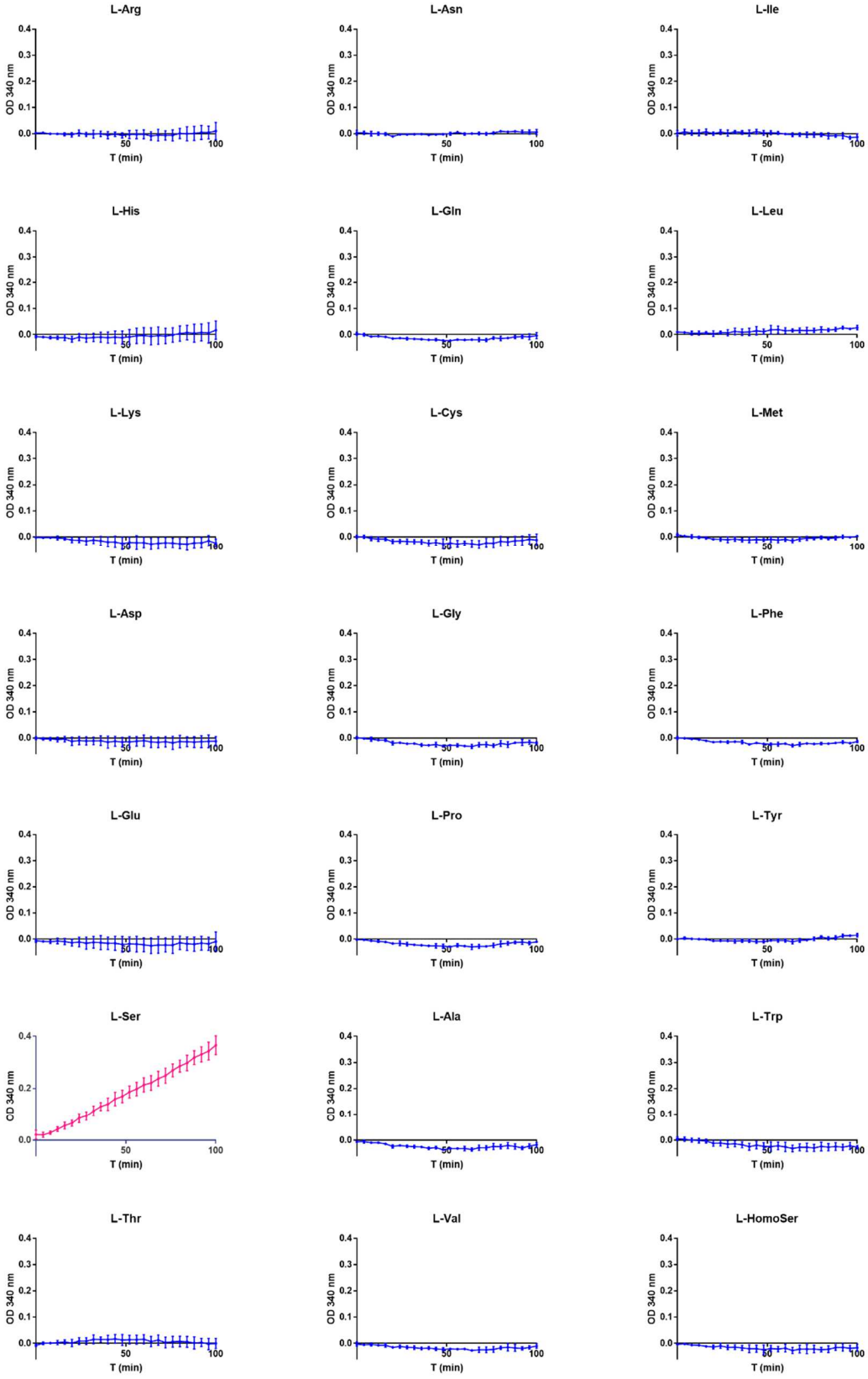

Figure S30. Time-course of AzeB_A2L catalysing pyrophosphorolysis of Ap4A with twenty proteinogenic amino acids, *L*-AZC, *D*-Pro and AdoMet.

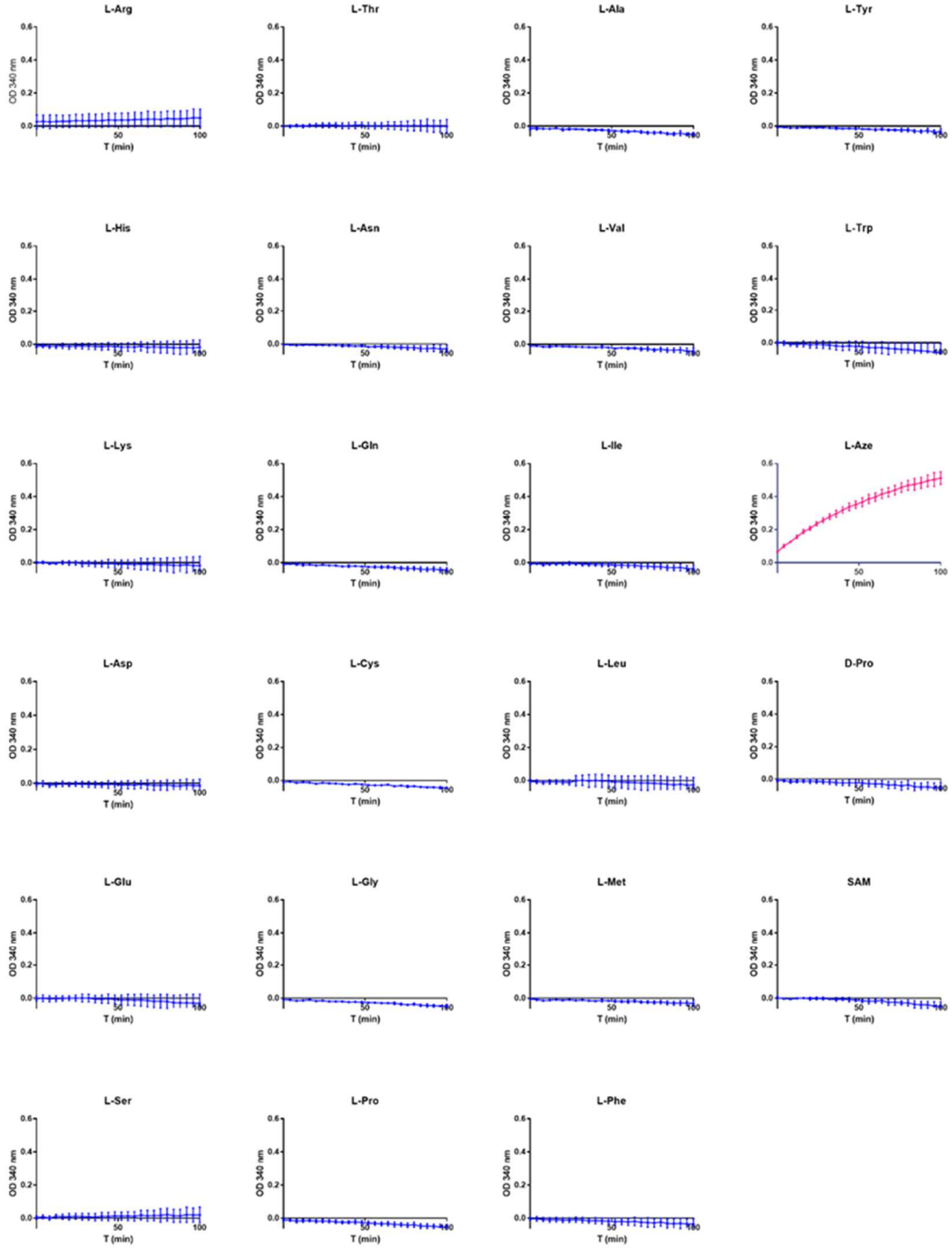

Figure S31. Characterization of AzeJ as AZC synthase *in vitro*. a) Reaction scheme; b) HPLC-UV traces at 254 nm.

a

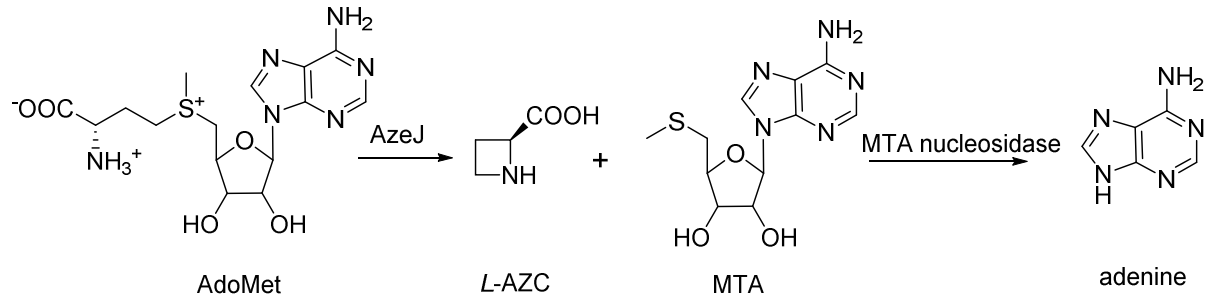

b

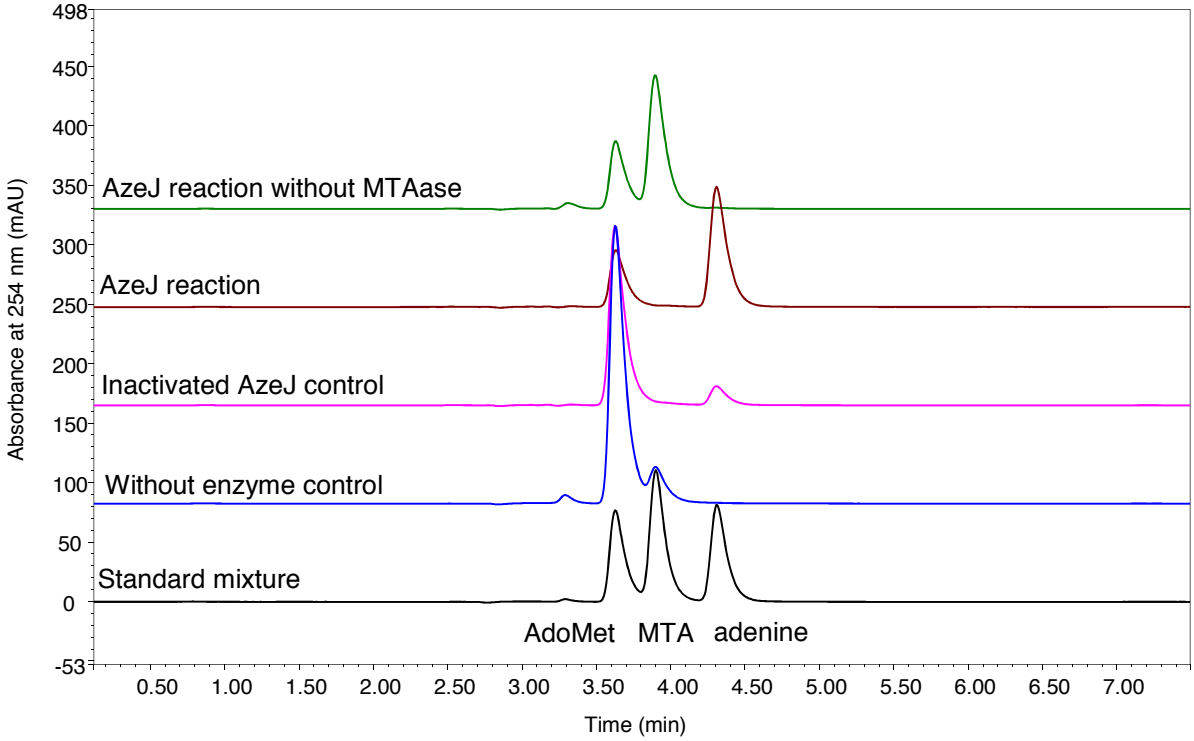

Figure S32. Detection of AZC by derivatization. a) Derivatization scheme and HRMS spectrum of derivatized product from AZC standard. b) Detection of AZC in *E. coli* cells expressing AzeJ. Extracted ion chromatography of $[M+Na]^+$ ion at *m/z* 258.0729 corresponding to the derivatized compound. Derivatized AZC standard (yellow), *E. coli* with pET28-PA3335N (blue), *E. coli* with pET29-PA3335C (red) and *E. coli* with pET28 as control (black).

a

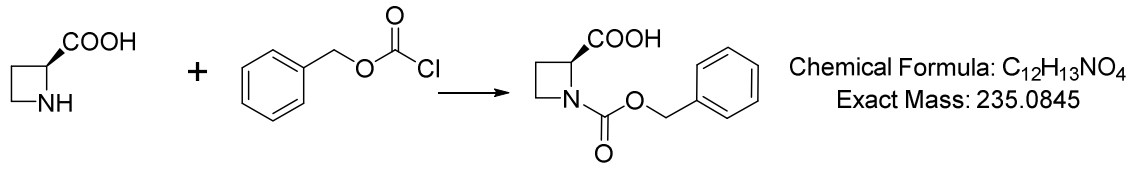

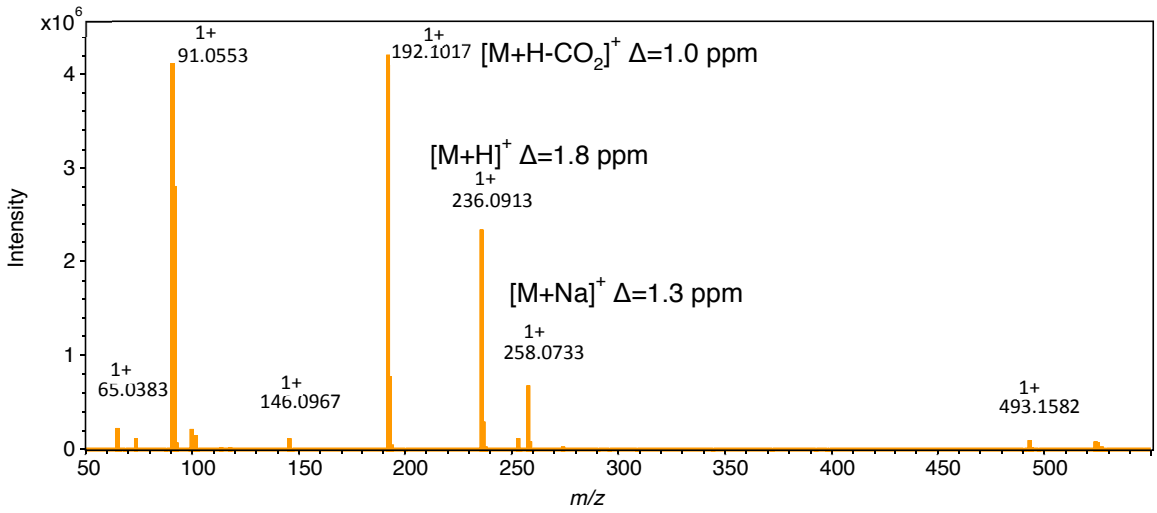

b

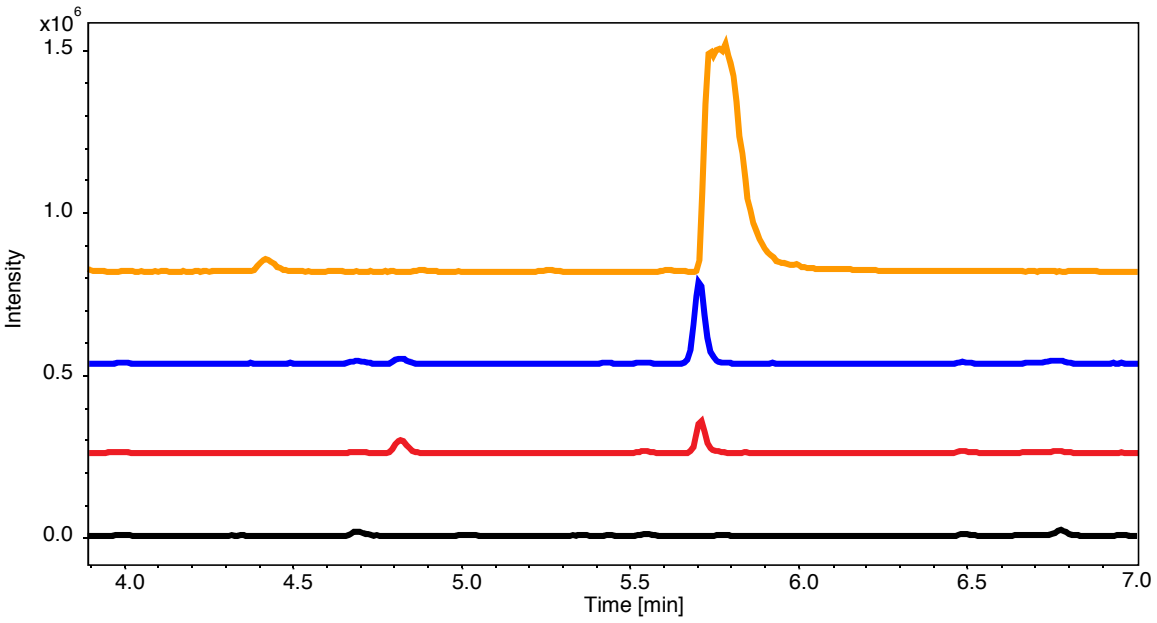

Figure S33. Michaelis-Menten plot to determine AzeJ kinetic parameters.

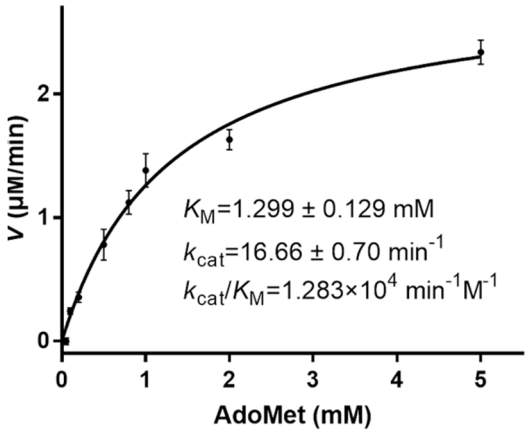

Figure S34. Biosynthetic pathway of related bacterial alkaloids: example of legonmycins produced by *Streptomyces*. [25h]

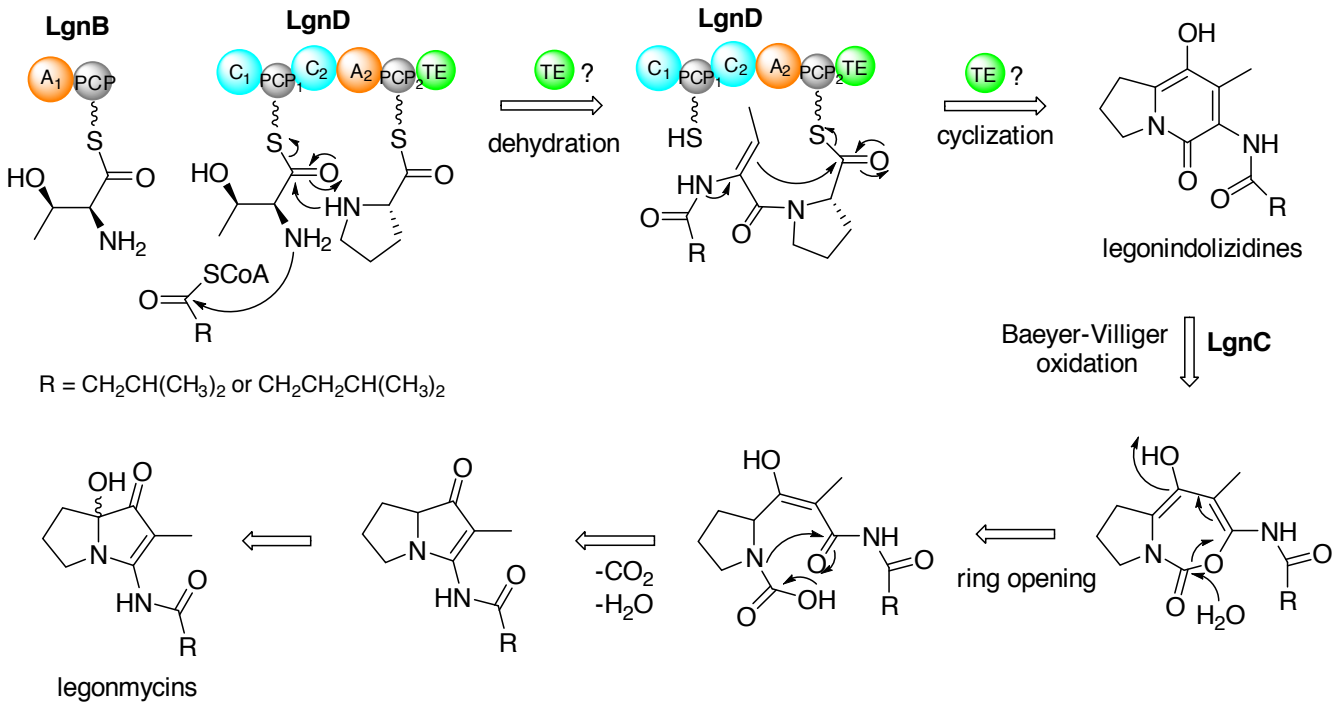

Figure S35. Identification of pyrrolizidine alkaloid 3 by LC-HR-MS/MSMS analysis. Red: synthetic compound; blue: compound identified in the AB16.2 extract. a) Extracted ion chromatography of ion $[M+H]^+$ at *m/z* 207.1128. b) MSMS spectra and fragment annotation.

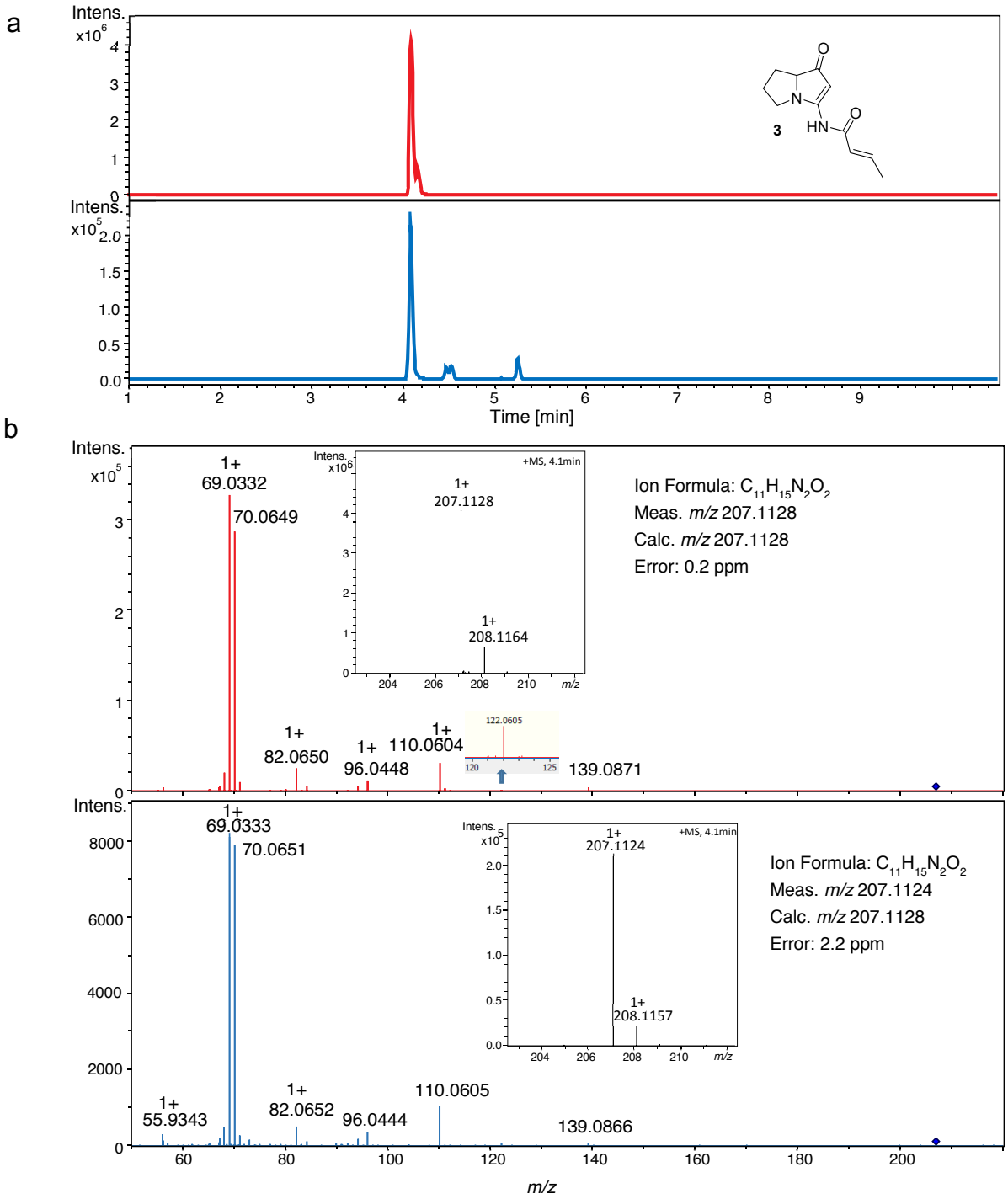

Figure S36. LC-MS analysis of putative cyclocarbamate compound 4. Extracted ion chromatograms (left panel) and mass spectra (right panel) of $[M+H]^+$ ion at *m/z* 251.1024 (ion formula: $C_{12}H_{15}N_2O_4$; calc. 251.1032) of extracts of AB16.2Δ27 (black), AB16.2 (blue) and AB16.2Δ35 (yellow).

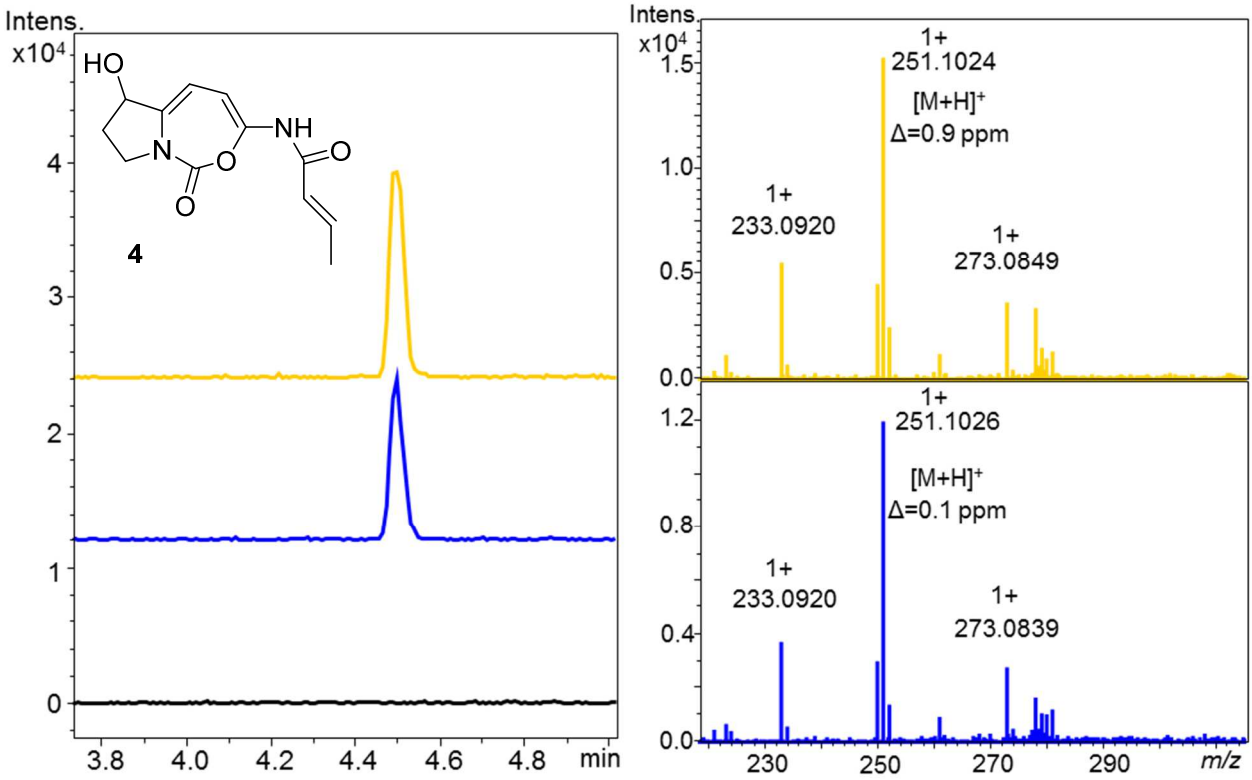

Figure S37. Genome mining of related azetidomonamide BGCs. Red: NRPS; blue: monooxygenase; purple: ring modification; yellow: acyl side chain synthesis as in the *aze* cluster; green: peptidase; brown: transporter; orange: PKS; black: others. Accession numbers for *azeB*-like genes are indicated below the strain names. PKS genes are not illustrated by their real scales for the purpose of clarity.

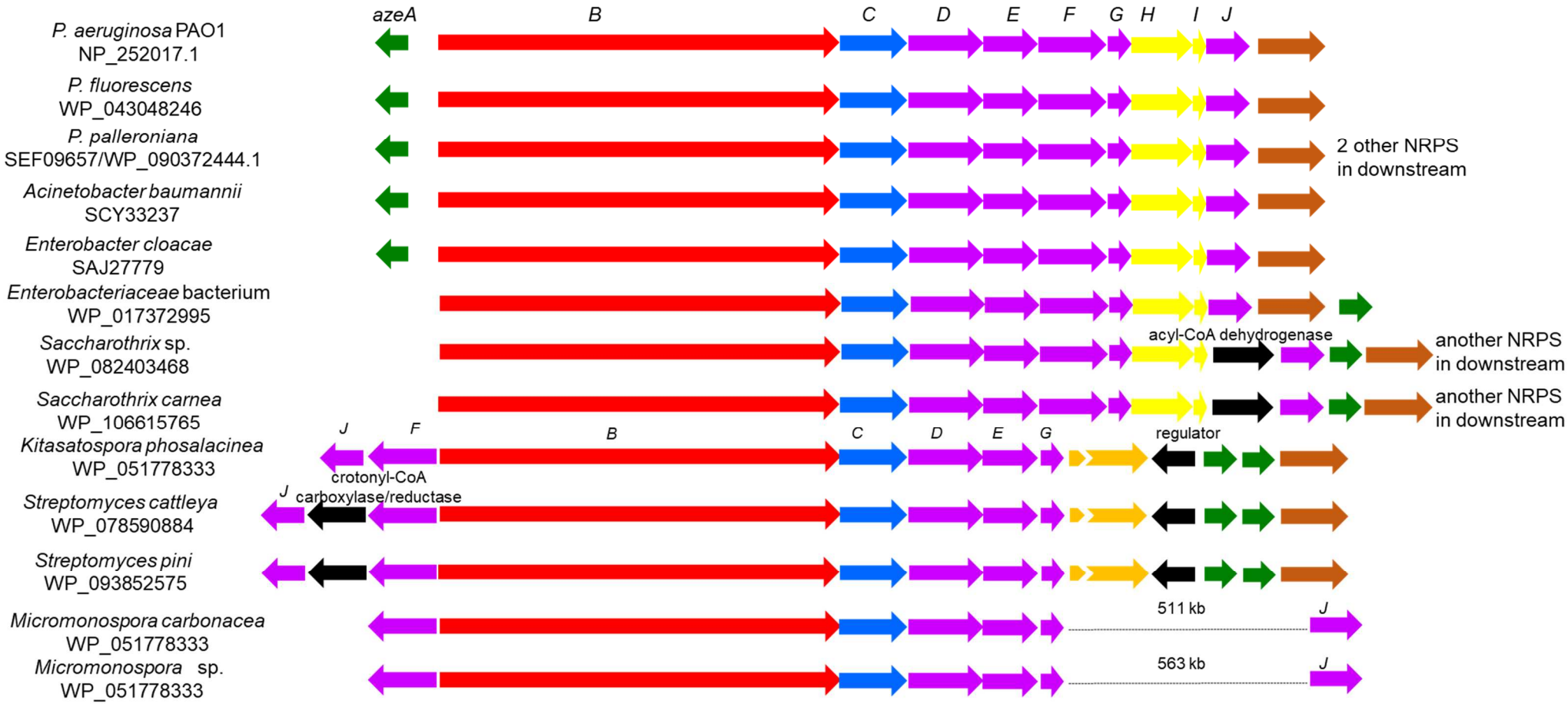

Figure S38. Phylogenetic tree of A2 domains of AzeB-like proteins. Underlined in red: characterized Pro-activating A2 domains involved in the biosynthesis of bacterial pyrrolizidine alkaloids or cyclocarbamates; in green: putative AZC-activating A2 domains in the related azetidomonamide pathways. Accession number of the AzeB-like NRPS is indicated after the strain name. Characterized AzeB_A2 from *P. aeruginosa* is highlighted in yellow.

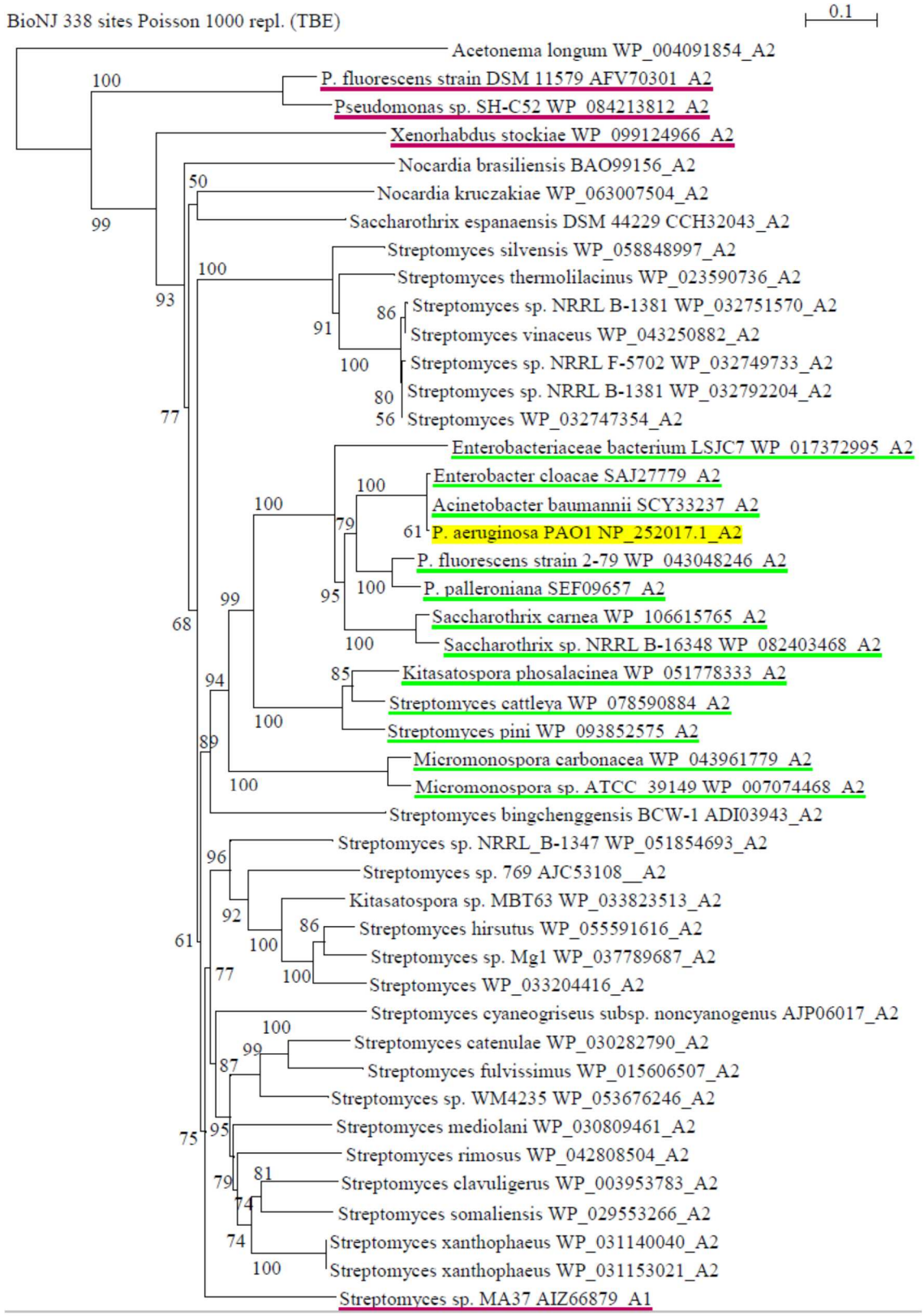

Figure S39. NMR spectra of synthetic new compounds.

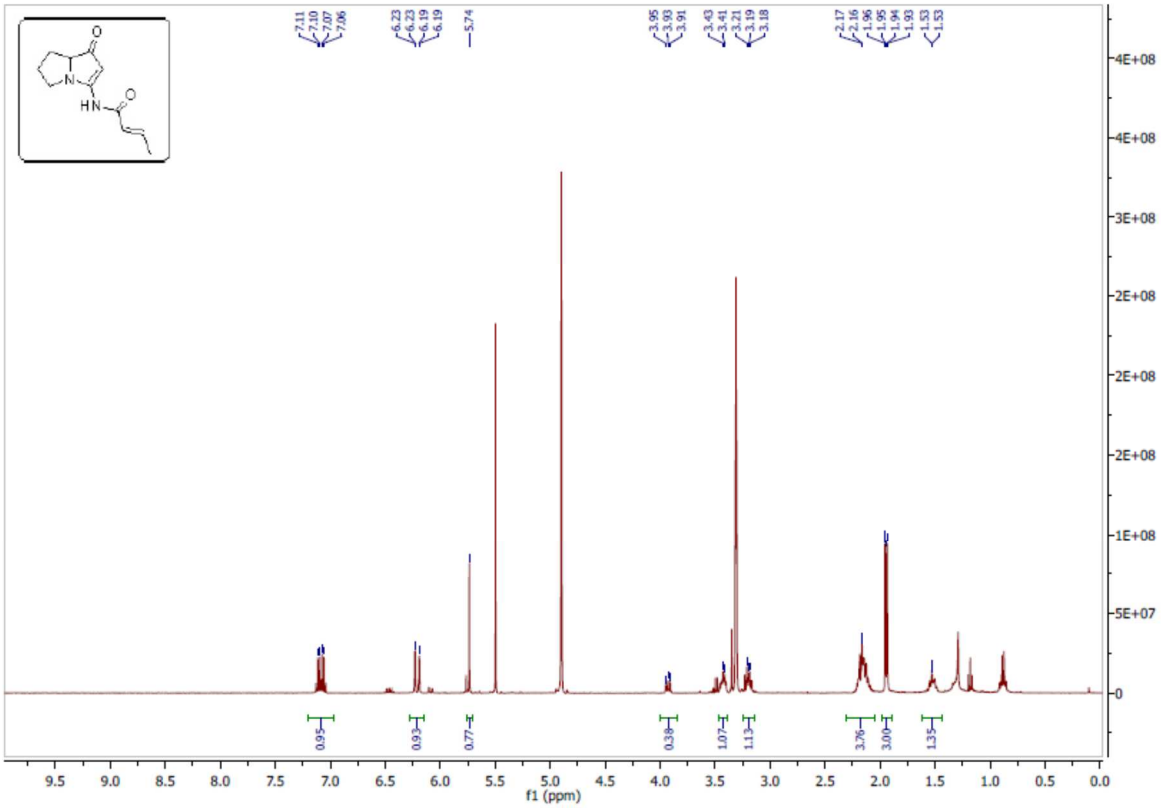

^{1}H NMR (CD_3OD, 400 MHz) of 3-(2*E*-butenoylamino)-5,6,7,7a-tetrahydro-1*H*-pyrrolizin-1-one (3)

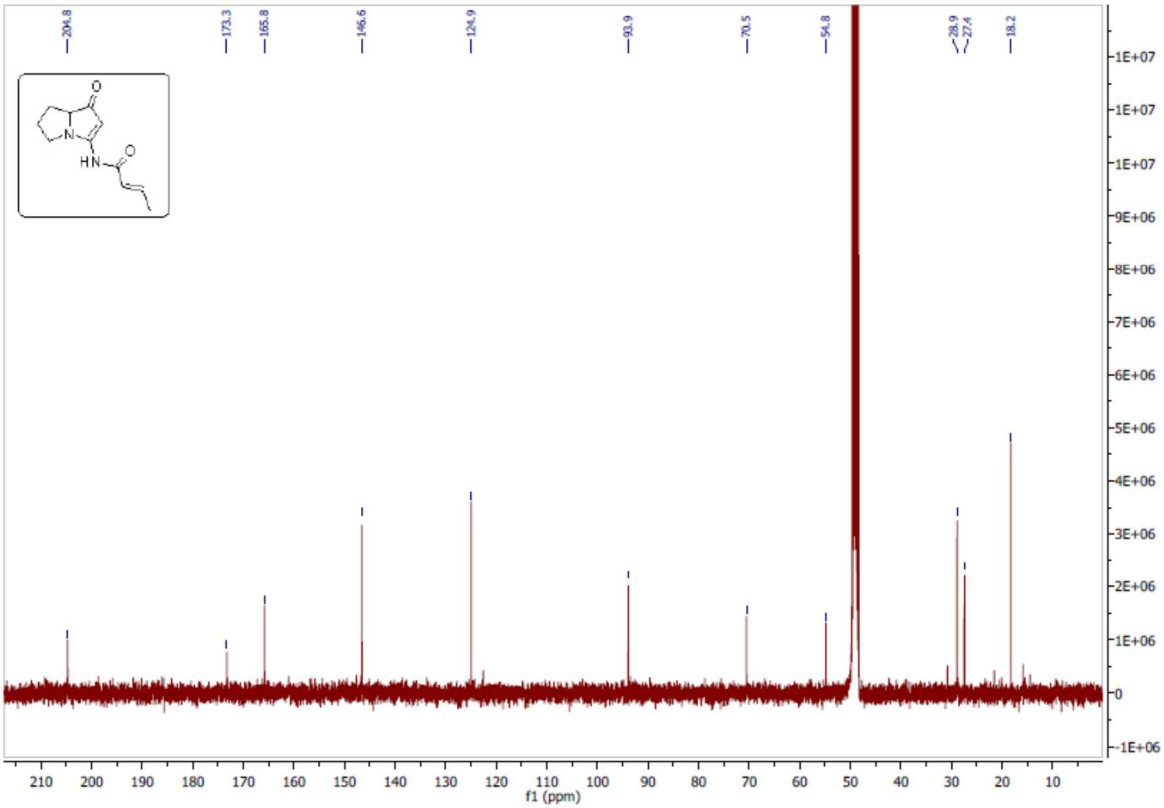

^{13}C NMR (CD_3OD, 101 MHz) of 3-(2*E*-butenoylamino)-5,6,7,7a-tetrahydro-1*H*-pyrrolizin-1-one (3)

Table S1. Fold change of concerned genes as revealed by RNAseq (PAO1_*vs*_AB16.2).[a]

Gene ID	log2 fold change	padj	Gene name
PA4777	-5.525	434.62	*pmrB*
PA4776	-7.327	622.76	*pmrA*
PA3335	-2.856	58.07	
PA3334	-4.721	230.29	
PA3333	-4.541	270.77	
PA3332	-4.518	181.25	
PA3331	-3.589	169.62	
PA3330	-4.507	171.01	
PA3329	-3.007	95.10	
PA3328	-3.776	127.51	
PA3327	-3.433	184.39	
PA3326	-4.407	296.44	
PA1000	-4.661	293.89	*pqsE*
PA0999	-4.149	227.29	*pqsD*
PA0998	-4.108	234.96	*pqsC*
PA0997	-4.572	288.18	*pqsB*
PA0996	-4.634	313.82	*pqsA*

[a] Full transcriptomic data will be reported in a separate publication.

Table S2. Predicted protein functions in the azetidomonamide biosynthetic gene cluster.

Gene ID	Protein name	Amino acid	Predicted function	Closest homologue (Protein ID; identity/similarity)
PA3326	AzeA	201	ATP-dependent ClpP2 protease	*Polyangium brachysporum* DSM 7029 (WP_047195047.1; 74%/91%)
PA3327	AzeB	2352	NRPS (C1-A1-PCP1-C2-A2-PCP2-TE)	*Acinetobacter baumannii* (SSU26971.1; 99%/99%)
PA3328	AzeC	388	FAD-dependent monooxygenase	*Saccharothrix sp.* NRRL B-16348 (WP_082403446.1; 76%/84%)
PA3329	AzeD	442	condensation domain protein	*Enterobacter cloacae* (SAJ27772.1; 99%/99%)
PA3330	AzeE	304	SDR family NAD(P)-dependent oxidoreductase	*Xenorhabdus miraniensis* (WP_099116035.1; 75%/86%)
PA3331	AzeF	418	cytochrome P450	*Acinetobacter baumannii* (SCY33085.1; 99%/99%)
PA3332	AzeG	141	hypothetical protein	*Xenorhabdus miraniensis* (WP_099116034.1; 81%/89%)
PA3333	AzeH	330	ketoacyl-ACP synthase III	*Saccharothrix sp.* NRRL B-16348 (WP_053716781.1; 71%, 81%)
PA3334	AzeI	79	acyl carrier protein	*Acinetobacter baumannii* (SST11212.1; 99%/100%)
PA3335	AzeJ	250	AdoMet-dependent class I methyltransferase	*Enterobacter cloacae* (SAJ27756.1; 99%/99%)

Table S3. ^{1}H (600 MHz) and ^{13}C NMR (150 MHz) data of azetidomonamide A (1) and B (2) in DMSO-d_6.

	1		**2**	
position	δ_C	δ_H (m, *J* in Hz)	δ_C	δ_H (m, *J* in Hz)
1	137.78, C		174.28, C	
2	98.22, CH	6.24 d (6.2)	99.10, CH	5.94 s
3	101.62, CH	5.46 dd (6.3, 1.5)	204.36, C	
4	148.04, C		65.84, CH	4.20 dd (9.8, 6.2)
5	66.04, CH	4.96 m	20.27, CH_2	2.60 m
				2.11 m
6	58.87, CH_2	4.19 dd (8.2, 6.7)	53.35, CH_2	3.38 m
		3.75 dd (8.2, 3.7)		4.03 dt (9.1, 8.9)
7	155.73, C			
1′	163.10, C		163.91, C	
2′	124.86, CH	6.08 dq (15.3, 1.7)	124.31, CH	6.16 dq (15.4, 1.7)
3′	140.91, CH	6.74 dq (15.2, 6.9)	143.75, CH	6.91 dq (15.2, 6.9)
4′	17.57, CH_3	1.81 dd (6.9, 1.6)	17.81, CH_3	1.87 dd (6.9, 1.6)
NH-1		9.99 s		10.74 s
OH-5		6.18 d (7.9)		

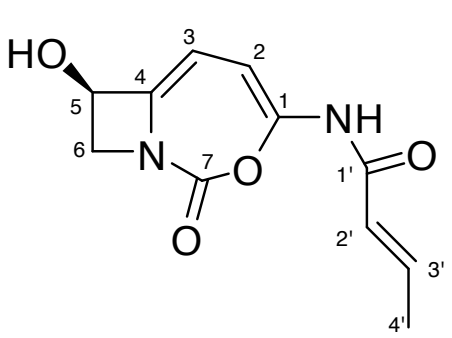

1

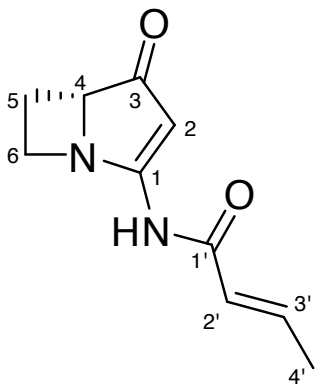

2

Table S4. Prediction of amino acid specificity of the AzeB A domains.

A domain	Predicted active site code	NRPSpredictor2	PKS/NRPS web server
AzeB_A1	D V W H F S L V D K	Ser	Ser
AzeB_A2	D M Q L V S Q Q V K	Pro	Not hit

Table S5. AzeJ homologs in Eukaryota and Archaea identified by hidden Markov models.*

Pfam Accession number	Organism name	Description
Eukaryotes		
A0A0M0K7E8_9EUKA	*Chrysochromulina* sp. CCMP291	Algae
A0A2D4BUJ7_PYTIN	*Pythium insidiosum*	Oomycetes
A4S1U4_OSTLU	*Ostreococcus lucimarinus* (strain CCE9901)	Algae
A0A074SLE0_HAMHA	*Hammondia hammondi*	Protozoa
A0A2P4YCA2_9STRA	*Phytophthora palmivora* var. *palmivora*	Fungi
W7TQE1_9STRA	*Nannochloropsis gaditana*	Algae
A0A0W8DZ72_PHYNI	*Phytophthora nicotianae*	Oomycetes
K8YR43_NANGC	*Nannochloropsis gaditana (strain CCMP526)*	Algae
Archaea		
A0A0V8RU57_PYROC	*Pyrodictium occultum*	
A2BJI4_HYPBU	*Hyperthermus butylicus* (strain DSM 5456 / JCM 9403 / PLM1-5)	
A0A151F6Z4_9EURY	*Theionarchaea archaeon* DG-70	
G0EDK1_PYRF1	*Pyrolobus fumarii* (strain DSM 11204 / 1A)	
A0A256Z8B0_9CREN	*Desulfurococcales archaeon* ex4484_42	

*As comparison, a total of 83 non-redundant bacterial homologs were found.

Table S6. Strains and plasmids used in this study.

Strain or plasmid	Relevant Characteristics	Source or reference
Pseudomonas aeruginosa		
PAO1	Wild-type reference strain	[20]
PAO1Δ27	PAO1 with in-frame deletion of 6,525 bp in gene PA3327	This study
AB16.2	Spontaneous mutant, colistin resistant exhibiting a deletion in-frame of 3 bp (Leucine 172) in gene *pmrB*	This study
AB16.2Δ*pqsA*	AB16.2 with in-frame deletion of 1,463 bp in gene *pqsA*	This study
AB16.2Δ27	AB16.2 with in-frame deletion of 6,525 bp in gene PA3327	This study
AB16.2Δ35	AB16.2 with in-frame deletion of 270 bp in gene PA3335	This study
AB16.2Δ35 *attB*::PA3335	Mutant AB16.2Δ35 *cis* complemented with PA3335 gene from PAO1 inserted at *attB* site, Tc^r	This study
Escherichia coli		
DH5α	F^- Φ80*lac*ZΔM15 Δ(*lac*ZYA-*arg*F) U169 *rec*A1 *end*A1 *hsd*R17(r_k^-, m_k^+) *pho*A *sup*E44 *thi*-1 *gyr*A96 *rel*A1 λ^-	Thermo Fischer Scientific™
CC118λ*pir*	Δ(*ara-leu*) *ara*D Δ*lac*X74 *gal*E *gal*K *pho*A20 *thi*-1 *rps*E *rpo*B *arg*E(Am) *rec*AI lysogenized with λ*pir* phage	[21]
HB101	*sup*E44 *hsd*S20(r_B^-, m_B^-) *rec*A13 *ara*-14 *pro*A2 *lac*Y1 *gal*K2 *rps*L20 *xyl*-5 *mtl*-1 *leu*B6 *thi*-1	[22]
BL21(DE3)	F^- *ompT gal dcm lon hsdS*$_B$($r_B^-m_B^-$) λ(DE3 [*lacI lacUV5-T7p07 ind1 sam7 nin5*]) [*malB*$^+$]$_{K\text{-}12}$(λ^S)	Novagen

Plasmids		
pKNG101	Marker exchange suicide vector in *P. aeruginosa*; *sac*BR *mob*RK2 *ori*R6K Str^r	[2b]
pRK2013	Helper plasmid for mobilization of non-self-transmissible plasmids; ColE1 Tra$^+$ Mob$^+$ Kan^r	[23]
pCR-Blunt	Blunt-end cloning vector *ccd*B *lac*Zα Zeo^r Kan^r	Thermo Fischer Scientific™
mini-CTX1	Self-proficient integration vector with *tet,* V-*FRT-attP,* MCS, *ori, int,* and *oriT*; Tc^r	[3]
mini-CTXPA3335	PA3335 (1.037-kb) from PAO1 cloned into mini-CTX1 at *BamHI/NotI* sites, Tc^r	This study
pKNGΔ*pqsA*	*XbaI*/*SpeI* 1.193-kb fragment composed of sequences flanking 5' and 3' ends of *pqsA*, cloned in pKNG101	This study
pKNGΔ3327	*BamHI/XbaI* 1.092-kb fragment composed of sequences 5' and 3' ends of PA3327, cloned in pKNG101	This study
pKNGΔ3335	*BamHI*/*Apa*I 1.065-kb fragment composed of sequences flanking 5' and 3' ends of PA3335, cloned in pKNG101	This study
pET28-PA3327A1L	*NdeI*/*HindIII* 3.141-kb fragment composed of C_1-A_1-PCP_1 domain sequences of PA3327, cloned in pET28a(+)	This study
pET28-PA3327A2L	*NdeI*/*HindIII* 3.150-kb fragment composed of C_2-A_2-PCP_2 domain sequences of PA3327, cloned in pET28a(+)	This study
pET28-PA3335N	*NdeI*/*Xho*I 750 bases fragment composed of the PA3335 ORF sequences, cloned in pET28a(+)	This study
pET29-PA3335C	*NdeI*/*Xho*I 747 bases fragment composed of the PA3335 ORF sequences without stop codon, cloned in pET29b(+)	This study
pACYC-SFP	*NdeI*/*Xho*I 675 bases fragment composed of the *sfp* ORF sequences, cloned in pACYC	This study

Tc^r, tetracycline resistance; Str^r, streptomycin resistance; Kan^r, kanamycin resistance; Zeo^r, zeocin resistance.

Table S7. Primers used in this study.

Primer name	Sequence (5'→3')[a]
Primers for genetic inactivation/complementation	
PCRi PA3327 A1	TCCATCCGGCAAACCTTTCA
PCRi PA3327 A2	GCAGGGCCCAGATGTCCCGTTGGTAGG
PCRi PA3327 A3	CATCTGGGCCCTGCTGCTGTTCTTCTA
PCRi PA3327 A4	CAGGGGATGTCTGCTCATGG
PCRi PA3335 A1	TTTCGATTCGCTGGTGGTCA
PCRi PA3335 A2	TAGCTCTCGAGATAGCGGGCATTGAG
PCRi PA3335 A3	TATCTCGAGAGCTACTACCGCCGTTG
PCRi PA3335 A4	AAGGTGACCAGGTAGCCGAT
PCRi pqsA A1	TACGCAATGGGATTTCAACA
PCRi pqsA A2	CAACATGTGGCCCCGATAGTGATAAAC
PCRi pqsA A3	GGGGCCACATGTTGATTCAGGCTGTGG

PCRi pqsA A4	AGGTTGAGGTGTCCCTTGAC
Primers for RT-qPCR	
uvrD1	CACGCCTCGCCCTACAGCA
uvrD2	GGATCTGGAAGTTCTCGCTCAGC
RT PA3327 AB1	ACCACCCTTTCCTACATGCG
RT PA3327 AB2	GAAGGTTTCGATATGCCGCG
Primers for protein expression[a]	
PA001_PA3335F	GATATGCATATGAGTCAGAACATGGATCTCACG
PA002_PA3335NR	GATATGCTCGAGTCATGCCGCCGACGAACC
PA003_PA3335CR	GATATGCTCGAGTGCCGCCGACGAACCGAAG
PA004_A1LF	GATATGCATATGGTTCGTTTCGCTCGCTTG
PA011_A1LR	GATATGAAGCTTTCACAGCCCTTCCAGGCGCG
PA013_A2LF	GATATGCATATGCTCGCGGAGCGAAGCTACC
PA015_A2LR	GATATGAAGCTTTCAGGCACGGATCGGTACCAGC

[a] restriction sites are underlined.

References

[1] R. G. Lageveen, G. W. Huisman, H. Preusting, P. Ketelaar, G. Eggink, B. Witholt, *Appl. Env. Microbiol.* **1988**, *54*, 2924-2932.

[2] a) C. Muller, P. Plésiat, K. Jeannot, *Antimicrob. Agents Chemother.* **2011**, *55*, 1211-1221; b) K. Kaniga, I. Delor, G. R. Cornelis, *Gene* **1991**, *109*, 137-141.

[3] T. T. Hoang, A. J. Kutchma, A. Becher, H. P. Schweizer, *Plasmid* **2000**, *43*, 59-72.

[4] C. Llanes, D. Hocquet, C. Vogne, D. Benali-Baitich, C. Neuwirth, P. Plesiat, *Antimicrob. Agents Chemother.* **2004**, *48*, 1797-1802.

[5] G. L. Winsor, E. J. Griffiths, R. Lo, B. K. Dhillon, J. A. Shay, F. S. Brinkman, *Nucleic Acids Res.* **2016**, *44*, D646-653.

[6] J. T. Jo, F. S. Brinkman, R. E. Hancock, *Antimicrob. Agents Chemother.* **2003**, *47*, 1101-1111.

[7] D. J. Busby, R. C. Copley, J. A. Hueso, S. A. Readshaw, A. Rivera, *J. Antibiot.* **2000**, *53*, 670-676.

[8] O. Schimming, V. L. Challinor, N. J. Tobias, H. Adihou, P. Gruen, L. Poeschel, C. Richter, H. Schwalbe, H. B. Bode, *Angew. Chem., Int. Ed.* **2015**, *54*, 12702-12705

[9] Gaussian 16, Revision B.01, M. J. Frisch, G. W. Trucks, H. B. Schlegel, G. E. Scuseria, M. A. Robb, J. R. Cheeseman, G. Scalmani, V. Barone, G. A. Petersson, H. Nakatsuji, X. Li, M. Caricato, A. V. Marenich, J. Bloino, B. G. Janesko, R. Gomperts, B. Mennucci, H. P. Hratchian, J. V. Ortiz, A. F. Izmaylov, J. L. Sonnenberg, D. Williams-Young, F. Ding, F. Lipparini, F. Egidi, J. Goings, B. Peng, A. Petrone, T. Henderson, D. Ranasinghe, V. G. Zakrzewski, J. Gao, N. Rega, G. Zheng, W. Liang, M. Hada, M. Ehara, K. Toyota, R. Fukuda, J. Hasegawa, M. Ishida, T. Nakajima, Y. Honda, O. Kitao, H. Nakai, T. Vreven, K. Throssell, J. A. Montgomery, Jr., J. E. Peralta, F. Ogliaro, M. J. Bearpark, J. J. Heyd, E. N. Brothers, K. N. Kudin, V. N. Staroverov, T. A. Keith, R. Kobayashi, J. Normand, K. Raghavachari, A. P. Rendell, J. C. Burant, S. S. Iyengar, J. Tomasi, M. Cossi, J. M. Millam, M. Klene, C. Adamo, R. Cammi, J. W. Ochterski, R. L. Martin, K. Morokuma, O. Farkas, J. B. Foresman, and D. J. Fox, Gaussian, Inc., Wallingford CT, **2016**.

[10] H. B. Bode, D. Reimer, S. W. Fuchs, F. Kirchner, C. Dauth, C. Kegler, W. Lorenzen, A. O. Brachmann, P. Grun, *Chemistry* **2012**, *18*, 2342-2348.

[11] Y. Li, N. M. Llewellyn, R. Giri, F. Huang, J. B. Spencer, *Chem. Biol.* **2005**, *12*, 665-675.

[12] B. P. Duckworth, D. J. Wilson, C. C. Aldrich, *Methods Mol. Biol.* **2016**, *1401*, 53-61.

[13] A. J. Lloyd, N. J. Potter, C. W. Fishwick, D. I. Roper, C. G. Dowson, *ACS Chem. Biol.* **2013**, *8*, 2157-2163.

[14] E. Tayama, K. Watanabe, Y. Matano, *Eur. J. Org. Chem.* **2016**, *2016*, 3631-3641.

[15] C. Guillaume, C. Payre, I. Jemel, L. Jeammet, S. Bezzine, G. S. Naika, J. Bollinger, P. Grellier, M. H. Gelb, J. Schrevel, G. Lambeau, C. Deregnaucourt, *Infect. Immun.* **2015**, *83*, 2453-2465.

[16] D. Dacheux, I. Attree, C. Schneider, B. Toussaint, *Infect. Immun.* **1999**, *67*, 6164-6167.

[17] T. Weber, K. Blin, S. Duddela, D. Krug, H. U. Kim, R. Bruccoleri, S. Y. Lee, M. A. Fischbach, R. Muller, W. Wohlleben, R. Breitling, E. Takano, M. H. Medema, *Nucleic Acids Res.* **2015**, *43*, W237-W243.

[18] M. Gouy, S. Guindon, O. Gascuel, *Mol. Biol. Evol.* **2010**, *27*, 221-224.

[19] B. B. Snider, J. R. Duvall, *Org. Lett.* **2005**, *7*, 4519-4522.

[20] C. K. Stover, X. Q. Pham, A. L. Erwin, S. D. Mizoguchi, P. Warrener, M. J. Hickey, F. S. Brinkman, W. O. Hufnagle, D. J. Kowalik, M. Lagrou, R. L. Garber, L. Goltry, E. Tolentino, S. Westbrock-Wadman, Y. Yuan, L. L. Brody, S. N. Coulter, K. R. Folger, A. Kas, K. Larbig, R. Lim, K. Smith, D. Spencer, G. K. Wong, Z. Wu, I. T. Paulsen, J. Reizer, M. H. Saier, R. E. Hancock, S. Lory, M. V. Olson, *Nature* **2000**, *406*, 959-964.

[21] M. Herrero, V. De Lorenzo, K. N. Timmis, *J. Bacteriol.* **1990**, *172*, 6557-6567.

[22] S. Lacks, B. Greenberg, *J. Mol. Biol.* **1977**, *114*, 153-168.

[23] G. Ditta, S. Stanfield, D. Corbin, D. R. Helinski, *Proc. Natl. Acad. Sci. USA*. **1980**, *77*, 7347-7351.

[24] a) K. Higuchi, K. Suzuki, H. Nakanishi, H. Yamaguchi, N.-K. Nishizawa, S. Mori, *Plant Physiol.* **1999**, *119*, 471-479; b) K. Isono, S. Suzuki, *Agr. Biol. Chem. (Tokyo)* **1968**, *32*, 1193-1197; c) C.-Y. Lai, I. W. Lo, R. T. Hewage, Y.-C. Chen, C.-T. Chen, C.-F. Lee, S. Lin, M.-C. Tang, H.-C. Lin, *Angew. Chem. Int. Ed.* **2017**, *56*, 9478-9482; d) G. Wu, J. M. Winter, J. R. Nielson, R. T. Peterson, *Mar. Drugs* **2017**, *15*; e) F. Yan, D. Auerbach, Y. Chai, L. Keller, Q. Tu, S. Huettel, A. Glemser, H. A. Grab, T. Bach, Y. Zhang, R. Mueller, *Angew. Chem. Int. Ed.* **2018**, *57*, 8754-8759.

[25] a) T. W. Doyle, D. E. Nettleton, D. M. Balitz, J. E. Moseley, R. E. Grulich, T. McCabe, J. Clardy, *J. Org. Chem.* **1980**, *45*, 1324-1326; b) A. Isogai, S. Sakuda, K. Shindo, S. Watanabe, A. Suzuki, S. Fujita, T. Furuya, *Tetrahedron Lett.* **1986**, *27*, 1161-1164; c) D. J. Busby, R. C. B. Copley, J. A. Hueso, S. A. Readshaw, A. Rivera, *J. Antibiot.* **2000**, *53*, 670-676; d) Q. Zhang, K. K. Schrader, H. N. ElSohly, S. Takamatsu, *J. Antibiot.* **2003**, *56*, 673-681; e) J.-F. Hu, D. Wunderlich, R. Thiericke, H.-M. Dahse, S. Grabley, X.-Z. Feng, I. Sattler, *J. Antibiot.* **2003**, *56*, 747-754; f) T. S. Bugni, M. Woolery, C. A. Kauffman, P. R. Jensen, W. Fenical, *J. Nat. Prod.* **2006**, *69*, 1626-1628; g) Y. Schmidt, M. van der Voort, M. Cruesemann, J. Piel, M. Josten, H.-G. Sahl, H. Miess, J. M. Raaijmakers, H. Gross, *ChemBioChem* **2014**, *15*, 259-266; h) S. Huang, J. Tabudravu, S. S. Elsayed, J. Travert, D. Peace, M. H. Tong, K. Kyeremeh, S. M. Kelly, L. Trembleau, R. Ebel, M. Jaspars, Y. Yu, H. Deng, *Angew. Chem. Int. Ed.* **2015**, *54*, 12697-12701; i) M. C. Kim, J. H. Lee, B. Shin, L. Subedi, J. W. Cha, J.-S. Park, D.-C. Oh, S. Y. Kim, H. C. Kwon, *Org. Lett.* **2015**, *17*, 5024-5027; j) P. Fu, J. B. MacMillan, *Org. Lett.* **2015**, *17*, 3046-3049; k) P. Fu, S. La, J. B. MacMillan, *J. Nat. Prod.* **2016**, *79*, 455-462; l) P. Fu, A. Legako, S. La, J. B. MacMillan, *Chem. - Eur. J.* **2016**, *22*, 3491-3495; m) B. Jiang, W. Zhao, S. Li, H. Liu, L. Yu, Y. Zhang, H. He, L. Wu, *J. Nat. Prod.* **2017**, *80*, 2825-2829.

Author Contributions

Z. H performed compound isolation/characterization and biochemical experiments; A. B performed genetic manipulation; C. G performed activity assays in caterpillar; S. P performed chemical synthesis; G. G-J performed ECD calculation; C. D tested phospholipase inhibition; S. H and K. J provided transcriptomic data; Z. H, C. G, K. J and Y. L analyzed data. K. J and Y. L conceived and supervised the project. Z. H, K. J and Y. L wrote the paper with contribution of all other authors.

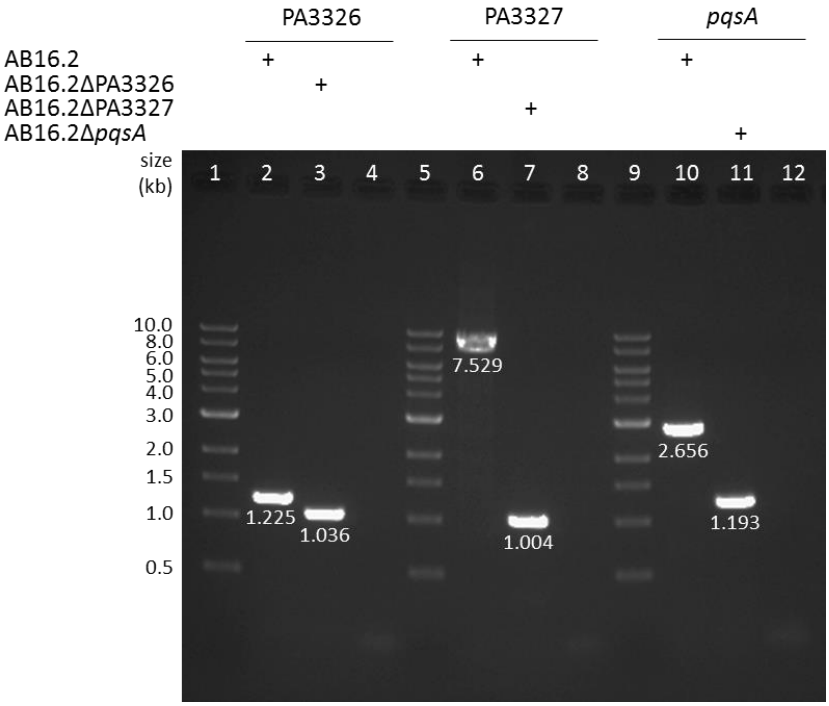

Figure 53: Agarose gel electrophoresis showing the inactivation of genes PA3326, PA3327 and *pqsA* in mutant AB16.2, by deletion of internal DNA fragments.

Lanes 1, 5 and 9: 1-kb DNA Ladder. Lanes 4, 8 and 12: negative controls.

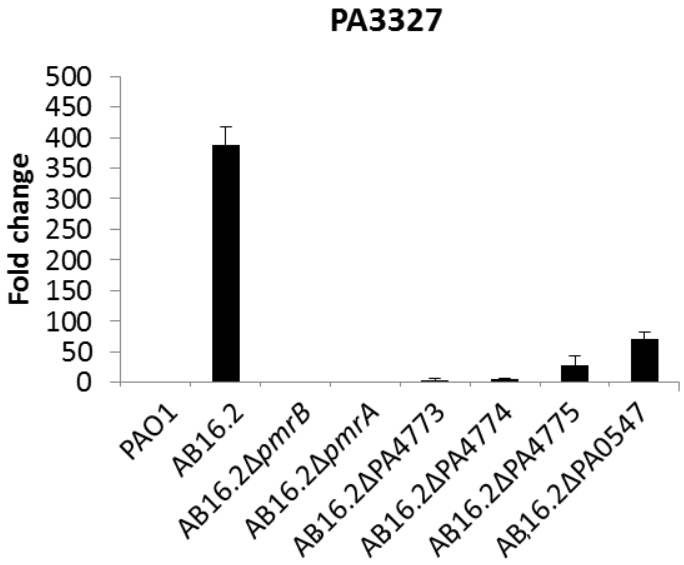

Figure 54: PA3327 gene expression in the *pmrB* mutant AB16.2 and various derivatives, as assessed by RT-qPCR.

Mean values were calculated from two bacterial cultures assessed twice.

3.2. Supplementary results

3.2.1. Characterization of nonribosomal peptide synthetase biosynthetic gene cluster PA3326-PA3335

The *pmrB* mutant AB16.2 overexpressed (from 7.2- to 26.4-fold *versus* strain PAO1) a relatively large locus that contains a gene (PA3327), determining a probable nonribosomal peptide synthetase (Hong *et al*., 2019). Considering the fact that the *pqsABCDE* operon was also upregulated in AB16.2, we hypothesized that the expression of this gene cluster could be under the control of PQS or HHQ (4-hydroxy-2-heptylquinoline). Deletion of 1.463-kb in gene *pqsA* of AB16.2 mutant (Figure 53, lanes 10 to 12) was associated with a significant 4.3-fold drop in PA3327 mRNA transcripts (Hong *et al*., 2019). Suppression of any of the genes PA4773 to *pmrB* almost completely abolished PA3327 transcription (Figure 54), which unambiguously confirmed that NRPS locus PA3326-35 was activated as a result of mutational activation of PmrAB and over production of polyamines (spermidine and/or norspermidine). Interestingly, inactivation of PA0547, a gene that codes for an ArsR-type transcriptional regulator and which is upregulated in AB16.2 (RNA seq data), led to a 6.6-fold decrease in PA3327 expression (Figure 54). Since PA0547 is cotranscribed with a gene, *metK*, that encodes an SAM synthetase (overexpressed 8.5-fold in AB16.2) (Figure 42), it is therefore possible that this second gene only is required for complete overexpression of cluster PA3326-35. Of note, ectopic plasmid-driven overexpression of *metK* has been reported to increase resistance of *P. aeruginosa* to aminoglycosides (Struble and Gill, 2009). Regulatory interplays between QS, polyamine synthesis, transcriptional regulator PA0547 and NRPs synthesized by PA3327 biosynthetic cluster remain to be established.

Next, in order to characterize the NRPs elaborated by the PA3326-35 genes, a 6.525-kb internal fragment was delted from gene PA3327 in mutant AB16.2 (Figure 53, lanes 6 to 8). Comparison of metabolomic profiles obtained by Liquid Chromatography coupled to High Resolution Mass Spectrometry (LC-HRMS) revealed the absence of four compounds in AB16.2ΔPA3327 mutant, subsequently identified as azetidomonamide A and B, and an analogue of each of them (compound 4 and 3, respectively) (Hong *et al*., 2019).

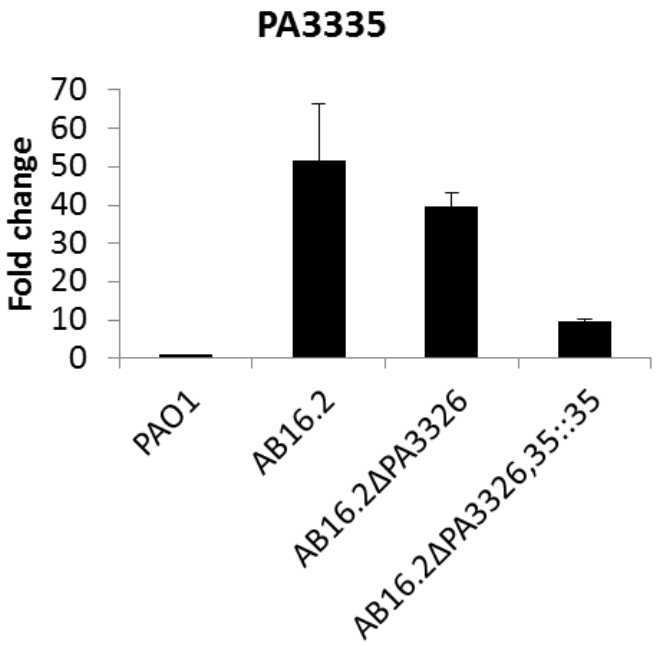

Figure 55: Gene expression of PA3335 in AB16.2ΔPA3326,35-complementated strain.

Data are expressed as a fold-change ratio to the value from reference strain PAO1.

Strains	MIC (µg ml^{-1})			
	GEN	CAZ	IMP	CST
PAO1	1	2	1	0.5
PAO1ΔPA3327	1	2	1	0.5
AB16.2	8	1	0.5	64
AB16.2ΔPA3327	8	1	0.5	64

Table 15: Contribution of the NRPS genetic cluster PA3327 in the susceptibility of *P. aeuginosa* to antibiotics.

GEN: gentamicin, CAZ: ceftazidime, IMP: imipenem, CST: colistin.

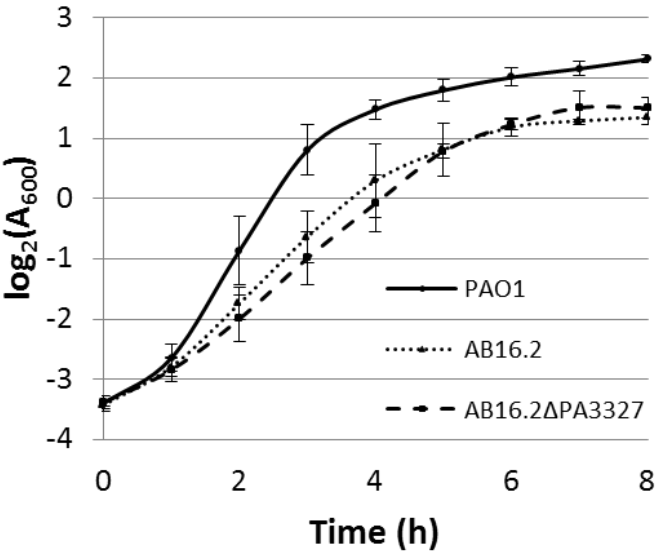

Figure 56: Growth curves of strains PAO1, AB16.2 and AB16.2ΔPA3327 cultivated in Mueller-Hinton broth at 37°C with shaking (250 rpm).

Azetidomonamide A and B contain an azetidine motif that was supposed to result from the incorporation by the NRPS PA3327 of L-azetidine 2-carboxylic acid (L-AZC) previously synthesized from the SAM-dependent enzyme PA3335. Thus, removal of a fragment of 270-bp in gene PA3335 was performed in the AB16.2ΔPA3326 mutant, which suppressed production of both compounds (Hong *et al*., 2019). This was verified by *trans*-complementation of mutant AB16.2ΔPA3326,35. Complementation of PA3335 carried by integrative plasmid mini-CTX::PA3335 was confirmed at a transcriptional level by RT-qPCR (9.6 ± 0.7 *versus* 1.0 ± 0.1 for reference strain PAO1) (Figure 55). Compared with mutant AB16.2ΔPA3326 (51.6 ± 14.9), this lower PA3335 expression could be due to a partial complementation, a hypothesis supported by the observation of lower production levels, found by LC-HRMS, of the two azetidomonamide compounds (Hong *et al*., 2019).

3.2.2. Nonribosomal peptides derived from the PA3327 biosynthesis cluster do not impact antibiotic resistance, plastic surface attachement or growth at low cell densities in AB16.2

NRPs are involved in various biological functions such as iron chelation, toxin and antibiotic production. In the AB16.2 mutant, NRPs synthesized by the PA3327 cluster are in part responsible for (i) a low growth rate at high cell densities, and (ii) reduced killing of *Galleria mellonella*, relative to strain PAO1 (Hong *et al*., 2019). However, they do not contribute to aminoglycoside and colistin cross-resistance in AB16.2, or the hypersusceptibility of this latter to β-lactams (as the inactivation of PA3327 gene in AB16.2 did not modify MICs of these antibiotics; Table 15). Furthermore, these NRPs do not impact the growth rate of AB16.2 at low cell densities (Figure 56). Finally, neither the constitutive activation (AB16.2) or disruption of this cluster (AB16.2ΔPA3327) modified the capacity of *P. aeruginosa* to attach to plastic surfaces when compared to PAO1 (Figure 57). The first stage of biofilm formation thus does not require the PA3327 locus at least for a *pmrB* mutant. However, we cannot rule out a role of this NRPS later on in biofilm formation or virulence factor production (e.g., pyocyanin, elastase, rhamnolipids) or motility (swarming, twitching).

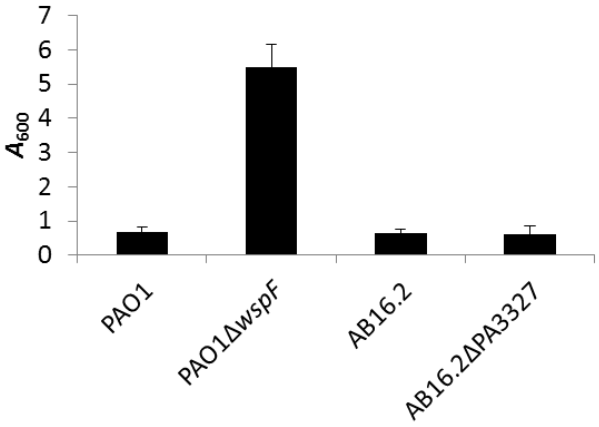

Figure 57: Characterization of the role of the NRPS genetic cluster PA3327 in the capacity of a *pmrB* mutant to adhere to a plastic surface.

PAO1Δ*wspF* strain was included as a positive control as *wspF* inactivation is known to induce a larger amount of biofilm biomass due to overproduction of Pel and Psl exopolysaccharides (Borlee *et al*., 2010).

Table 16: Effects of PmrAB substitutions on expression of gene PA3327 and two PmrAB regulated genes (PA4774 and *arnA*).

PAO1Δ*pmrAB* transformed with pME6012 derivates[a]	PmrA substitution	PmrB substitution	Transcript levels[b]		
			PA3327	PA4774	*arnA*
-	Δ	Δ	1.1 ± 0.8	1.1 ± 0.7	0.9 ± 0.1
pME6012	Δ	Δ	1.3 ± 0.2	1.0 ± 0.5	0.9 ± 0.1
pABWT	-	-	1.5 ± 0.5	1.5 ± 0.9	1.0 ± 0.0
pAB8.2	-	$V_{28}G$	**62** ± 8	**1,261** ± 188	**166** ± 30
pAB16.1	-	$F_{408}L$	**74** ± 38	**2,475** ± 859	**285** ± 95
pAB16.1.1	-	$F_{408}L$ (K_{428}-V_{431})[c]	2.1 ± 1.4	2.7 ± 2.3	1.1 ± 0.3
pAB16.1.2	-	$F_{408}L$ ΔNtG_{1175}	1.5 ± 0.6	4.7 ± 3.1	1.3 ± 0.1
pAB16.2	-	ΔL_{172}	**647** ± 19	**7,451** ± 1,826	**1159** ± 515
pAB3095	-	V_6A	1.9 ± 1.5	1.7 ± 1.0	1.0 ± 0.1
pAB3092	-	V_6A $L_{37}P$	**425** ± 313	**5,239** ± 448	**581** ± 32
pAB3091	$L_{12}I$	V_6A	**26.9** ± 16.2	**1,143** ± 181	**148** ± 43
pAB3890	-	$D_{45}E$	**19.8** ± 0.1	**1,825** ± 661	**207** ± 53
pAB2243	-	$Q_{105}P$	**899** ± 458	**5,276** ± 1,477	**672** ± 93
pAB3795	-	$G_{188}D$	**644** ± 74	**6,615** ± 3,738	**816** ± 459

[a] pME6012 plasmids carrying *pmrAB* alleles from strain PAO1 (WT), *in vitro* mutants (8.2, 16.1, 16.2), AB16.1 revertants (16.1.1, 16.1.2) and clinical strains (3095, 3092, 3091, 3890, 2243, 3795).
[b] data are expressed as a fold-change ratio to the value from reference strain PAO1.
[c] *pmrAB* allele contains a 12-bp insertion leading to a K_{428} to V_{431} insertion.
Δ: absence of protein.

3.2.3. *pmrAB* mutations identified from *in vitro* mutants and clinical strains activate the expression of PA3327 gene

A number of PmrAB sequence variants confer a cross-resistance to aminoglycosides and colistin when produced from plasmid pME6012 in mutant PAO1Δ*pmrAB*. In order to evaluate the capacity of additional mutations to activate the PA3327 biosynthesis cluster, we measured by RT-qPCR the transcripts levels of PA3327 in our *in vitro* collection of PAO1Δ*pmrAB*-complemented mutants (Table 16). These results showed that all studied PmrB ($V_{28}G$, $F_{408}L$, ΔL_{172}, $L_{37}P$, $D_{45}E$, $Q_{105}P$ and $G_{188}D$) and PmrA ($L_{12}I$) mutations activated expression of gene PA3327 as well as PmrAB-regulated genes PA4774 and *arnA*. Overall, this confirms that the PA3327 cluster is PmrAB-regulated.

4. Conclusion

This collaborative study revealed two rare azetidine-containing alkaloids produced by *P. aeruginosa*. Biosynthesis of the azetidine motif of azetidomonamide A and B is governed by the activity of a new SAM-dependent enzyme (PA3335). This enzyme produces azetidine 2-carboxylic acid which is subsequently integrated as an unusual building block by the NRPS PA3327. Inactivation of PA3327 gene in a *pmrB* mutant was beneficial for bacterial growth at high cell density and increased virulence in the infection model *G. mellonella*. Finally, we showed that the gene cluster PA3326-PA3335 is under the control of QS.

IV. Discussion and perspectives

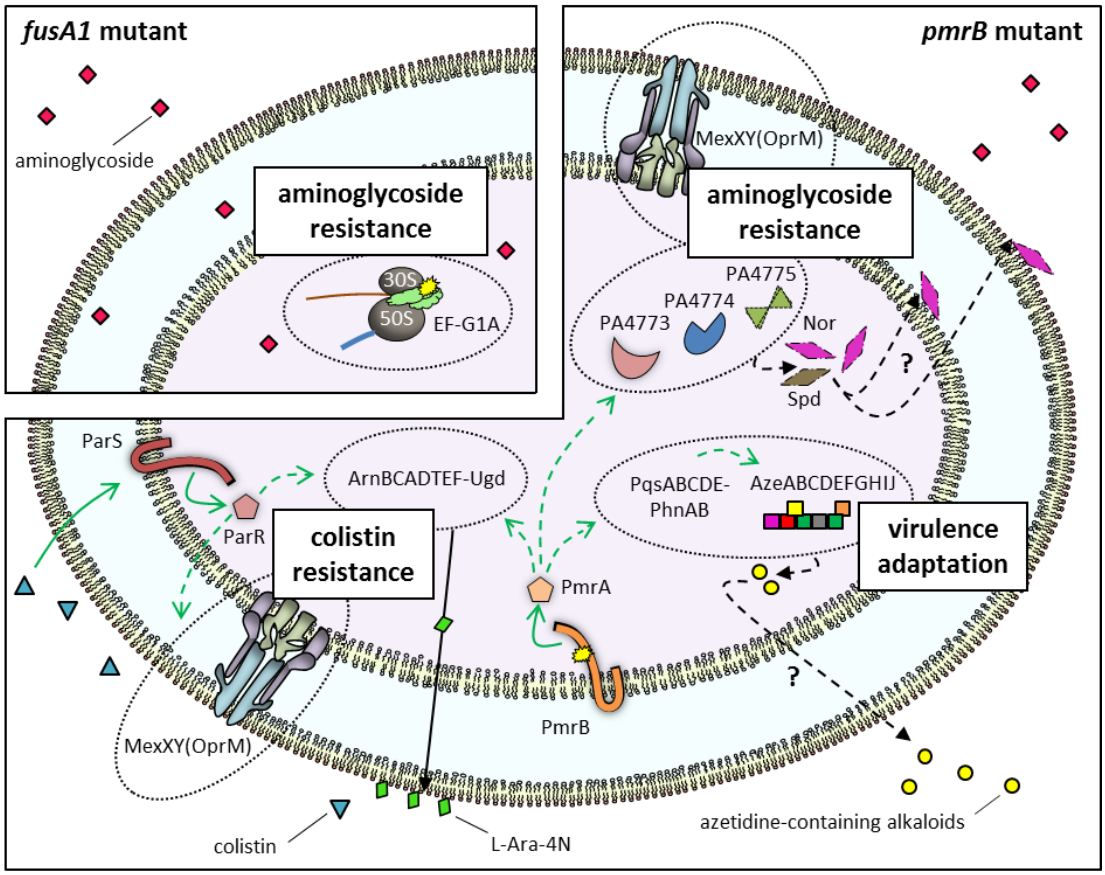

Figure 58: Schematic representation of *P. aeruginosa* adaptation mediated by mutations in genes *fusA1* and *pmrB*.

Nor: norspermidine, Spd: spermidine.

By many aspects, *P. aeruginosa* is as a paradigm to study adaptation, survival, and persistence of opportunistic pathogens (Moradali *et al*., 2017). This bacterium can cause severe infections in immunocompromised patients and has a major impact on morbidity and mortality in CF patients (McCarthy, 2015). Several complex mechanisms contribute to its capacity to colonize the human host, such as multiple metabolic pathways, production of a plethora of virulence factors, cell-to-cell communication by *quorum*-sensing, biofilm formation, and antibiotic resistance (Moradali *et al*., 2017). To survive and adapt to environmental changes and stress, this pathogen can sense external and internal signals through dozens of TCSs which when activated induce specific adaptive responses (Bhagirath *et al*., 2019).

The fact that *P. aeruginosa* is intrinsically resistant to a wide range of antibiotics results from mechanisms that have likely been acquired and selected all over the evolution, even though the primary function of these mechanisms may not have been to protect the bacterium from antimicrobials (as illustrated by the poly-specificity of bacterial efflux transporters). Thus, the many physiological processes that are coupled with extended regulatory networks account in part for the exceptional adaptation and survival of *P. aeruginosa* to bactericidal antibiotics such as aminoglycosides and colistin. In chronic infections, gain-/loss-of-function mutations and horizontal gene transfers to this pathogen may confer an increased resistance to antibiotics and consequently, lead to therapeutic failure (Moradali *et al*., 2017).

Characterization of the molecular mechanisms contributing to the tolerance or resistance to antibiotics should, in theory, facilitate the development of novel or next-generation molecules active against this species. From a fundamental research perspective, deciphering of the physiological processes responsible of the adaptation of *P. aeruginosa* to its environment is also noteworthy. In this context, we investigated two clinically-relevant types of *P. aeruginosa* mutants, namely *fusA1* (encoding EF-G1A) and *pmrB* (PmrB) (Figure 58).

Role of elongation factors EF-G1A and EF-G1B in adaptation of *P. aeruginosa* to antibiotics

Elongation factor G belongs to the GTPase superfamily and is the target of mechanistically-related antibiotics fusidic acid and argyrins (Jones *et al*., 2017). Fusidic acid inhibits protein synthesis by binding to EF-G during its interaction with the ribosome (Gao *et al*., 2009). The role of mutations in EF-G in acquired resistance to fusidic acid has been well established in several species such as *Thermus thermophilus* (Martemyanov *et al*., 2001), *Salmonella* Typhimurium (Johanson and Hughes, 1994) and *Staphylococcus aureus* (Chen *et al*., 2010). In *P. aeruginosa*, this antibiotic impacts the GTPase activity of EF-G1B but not that of EF-G1A (Palmer *et al*., 2013).

The natural cyclic peptides argyrins also target EF-G but bind to a protein domain distinct from that of fusidic acid (Nyfeler *et al*., 2012). Some amino acid substitutions in EF-G1A of *P. aeruginosa* are known to confer an increased resistance to these peptides (Bielecki *et al*., 2012; Nyfeler *et al*., 2012). Until now, resistance to argyrins has not been associated with alterations in EF-G1B, suggesting that this second elongation factor is not a target for these protein synthesis inhibitors (Jones *et al*., 2017).

Whole genome sequencing of *P. aeruginosa* CF isolates revealed that amino acid substitutions in EF-G1A and/or EF-G1B might help *P. aeruginosa* to resist aminoglycoside treatments (López-Causapé *et al*., 2017). In order to evaluate the relevance of amino acid variations in EF-G1A, we first compared the sequences of *fusA1* alleles from environmental strains to that of aminoglycoside-susceptible strains from PATRIC database (https://www.patricbrc.org/). It appeared that gene *fusA1* has a highly conserved sequence, which is consistent with the crucial ribosome recycling function of EF-G1A in the cell. Supporting this notion, we were unable to inactivate *fusA1* by gene replacement experiments. Moreover, we showed for the first time that, in strain PAO1, single amino acid substitutions in any domain of EF-G1A can confer a 2- to 16-fold increase in MICs of the four subclasses of aminoglycosides (streptomycin, apramycin, neomycin and tobramycin) (Bolard *et al*., 2018). Thus, we could confirm that if targeted by mutations, *fusA1* is a potential resistance mechanism to aminoglycosides in non-CF and CF isolates (Bolard *et al*., 2018). Of note, the characterized substitutions in EF-G1A did not impact the bacterial susceptibility to

other antibiotic families [β-lactams (ceftazidime, cefepime), carbapenems (imipenem), fluoroquinolones (ciprofloxacin)]. We also found that *fusA1* mutations have unequal effects on resitance depending upon the aminoglycoside molecules considered [e.g., substitution $R_{371}C$ increases MICs of 2-fold (streptomycin), 4-fold (apramycin, neomycin) and 8-fold (tobramycin)]. Levels of resistance also depend on the location and type of the amino acid substitution (e.g., MICs to amikacin from 4 to 32 µg ml^{-1}).

Altogether, our data suggest that certain EF-G1A substitutions could reduce the interaction of aminoglycosides with the elongation factor or allow the ribosome to adapt to the presence of aminoglycosides in the peptidyl center. EF-G1A is not a known target for aminoglycosides and we did not see a correlation between the level of aminoglycoside resistance and which domain of protein EF-G1A was mutated. However, substitution $T_{671}A$ can confer a cross-resistance to both aminoglycosides and argyrin B (Nyfeler *et al*., 2012). Thus, it is tempting to speculate that aminoglycosides directly interact with EF-G1A and that a part of their inhibitory activity on protein synthesis is dependent upon this binding. As the activation of *mexXY* operon resulting from deletion of repressor gene *mexZ* increases the MIC of aminoglycosides, mutations in EF-G1A act cooperatively to further augment these resistance levels in *in vitro*-selected mutants. We were unable to demonstrate the presence of *fusA1* mutations in a collection of non-CF *agrZ* and *agrW*-type clinical strains showing a relatively high resistance to aminoglycosides. The low prevalence of *fusA1* mutants in non-CF patients is likely due to the fitness cost associated with these mutations. While a deficient growth is detrimental to such mutants in acute infections, it can have a minor impact in chronic infections where a biofilm mode of life is frequent. The occurrence of *fusA1* mutants in various chronic infections (e.g., osteo-articular infections) remains to be established.

During this project, we did not evaluate the impact of *fusA2* mutations, as they might also confer aminoglycoside resistance as suggested by López-Causapé *et al*. (López-Causapé *et al*., 2017). If this is confirmed, it would provide a new insight into how *P. aeruginosa* adapt during infection. Indeed, if *fusA2* mutations increase aminoglycoside resistance but with a low impact on bacterial fitness, selection of *fusA2 versus fusA1* mutations might be more advantageous for *P. aeruginosa*. Sequence analysis of gene *fusA2* from clinical strains overexpressing operon *mexXY* might explain

the high resistance of some of them to aminoglycosides. From a clinical point of view, it would also be interesting to evaluate the aminoglycoside resistance levels exhibited by a strain harboring mutations in both genes, to see if the mechanisms are relevant.

From another point of view, it is conceivable that substitutions in EF-G1B might have no impact on the susceptibility to aminoglycosides. Indeed, as previously mentioned, the action of fusidic acid and argyrins on both EF-G (EF-G1A or EF-G1B) is unlikely because these factors achieve complementary but distinct functions. Palmer *et al*. suggested that despite both elongation factors exhibit GTPase activities in ribosome-dependent reactions, EF-G1A would play a role in ribosome recycling, while EF-G1B would be the sole translocase in the elongation phase of protein biosynthesis in *P. aeruginosa* (Palmer *et al*., 2013). However, the fact that gene *fusA2* could be inactivated by genetic manipulations (Jones *et al*., 2017), together with the observation that inactivating mutations may be present in clinical strains (Greipel *et al*., 2016; López-Causapé *et al*., 2017), also suggest that EF-G1A can compensate for EF-G1B deficiency. This assumption is supported by experiments showing that EF-G1A, though 75-fold less active than EF-G1B, was functional in a poly(U)-directed poly-phenylalanine translation system (Palmer *et al*., 2013). In the same study, EF-G1B failed to separate the ribosomal subunits in concert with RRF, which might explain why *fusA1* cannot be inactivated. Thus, only EF-G1A variations might impact the susceptibility to aminoglycosides and argyrins through its specific role during the recycling process.

The presence of two elongation factors in *P. aeruginosa* is not an exception in bacteria. An analysis of 191 bacterial genomes revealed that 24.6% harbored two genes encoding proteins of the EF-G subfamily (e.g., *T. thermophilus*, *Mycobacterium smegmatis*, *Vibrio cholerae* and *Borrelia burgdorferi*) (Margus *et al*., 2007). Moreover, 5.2% of the studied genomes possessed three copies of these genes (e.g., *Streptomyces avermitilis*, *V. parahaemolyticus*, *Treponema denticola*) (Margus *et al*., 2007). Usually, the EF-G proteins produced by a same organism differ extensively at the sequence level, with amino acid sequence identities ranging from 29% in *Mycobacterium smegmatis* to 56% in *Methylococcus capsulatus*. In contrast, EF-G1A and EF-G1B from *P. aeruginosa* are 84% identical (Palmer *et al*., 2013). This high sequence proximity could support common functions (Margus *et al*., 2011). Obviously, further studies are needed to better

understand the respective roles of these two elongation factors.

From an evolutionary perspective, it is commonly believed that several mechanisms generate new genes involved in adaptation and in lineage-specific phenotypes, such as duplication-divergence, deletion, lateral gene transfer, gene fusion/fission, and *de novo* origin (Andersson *et al*., 2015). Mechanisms of gene duplication and subsequent divergence are major contributors to the emergence of new genes (Andersson *et al*., 2015). The size of duplicated DNA can vary from very short regions (bp) to very large sequences, but duplication of regions of intermediate size (kb-Mb) is the most common. Subsequently to gene duplication, the frequency of an extra copy in the bacterial population can be reduced (due to fitness cost, instability, non-functionality) or maintained (sub-functionalization, neo-functionalization) depending notably on the resulting advantages or disadvantages provided for bacterial adaptation (Andersson *et al*., 2015). Nevertheless, duplication was shown to result more frequently from lateral gene transfers than from indigenous gene duplications, and was suggested to accelerate the evolutionary process of duplication by bringing foreign genes that have mainly weak or no function into the genome (Hooper and Berg, 2003). Treangen *et al*. suggested that gene transfers would permit the acquisition of new functions while duplication would lead to higher gene dosage (Treangen and Rocha, 2011).

The presence of the two elongation factors in *P. aeruginosa* would result from lateral gene transfers (Margus *et al*., 2011). This is consistent with the fact that genes *fusA1* and *fusA2* are located in two distinct regions of the genome, while new genes acquired through duplication/divergence mechanisms are typically arranged in tandem (Andersson *et al*., 2015).

Activation of the two-component system PmrAB protects *P. aeruginosa* from the bactericidal action of colistin and aminoglycosides by MexXY(OprM)-dependent mechanisms

In *P. aeruginosa*, resistance to colistin results from the activation of operon *arn*, and subsequent OM impermeability (Jeannot *et al*., 2017). Environmental changes such as a Mg^{2+}/Ca^{2+} depletion or the presence of cationic antimicrobial peptides (polymyxins, indolicidin) are sensed by several TCSs which, in turn, activate this operon (Jeannot *et al*., 2017). This is the case of TCS PmrAB, which responds to low Mg^{2+}, and to indolicidin and LL-37. Activating mutations in gene *pmrB* were identified in *in vitro*-selected mutants and in clinical strains. They enable the constitutive activation of PmrA regulon for adequate adaptation to these OM stressors. In this context, we selected *in vitro* colistin-resistant mutants with gain-of-function mutations in *pmrB*. First, we confirmed that the alterations identified in sensor PmrB ($V_{28}G$, ΔL_{172} and $F_{408}L$) were responsible for the higher resistance to colistin as a result of operon *arn* upregulation. Inactivation of this operon in mutant AB16.2 restored the wild-type susceptibility to colistin. Phenotypic analysis of these mutants suggested a role of the PmrB variants in protection against aminoglycosides (tobramycin, gentamicin and amikacin). For the first time, we confirmed by *cis*-complementation of mutant PAO1Δ*pmrAB* that mutations in *pmrB* can lead to cross-resistance to colistin and aminoglycosides. Moreover, analysis of a collection of colistin resistant clinical isolates revealed the presence of *pmrAB* mutations in eighteen of them. We found that some of these alterations represent a so far uncharacterized mechanism of resistance to aminoglycosides in hospital isolates. Cross-resistance in *pmrB* mutants is mediated by two mechanisms discussed below.

Resistance to aminoglycosides results from PmrAB-dependent activation of genes PA4773, PA4774 and PA4775. Bioinformatics analysis suggest that protein PA4773 is an SAM decarboxylase and that PA4774 is a spermidine synthase. For this reason, these enzymes were previously considered as SpeD (PA0654) and SpeE (PA1687) homologs, respectively (Johnson *et al*., 2012). This assumption was reinforced by experimental data showing that these proteins contribute to spermidine biosynthesis (Johnson *et al*., 2012). However, our findings suggest that the primary role of these enzymes might not be to synthetize spermidine but rather the shorter structural analog, norspermidine. Based on our results, we propose an updated model for the biosynthesis of spermidine

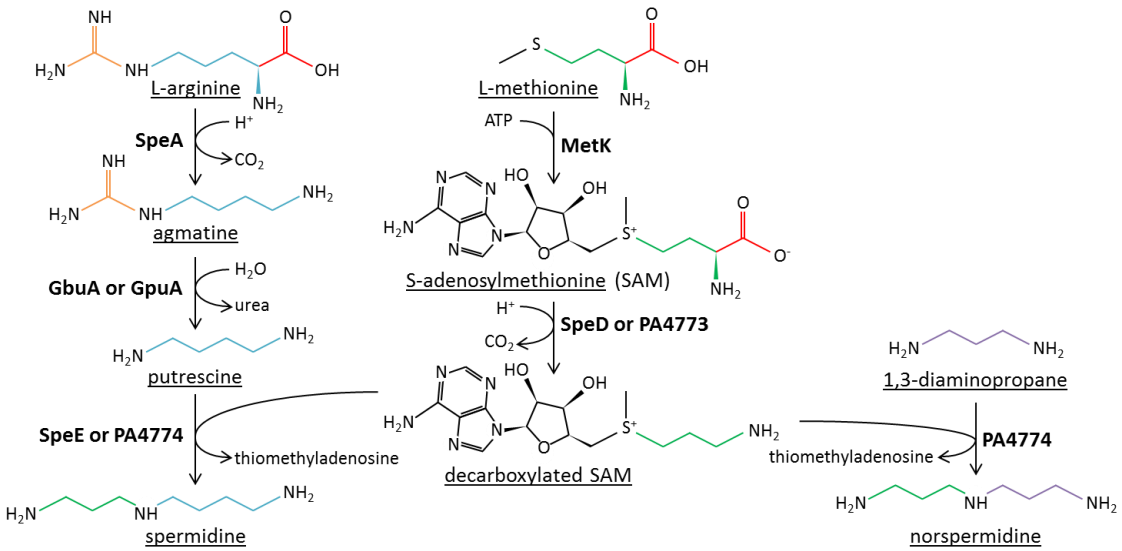

Figure 59: Proposed model for the synthesis of spermidine and norspermidine in *P. aeruginosa*.

and norspermidine in *P. aeruginosa* where (i) SAM would be decarboxylated by SpeD and PA4773, (ii) SpeE and PA4774 would convert putrescine into spermidine and (iii) PA4774 would synthesize norspermidine from 1,3-diaminopropane (Figure 59). In order to validate this model, we are planning to characterize the enzymatic activities of PA4773 and PA4774, and compare them with the ones of SpeD and SpeE. In this objective, the four enzymes will be produced, purified and their substrates specificities assessed. If this model is correct, proteins PA4773, PA4774 and PA4775 would be the main pathway for norspermidine biosynthesis in *P. aeruginosa*. In *Vibrio* species, norspermidine is synthetized through an L-aspartate β-semialdehyde-dependent pathway where a carboxynorspermidine dehydrogenase (CANSDH) catalyzes the formation of carboxynorspermidine from 1,3-diaminopropane and L-aspartate β-semialdehyde; a subsequent step involving a carboxynorspermidine decarboxylase (CANSDC), enables the production of norspermidine (Yamamoto *et al*., 1986).

Our model relies on the presence of 1,3-diaminopropane in the cytoplasm. Polyamines are either synthesized by the bacterial cells in the cytoplasm or imported from the external medium (Miller-Fleming *et al*., 2015). In some bacterial species, 1,3-diaminopropane is formed from L-aspartate β-semialdehyde by a two-step reaction that first implies an L-2,4-diaminobutyrate:2-ketoglutarate 4-aminotransferase (DABA AT), with production of the intermediate L-2,4-diaminobutyrate (DABA), and then, an L-2,4-diaminobutyrate decarboxylase (DABA DC) that converts DABA into 1,3-diaminopropane (Michael, 2016). These two enzymes, DABA AT and DABA DC, are present in *Vibrio cholerae*, *Acinetobacter baumanii* and *Klebsiella pneumoniae* but absent in *P. aeruginosa*, suggesting that this latter pathogen would need to import this diamine to produce norspermidine. So far, no uptake system for 1,3-diaminopropane has been characterized in bacteria. A plausible hypothesis would be that protein PA4775, which is predicted to contain a TM domain, transports 1,3-diaminopropane and might contribute to the uptake from the extracellular environment into the cytoplasm. As a first step in the characterization of this protein, we constructed a truncated PA4775 peptide lacking the predicted TM and tagged with a 6x-His, in the *E. coli* system (data not shown). Purification of the recombinant peptide will be optimized to subsequently generate specific antibodies. Western-blot analysis of subcellular fractions using these antibodies should allow us to conclude on whether

PA4775 is an IM or an OM protein. In any case, the fact that *P. aeruginosa* produces norspermidine in addition to spermidine is not an exception in the bacterial world, as other organisms such as *V. cholerae* can synthesize both (Lee *et al*., 2009a). The existence of a norspermidine biosynthesis pathway raises the question of physiological functions of the multiple polyamines elaborated by bacteria. Polyamines can modulate gene expression by binding to nucleic acids and proteins, they are important for cell growth, survival, stress response and proliferation (Gevrekci, 2017). Some organisms, particularly Gram-positive bacteria, do not synthesize polyamines but encode polyamine uptake transporters instead (Michael, 2016).

In *pmrB* mutants of *P. aeruginosa*, synthesis of norspermidine and/or spermidine contributes to aminoglycoside resistance by a mechanism that remain to be elucidated. It has been proposed that spermidine (synthesized by PA4773 and PA4774) is transported to the cell surface or possibly secreted before its binding to LPS molecules (Johnson *et al*., 2012). As a result, the electrostatic interaction of aminoglycosides with the OM would be reduced and their activity impaired (Johnson *et al*., 2012). This hypothesis is supported by the observation that the addition of exogenous spermidine (20 mM) decreases *P. aeruginosa* susceptibility to aminoglycosides (Kwon and Lu, 2006). Moreover, PA4774-dependent spermidine was isolated from the cell surface of *P. aeruginosa* under conditions that induce TCS PmrAB (0.02 mM Mg^{2+}) (Johnson *et al*., 2012). However, while the authors provided evidence of the integrity of IM by measuring the activity of the cytoplasmic protein XylE, they did not reported data on a possible leakage of the polyamines through the OM under those conditions (Johnson *et al*., 2012). In our hands, the extraction protocole proved to cause the leakage of periplasmic protein DsbA across the OM.

Thus, the subcellular localization of spermidine and norspermidine by this method should be considered with caution. Nevertheless, if these polyamines actually bind to LPS, the transport systems allowing the export of spermidine to the OM await to be identified (Johnson *et al*., 2012). Our observation that resistance to aminoglycosides in *pmrB* mutants is dependent upon efflux pump MexXY(OprM) could suggest that this pump is able to extrude norspermidine and/or spermidine outside the cell. However, preliminary data do not corroborate this hypothesis as (i) the supernatant from a *pmrB*-

mutant culture did not confer resistance to aminoglycosides as compared with the one from a wild-type strain (data not shown), (ii) mutant PAO1Δ*mexXY* exhibited the same susceptibility to spermidine and norspermidine as strain PAO1 (MICs = 2,048 µg ml^{-1}) and (iii) inactivation of operon *mexXY* in AB16.2 did not significantly impact the amounts of spermidine and norspermidine in cell surface extracts (data not shown), but in that particular case, OM permeabilization might lead to a misinterpretation of results. Overall, the MexXY(OprM)-dependent aminoglycoside resistance seen in *pmrB* mutants might only result from the well-characterized capacity of the pump to extrude aminoglycosides outside the bacterial cell. An attractive hypothesis is that the lower OM permeability to aminoglycosides caused by membrane bound polyamines potentiates the efflux of these antibiotics *via* MexXY(OprM).

Unexpectedly, MexXY(OprM) was found (in addition to its role in acquired resistance to aminoglycosides) to contribute to the acquired resistance of laboratory and clinical *pmrB* mutants to colistin. Previous characterization of the polymyxin B resistome failed to demonstrate a role of efflux in polymyxin resistance (Fernández *et al*., 2013). This is not surprising as the study was performed on wild-type strain PA14. Screening of transposon-insertion mutants constructed from a *pmrB* mutant, could allow the identification of additional cellular determinants involved in polymyxin resistance, including efflux systems other than MexAB-OprM, MexCD-OprJ and MexXY(OprM). Several questions remain to be addressed concerning the involvement of MexXY(OprM) in (i) bacterial protection against antimicrobial peptides such as indolicidin and LL-37, (ii) resistance development to polymyxins mediated by alteration of other TCS (e.g., PhoPQ and CprRS), and (iii) possible interplays with plasmidic resistance to colistin due to genes *mcr*, that encode phosphoethanolamine transferases mediating the addition of phosphoetanolamine to the lipid A. A first strain of *P. aeruginosa* harboring gene *mcr-5* has been reported recently (Snesrud *et al*., 2018).

Our findings corroborate the results of Gutu *et al*., showing that *arn*-mediated LPS modification by L-Ara-4N is required but not sufficient to provide high levels of resistance to polymyxins (Gutu *et al*., 2015). Indeed, some clinical strains lose their polymyxin resistance after drug-free passage despite preserved lipid A modification (Moskowitz *et al*., 2012). Pump MexXY(OprM) is not the first system identified as mediating high resistance to polymyxins. Inactivation of gene *cprA* in strain PAK was

shown to influence polymyxin resistance conferred by mutations activating TCSs PmrAB, PhoPQ and CprRS (Gutu *et al*., 2015). As for MexXY(OprM), protein CprA does not contribute to the canonical modification of lipid A by aminoarabinose, but would be implicated in other LPS modification(s) and in formation of OM vesicules (Gutu *et al*., 2015). Consequently, further investigations are needed to decipher the interplays between the three systems [(Arn, CprA and MexXY(OprM)] and to fully apprehend the adaptive responses of *P. aeruginosa* to polymyxins, cationic antimicrobial peptides and stress such as Mg^{2+} depletion. A first step in this direction was achieved in 2015 by Poole and collaborators who showed that the expression of *arn* operon was negatively impacted by *mexXY* overexpression in bacteria exposed to spectinomycin (Poole *et al*., 2015). The authors discussed about the possible existence of MexXY(OprM)-dependent mechanisms able to promote polymyxin hyper-susceptibility through distinct and so far unknown LPS modifications (Poole *et al*., 2015). This mechanism was shown to be *arn*- and PA4773-PA4774-independent, and likely CprA unrelated as the study was performed in PAO1 background where *cprA* is disrupted (Gutu *et al*., 2015).

Overall, our and other data reveal that *P. aeruginosa* can count on an impressive diversity of adaptive mechanisms mediated by TCS PmrAB to resist aminoglycosides and polymyxins, among which pump MexXY(OprM) is crucial.

Biosynthesis of azetidine-containing alkaloids through a nonribosomal peptide synthetase pathway impaired the capacity of *P. aeruginosa* to infect *Galleria mellonella* larvae

Adaptation of *P. aeruginosa* to its host does not exclusively rely on mechanisms conferring an increased resistance to antibiotics (Moradali *et al*., 2017). We showed that in *pmrB* mutants, *pqsA*-dependent activation of the NRPS genetic cluster *azeABCDEFGHIJ* impacts the capacity of this bacterium to grow at high cell densities and to infect *G. mellonella* larvae through the biosynthesis of novel azetidine-containing alkaloids (i.e., azetidomonamide A and B) (Hong *et al*., 2019). *G. mellonella* is now widely used as a surrogate for murine models in the study of microbial infections (Tsai *et al*., 2016). This invertebrate presents the advantage to survive at 37°C, which enables the study of temperature-dependent virulence factors (Pereira *et al*., 2018). However, the secreted-NRPs identified during the thesis should also be assessed in other infection models. Indeed, insects are devoid of adaptive immune response (Tsai *et al*., 2016), and an azetidomonamides-dependent advantage in infections of vertebrates cannot be excluded (i.e., mice).

In parallel, it would be interesting to determine whether these NRPs modify the expression of the *pqsABCDE-phnAB* locus. If they are responsible for a negative feedback, these molecules could inhibit production of PQS-dependent virulence factors (e.g., phenazine, pyocyanin, hydrogen cyanide, lectin) (Lee and Zhang, 2015). Further investigations would be useful to clarify the role(s) of these azetidomonamides in virulence of *P. aeruginosa* and determine their concentration in the sputa of CF patients during lung colonisation. The secretion and possibly uptake systems of these molecules remain to be characterized. Finally, as NRPs are known to exhibit multiple functions, determining of the properties of azetidomonamides can potentially lead to therapeutic applications.

In summary, this work on *fusA1* and *pmrB* mutants enlarged our knowledge on the highly adaptive, opportunistic pathogen, *P. aeruginosa*.

V. Materials and methods

1. Microbiology

1.1. Bacterial strains

The bacterial strains used in this project are reported in Tables 17, 18, 19, 20 and 21.

Table 17: Bacterial strains used to characterize the role of elongation factor EF-G1A in aminoglycoside resistance of *P. aeruginosa* clinical strains.

Strains	Relevant characteristics	Source or reference
Escherichia coli		
DH5α-T1^{R}	F^{-} Φ80*lac*ZΔM15 Δ(*lac*ZYA-*arg*F)U169 *rec*A1 *end*A1 *hsd*R17 (r_k^-, m_k^+) *pho*A *sup*E44 *thi*-1 *gyr*A96 *rel*A1 *ton*A	Invitrogen^{TM}
Pseudomonas aeruginosa		
Reference strain		
PAO1	Wild-type reference strain	(Stover *et al*., 2000)
Environmental strains		
591	Environmental strain serotype O:1	Juarez's PhD
142951	Environmental strain serotype O:10	Juarez's PhD
1053	Environmental strain serotype O:5	Juarez's PhD
2140	Environmental strain serotype O:3	Juarez's PhD
114793	Environmental strain serotype O:8	Juarez's PhD
1033	Environmental strain serotype O:12	Juarez's PhD
2531	Environmental strain serotype O:16	Juarez's PhD
986-36	Environmental strain serotype O:6	Juarez's PhD
201	Environmental strain serotype O:4, with Ala_{175}-to-Ser change in EF-G1A	Juarez's PhD
1281G	Environmental strain serotype O:13, with Ile_{186}-to-Val change in EF-G1A	Juarez's PhD
2112	Environmental strain serotype O:11	Juarez's PhD
1972G	Environmental strain serotype O:2	Juarez's PhD
2910	Environmental strain non-agglutinable	Juarez's PhD
2998x	Environmental strain poly-agglutinable	Juarez's PhD
Clinical strains with amino acid substitutions in EF-G1A		
5910	Clinical strain with Ala_{555}-to-Glu change in EF-G1A	(Bolard *et al*., 2018)
6233	Clinical strain with Thr_{671}-to-Ala change in EF-G1A	(Bolard *et al*., 2018)
6253	Clinical strain with Val_{93}-to-Ala and Ile_{186}-to-Val changes in EF-G1A	(Bolard *et al*., 2018)
Spontaneous aminoglycoside resistant mutants		
PAOR10	PAO1 spontaneous amikacin-resistant mutant with Arg_{680}-to-Cys change in EF-G1A	(Bolard *et al*., 2018)
PAOR13	PAO1 spontaneous amikacin-resistant mutant with Thr_{456}-to-Ala change in EF-G1A	(Bolard *et al*., 2018)
PAOR15	PAO1 spontaneous amikacin-resistant mutant with Arg_{371}-to-Cys change in EF-G1A	(Bolard *et al*., 2018)
***In vitro* mutants**		
PAO1 derivatives		
ABR10	PAO1 with allele *fusA1* from PAOR10	(Bolard *et al*., 2018)
ABR13	PAO1 with allele *fusA1* from PAOR13	(Bolard *et al*., 2018)
ABR15	PAO1 with allele *fusA1* from PAOR15	(Bolard *et al*., 2018)
ABR5910	PAO1 with allele *fusA1* from 5910	(Bolard *et al*., 2018)
ABR6233	PAO1 with allele *fusA1* from 6233	(Bolard *et al*., 2018)

ABR6253	PAO1 with allele *fusA1* from 6253	(Bolard *et al*., 2018)
ABR_mutL40Q	PAO1 with allele $fusA1_{T119A}$	(Bolard *et al*., 2018)
ABR_mutG118S	PAO1 with allele $fusA1_{G352A}$	(Bolard *et al*., 2018)
ABR_mutN592I	PAO1 with allele $fusA1_{A1775T}$	(Bolard *et al*., 2018)
PAO1Δ*mexXY*	PAO1 with in-frame deletion of 4,185-bp in operon *mexXY*	(Guénard *et al*., 2014)
PAO1Δ*mexZ*	PAO1 with in-frame deletion of 627-bp in gene *mexZ*	(Muller *et al*., 2011)
PAOR13 derivatives		
PAOR13Δ*mexXY*	PAOR13 with in-frame deletion of 4,185-bp in operon *mexXY*	(Bolard *et al*., 2018)
PAOR13Δ*mexZ*	PAOR13 with in-frame deletion of 627-bp in gene *mexZ*	(Bolard *et al*., 2018)
PAOR15 derivatives		
PAOR15Δ*mexXY*	PAOR15 with in-frame deletion of 4,185-bp in operon *mexXY*	(Bolard *et al*., 2018)
PAOR15Δ*mexZ*	PAOR15 with in-frame deletion of 627-bp in gene *mexZ*	(Bolard *et al*., 2018)

Table 18: Bacterial strains used to characterize the role of PmrB protein in cross-resistance to aminoglycosides and colistin.

Strains	Relevant characteristics	Source or reference
Escherichia coli		
BL21 Star™ (DE3)	F^- *ompT hsdS*$_B$ (r_B^-, m_B^-) *gal dcm rne131* (DE3)	Invitrogen™
Pseudomonas aeruginosa		
Reference strain		
PAO1	Wild-type reference strain	(Stover *et al*., 2000)
Clinical strains with amino acid substitutions in PmrAB		
3095	Clinical strain with Val_6-to-Ala change in PmrB	This study
3094	Clinical strain with Val_6-to-Ala change in PmrB	This study
3093	Clinical strain with Val_6-to-Ala and Leu_{37}-to-Pro changes in PmrB	This study
3092	Clinical strain with Val_6-to-Ala and Leu_{37}-to-Pro changes in PmrB	This study
3091	Clinical strain with Leu_{12}-to-Ile change in PmrA, Val_6-to-Ala change in PmrB	This study
3090	Clinical strain with Leu_{12}-to-Ile change in PmrA, Val_6-to-Ala change in PmrB	This study
3089	Clinical strain with Leu_{12}-to-Ile change in PmrA, Val_6-to-Ala change in PmrB	This study
2243	Clinical strain with Gln_{105}-to-Pro change in PmrB	This study
3795	Clinical strain with Gly_{188}-to-Asp change in PmrB	This study
3890	Clinical strain with Asp_{45}-to-Glu change in PmrB	This study
Spontaneous colistin resistant mutants		
AB8.2	PAO1 spontaneous colistin-resistant mutant with Val_{28}-to-Gly change in PmrB	This study
AB16.1	PAO1 spontaneous colistin-resistant mutant with Phe_{408}-to-Leu change in PmrB	This study
AB16.2	PAO1 spontaneous colistin-resistant mutant with ΔLeu_{172} in PmrB	(Hong *et al*., 2019)
***In vitro* mutants**		
PAO1 derivatives		
PAO1Δ*oprM*	PAO1 with in-frame deletion of 1,408-bp in gene *oprM*	(Guénard *et al*., 2014)
PAO1ΔPA0547	PAO1 with in-frame deletion of 951-bp in gene PA0547	This study
PAO1Δ*mexXY*	PAO1 with in-frame deletion of 4,185-bp in operon *mexXY*	(Guénard *et al*., 2014)
PAO1Δ*mexZ*	PAO1 with in-frame deletion of 627-bp in gene *mexZ*	(Muller *et al*., 2011)
PAO1Δ*pslB*	PAO1 with in-frame deletion of 1,434-bp in gene *pslB*	This study

PAO1Δ*pelB*	PAO1 with in-frame deletion of 3,488-bp in gene *pelB*	This study
PAO1Δ*arn*	PAO1 with in-frame deletion of 8,755-bp in operon *arn*	Noguès' PhD
PAO1ΔPA4133	PAO1 with in-frame deletion of 1,113-bp in gene PA4133	This study
PAO1Δ*cdrB*	PAO1 with in-frame deletion of 1,599-bp in gene *cdrB*	This study
PAO1Δ*cdrA*	PAO1 with in-frame deletion of 6,264-bp in gene *cdrA*	This study
PAO1ΔPA4773	PAO1 with in-frame deletion of 465-bp in gene PA4773	This study
PAO1ΔPA4774	PAO1 with in-frame deletion of 921-bp in gene PA4774	This study
PAO1ΔPA4775	PAO1 with in-frame deletion of 714-bp in gene PA4775	This study
PAO1Δ*pmrA*	PAO1 with in-frame deletion of 642-bp in gene *pmrA*	This study
PAO1Δ*pmrB*	PAO1 with in-frame deletion of 915-bp in gene *pmrB*	This study
PAO1Δ*pmrAB*	PAO1 with in-frame deletion of 1,941-bp in operon *pmrAB*	(Muller *et al*., 2011)
PAO1Δ*pmrAB*Δ*amgRS*	PAO1Δ*pmrAB* with in-frame deletion of 1,687-bp in operon *amgRS*	This study
PAO1ΔPA4781	PAO1 with in-frame deletion of 963-bp in gene PA4781	This study
PAO1ΔPA4782	PAO1 with in-frame deletion of 78-bp in gene PA4782	This study
PAO1Δ*amgRS*	PAO1 with in-frame deletion of 1,687-bp in operon *amgRS*	This study
PAO1Δ*armZ*	PAO1 with in-frame deletion of 961-bp in gene *armZ*	(Muller *et al*., 2011)
AB16.2 derivatives		
AB16.2Δ*oprM*	AB16.2 with in-frame deletion of 1,408-bp in gene *oprM*	This study
AB16.2ΔPA0547	AB16.2 with in-frame deletion of 951-bp in gene PA0547	This study
AB16.2Δ*pqsA*	AB16.2 with in-frame deletion of 1,463-bp in gene *pqsA*	This study
AB16.2Δ*mexXY*	AB16.2 with in-frame deletion of 4,185-bp in operon *mexXY*	This study
AB16.2Δ*mexZ*	AB16.2 with in-frame deletion of 627-bp in gene *mexZ*	This study
AB16.2Δ*hcnB*	AB16.2 with in-frame deletion of 1,062-bp in gene *hcnB*	This study
AB16.2Δ*pslB*	AB16.2 with in-frame deletion of 1,434-bp in gene *pslB*	This study
AB16.2Δ*rmf*	AB16.2 with in-frame deletion of 183-bp in gene *rmf*	This study
AB16.2Δ*pelB*	AB16.2 with in-frame deletion of 3,488-bp in gene *pelB*	This study
AB16.2Δ*arn*	AB16.2 with in-frame deletion of 8,755-bp in operon *arn*	This study
AB16.2Δ*oprC*	AB16.2 with in-frame deletion of 2,025-bp in gene *oprC*	This study
AB16.2ΔPA4133	AB16.2 with in-frame deletion of 1,113-bp in gene PA4133	This study
AB16.2Δ*cdrB*	AB16.2 with in-frame deletion of 1,599-bp in gene *cdrB*	This study
AB16.2Δ*cdrA*	AB16.2 with in-frame deletion of 6,264-bp in gene *cdrA*	This study
AB16.2ΔPA4773	AB16.2 with in-frame deletion of 465-bp in gene PA4773	This study
AB16.2ΔPA4773::73-75	AB16.2Δ*PA4773* complemented with PA4773-75	This study
AB16.2ΔPA4774	AB16.2 with in-frame deletion of 921-bp in gene PA4774	This study
AB16.2ΔPA4774::73-75	AB16.2ΔPA4774 complemented with PA4773-75	This study
AB16.2ΔPA4775	AB16.2 with in-frame deletion of 714-bp in gene PA4775	This study
AB16.2ΔPA4775::73-75	AB16.2Δ*PA4775* complemented with PA4773-75	This study
AB16.2Δ*pmrA*	AB16.2 with in-frame deletion of 642-bp in gene *pmrA*	This study
AB16.2Δ*pmrB*	AB16.2 with in-frame deletion of 915-bp in gene *pmrB*	This study
AB16.2Δ*pmrAB*	AB16.2 with in-frame deletion of 1,941-bp in operon *pmrAB*	This study
AB16.2Δ*cueR*	AB16.2 with in-frame deletion of 306-bp in gene *cueR*	This study
AB16.2ΔPA4781	AB16.2 with in-frame deletion of 963-bp in gene PA4781	This study
AB16.2ΔPA4782	AB16.2 with in-frame deletion of 78-bp in gene PA4782	This study
AB16.2Δ*armZ*	AB16.2 with in-frame deletion of 961-bp in gene *armZ*	This study

Table 19: Bacterial strains used to characterize novel genetic determinants involved in the protection of *P. aeruginosa* from colistin.

Strains	Relevant characteristics	Source or reference
Pseudomonas aeruginosa		
Reference strain		
PAO1	Wild-type reference strain	(Stover *et al*., 2000)
Clinical strains		
2243	Clinical strain with Gln_{105}-to-Pro change in PmrB	This study
3795	Clinical strain with Gly_{188}-to-Asp change in PmrB	This study
5345	CF clinical isolate	This study
5769	CF clinical isolate	This study
6029	Non-CF clinical isolate	This study
6181	Non-CF clinical isolate	This study
Spontaneous colistin resistant mutants		
AB8.2	PAO1 spontaneous colistin-resistant mutant with Val_{28}-to-Gly change in PmrB	This study
AB16.2	PAO1 spontaneous colistin-resistant mutant with ΔLeu_{172} change in PmrB	(Hong *et al*., 2019)
***In vitro* mutants**		
PAO1 derivatives		
PAO1Δ*mexAB*	PAO1 with in-frame deletion in operon *mexAB*	Smaltis
PAO1Δ*oprM*	PAO1 with in-frame deletion of 1,408-bp in gene *oprM*	(Guénard *et al*., 2014)
PAO1ΔPA0929-30	PAO1 with in-frame deletion of 1,775-bp in operon PA0929-30	This study
PAO1Δ*pqsA*	PAO1 with in-frame deletion of 1,463-bp in gene *pqsA*	Smaltis
PAO1Δ*phoPQ*	PAO1 with in-frame deletion of 1,984-bp in operon *phoPQ*	Noguès' PhD
PAO1Δ*parRS*	PAO1 with in-frame deletion of 1,815-bp in operon *parRS*	(Muller *et al*., 2011)
PAO1Δ*mexXY*	PAO1 with in-frame deletion of 4,185-bp in operon *mexXY*	(Guénard *et al*., 2014)
PAO1Δ*mexZ*	PAO1 with in-frame deletion of 627-bp in gene *mexZ*	(Muller *et al*., 2011)
PAO1Δ*pslB*	PAO1 with in-frame deletion of 1,434-bp in gene *pslB*	This study
PAO1Δ*pslB*Δ*pelB*	PAO1Δ*pslB* with in-frame deletion of 3,488-bp in gene *pelB*	This study
PAO1Δ*pelB*	PAO1 with in-frame deletion of 3,488-bp in gene *pelB*	This study
PAO1Δ*cprRS*	PAO1 with in-frame deletion of 1,497-bp in operon *cprRS*	Puja's PhD
PAO1Δ*arn*	PAO1 with in-frame deletion of 8,755-bp in operon *arn*	Noguès' PhD
PAO1Δ*wspF*	PAO1 with in-frame deletion of 780-bp in gene *wspF*	This study
PAO1Δ*mexCD-oprJ*	PAO1 with in-frame deletion of 5,706-bp in locus *mexCD-oprJ*	This study
PAO1Δ*cdrB*	PAO1 with in-frame deletion of 1,599-bp in gene *cdrB*	This study
PAO1Δ*cdrA*	PAO1 with in-frame deletion of 6,264-bp in gene *cdrA*	This study
PAO1ΔPA4773	PAO1 with in-frame deletion of 465-bp in gene PA4773	This study
PAO1ΔPA4774	PAO1 with in-frame deletion of 921-bp in gene PA4774	This study
PAO1ΔPA4775	PAO1 with in-frame deletion of 714-bp in gene PA4775	This study
PAO1Δ*pmrA*	PAO1 with in-frame deletion of 642-bp in gene *pmrA*	This study
PAO1Δ*pmrB*	PAO1 with in-frame deletion of 915-bp in gene *pmrB*	This study
PAO1Δ*pmrAB*	PAO1 with in-frame deletion of 1,941-bp in operon *pmrAB*	(Muller *et al*., 2011)
PAO1Δ*armZ*	PAO1 with in-frame deletion of 961-bp in gene *armZ*	(Muller *et al*., 2011)
AB16.2 derivatives		
AB16.2Δ*mexAB*	AB16.2 with in-frame deletion of in operon *mexAB*	This study
AB16.2Δ*oprM*	AB16.2 with in-frame deletion of 1,408-bp in gene *oprM*	This study
AB16.2Δ*phoPQ*	AB16.2 with in-frame deletion of 1,984-bp in operon *phoPQ*	This study
AB16.2Δ*parRS*	AB16.2 with in-frame deletion of 1,815-bp in operon *parRS*	This study
AB16.2Δ*mexXY*	AB16.2 with in-frame deletion of 4,185-bp in operon *mexXY*	This study
AB16.2Δ*mexZ*	AB16.2 with in-frame deletion of 627-bp in gene *mexZ*	This study
AB16.2Δ*cprRS*	AB16.2 with in-frame deletion of 1,497-bp in operon *cprRS*	This study
AB16.2Δ*arn*	AB16.2 with in-frame deletion of 8,755-bp in operon *arn*	This study
AB16.2Δ*mexCD-oprJ*	AB16.2 with in-frame deletion of 5,706-bp in locus *mexCD-oprJ*	This study

AB16.2Δ*pmrAB*	AB16.2 with in-frame deletion of 1,941-bp in operon *pmrAB*	This study
AB16.2Δ*armZ*	AB16.2 with in-frame deletion of 961-bp in gene *armZ*	This study
AB8.2 derivatives		
AB8.2Δ*mexXY*	AB8.2 with in-frame deletion of 4,185-bp in operon *mexXY*	This study
Clinical strain derivatives		
2243Δ*mexXY*	2243 with in-frame deletion of 4,185-bp in operon *mexXY*	This study
3795Δ*mexXY*	3795 with in-frame deletion of 4,185-bp in operon *mexXY*	This study
5345*lux*	Bioluminescent clinical strain 5345	This study
5769*lux*	Bioluminescent clinical strain 5769	This study
6029*lux*	Bioluminescent clinical strain 6029	This study
6181*lux*	Bioluminescent clinical strain 6181	This study
5345*lux*Δ*mexXY*	5345*lux* with in-frame deletion of 4,185-bp in operon *mexXY*	This study
5769*lux*Δ*mexXY*	5769*lux* with in-frame deletion of 4,185-bp in operon *mexXY*	This study
6029*lux*Δ*mexXY*	6029*lux* with in-frame deletion of 4,185-bp in operon *mexXY*	This study

Table 20: Bacterial strains used to characterize a novel NRPS genetic cluster present in *P. aeruginosa*.

Strains	Relevant characteristics	Source or reference
Pseudomonas aeruginosa		
Reference strain		
PAO1	Wild-type reference strain	(Stover *et al*., 2000)
Spontaneous colistin resistant mutant		
AB16.2	PAO1 spontaneous colistin-resistant mutant with ΔLeu_{172} in PmrB	(Hong *et al*., 2019)
***In vitro* mutants**		
PAO1 derivatives		
PAO1Δ*pqsA*	PAO1 with in-frame deletion of 1,463-bp in gene *pqsA*	Smaltis
PAO1ΔPA3327	PAO1 with in-frame deletion of 6,525-bp in gene PA3327	(Hong *et al*., 2019)
AB16.2 derivatives		
AB16.2Δ*pqsA*	AB16.2 with in-frame deletion of 1,463-bp in gene *pqsA*	(Hong *et al*., 2019)
AB16.2ΔPA3326	AB16.2 with in-frame deletion of 189-bp in gene PA3326	This study
AB16.2ΔPA3327	AB16.2 with in-frame deletion of 6,525-bp in gene PA3327	(Hong *et al*., 2019)
AB16.2ΔPA3326,28	AB16.2ΔPA3326 with in-frame deletion of 276-bp in gene PA3328	This study
AB16.2ΔPA3326,29	AB16.2ΔPA3326 with in-frame deletion of 621-bp in gene PA3329	This study
AB16.2ΔPA3326,30	AB16.2ΔPA3326 with in-frame deletion of 366-bp in gene PA3330	This study
AB16.2ΔPA3326,31	AB16.2ΔPA3326 with in-frame deletion of 444-bp in gene PA3331	This study
AB16.2ΔPA3326,32	AB16.2ΔPA3326 with in-frame deletion of 225-bp in gene PA3332	This study
AB16.2ΔPA3326,35	AB16.2ΔPA3326 with in-frame deletion of 270-bp in gene PA3335	(Hong *et al*., 2019)
AB16.2ΔPA3326,35::35	AB16.2ΔPA3326,35 complemented with PA3335	(Hong *et al*., 2019)

Table 21: List of bacterial strains used in all projects.

Strains	Relevant characteristics	Source or reference
Escherichia coli		
DH5α	F^- Φ80*lac*ZΔM15 Δ(*lac*ZYA-*arg*F) U169 *rec*A1 *end*A1 *hsd*R17(r_k^-, m_k^+) *pho*A *sup*E44 *thi*-1 *gyr*A96 *rel*A1 λ^-	Invitrogen™
CC118	Δ(*ara*-*leu*) *ara*D Δ*lac*X74 *gal*E *gal*K *pho*A20 *thi*-1 *rps*E *rpo*B *arg*E(Am) *rec*Al	(Manoil and Beckwith, 1985)
CC118 λ*pir*	CC118 lysogenized with λ*pir* phage	(Herrero *et al*., 1990)
HB101	*sup*E44 *hsd*S20(r_B^-, m_B^-) *rec*A13 *ara*-14 *pro*A2 *lac*Y1 *gal*K2 *rps*L20 *xyl*-5 *mtl*-1 *leu*B6 *thi*-1	(Lacks and Greenberg, 1977)

1.2. Plasmids

The plasmids used in these studies are listed in Tables 22, 23, 24, 25 and 26.

Table 22: Plasmids used in all projects.

Plasmids	Relevant characteristics	Source or reference
pCR-Blunt	Blunt-end cloning vector; *ccd*B *lac*Zα Zeo^r Kan^r	Life technologies
pME6012	Broad-host-range expression plasmid; Tet^r	(Heeb *et al*., 2000)
pKNG101	Marker exchange suicide vector in *P. aeruginosa*; *sacB mob*RK2 *ori*R6K Str^r	(Kaniga *et al*., 1991)
pRK2013	Helper plasmid for mobilization of non-self-transmissible plasmids; ColE1 Tra$^+$ Mob$^+$ Kan^r	(Ditta *et al*., 1980)
pAK1900	Broad-host-range expression plasmid; Amp^r	(Poole *et al*., 1993)
mini-CTX1	Self-proficient integration vector ; Ω-*FRT-attP*-MCS *ori int oriT* Tet^r	(Hoang *et al*., 2000)
pFLP2	Source of FLP recombinase; Amp^r	(Hoang *et al*., 1998)
pTNS3	*tnsABCD* genes for mini-Tn7 transposition; Amp^r	(Choi *et al*., 2008)
pUC18-mini-Tn7T-Gm^R-P$_{lac}$-*lux*	Mobilizable mini-Tn7 overexpressing *luxCDABE* from promoter P$_{lac}$; Gm^r	Noguès' PhD
pET-28a	Expression plasmid; Kan^r	Novagen

Zeo^r: zeocin resistance, Kan^r: kanamycin resistance, Tet^r: tetracycline resistance, Str^r: streptomycin resistance, Amp^r: ampicillin resistance, Gm^r: gentamicin resistance.

Table 23: Plasmids used to study the impact of EF-G1A amino acid substitutions *in vitro*.

Plasmids	Relevant characteristics	Source or reference
<u>pCR-Blunt-derivatives</u>		
pCR-Blunt::*fusA1*	Template plasmid for site-directed mutagenesis of *fusA1* from PAO1	(Bolard *et al*., 2018)
<u>pKNG101-derivatives</u>		
pKNG::*fusA1*$_{C2038T}$	Mutator plasmid for substitution Arg$_{680}$-to-Cys in EF-G1A	(Bolard *et al*., 2018)
pKNG::*fusA1*$_{A1366G}$	Mutator plasmid for substitution Thr$_{456}$-to-Ala in EF-G1A	(Bolard *et al*., 2018)
pKNG::*fusA1*$_{C1111T}$	Mutator plasmid for substitution Arg$_{371}$-to-Cys in EF-G1A	(Bolard *et al*., 2018)
pKNG::*fusA1*$_{C1664A}$	Mutator plasmid for substitution Ala$_{555}$-to-Glu in EF-G1A	(Bolard *et al*., 2018)
pKNG::*fusA1*$_{A2011G}$	Mutator plasmid for substitution Thr$_{671}$-to-Ala in EF-G1A	(Bolard *et al*., 2018)
pKNG::*fusA1*$_{T278C,A556G}$	Mutator plasmid for substitutions Val$_{93}$-to-Ala and Ile$_{186}$-to-Val in EF-G1A	(Bolard *et al*., 2018)
pKNG::*fusA1*$_{T119A}$	Mutator plasmid for substitution Leu$_{40}$-to-Gln in EF-G1A	(Bolard *et al*., 2018)
pKNG::*fusA1*$_{G352A}$	Mutator plasmid for substitution Gly$_{118}$-to-Ser in EF-G1A	(Bolard *et al*., 2018)
pKNG::*fusA1*$_{A1775T}$	Mutator plasmid for substitution Asn$_{592}$-to-Ile in EF-G1A	(Bolard *et al*., 2018)
pKNGΔ*mexXY*	BamHI/ApaI 1.756-kb fragment composed of sequences flanking 5' and 3' ends of *mexXY*, cloned into pKNG101	(Guénard *et al*., 2014)
pKNGΔ*mexZ*	BamHI/ApaI 1.111-kb fragment composed of sequences flanking 5' and 3' ends of *mexZ*, cloned into pKNG101	(Muller *et al*., 2011)
pKNGΔ*fusA1*	BamHI/ApaI 1.033-kb fragment composed of sequences flanking 5' and 3' ends of *fusA1*, cloned into pKNG101	This study

Table 24: Plasmids used to study the impact of PmrAB amino acid substitutions.

Plasmids	Relevant characteristics	Source or reference
pME6012-derivatives		
pABWT	pME6012::*pmrAB*	This study
pAB8.2	pME6012::$pmrAB_{Val28\text{-}to\text{-}Gly}$	This study
pAB16.1	pME6012::$pmrAB_{Phe408\text{-}to\text{-}Leu}$	This study
pAB16.1.1	pME6012::$pmrAB_{Phe408\text{-}to\text{-}Leu + Lys428\text{-}to\text{-}Val431 duplication}$	This study
pAB16.1.2	pME6012::$pmrAB_{Phe408\text{-}to\text{-}Leu + \Delta G1178}$	This study
pAB16.2	pME6012::$pmrAB_{\Delta Leu172}$	This study
pAB3095	pME6012::$pmrAB_{Val6\text{-}to\text{-}Ala}$	This study
pAB3092	pME6012::$pmrAB_{Val6\text{-}to\text{-}Ala + Leu37\text{-}to\text{-}Pro}$	This study
pAB3091	pME6012::$pmrA_{Leu12\text{-}to\text{-}Ile}B_{Val6\text{-}to\text{-}Ala}$	This study
pAB3890	pME6012::$pmrAB_{Asp45\text{-}to\text{-}Glu}$	This study
pAB2243	pME6012::$pmrAB_{Gln105\text{-}to\text{-}Pro}$	This study
pAB3795	pME6012::$pmrAB_{Gly188\text{-}to\text{-}Asp}$	This study
pKNG101-derivatives		
pKNGΔ*metK*	BamHI/ApaI 1.092-kb fragment composed of sequences flanking 5' and 3' ends of *metK*, cloned into pKNG101	This study
pKNGΔPA0547	BamHI/ApaI 1.073-kb fragment composed of sequences flanking 5' and 3' ends of PA0547, cloned into pKNG101	This study
pKNGΔ*ccoN2*	BamHI/ApaI 1.049-kb fragment composed of sequences flanking 5' and 3' ends of *ccoN2*, cloned into pKNG101	This study
pKNGΔ*mexXY*	BamHI/ApaI 1.756-kb fragment composed of sequences flanking 5' and 3' ends of *mexXY*, cloned into pKNG101	(Guénard *et al*., 2014)
pKNGΔ*mexZ*	BamHI/ApaI 1.111-kb fragment composed of sequences flanking 5' and 3' ends of *mexZ*, cloned into pKNG101	(Muller *et al*., 2011)
pKNGΔ*hcnB*	BamHI/ApaI 1.069-kb fragment composed of sequences flanking 5' and 3' ends of *hcnB*, cloned into pKNG101	This study
pKNGΔ*pslB*	BamHI/ApaI 1.029-kb fragment composed of sequences flanking 5' and 3' ends of *pslB*, cloned into pKNG101	This study
pKNGΔ*rmf*	BamHI/ApaI 1.057-kb fragment composed of sequences flanking 5' and 3' ends of *rmf*, cloned into pKNG101	This study
pKNGΔ*pelB*	BamHI/ApaI 1.061-kb fragment composed of sequences flanking 5' and 3' ends of *pelB*, cloned into pKNG101	This study
pKNGΔ*arn*	BamHI/ApaI 1.135-kb fragment composed of sequences flanking 5' and 3' ends of *arn*, cloned into pKNG101	Noguès' PhD
pKNGΔ*oprC*	BamHI/XbaI 1.077-kb fragment composed of sequences flanking 5' and 3' ends of *oprC*, cloned into pKNG101	This study
pKNGΔ*cioA*	BamHI/XbaI 1.081-kb fragment composed of sequences flanking 5' and 3' ends of *cioA* cloned into pKNG101	This study
pKNGΔPA4133	BamHI/ApaI 1.055-kb fragment composed of sequences flanking 5' and 3' ends of PA4133, cloned into pKNG101	This study
pKNGΔ*cdrB*	BamHI/ApaI 1.086-kb fragment composed of sequences flanking 5' and 3' ends of *cdrB* cloned into pKNG101	This study
pKNGΔ*cdrA*	BamHI/ApaI 1.099-kb fragment composed of sequences flanking 5' and 3' ends of *cdrA* cloned into pKNG101	This study
pKNGΔPA4773	BamHI/ApaI 1.045-kb fragment composed of sequences flanking 5' and 3' ends of PA4773, cloned into pKNG101	This study
pKNGΔPA4774	BamHI/ApaI 1.070-kb fragment composed of sequences flanking 5' and 3' ends of PA4774, cloned into pKNG101	This study
pKNGΔPA4775	BamHI/ApaI 1.027-kb fragment composed of sequences flanking 5' and 3' ends of PA4775, cloned into pKNG101	This study
pKNGΔ*pmrA*	ApaI 851-bp fragment composed of sequences flanking 5' and 3' ends of *pmrA*, cloned into pKNG101	This study
pKNGΔ*pmrB*	BamHI/XbaI 1.074-kb fragment composed of sequences flanking 5' and 3' ends of *pmrB*, cloned into pKNG101	This study

pKNGΔ*pmrAB*	BamHI/ApaI 1.028-kb fragment composed of sequences flanking 5' and 3' ends of *pmrAB*, cloned into pKNG101	(Muller *et al*., 2011)
pKNGΔ*cueR*	BamHI/XbaI 1.038-kb fragment composed of sequences flanking 5' and 3' ends of *cueR*, cloned into pKNG101	This study
pKNGΔPA4781	BamHI/ApaI 1.121-kb fragment composed of sequences flanking 5' and 3' ends of PA4781, cloned into pKNG101	This study
pKNGΔPA4782	BamHI/ApaI 1.119-kb fragment composed of sequences flanking 5' and 3' ends of PA4782, cloned into pKNG101	This study
pKNGΔ*amgRS*	BamHI/ApaI 1.113-kb fragment composed of sequences flanking 5' and 3' ends of *amgRS*, cloned into pKNG101	This study
pKNGΔ*armZ*	BamHI/ApaI 1.241-kb fragment composed of sequences flanking 5' and 3' ends of *armZ*, cloned into pKNG101	(Muller *et al*., 2011)
mini-CTX1-derivatives		
mini-CTX::PA4773-75	PA4773 to PA4775 cloned into mini-CTX1 at sites BamHI/NotI	This study
pET-28a-derivatives		
pET-28a_PA4775	NcoI/NotI 0.757-kb fragment composed of PA4775 gene sequence cloned in frame with N-ter His_6-tag encoding sequence in pET-28a	This study

Table 25: Plasmids used to characterize the colistin resistome in *P. aeruginosa*.

Plasmids	Relevant characteristics	Source or reference
pKNG101-derivatives		
pKNGΔ*mexAB*	Fragment composed of sequences flanking 5' and 3' ends of *mexAB*, cloned into pKNG101	Smaltis
pKNGΔ*oprM*	SpeI/ApaI 1.162-kb fragment composed of sequences flanking 5' and 3' ends of *oprM*, cloned into pKNG101	(Guénard *et al*., 2014)
pKNGΔ*metK*	BamHI/ApaI 1.092-kb fragment composed of sequences flanking 5' and 3' ends of *metK*, cloned into pKNG101	This study
pKNGΔPA0547	BamHI/ApaI 1.073-kb fragment composed of sequences flanking 5' and 3' ends of PA0547, cloned into pKNG101	This study
pKNGΔPA0929-30	BamHI/ApaI 1.074-kb fragment composed of sequences flanking 5' and 3' ends of PA0929-30, cloned into pKNG101	This study
pKNGΔ*phoPQ*	BamHI/ApaI 1.551-kb fragment composed of sequences flanking 5' and 3' ends of *phoPQ*, cloned into pKNG101	Noguès' PhD
pKNGΔ*ccoN2*	BamHI/ApaI 1.049-kb fragment composed of sequences flanking 5' and 3' ends of *ccoN2*, cloned into pKNG101	This study
pKNGΔ*parRS*	ApaI 1.045-kb fragment composed of sequences flanking 5' and 3' ends of *parRS*, cloned into pKNG101	(Muller *et al*., 2011)
pKNGΔ*mexXY*	BamHI/ApaI 1.756-kb fragment composed of sequences flanking 5' and 3' ends of *mexXY*, cloned into pKNG101	(Guénard *et al*., 2014)
pKNGΔ*mexZ*	BamHI/ApaI 1.111-kb fragment composed of sequences flanking 5' and 3' ends of *mexZ*, cloned into pKNG101	(Muller *et al*., 2011)
pKNGΔ*hcnB*	BamHI/ApaI 1.069-kb fragment composed of sequences flanking 5' and 3' ends of *hcnB*, cloned into pKNG101	This study
pKNGΔ*pslB*	BamHI/ApaI 1.029-kb fragment composed of sequences flanking 5' and 3' ends of *pslB*, cloned into pKNG101	This study
pKNGΔ*pelB*	BamHI/ApaI 1.061-kb fragment composed of sequences flanking 5' and 3' ends of *pelB*, cloned into pKNG101	This study
pKNGΔ*cprRS*	BamHI/ApaI 0.959-kb fragment composed of sequences flanking 5' and 3' ends of *cprRS*, cloned into pKNG101	Noguès' PhD
pKNGΔ*arn*	BamHI/ApaI 1.135-kb fragment composed of sequences flanking 5' and 3' ends of *arn*, cloned into pKNG101	Noguès' PhD
pKNGΔ*wspF*	BamHI/XbaI 1.103-kb fragment composed of sequences flanking 5' and 3' ends of *wspF*, cloned into pKNG101	This study

pKNGΔ*mexCD-oprJ*	BamHI/ApaI 1.121-kb fragment composed of sequences flanking 5' and 3' ends of *mexCD-oprJ*, cloned into pKNG101	Noguès' PhD
pKNGΔ*cdrB*	BamHI/ApaI 1.086-kb fragment composed of sequences flanking 5' and 3' ends of *cdrB* cloned into pKNG101	This study
pKNGΔ*cdrA*	BamHI/ApaI 1.099-kb fragment composed of sequences flanking 5' and 3' ends of *cdrA* cloned into pKNG101	This study
pKNGΔPA4773	BamHI/ApaI 1.045-kb fragment composed of sequences flanking 5' and 3' ends of PA4773, cloned into pKNG101	This study
pKNGΔPA4774	BamHI/ApaI 1.070-kb fragment composed of sequences flanking 5' and 3' ends of PA4774, cloned into pKNG101	This study
pKNGΔPA4775	BamHI/ApaI 1.027-kb fragment composed of sequences flanking 5' and 3' ends of PA4775, cloned into pKNG101	This study
pKNGΔ*pmrAB*	BamHI/ApaI 1.028-kb fragment composed of sequences flanking 5' and 3' ends of *pmrAB*, cloned into pKNG101	(Muller *et al*., 2011)
pKNGΔ*armZ*	BamHI/ApaI 1.241-kb fragment composed of sequences flanking 5' and 3' ends of *armZ*, cloned into pKNG101	(Muller *et al*., 2011)
pAK1900-derivatives		
pAGH97	pAK1900-derived *mexXY* expression vector	(Aires *et al*., 1999)
pAK1900::*arn*	pAK1900-derived *arn* expression vector	This study

Table 26: Plasmids used to characterize the biosynthesis of new azetidine-containing alkaloids.

Plasmids	Relevant characteristics	Source or reference
pKNG101-derivatives		
pKNGΔ*pqsA*	XbaI/SpeI fragment composed of sequences flanking 5' and 3' ends of *pqsA*, cloned into pKNG101	Smaltis
pKNGΔPA3326	BamHI/ApaI 1.134-kb fragment composed of sequences flanking 5' and 3' ends of PA3326, cloned into pKNG101	This study
pKNGΔPA3327	BamHI/XbaI 1.092-kb fragment composed of sequences flanking 5' and 3' ends of PA3327, cloned into pKNG101	(Hong *et al*., 2019)
pKNGΔPA3328	BamHI/ApaI 1.063-kb fragment composed of sequences flanking 5' and 3' ends of PA3328, cloned into pKNG101	This study
pKNGΔPA3329	BamHI/ApaI 1.063-kb fragment composed of sequences flanking 5' and 3' ends of PA3329, cloned into pKNG101	This study
pKNGΔPA3330	BamHI/ApaI 1.072-kb fragment composed of sequences flanking 5' and 3' ends of PA3330, cloned into pKNG101	This study
pKNGΔPA3331	BamHI/ApaI 1.006-kb fragment composed of sequences flanking 5' and 3' ends of PA3331, cloned into pKNG101	This study
pKNGΔPA3332	BamHI/ApaI 1.067-kb fragment composed of sequences flanking 5' and 3' ends of PA3332, cloned into pKNG101	This study
pKNGΔPA3335	BamHI/ApaI 1.065-kb fragment composed of sequences flanking 5' and 3' ends of PA3335, cloned into pKNG101	(Hong *et al*., 2019)
mini-CTX1-derivatives		
mini-CTX::PA3335	PA3335 cloned into mini-CTX1 at sites BamHI/NotI	(Hong *et al*., 2019)

1.3. Culture media

The culture media, indicated in Table 27, were supplemented with antibiotics as required (Table 28).

Table 27: Composition of culture media.

Media abbreviation	Media	Composition	Source or reference
MHBc	Mueller-Hinton Broth (cation-adjusted)	0.3% beef extract, 1.75% acid hydrolysate of casein, 0.15% starch with adjusted concentrations of the divalent cations Ca^{2+} (from 20 to 25 µg ml^{-1}) and Mg^{2+} (from 10 to 12.5 µg ml^{-1})	Becton, Dickinson and Company, Sparks, MD
MHA	Mueller-Hinton Agar	0.2% beef extract, 1.75% acid hydrolysate of casein, 0.15% starch, 1.7% agar	Becton, Dickinson and Company
LB	LB broth, Miller	1% tryptone, 0.5% yeast extract, 1% NaCl	Becton, Dickinson and Company
M9-sucrose	M9 minimal broth medium with sucrose	8.54 mM NaCl, 25.18 mM NaH_2PO_4, 18.68 mM NH_4Cl, 22 mM KH_2PO_4, 2 mM $MgSO_4$, 5% sucrose, 0.8% agar	(Kaniga *et al.*, 1991)
PIA	*Pseudomonas* isolation agar	2% bacto peptone, 14.70 mM $MgCl_2$, 57.39 mM K_2SO_4, 25 µg ml^{-1} Irgasan®, 1.36% agar, 2% glycerol	Becton, Dickinson and Company

Table 28: Antibiotic concentrations used to maintain plasmids in cultures of *E. coli* and *P. aeruginosa* strains.

Antibiotics	Plasmids	Concentration in bacterial hosts (µg ml^{-1})	
		E. coli	***P. aeruginosa***
Kanamycin	pCR-Blunt pRK2013 pET-28a	50	NA
Tetracycline	pME6012 mini-CTX1	5	200
Ampicillin	pAK1900 pFLP2	100	NA
Ticarcillin	pAK1900 pFLP2	NA	150
Streptomycin	pKNG101	50	2,000

NA: non applicable.

1.4. Selection of antibiotic-resistant mutants

In vitro selection of spontaneous mutants resistant to aminoglycosides was obtained by plating an overnight culture of reference strain PAO1 (about 10^8 CFU) on MHA plates supplemented with 6 µg ml^{-1} of amikacin. Colistin-resistant mutants were selected by plating 100 µl of an overnight culture of strain PAO1 on MHA plates supplemented with colistin (8 or 16 µg ml^{-1}). In both cases, colonies were grown at 37°C for 18-24 h.

1.5. Drug susceptibility testing

1.5.1. Antibiograms

Bacterial susceptibility to antibiotics was assessed by the disk diffusion method (antibiograms). Briefly, a bacterial suspension adjusted to 0.2 McF opacity was diluted 1,000-fold into 10 ml of MHBc, spread onto MHA plate and removed. Disks of antibiotics (Bio-Rad, Marnes-la-Coquette, France) were placed on the dried seeded-plate and bacteria were grown at 35°C ± 2°C for 18 h. The diameter of inhibition zones was measured to evaluate drug susceptibility.

1.5.2. Minimum Inhibitory Concentration (MIC)

The Minimum Inhibitory Concentration (MIC) of antibiotics was determined by the standard 2-fold serial microdilution method in 200 µl MHBc, according to the Clinical and Laboratory Standards Institute (CLSI, 2014) recommendations. Briefly, a microplate with 2-fold serial dilutions of antibiotic MHBc (100 µl per well) was prepared. A bacterial suspension adjusted to 0.5 McF opacity (1 to 2 x 10^8 CFU ml^{-1}) was diluted into 10 ml of MHBc. One hundred microliter volumes of this dilution were then distributed in the wells in order to obtain a final concentration around 5 x 10^5 CFU ml^{-1}. After 18 h at 35°C ± 2°C, MIC values were visually determined as the lowest concentrations of antibiotic that inhibit bacterial growth.

1.6. Growth curves

Thirty milliliters of prewarmed MHBc were inoculated with exponentially growing bacteria to obtain an absorbance A_{600} equal to 0.1, and then incubated for 8 h at 37°C with shaking (250 rpm). The A_{600} of bacterial cultures was recorded every hour. For

each strain, triplicates were performed.

1.7. Cytochrome *c* binding assay

Horse heart cytochrome *c* (Sigma-Aldrich), a highly cationic protein exhibiting a specific absorbance, and that is able to bind to anionic surfaces in a charge-dependent manner was used to assess the net charge of the bacterial surface. The protocol applied was the one described by Peschel *et al*. (Peschel *et al*., 1999) and modified as follows. Thirteen milliliters of MHBc were inoculated with a single colony of *P. aeruginosa* and incubated overnight at 37°C, with shaking at 250 rpm. Bacteria were centrifuged at 4,000 rpm for 25 min at 20°C. Pelleted cells were washed twice by resuspension in 20 mM 3-(N-morpholino)propanesulfonic acid (MOPS) buffer, pH = 7.0 and finally resuspended in the same buffer at an A_{600} equal to 6. Nine hundred microliters of this concentrate were mixed with 100 µl of a MOPS-cytochrome *c* solution (5 mg ml^{-1}) and left at room temperature for 15 min in the dark. The sample was centrifuged (8,000 rpm, 20 min, 20°C) and the absorbance at 530 nm (A_{530}) of supernatant was measured in a microplate by using a *Synergy™ H1 Hybrid Multi-Mode Reader* (BioTek™ Instruments, Inc., Winooski, VT, USA). As blank controls, the A_{530} of MOPS buffer and MOPS-cytochrome *c* solution (cyt c) were measured. The percentage of cytochrome *c* bound to the cells was calculated as follows: % of bound cytochrome *c* = 100 - ($A_{530sample}$ - $A_{530MOPS}$) / $A_{530cyt\ c}$ x 100. The results presented are mean values of three experiments.

2. Molecular biology

2.1. Primers

A list of the primers used in the study is presented in Tables 29, 30, 31, 32 and 33.

Table 29: Primers used in the study of elongation factor EF-G1A.

Name	Sequence (5'→3')	Reference
Gene sequencing		
fusA1		
PCR_screen_fusA1_AB1	TGCCAAGACGTCGTGTAGC	(Bolard *et al*., 2018)
PCR_screen_fusA1_AB2	GCGAACTTCCATCTCGACCA	(Bolard *et al*., 2018)
Seq_fusA1_AB1	AGGAAGGCCTGCGTCTG	(Bolard *et al*., 2018)
Seq_fusA1_AB2	GGTCGGTAGCGATCTTGAAC	(Bolard *et al*., 2018)

Gene inactivation		
fusA1		
PCRi fusA1 A1	GCTGATCCGAAATACGGAAG	This study
PCRi fusA1 A2	TGAATCAATTACGGTAGCGGTTGATGG	This study
PCRi fusA1 A3	CCGTAATTGATTCAGCCCTTTAAGTAA	This study
PCRi fusA1 A4	AGGAACACGACGATGTAGGG	This study
Gene complementation		
fusA1		
PCR fusA1 AB1	TCAAGAAGCGTGAAGACGTG	(Bolard *et al*., 2018)
PCR fusA1 AB2	GTTGACGTGCGGTTTGTTAC	(Bolard *et al*., 2018)
Site-directed mutagenesis		
$fusA1_{L40Q}$		
Mut_L40Q_AB1	GCGTCAACCACAAGC**A**GGGCGAAGTGCATGA	(Bolard *et al*., 2018)
Mut_L40Q_AB2	TCATGCACTTCGCCC**T**GCTTGTGGTTGACGC	(Bolard *et al*., 2018)
$fusA1_{G118S}$		
Mut_G118S_AB1	TTCTGTGGCACCTCC**A**GCGTAGAGCCGCAGT	(Bolard *et al*., 2018)
Mut_G118S_AB2	ACTGCGGCTCTACGC**T**GGAGGTGCCACAGAA	(Bolard *et al*., 2018)
$fusA1_{N592I}$		
Mut_N592I_AB1	ATGACGTCGACTCCA**T**CGAGATGGCGTTCAA	(Bolard *et al*., 2018)
Mut_N592I_AB2	TTGAACGCCATCTCG**A**TGGAGTCGACGTCAT	(Bolard *et al*., 2018)
qPCR		
mexY		
mexY1A	TTACCTCCTCCAGCGGC	(Jeannot *et al*., 2005)
mexY1B	GTGAGGCGGGCGTTGTG	(Jeannot *et al*., 2005)
fusA2		
RT fusA2 AB1	GCCAACAAGTACCATGTGCC	This study
RT fusA2 AB2	GAAGTTTTCCTCCGAGCCGA	This study
fusA1		
RT fusA1 AB1	GGCCACGTAGACTTCACCAT	This study
RT fusA1 AB2	GTATGACCCAGGCGCTTCTT	This study
armZ		
PA5471A	AGCTACAGCAGGTCGAGACG	(El'Garch *et al*., 2007)
PA5471B	TTGATGTCGAGCAGTTCCAG	(El'Garch *et al*., 2007)

Table 30: Primers used in the project related to PmrAB substitutions and increased resistance to aminoglycosides.

Name	Sequence (5'→3')	Reference
Gene sequencing		
phoPQ		
PCR-phoP1	AGCTCGCAATTCTACCTGGG	This study
PhoQ1	GCTGGTCGAGGAGCAACC	(Sautrey *et al*., 2014)
PhoQ2	CTGGCGCGACAGGTAGAT	(Sautrey *et al*., 2014)
SeqPhoQ1	GTAGAGCTGCTCGCGGAAC	(Sautrey *et al*., 2014)
SeqPhoQ2	AACTACACGCCGCGCTAC	(Sautrey *et al*., 2014)
parRS		
CloparRSC1	CTTCCGGCTCCCAGAATC	This study
CloparRSC2	CGAGGTGTCCCATGCTAGG	(Guénard *et al*., 2014)
Seq-parRC2	GGTCGACCACGAAGATCG	(Guénard *et al*., 2014)
Seq-parSC1	GCCAGGCAGGGGAAATACT	(Guénard *et al*., 2014)
Seq-parSC4	ATGCGGATCTGTTCGACCT	(Guénard *et al*., 2014)
Seq-parSC5	CGAACTGGAGGAAATGGTCT	(Guénard *et al*., 2014)

cprRS		
CprRS1	CACCTGGAAGCTGTTCGATG	(Sautrey *et al*., 2014)
iPCR4-cprRS	TTCATGCTGCTCTGGAACAT	Noguès' thesis
SeqCprS1	CGACGATGAACCAGACCAG	(Sautrey *et al*., 2014)
SeqCprS2	CTGTCCGACGCCATCATC	(Sautrey *et al*., 2014)
SeqCprS3	GGAAAGCAACACCCTCAACG	(Sautrey *et al*., 2014)
SeqCprS4	GCATGAACCTGGAGTTGCTC	This study
SeqCprS5	GCCGACCTCGATGTGTCC	This study
PA4773 to PA4775		
Seqi PA4773-75 AB1	AACTGAACGCTCACTCCCTG	This study
Seqi PA4773-75 AB2	CTCGCCGTGCACCAGTTG	This study
pmrAB		
PCR-pmrAB1	GATCGTCGCCATCCTCCTG	This study
PCR-pmrAB4	TTCACCGATGTTCATCCGGG	This study
PmrB1	GCAACCAACTGGAGCAGAG	(Sautrey *et al*., 2014)
SeqpmrB1	GAAGTGCAGGCCGAGGTC	(Sautrey *et al*., 2014)
SeqpmrB2	TCCAGCAGGAGGTTGAGTTC	(Sautrey *et al*., 2014)
amgS		
Seq_amgS_AB1	GTTCCCGCAAAGCTTCTTCG	This study
Gene inactivation		
metK		
PCRi PA0546 A1	GCAAGGAAGAAGGATTGGGC	This study
PCRi PA0546 A2	GGTGAACATCTGGTCCGCGATCTTGTC	This study
PCRi PA0546 A3	ACCAGATGTTCACCTGGGAGAAGACCG	This study
PCRi PA0546 A4	ATACGGCTGCTTCGACTTCC	This study
PA0547		
PCRi PA0547 A1	GGTGCAGCAGGGAGTAGATC	This study
PCRi PA0547 A2	CGGTGGGCGTAGTCGTCTGGTCGTATCG	This study
PCRi PA0547 A3	GACTACGCCCACCGGTAATGTAGGAACC	This study
PCRi PA0547 A4	CGGTGGGAGAAACAGATCGG	This study
ccoN2		
PCRi PA1557 A1	TGTAGGGAAACTCGAAGCGC	This study
PCRi PA1557 A2	TCCTCAGGGCAAGCCGAAGTTCAGGTC	This study
PCRi PA1557 A3	GCTTGCCCTGAGGAGCCGAGCATGAAA	This study
PCRi PA1557 A4	GTCGAGCTTGTTCTCCACCA	This study
hcnB		
PCRi PA2194 A1	CATGACCATCCACCTCAATG	This study
PCRi PA2194 A2	GCACATCCGCAGTTTTTCCAGCATCC	This study
PCRi PA2194 A3	AACTGCGGATGTGCATCGGCTACTGC	This study
PCRi PA2194 A4	CTCGAACTTGAAGTCCATCC	This study
pslB		
PCRi pslB A1	TGGGTCTTCAAGTTCCGCTC	This study
PCRi pslB A2	TCGTCGCCGACGGCGTTCATCAGTAGA	This study
PCRi pslB A3	GCCGTCGGCGACGAGAAGAAAGCCTGA	This study
PCRi pslB A4	GGTCTTGATCCCCAGTTCCG	This study
rmf		
PCRi PA3049 A1	ACATCAGCCATATCGCCTTC	This study
PCRi PA3049 A2	TGAGACGCATAGGGTGTTGCCCTCACT	This study
PCRi PA3049 A3	CCCTATGCGTCTCAATCAACTCCAGCA	This study
PCRi PA3049 A4	ACATGACCGACGAAGAGACC	This study
pelB		
PCRi pelB A1	GATTACATCCCGCGCCTGG	This study
PCRi pelB A2	GGTGAACGCCTGGGGATGCTTGTCAG	This study
PCRi pelB A3	CCCAGGCGTTCACCTTCGGCTACCAGT	This study
PCRi pelB A4	TTGTACTGCCACTCCTCGAC	This study

wspF		
PCRi wspF A1	GCTGATCCTGGACGTCGAG	This study
PCRi wspF A2	AATAATTCAACCCTGTGCTTCTCCGAT	This study
PCRi wspF A3	AGGGTTGAATTATTGGCGTGGCGATGC	This study
PCRi wspF A4	ATCACCGTCGGCTTGATCTG	This study
oprC		
PCRi PA3790 A1	ATGTCCCACGAGAACATGG	This study
PCRi PA3790 A2	GGTGTAAGCCGCTCGTTGTTGAGTAG	This study
PCRi PA3790 A3	GAGCGGCTTACACCGAGCACCTGAACA	This study
PCRi PA3790 A4	TGTAGGGATCGACGAAGAGG	This study
cioA		
PCRi PA3930 A1	GCTTGAAGGGGAGAGTAGCG	This study
PCRi PA3930 A2	ACCACCACGTTCGTTTTCAGCCAGAGG	This study
PCRi PA3930 A3	ACGAACGTGGTGGTGTACTTCTCGCTG	This study
PCRi PA3930 A4	GCATGAAGATCAACGGCAGG	This study
PA4133		
PCRi PA4133 A1	CAGGAGAAGGCGATGGAGAC	This study
PCRi PA4133 A2	GAAGGAGCAGGGCAGGTCGAAGTTCAT	This study
PCRi PA4133 A3	TGCCCTGCTCCTTCGTCGAGTCGCTG	This study
PCRi PA4133 A4	CATGCCGGCCAATTCTTGTC	This study
cdrB		
PCRi cdrB A1	CGGCAACTACCAGCTCAACT	This study
PCRi cdrB A2	TGAACGACATCATTCACCTCGGGCAGA	This study
PCRi cdrB A3	AATGATGTCGTTCAACCCGGAGATTGC	This study
PCRi cdrB A4	GCGATCAGTTGTTGGGCAC	This study
cdrA		
PCRi cdrA A1	GGAGGCATGGTCGAGGAAAA	This study
PCRi cdrA A2	TAGTCGGTCTCGTTGGGGTTGAACTGG	This study
PCRi cdrA A3	AACGAGACCGACTACTGGAGCTGCTTC	This study
PCRi cdrA A4	GGGTCAACAGGAAGCCGTC	This study
PA4773		
PCRi PA4773 A1	GTATCCACCAGCCGTACCTG	This study
PCRi PA4773 A2	ATCCATCACGGTTGAATTGCCATGAAG	This study
PCRi PA4773 A3	CAACCGTGATGGATACGCCGATCGAA	This study
PCRi PA4773 A4	GTCGAGATCGACCATCACC	This study
PA4774		
PCRi PA4774 A1	CAGTGGATCGAGGAAAGCAT	This study
PCRi PA4774 A2	ATCCGGCTCCGGCGGATAGAAATAGAA	This study
PCRi PA4774 A3	CGCCGGAGCCGGATATCGAGGAGATCG	This study
PCRi PA4774 A4	GGGTTGCCGATGACCAG	This study
PA4775		
PCRi PA4775 A1	GGCTCTCTATACCCGCCAGT	This study
PCRi PA4775 A2	TCCTGCACGGACATCTTCAGGTCCTC	This study
PCRi PA4775 A3	ATGTCCGTGCAGGACCTCTACGAACTG	This study
PCRi PA4775 A4	GGCTTGGTCAGGTAGTCGTC	This study
pmrA		
PCRi pmrA A1	GTCGAACTGACCCAGCTACC	This study
PCRi pmrA A2	GTTTTCACTCGGCCAGCAGTATTCTCA	This study
PCRi pmrA A3	GGCCGAGTGAAAACTGCCTACCGGAGT	This study
PCRi pmrA A4	ATCAGGTTTTCGCTGATCCA	This study
pmrB		
PCRi pmrB A1	GCGCCCTGAAAACTGCCTA	This study
PCRi pmrB A2	CCGCCCGAGCGAGTAGAACAGCAGCAG	This study
PCRi pmrB A3	ACTCGCTCGGGCGGTCACATATCTGAT	This study
PCRi pmrB A4	CTTGAGGATCGGGCAGTCG	This study

cueR		
PCRi cueR A1	CATCGACCTGTGGCTGAAG	This study
PCRi cueR A2	GGTCCTGGATGTTCATCCGGGTCTCC	This study
PCRi cueR A3	GAACATCCAGGACCTGGTCGAGCACT	This study
PCRi cueR A4	GACCATCTGCATGGCTACG	This study
PA4781		
PCRi PA4781 A1	ACGAAGATGAAAGCGCTGGT	This study
PCRi PA4781 A2	TGCTTTCCACATCGAGCAGGATCAGGT	This study
PCRi PA4781 A3	CGATGTGGAAAGCATCGAACTCACCGC	This study
PCRi PA4781 A4	CCAGTTCCATCAGCAACACG	This study
PA4782		
PCRi PA4782 A1	CCGGCCTGATCCTGTTCG	This study
PCRi PA4782 A2	CTCCTTGACCAGCGCTTTCATCTTCGT	This study
PCRi PA4782 A3	CGCTGGTCAAGGAGTATTTCGGCCAGGA	This study
PCRi PA4782 A4	GCGGGCAGTGAGGAACAT	This study
amgRS		
PCRi amgRS A1	CAACTGGGTATCGTCGAGGC	This study
PCRi amgRS A2	GATCAGGCGATCCATCTGCTCGGTGTT	This study
PCRi amgRS A3	TGGATCGCCTGATCGACAATGCCCTGA	This study
PCRi amgRS A4	CATCGAGGTGCCGCTCTAC	This study
Gene complementation		
PA4773 to PA4775		
PCR PA4773 AB1	CGCCTATCGTGCCTTCCA	This study
PCR PA4775 AB2	GGCAGCCTCGTTTCAGTGAT	This study
pmrAB		
PCRpmrAB1	GATCGTCGCCATCCTCCTG	This study
PCRpmrAB4	TTCACCGATGTTCATCCGGG	This study
qPCR		
metK		
RT metK AB1	ATGCGAAACCCTGGTCAAGA	This study
RT metK AB2	GCTTGCCGATGATGTTCAGC	This study
PA0547		
RT PA0547 AB1	ATACCGTGAGAGCGTGTTGG	This study
RT PA0547 AB2	GGACGTTGCCCAATCCTTCT	This study
ccoN2		
RT PA1557 AB1	GGCTTCCTCGGCATGATGTA	This study
RT PA1557 AB2	AGAGGGTCATCATGCCGTTG	This study
mexY		
mexY1A	TTACCTCCTCCAGCGGC	(Jeannot *et al*., 2005)
mexY1B	GTGAGGCGGGCGTTGTG	(Jeannot *et al*., 2005)
hcnB		
RT PA2194 AB1	GAATGCAACGTCTGGCAGC	This study
RT PA2194 AB2	AGATGGGATTCTCGGCGTTC	This study
pslB		
RT pslB AB1	AGTTGCTGATCCTTCCCGC	This study
RT pslB AB2	GGGCGCCCTGTTCGATATAG	This study
rmf		
RT PA3049 AB1	TTTGTCCGTTCACCCATCCT	This study
RT PA3049 AB2	TGCTGGAGTTGATTGAGACGT	This study
pelB		
RT pelB AB1	CGGAGGATGAATCGACCCTG	This study
RT pelB AB2	GCCATGTTCAGACGCAGGT	This study
arnA		
RT PA3554 AB1	TTCATCGGCAACCACCTGTC	This study
RT PA3554 AB2	ATGGTATTCGAGCCACTCCG	This study

wspF		
RT wspF AB1	TCGGATCATGGCGGAAAGTC	This study
RT wspF AB2	CTGGACCTTGCCACGGTTAT	This study
oprC		
RT PA3790 AB1	GAACACTCACAGCACCAGGA	This study
RT PA3790 AB2	TTGGTGAGGATGTTCAGGCG	This study
cioA		
RT PA3930 AB1	GGTGATCTTCAACCCGTCGT	This study
RT PA3930 AB2	GGTGCTCCAGGGTATTGAGG	This study
PA4133		
RT PA4133 AB1	GACTGTTCTCCGACACCCTG	This study
RT PA4133 AB2	GATCAGGGTGCCGAAGAACA	This study
cdrB		
RT cdrB AB1	GCAACAGCAGCGATACGAAG	This study
RT cdrB AB2	ATGATCTGCAGGGTATCGCC	This study
cdrA		
RT cdrA AB1	CGAACATCAGCGACGAACAC	This study
RT cdrA AB2	GTTGATCACGCCGTTGTTGG	This study
PA4773		
PA4773RTAB1	TCCACAAGTTCAGCCCGATC	This study
PA4773RTAB2	GGTCCATGCTCGAGATCAGG	This study
PA4774		
PA4774RTAB1	TGATCGCCGACACCTACAAC	This study
PA4774RTAB2	GACACAGTTCCACCAGCTCC	This study
PA4775		
PA4775RTAB1	ACGAGCTGCTGGTGATCTTC	This study
PA4775RTAB2	CAGGTGACCTTCGTGCCAG	This study
pmrA		
pmrARTAB1	GTTCGACCTGCTGGTGCT	This study
pmrARTAB2	TCGAGATCGAAGGGCTTG	This study
pmrB		
pmrBRTAB1	ACGAACTCAACCTCCTGCTG	This study
pmrBRTAB2	ATCAAGGTGCTGATCCGCTC	This study
cueR		
RT cueR AB1	GCGAAGAAAAGCGGACTGAC	This study
RT cueR AB2	GATGAACGCCAGGGTATGCA	This study
PA4781		
RT PA4781 AB1	GATTTCCTGCGCGACAAGAG	This study
RT PA4781 AB2	GCCTGACATAGCGCTCGATA	This study
PA4782		
RT PA4782 AB1	GGGTACGAAGATGAAAGCGC	This study
RT PA4782 AB2	ATGGGGTCCTGGCCGAAATA	This study
amgR		
RT amgR AB1	AGGTGCCGATCATCATGCTC	This study
RT amgR AB2	GTACCTCGTCGCCCTTCTTC	This study
armZ		
PA5471A	AGCTACAGCAGGTCGAGACG	(El'Garch *et al*., 2007)
PA5471B	TTGATGTCGAGCAGTTCCAG	(El'Garch *et al*., 2007)
Protein production		
PA4775		
NcoI_PA4775_Fw	CGCCATGGCGCCCTGCCTGCTGCACCG	This study
NotI_PA4775_Rv	GCGCGGCCGCGACCCGCAGTTCGCCCCGG	This study

Table 31: Primers used for investigating the role of pump MexXY(OprM) as determinant of acquired and adaptive resistance to colistin.

Name	Sequence (5'→3')	Reference
Gene inactivation		
PA0929-30		
PCRi PA0929-30 A1	GTTGTTCGGCGATCAGTTGC	This study
PCRi PA0929-30 A2	CCAGGCCCAGGATCAGGTCATAGCCGC	This study
PCRi PA0929-30 A3	GATCCTGGGCCTGGGACTGAGCATTG	This study
PCRi PA0929-30 A4	GCGTTCGTCCAGTTCTTCCA	This study
pslB		
PCRi pslB A1	TGGGTCTTCAAGTTCCGCTC	This study
PCRi pslB A2	TCGTCGCCGACGGCGTTCATCAGTAGA	This study
PCRi pslB A3	GCCGTCGGCGACGAGAAGAAAGCCTGA	This study
PCRi pslB A4	GGTCTTGATCCCCAGTTCCG	This study
pelB		
PCRi pelB A1	GATTACATCCCGCGCCTGG	This study
PCRi pelB A2	GGTGAACGCCTGGGGATGCTTGTCAG	This study
PCRi pelB A3	CCCAGGCGTTCACCTTCGGCTACCAGT	This study
PCRi pelB A4	TTGTACTGCCACTCCTCGAC	This study
wspF		
PCRi wspF A1	GCTGATCCTGGACGTCGAG	This study
PCRi wspF A2	AATAATTCAACCCTGTGCTTCTCCGAT	This study
PCRi wspF A3	AGGGTTGAATTATTGGCGTGGCGATGC	This study
PCRi wspF A4	ATCACCGTCGGCTTGATCTG	This study
cdrB		
PCRi cdrB A1	CGGCAACTACCAGCTCAACT	This study
PCRi cdrB A2	TGAACGACATCATTCACCTCGGGCAGA	This study
PCRi cdrB A3	AATGATGTCGTTCAACCCGGAGATTGC	This study
PCRi cdrB A4	GCGATCAGTTGTTGGGCAC	This study
cdrA		
PCRi cdrA A1	GGAGGCATGGTCGAGGAAAA	This study
PCRi cdrA A2	TAGTCGGTCTCGTTGGGGTTGAACTGG	This study
PCRi cdrA A3	AACGAGACCGACTACTGGAGCTGCTTC	This study
PCRi cdrA A4	GGGTCAACAGGAAGCCGTC	This study
PA4773		
PCRi PA4773 A1	GTATCCACCAGCCGTACCTG	This study
PCRi PA4773 A2	ATCCATCACGGTTGAATTGCCATGAAG	This study
PCRi PA4773 A3	CAACCGTGATGGATACGCCGATCGAA	This study
PCRi PA4773 A4	GTCGAGATCGACCATCACC	This study
PA4774		
PCRi PA4774 A1	CAGTGGATCGAGGAAAGCAT	This study
PCRi PA4774 A2	ATCCGGCTCCGGCGGATAGAAATAGAA	This study
PCRi PA4774 A3	CGCCGGAGCCGGATATCGAGGAGATCG	This study
PCRi PA4774 A4	GGGTTGCCGATGACCAG	This study
PA4775		
PCRi PA4775 A1	GGCTCTCTATACCCGCCAGT	This study
PCRi PA4775 A2	TCCTGCACGGACATCTTCAGGTCCTC	This study
PCRi PA4775 A3	ATGTCCGTGCAGGACCTCTACGAACTG	This study
PCRi PA4775 A4	GGCTTGGTCAGGTAGTCGTC	This study
Gene complementation		
arn		
PCR PA3552 Fw	GCAGCATTCAGCGACATATAA	This study
PCR PA3559 Rv	GGAGAACCGGCGGATAAC	This study

qPCR		
PA0929		
RT PA0929 AB1	GATGTCTGCGATGTCAGCCT	This study
RT PA0929 AB2	ATGTCCAGGCTGCGATCATG	This study
PA0930		
RT PA0930 AB1	CAACTGCTCCGCGATCTCTC	This study
RT PA0930 AB2	ATGTCCTCCAGCGCCAATAC	This study
pslB		
RT pslB AB1	AGTTGCTGATCCTTCCCGC	This study
RT pslB AB2	GGGCGCCCTGTTCGATATAG	This study
pelB		
RT pelB AB1	CGGAGGATGAATCGACCCTG	This study
RT pelB AB2	GCCATGTTCAGACGCAGGT	This study
arnA		
RT PA3554 AB1	TTCATCGGCAACCACCTGTC	This study
RT PA3554 AB2	ATGGTATTCGAGCCACTCCG	This study
wspF		
RT wspF AB1	TCGGATCATGGCGGAAAGTC	This study
RT wspF AB2	CTGGACCTTGCCACGGTTAT	This study
cdrB		
RT cdrB AB1	GCAACAGCAGCGATACGAAG	This study
RT cdrB AB2	ATGATCTGCAGGGTATCGCC	This study
cdrA		
RT cdrA AB1	CGAACATCAGCGACGAACAC	This study
RT cdrA AB2	GTTGATCACGCCGTTGTTGG	This study
PA4773		
PA4773RTAB1	TCCACAAGTTCAGCCCGATC	This study
PA4773RTAB2	GGTCCATGCTCGAGATCAGG	This study
PA4774		
PA4774RTAB1	TGATCGCCGACACCTACAAC	This study
PA4774RTAB2	GACACAGTTCCACCAGCTCC	This study
PA4775		
PA4775RTAB1	ACGAGCTGCTGGTGATCTTC	This study
PA4775RTAB2	CAGGTGACCTTCGTGCCAG	This study
pmrB		
pmrBRTAB1	ACGAACTCAACCTCCTGCTG	This study
pmrBRTAB2	ATCAAGGTGCTGATCCGCTC	This study

Table 32: Primers used for the characterization of the PA3327 cluster.

Name	Sequence (5'→3')	Reference
Gene sequencing		
azeA		
Screen iPA3326 AB1	GAGCGAAACGAACCATCCCT	This study
Screen iPA3326 AB2	GGGATTCCTACGAACCTGGTG	This study
azeC		
Screen iPA3328 AB1	GCTATCGCCCGGAAGTCAG	This study
Screen iPA3328 AB2	GGAGAACTGGTCGCTGAGC	This study
azeD		
Screen iPA3329 AB1	CATCGAGCAGTTGGAGCATC	This study
Screen iPA3329 AB2	GTAGGGAATGGCGACCGAG	This study

azeE		
Screen iPA3330 AB1	TCAACCTGTGCTCCTCCAAC	This study
Screen iPA3330 AB2	AGCAATGCCTCGGTGATCC	This study
azeF		
Screen iPA3331 AB1	CTCGGTCGCCATTCCCTAC	This study
Screen iPA3331 AB2	CACCGAGATGTAGTCCTGCG	This study
azeG		
Screen iPA3332 AB1	CAACGCCATGGAAGAACTGG	This study
Screen iPA3332 AB2	GGTCATCAGCAGGTCGAACT	This study
azeJ		
Screen iPA3335 AB1	CCGACAATGGACTGAAGAGGG	This study
Screen iPA3335 AB2	GACCATCACCGCATAGCCC	This study
Gene inactivation		
pqsA		
PCRi pqsA A1	TACGCAATGGGATTTCAACA	(Hong *et al*., 2019)
PCRi pqsA A2	CAACATGTGGCCCCGATAGTGATAAAC	(Hong *et al*., 2019)
PCRi pqsA A3	GGGGCCACATGTTGATTCAGGCTGTGG	(Hong *et al*., 2019)
PCRi pqsA A4	AGGTTGAGGTGTCCCTTGAC	(Hong *et al*., 2019)
azeA		
PCRi PA3326 A1	CGCCGGTCTTTTCGAAGTTG	This study
PCRi PA3326 A2	GCCGTACCGGGTATTGGGCAGCGAATA	This study
PCRi PA3326 A3	ATACCCGGTACGGCCTGGTCAACAAGA	This study
PCRi PA3326 A4	CGCCCGTTACTTCAATCCCT	This study
azeB		
PCRi PA3327 A1	TCCATCCGGCAAACCTTTCA	(Hong *et al*., 2019)
PCRi PA3327 A2	GCAGGGCCCAGATGTCCCGTTGGTAGG	(Hong *et al*., 2019)
PCRi PA3327 A3	CATCTGGGCCCTGCTGCTGTTCTTCTA	(Hong *et al*., 2019)
PCRi PA3327 A4	CAGGGGATGTCTGCTCATGG	(Hong *et al*., 2019)
azeC		
PCRi PA3328 A1	GAACCCTATGTCGAGACGGTC	This study
PCRi PA3328 A2	ACGTTGCCCAGTTCGATGCGGCAGTC	This study
PCRi PA3328 A3	GAACTGGGCAACGTCTATTGGTGGGGC	This study
PCRi PA3328 A4	TTCGACTCCTGGGAAGGTCA	This study
azeD		
PCRi PA3329 A1	AACGAACTGGCACTGACCTT	This study
PCRi PA3329 A2	AGGTTGAATTGTTCGGCGAGGGTCAG	This study
PCRi PA3329 A3	GAACAATTCAACCTGTGCTCCTCCAAC	This study
PCRi PA3329 A4	CCAATGGATTCCTCGTCGGT	This study
azeE		
PCRi PA3330 A1	CGCCATCAACTCCAGCCAT	This study
PCRi PA3330 A2	GGTATCGCAGATCCCGGCGTTGTTCA	This study
PCRi PA3330 A3	GGATCTGCGATACCTACCTGCGCTTCC	This study
PCRi PA3330 A4	TCGAGGTTGAGCATGTGGTG	This study
azeF		
PCRi PA3331 A1	ACCAAGCCCGCCGATGTC	This study
PCRi PA3331 A2	CGAAGCCCATGTGGTGGCTGAGTCCC	This study
PCRi PA3331 A3	CCACATGGGCTTCGAGACCACCATGAA	This study
PCRi PA3331 A4	GGAGGAAGGTGATCGGCAG	This study
azeG		
PCRi PA3332 A1	GCGAATACATCCTGGTCTCCA	This study
PCRi PA3332 A2	AGAGCAGGGCGTAGGGGAATTCGAGTAC	This study
PCRi PA3332 A3	CTACGCCCTGCTCTACCGCGACTTCTG	This study
PCRi PA3332 A4	CTGAAAGTGTCCACCCCGAC	This study

azeJ		
PCRi PA3335 A1	TTTCGATTCGCTGGTGGTCA	(Hong *et al.*, 2019)
PCRi PA3335 A2	TAGCTCTCGAGATAGCGGGCATTGAG	(Hong *et al.*, 2019)
PCRi PA3335 A3	TATCTCGAGAGCTACTACCGCCGTTG	(Hong *et al.*, 2019)
PCRi PA3335 A4	AAGGTGACCAGGTAGCCGAT	(Hong *et al.*, 2019)
Gene complementation		
azeJ		
PCRi PA3335 A1	TTTCGATTCGCTGGTGGTCA	(Hong *et al.*, 2019)
PCRi PA3335 A4	AAGGTGACCAGGTAGCCGAT	(Hong *et al.*, 2019)
qPCR		
pqsA		
RT pqsA AB1	CGCGAAGGACACACTATCGA	This study
RT pqsA AB2	TGAACAGATCGTCTTCCCGC	This study
azeA		
RT PA3326 AB1	GCCCAATACCCGCTTCCTC	This study
RT PA3326 AB2	GCTGATCTTTTCCGGCGTCT	This study
azeB		
RT PA3327 AB1	ACCACCCTTTCCTACATGCG	(Hong *et al.*, 2019)
RT PA3327 AB2	GAAGGTTTCGATATGCCGCG	(Hong *et al.*, 2019)
azeC		
RT PA3328 AB1	GGCTTCAACTCGGCGATCC	This study
RT PA3328 AB2	ATAGACGTTGCCTTCGCCG	This study
azeD		
RT PA3329 AB1	CTGAACGTGATTTCCCGGGT	This study
RT PA3329 AB2	TTGATTTCCCGCAGCCATTG	This study
azeE		
RT PA3330 AB1	AACGCCGGGATCTGCATTT	This study
RT PA3330 AB2	CAGGTAGGGAATGGCGACC	This study
azeF		
RT PA3331 AB1	CGGTGATCTTCGAGCTGCT	This study
RT PA3331 AB2	AGTTCCGCTTCGCTCAACT	This study
azeG		
RT PA3332 AB1	CTGTTTCCCGAGCACCTGAC	This study
RT PA3332 AB2	GGATTCCAGAAGTCGCGGTA	This study
azeJ		
RT PA3335 AB1	CGACATCCTCAACCACACCA	This study
RT PA3335 AB2	GAACACCGAGACCACCGC	This study

Table 33: Primers used in several projects.

Name	Sequence (5'→3')	Reference
Gene sequencing		
pCR-Blunt vectors		
M13 Forward	GTAAAACGACGGCCAG	Life technologies
M13 Reverse	CAGGAAACAGCTATGAC	Life technologies
qPCR		
uvrD		
uvrD1	CACGCCTCGCCCTACAGCA	(Jo *et al.*, 2003)
uvrD2	GGATCTGGAAGTTCTCGCTCAGC	(Jo *et al.*, 2003)

2.2. Nucleic acid purification

2.2.1. Genomic DNA extraction

Bacterial genomic DNA was extracted by using the *Wizard® genomic DNA purification* kit (Promega Corporation, Charbonnières-les-Bains, France) according to the manufacturer's recommendations.

2.2.2. Plasmid DNA preparation

Plasmid DNA was extracted by using the *Wizard® plus SV Minipreps DNA purification system* kit (Promega Corporation), according to the supplier's instructions.

2.3. DNA amplification *via* Polymerase Chain Reaction (PCR)

Genic amplifications by PCR were achieved on a Biometra T3 termocycler (Biolabs Scientific Instrument, Lausanne, Switzerland) using either *MyTaq Red DNA polymerase* (Bioline, London, UK) or *iProof™ High-Fidelity Master Mix* (Bio-Rad). With *MyTaq Red DNA polymerase*, the 50 µl reaction mixtures contained 1x Reaction Buffer, 2 µM of each primer, 2.5 U of DNA polymerase and 100 ng of template DNA. The PCR conditions were as follows: (i) an initial denaturation step of 1 min at 95°C and (ii) 30 cycles of amplification each composed of 15 s at 95°C, 15 s at the optimal Tm of individual pairs of primers and 10 s at 72°C. For *iProof™* reactions, the conditions were modified as follows: 1x *iProof HF Master Mix*, 3% dimethyl sulfoxide (DMSO), 0.5 µM of each primer and 100 ng of template DNA. After 3 min of denaturation at 98°C, the amplification reaction was carried out with 30 cycles, each consisting in 10 s at 98°C, 30 s at the optimal Tm and 45 s at 72°C, with a final extension step of 7 min at 72°C.

2.4. DNA cloning

2.4.1. Enzymatic restriction of DNA

Plasmids or PCR fragments were digested using specific restriction endonucleases following manufacturers recommendations. Briefly, 1 µg of DNA was digested in a reaction mixture of 25 µl containing 1x specific buffer and an appropriate volume of restriction enzymes (Promega Corporation).

2.4.2. Separation of DNA fragments by agarose gel electrophoresis

DNA fragments were separated and their length determined by electrophoresis in 0.8% agarose gel containing 1x SYBR Safe™ intercalating dye (Invitrogen™, St. Aubin, France). Migration was achieved in 1x TAE buffer (Tris-acetate 40 mM, EDTA 1 mM, pH = 8.0) during 45 min at 100 V. DNA bands were visualized under UV light by using *UV ChemiDoc XRS transilluminator* (Bio-Rad).

2.4.3. Extraction of DNA fragments from agarose gels

Digested fragments were extracted and purified by using the *Wizard® SV Gel and PCR clean up system* kit (Promega Corporation) according to the manufacturer's instructions.

2.4.4. Ligation of DNA fragments

Digested fragments with blunt or cohesive ends were ligated to cleaved linear plasmids using T4 DNA ligase (Promega Corporation) as required by enzyme supplier. Ligation reactions were incubated overnight at 15°C.

2.5. Bacterial DNA transfer

2.5.1. Heat-shock method

E. coli DH5α and DH5α-T1^{R} ready-to-use competent cells were obtained from Invitrogen™ (*Cloning Efficiency® DH5α Competent Cells* and *GeneArt™ Site-Directed Mutagenesis System* kit). They were transformed by recombinant DNA as following recommended protocols. *E. coli* strains CC118 and CC118 *λpir* were rendered competent by using the rubidium chloride protocol described by Hanaham *et al*. (Hanahan, 1983). They were transformed with plasmids (10 ng) or ligation mixtures (2 µl) by a treatment composed of a first step of 30 min in ice, then a heat shock at 42°C for 1 min, and 10 min at 0°C. Finally, 900 µl of MHBc were added to the cells. After 1h30 of incubation at 37°C, bacteria were plated on MHA supplemented with selective antibiotic markers (Table 28).

2.5.2. Electro-competent method

P. aeruginosa strains were made electro-competent by using the sucrose protocol of Choi *et al*. (Choi *et al*., 2006). When needed, electro-competent cells were transformed with 20 ng of plasmid in the MicoPulser™ Electroporator (Bio-Rad) set with the following parameters: 2.5 kV cm^{-1}, 200 Ω and 25 µF for 4.5-5 ms. Then, they were cultured in 1 ml of MHBc for 1 h at 37°C with shaking (250 rpm), and finally plated onto MHA medium supplemented with required antibiotics (Table 28).

2.5.3. Conjugation method

Bacterial conjugations were performed by triparental mating with *P. aeruginosa* as the recipient strain, *E. coli* HB101 containing broad-host-range plasmid pRK2013 as a helper strain, and *E. coli* CC118 (containing a mini-CTX1 derivated-plasmid) or CC118 *λpir* (containing a pKNG101 derivated-plasmid) as a donor. Each strain was individually cultured overnight in 10 ml of MHBc at 37°C with shaking (250 rpm). 100 µl of the helper and of the donor strains were mixed and spotted onto the surface of MHA plate, and incubated 2 h at 37°C. In the meantime, the recipient strain was incubated 2 h at 42°C (to induce *pili* formation) and then added to the bacterial spot. After 2h30 at 37°C, the bacterial spot was collected, resuspended in 1 ml of MHBc and cultured at 37°C with shaking for 1h30. Transconjugants were selected on PIA medium supplemented with selective antibiotics (Table 28).

2.6. Gene inactivation

Gene inactivation was carried out by using overlapping PCR and homologous recombination events (see steps in Figure 60). First, two DNA sequences of about 500-bp in length, flanking the target gene, were amplified by PCR. The amplicons were used as a template to synthesize, by an overlapping PCR, a fragment of about 1,000-bp which was subsequently cloned into plasmid pCR-Blunt, sequenced with M13 Forward and M13 Reverse primers (Table 33), and sub-cloned into suicide vector pKNG101. Then, the recombinant pKNG101 plasmid was transferred from *E. coli* CC118 *λpir* to *P. aeruginosa* by triparental conjugation as mentioned above. Excision of pKNG101 from the chromosome of transconjugants was obtained by positive selection on M9-sucrose medium, which is lethal for cells that still harbor the *sacB* gene present on

pKNG101. The allelic exchange of streptomycin-susceptible clones was confirmed by PCR and DNA sequencing.

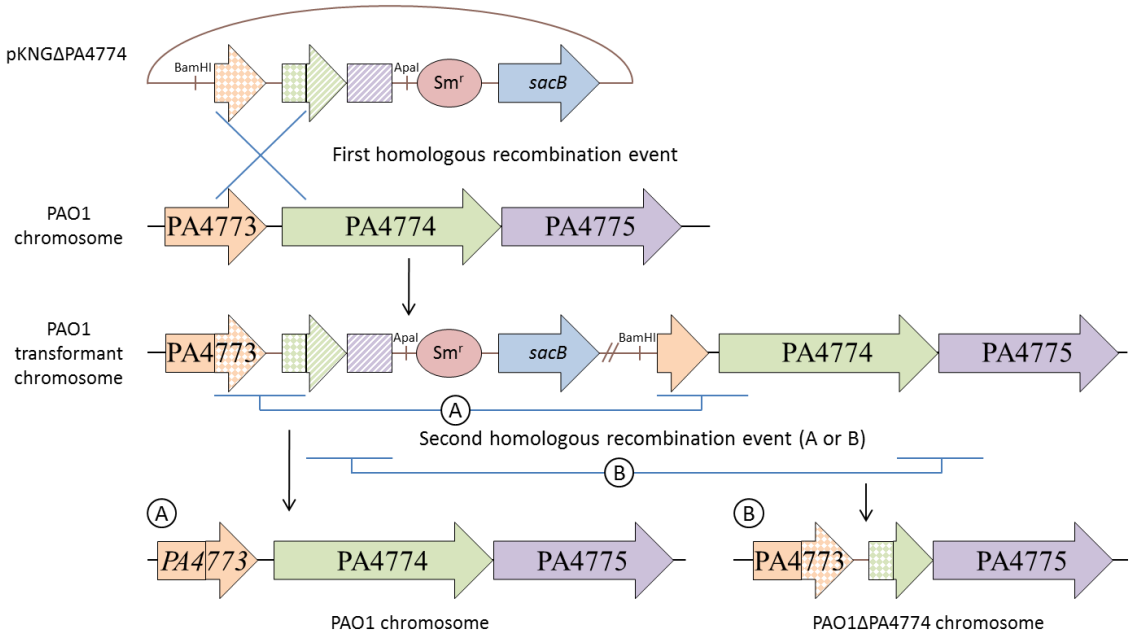

Figure 60: Gene inactivation by homologous recombination between a recombinant derivative of plasmid pKNG101 and the *P. aeruginosa* chromosome. Example is given of the inactivation of PA4774 gene.

2.7. Gene complementation and mutagenesis

2.7.1. Chromosomal complementation

Genes PA4773 to PA4775 and the PA3335 gene were amplified by PCR and cloned into vector pCR-Blunt, and then ligated to BamHI/NotI restriction sites of cleaved mini-CTX1 plasmid. *E. coli* CC118 competent cells were transformed with the recombinant plasmids, and transformants were selected on MHA plates containing tetracycline (5 µg ml^{-1}). Once checked by PCR and sequencing, the recombinant plasmids were transferred to *P. aeruginosa* by triparental mating. Excision of the tetracycline resistance cassette was obtained by introducing the pFLP2 vector that codes for the Flp flippase into the transconjugants by electroporation (Table 22). Transformants were selected on MHA plates supplemented with ticarcillin (150 µg ml^{-1}). pFLP2 excision was selected by culturing the transformants on M9-sucrose plate. Finally, the chromosomal insertion was verified by PCR and sequencing on both DNA strands.

2.7.2. Plasmid-based complementation

The *pmrAB* genes of different genetic backgrounds (PAO1, *in vitro*-selected mutants and clinical strains) were amplified by PCR with primers PCRpmrAB1 and PCRpmrAB4 (Table 30). The amplicons were cloned into vector pCR-Blunt, and then subcloned into EcoRI-linearized plasmid pME6012. After checking sequences of *pmrAB* alleles, the recombinant plasmids were transferred into mutant PAO1Δ*pmrAB* by electroporation. Selection of transformants was achieved on MHA supplemented with 200 µg ml^{-1} tetracycline.

The *arnBCADTEF-ugd* (*arn*) operon was amplified by PCR, with primers PCR_PA3552_Fw and PCR_PA3559_Rv (Table 31). The product of amplification was cloned into vector pCR-Blunt, and ligated to the HindIII/XbaI restriction sites of linearized vector pAK1900 (Table 22). The recombinant plasmid was transferred into strain PAO1 by electroporation and transformants were selected by 150 µg ml^{-1} ticarcillin on MHA.

2.7.3. Mutagenesis of *fusA1* gene by homologous recombination

Variants of gene *fusA1* exhibiting significant allelic variations were amplified by PCR using primers PCR_fusA1_AB1 and PCR_fusA1_AB2 (Table 31). The resultant amplicons were cloned into vector pCR-Blunt, next sequenced and then subcloned as SpeI/ApaI fragments of 2,383-bp in length into plasmid pKNG101 by using *E. coli* CC118 *λpir* as a host. The recombinant plasmids were transferred into strain PAO1 by triparental conjugation. The excision of pKNG101 from the bacterial chromosome was obtained as described above. The allelic exchanges and the presence of desired mutations were verified by PCR using primers PCR_screen_fusA1_AB1 and PCR_screen_fusA1_AB2 (Table 31) and sequencing experiments.

2.7.4. Site-directed mutagenesis

Plasmids pKNG::$fusA1_{T119A}$, pKNG::$fusA1_{G352A}$ and pKNG::$fusA1_{A1775T}$ (Table 23) were constructed from pCR-Blunt::*fusA1* using the *GENEART Site-Directed Mutagenesis System* kit (Invitrogen™) and specific primers (Table 31). Briefly, a first reaction led to the methylation and mutagenesis of template vector under the indicated conditions: plasmid DNA methylation at 37°C for 20 min, inactivation of the DNA

methylase at 94°C for 2 min, followed by 18 cycles of amplification, each composed of 20 s at 94°C, 30 s at 57°C, 3 min at 68°C with a final extension of 5 min at 68°C.

The reaction mixtures contained 1x *accuPrime Pfx reaction mix*, 1x enhancer, 0.3 µM of each primer, 20 ng of plasmid pCR-Blunt::*fusA1*, 4 U DNA methylase, 1x SAM (S-adenosylmethionine), and 1 U AccuPrime Pfx. Then, a second recombination step is performed at room temperature for 10 min by mixing 4 µl of PCR mixture, 1x reaction buffer and 1x enzymer mix. The reaction was stopped by adding 1 µl of 0.5 M EDTA. Two microliters of mixture were used to transform *E. coli* DH5α-T1^{R} by the heat shock method, enabling circularization of the linear mutated DNA by *E. coli* and digestion of the methylated template DNA by McrBC endonuclease. Resultant transformants were selected on MHA plates supplemented with 50 µg ml^{-1} kanamycin.Their plasmids were sequenced in both strands to confirm the presence of desired mutation.

2.8. Quantification of mRNA transcripts by RT-qPCR

Ten microliters of an overnight bacterial culture were diluted in 10 ml of MHBc subsequently incubated aerobically at 37°C to reach an absorbance of A_{600} = 0.8. The A_{600} was monitored in an *Eppendorf BioPhotometer 6131* (Eppendorf, Hamburg, Germany). Five hundred microliters of culture were added to 1 ml of *RNA Protect Bacteria Reagent* (Qiagen), then vortexed 5 s, and incubated at room temperature for 5 min before a 5 min centrifugation at 10,000 rpm. Total RNAs from the *P. aeruginosa* pellet were extracted with the *RNeasy Plus Mini* kit (Qiagen) according the manufacturer's instructions. A step of in-column DNA digestion was added to the protocole to completely eliminate genomic DNA (*RNAse free DNase Set*, Qiagen). Thus, 27 Kunitz units of DNase I were applied to the *RNeasy column* and left in contact with the RNA extract for 45 min at room temperature. Total RNAs were stored at -80°C until use. When required, 2 µg of RNAs were reverse transcribed (RT, reverse transcription sample) with an *ImProm-II^{TM} Reverse Transcription System* (Promega Corporation). A control free of reverse transcriptase (NRT, non-reverse transcription sample) was made in parallel to confirm the absence of contamination of samples by genomic DNA. Synthesized cDNA were stored frozen at -20°C. Quantitative PCR was performed in duplicates on a *Rotor-Gene Q* apparatus (Qiagen) by using the *QuantiFast SYBR® Green PCR dye* (Qiagen). 3 µl of 10^{-1} diluted NRT sample were amplified with

1x *QuantiFast SYBR Green PCR Master* mix (Qiagen) and 1 µM of each primer (Tables 30 to 33) in a final volume of 15 µl. The amplification setting was the following: (i) 5 min of initiation at 95°C (ii) 35 cycles of amplification each composed of 10 s at 95°C and 30 s at 60°C. Ten-fold serial dilutions of RT cDNA samples from reference strain PAO1 (10^{-1}, 2.10^{-2}, 10^{-2}, 2.10^{-3} and 10^{-3}) were included as calibrators. A negative control with *RNase free water* (Qiagen) without cDNA was introduced in every experimental series. Finally, the specificity of amplification was checked by doing a melting curve analysis. Gene transcripts were normalized in each strain to the transcript levels of housekeeping gene *uvrD*. This quantification method takes into account the reaction efficacy of the reference gene (E_{uvrD}) and those of the target gene (E_{target}). The cycle threshold (Ct) was determined automatically by *Rotor-Gene Q software 1.7* (Qiagen) and the fold-change in gene expression was calculated with the above formula from two to three experiments and is presented as an average:

$$\text{Fold-change} = (E_{target})^{\Delta Ct_{target}} / (E_{uvrD})^{\Delta Ct_{uvrD}} \qquad \text{with } \Delta Ct = Ct_{PAO1} - Ct_{sample}$$

2.9. Quantification of mRNA transcripts by RNA seq

RNA sequencing data were analyzed by Monika Schniederjans at the Helmholtz Centre for Infection Research, Molecular Bacteriology Department, Braunschweig (Germany) under the supervision of Susanne Häussler.

2.9.1. Sample preparation

Bacterial pellets of strains PAO1 and AB16.2 were prepared in duplicates as described above in the **2.8.** section and were stored at -80°C until shipping.

2.9.2. Sample analysis and mRNA transcripts quantification

Total RNA was extracted from pelleted cells using the *RNeasy Mini* kit (Qiagen) with *QIAshredder homogenizer* (Qiagen). Ribosomal RNA sequences were depleted and cDNA libraries were prepared and sequenced as described by Dötsch *et al*. (Dötsch *et al*., 2012) using a *HiSeq® 2500 Sequencing System* (Illumina®). Reads were aligned to the genome of strain PAO1 using *Stampy* algorithm software (Lunter and Goodson, 2011) and differential gene expression analysis was performed with *DESeq package* from *R* software.

3. DNA sequencing

All the Sanger sequencing and whole genome sequencing experiments (PGM, Iontorrent, Life technologies, Thermo Fisher Scientific) were performed by *la Plateforme Genomique*, Université de Franche-Comté, Besançon, France.

PCR fragments were sequenced on both strands on an *Applied Biosystems® 3130 Genetic Analyzer* (Thermo Fisher Scientific, Waltham, MA, USA) according to manufacturer's guidelines. Electropherogram and DNA sequences were analyzed with *SnapGene* software (version 4.0.6, GSL Biotech LLC, Chicago, USA).

Genomic DNA from *in vitro*-selected mutants PAOR10, PAOR13 and PAOR15 was extracted with *PureLink™ Genomic DNA Mini* as recommended by Invitrogen™. Genomic libraries of 250-bp fragments were generated with a cocktail of restriction enzymes and were subsequently amplified by emulsion PCR, and sequenced with *Ion Personal Genome Machine*™ (*PGM*™) *System* (Thermo Fisher). The sequence reads (PAOR10 = 13,603,185; PAOR13 = 10,768,909 and, PAOR15 = 11,708,879) were aligned with the sequence of PAO1 genome (NCBI accession number NC_002516) using *CLC Genomics Workbench* software (Qiagen, Aarhus, Denmark). A single nucleotide polymorphism (SNP) with a coverage >5-fold and with a percentage >90% of reads was considered as significant and submitted to resequencing by the Sanger method.

4. Purification of His_6-tagged protein

A fragment of gene PA4775 was amplified by PCR with primers NcoI_PA4775_Fw and NotI_PA4775_Rv (Table 30). The amplicon (764-bp) was then cloned within the NcoI/NotI restriction sites and under the IPTG-inducible promoter of pET28a plasmid. The recombinant plasmid was transferred into One Shot™ BL21 Star™ (DE3) competent *E. coli* strain (Table 18). Bacteria producing the His_6-PA4775 protein were grown at 37°C in 200 ml of LB medium supplemented with kanamycin (50 µg ml^{-1}) up to an A_{600} = 0.7. Then, protein production was triggered by addition of 1 mM isopropyl-β-D-thiogalactopyranoside (IPTG) to the culture for 3 h. Bacteria from 1 ml of culture were collected by centrifugation (6,500 g, 10 min), and resuspended in 100 µl of

1x *Laemmli Sample Buffer* (Bio-Rad) containing 2.5% (vol/vol) β-mercaptoethanol (Sigma-Aldrich). The sample was heated for 3 min at 95°C before loading on a 4-20% polyacrylamide *Mini-PROTEAN® TGX™ Precast Gel* (Bio-Rad) with 5 µl of molecular weight marker *Precision Plus Protein™ Dual Color Standards* (Bio-Rad). SDS-PAGE was run at 200 V for 35 min in a *Mini-PROTEAN Tetra Cell* (Bio-Rad) in TGS buffer (25 mM Tris, 192 mM glycine, 0.1% SDS, pH = 8.3). The gel was washed 3 times for 5 min in water and colored with *Bio-Safe™ Coomassie G-250 stain* (Bio-Rad) for 1 h. Finally, the gel was left soaked in water overnight. Images were acquired by using *Molecular Imager® GS-800™ Calibrated Densitometer* (Bio-Rad) and *Quantity One® 1-D analysis* software. His-tagged proteins were isolated by using *Protino® Ni-IDA 150 Packed Columns* (Machery-Nagel) or *Dynabeads™ His-Tag Isolation & Pulldown* (Invitrogen™) by following supplier's recommendations.

5. Surface polyamine analysis

5.1. Surface polyamine sample preparation

Surface-associated polyamines were extracted as previously described (Johnson *et al.*, 2012) with the following modifications. 1 ml of an overnight *P. aeruginosa* culture in MHBc were sub-cultivated aerobically in 100 ml of fresh medium at 37°C (250 rpm) up to mid-log phase (A_{600} = 0.8). Bacteria from 50 ml of culture were then harvested by centrifugation and resuspended in 250 µl of prewarmed 10 mM HEPES buffer pH = 7.4 (4-(2-hydroxyethyl)-1-piperazineethanesulfonic acid) or in HEPES buffer containig 1 M NaCl. After a 10 min incubation at 37°C with shaking (250 rpm), the bacterial suspensions were centrifuged three times (10 min, room temperature, 5,000 g) to remove whole cells. The supernatants of each strain were collected in triplicate. 2 µl of the samples were analyzed on a SDS-PAGE gel and colored with *Bio-Safe™ Coomassie G-250 stain* (Bio-Rad) as described in the **4.** section. Additionally, Western blotting was performed on SDS-PAGE gel using anti-DsbA antibody (kindly provided by Dr Ina Attrée) diluted at 1:10,000 and with a secondary alkaline phosphatase conjugated-antibody against rabbit diluted at 1:20,000 (Sigma-Aldrich).

5.2. Surface polyamine sample analysis

Liquid Chromatography-ElectroSpray Ionization-Mass Spectrometry (LC-ESI-MS) analysis was performed by *la Plateforme BioPark d'Archamps* of the Archamps Technopole located in St-Julien en Genevois, France.

5.2.1. Principle

Amounts of putrescine, cadaverine, spermidine, norspermidine, spermine and 1,3-diaminopropane were measured by LC-ESI-MS. Purified standard polyamines and polyamines contained in the tested biological samples were covalently modified by addition of N-succinimidyloxycarbonylmethyl)-tris-(2,4,6-trimethoxyphenyl)-phosphonium bromide (TMPP) to facilitate their detection by mass spectrometry. Derivatization by TMPP increases ionization of the molecules in the electrospray interface. Modified molecules with an extra nominal mass of 572.18 Da (Table 34) were separated through a standard reverse-phase chromatography column (C18 phase) and eluted by a water:acetonitrile gradient. Molecules were detected by a mass spectrometer connected to the chromatography column exit *via* an electrospray ionization interface. Extracted ion chromatograms were used to identify the mass/charge ratio (*m*/*z*) of each TMPP-amine ion. Areas under the peaks were compared between strains.

Table 34: TMPP-modified standard amines.

Amines	Formula	Molecular weight (Da)	TMPP-modified weight (Da)
1,3-diaminopropane	$C_3H_{10}N_2$	74.13	646.264
putrescine	$C_4H_{12}N_2$	88.15	660.280
cadaverine	$C_5H_{14}N_2$	102.18	674.296
norspermidine	$C_6H_{17}N_3$	131.22	703.322
spermidine	$C_7H_{19}N_3$	145.25	717.338
spermine	$C_{10}H_{26}N_4$	202.35	774.396

5.2.2. Polyamine standards analysis

An equimolar mixture (83 pmol μl^{-1} each) of the six polyamines was prepared in Milli-Q water (Merck Millipore, Billerica, MA), and diluted at 10^{-1} and 10^{-2}, respectively. Twelve microliters of each of the three solutions were mixed with 10 µl of 20 mM TMPP (Sigma-Aldrich) in water:acetonitrile 80:20, and incubated 1 h at room temperature. Reactions were stopped by addition of 15 µl of NH_4OH (405 mM final concentration). Then, the samples were incubated for 30 min at room temperature

before the addition of 12 µl of 10% trifluoroacetic acid (TFA). A 10 µl volume of the final reaction was removed, desiccated, and resuspended in 100 µl of 2% acetonitrile (ACN)/0.1% TFA solution before injection (10 µl fractions) in LC-ESI-MS instrument (Thermo Scientific, Bremen, Germany). For that purpose, an Ultimate 3000 nanoflow high performance LC system online coupled to a Q-Exactive Orbitrap was used with a 75 µm x 150 mm Acclaim Pepmap 100 C18 3 µm nanoviper column, maintained at 35°C. Samples were loaded at 10 µl min^{-1} for 6 min on a 300 µm x 5 mm Pepmap 100 C18 5 µm microcolumn and then resolved at 300 nl min^{-1} using a linear gradient ranging from 2% to 35% acetonitrile in 0.1% (v/v) formic acid (Biosolve Chimie, Dieuze, France) during 33 min, and then from 35% to 85% during 3 min. Operating in positive polarity mode, the Q-Exactive Orbitrap acquired a full-range scan from 310 to 2000 Th (70,000 resolution, AGC target 3.10^6, maximum IT 200 ms). Softwares *Xcalibur™ 2.2* and *Chromeleon® Xpress* were used to control the LC-ESI-MS/MS instrument.

5.2.3. Surface-washed polyamines analysis

The biological samples were treated similarly to the standard amines with the following modifications. One hundred microliters of polyamines washed-out from the bacterial surface were mixed to 90 µl of TMPP. 150 µl of 1M NH_4OH and 160 µl of 10% TFA were added to the solution. Samples were then desalted by solid phase extraction using an Omics Bond Elute/C18/100 µl tip (Waters), according to the manufacturer's instructions. Amines were eluted using 50 µl of 60% ACN/0.1% TFA. Prior to LC-MS analysis, TMPP-modified samples were desiccated in a Speed vac evaporator and were re-suspended in 20 µl of 2% ACN/0.1% TFA solution. Finally, 2 µl were injected on LC-ESI-MS which corresponds to 10 µl of the initial "surface-washed" polyamines sample before reaction.

5.3. Surface polyamine sample quantification

The *m/z* ions expected for the TMPP-derivatized amines were identified from extracted ion chromatograms. Area under the peaks were collected to compare the amounts of the present amines. Data were represented as means of normalized values (log scale) of three independent experiments. A statistical Tukey's test was performed and results are presented as *P<0.05 and **P<0.01.

VI. Appendix

International Journal of Antimicrobial Agents 49 (2017) 526–535

Contents lists available at ScienceDirect

International Journal of Antimicrobial Agents

journal homepage: www.elsevier.com/locate/ijantimicag

Themed Issue: Resurrection of old antibiotics

Resistance to polymyxins in Gram-negative organisms

Katy Jeannot *, Arnaud Bolard, Patrick Plésiat

Laboratoire de bactériologie, Centre national de référence (CNR) de la résistance aux antibiotiques, Centre hospitalier universitaire (CHRU) de Besançon, boulevard Fleming, 25000 Besançon, France

ARTICLE INFO

Keywords:
Enterobacteriaceae
Pseudomonas aeruginosa
Acinetobacter baumannii
Colistin resistance
MCR-1
Two-components systems

ABSTRACT

Polymyxins have recently been re-introduced into the therapeutic arsenal to combat infections caused by multidrug-resistant Gram-negative bacteria. However, the emergence of strains resistant to these last-resort drugs is becoming a critical issue in a growing number of countries. Both intrinsic and transferable mechanisms of polymyxin resistance have been characterised. These mechanisms as well as the epidemiological data regarding four relevant bacterial pathogens (*Escherichia coli*, *Klebsiella pneumoniae*, *Acinetobacter baumannii* and *Pseudomonas aeruginosa*) are considered in this review. A special focus is made on plasmid-mediated resistance and the spread of *mcr* genes.

1. Introduction

The gradual increase in antibiotic resistance that started in the 1970s among Gram-negative bacteria is becoming a critical global issue [1–3]. Multidrug-resistant (MDR), extensively drug-resistant (XDR) and pandrug-resistant (PDR) strains of *Escherichia coli*, *Klebsiella pneumoniae*, *Acinetobacter baumannii* and *Pseudomonas aeruginosa* are now reported worldwide. Interspecies transfer of mobile genes conferring resistance to broad-spectrum β-lactams and aminoglycosides are one of the factors accounting for the progressive erosion of antimicrobial activity both in the community and hospital settings [4–6]. Because of the current shortage of novel anti-infective drugs to combat infections caused by recalcitrant isolates, the polymyxins (colistin and polymyxin B) have been re-introduced into the therapeutic arsenal as last-resort drugs [7,8]. However, as the use of these polycationic agents is increasing to treat humans and animals, bacterial resistance has emerged in many parts of the world, leaving clinicians unarmed to treat patients.

Polymyxin resistance in Gram-negative bacteria is primarily due to post-translational modification of the lipopolysaccharide (LPS) molecules that form the outer layer of the outer membrane. In most resistant strains, substituents such as 4-amino-4-deoxy-L-arabinose (L-Ara4N), phosphoethanolamine (pEtN) or galactosamine are enzymatically added to the lipid A or the LPS core; alternatively, the LPS part of the outer membrane may be completely lost in some other isolates [9–13]. By decreasing the net negative charge of phosphate residues, these LPS alterations tend to prevent the binding of polymyxin molecules to the bacterial surface and their further penetration into the cell interior where they are supposed to exert their bactericidal activity. Expression of most of the genes of the LPS modification pathway is under the control of a variety of two-component systems (TCSs) such as PhoP–PhoQ (PhoPQ) and PmrA–PmrB (PmrAB). Each of these phosphorelays is composed of a transmembrane sensor histidine kinase (e.g. PhoQ, PmrB), which is subject to self-phosphorylation under specific stress conditions, and a cognate cytoplasmic response regulator (e.g. PhoP, PmrA), which when phosphorylated by the kinase in turn modulates the expression of target genes. Some mutations in the genes encoding these TCSs result in constitutive upregulation of the LPS modification pathway and thus polymyxin resistance because of membrane impermeability. Polymyxin resistance rates are still low in many countries but are increasing steadily in some others such as Greece and Italy [14]. However, the recent identification of a plasmid-borne colistin resistance gene (*mcr-1*) in human, animal and environmental strains of Enterobacteriaceae may potentially worsen this situation at the global scale [15]. Indeed, reports from all continents multiply on the isolation of *mcr-1*-positive strains [16]. The goal of the present review is to provide readers with the most recent mechanistic and epidemiological data on polymyxin resistance in human Gram-negative pathogens.

2. Intrinsic resistance mechanisms to polymyxins in Enterobacteriaceae

2.1. Escherichia coli

The lipid A of *E. coli* contains a β-1′-6-linked glucosamine disaccharide backbone phosphorylated at the 1′ and 4′ positions, which is decorated by six fatty acyl chains. It is now well established that addition of pEtN and L-Ara4N molecules to the LPS phosphate groups by enzymes EptA and ArnT, respectively, strongly increases the

* Corresponding author. Laboratoire de bactériologie, Centre national de référence (CNR) de la résistance aux antibiotiques, Centre hospitalier universitaire (CHRU) de Besançon, boulevard Fleming, 25000 Besançon, France. Fax: +33 3 81 66 89 14.
E-mail address: katy.jeannot@univ-fcomte.fr (K. Jeannot).

http://dx.doi.org/10.1016/j.ijantimicag.2016.11.029
0924-8579/

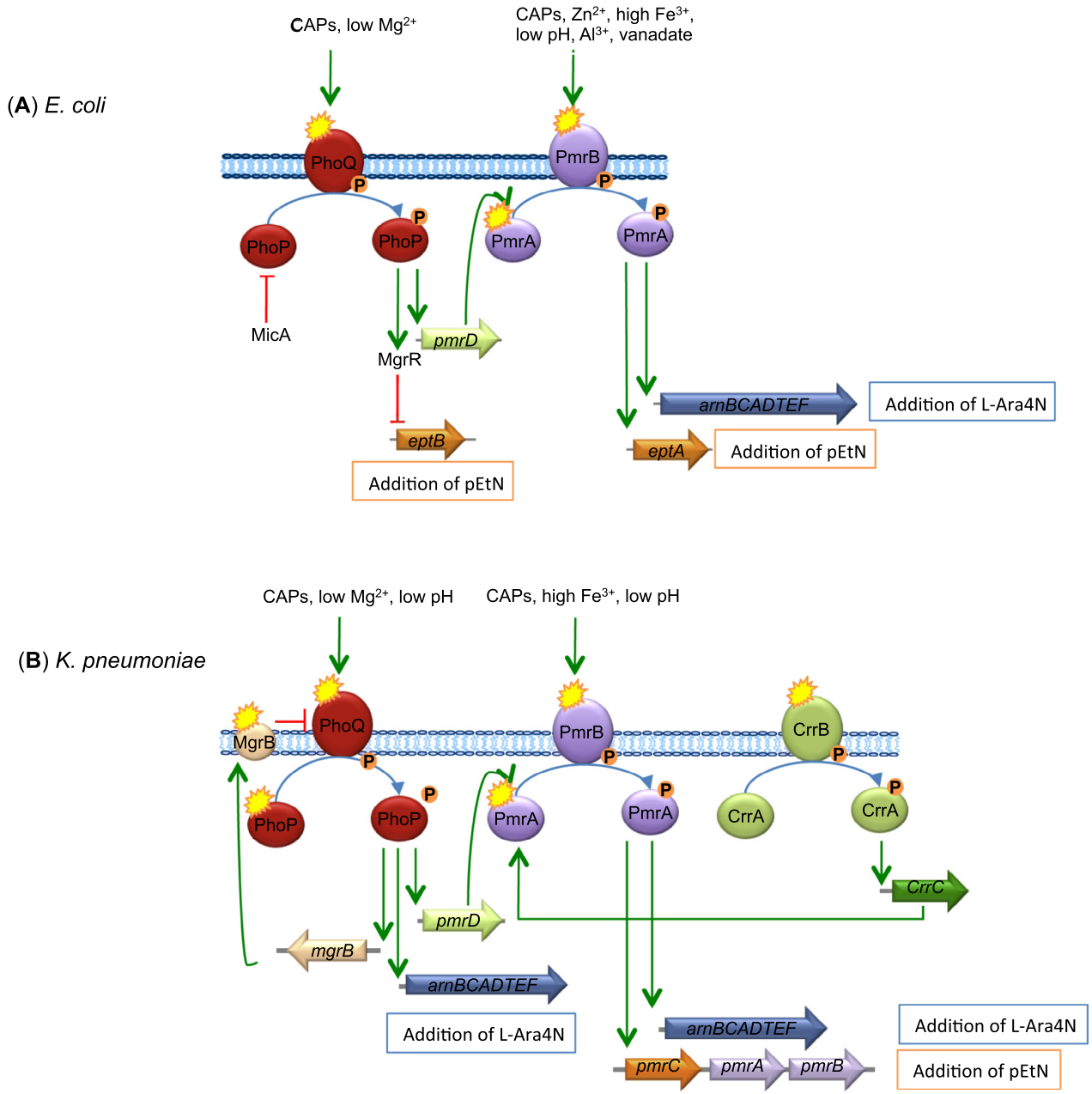

Fig. 1. Schematic representation of regulation of genes involved in polymyxin resistance in clinical isolates of (A) *Escherichia coli* and (B) *Klebsiella pneumoniae*. In both species, resistance to polymyxins is induced by cationic compounds such as colistin, low Mg^{2+} concentrations, acidic pH and high Fe^{3+} concentrations, which activate the two-component systems (TCSs) PhoPQ and/or PmrAB. Subsequent activation of operon *arnBCADTEF* (also called *pmrHFIJKLM*), the *eptA* gene or the *pmrC* gene triggers the synthesis and addition of 4-amino-4-deoxy-L-arabinose (L-Ara4N) and phosphoethanolamine (pEtN) to lipid A, respectively. PmrAB is also activated by PhoPQ via the product of the *pmrD* gene. In *K. pneumoniae* (B), the *arnBCADTEF* operon can be directly activated by PhoP. In *E. coli* only (A), a first small RNA, MgrR, directly represses the expression of *eptB*, a gene required for addition of pEtN to the lipopolysaccharide (LPS) core, whilst a second small RNA, MicA, represses the *phoP* gene. In both *E. coli* and *K. pneumoniae* (A and B) clinical isolates, alterations (represented by yellow asterisks) in histidine kinases PhoQ and PmrB or in the response regulator PmrA lead to constitutive activation of the TCSs PmrAB or PhoPQ. Furthermore, in *K. pneumoniae* (B), inactivation of *mgrB* results in colistin resistance through activation of PhoPQ, whilst mutations in histidine kinase CrrB activate PmrAB through CrrC. CAPs, cationic antimicrobial peptides (including polymyxins). (For interpretation of the references to color in this figure legend, the reader is referred to the web version of this article.)

resistance of *E. coli* to cationic antimicrobial peptides (CAPs) including colistin [minimum inhibitory concentration (MIC) × 4- to 32-fold) [9]. Various membrane stress conditions are also known to trigger LPS modification through activation of the TCSs PhoPQ and PmrAB. The inner membrane sensor PhoQ is activated when bacteria grow in low Mg^{2+} environments or in the presence of CAPs, whereas PmrB senses molecular signals generated by exposure to CAPs, acidic pH, Zn^{2+}, Al^{3+}, vanadate (VO_3^-) or high Fe^{3+} concentrations (Fig. 1A) [17–21]. As mentioned above, mutations in operons *pmrAB* and *phoPQ* or several loci (*micA*, *mgrR*, *etk*) involved in complex regulatory pathways may potentially result in constitutive activation of the *eptA* and *arnT* genes [22] (Fig. 1A). Analysis of polymyxin-resistant *E. coli* strains of human (urine, stools) or animal (swine) origin revealed the occurrence of mutations in the genes *pmrA* (R81S), *pmrB* (T156K, A159V, G161V, +I92, Δ7–12) and *phoQ* (E375K) [23–25]. More surprisingly, some of these mutations seemingly emerged in the absence of colistin treatment, thus suggesting that factors other than the polymyxin itself might select for such mutants

in vivo [26,27]. Supporting this notion, resistant *E. coli* strains (MICs of 4–16 mg/L) have been isolated in polymyxin untreated patients from Spain, Laos, the USA, Thailand, France and Nigeria [24,28,29]. The same observation was made regarding strains recovered from wild animals such as rabbits and hares [29]. Large-scale epidemiological studies show that the rates of polymyxin resistance, as defined by the European Committee on Antimicrobial Susceptibility Testing (EUCAST) (MIC > 2 mg/L), are still rather low in *E. coli* (from 0.1% to 0.6% between 2006 and 2012) [14,27,30,31].

2.2. Klebsiella pneumoniae

Polymyxin resistance would be more critical in *K. pneumoniae* than in *E. coli*, with high rates reported for this species in Europe by the European Centre for Disease Prevention and Control (ECDC) (8.2% in 2014) [14]. However, some European countries are more deeply impacted than others by colistin-resistant *K. pneumoniae*, such as Romania (25.8%), Greece (19.9%) and Italy (15.4%). According to the global SENTRY Antimicrobial Surveillance Program, the overall colistin resistance rates in the USA for *K. pneumoniae* reached 2.7% over the period 2009–2012. These rates were higher among extended-spectrum β-lactamase (ESBL)-producers (11.5%) [31]. Other data indicate that polymyxin resistance occurs more frequently among carbapenem-resistant than carbapenem-susceptible strains (29% vs. 3%) [14,32]. The increased use of colistin to combat infections caused by carbapenemase-positive *K. pneumoniae* (KPC- and VIM-producers) may have contributed to this situation in countries such as Italy (from 22.4% in 2011 to 43% in 2013–2014), Greece (from 3.5% in 2008 to 20.8% in 2010), Spain (from 13.15% in 2010 to 31.70% in 2012) and Taiwan (17% in 2012) [32–38]. In line with this, a number of hospital outbreaks due to colistin-resistant carbapenemase-producing *K. pneumoniae* have been described in Italy (KPC-2, KPC3), The Netherlands (KPC-2), the USA (KPC-2), Greece (KPC-2, VIM-1) and Israel (KPC-3) [32,39–41]. Resistance to both carbapenems and colistin is especially high, with rates ranging from 20% to 55.2% among strains from intensive care units [32,42]. However, these data should be taken with caution as the results of susceptibility testing for polymyxins are strongly dependent upon the methods and breakpoints used.

As in *E. coli*, acquisition of polymyxin resistance in *K. pneumoniae* results from the addition of L-Ara4N and/or pEtN to the lipid A. The *arnBCADTEF* operon (also called *pmrHFIJKLM* or *pbgPE*) and the *pmrC* gene that promote these modifications, respectively, are under positive control of the TCSs PhoPQ and PmrAB (Fig. 1B). Single point mutations in both TCSs have been held responsible for polymyxin resistance in clinical *K. pneumoniae*, but the real impact of these changes on the activity of the TCSs awaits further confirmation [43–47]. More evidence has accumulated on the role played by *mgrB*, a gene encoding a small regulatory transmembrane protein, MgrB, that negatively regulates the kinase activity of PhoQ and whose inactivation increases colistin resistance [48]. Whatever the genetic events leading to *mgrB* inactivation, a phosphorylation cascade involving PhoQ, PhoP, PmrD and/or PmrAB is activated that finally triggers expression of the operon *arnBCADTEF* and LPS modification (Fig. 1B) [48,49]. Alteration of the *mgrB* gene by insertion sequences (IS*5*-like, IS*1F*, IS*Kpn13*, IS*Kpn14*, IS*10R*), point mutations or indels thus represents the most common cause of polymyxin resistance in clinical *K. pneumoniae* strains [40,44,46,47,49–52]. On the other hand, the wide range of susceptibility levels (colistin MICs from 4 mg/L to >256 mg/L) exhibited by strains harbouring mutations in the genes *phoPQ*, *pmrAB* or *mgrB* suggests a role for other genetic loci in resistance. For instance, mutations (L94M, Q10L, Y31H, W140R, N141I, P151S and S195) in CrrB, the sensor kinase partner of the TCS CrrAB (for Colistin resistance regulation), were recently shown to confer elevated resistance to colistin in clinical strains (16 mg/L to >2048 mg/L) [47,52]. However, the *crrAB* genes that code for these proteins are not present in all of the genomes of *K. pneumoniae* and are absent in *E. coli*. These findings support the notion that strain-specific pathways or mechanisms might be involved in polymyxin resistance [47]. So far, *crrB* mutations have been detected in strains belonging to sequence types ST11, ST29 and ST258 only [47,52]. The mutated sensor CrrB activates PmrAB through a recently characterised connector, named CrrC, which does not contribute to but is necessary for CrrB-mediated resistance to colistin (Fig. 1B) [52]. Heteroresistance to polymyxins also illustrates the complexity of phenotypes that may arise in clinical strains of *K. pneumoniae* upon mutation. Whilst 'classical' mutants form uniform populations with individual cells exhibiting the same phenotype, heteroresistant strains give rise to subpopulations showing different susceptibility levels to polymyxins [53]. Whilst analysis of population profiles remains the gold-standard method to demonstrate heteroresistance, this can also be achieved by microdilution assays [53]. A 'skipped wells' phenomenon (wells exhibiting no growth although growth still occurs at higher concentrations) is observed with heteroresistant strains. Strains of *K. pneumoniae* with this particular phenotype should be considered resistant in light of clinical experience [54,55]. At a mechanistic level, data suggest that heteroresistance to polymyxins might result from mutations affecting the response regulator PhoP [56]. In support of this, a colistin-resistant population (MIC = 128 mg/L) exhibiting a PhoP alteration (N191T) was found to coexist with a colistin-susceptible population (0.12 mg/L) harbouring an additional mutation that inactivated PhoP and thus prevented the PhoQ-dependent activation of LPS modification [56].

2.3. Acinetobacter baumannii

Since the first description of colistin-resistant *Acinetobacter* spp. strains in the Czech Republic in 1999, similar reports from all over the world never stop increasing [57]. Global rates of colistin resistance from 0.9% to 3.3% were recorded in *A. baumannii* between 2001 and 2011 [58], although substantial differences were noted between the countries covered by the survey. For instance, polymyxin-resistant *Acinetobacter* spp. were more frequent in North America (3.5% between 2009 and 2011, 4.8% between 2009 and 2012, and 5.3% in 2010) than in Latin America (2%) [31,59–62]. These frequencies were somewhat higher in Canada (6.5%), but the panel of tested strains was too small ($n = 31$) to draw more general conclusions [27]. In Europe, the rates varied from 0.7 % to 3.9% over the period 2009–2012 [31,59,63]. However, the epidemiological situation is particularly critical in some geographical areas [14]. Among the 4% of strains reported as resistant to polymyxins in Europe, 80% were from Greece and Italy [14]. More alarming are the reports mentioning the emergence of *A. baumannii* strains resistant to both colistin and carbapenems (as a result of production of carbapenemase OXA-23 or OXA-24/40), especially in Greece (from 1% in 2012 to 21.4% in 2014) [64–71]. Some PDR bacteria were involved in hospital outbreaks in Italy and Greece [64,66,72].

Resistance to polymyxins in *A. baumannii* is primarily caused by mutations in the genes *pmrA* and/or *pmrB*. Such mutations constitutively activate the PmrAB regulatory system, which in turn upregulates expression of its own operon, *pmrCAB* [22,73–75] (Fig. 2A). The *pmrC* gene encodes an EptA-like phosphoethanolamine transferase that catalyses the addition of pEtN to the 1′- or 4′-phosphate group of lipid A. Colistin MICs ranging from 4 mg/L to up 256 mg/L were recorded in clinical strains with *pmrA*/*B* mutations, strongly suggesting that as yet unknown factors contribute to the resistance levels of hospital isolates, in addition to pEtN-mediated LPS modification. Interestingly, it was found that colistin-resistant clinical strains are able to revert to a susceptible phenotype via mutations in *pmrA*/*B*, downregulating operon *pmrCAB* expression [73,76,77].

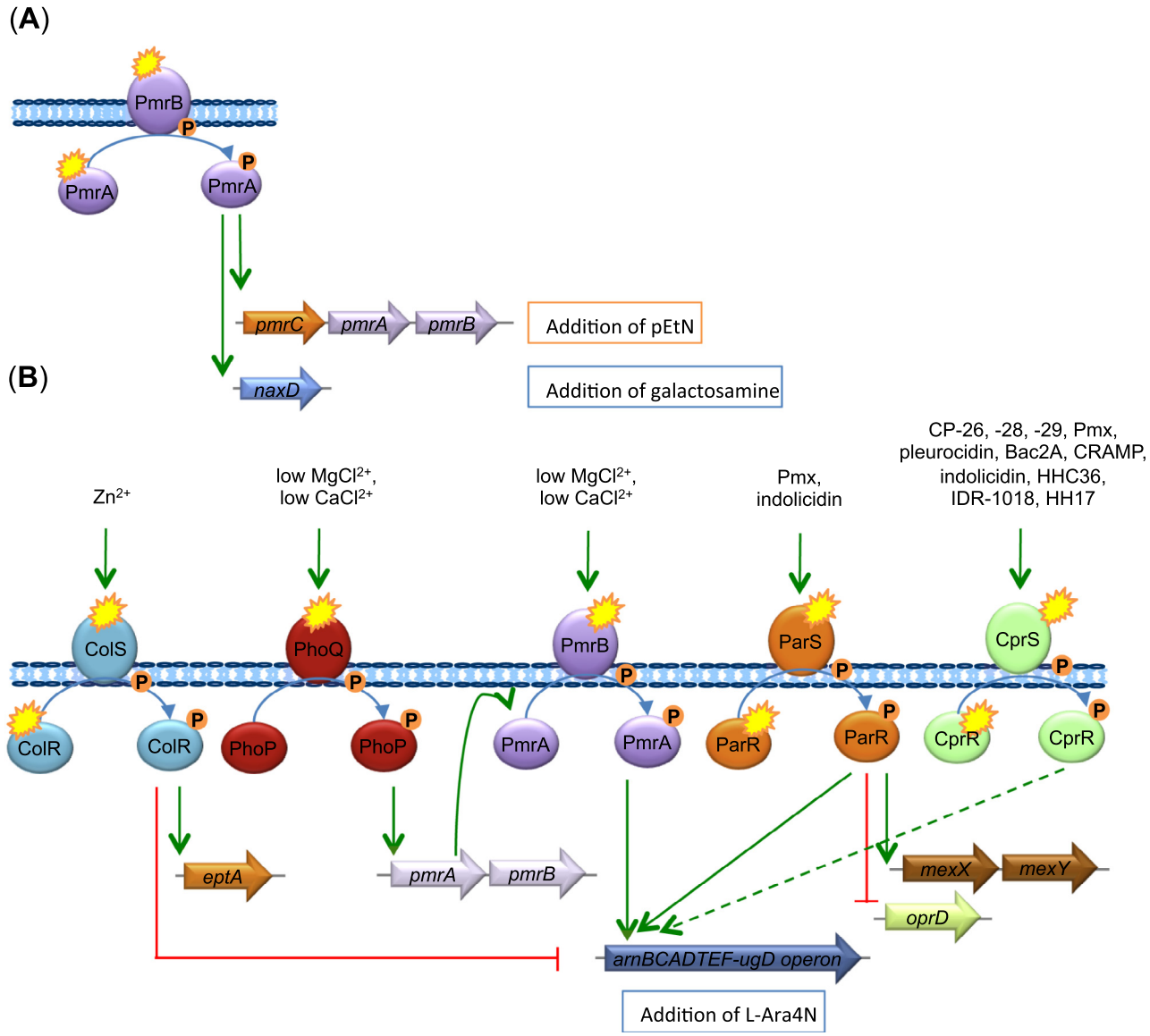

Fig. 2. Schematic representation of regulation of genes contributing to colistin resistance in clinical strains of (A) *Acinetobacter baumannii* and (B) *Pseudomonas aeruginosa*. Unlike *P. aeruginosa*, *A. baumannii* (A) does not have chromosomal genes for synthesis and transport of 4-amino-4-deoxy-L-arabinose molecules (L-Ara4N). Colistin resistance in clinical isolates is due to alterations in histidine kinase PmrB or response regulator PmrA, which activate the two-component system (TCS) PmrAB. Once activated, PmrAB upregulates *pmrC* gene expression, thus promoting addition of phosphoethanolamine (pEtN) to lipid A, and upregulates *naxD*, a gene involved in galactosamine biosynthesis. This amino sugar is added to lipid A by an unknown enzyme. In *P. aeruginosa* (B), no less than five TCSs are involved in polymyxin resistance. Two of them (ParRS and CprRS) are activated in response to polymyxin or cationic antimicrobial peptide (CAP) exposure, whereas ColRS, PhoPQ and PmrAB are activated when bacteria develop in the presence of zinc or low concentrations of divalent cations. Activation of these TCSs leads to overexpression of the operon *arnBCADTEF-ugd* and synthesis of L-Ara4N, except for ColRS that promotes the addition of pEtN and represses L-Ara4N synthesis. In clinical strains, alterations in histidine kinases PmrB, ParS and PhoQ and in the response regulator ParR (represented by yellow asterisks) result in constitutive activation of these TCSs. Mutations in CprRS and ColRS are associated with polymyxin resistance only in *phoQ* mutants. Activation of ParRS results in multidrug resistance through the induction of operons *arnBCADTEF-ugd* and *mexXY*, concomitant with gene *oprD* downregulation. Pmx, polymyxins (including colistin and polymyxin B). (For interpretation of the references to color in this figure legend, the reader is referred to the web version of this article.)

Alternatively, low to moderate colistin resistance levels in *A. baumannii* (MICs from 1.5 mg/L to 48 mg/L) may result from the addition of galactosamine to the 1′-phosphate position of lipid A, when sensor kinase PmrB is activated [12]. Recently, Chin et al. showed that expression of *naxD*, a gene encoding a deacetylase required to convert *N*-acetylgalactosamine into galactosamine prior to its addition to lipid A, depends on PmrB [78]. It is worth mentioning that unlike Enterobacteriaceae and *P. aeruginosa*, *A. baumannii* lacks all the genes required for L-Ara4N biosynthesis.

Finally, analysis of in vitro-selected mutants demonstrated that very high colistin MICs (128 mg/L) were caused by the inactivation of LPS biosynthesis genes *lpxA*, *lpxC*, *lpxD* and *lpsB*, respectively, resulting in complete loss of lipid A or the LPS core [13,79–82]. Because of their impaired fitness, as evidenced by defective growth and poor competitiveness in vitro, such mutants are rarely encountered in the clinical setting [83,84].

2.4. Pseudomonas aeruginosa

With reference to the EUCAST breakpoints, no trends in higher polymyxin resistance rates were noticed in *P. aeruginosa* strains from the USA (1.1% in 2009–2012), Canada (1.06% in 2007–2008), Europe (1.0% in 2009–2012) and Latin America (0.5% in 2011) [27,30,31,59,61–63,85]. In contrast, the situation is more worrying

Table 1
Colistin-resistant strains producing MCR-1 from several sources.

Organism	Source	Country	Year of isolation	Colistin MIC (mg/L)	Associated β-lactam resistance	Plasmid classification	Reference
Human							
Escherichia coli	Blood, faeces, bile, ascites, catheter, urine, pulmonary	China	2010–2016	4–16	TEM-1, NDM-1, NDM-5, CMY-2, CTX-M-1, CTX-M-14, CTX-M-15	IncX4, IncI2	[15,94–98]
	Blood, urine, ascites, abscess	Taiwan	2010–2014	1.5–8	CTX-M group 1	Plasmid	[99]
	Gastrostomy tube, rectum	Canada	2011	4	OXA-48	IncI2	[100]
	Faeces	Laos	2012	6–16	NA	NA	[101]
	Faeces	Thailand	2012	4–6	NA	NA	[101]
	Faeces	Cambodia	2012	–	CTX-M-55	NA	[102]
	Faeces	Netherlands [a]	2012–2013	4–8	CTX-M-1, CTX-M-14, CTX-M-55, CTX-M-65	NA	[103]
	Urine, sputum, blood, wound	Spain	2012–2015	4–12	ESBL [b]	–	[104]
	NA	Argentina	2012–2016	8–16	CTX-M-2, -14, -15	Plasmid conjugable	[105]
	Faeces, intraoperative sacral tissue	Singapore	2013	4	TEM-1A, KPC-2	IncFII, IncXI, ColpVC, IncI2, IncN	[106]
	Urine	Malaysia	2013	13	TEM-1B, DHA-1	ColRNAI, Col(MGD2), IncN, IncFIA(HI1), IncX1, IncFIB(K), IncQ1	[107]
	Blood, faeces	England, Wales	2013–2014	4	TEM-1, CTX-M-14, CTX-M-27	IncHI2, IncI2	[108]
	Faeces, urine, surgical wound	Italy	2013–2015	8	SHV-12, CTX-M-15	Non-typeable	[109,110]
	Wound	Germany	2014	2	KPC-2	IncHI2	[111]
	Blood, urine, wound, pus	South Africa	2014–2016	4–8	ESBL [b], TEM-1, CTX-M-55, CMY-2	IncI2, IncHI2, IncX4	[112,113]
	Urine	Poland	2015	3	CMY-2	IncFIB	[114]
	Blood, faeces [c], urine	Switzerland	2015	4–16	TEM, TEM-1, TEM-52, VIM-1	IncFIB, IncHI2, IncFII, IncFIB, IncX	[115–117]
	Blood	Denmark	2015	>4	TEM-1B, CMY-2, CTX-M-55	IncI2	[118]
	Sputum	Egypt	2015	16	CTX-M-15	Plasmid transferable	[119]
	Faeces	Venezuela	2015	4	TEM-1, NDM-1, ACT-15, OXA-1, CTX-M-15	IncI2	[120]
	Urine	USA	2016	4	TEM-1B, CTX-M-55	IncF	[121]
	Blood, urine, faeces	Hong Kong	2016	3–64	ESBL [b]	NA	[122]
	Wound	Brazil	2016	>4	CTX-M-8	IncX4	[123]
Enterobacter cloacae	Urine	China	2014	16	TEM-1, CTX-M-15	IncFI	[124]
	Faeces	Hong Kong	2016	64	–	NA	[122]
Enterobacter aerogenes	Vaginal secretion	China	2014	16	TEM-1, CTX-M-15	IncFI	[124]
	Urine	Singapore	2014	4	TEM-1B, KPC-2, CTX-M-15, OXA-1	IncFII, IncX4	[106]
Shigella sonnei	Faeces	Vietnam	2008	32	NA	IncI2	[125]
Salmonella serotype 1,4 [5],,12:i-	Faeces, blood	Portugal	2011–2012	4–8	TEM	IncHI2, IncX4	[126]
Salmonella Typhimurium	Faeces	England, Wales	2012–2015	4–8	TEM-1, CMY-2	IncX4, IncI, IncI2	[108]
Salmonella Paratyphi B	Faeces	England	2015	8	–	IncI2	[108]
Salmonella Virchow PT31	Faeces	England	2014	8	TEM-1	IncHI2	[108]
Klebsiella pneumoniae	Wound, peritoneal fluid	China	2014–2015	>2	NDM-5, CTX-M-1	NA	[15,95]
Foodborne							
E. coli	Chicken	Netherlands	2009–2014	3 to ≥16	TEM-1B, SHV-12, CTX-M-1	FIB, FII, HI2, HI2A, I1, I2, P, p0111	[127]
	Lean ground beef	Canada	2010	NA	None	IncHIA2	[100]
	Chicken, pork	China	2011–2014	4–8	NA	IncI2	[15]
	Vegetables	Switzerland	2012	6	CTX-M-55, CTX-M-65	Plasmid transferable	[128]
	Turkey, chicken, beef	Germany	2012–2013	4	TEM-1B, TEM-52C, OXA-1, CTX-M-1, CTX-M-14, CTX-M-15	IncHI2, IncX4	[129]
	Chicken	Denmark	2012–2014	>4	SHV-12, CMY-2	IncI2, IncX4	[118]
	Chicken, ground beef, pork	Taiwan	2012–2015	3–4	CTX-M group 1 and group 9	Plasmid	[99]
	Chicken	China	2014	8	NDM-9, CTX-M-65	IncI2	[130]
Salmonella Java	Chicken	Netherlands	2010–2015	4–16	NA	IncX4	[131]
Salmonella Anatum	Turkey	Netherlands	2013	4–16	NA	IncX4	[131]
Salmonella Schwarzengrund	Chicken breast	France	2012	≥4	NA	IncX4	[132]
Salmonella Schwarzengrund	Broiler and turkey	Netherlands	2010–2015	4–16	NA	IncX4	[131]
Salmonella enterica	Food sample	NA	2011	NA	NA	NA	[133]
Salmonella Typhimurium	Pork, poultry, cattle	Portugal	2011–2012	>4	CTX-M-1	IncHI2	[133,134]

(*continued on next page*)

Table 1 (*continued*)

Organism	Source	Country	Year of isolation	Colistin MIC (mg/L)	Associated β-lactam resistance	Plasmid classification	Reference
Salmonella Paratyphi B	Guinea fowl pie	France	2012	≥4	NA	IncX4	[132]
	Poultry	Great Britain [d]	2014	8	TEM-1	IncHI2	[108]
Salmonella Derby	Chipolata sausage	France	2013	≥4	NA	IncP	[132]
Salmonella serotype 1,4 [5],,12:i-	Boot swabs from broiler farm	France	2013	≥4	NA	IncP	[132]
	Pork	Portugal	2014–2015	4–8	TEM	IncHI2, IncX4	[126]
Salmonella Rissen	Pork	Portugal	2014–2015	4	TEM	IncX4	[126]
Animals							
E. coli	Chicken	China	1980s–2014	NA	NA	NA	[135]
	Veal calves	France	2005–2014	NA	CTX-M-1	NA	[136]
	Cattle	France	2007	4	TEM-1A, TEM-1B	IncHI2	[137]
	Swine, turkeys, broilers	France	2007–2014	4–16	CMY-2	NA	[138]
	Swine	Japan	2007–2014	8–128	NA	NA	[139]
	Swine	Germany	2010–2011	2–16	CTX-M-1	IncHI2, IncX4	[111]
	Veal calves, broilers, turkeys	Netherlands	2010–2013	4–16	–	IncHI2/ST4, IncHI2/ST2, IncHI2/P/ST3, IncHI2/P/ST4, IncHI2/P/ST6, IncX4, chromosomal	[131]
	Turkeys, swine	Spain	2010–2014	4–8	–	Plasmid	[140]
	Piglets, calves	Belgium	2011–2012	8–16	–	IncP, IncFII	[141,142]
	Swine, broilers, turkeys	France	2011–2014	4–16	CMY-2	NA	[138]
	Swine	Laos	2012	4–6	NA	NA	[101]
	Chicken, swine, poultry	Brazil	2012–2015	0.25–16	CTX-M-1, CTX-M-8, CTX-M-15, CMY-2	NA, transferable plasmid	[143,144]
	Cattle	Japan	2012–2013	4	CTX-M-27	IncHI2	[145]
	Swine	China	2012–2014	4–8	NA	IncI2	[15]
	Dairy cow	Egypt	2014	–	TEM-1	Plasmid	[146]
	Chicken	Malaysia	2013	8	TEM-1B, CTX-M-55	IncHI1A, ColpVC, IncHIB(R27), IncQ1, IncFIA(HI1), p0111, IncFIB, IncI1, IncI2, IncFIC(FII)	[107,133]
	Swine	Malaysia	2013	12	TEM-1B	IncHIB, IncHI1A, IncFIB, IncX1, IncFIC, IncFIA, IncY	[107,133]
	Swine	Vietnam	2014–2015	4–8	CTX-M-55	IncFII, IncF1A(H1), IncF1B(K), IncX1	[147]
	Chicken	Tunisia	2015	2–6	CTX-M-1	IncHI2	[148]
	Broiler	South Africa	2015	>4	CMY-2	IncI2	[149]
	Swine	Great Britain	–	8	TEM-1, LAT-1	RepB	[150]
	Chicken	Algeria	2015	4	NA	NA	[101]
	Swine	Venezuela	2015	4	NDM-1, CTX-M-2	IncI2	[120]
	Muscovy duck	China	2016	NA	TEM-1, NDM-5, CTX-M-55	IncHI2, IncI2	[151]
Salmonella Typhimurium	Swine	Spain	2009–2011	8	–	Plasmid	[140]
Salmonella Rissen	Swine	Spain	2010	8	–	Plasmid	[140]
Salmonella Typhimurium	Swine	Great Britain	–	8	TEM-1	IncI2	[150]
Salmonella Typhimurium	Swine	Japan	2013	32	NA	IncI2	[145]
Wildlife							
E. coli	Kelp gulls	Argentina	2012	4–8	CTX-M-2, CTX-M-14	IncI2	[152]
	Herring gull	Lithuania	2016	4–8	NA	NA	[153]
Environment							
E. coli	River water	Switzerland	2012	6	SHV-12	Plasmid transferable	[128]
	Pond water	Malaysia	2013	8	TEM-1B	IncFII(29), IncI2, ColRNAI, IncFIB	[107]
	Water	Malaysia	2013	NA	NA	14 kb identical to pHNSHP45	[133]
	Lairage area	Vietnam	2014–2015	4–8	NA	NA	[147]

MIC, minimum inhibitory concentration; NA, not available; ESBL, extended-spectrum β-lactamase.

[a] After travelling in Tunisia, Peru, Bolivia, Colombia, Thailand, Vietnam, Cambodia or Laos.

[b] The type of ESBL was not determined.

[c] After travelling in India.

[d] Imported from Europe.

in China where 22.2% of XDR bacteraemic *P. aeruginosa* turned out to be resistant to polymyxin B in a 2013 study [86].

In *P. aeruginosa*, development of polymyxin resistance relies on the covalent addition of L-Ara4N to the phosphate groups of lipid A [11]. As in Enterobacteriaceae, a large operon called *arnBCADTEF-ugd* encodes all of the enzymes needed for synthesis, transmembrane transport and attachment of L-Ara4N [87]. Intensive research in the field has demonstrated that at least five TCSs may potentially play a role in polymyxin resistance, namely PhoPQ, PmrAB, ParRS, CprRS and ColRS (Fig. 2B) [22]. Mutational alterations of proteins PmrB, PhoQ, ParR and ParS are found in clinical strains exhibiting various degrees of colistin resistance (from 2 mg/L to >512 mg/L). All of the reported mutations cause constitutive overexpression of the LPS modification operon *arn*, either by activating one of the components of an individual TCS (e.g. PmrB, ParS, ParR) or by inactivating sensor kinase PhoQ [88–91]. Indeed, PhoQ acts as a repressor of PhoP transcriptional activity. Loss-of-function mutations in PhoQ thus allow PhoP to induce *arn* operon expression. This explains why secondary mutations that inactivate PhoP completely restore polymyxin susceptibility in clinical strains [91]. Higher polymyxin MICs may be reached in PhoQ-deficient mutants when additional alterations affect CprS, CprR, ColS or ColR [92]. Interestingly too is the observation that mutations in ParS or ParR not only lead to modification of LPS but also to increased production of the multidrug efflux system MexXY(OprM) and concomitant downregulation of carbapenem-specific porin OprD, mechanisms that together confer low to moderate resistance levels to four classes of antibiotics, namely polymyxins, aminoglycosides, fluoroquinolones and β-lactams (Fig. 2B) [93].

3. Acquisition of foreign DNA (*mcr* genes)

In addition to the mutation-based mechanisms described above, acquisition of plasmid-borne genes *mcr-1*, *mcr-1.2* and *mcr-2* very recently turned out to be a major cause of polymyxin resistance in *E. coli*, *K. pneumoniae*, *Shigella sonnei* and *Salmonella enterica*. Since its first report in China in November 2015 [15], *mcr-1* has been detected in Enterobacteriaceae strains from five continents, both from colonised and infected humans, from food (meat and vegetables), from farm and wild animals, and from aquatic environments (Table 1). The *mcr-2* gene was next detected in bovine and porcine *E. coli* isolates from Belgium [154]. However, the emergence and diffusion of the MCR enzymes is not recent and could be traced back to the 1980s in China and in 2005 in France, in isolates recovered from chickens and veal calves, respectively [135,136]. MCR enzymes generally confer low to moderate polymyxin resistance (from 4 mg/L to 16 mg/L). However, it should be noted that some *mcr-1*-positive *E. coli* are classified as susceptible with reference to the EUCAST breakpoint of 2 mg/L as their resistance levels to polymyxins range from 0.25 mg/L to 2 mg/L [99,143].

The phosphoethanolamine transferases encoded by genes *mcr-1* and *mcr-2*, respectively, share 80.65% identity at the amino acid sequence level. Their closest homologues have been found in *Paenibacillus sophorae* (63% identity) and *Moraxella osloensis* (64% identity). Predictive models of protein structure as well as analysis of key residues located in the catalytic site of MCR-1 suggest structural similarities with enzymes LptA and EptC from *Neisseria meningitidis* and *Campylobacter jejuni*, respectively [15,154–156]. A domain of the enzyme is inserted in the inner membrane, whilst the C-terminal catalytic sulfatase domain is periplasmic. This latter allows the addition of a pEtN moiety resulting from the cleavage of phosphatidylethanolamine to the outer 3-deoxy-D-manno-octulosonic acid (Kdo) residue of LPS [157]. The mechanism by which the MCR enzymes promote polymyxin resistance is not different from that found in intrinsically resistant Gram-negative species. The same strategy based on the addition of pEtN to LPS is seen in resistant strains of *E. coli*, *K. pneumoniae* or *A. baumannii* with mutations in regulatory genes *ept*.

A major concern with *mcr* genes is their location on transferable plasmids such as pHNSHP45 (*mcr-1* gene, IncI2; 64 105 bp) and pKP37-BE (*mcr-2* gene, IncX4; 35 104 bp), which can both easily propagate (10^{-1} to 10^{-3}) by conjugation among *E. coli* strains [15,154]. Furthermore, pHNSHP45 could be transmitted to *K. pneumoniae* and *P. aeruginosa* by in vitro transformation. Unlike *K. pneumoniae*, so far no clinical or environmental strains of *P. aeruginosa* or *A. baumannii* has been reported to harbour *mcr* genes, but this may be just a matter of time. Most of the plasmids carrying *mcr-1* belong to the incompatibility groups IncI2, IncHI2 and IncX4, whilst some belong to the groups IncF, IncN, IncP, IncQ and IncX. To date, the *mcr-2* gene was detected on an IncX4 plasmid only [154]. Investigations on the genetic environment of *mcr* genes revealed the presence of the insertion sequence IS*Apl1* upstream of *mcr-1* and of an IS belonging to the IS*1595* superfamily ahead of *mcr-2*, suggesting that both genes can be mobilised by these elements. The variety of *mcr-1*-bearing plasmids discovered in Enterobacteriaceae from different continents highlights the capacity of this gene to spread. Its integration into the bacterial chromosome occurs in some strains. Its higher occurrence in bacteria harbouring genes coding for carbapenemases and/or ESBLs (e.g. CTX-M-15 and CTX-M-55) likely results from multiple and complex genetic events selected under antibiotic pressure (Table 1). For instance, the *mcr-1* gene was detected in *E. coli* strains producing various carbapenemases such as NDM-1 (China, Venezuela), NDM-5 (China), KPC-2 (Germany, Singapore), OXA-48 (Canada) and VIM-1 (Switzerland) [94,100,111,115]. Similarly, a clinical isolate of *K. pneumoniae* producing the metallo-β-lactamase NDM-5 was found to be *mcr-1*-positive [95]. In a large-scale SENTRY survey conducted in 2014 and 2015, 4.4% (331/7480 strains) of *K. pneumoniae* and 0.4% (59/13 526) of *E. coli* from Europe, Latin America, North America and the Asia-Pacific region were scored colistin-resistant (MIC ≥ 4 mg/L). All of the *mcr-1*-positive strains (19/59; 32.2%) belonged to the species *E. coli*, with an overall prevalence of 0.1% in this species, and were susceptible to carbapenems [158]. New surveys will be needed in the future to determine whether *mcr* genes continue to spread among Enterobacteriaceae and will diffuse in non-fermenters such as *P. aeruginosa* and *A. baumannii*.

Funding: The French National Reference Centre for Antibiotic Resistance is funded by the French Ministry of Health through the agency Santé publique France.

Competing interests: None declared.

Ethical approval: Not required.

References

[1] Boucher HW, Talbot GH, Bradley JS, Edwards JE, Gilbert D, Rice LB, et al. Bad bugs, no drugs: no ESKAPE! An update from the Infectious Diseases Society of America. Clin Infect Dis 2009;48:1–12.
[2] US Centers for Disease Control and Prevention (CDC). Antibiotic resistance threats in the United States. Atlanta, GA: CDC; 2013.
[3] Shlaes DM, Sahm D, Opiela C, Spellberg B. The FDA reboot of antibiotic development. Antimicrob Agents Chemother 2013;57:4605–7.
[4] Tzouvelekis LS, Markogiannakis A, Psichogiou M, Tassios PT, Daikos GL. Carbapenemases in *Klebsiella pneumoniae* and other Enterobacteriaceae: an evolving crisis of global dimensions. Clin Microbiol Rev 2012;25:682–707.
[5] Munoz-Price LS, Poirel L, Bonomo RA, Schwaber MJ, Daikos GL, Cormican M, et al. Clinical epidemiology of the global expansion of *Klebsiella pneumoniae* carbapenemases. Lancet Infect Dis 2013;13:785–96.
[6] Kempf M, Rolain JM. Emergence of resistance to carbapenems in *Acinetobacter baumannii* in Europe: clinical impact and therapeutic options. Int J Antimicrob Agents 2012;39:105–14.
[7] European Centre for Disease Prevention and Control (ECDC). Summary of the latest data on antibiotic consumption in the European Union. ESAC-Net data. Stockholm, Sweden: ECDC; 2015.
[8] Biswas S, Brunel JM, Dubus JC, Reynaud-Gaubert M, Rolain JM. Colistin: an update on the antibiotic of the 21st century. Expert Rev Anti Infect Ther 2012;10:917–34.

[9] Trent MS. Biosynthesis, transport, and modification of lipid A. Biochem Cell Biol 2004;82:71–86.
[10] Ernst RK, Guina T, Miller SI. *Salmonella* Typhimurium outer membrane remodeling: role in resistance to host innate immunity. Microbes Infect 2001;3:1327–34.
[11] Moskowitz SM, Ernst RK, Miller SI. PmrAB, a two-component regulatory system of *Pseudomonas aeruginosa* that modulates resistance to cationic antimicrobial peptides and addition of aminoarabinose to lipid A. J Bacteriol 2004;186:575–9.
[12] Pelletier MR, Casella LG, Jones JW, Adams MD, Zurawski DV, Hazlett KR, et al. Unique structural modifications are present in the lipopolysaccharide from colistin-resistant strains of *Acinetobacter baumannii*. Antimicrob Agents Chemother 2013;57:4831–40.
[13] Moffatt JH, Harper M, Harrison P, Hale JD, Vinogradov E, Seemann T, et al. Colistin resistance in *Acinetobacter baumannii* is mediated by complete loss of lipopolysaccharide production. Antimicrob Agents Chemother 2010;54: 4971–7.
[14] European Centre for Disease Prevention and Control (ECDC). Antimicrobial resistance surveillance in Europe 2014. Annual report of the European Antimicrobial Resistance Surveillance Network (EARS-Net). Stockholm, Sweden: ECDC; 2015.
[15] Liu YY, Wang Y, Walsh TR, Yi LX, Zhang R, Spencer J, et al. Emergence of plasmid-mediated colistin resistance mechanism MCR-1 in animals and human beings in China: a microbiological and molecular biological study. Lancet Infect Dis 2016;16:161–8.
[16] Skov RL, Monnet DL. Plasmid-mediated colistin resistance (*mcr-1* gene): three months later, the story unfolds. Euro Surveill 2016;21:doi:10.2807/1560-7917.ES.2016.21.9.30155.
[17] Gunn JS, Richards SM. Recognition and integration of multiple environmental signals by the bacterial sensor kinase PhoQ. Cell Host Microbe 2007;1:163–5.
[18] Wosten MM, Kox LF, Chamnongpol S, Soncini FC, Groisman EA. A signal transduction system that responds to extracellular iron. Cell 2000;103:113–25.
[19] Perez JC, Groisman EA. Acid pH activation of the PmrA/PmrB two-component regulatory system of *Salmonella enterica*. Mol Microbiol 2007;63:283–93.
[20] Zhou Z, Lin S, Cotter RJ, Raetz CR. Lipid A modifications characteristic of *Salmonella typhimurium* are induced by NH_4VO_3 in *Escherichia coli* K12. Detection of 4-amino-4-deoxy-L-arabinose, phosphoethanolamine and palmitate. J Biol Chem 1999;274:18503–14.
[21] Nishino K, Hsu FF, Turk J, Cromie MJ, Wosten MM, Groisman EA. Identification of the lipopolysaccharide modifications controlled by the *Salmonella* PmrA/PmrB system mediating resistance to Fe(III) and Al(III). Mol Microbiol 2006;61:645–54.
[22] Olaitan AO, Morand S, Rolain JM. Mechanisms of polymyxin resistance: acquired and intrinsic resistance in bacteria. Front Microbiol 2014;5:643.
[23] Olaitan AO, Thongmalayvong B, Akkhavong K, Somphavong S, Paboriboune P, Khounsy S, et al. Clonal transmission of a colistin-resistant *Escherichia coli* from a domesticated pig to a human in Laos. J Antimicrob Chemother 2015;70:3402–4.
[24] Olaitan AO, Morand S, Rolain JM. Emergence of colistin-resistant bacteria in humans without colistin usage: a new worry and cause for vigilance. Int J Antimicrob Agents 2016;47:1–3.
[25] Quesada A, Porrero MC, Tellez S, Palomo G, Garcia M, Dominguez L. Polymorphism of genes encoding PmrAB in colistin-resistant strains of *Escherichia coli* and *Salmonella enterica* isolated from poultry and swine. J Antimicrob Chemother 2015;70:71–4.
[26] Urban C, Tiruvury H, Mariano N, Colon-Urban R, Rahal JJ. Polymyxin-resistant clinical isolates of *Escherichia coli*. Antimicrob Agents Chemother 2011;55: 388–9.
[27] Walkty A, DeCorby M, Nichol K, Karlowsky JA, Hoban DJ, Zhanel GG. In vitro activity of colistin (polymyxin E) against 3,480 isolates of Gram-negative bacilli obtained from patients in Canadian hospitals in the CANWARD study, 2007–2008. Antimicrob Agents Chemother 2009;53:4924–6.
[28] Prim N, Rivera A, Espanol M, Mirelis B, Coll P. In vivo adaptive resistance to colistin in *Escherichia coli* isolates. Clin Infect Dis 2015;61:1628–9.
[29] Dotto G, Giacomelli M, Grilli G, Ferrazzi V, Carattoli A, Fortini D, et al. High prevalence of *oqxAB* in *Escherichia coli* isolates from domestic and wild lagomorphs in Italy. Microb Drug Resist 2014;20:118–23.
[30] Gales AC, Jones RN, Sader HS. Contemporary activity of colistin and polymyxin B against a worldwide collection of Gram-negative pathogens: results from the SENTRY Antimicrobial Surveillance Program (2006–09). J Antimicrob Chemother 2011;66:2070–4.
[31] Sader HS, Farrell DJ, Flamm RK, Jones RN. Antimicrobial susceptibility of Gram-negative organisms isolated from patients hospitalised with pneumonia in US and European hospitals: results from the SENTRY Antimicrobial Surveillance Program, 2009–2012. Int J Antimicrob Agents 2014;43:328–34.
[32] Ah YM, Kim AJ, Lee JY. Colistin resistance in *Klebsiella pneumoniae*. Int J Antimicrob Agents 2014;44:8–15.
[33] Monaco M, Giani T, Raffone M, Arena F, Garcia-Fernandez A, Pollini S, et al. Colistin resistance superimposed to endemic carbapenem-resistant *Klebsiella pneumoniae*: a rapidly evolving problem in Italy, November 2013 to April 2014. Euro Surveill 2014;19:pii: 20939.
[34] Parisi SG, Bartolini A, Santacatterina E, Castellani E, Ghirardo R, Berto A, et al. Prevalence of *Klebsiella pneumoniae* strains producing carbapenemases and increase of resistance to colistin in an Italian teaching hospital from January 2012 to December 2014. BMC Infect Dis 2015;15:244.
[35] Zagorianou A, Sianou E, Iosifidis E, Dimou V, Protonotariou E, Miyakis S, et al. Microbiological and molecular characteristics of carbapenemase-producing *Klebsiella pneumoniae* endemic in a tertiary Greek hospital during 2004–2010. Euro Surveill 2012;17:pii: 20088.
[36] Pena I, Picazo JJ, Rodriguez-Avial C, Rodriguez-Avial I. Carbapenemase-producing Enterobacteriaceae in a tertiary hospital in Madrid, Spain: high percentage of colistin resistance among VIM-1-producing *Klebsiella pneumoniae* ST11 isolates. Int J Antimicrob Agents 2014;43:460–4.
[37] Capone A, Giannella M, Fortini D, Giordano A, Meledandri M, Ballardini M, et al. High rate of colistin resistance among patients with carbapenem-resistant *Klebsiella pneumoniae* infection accounts for an excess of mortality. Clin Microbiol Infect 2013;19:E23–30.
[38] Chiu SK, Wu TL, Chuang YC, Lin JC, Fung CP, Lu PL, et al. National surveillance study on carbapenem non-susceptible *Klebsiella pneumoniae* in Taiwan: the emergence and rapid dissemination of KPC-2 carbapenemase. PLoS ONE 2013;8:e69428.
[39] Giani T, Arena F, Vaggelli G, Conte V, Chiarelli A, Henrici De Angelis L, et al. Large nosocomial outbreak of colistin-resistant, carbapenemase-producing *Klebsiella pneumoniae* traced to clonal expansion of an *mgrB* deletion mutant. J Clin Microbiol 2015;53:3341–4.
[40] Cannatelli A, Giani T, D'Andrea MM, Di Pilato V, Arena F, Conte V, et al. MgrB inactivation is a common mechanism of colistin resistance in KPC-producing *Klebsiella pneumoniae* of clinical origin. Antimicrob Agents Chemother 2014;58:5696–703.
[41] Weterings V, Zhou K, Rossen JW, van Stenis D, Thewessen E, Kluytmans J, et al. An outbreak of colistin-resistant *Klebsiella pneumoniae* carbapenemase-producing *Klebsiella pneumoniae* in The Netherlands (July to December 2013), with inter-institutional spread. Eur J Clin Microbiol Infect Dis 2015;34:1647–55.
[42] Meletis G, Oustas E, Botziori C, Kakasi E, Koteli A. Containment of carbapenem resistance rates of *Klebsiella pneumoniae* and *Acinetobacter baumannii* in a Greek hospital with a concomitant increase in colistin, gentamicin and tigecycline resistance. New Microbiol 2015;38:417–21.
[43] Cannatelli A, Di Pilato V, Giani T, Arena F, Ambretti S, Gaibani P, et al. In vivo evolution to colistin resistance by PmrB sensor kinase mutation in KPC-producing *Klebsiella pneumoniae* is associated with low-dosage colistin treatment. Antimicrob Agents Chemother 2014;58:4399–403.
[44] Olaitan AO, Diene SM, Kempf M, Berrazeg M, Bakour S, Gupta SK, et al. Worldwide emergence of colistin resistance in *Klebsiella pneumoniae* from healthy humans and patients in Lao PDR, Thailand, Israel, Nigeria and France owing to inactivation of the PhoP/PhoQ regulator *mgrB*: an epidemiological and molecular study. Int J Antimicrob Agents 2014;44:500–7.
[45] Jayol A, Poirel L, Brink A, Villegas MV, Yilmaz M, Nordmann P. Resistance to colistin associated with a single amino acid change in protein PmrB among *Klebsiella pneumoniae* isolates of worldwide origin. Antimicrob Agents Chemother 2014;58:4762–6.
[46] Cheng YH, Lin TL, Pan YJ, Wang YP, Lin YT, Wang JT. Colistin resistance mechanisms in *Klebsiella pneumoniae* strains from Taiwan. Antimicrob Agents Chemother 2015;59:2909–13.
[47] Wright MS, Suzuki Y, Jones MB, Marshall SH, Rudin SD, van Duin D, et al. Genomic and transcriptomic analyses of colistin-resistant clinical isolates of *Klebsiella pneumoniae* reveal multiple pathways of resistance. Antimicrob Agents Chemother 2015;59:536–43.
[48] Lippa AM, Goulian M. Feedback inhibition in the PhoQ/PhoP signaling system by a membrane peptide. PLoS Genet 2009;5:e1000788.
[49] Cannatelli A, D'Andrea MM, Giani T, Di Pilato V, Arena F, Ambretti S, et al. In vivo emergence of colistin resistance in *Klebsiella pneumoniae* producing KPC-type carbapenemases mediated by insertional inactivation of the PhoQ/PhoP *mgrB* regulator. Antimicrob Agents Chemother 2013;57:5521–6.
[50] Lopez-Camacho E, Gomez-Gil R, Tobes R, Manrique M, Lorenzo M, Galvan B, et al. Genomic analysis of the emergence and evolution of multidrug resistance during a *Klebsiella pneumoniae* outbreak including carbapenem and colistin resistance. J Antimicrob Chemother 2014;69:632–6.
[51] Poirel L, Jayol A, Bontron S, Villegas MV, Ozdamar M, Turkoglu S, et al. The *mgrB* gene as a key target for acquired resistance to colistin in *Klebsiella pneumoniae*. J Antimicrob Chemother 2015;70:75–80.
[52] Cheng YH, Lin TL, Lin YT, Wang JT. Amino acid substitutions of CrrB responsible for resistance to colistin through CrrC in *Klebsiella pneumoniae*. Antimicrob Agents Chemother 2016;60:3709–16.
[53] El-Halfawy OM, Valvano MA. Antimicrobial heteroresistance: an emerging field in need of clarity. Clin Microbiol Rev 2015;28:191–207.
[54] Poudyal A, Howden BP, Bell JM, Gao W, Owen RJ, Turnidge JD, et al. In vitro pharmacodynamics of colistin against multidrug-resistant *Klebsiella pneumoniae*. J Antimicrob Chemother 2008;62:1311–18.
[55] Meletis G, Tzampaz E, Sianou E, Tzavaras I, Sofianou D. Colistin heteroresistance in carbapenemase-producing *Klebsiella pneumoniae*. J Antimicrob Chemother 2011;66:946–7.
[56] Jayol A, Nordmann P, Brink A, Poirel L. Heteroresistance to colistin in *Klebsiella pneumoniae* associated with alterations in the PhoPQ regulatory system. Antimicrob Agents Chemother 2015;59:2780–4.
[57] Hejnar P, Kolar M, Hajek V. Characteristics of *Acinetobacter* strains (phenotype classification, antibiotic susceptibility and production of β-lactamases) isolated from haemocultures from patients at the Teaching Hospital in Olomouc. Acta Univ Palacki Olomuc Fac Med 1999;142:73–7.
[58] Cai Y, Chai D, Wang R, Liang B, Bai N. Colistin resistance of *Acinetobacter baumannii*: clinical reports, mechanisms and antimicrobial strategies. J Antimicrob Chemother 2012;67:1607–15.
[59] Sader HS, Farrell DJ, Flamm RK, Jones RN. Antimicrobial susceptibility of Gram-negative organisms isolated from patients hospitalized in intensive care

units in United States and European hospitals (2009–2011). Diagn Microbiol Infect Dis 2014;78:443–8.
[60] Queenan AM, Pillar CM, Deane J, Sahm DF, Lynch AS, Flamm RK, et al. Multidrug resistance among *Acinetobacter* spp. in the USA and activity profile of key agents: results from CAPITAL Surveillance 2010. Diagn Microbiol Infect Dis 2012;73:267–70.
[61] Gales AC, Castanheira M, Jones RN, Sader HS. Antimicrobial resistance among Gram-negative bacilli isolated from Latin America: results from SENTRY Antimicrobial Surveillance Program (Latin America, 2008–2010). Diagn Microbiol Infect Dis 2012;73:354–60.
[62] Jones RN, Guzman-Blanco M, Gales AC, Gallegos B, Castro AL, Martino MD, et al. Susceptibility rates in Latin American nations: report from a regional resistance surveillance program (2011). Braz J Infect Dis 2013;17:672–81.
[63] Jones RN, Flonta M, Gurler N, Cepparulo M, Mendes RE, Castanheira M. Resistance surveillance program report for selected European nations (2011). Diagn Microbiol Infect Dis 2014;78:429–36.
[64] Oikonomou O, Sarrou S, Papagiannitsis CC, Georgiadou S, Mantzarlis K, Zakynthinos E, et al. Rapid dissemination of colistin and carbapenem resistant *Acinetobacter baumannii* in Central Greece: mechanisms of resistance, molecular identification and epidemiological data. BMC Infect Dis 2015;15:559.
[65] Mavroidi A, Likousi S, Palla E, Katsiari M, Roussou Z, Maguina A, et al. Molecular identification of tigecycline- and colistin-resistant carbapenemase-producing *Acinetobacter baumannii* from a Greek hospital from 2011 to 2013. J Med Microbiol 2015;64:993–7.
[66] Agodi A, Voulgari E, Barchitta M, Quattrocchi A, Bellocchi P, Poulou A, et al. Spread of a carbapenem- and colistin-resistant *Acinetobacter baumannii* ST2 clonal strain causing outbreaks in two Sicilian hospitals. J Hosp Infect 2014;86:260–6.
[67] Bakour S, Olaitan AO, Ammari H, Touati A, Saoudi S, Saoudi K, et al. Emergence of colistin- and carbapenem-resistant *Acinetobacter baumannii* ST2 clinical isolate in Algeria: first case report. Microb Drug Resist 2015;21:279–85.
[68] Rolain JM, Diene SM, Kempf M, Gimenez G, Robert C, Raoult D. Real-time sequencing to decipher the molecular mechanism of resistance of a clinical pan-drug-resistant *Acinetobacter baumannii* isolate from Marseille, France. Antimicrob Agents Chemother 2013;57:592–6.
[69] Qureshi ZA, Hittle LE, O'Hara JA, Rivera JI, Syed A, Shields RK, et al. Colistin-resistant *Acinetobacter baumannii*: beyond carbapenem resistance. Clin Infect Dis 2015;60:1295–303.
[70] Park YK, Choi JY, Jung SI, Park KH, Lee H, Jung DS, et al. Two distinct clones of carbapenem-resistant *Acinetobacter baumannii* isolates from Korean hospitals. Diagn Microbiol Infect Dis 2009;64:389–95.
[71] Mahamat A, Bertrand X, Moreau B, Hommel D, Couppie P, Simonnet C, et al. Clinical epidemiology and resistance mechanisms of carbapenem-resistant *Acinetobacter baumannii*, French Guiana, 2008–2014. Int J Antimicrob Agents 2016;48:51–5.
[72] Valencia R, Arroyo LA, Conde M, Aldana JM, Torres MJ, Fernandez-Cuenca F, et al. Nosocomial outbreak of infection with pan-drug-resistant *Acinetobacter baumannii* in a tertiary care university hospital. Infect Control Hosp Epidemiol 2009;30:257–63.
[73] Adams MD, Nickel GC, Bajaksouzian S, Lavender H, Murthy AR, Jacobs MR, et al. Resistance to colistin in *Acinetobacter baumannii* associated with mutations in the PmrAB two-component system. Antimicrob Agents Chemother 2009;53:3628–34.
[74] Lesho E, Yoon EJ, McGann P, Snesrud E, Kwak Y, Milillo M, et al. Emergence of colistin-resistance in extremely drug-resistant *Acinetobacter baumannii* containing a novel *pmrCAB* operon during colistin therapy of wound infections. J Infect Dis 2013;208:1142–51.
[75] Lim TP, Ong RT, Hon PY, Hawkey J, Holt KE, Koh TH, et al. Multiple genetic mutations associated with polymyxin resistance in *Acinetobacter baumannii*. Antimicrob Agents Chemother 2015;59:7899–902.
[76] Snitkin ES, Zelazny AM, Gupta J, Program NCS, Palmore TN, Murray PR, et al. Genomic insights into the fate of colistin resistance and *Acinetobacter baumannii* during patient treatment. Genome Res 2013;23:1155–62.
[77] Cheah SE, Johnson MD, Zhu Y, Tsuji BT, Forrest A, Bulitta JB, et al. Polymyxin resistance in *Acinetobacter baumannii:* genetic mutations and transcriptomic changes in response to clinically relevant dosage regimens. Sci Rep 2016;6:26233.
[78] Chin CY, Gregg KA, Napier BA, Ernst RK, Weiss DS. A PmrB-regulated deacetylase required for lipid A modification and polymyxin resistance in *Acinetobacter baumannii*. Antimicrob Agents Chemother 2015;59:7911–14.
[79] Moffatt JH, Harper M, Adler B, Nation RL, Li J, Boyce JD. Insertion sequence IS*Aba11* is involved in colistin resistance and loss of lipopolysaccharide in *Acinetobacter baumannii*. Antimicrob Agents Chemother 2011;55:3022–4.
[80] Hood MI, Becker KW, Roux CM, Dunman PM, Skaar EP. Genetic determinants of intrinsic colistin tolerance in *Acinetobacter baumannii*. Infect Immun 2013;81:542–51.
[81] Lean SS, Suhaili Z, Ismail S, Rahman NI, Othman N, Abdullah FH, et al. Prevalence and genetic characterization of carbapenem- and polymyxin-resistant *Acinetobacter baumannii* isolated from a tertiary hospital in Terengganu, Malaysia. ISRN Microbiol 2014;2014:953417.
[82] Lean SS, Yeo CC, Suhaili Z, Thong KL. Comparative genomics of two ST 195 carbapenem-resistant *Acinetobacter baumannii* with different susceptibility to polymyxin revealed underlying resistance mechanism. Front Microbiol 2015;6:1445.
[83] Beceiro A, Moreno A, Fernandez N, Vallejo JA, Aranda J, Adler B, et al. Biological cost of different mechanisms of colistin resistance and their impact on virulence in *Acinetobacter baumannii*. Antimicrob Agents Chemother 2014;58:518–26.
[84] Durante-Mangoni E, Del Franco M, Andini R, Bernardo M, Giannouli M, Zarrilli R. Emergence of colistin resistance without loss of fitness and virulence after prolonged colistin administration in a patient with extensively drug-resistant *Acinetobacter baumannii*. Diagn Microbiol Infect Dis 2015;82:222–6.
[85] Mendes RE, Mendoza M, Banga Singh KK, Castanheira M, Bell JM, Turnidge JD, et al. Regional resistance surveillance program results for 12 Asia-Pacific nations (2011). Antimicrob Agents Chemother 2013;57:5721–6.
[86] Xu A, Zheng B, Xu YC, Huang ZG, Zhong NS, Zhuo C. National epidemiology of carbapenem-resistant and extensively drug-resistant Gram-negative bacteria isolated from blood samples in China in 2013. Clin Microbiol Infect 2016;22(Suppl. 1):S1–8.
[87] Gunn JS, Lim KB, Krueger J, Kim K, Guo L, Hackett M, et al. *pmrA–pmrB*-regulated genes necessary for 4-aminoarabinose lipid A modification and polymyxin resistance. Mol Microbiol 1998;27:1171–82.
[88] Moskowitz SM, Brannon MK, Dasgupta N, Pier M, Sgambati N, Miller AK, et al. PmrB mutations promote polymyxin resistance of *Pseudomonas aeruginosa* isolated from colistin-treated cystic fibrosis patients. Antimicrob Agents Chemother 2012;56:1019–30.
[89] Abraham N, Kwon DH. A single amino acid substitution in PmrB is associated with polymyxin B resistance in clinical isolate of *Pseudomonas aeruginosa*. FEMS Microbiol Lett 2009;298:249–54.
[90] Barrow K, Kwon DH. Alterations in two-component regulatory systems of *phoPQ* and *pmrAB* are associated with polymyxin B resistance in clinical isolates of *Pseudomonas aeruginosa*. Antimicrob Agents Chemother 2009;53:5150–4.
[91] Miller AK, Brannon MK, Stevens L, Johansen HK, Selgrade SE, Miller SI, et al. PhoQ mutations promote lipid A modification and polymyxin resistance of *Pseudomonas aeruginosa* found in colistin-treated cystic fibrosis patients. Antimicrob Agents Chemother 2011;55:5761–9.
[92] Gutu AD, Sgambati N, Strasbourger P, Brannon MK, Jacobs MA, Haugen E, et al. Polymyxin resistance of *Pseudomonas aeruginosa phoQ* mutants is dependent on additional two-component regulatory systems. Antimicrob Agents Chemother 2013;57:2204–15.
[93] Muller C, Plésiat P, Jeannot K. A two-component regulatory system interconnects resistance to polymyxins, aminoglycosides, fluoroquinolones, and β-lactams in *Pseudomonas aeruginosa*. Antimicrob Agents Chemother 2011;55:1211–21.
[94] Yu H, Qu F, Shan B, Huang B, Jia W, Chen C, et al. Detection of *mcr-1* colistin resistance gene in carbapenem-resistant Enterobacteriaceae (CRE) from different hospitals in China. Antimicrob Agents Chemother 2016;60:5033–5.
[95] Du H, Chen L, Tang YW, Kreiswirth BN. Emergence of the *mcr-1* colistin resistance gene in carbapenem-resistant Enterobacteriaceae. Lancet Infect Dis 2016;16:287–8.
[96] Ruppe E, Chatelier EL, Pons N, Andremont A, Ehrlich SD. Dissemination of the *mcr-1* colistin resistance gene. Lancet Infect Dis 2016;16:290–1.
[97] Zhang R, Huang Y, Chan EW, Zhou H, Chen S. Dissemination of the *mcr-1* colistin resistance gene. Lancet Infect Dis 2016;16:291–2.
[98] Zheng B, Dong H, Xu H, Lv J, Zhang J, Jiang X, et al. Coexistence of MCR-1 and NDM-1 in clinical *Escherichia coli* isolates. Clin Infect Dis 2016;9:pii: ciw553.
[99] Kuo SC, Huang WC, Wang HY, Shiau YR, Cheng MF, Lauderdale TL. Colistin resistance gene *mcr-1* in *Escherichia coli* isolates from humans and retail meats, Taiwan. J Antimicrob Chemother 2016;71:2327–9.
[100] Mulvey MR, Mataseje LF, Robertson J, Nash JH, Boerlin P, Toye B, et al. Dissemination of the *mcr-1* colistin resistance gene. Lancet Infect Dis 2016;16:289–90.
[101] Olaitan AO, Chabou S, Okdah L, Morand S, Rolain JM. Dissemination of the *mcr-1* colistin resistance gene. Lancet Infect Dis 2016;16:147.
[102] Stoesser N, Mathers AJ, Moore CE, Day NP, Crook DW. Colistin resistance gene *mcr-1* and pHNSHP45 plasmid in human isolates of *Escherichia coli* and *Klebsiella pneumoniae*. Lancet Infect Dis 2016;16:285–6.
[103] Arcilla MS, van Hattem JM, Matamoros S, Melles DC, Penders J, de Jong MD, et al. Dissemination of the *mcr-1* colistin resistance gene. Lancet Infect Dis 2016;16:147–9.
[104] Prim N, Rivera A, Rodriguez-Navarro J, Espanol M, Turbau M, Coll P, et al. Detection of *mcr-1* colistin resistance gene in polyclonal *Escherichia coli* isolates in Barcelona, Spain, 2012 to 2015. Euro Surveill 2016;21:doi:10.2807/1560-7917.ES.2016.21.13.30183.
[105] Rapoport M, Faccone D, Pasteran F, Ceriana P, Albornoz E, Petroni A, et al. *mcr-1*-mediated colistin resistance in human infections caused by *Escherichia coli*: first description in Latin America. Antimicrob Agents Chemother 2016;60:4412–13.
[106] Teo JQ, Ong RT, Xia E, Koh TH, Khor CC, Lee SJ, et al. *mcr-1* in multidrug-resistant bla_{KPC-2} clinical Enterobacteriaceae isolates in Singapore. Antimicrob Agents Chemother 2016;8:pii: AAC.
[107] Yu CY, Ang GY, Chin PS, Ngeow YF, Yin WF, Chan KG. Emergence of *mcr-1*-mediated colistin resistance in *Escherichia coli* in Malaysia. Int J Antimicrob Agents 2016;47:504–5.
[108] Doumith M, Godbole G, Ashton P, Larkin L, Dallman T, Day M, et al. Detection of the plasmid-mediated *mcr-1* gene conferring colistin resistance in human and food isolates of *Salmonella enterica* and *Escherichia coli* in England and Wales. J Antimicrob Chemother 2016;71:2300–5.
[109] Giufre M, Monaco M, Accogli M, Pantosti A, Cerquetti M. PAMURSA Study Group. Emergence of the colistin resistance *mcr-1* determinant in commensal *Escherichia coli* from residents of long-term-care facilities in Italy. J Antimicrob Chemother 2016;71:2329–31.

[110] Cannatelli A, Giani T, Antonelli A, Principe L, Luzzaro F, Rossolini GM. First detection of the *mcr-1* colistin resistance gene in *Escherichia coli* in Italy. Antimicrob Agents Chemother 2016;60:3257–8.

[111] Falgenhauer L, Waezsada SE, Yao Y, Imirzalioglu C, Kasbohrer A, Roesler U, et al. Colistin resistance gene *mcr-1* in extended-spectrum β-lactamase-producing and carbapenemase-producing Gram-negative bacteria in Germany. Lancet Infect Dis 2016;16:282–3.

[112] Coetzee J, Corcoran C, Prentice E, Moodley M, Mendelson M, Poirel L, et al. Emergence of plasmid-mediated colistin resistance (MCR-1) among *Escherichia coli* isolated from South African patients. S Afr Med J 2016;106:449–50.

[113] Poirel L, Kieffer N, Brink A, Coetze J, Jayol A, Nordmann P. Genetic features of MCR-1-producing colistin-resistant *Escherichia coli* isolates, South Africa. Antimicrob Agents Chemother 2016;60:4394–7.

[114] Izdebski R, Baraniak A, Bojarska K, Urbanowicz P, Fiett J, Pomorska-Wesolowska M, et al. Mobile MCR-1-associated resistance to colistin in Poland. J Antimicrob Chemother 2016;71:2331–3.

[115] Poirel L, Kieffer N, Liassine N, Thanh D, Nordmann P. Plasmid-mediated carbapenem and colistin resistance in a clinical isolate of *Escherichia coli*. Lancet Infect Dis 2016;16:281.

[116] Nordmann P, Lienhard R, Kieffer N, Clerc O, Poirel L. Plasmid-mediated colistin-resistant *Escherichia coli* in bacteremia in Switzerland. Clin Infect Dis 2016;62:1322–3.

[117] Bernasconi OJ, Kuenzli E, Pires J, Tinguely R, Carattoli A, Hatz C, et al. Travelers can import colistin-resistant Enterobacteriaceae including those possessing the plasmid-mediated *mcr-1* gene. Antimicrob Agents Chemother 2016; 60:5080–4.

[118] Hasman H, Hammerum AM, Hansen F, Hendriksen RS, Olesen B, Agerso Y, et al. Detection of *mcr-1* encoding plasmid-mediated colistin-resistant *Escherichia coli* isolates from human bloodstream infection and imported chicken meat, Denmark 2015. Euro Surveill 2015;20:doi:10.2807/1560-7917.ES.2015.20.49.30085.

[119] Elnahriry SS, Khalifa HO, Soliman AM, Ahmed AM, Hussein AM, Shimamoto T, et al. Emergence of plasmid-mediated colistin resistance gene *mcr-1* in a clinical *Escherichia coli* isolate from Egypt. Antimicrob Agents Chemother 2016;60:3249–50.

[120] Delgado-Blas JF, Ovejero CM, Abadia Patino L, Gonzalez-Zorn B. Coexistence of *mcr-1* and bla_{NDM-1} in *Escherichia coli* from Venezuela. Antimicrob Agents Chemother 2016;60:6356–8.

[121] McGann P, Snesrud E, Maybank R, Corey B, Ong AC, Clifford R, et al. *Escherichia coli* harboring *mcr-1* and bla_{CTX-M} on a novel IncF plasmid: first report of *mcr-1* in the USA. Antimicrob Agents Chemother 2016;60:4420–1.

[122] Wong SC, Tse H, Chen JH, Cheng VC, Ho PL, Yuen KY. Colistin-resistant Enterobacteriaceae carrying the *mcr-1* gene among patients in Hong Kong. Emerg Infect Dis 2016;22:1667–9.

[123] Fernandes MR, McCulloch JA, Vianello MA, Moura Q, Pérez-Chaparro PJ, Esposito F, et al. First report of the globally disseminated IncX4 plasmid carrying the *mcr-1* gene in a colistin-resistant *Escherichia coli* sequence type 101 isolate from a human infection in Brazil. Antimicrob Agents Chemother 2016;60:6415–17.

[124] Zeng KJ, Doi Y, Patil S, Huang X, Tian GB. Emergence of the plasmid-mediated *mcr-1* gene in colistin-resistant *Enterobacter aerogenes* and *Enterobacter cloacae*. Antimicrob Agents Chemother 2016;60:3862–3.

[125] Pham Thanh D, Thanh Tuyen H, Nguyen Thi Nguyen T, Chung The H, Wick RR, Thwaites GE, et al. Inducible colistin resistance via a disrupted plasmid-borne *mcr-1* gene in a 2008 Vietnamese *Shigella sonnei* isolate. J Antimicrob Chemother 2016;71:2314–17.

[126] Campos JCL, Peixe L, Antunes P. MCR-1 in multidrug-resistant and copper-tolerant clinically relevant *Salmonella* 1,4,[5],12:i:- and *S.* Rissen clones in Portugal, 2011 to 2015. Euro Surveill 2016;21:doi:10.2807/1560-7917.ES.2016.21.26.30270.

[127] Kluytmans-van den Bergh MF, Huizinga P, Bonten MJ, Bos M, De Bruyne K, Friedrich AW, et al. Presence of *mcr-1*-positive Enterobacteriaceae in retail chicken meat but not in humans in The Netherlands since 2009. Euro Surveill 2016;21. doi:10.2807/1560-7917.ES.2016.21.9.30149.

[128] Zurfuh K, Poirel L, Nordmann P, Nuesch-Inderbinen M, Hachler H, Stephan R. Occurrence of the plasmid-borne *mcr-1* colistin resistance gene in extended-spectrum-β-lactamase-producing Enterobacteriaceae in river water and imported vegetable samples in Switzerland. Antimicrob Agents Chemother 2016;60:2594–5.

[129] Falgenhauer L, Waezsada SE, Gwozdzinski K, Ghosh H, Doijad S, Bunk B, et al. Chromosomal locations of *mcr-1* and $bla_{CTX-M-15}$ in fluoroquinolone-resistant *Escherichia coli* ST410. Emerg Infect Dis 2016;22:1689–91.

[130] Yao X, Doi Y, Zeng L, Lv L, Liu JH. Carbapenem-resistant and colistin-resistant *Escherichia coli* co-producing NDM-9 and MCR-1. Lancet Infect Dis 2016;16:288–9.

[131] Veldman K, van Essen-Zandbergen A, Rapallini M, Wit B, Heymans R, van Pelt W, et al. Location of colistin resistance gene *mcr-1* in Enterobacteriaceae from livestock and meat. J Antimicrob Chemother 2016;71:2340–2.

[132] Webb HE, Granier SA, Marault M, Millemann Y, den Bakker HC, Nightingale KK, et al. Dissemination of the *mcr-1* colistin resistance gene. Lancet Infect Dis 2016;16:144–5.

[133] Petrillo M, Angers-Loustau A, Kreysa J. Possible genetic events producing colistin resistance gene *mcr-1*. Lancet Infect Dis 2016;16:280.

[134] Figueiredo R, Card RM, Nunez J, Pomba C, Mendonca N, Anjum MF, et al. Detection of an *mcr-1*-encoding plasmid mediating colistin resistance in *Salmonella enterica* from retail meat in Portugal. J Antimicrob Chemother 2016;71:2338–40.

[135] Shen Z, Wang Y, Shen Y, Shen J, Wu C. Early emergence of *mcr-1* in *Escherichia coli* from food-producing animals. Lancet Infect Dis 2016;16:293.

[136] Haenni M, Poirel L, Kieffer N, Chatre P, Saras E, Metayer V, et al. Co-occurrence of extended spectrum β lactamase and MCR-1 encoding genes on plasmids. Lancet Infect Dis 2016;16:281–2.

[137] Brennan E, Martins M, McCusker MP, Wang J, Alves BM, Hurley D, et al. Multidrug-resistant *Escherichia coli* in bovine animals, Europe. Emerg Infect Dis 2016;22:1650–2.

[138] Perrin-Guyomard A, Bruneau M, Houee P, Deleurme K, Legrandois P, Poirier C, et al. Prevalence of *mcr-1* in commensal *Escherichia coli* from French livestock, 2007 to 2014. Euro Surveill 2016;21:doi:10.2807/1560-7917.ES.2016.21.6.30135.

[139] Kusumoto M, Ogura Y, Gotoh Y, Iwata T, Hayashi T, Akiba M. Colistin-resistant *mcr-1*-positive pathogenic *Escherichia coli* in swine, Japan, 2007–2014. Emerg Infect Dis 2016;22:1315–17.

[140] Quesada A, Ugarte-Ruiz M, Iglesias MR, Porrero MC, Martinez R, Florez-Cuadrado D, et al. Detection of plasmid mediated colistin resistance (MCR-1) in *Escherichia coli* and *Salmonella enterica* isolated from poultry and swine in Spain. Res Vet Sci 2016;105:134–5.

[141] Malhotra-Kumar S, Xavier BB, Das AJ, Lammens C, Butaye P, Goossens H. Colistin resistance gene *mcr-1* harboured on a multidrug resistant plasmid. Lancet Infect Dis 2016;16:283–4.

[142] Xavier BB, Lammens C, Butaye P, Goossens H, Malhotra-Kumar S. Complete sequence of an IncFII plasmid harbouring the colistin resistance gene *mcr-1* isolated from Belgian pig farms. J Antimicrob Chemother 2016;71:2342–4.

[143] Lentz SA, de Lima-Morales D, Cuppertino VM, Nunes L, da Motta AS, Zavascki AP, et al. *Escherichia coli* harbouring *mcr-1* gene isolated from poultry not exposed to polymyxins in Brazil. Euro Surveill 2016;21:doi:10.2807/1560-7917.ES.2016.21.26.30267.

[144] Fernandes MR, Moura Q, Sartori L, Silva KC, Cunha MP, Esposito F, et al. Silent dissemination of colistin-resistant *Escherichia coli* in South America could contribute to the global spread of the *mcr-1* gene. Euro Surveill 2016;21: doi:10.2807/1560-7917.ES.2016.21.17.302.

[145] Suzuki S, Ohnishi M, Kawanishi M, Akiba M, Kuroda M. Investigation of a plasmid genome database for colistin-resistance gene *mcr-1*. Lancet Infect Dis 2016;16:284–5.

[146] Khalifa HO, Ahmed AM, Oreiby AF, Eid AM, Shimamoto T, Shimamoto T. Characterisation of the plasmid-mediated colistin resistance gene *mcr-1* in *Escherichia coli* isolated from animals in Egypt. Int J Antimicrob Agents 2016;47:413–14.

[147] Malhotra-Kumar S, Xavier BB, Das AJ, Lammens C, Hoang HT, Pham NT, et al. Colistin-resistant *Escherichia coli* harbouring *mcr-1* isolated from food animals in Hanoi, Vietnam. Lancet Infect Dis 2016;16:286–7.

[148] Grami R, Mansour W, Mehri W, Bouallegue O, Boujaafar N, Madec JY, et al. Impact of food animal trade on the spread of *mcr-1*-mediated colistin resistance, Tunisia. Euro Surveill 2015;2016:21. doi:10.2807/1560-7917.ES.2016.21.8.30144.

[149] Perreten V, Strauss C, Collaud A, Gerber D. Colistin resistance gene *mcr-1* in avian pathogenic *Escherichia coli* in South Africa. Antimicrob Agents Chemother 2016;60:4414–15.

[150] Anjum MF, Duggett NA, AbuOun M, Randall L, Nunez-Garcia J, Ellis RJ, et al. Colistin resistance in *Salmonella* and *Escherichia coli* isolates from a pig farm in Great Britain. J Antimicrob Chemother 2016;71:2306–13.

[151] Yang RS, Feng Y, Lv XY, Duan JH, Chen J, Fang LX, et al. Emergence of NDM-5- and MCR-1-producing *Escherichia coli* clones ST648 and ST156 from a single muscovy duck (*Cairina moschata*). Antimicrob Agents Chemother 2016;60:6899–902.

[152] Liakopoulos A, Mevius DJ, Olsen B, Bonnedahl J. The colistin resistance *mcr-1* gene is going wild. J Antimicrob Chemother 2016;71:2335–6.

[153] Ruzauskas M. Vaskeviciute L. Detection of the *mcr-1* gene in *Escherichia coli* prevalent in the migratory bird species *Larus argentatus*. J Antimicrob Chemother 2016;71:2333–4.

[154] Xavier BB, Lammens C, Ruhal R, Kumar-Singh S, Butaye P, Goossens H, et al. Identification of a novel plasmid-mediated colistin-resistance gene, *mcr-2*, in *Escherichia coli*, Belgium, June 2016. Euro Surveill 2016;21. doi:10.2807/1560-7917.ES.2016.21.27.30280.

[155] Wanty C, Anandan A, Piek S, Walshe J, Ganguly J, Carlson RW, et al. The structure of the neisserial lipooligosaccharide phosphoethanolamine transferase A (LptA) required for resistance to polymyxin. J Mol Biol 2013;425:3389–402.

[156] Fage CD, Brown DB, Boll JM, Keatinge-Clay AT, Trent MS. Crystallographic study of the phosphoethanolamine transferase EptC required for polymyxin resistance and motility in *Campylobacter jejuni*. Acta Crystallogr D Biol Crystallogr 2014;70:2730–9.

[157] Reynolds CM, Kalb SR, Cotter RJ, Raetz CR. A phosphoethanolamine transferase specific for the outer 3-deoxy-D-manno-octulosonic acid residue of *Escherichia coli* lipopolysaccharide. Identification of the *eptB* gene and Ca^{2+} hypersensitivity of an *eptB* deletion mutant. J Biol Chem 2005;280:21202–11.

[158] Castanheira M, Griffin MA, Deshpande LM, Mendes RE, Jones RN, Flamm RK. Detection of *mcr-1* among *Escherichia coli* clinical isolates collected worldwide as part of the SENTRY Antimicrobial Surveillance Program in 2014 and 2015. Antimicrob Agents Chemother 2016;60:5623–4.

VII. References

Abraham, N., and Kwon, D.H. (2009). A single amino acid substitution in PmrB is associated with polymyxin B resistance in clinical isolate of *Pseudomonas aeruginosa*. FEMS Microbiol Lett *298*, 249-254.

Aires, J.R., Köhler, T., Nikaido, H., and Plésiat, P. (1999). Involvement of an active efflux system in the natural resistance of *Pseudomonas aeruginosa* to aminoglycosides. Antimicrob Agents Chemother *43*, 2624-2628.

Akama, H., Matsuura, T., Kashiwagi, S., Yoneyama, H., Narita, S., Tsukihara, T., Nakagawa, A., and Nakae, T. (2004). Crystal structure of the membrane fusion protein, MexA, of the multidrug transporter in *Pseudomonas aeruginosa*. J Biol Chem *279*, 25939-25942.

Andersson, D.I., Jerlström-Hultqvist, J., and Näsvall, J. (2015). Evolution of new functions *de novo* and from preexisting genes. Cold Spring Harb Perspect Biol *7*.

Arenz, S., and Wilson, D.N. (2016). Bacterial Protein Synthesis as a Target for Antibiotic Inhibition. Cold Spring Harb Perspect Med *6*.

Bader, M.W., Sanowar, S., Daley, M.E., Schneider, A.R., Cho, U., Xu, W., Klevit, R.E., Le Moual, H., and Miller, S.I. (2005). Recognition of antimicrobial peptides by a bacterial sensor kinase. Cell *122*, 461-472.

Baraquet, C., Théraulaz, L., Guiral, M., Lafitte, D., Méjean, V., and Jourlin-Castelli, C. (2006). TorT, a member of a new periplasmic binding protein family, triggers induction of the Tor respiratory system upon trimethylamine N-oxide electron-acceptor binding in *Escherichia coli*. J Biol Chem *281*, 38189-38199.

Barrow, K., and Kwon, D.H. (2009). Alterations in two-component regulatory systems of *phoPQ* and *pmrAB* are associated with polymyxin B resistance in clinical isolates of *Pseudomonas aeruginosa*. Antimicrob Agents Chemother *53*, 5150-5154.

Becker, B., and Cooper, M.A. (2013). Aminoglycoside antibiotics in the 21st century. ACS Chem Biol *8*, 105-115.

Bhagirath, A.Y., Li, Y., Patidar, R., Yerex, K., Ma, X., Kumar, A., and Duan, K. (2019). Two Component Regulatory Systems and Antibiotic Resistance in Gram-Negative Pathogens. Int J Mol Sci *20*.

Bhate, M.P., Molnar, K.S., Goulian, M., and DeGrado, W.F. (2015). Signal transduction in histidine kinases: insights from new structures. Structure *23*, 981-994.

Bielecki, P., Lukat, P., Hüsecken, K., Dötsch, A., Steinmetz, H., Hartmann, R.W., Müller, R., and Häussler, S. (2012). Mutation in elongation factor G confers resistance to the antibiotic argyrin in the opportunistic pathogen *Pseudomonas aeruginosa*. Chembiochem *13*, 2339-2345.

Bina, X.R., Provenzano, D., Nguyen, N., and Bina, J.E. (2008). *Vibrio cholerae* RND family efflux systems are required for antimicrobial resistance, optimal virulence factor production, and colonization of the infant mouse small intestine. Infect Immun *76*, 3595-3605.

Bolard, A., Plésiat, P., and Jeannot, K. (2018). Mutations in Gene *fusA1* as a Novel Mechanism of Aminoglycoside Resistance in Clinical Strains of *Pseudomonas aeruginosa*. Antimicrob Agents Chemother *62*.

Borlee, B.R., Goldman, A.D., Murakami, K., Samudrala, R., Wozniak, D.J., and Parsek, M.R. (2010). *Pseudomonas aeruginosa* uses a cyclic-di-GMP-regulated adhesin to reinforce the biofilm extracellular matrix. Mol Microbiol *75*, 827-842.

Borovinskaya, M.A., Pai, R.D., Zhang, W., Schuwirth, B.S., Holton, J.M., Hirokawa, G., Kaji, H., Kaji, A., and Cate, J.H. (2007). Structural basis for aminoglycoside inhibition of bacterial ribosome recycling. Nat Struct Mol Biol *14*, 727-732.

Braud, A., Hannauer, M., Mislin, G.L., and Schalk, I.J. (2009). The *Pseudomonas aeruginosa* pyochelin-iron uptake pathway and its metal specificity. J Bacteriol *191*, 3517-3525.

Bryan, L.E., O'Hara, K., and Wong, S. (1984). Lipopolysaccharide changes in impermeability-type aminoglycoside resistance in *Pseudomonas aeruginosa*. Antimicrob Agents Chemother *26*, 250-255.

Caille, O., Rossier, C., and Perron, K. (2007). A copper-activated two-component system interacts with zinc and imipenem resistance in *Pseudomonas aeruginosa*. J Bacteriol *189*, 4561-4568.

Cao, L., Srikumar, R., and Poole, K. (2004). MexAB-OprM hyperexpression in NalC-type multidrug-resistant *Pseudomonas aeruginosa*: identification and characterization of the *nalC* gene encoding a repressor of PA3720-PA3719. Mol Microbiol *53*, 1423-1436.

Carter, A.P., Clemons, W.M., Brodersen, D.E., Morgan-Warren, R.J., Wimberly, B.T., and Ramakrishnan, V. (2000). Functional insights from the structure of the 30S ribosomal subunit and its interactions with antibiotics. Nature *407*, 340-348.

Caughlan, R.E., Sriram, S., Daigle, D.M., Woods, A.L., Buco, J., Peterson, R.L., Dzink-Fox, J., Walker, S., and Dean, C.R. (2009). Fmt bypass in *Pseudomonas aeruginosa* causes induction of MexXY efflux pump expression. Antimicrob Agents Chemother *53*, 5015-5021.

Chen, X., Schauder, S., Potier, N., Van Dorsselaer, A., Pelczer, I., Bassler, B.L., and Hughson, F.M. (2002). Structural identification of a bacterial *quorum*-sensing signal containing boron. Nature *415*, 545-549.

Chen, Y., Koripella, R.K., Sanyal, S., and Selmer, M. (2010). *Staphylococcus aureus* elongation factor G - structure and analysis of a target for fusidic acid. FEBS J *277*, 3789-3803.

Cheung, J., and Hendrickson, W.A. (2009). Structural analysis of ligand stimulation of the histidine kinase NarX. Structure *17*, 190-201.

Choi, K.H., Kumar, A., and Schweizer, H.P. (2006). A 10-min method for preparation of highly electrocompetent *Pseudomonas aeruginosa* cells: application for DNA fragment transfer between chromosomes and plasmid transformation. J Microbiol Methods *64*, 391-397.

Choi, K.H., Mima, T., Casart, Y., Rholl, D., Kumar, A., Beacham, I.R., and Schweizer, H.P. (2008). Genetic tools for select-agent-compliant manipulation of *Burkholderia pseudomallei*. Appl Environ Microbiol *74*, 1064-1075.

Chua, S.L., Tan, S.Y., Rybtke, M.T., Chen, Y., Rice, S.A., Kjelleberg, S., Tolker-Nielsen, T., Yang, L., and Givskov, M. (2013). Bis-(3'-5')-cyclic dimeric GMP regulates antimicrobial peptide resistance in *Pseudomonas aeruginosa*. Antimicrob Agents Chemother *57*, 2066-2075.

Chugani, S., Kim, B.S., Phattarasukol, S., Brittnacher, M.J., Choi, S.H., Harwood, C.S., and Greenberg, E.P. (2012). Strain-dependent diversity in the *Pseudomonas aeruginosa quorum*-sensing regulon. Proc Natl Acad Sci U S A *109*, E2823-2831.

Chung, J.C., Becq, J., Fraser, L., Schulz-Trieglaff, O., Bond, N.J., Foweraker, J., Bruce, K.D., Smith, G.P., and Welch, M. (2012). Genomic variation among contemporary *Pseudomonas aeruginosa* isolates from chronically infected cystic fibrosis patients. J Bacteriol *194*, 4857-4866.

Cybulski, L.E., Martín, M., Mansilla, M.C., Fernández, A., and de Mendoza, D. (2010). Membrane thickness cue for cold sensing in a bacterium. Curr Biol *20*, 1539-1544.

Davis, B.D. (1987). Mechanism of bactericidal action of aminoglycosides. Microbiol Rev *51*, 341-350.

Dean, C.R., and Goldberg, J.B. (2002). *Pseudomonas aeruginosa galU* is required for a complete lipopolysaccharide core and repairs a secondary mutation in a PA103 (serogroup O11) *wbpM* mutant. FEMS Microbiol Lett *210*, 277-283.

Del Barrio-Tofiño, E., López-Causapé, C., Cabot, G., Rivera, A., Benito, N., Segura, C., Montero, M.M., Sorlí, L., Tubau, F., Gómez-Zorrilla, S.*, et al.* (2017). Genomics and Susceptibility Profiles of Extensively Drug-Resistant *Pseudomonas aeruginosa* Isolates from Spain. Antimicrob Agents Chemother *61*.

Ditta, G., Stanfield, S., Corbin, D., and Helinski, D.R. (1980). Broad host range DNA cloning system for Gram-negative bacteria: construction of a gene bank of *Rhizobium meliloti*. Proc Natl Acad Sci U S A *77*, 7347-7351.

Dorrestein, P.C., Poole, K., and Begley, T.P. (2003). Formation of the chromophore of the pyoverdine siderophores by an oxidative cascade. Org Lett *5*, 2215-2217.

Dorrestein, P.C., Yeh, E., Garneau-Tsodikova, S., Kelleher, N.L., and Walsh, C.T. (2005). Dichlorination of a pyrrolyl-S-carrier protein by FADH2-dependent halogenase PltA during pyoluteorin biosynthesis. Proc Natl Acad Sci U S A *102*, 13843-13848.

Drake, E.J., Cao, J., Qu, J., Shah, M.B., Straubinger, R.M., and Gulick, A.M. (2007). The 1.8 Å crystal structure of PA2412, an MbtH-like protein from the pyoverdine cluster of *Pseudomonas aeruginosa*. J Biol Chem *282*, 20425-20434.

Dubern, J.F., Cigana, C., De Simone, M., Lazenby, J., Juhas, M., Schwager, S., Bianconi, I., Döring, G., Eberl, L., Williams, P.*, et al.* (2015). Integrated whole-genome screening for *Pseudomonas aeruginosa* virulence genes using multiple disease models reveals that pathogenicity is host specific. Environ Microbiol *17*, 4379-4393.

Dötsch, A., Eckweiler, D., Schniederjans, M., Zimmermann, A., Jensen, V., Scharfe, M., Geffers, R., and Häussler, S. (2012). The *Pseudomonas aeruginosa* transcriptome in planktonic cultures and static biofilms using RNA sequencing. PLoS One *7*, e31092.

Dößelmann, B., Willmann, M., Steglich, M., Bunk, B., Nübel, U., Peter, S., and Neher, R.A. (2017). Rapid and Consistent Evolution of Colistin Resistance in Extensively Drug-Resistant *Pseudomonas aeruginosa* during Morbidostat Culture. Antimicrob Agents Chemother *61*.

El'Garch, F., Jeannot, K., Hocquet, D., Llanes-Barakat, C., and Plésiat, P. (2007). Cumulative effects of several nonenzymatic mechanisms on the resistance of *Pseudomonas aeruginosa* to aminoglycosides. Antimicrob Agents Chemother *51*, 1016-1021.

Feng, Y., Jonker, M.J., Moustakas, I., Brul, S., and Ter Kuile, B.H. (2016). Dynamics of Mutations during Development of Resistance by *Pseudomonas aeruginosa* against Five Antibiotics. Antimicrob Agents Chemother *60*, 4229-4236.

Fernández, L., Alvarez-Ortega, C., Wiegand, I., Olivares, J., Kocíncová, D., Lam, J.S., Martínez, J.L., and Hancock, R.E. (2013). Characterization of the polymyxin B resistome of *Pseudomonas aeruginosa*. Antimicrob Agents Chemother *57*, 110-119.

Fernández, L., Gooderham, W.J., Bains, M., McPhee, J.B., Wiegand, I., and Hancock, R.E. (2010). Adaptive resistance to the "last hope" antibiotics polymyxin B and colistin in *Pseudomonas aeruginosa* is mediated by the novel two-component regulatory system ParR-ParS. Antimicrob Agents Chemother *54*, 3372-3382.

Fernández, L., Jenssen, H., Bains, M., Wiegand, I., Gooderham, W.J., and Hancock, R.E. (2012). The two-component system CprRS senses cationic peptides and triggers adaptive resistance in *Pseudomonas aeruginosa* independently of ParRS. Antimicrob Agents Chemother *56*, 6212-6222.

Finking, R., and Marahiel, M.A. (2004). Biosynthesis of nonribosomal peptides. Annu Rev Microbiol *58*, 453-488.

Fourmy, D., Recht, M.I., Blanchard, S.C., and Puglisi, J.D. (1996). Structure of the A site of *Escherichia coli* 16S ribosomal RNA complexed with an aminoglycoside antibiotic. Science *274*, 1367-1371.

Galperin, M.Y. (2004). Bacterial signal transduction network in a genomic perspective. Environ Microbiol *6*, 552-567.

Fruci, M., and Poole, K. (2018). Aminoglycoside-inducible expression of the *mexAB-oprM* multidrug efflux operon in *Pseudomonas aeruginosa*: Involvement of the envelope stress-responsive AmgRS two-component system. PLoS One *13*, e0205036.

Gao, R., Mack, T.R., and Stock, A.M. (2007). Bacterial response regulators: versatile regulatory strategies from common domains. Trends Biochem Sci *32*, 225-234.

Gao, R., and Stock, A.M. (2009). Biological insights from structures of two-component proteins. Annu Rev Microbiol *63*, 133-154.

Gao, Y.G., Selmer, M., Dunham, C.M., Weixlbaumer, A., Kelley, A.C., and Ramakrishnan, V. (2009). The structure of the ribosome with elongation factor G trapped in the posttranslocational state. Science *326*, 694-699.

Gasser, V., Guillon, L., Cunrath, O., and Schalk, I.J. (2015). Cellular organization of siderophore biosynthesis in *Pseudomonas aeruginosa*: Evidence for siderosomes. J Inorg Biochem *148*, 27-34.

Ge, L., and Seah, S.Y. (2006). Heterologous expression, purification, and characterization of an L-ornithine N(5)-hydroxylase involved in pyoverdine siderophore biosynthesis in *Pseudomonas aeruginosa*. J Bacteriol *188*, 7205-7210.

Gevrekci, A. (2017). The roles of polyamines in microorganisms. World J Microbiol Biotechnol *33*, 204.

Gilbert, K.B., Kim, T.H., Gupta, R., Greenberg, E.P., and Schuster, M. (2009). Global position analysis of the *Pseudomonas aeruginosa quorum*-sensing transcription factor LasR. Mol Microbiol *73*, 1072-1085.

Goldberg, S.D., Clinthorne, G.D., Goulian, M., and DeGrado, W.F. (2010). Transmembrane polar interactions are required for signaling in the *Escherichia coli* sensor kinase PhoQ. Proc Natl Acad Sci U S A *107*, 8141-8146.

Gooderham, W.J., Gellatly, S.L., Sanschagrin, F., McPhee, J.B., Bains, M., Cosseau, C., Levesque, R.C., and Hancock, R.E. (2009). The sensor kinase PhoQ mediates virulence in *Pseudomonas aeruginosa*. Microbiology *155*, 699-711.

Gooderham, W.J., and Hancock, R.E. (2009). Regulation of virulence and antibiotic resistance by two-component regulatory systems in *Pseudomonas aeruginosa*. FEMS Microbiol Rev *33*, 279-294.

Greipel, L., Fischer, S., Klockgether, J., Dorda, M., Mielke, S., Wiehlmann, L., Cramer, N., and Tümmler, B. (2016). Molecular Epidemiology of Mutations in Antimicrobial Resistance Loci of *Pseudomonas aeruginosa* Isolates from Airways of Cystic Fibrosis Patients. Antimicrob Agents Chemother *60*, 6726-6734.

Gulick, A.M. (2017). Nonribosomal peptide synthetase biosynthetic clusters of ESKAPE pathogens. Nat Prod Rep *34*, 981-1009.

Gutierrez, B., Douthwaite, S., and Gonzalez-Zorn, B. (2013). Indigenous and acquired modifications in the aminoglycoside binding sites of *Pseudomonas aeruginosa* rRNAs. RNA Biol *10*, 1324-1332.

Gutu, A.D., Rodgers, N.S., Park, J., and Moskowitz, S.M. (2015). *Pseudomonas aeruginosa* high-level resistance to polymyxins and other antimicrobial peptides requires *cprA*, a gene that is disrupted in the PAO1 strain. Antimicrob Agents Chemother *59*, 5377-5387.

Gutu, A.D., Sgambati, N., Strasbourger, P., Brannon, M.K., Jacobs, M.A., Haugen, E., Kaul, R.K., Johansen, H.K., Høiby, N., and Moskowitz, S.M. (2013). Polymyxin resistance of *Pseudomonas aeruginosa phoQ* mutants is dependent on additional two-component regulatory systems. Antimicrob Agents Chemother *57*, 2204-2215.

Guénard, S., Muller, C., Monlezun, L., Benas, P., Broutin, I., Jeannot, K., and Plésiat, P. (2014). Multiple mutations lead to MexXY-OprM-dependent aminoglycoside resistance in clinical strains of *Pseudomonas aeruginosa*. Antimicrob Agents Chemother *58*, 221-228.

Ha, D.G., and O'Toole, G.A. (2015). c-di-GMP and its Effects on Biofilm Formation and Dispersion: a *Pseudomonas aeruginosa* Review. Microbiol Spectr *3*, MB-0003-2014.

Hall, B.M., Breidenstein, E.B.M., de la Fuente-Núñez, C., Reffuveille, F., Mawla, G.D., Hancock, R.E.W., and Baker, T.A. (2017). Two Isoforms of Clp Peptidase in *Pseudomonas aeruginosa* Control Distinct Aspects of Cellular Physiology. J Bacteriol *199*.

Hamada, M., Toyofuku, M., Miyano, T., and Nomura, N. (2014). cbb3-type cytochrome *c* oxidases, aerobic respiratory enzymes, impact the anaerobic life of *Pseudomonas aeruginosa* PAO1. J Bacteriol *196*, 3881-3889.

Hanahan, D. (1983). Studies on transformation of *Escherichia coli* with plasmids. J Mol Biol *166*, 557-580.

Hancock, R.E. (1981). Aminoglycoside uptake and mode of action-with special reference to streptomycin and gentamicin. I. Antagonists and mutants. J Antimicrob Chemother *8*, 249-276.

Hancock, R.E., Mutharia, L.M., Chan, L., Darveau, R.P., Speert, D.P., and Pier, G.B. (1983). *Pseudomonas aeruginosa* isolates from patients with cystic fibrosis: a class of serum-sensitive, nontypable strains deficient in lipopolysaccharide O side chains. Infect Immun *42*, 170-177.

Hannauer, M., Schäfer, M., Hoegy, F., Gizzi, P., Wehrung, P., Mislin, G.L., Budzikiewicz, H., and Schalk, I.J. (2012). Biosynthesis of the pyoverdine siderophore of *Pseudomonas aeruginosa* involves precursors with a myristic or a myristoleic acid chain. FEBS Lett *586*, 96-101.

Hannauer, M., Yeterian, E., Martin, L.W., Lamont, I.L., and Schalk, I.J. (2010). An efflux pump is involved in secretion of newly synthesized siderophore by *Pseudomonas aeruginosa*. FEBS Lett *584*, 4751-4755.

Hay, T., Fraud, S., Lau, C.H., Gilmour, C., and Poole, K. (2013). Antibiotic inducibility of the *mexXY* multidrug efflux operon of *Pseudomonas aeruginosa*: involvement of the MexZ anti-repressor ArmZ. PLoS One *8*, e56858.

Hayden, H.S., Gillett, W., Saenphimmachak, C., Lim, R., Zhou, Y., Jacobs, M.A., Chang, J., Rohmer, L., D'Argenio, D.A., Palmieri, A.*, et al.* (2008). Large-insert genome analysis technology detects structural variation in *Pseudomonas aeruginosa* clinical strains from cystic fibrosis patients. Genomics *91*, 530-537.

Hazan, R., He, J., Xiao, G., Dekimpe, V., Apidianakis, Y., Lesic, B., Astrakas, C., Déziel, E., Lépine, F., and Rahme, L.G. (2010). Homeostatic interplay between bacterial cell-cell signaling and iron in virulence. PLoS Pathog *6*, e1000810.

Heeb, S., Itoh, Y., Nishijyo, T., Schnider, U., Keel, C., Wade, J., Walsh, U., O'Gara, F., and Haas, D. (2000). Small, stable shuttle vectors based on the minimal pVS1 replicon for use in Gram-negative, plant-associated bacteria. Mol Plant Microbe Interact *13*, 232-237.

Herrero, M., de Lorenzo, V., and Timmis, K.N. (1990). Transposon vectors containing non-antibiotic resistance selection markers for cloning and stable chromosomal insertion of foreign genes in Gram-negative bacteria. J Bacteriol *172*, 6557-6567.

Hoang, T.T., Karkhoff-Schweizer, R.R., Kutchma, A.J., and Schweizer, H.P. (1998). A broad-host-range Flp-FRT recombination system for site-specific excision of chromosomally-located DNA sequences: application for isolation of unmarked *Pseudomonas aeruginosa* mutants. Gene *212*, 77-86.

Hoang, T.T., Kutchma, A.J., Becher, A., and Schweizer, H.P. (2000). Integration-proficient plasmids for *Pseudomonas aeruginosa*: site-specific integration and use for engineering of reporter and expression strains. Plasmid *43*, 59-72.

Hocquet, D., Muller, A., Blanc, K., Plésiat, P., Talon, D., Monnet, D.L., and Bertrand, X. (2008). Relationship between antibiotic use and incidence of MexXY-OprM overproducers among clinical isolates of *Pseudomonas aeruginosa*. Antimicrob Agents Chemother *52*, 1173-1175.

Hocquet, D., Vogne, C., El Garch, F., Vejux, A., Gotoh, N., Lee, A., Lomovskaya, O., and Plésiat, P. (2003). MexXY-OprM efflux pump is necessary for a adaptive resistance of *Pseudomonas aeruginosa* to aminoglycosides. Antimicrob Agents Chemother *47*, 1371-1375.

Hoffman, L.R., D'Argenio, D.A., MacCoss, M.J., Zhang, Z., Jones, R.A., and Miller, S.I. (2005). Aminoglycoside antibiotics induce bacterial biofilm formation. Nature *436*, 1171-1175.

Hong, Z., Bolard, A., Giraud, C., Prévost, S., Genta-Jouve, G., Deregnaucourt, C., Häussler, S., Jeannot, K., and Li, Y. (2019). Azetidine-Containing Alkaloids Produced by a *Quorum*-Sensing Regulated Nonribosomal Peptide Synthetase Pathway in *Pseudomonas aeruginosa*. Angew Chem Int Ed Engl *58*, 3178-3182.

Hooper, S.D., and Berg, O.G. (2003). Duplication is more common among laterally transferred genes than among indigenous genes. Genome Biol *4*, R48.

Huang, X., Yan, A., Zhang, X., and Xu, Y. (2006). Identification and characterization of a putative ABC transporter PltHIJKN required for pyoluteorin production in *Pseudomonas sp*. M18. Gene *376*, 68-78.

Jeannot, K., Bolard, A., and Plésiat, P. (2017). Resistance to polymyxins in Gram-negative organisms. Int J Antimicrob Agents *49*, 526-535.

Jeannot, K., Sobel, M.L., El Garch, F., Poole, K., and Plésiat, P. (2005). Induction of the MexXY efflux pump in *Pseudomonas aeruginosa* is dependent on drug-ribosome interaction. J Bacteriol *187*, 5341-5346.

Jo, J.T., Brinkman, F.S., and Hancock, R.E. (2003). Aminoglycoside efflux in *Pseudomonas aeruginosa*: involvement of novel outer membrane proteins. Antimicrob Agents Chemother *47*, 1101-1111.

Jochumsen, N., Marvig, R.L., Damkiær, S., Jensen, R.L., Paulander, W., Molin, S., Jelsbak, L., and Folkesson, A. (2016). The evolution of antimicrobial peptide resistance in *Pseudomonas aeruginosa* is shaped by strong epistatic interactions. Nat Commun *7*, 13002.

Johanson, U., and Hughes, D. (1994). Fusidic acid-resistant mutants define three regions in elongation factor G of *Salmonella typhimurium*. Gene *143*, 55-59.

Johnson, L., Mulcahy, H., Kanevets, U., Shi, Y., and Lewenza, S. (2012). Surface-localized spermidine protects the *Pseudomonas aeruginosa* outer membrane from antibiotic treatment and oxidative stress. J Bacteriol *194*, 813-826.

Jones, A.K., Woods, A.L., Takeoka, K.T., Shen, X., Wei, J.R., Caughlan, R.E., and Dean, C.R. (2017). Determinants of Antibacterial Spectrum and Resistance Potential of the Elongation Factor G Inhibitor Argyrin B in Key Gram-Negative Pathogens. Antimicrob Agents Chemother *61*.

Juarez, P., Jeannot, K., Plésiat, P., and Llanes, C. (2017). Toxic Electrophiles Induce Expression of the Multidrug Efflux Pump MexEF-OprN in *Pseudomonas aeruginosa* through a Novel Transcriptional Regulator, CmrA. Antimicrob Agents Chemother *61*.

Kadurugamuwa, J.L., Lam, J.S., and Beveridge, T.J. (1993). Interaction of gentamicin with the A band and B band lipopolysaccharides of *Pseudomonas aeruginosa* and its possible lethal effect. Antimicrob Agents Chemother *37*, 715-721.

Kang, T.J., and Suga, H. (2008). Ribosomal synthesis of nonstandard peptides. Biochem Cell Biol *86*, 92-99.

Kaniga, K., Delor, I., and Cornelis, G.R. (1991). A wide-host-range suicide vector for improving reverse genetics in Gram-negative bacteria: inactivation of the *blaA* gene of *Yersinia enterocolitica*. Gene *109*, 137-141.

Kashiwagi, K., Miyamoto, S., Nukui, E., Kobayashi, H., and Igarashi, K. (1993). Functions of PotA and PotD proteins in spermidine-preferential uptake system in *Escherichia coli*. J Biol Chem *268*, 19358-19363.

Kazmierczak, B.I., Schniederberend, M., and Jain, R. (2015). Cross-regulation of *Pseudomonas* motility systems: the intimate relationship between flagella, pili and virulence. Curr Opin Microbiol *28*, 78-82.

Kidarsa, T.A., Goebel, N.C., Zabriskie, T.M., and Loper, J.E. (2011). Phloroglucinol mediates cross-talk between the pyoluteorin and 2,4-diacetylphloroglucinol biosynthetic pathways in *Pseudomonas fluorescens* Pf-5. Mol Microbiol *81*, 395-414.

King, J.D., Kocíncová, D., Westman, E.L., and Lam, J.S. (2009). Review: Lipopolysaccharide biosynthesis in *Pseudomonas aeruginosa*. Innate Immun *15*, 261-312.

Klockgether, J., Munder, A., Neugebauer, J., Davenport, C.F., Stanke, F., Larbig, K.D., Heeb, S., Schöck, U., Pohl, T.M., Wiehlmann, L.*, et al.* (2010). Genome diversity of *Pseudomonas aeruginosa* PAO1 laboratory strains. J Bacteriol *192*, 1113-1121.

Kohanski, M.A., Dwyer, D.J., and Collins, J.J. (2010). How antibiotics kill bacteria: from targets to networks. Nat Rev Microbiol *8*, 423-435.

Korycinski, M., Albrecht, R., Ursinus, A., Hartmann, M.D., Coles, M., Martin, J., Dunin-Horkawicz, S., and Lupas, A.N. (2015). STAC-A New Domain Associated with Transmembrane Solute Transport and Two-Component Signal Transduction Systems. J Mol Biol *427*, 3327-3339.

Krahn, T., Gilmour, C., Tilak, J., Fraud, S., Kerr, N., Lau, C.H., and Poole, K. (2012). Determinants of intrinsic aminoglycoside resistance in *Pseudomonas aeruginosa*. Antimicrob Agents Chemother *56*, 5591-5602.

Krause, K.M., Serio, A.W., Kane, T.R., and Connolly, L.E. (2016). Aminoglycosides: An Overview. Cold Spring Harb Perspect Med *6*.

Kwon, D.H., and Lu, C.D. (2006). Polyamines induce resistance to cationic peptide, aminoglycoside, and quinolone antibiotics in *Pseudomonas aeruginosa* PAO1. Antimicrob Agents Chemother *50*, 1615-1622.

Lacks, S., and Greenberg, B. (1977). Complementary specificity of restriction endonucleases of *Diplococcus pneumoniae* with respect to DNA methylation. J Mol Biol *114*, 153-168.

Lam, J.S., Taylor, V.L., Islam, S.T., Hao, Y., and Kocíncová, D. (2011). Genetic and Functional Diversity of *Pseudomonas aeruginosa* Lipopolysaccharide. Front Microbiol *2*, 118.

Lambert, P.A. (1988). Enterobacteriaceae: composition, structure and function of the cell envelope. Soc Appl Bacteriol Symp Ser *17*, 21S-34S.

Lamont, I.L., Martin, L.W., Sims, T., Scott, A., and Wallace, M. (2006). Characterization of a gene encoding an acetylase required for pyoverdine synthesis in *Pseudomonas aeruginosa*. J Bacteriol *188*, 3149-3152.

Landman, D., Bratu, S., Alam, M., and Quale, J. (2005). Citywide emergence of *Pseudomonas aeruginosa* strains with reduced susceptibility to polymyxin B. J Antimicrob Chemother *55*, 954-957.

Lau, C.H., Fraud, S., Jones, M., Peterson, S.N., and Poole, K. (2012). Reduced expression of the *rplU-rpmA* ribosomal protein operon in *mexXY*-expressing pan-aminoglycoside-resistant mutants of *Pseudomonas aeruginosa*. Antimicrob Agents Chemother *56*, 5171-5179.

Lau, C.H., Fraud, S., Jones, M., Peterson, S.N., and Poole, K. (2013). Mutational activation of the AmgRS two-component system in aminoglycoside-resistant *Pseudomonas aeruginosa*. Antimicrob Agents Chemother *57*, 2243-2251.

Lau, C.H., Krahn, T., Gilmour, C., Mullen, E., and Poole, K. (2015). AmgRS-mediated envelope stress-inducible expression of the *mexXY* multidrug efflux operon of *Pseudomonas aeruginosa*. Microbiologyopen *4*, 121-135.

Lee, J., Sperandio, V., Frantz, D.E., Longgood, J., Camilli, A., Phillips, M.A., and Michael, A.J. (2009a). An alternative polyamine biosynthetic pathway is widespread in bacteria and essential for biofilm formation in *Vibrio cholerae*. J Biol Chem *284*, 9899-9907.

Lee, J., and Zhang, L. (2015). The hierarchy *quorum* sensing network in *Pseudomonas aeruginosa*. Protein Cell *6*, 26-41.

Lee, J.Y., Choi, M.J., Choi, H.J., and Ko, K.S. (2016). Preservation of Acquired Colistin Resistance in Gram-Negative Bacteria. Antimicrob Agents Chemother *60*, 609-612.

Lee, J.Y., and Ko, K.S. (2014). Mutations and expression of PmrAB and PhoPQ related with colistin resistance in *Pseudomonas aeruginosa* clinical isolates. Diagn Microbiol Infect Dis *78*, 271-276.

Lee, S., Hinz, A., Bauerle, E., Angermeyer, A., Juhaszova, K., Kaneko, Y., Singh, P.K., and Manoil, C. (2009b). Targeting a bacterial stress response to enhance antibiotic action. Proc Natl Acad Sci U S A *106*, 14570-14575.

Lee, X., Fox, A., Sufrin, J., Henry, H., Majcherczyk, P., Haas, D., and Reimmann, C. (2010). Identification of the biosynthetic gene cluster for the *Pseudomonas aeruginosa* antimetabolite L-2-amino-4-methoxy-trans-3-butenoic acid. J Bacteriol *192*, 4251-4255.

Li, X.Z., Plésiat, P., and Nikaido, H. (2015). The challenge of efflux-mediated antibiotic resistance in Gram-negative bacteria. Clin Microbiol Rev *28*, 337-418.

Lin, J., Gagnon, M.G., Bulkley, D., and Steitz, T.A. (2015). Conformational changes of elongation factor G on the ribosome during tRNA translocation. Cell *160*, 219-227.

Ling, C., and Ermolenko, D.N. (2016). Structural insights into ribosome translocation. Wiley Interdiscip Rev RNA *7*, 620-636.

Lister, P.D., Wolter, D.J., and Hanson, N.D. (2009). Antibacterial-resistant *Pseudomonas aeruginosa*: clinical impact and complex regulation of chromosomally encoded resistance mechanisms. Clin Microbiol Rev *22*, 582-610.

Llanes, C., Hocquet, D., Vogne, C., Benali-Baitich, D., Neuwirth, C., and Plésiat, P. (2004). Clinical strains of *Pseudomonas aeruginosa* overproducing MexAB-OprM and MexXY efflux pumps simultaneously. Antimicrob Agents Chemother *48*, 1797-1802.

Lunter, G., and Goodson, M. (2011). Stampy: a statistical algorithm for sensitive and fast mapping of Illumina sequence reads. Genome Res *21*, 936-939.

López-Causapé, C., Rubio, R., Cabot, G., and Oliver, A. (2018). Evolution of the *Pseudomonas aeruginosa* Aminoglycoside Mutational Resistome. Antimicrob Agents Chemother *62*.

López-Causapé, C., Sommer, L.M., Cabot, G., Rubio, R., Ocampo-Sosa, A.A., Johansen, H.K., Figuerola, J., Cantón, R., Kidd, T.J., Molin, S.*, et al.* (2017). Evolution of the *Pseudomonas aeruginosa* mutational resistome in an international Cystic Fibrosis clone. Sci Rep *7*, 5555.

Macfarlane, E.L., Kwasnicka, A., and Hancock, R.E. (2000). Role of *Pseudomonas aeruginosa* PhoP-phoQ in resistance to antimicrobial cationic peptides and aminoglycosides. Microbiology *146 (Pt 10)*, 2543-2554.

Macfarlane, E.L., Kwasnicka, A., Ochs, M.M., and Hancock, R.E. (1999). PhoP-PhoQ homologues in *Pseudomonas aeruginosa* regulate expression of the outer-membrane protein OprH and polymyxin B resistance. Mol Microbiol *34*, 305-316.

Magiorakos, A.P., Srinivasan, A., Carey, R.B., Carmeli, Y., Falagas, M.E., Giske, C.G., Harbarth, S., Hindler, J.F., Kahlmeter, G., Olsson-Liljequist, B.*, et al.* (2012). Multidrug-resistant, extensively drug-resistant and pandrug-resistant bacteria: an international expert proposal for interim standard definitions for acquired resistance. Clin Microbiol Infect *18*, 268-281.

Mah, T.F., Pitts, B., Pellock, B., Walker, G.C., Stewart, P.S., and O'Toole, G.A. (2003). A genetic basis for *Pseudomonas aeruginosa* biofilm antibiotic resistance. Nature *426*, 306-310.

Manoil, C., and Beckwith, J. (1985). TnphoA: a transposon probe for protein export signals. Proc Natl Acad Sci U S A *82*, 8129-8133.

Margus, T., Remm, M., and Tenson, T. (2007). Phylogenetic distribution of translational GTPases in bacteria. BMC Genomics *8*, 15.

Margus, T., Remm, M., and Tenson, T. (2011). A computational study of elongation factor G (EF-G) duplicated genes: diverged nature underlying the innovation on the same structural template. PLoS One *6*, e22789.

Markussen, T., Marvig, R.L., Gómez-Lozano, M., Aanæs, K., Burleigh, A.E., Høiby, N., Johansen, H.K., Molin, S., and Jelsbak, L. (2014). Environmental heterogeneity drives within-host diversification and evolution of *Pseudomonas aeruginosa*. MBio *5*, e01592-01514.

Martemyanov, K.A., Liljas, A., Yarunin, A.S., and Gudkov, A.T. (2001). Mutations in the G-domain of elongation factor G from *Thermus thermophilus* affect both its interaction with GTP and fusidic acid. J Biol Chem *276*, 28774-28778.

Marvig, R.L., Johansen, H.K., Molin, S., and Jelsbak, L. (2013). Genome analysis of a transmissible lineage of *Pseudomonas aeruginosa* reveals pathoadaptive mutations and distinct evolutionary paths of hypermutators. PLoS Genet *9*, e1003741.

Mascher, T. (2006). Intramembrane-sensing histidine kinases: a new family of cell envelope stress sensors in *Firmicutes bacteria*. FEMS Microbiol Lett *264*, 133-144.

Masuda, N., Sakagawa, E., Ohya, S., Gotoh, N., Tsujimoto, H., and Nishino, T. (2000). Contribution of the MexX-MexY-OprM efflux system to intrinsic resistance in *Pseudomonas aeruginosa*. Antimicrob Agents Chemother *44*, 2242-2246.

Matsuo, Y., Eda, S., Gotoh, N., Yoshihara, E., and Nakae, T. (2004). MexZ-mediated regulation of *mexXY* multidrug efflux pump expression in *Pseudomonas aeruginosa* by binding on the *mexZ-mexX* intergenic DNA. FEMS Microbiol Lett *238*, 23-28.

Matt, T., Ng, C.L., Lang, K., Sha, S.H., Akbergenov, R., Shcherbakov, D., Meyer, M., Duscha, S., Xie, J., Dubbaka, S.R.*, et al.* (2012). Dissociation of antibacterial activity and aminoglycoside ototoxicity in the 4-monosubstituted 2-deoxystreptamine apramycin. Proc Natl Acad Sci U S A *109*, 10984-10989.

McCarthy, K. (2015). *Pseudomonas aeruginosa*: evolution of antimicrobial resistance and implications for therapy. Semin Respir Crit Care Med *36*, 44-55.

McLaughlin, H.P., Caly, D.L., McCarthy, Y., Ryan, R.P., and Dow, J.M. (2012). An orphan chemotaxis sensor regulates virulence and antibiotic tolerance in the human pathogen *Pseudomonas aeruginosa*. PLoS One *7*, e42205.

McMorran, B.J., Shanta Kumara, H.M., Sullivan, K., and Lamont, I.L. (2001). Involvement of a transformylase enzyme in siderophore synthesis in *Pseudomonas aeruginosa*. Microbiology *147*, 1517-1524.

McPhee, J.B., Bains, M., Winsor, G., Lewenza, S., Kwasnicka, A., Brazas, M.D., Brinkman, F.S., and Hancock, R.E. (2006). Contribution of the PhoP-PhoQ and PmrA-PmrB two-component regulatory systems to Mg^{2+}-induced gene regulation in *Pseudomonas aeruginosa*. J Bacteriol *188*, 3995-4006.

McPhee, J.B., Lewenza, S., and Hancock, R.E. (2003). Cationic antimicrobial peptides activate a two-component regulatory system, PmrA-PmrB, that regulates resistance to polymyxin B and cationic antimicrobial peptides in *Pseudomonas aeruginosa*. Mol Microbiol *50*, 205-217.

Melnikov, S., Ben-Shem, A., Garreau de Loubresse, N., Jenner, L., Yusupova, G., and Yusupov, M. (2012). One core, two shells: bacterial and eukaryotic ribosomes. Nat Struct Mol Biol *19*, 560-567.

Meneely, K.M., Barr, E.W., Bollinger, J.M., and Lamb, A.L. (2009). Kinetic mechanism of ornithine hydroxylase (PvdA) from *Pseudomonas aeruginosa*: substrate triggering of O2 addition but not flavin reduction. Biochemistry *48*, 4371-4376.

Michael, A.J. (2016). Biosynthesis of polyamines and polyamine-containing molecules. Biochem J *473*, 2315-2329.

Miller, A.K., Brannon, M.K., Stevens, L., Johansen, H.K., Selgrade, S.E., Miller, S.I., Høiby, N., and Moskowitz, S.M. (2011). PhoQ mutations promote lipid A modification and polymyxin resistance of *Pseudomonas aeruginosa* found in colistin-treated cystic fibrosis patients. Antimicrob Agents Chemother *55*, 5761-5769.

Miller-Fleming, L., Olin-Sandoval, V., Campbell, K., and Ralser, M. (2015). Remaining Mysteries of Molecular Biology: The Role of Polyamines in the Cell. J Mol Biol *427*, 3389-3406.

Mine, T., Morita, Y., Kataoka, A., Mizushima, T., and Tsuchiya, T. (1999). Expression in *Escherichia coli* of a new multidrug efflux pump, MexXY, from *Pseudomonas aeruginosa*. Antimicrob Agents Chemother *43*, 415-417.

Mingeot-Leclercq, M.P., Glupczynski, Y., and Tulkens, P.M. (1999). Aminoglycosides: activity and resistance. Antimicrob Agents Chemother *43*, 727-737.

Mitchell, C.A., Shi, C., Aldrich, C.C., and Gulick, A.M. (2012). Structure of PA1221, a nonribosomal peptide synthetase containing adenylation and peptidyl carrier protein domains. Biochemistry *51*, 3252-3263.

Moore, J.O., and Hendrickson, W.A. (2012). An asymmetry-to-symmetry switch in signal transmission by the histidine kinase receptor for TMAO. Structure *20*, 729-741.

Moradali, M.F., Ghods, S., and Rehm, B.H. (2017). *Pseudomonas aeruginosa* Lifestyle: A Paradigm for Adaptation, Survival, and Persistence. Front Cell Infect Microbiol *7*, 39.

Morita, Y., Gilmour, C., Metcalf, D., and Poole, K. (2009). Translational control of the antibiotic inducibility of the PA5471 gene required for *mexXY* multidrug efflux gene expression in *Pseudomonas aeruginosa*. J Bacteriol *191*, 4966-4975.

Moskowitz, S.M., Brannon, M.K., Dasgupta, N., Pier, M., Sgambati, N., Miller, A.K., Selgrade, S.E., Miller, S.I., Denton, M., Conway, S.P.*, et al.* (2012). PmrB mutations promote polymyxin resistance of *Pseudomonas aeruginosa* isolated from colistin-treated cystic fibrosis patients. Antimicrob Agents Chemother *56*, 1019-1030.

Moskowitz, S.M., Ernst, R.K., and Miller, S.I. (2004). PmrAB, a two-component regulatory system of *Pseudomonas aeruginosa* that modulates resistance to cationic antimicrobial peptides and addition of aminoarabinose to lipid A. J Bacteriol *186*, 575-579.

Mulcahy, H., Charron-Mazenod, L., and Lewenza, S. (2008). Extracellular DNA chelates cations and induces antibiotic resistance in *Pseudomonas aeruginosa* biofilms. PLoS Pathog *4*, e1000213.

Muller, C., Plésiat, P., and Jeannot, K. (2011). A two-component regulatory system interconnects resistance to polymyxins, aminoglycosides, fluoroquinolones, and β-lactams in *Pseudomonas aeruginosa*. Antimicrob Agents Chemother *55*, 1211-1221.

Möglich, A., Ayers, R.A., and Moffat, K. (2009). Structure and signaling mechanism of Per-ARNT-Sim domains. Structure *17*, 1282-1294.

Nadal-Jimenez, P., Koch, G., Reis, C.R., Muntendam, R., Raj, H., Jeronimus-Stratingh, C.M., Cool, R.H., and Quax, W.J. (2014). PvdP is a tyrosinase that drives maturation of the pyoverdine chromophore in *Pseudomonas aeruginosa*. J Bacteriol *196*, 2681-2690.

Needham, B.D., and Trent, M.S. (2013). Fortifying the barrier: the impact of lipid A remodelling on bacterial pathogenesis. Nat Rev Microbiol *11*, 467-481.

Nishijyo, T., Haas, D., and Itoh, Y. (2001). The CbrA-CbrB two-component regulatory system controls the utilization of multiple carbon and nitrogen sources in *Pseudomonas aeruginosa*. Mol Microbiol *40*, 917-931.

Novichkov, P.S., Li, X., Kuehl, J.V., Deutschbauer, A.M., Arkin, A.P., Price, M.N., and Rodionov, D.A. (2014). Control of methionine metabolism by the SahR transcriptional regulator in Proteobacteria. Environ Microbiol *16*, 1-8.

Nowak-Thompson, B., Chaney, N., Wing, J.S., Gould, S.J., and Loper, J.E. (1999). Characterization of the pyoluteorin biosynthetic gene cluster of *Pseudomonas fluorescens* Pf-5. J Bacteriol *181*, 2166-2174.

Nowak-Thompson, B., Gould, S.J., and Loper, J.E. (1997). Identification and sequence analysis of the genes encoding a polyketide synthase required for pyoluteorin biosynthesis in *Pseudomonas fluorescens* Pf-5. Gene *204*, 17-24.

Nyfeler, B., Hoepfner, D., Palestrant, D., Kirby, C.A., Whitehead, L., Yu, R., Deng, G., Caughlan, R.E., Woods, A.L., Jones, A.K.*, et al.* (2012). Identification of elongation factor G as the conserved cellular target of argyrin B. PLoS One *7*, e42657.

Ochsner, U.A., Wilderman, P.J., Vasil, A.I., and Vasil, M.L. (2002). GeneChip expression analysis of the iron starvation response in *Pseudomonas aeruginosa*: identification of novel pyoverdine biosynthesis genes. Mol Microbiol *45*, 1277-1287.

Owusu-Anim, D., and Kwon, D.H. (2012). Differential Role of Two-Component Regulatory Systems (*phoPQ* and *pmrAB*) in polymyxin B Susceptibility of *Pseudomonas aeruginosa*. Adv Microbiol *2*.

Padilla, E., Llobet, E., Doménech-Sánchez, A., Martínez-Martínez, L., Bengoechea, J.A., and Albertí, S. (2010). *Klebsiella pneumoniae* AcrAB efflux pump contributes to antimicrobial resistance and virulence. Antimicrob Agents Chemother *54*, 177-183.

Palmer, S.O., Rangel, E.Y., Hu, Y., Tran, A.T., and Bullard, J.M. (2013). Two homologous EF-G proteins from *Pseudomonas aeruginosa* exhibit distinct functions. PLoS One *8*, e80252.

Pamp, S.J., Gjermansen, M., Johansen, H.K., and Tolker-Nielsen, T. (2008). Tolerance to the antimicrobial peptide colistin in *Pseudomonas aeruginosa* biofilms is linked to metabolically active cells, and depends on the *pmr* and *mexAB-oprM* genes. Mol Microbiol *68*, 223-240.

Pappalardo, L., Janausch, I.G., Vijayan, V., Zientz, E., Junker, J., Peti, W., Zweckstetter, M., Unden, G., and Griesinger, C. (2003). The NMR structure of the sensory domain of the membranous two-component fumarate sensor (histidine protein kinase) DcuS of *Escherichia coli*. J Biol Chem *278*, 39185-39188.

Patel, H.M., Tao, J., and Walsh, C.T. (2003). Epimerization of an L-cysteinyl to a D-cysteinyl residue during thiazoline ring formation in siderophore chain elongation by pyochelin synthetase from *Pseudomonas aeruginosa*. Biochemistry *42*, 10514-10527.

Patel, H.M., and Walsh, C.T. (2001). *In vitro* reconstitution of the *Pseudomonas aeruginosa* nonribosomal peptide synthesis of pyochelin: characterization of backbone tailoring thiazoline reductase and N-methyltransferase activities. Biochemistry *40*, 9023-9031.

Patteson, J.B., Dunn, Z.D., and Li, B. (2018). *In Vitro* Biosynthesis of the Nonproteinogenic Amino Acid Methoxyvinylglycine. Angew Chem Int Ed Engl *57*, 6780-6785.

Pereira, T.C., de Barros, P.P., Fugisaki, L.R.O., Rossoni, R.D., Ribeiro, F.C., de Menezes, R.T., Junqueira, J.C., and Scorzoni, L. (2018). Recent Advances in the Use of *Galleria mellonella* Model to Study Immune Responses against Human Pathogens. J Fungi (Basel) *4*.

Perron, K., Caille, O., Rossier, C., Van Delden, C., Dumas, J.L., and Köhler, T. (2004). CzcR-CzcS, a two-component system involved in heavy metal and carbapenem resistance in *Pseudomonas aeruginosa*. J Biol Chem *279*, 8761-8768.

Peschel, A., Otto, M., Jack, R.W., Kalbacher, H., Jung, G., and Götz, F. (1999). Inactivation of the *dlt* operon in *Staphylococcus aureus* confers sensitivity to defensins, protegrins, and other antimicrobial peptides. J Biol Chem *274*, 8405-8410.

Piddock, L.J. (2006). Clinically relevant chromosomally encoded multidrug resistance efflux pumps in bacteria. Clin Microbiol Rev *19*, 382-402.

Poole, K. (2005). Aminoglycoside resistance in *Pseudomonas aeruginosa*. Antimicrob Agents Chemother *49*, 479-487.

Poole, K., Krebes, K., McNally, C., and Neshat, S. (1993). Multiple antibiotic resistance in *Pseudomonas aeruginosa*: evidence for involvement of an efflux operon. J Bacteriol *175*, 7363-7372.

Poole, K., Lau, C.H., Gilmour, C., Hao, Y., and Lam, J.S. (2015). Polymyxin Susceptibility in *Pseudomonas aeruginosa* Linked to the MexXY-OprM Multidrug Efflux System. Antimicrob Agents Chemother *59*, 7276-7289.

Prokhorova, I., Altman, R.B., Djumagulov, M., Shrestha, J.P., Urzhumtsev, A., Ferguson, A., Chang, C.T., Yusupov, M., Blanchard, S.C., and Yusupova, G. (2017). Aminoglycoside interactions and impacts on the eukaryotic ribosome. Proc Natl Acad Sci U S A *114*, E10899-E10908.

Reimmann, C., Patel, H.M., Serino, L., Barone, M., Walsh, C.T., and Haas, D. (2001). Essential PchG-dependent reduction in pyochelin biosynthesis of *Pseudomonas aeruginosa*. J Bacteriol *183*, 813-820.

Reimmann, C., Patel, H.M., Walsh, C.T., and Haas, D. (2004). PchC thioesterase optimizes nonribosomal biosynthesis of the peptide siderophore pyochelin in *Pseudomonas aeruginosa*. J Bacteriol *186*, 6367-6373.

Reimmann, C., Serino, L., Beyeler, M., and Haas, D. (1998). Dihydroaeruginoic acid synthetase and pyochelin synthetase, products of the *pchEF* genes, are induced by extracellular pyochelin in *Pseudomonas aeruginosa*. Microbiology *144 (Pt 11)*, 3135-3148.

Reinelt, S., Hofmann, E., Gerharz, T., Bott, M., and Madden, D.R. (2003). The structure of the periplasmic ligand-binding domain of the sensor kinase CitA reveals the first extracellular PAS domain. J Biol Chem *278*, 39189-39196.

Rieg, S., Huth, A., Kalbacher, H., and Kern, W.V. (2009). Resistance against antimicrobial peptides is independent of *Escherichia coli* AcrAB, *Pseudomonas aeruginosa MexAB* and *Staphylococcus aureus* NorA efflux pumps. Int J Antimicrob Agents *33*, 174-176.

Ringel, M.T., Dräger, G., and Brüser, T. (2016). PvdN Enzyme Catalyzes a Periplasmic Pyoverdine Modification. J Biol Chem *291*, 23929-23938.

Rivera-Cancel, G., Ko, W.H., Tomchick, D.R., Correa, F., and Gardner, K.H. (2014). Full-length structure of a monomeric histidine kinase reveals basis for sensory regulation. Proc Natl Acad Sci U S A *111*, 17839-17844.

Rodrigue, A., Quentin, Y., Lazdunski, A., Méjean, V., and Foglino, M. (2000). Two-component systems in *Pseudomonas aeruginosa*: why so many? Trends Microbiol *8*, 498-504.

Rojas Murcia, N., Lee, X., Waridel, P., Maspoli, A., Imker, H.J., Chai, T., Walsh, C.T., and Reimmann, C. (2015). The *Pseudomonas aeruginosa* antimetabolite L -2-amino-4-methoxy-trans-3-butenoic acid (AMB) is made from glutamate and two alanine residues *via* a thiotemplate-linked tripeptide precursor. Front Microbiol *6*, 170.

Ronnebaum, T.A., and Lamb, A.L. (2018). Nonribosomal peptides for iron acquisition: pyochelin biosynthesis as a case study. Curr Opin Struct Biol *53*, 1-11.

Sahm, U., Knobloch, G., and Wagner, F. (1973). Isolation and characterization of the methionine antagonist L-2-amino-4-methoxy-trans-3-butenoic acid from *Pseudomonas aeruginosa* grown on n-paraffin. J Antibiot (Tokyo) *26*, 389-390.

Saita, E., Albanesi, D., and de Mendoza, D. (2016). Sensing membrane thickness: Lessons learned from cold stress. Biochim Biophys Acta *1861*, 837-846.

Salunkhe, P., Smart, C.H., Morgan, J.A., Panagea, S., Walshaw, M.J., Hart, C.A., Geffers, R., Tümmler, B., and Winstanley, C. (2005). A cystic fibrosis epidemic strain of *Pseudomonas aeruginosa* displays enhanced virulence and antimicrobial resistance. J Bacteriol *187*, 4908-4920.

Sautrey, G., Zimmermann, L., Deleu, M., Delbar, A., Souza Machado, L., Jeannot, K., Van Bambeke, F., Buyck, J.M., Decout, J.L., and Mingeot-Leclercq, M.P. (2014). New amphiphilic neamine derivatives active against resistant *Pseudomonas aeruginosa* and their interactions with lipopolysaccharides. Antimicrob Agents Chemother *58*, 4420-4430.

Scannell, J.P., Ax, H.A., Pruess, D.L., Williams, T., and Demny, T.C. (1972). Antimetabolites produced by microorganisms. VI. L-N 5 -(1-iminoethyl) ornithine. J Antibiot (Tokyo) *25*, 179-184.

Schalk, I.J., and Cunrath, O. (2016). An overview of the biological metal uptake pathways in *Pseudomonas aeruginosa*. Environ Microbiol *18*, 3227-3246.

Schalk, I.J., and Guillon, L. (2013). Pyoverdine biosynthesis and secretion in *Pseudomonas aeruginosa*: implications for metal homeostasis. Environ Microbiol *15*, 1661-1673.

Schniederjans, M., Koska, M., and Häussler, S. (2017). Transcriptional and Mutational Profiling of an Aminoglycoside-Resistant *Pseudomonas aeruginosa* Small-Colony Variant. Antimicrob Agents Chemother *61*.

Schurek, K.N., Marr, A.K., Taylor, P.K., Wiegand, I., Semenec, L., Khaira, B.K., and Hancock, R.E. (2008). Novel genetic determinants of low-level aminoglycoside resistance in *Pseudomonas aeruginosa*. Antimicrob Agents Chemother *52*, 4213-4219.

Schurek, K.N., Sampaio, J.L., Kiffer, C.R., Sinto, S., Mendes, C.M., and Hancock, R.E. (2009). Involvement of *pmrAB* and *phoPQ* in polymyxin B adaptation and inducible resistance in non-cystic fibrosis clinical isolates of *Pseudomonas aeruginosa*. Antimicrob Agents Chemother *53*, 4345-4351.

Schuster, M., Lostroh, C.P., Ogi, T., and Greenberg, E.P. (2003). Identification, timing, and signal specificity of *Pseudomonas aeruginosa quorum*-controlled genes: a transcriptome analysis. J Bacteriol *185*, 2066-2079.

Schwarzer, D., Finking, R., and Marahiel, M.A. (2003). Nonribosomal peptides: from genes to products. Nat Prod Rep *20*, 275-287.

Selva, E., Gastaldo, L., Saddler, G.S., Toppo, G., Ferrari, P., Carniti, G., and Goldstein, B.P. (1996). Antibiotics A21459 A and B, new inhibitors of bacterial protein synthesis. I. Taxonomy, isolation and characterization. J Antibiot (Tokyo) *49*, 145-149.

Shafer, W.M., Qu, X., Waring, A.J., and Lehrer, R.I. (1998). Modulation of *Neisseria gonorrhoeae* susceptibility to vertebrate antibacterial peptides due to a member of the resistance/nodulation/division efflux pump family. Proc Natl Acad Sci U S A *95*, 1829-1833.

Shajani, Z., Sykes, M.T., and Williamson, J.R. (2011). Assembly of bacterial ribosomes. Annu Rev Biochem *80*, 501-526.

Shi, J., Jin, Y., Bian, T., Li, K., Sun, Z., Cheng, Z., Jin, S., and Wu, W. (2015). SuhB is a novel ribosome associated protein that regulates expression of MexXY by modulating ribosome stalling in *Pseudomonas aeruginosa*. Mol Microbiol *98*, 370-383.

Silhavy, T.J., Kahne, D., and Walker, S. (2010). The bacterial cell envelope. Cold Spring Harb Perspect Biol *2*, a000414.

Sitaraman, R. (2015). *Pseudomonas spp*. as models for plant-microbe interactions. Front Plant Sci *6*, 787.

Sivaneson, M., Mikkelsen, H., Ventre, I., Bordi, C., and Filloux, A. (2011). Two-component regulatory systems in *Pseudomonas aeruginosa*: an intricate network mediating fimbrial and efflux pump gene expression. Mol Microbiol *79*, 1353-1366.

Smith, W.D., Bardin, E., Cameron, L., Edmondson, C.L., Farrant, K.V., Martin, I., Murphy, R.A., Soren, O., Turnbull, A.R., Wierre-Gore, N.*, et al.* (2017). Current and future therapies for *Pseudomonas aeruginosa* infection in patients with cystic fibrosis. FEMS Microbiol Lett *364*.

Snesrud, E., Maybank, R., Kwak, Y.I., Jones, A.R., Hinkle, M.K., and McGann, P. (2018). Chromosomally Encoded *mcr-5* in Colistin-Nonsusceptible *Pseudomonas aeruginosa*. Antimicrob Agents Chemother *62*.

Stover, C.K., Pham, X.Q., Erwin, A.L., Mizoguchi, S.D., Warrener, P., Hickey, M.J., Brinkman, F.S., Hufnagle, W.O., Kowalik, D.J., Lagrou, M.*, et al.* (2000). Complete genome sequence of *Pseudomonas aeruginosa* PAO1, an opportunistic pathogen. Nature *406*, 959-964.

Strehmel, J., Neidig, A., Nusser, M., Geffers, R., Brenner-Weiss, G., and Overhage, J. (2015). Sensor kinase PA4398 modulates swarming motility and biofilm formation in *Pseudomonas aeruginosa* PA14. Appl Environ Microbiol *81*, 1274-1285.

Strieker, M., Tanović, A., and Marahiel, M.A. (2010). Nonribosomal peptide synthetases: structures and dynamics. Curr Opin Struct Biol *20*, 234-240.

Struble, J.M., and Gill, R.T. (2009). Genome-scale identification method applied to find cryptic aminoglycoside resistance genes in *Pseudomonas aeruginosa*. PLoS One *4*, e6576.

Süssmuth, R.D., and Mainz, A. (2017). Nonribosomal Peptide Synthesis-Principles and Prospects. Angew Chem Int Ed Engl *56*, 3770-3821.

Taber, H.W., Mueller, J.P., Miller, P.F., and Arrow, A.S. (1987). Bacterial uptake of aminoglycoside antibiotics. Microbiol Rev *51*, 439-457.

Tacconelli, E., Carrara, E., Savoldi, A., Harbarth, S., Mendelson, M., Monnet, D.L., Pulcini, C., Kahlmeter, G., Kluytmans, J., Carmeli, Y.*, et al.* (2018). Discovery, research, and development of new antibiotics: the WHO priority list of antibiotic-resistant bacteria and tuberculosis. Lancet Infect Dis *18*, 318-327.

Takeda, R. (1958). Structure of a new antibiotic, pyoluteorin. Journal of the American Chemical Society *80*, 4749-4750.

Tamma, P.D., Cosgrove, S.E., and Maragakis, L.L. (2012). Combination therapy for treatment of infections with Gram-negative bacteria. Clin Microbiol Rev *25*, 450-470.

Taylor, B.L., and Zhulin, I.B. (1999). PAS domains: internal sensors of oxygen, redox potential, and light. Microbiol Mol Biol Rev *63*, 479-506.

Taylor, P.K., Yeung, A.T., and Hancock, R.E. (2014). Antibiotic resistance in *Pseudomonas aeruginosa* biofilms: towards the development of novel anti-biofilm therapies. J Biotechnol *191*, 121-130.

Thomas, M.G., Burkart, M.D., and Walsh, C.T. (2002). Conversion of L-proline to pyrrolyl-2-carboxyl-S-PCP during undecylprodigiosin and pyoluteorin biosynthesis. Chem Biol *9*, 171-184.

Treangen, T.J., and Rocha, E.P. (2011). Horizontal transfer, not duplication, drives the expansion of protein families in prokaryotes. PLoS Genet *7*, e1001284.

Trias, J., and Nikaido, H. (1990). Outer membrane protein D2 catalyzes facilitated diffusion of carbapenems and penems through the outer membrane of *Pseudomonas aeruginosa*. Antimicrob Agents Chemother *34*, 52-57.

Tsai, C.J., Loh, J.M., and Proft, T. (2016). *Galleria mellonella* infection models for the study of bacterial diseases and for antimicrobial drug testing. Virulence *7*, 214-229.

Tzeng, Y.L., Ambrose, K.D., Zughaier, S., Zhou, X., Miller, Y.K., Shafer, W.M., and Stephens, D.S. (2005). Cationic antimicrobial peptide resistance in *Neisseria meningitidis*. J Bacteriol *187*, 5387-5396.

Vakulenko, S.B., and Mobashery, S. (2003). Versatility of aminoglycosides and prospects for their future. Clin Microbiol Rev *16*, 430-450.

Vandenende, C.S., Vlasschaert, M., and Seah, S.Y. (2004). Functional characterization of an aminotransferase required for pyoverdine siderophore biosynthesis in *Pseudomonas aeruginosa* PAO1. J Bacteriol *186*, 5596-5602.

Vettoretti, L., Plésiat, P., Muller, C., El Garch, F., Phan, G., Attrée, I., Ducruix, A., and Llanes, C. (2009). Efflux unbalance in *Pseudomonas aeruginosa* isolates from cystic fibrosis patients. Antimicrob Agents Chemother *53*, 1987-1997.

Visca, P., Imperi, F., and Lamont, I.L. (2007). Pyoverdine siderophores: from biogenesis to biosignificance. Trends Microbiol *15*, 22-30.

Wagner, V.E., Bushnell, D., Passador, L., Brooks, A.I., and Iglewski, B.H. (2003). Microarray analysis of *Pseudomonas aeruginosa quorum*-sensing regulons: effects of growth phase and environment. J Bacteriol *185*, 2080-2095.

Wang, D., Seeve, C., Pierson, L.S., and Pierson, E.A. (2013). Transcriptome profiling reveals links between ParS/ParR, MexEF-OprN, and *quorum* sensing in the regulation of adaptation and virulence in *Pseudomonas aeruginosa*. BMC Genomics *14*, 618.

Wang, Y., Ha, U., Zeng, L., and Jin, S. (2003). Regulation of membrane permeability by a two-component regulatory system in *Pseudomonas aeruginosa*. Antimicrob Agents Chemother *47*, 95-101.

Westbrock-Wadman, S., Sherman, D.R., Hickey, M.J., Coulter, S.N., Zhu, Y.Q., Warrener, P., Nguyen, L.Y., Shawar, R.M., Folger, K.R., and Stover, C.K. (1999). Characterization of a *Pseudomonas aeruginosa* efflux pump contributing to aminoglycoside impermeability. Antimicrob Agents Chemother *43*, 2975-2983.

Whiteley, M., Bangera, M.G., Bumgarner, R.E., Parsek, M.R., Teitzel, G.M., Lory, S., and Greenberg, E.P. (2001). Gene expression in *Pseudomonas aeruginosa* biofilms. Nature *413*, 860-864.

Wilson, D.N. (2014). Ribosome-targeting antibiotics and mechanisms of bacterial resistance. Nat Rev Microbiol *12*, 35-48.

Wilton, M., Charron-Mazenod, L., Moore, R., and Lewenza, S. (2016). Extracellular DNA Acidifies Biofilms and Induces Aminoglycoside Resistance in *Pseudomonas aeruginosa*. Antimicrob Agents Chemother *60*, 544-553.

Winstanley, C., Langille, M.G., Fothergill, J.L., Kukavica-Ibrulj, I., Paradis-Bleau, C., Sanschagrin, F., Thomson, N.R., Winsor, G.L., Quail, M.A., Lennard, N.*, et al.* (2009). Newly introduced genomic prophage islands are critical determinants of *in vivo* competitiveness in the Liverpool Epidemic Strain of *Pseudomonas aeruginosa*. Genome Res *19*, 12-23.

Wu, R., Gu, M., Wilton, R., Babnigg, G., Kim, Y., Pokkuluri, P.R., Szurmant, H., Joachimiak, A., and Schiffer, M. (2013). Insight into the sporulation phosphorelay: crystal structure of the sensor domain of *Bacillus subtilis* histidine kinase, KinD. Protein Sci *22*, 564-576.

Yamamoto, M., Ueda, A., Kudo, M., Matsuo, Y., Fukushima, J., Nakae, T., Kaneko, T., and Ishigatsubo, Y. (2009). Role of MexZ and PA5471 in transcriptional regulation of *mexXY* in *Pseudomonas aeruginosa*. Microbiology *155*, 3312-3321.

Yamamoto, S., Hamanaka, K., Suemoto, Y., Ono, B., and Shinoda, S. (1986). Evidence for the presence of a novel biosynthetic pathway for norspermidine in *Vibrio*. Can J Microbiol *32*, 99-103.

Yeterian, E., Martin, L.W., Guillon, L., Journet, L., Lamont, I.L., and Schalk, I.J. (2010). Synthesis of the siderophore pyoverdine in *Pseudomonas aeruginosa* involves a periplasmic maturation. Amino Acids *38*, 1447-1459.

Yeung, A.T., Bains, M., and Hancock, R.E. (2011). The sensor kinase CbrA is a global regulator that modulates metabolism, virulence, and antibiotic resistance in *Pseudomonas aeruginosa*. J Bacteriol *193*, 918-931.

Yokoyama, K., Doi, Y., Yamane, K., Kurokawa, H., Shibata, N., Shibayama, K., Yagi, T., Kato, H., and Arakawa, Y. (2003). Acquisition of 16S rRNA methylase gene in *Pseudomonas aeruginosa*. Lancet *362*, 1888-1893.

Zaborin, A., Gerdes, S., Holbrook, C., Liu, D.C., Zaborina, O.Y., and Alverdy, J.C. (2012). *Pseudomonas aeruginosa* overrides the virulence inducing effect of opioids when it senses an abundance of phosphate. PLoS One *7*, e34883.

Zaoui, C., Overhage, J., Löns, D., Zimmermann, A., Müsken, M., Bielecki, P., Pustelny, C., Becker, T., Nimtz, M., and Häussler, S. (2012). An orphan sensor kinase controls quinolone signal production *via* MexT in *Pseudomonas aeruginosa*. Mol Microbiol *83*, 536-547.

Zhang, L., Fritsch, M., Hammond, L., Landreville, R., Slatculescu, C., Colavita, A., and Mah, T.F. (2013). Identification of genes involved in *Pseudomonas aeruginosa* biofilm-specific resistance to antibiotics. PLoS One *8*, e61625.

Zhang, L., Hinz, A.J., Nadeau, J.P., and Mah, T.F. (2011). *Pseudomonas aeruginosa* tssC1 links type VI secretion and biofilm-specific antibiotic resistance. J Bacteriol *193*, 5510-5513.

Zhang, L., and Mah, T.F. (2008). Involvement of a novel efflux system in biofilm-specific resistance to antibiotics. J Bacteriol *190*, 4447-4452.

Zhang, W., Heemstra, J.R., Walsh, C.T., and Imker, H.J. (2010). Activation of the pacidamycin PacL adenylation domain by MbtH-like proteins. Biochemistry *49*, 9946-9947.

Zhang, X.X., and Rainey, P.B. (2008). Dual involvement of CbrAB and NtrBC in the regulation of histidine utilization in *Pseudomonas fluorescens* SBW25. Genetics *178*, 185-195.

Zschiedrich, C.P., Keidel, V., and Szurmant, H. (2016). Molecular Mechanisms of Two-Component Signal Transduction. J Mol Biol *428*, 3752-3775.

Identification of novel regulatory pathways involved in non-enzymatic resistance to aminoglycosides in *Pseudomonas aeruginosa*

Antibiotics are invaluable drugs to combat bacterial infections. Emergence and spread of antibiotic resistance in the opportunistic pathogen *Pseudomonas aeruginosa* have led the World Health Organization to consider as a crucial priority the development of new therapeutic approaches to fight this bacterium. In addition to other alternatives, preservation of activity of major antibiotics such as aminoglycosides and colistin is primordial. Consequently, characterization of the resistance mechanisms to these drugs is a prerequisite to design novel molecules, and improve patient care. In this context, we show that mutations in gene *fusA1* (encoding elongation factor EF-G1A) and in operon *pmrAB* (two-component system PmrAB) lead to an increased resistance to aminoglycosides in *in vitro*-selected mutants and strains isolated from cystic fibrosis (CF) and non-CF patients. Certain amino acid substitutions in EF-G1A confer a 2- to 16-fold increased resistance to the four aminoglycoside subclasses. On the other hand, amino acid variations in two-component system PmrAB activate the expression of genes PA4773-PA4774-PA4775, and production of norspermidine and spermidine. This upregulated polyamine biosynthesis is associated with a 4- to 16-fold decreased susceptibility to 4,6-di-substituted deoxystreptamine aminoglycosides (gentamicin, amikacin and tobramycin). Moreover, our work reveals that the acquired resistance of *pmrB* mutants to colistin partially depends upon pump MexXY(OprM), a system that otherwise mediates intrinsic, adaptive and acquired resistance to aminoglycosides. Finally, we show that *pmrB* mutants overproduce azetidine-containing alkaloids by a *quorum*-sensing-regulated, nonribosomal peptide synthetase pathway. These alkaloids impair the virulence of *P. aeruginosa* in a *Galleria mellonella* infection model.

Identification de nouvelles voies de régulation impliquées dans la résistance non enzymatique aux aminosides chez *Pseudomonas aeruginosa*

Les antibiotiques sont des molécules incontournables dans le traitement des infections bactériennes. L'émergence et la dissémination de la résistance aux antibiotiques chez la pathogène opportuniste *Pseudomonas aeruginosa*, ont amené l'Organisation Mondiale de la Santé à déclarer indispensable le développement de nouvelles approches thérapeutiques pour lutter contre cette bactérie. Bien que certaines alternatives aient été envisagées, la préservation de l'activité d'antibiotiques majeurs tels que les aminosides et la colistine est primordiale. La caractérisation des mécanismes de résistance à ces médicaments est nécessaire pour la mise au point de nouvelles molécules et mieux prendre en charge les patients. Dans ce contexte, nous montrons que des mutations dans le gène *fusA1* (codant le facteur d'élongation EF-G1A) et dans l'opéron *pmrAB* (système à deux composants PmrAB) entrainent une augmentation de la résistance aux aminosides chez des mutants isolés au laboratoire et des souches issues de patients, atteints ou non, de mucoviscidose. Certaines substitutions d'acide aminé dans EF-G1A accroissent les niveaux de résistance de 2 à 16 fois aux quatre sous-classes d'aminosides. Par ailleurs, des changements d'acide aminé dans le système à deux composants PmrAB activent l'expression des gènes PA4773-PA4774-PA4775, et la production de norspermidine et de spermidine. La synthèse de ces polyamines va de pair avec une baisse de 4 à 16 fois de la sensibilité aux aminosides à noyan 2-désoxystreptamine bisubstitué en 4,6 (gentamicine, amikacine et tobramycine). De plus, il apparaît que la résistance des mutants *pmrB* à la colistine est en partie dépendante de la pompe d'efflux MexXY(OprM), un système impliqué dans la résistance naturelle, adaptative ou acquise aux aminosides. Enfin, nous montrons que les mutants *pmrB* surproduisent des alcaloïdes contenant un motif azétidine, par une voie de synthèse non-ribosomale et dépendante du *quorum* sensing. Ces alcaloïdes diminuent la virulence de *P. aeruginosa* dans le modèle *Galleria mellonella*.

ÉCOLE DOCTORALE
Environnements - Santé
Bourgogne | Franche-Comté